EXPLORING IN AERONAUTICS

An Introduction to Aeronautical Sciences

NATIONAL AERONAUTICS AND SPACE ADMINISTRATION

EXPLORING IN AERONAUTICS

an Introduction to Aeronautical Sciences developed at the NASA Lewis Research Center, Cleveland, Ohio.

National Aeronautics and Space Administration, Washington, D.C. 20546
1971

For sale by the Superintendent of Documents, U.S. Government Printing Office
Washington, D.C. 20402 - Price $3.50
Stock Number 3300-0395

PREFACE

"Exploring in Aeronautics" is the second publication resulting from the NASA-Lewis Aerospace Explorer program; the first is titled "Exploring in Aerospace Rocketry" (NASA EP-88). Both publications are based on the lectures and projects of a contemporary, special-interest Explorer program sponsored by the NASA-Lewis Research Center. The principal objective of this program is to provide promising students from local schools with an opportunity for meaningful career guidance and motivation over a wide spectrum of aerospace engineering and scientific professions. Each year, candidates (ages 15 to 19 years) for the program are selected by school officials on the basis of their demonstrated interest and proficiency in mathematics and science.

In this adult-oriented program, we attempt to provide the young people with a meaningful career exposure through adult associations in a professional environment. Instead of merely lecturing to them, we try to involve the youths directly in the aerospace technology and to stress attendant project activity and teamwork. Fundamental scientific principles are explained through lectures and demonstrations. Technical sophistication and rigorous mathematical developments are generally avoided. The youths are committed to a realistic simulation of the "research-and-development" environment. Project activities are assigned, planned, implemented, analyzed, and reported on in significant detail. In effect, the youths are taken behind the scenes for a full view of the real engineering world.

Throughout the program, emphasis is placed on communication. The art of effective communication, of course, is vital to almost any career. To generate a high level of interest, to ensure clarity and understanding in the presentations, and to achieve a rapport with the lecturers, the participants are encouraged to raise questions. Explorer "project engineers" are periodically required to report to the membership on current project status and progress. Each year, the culmination of the program is a research symposium, in which the youths report the results of their researches to an audience of parents, teachers, and Lewis management officials.

NASA-Lewis employee participation in the program is considerable. Many employees enthusiastically and sincerely guide the young people in their scientific endeavors. Thus, the youths are exposed to a wide range of aerospace-oriented personnel - technicians, engineers, scientists, and administrators. The time donated to the program by these NASA employees is their personal contribution to the future well-being and success of our youth and our nation. In a very real sense, this effort goes hand in hand with the academic programs to focus and develop the interests and skills of our young men and women.

Lewis management believes that this work with young people is clearly in keeping with the spirit of the NASA Charter, wherein NASA is commissioned "to contribute materially to . . . the expansion of human knowledge of phenomena in the atmosphere and space." NASA is also charged with the "widest practicable . . . dissemination of information concerning its activities and the results thereof."

This publication is intended not only to provide a basic explanation of some of the fundamentals of aerodynamics but also to stimulate other government agencies, educational institutions, private industry, and business to establish career-motivation programs within their own special fields of knowledge.

The basis of this publication was just one year of the Lewis Explorer program. The various NASA-Lewis employees who lectured to the Explorers, and also served as associate advisers, during that year are identified as authors of the chapters of this publication. Other employees who donated their time and talents to the program included Dr. Abe Silverstein (Explorer Post sponsor); Billy R. Harrison, William J. Masica, Roy A. Maurer, Edward T. Meleason, Brent A. Miller, Larry E. Smith, and Calvin W. Weiss (all associate advisers for wind-tunnel projects); John F. Staggs and Michael C. Thompson (associate advisers for flight projects); Harold D. Wharton (institutional representative); Joseph F. Hobzek, Jr., (Chairman, Explorer Post Committee); William A. Brahms, Charles E. Kelsey, Donald A. Kelsey, Clair R. King, and Horace C. Moore, Jr., (all members of Explorer Post Committee); and Clifford W. Brooks (photographer for the program and associate adviser for flight projects).

James F. Connors
Director of Technical Services
(Adviser, Lewis Aerospace Explorer Post)

INTRODUCTION

The history of the airplane is much better known than the history of rockets and satellites. Aircraft flying overhead are a common sight in all technologically advanced countries. It is quite appropriate, therefore, that an educational publication on the principles of aeronautics should be made available by NASA.

An important use of this book could be as a curriculum resource for teachers in high schools and colleges. It might also be helpful to curriculum committees and textbook writers. It discusses many topics which teachers in various disciplines can use to supplement their regular courses. The comprehensive history of aviation given in the first chapter could enrich courses in general or physical science or the history of science. The chapter on weather safety and navigation in severe storms would be useful in Earth science courses. Many examples of applications of mathematics are found in the book. But the discipline which would find the most usefulness in the book is physics. Even a cursory glance through the book impresses one with the fact that the design and operation of aircraft would be impossible without an understanding of complex physical concepts.

A course in aeronautics for college-capable students in high school could be built around the book, especially if the teacher refers to related literature for problem material to reinforce the concepts presented. At the college level it could provide appropriate material for introductory courses in the science of aeronautics. With some modification, it could be used with vocationally oriented student groups in high school. Student and adult hobbyists in aeronautics will find much of the book relevant to their interests.

It is hoped that one outcome of the use of this book, and of the companion volume, "Exploring in Aerospace Rocketry" (NASA EP-88), will be to stimulate the interest and imagination of capable students so that many of them will be interested in following developments in the rapidly changing aerospace field.

CONTENTS

1. AERONAUTICS IN HISTORICAL PERSPECTIVE

James F. Connors*

The airplane has had a tremendous impact upon our society and our way of life. The world is smaller for it, people and nations are less isolated. Previous obstacles of distance have been virtually eradicated. In 1969 alone, there were 57 certified American airlines, which carried approximately 164 million originating passengers and some 20 billion revenue ton-miles of freight. Aso, the airplane is a vital element in our national defense.

How did all this come about? What can we learn from the dramatic accomplishments that have taken place in manned, powered flight?

With history going back many thousands of years, the extremely short time within which manned flight achievements have taken place is certainly impressive. For ages, man aspired to sustained flight. But, in terms of accomplishment, only one average lifespan has elapsed between the first, manned, powered flight of the Wright brothers, in 1903, and the current era of supersonic flight. Man has even penetrated successfully the Earth's atmosphere and has ventured out into the vastness of space. Viewed on a time scale, these achievements are representative of the "technological explosion" that is popularly referred to in current writings.

Here, we will only briefly touch upon technical highlights in the evolution of the airplane and point out some of the major events in aviation history. Many excellent books and documentaries have been written on this subject. Some of them have been used as information sources for this chapter and are listed in the bibliography. For convenience, a brief aviation chronology is provided in appendix A. Some of the airplane terminology is defined in appendix B.

Over the years, truly prodigious numbers and kinds of aircraft have been designed and built. Some historical airplanes used by the United States Air Force are shown in figures 1-1 to 1-45 in more or less chronological order. The modern stable of USAF aircraft is illustrated in figures 1-46 to 1-70. These are but a small sampling. Many other configurations have been used by the Air Force and the other services, notably the Navy, and in the commercial, business, and sports-flying fields.

---

*Director of Technical Services.

The story of the airplane can be broken down logically into the following phases or time periods: before the Wright brothers; the era of the Wright brothers; World War I; the late '20's and the '30's; World War II; post-World War II; and the future.

Speed has always been the prime measuring stick for aircraft performance, especially to the military. The Wright Flyer flew at about 30 miles per hour (mph); World War I aircraft averaged about 100 mph. In the late 1930's, bombers operated at slightly above 200 mph, with fighters at 300 to 350 mph. By 1945, bombers traveled at approximately 350 mph, top fighters at 500 mph, and some jet-propelled fighters exceeded 550 mph. The Douglas D-558-II Skyrocket went 1238 mph in 1951, and the experimental, rocket-powered North American X-15 (fig. 1-60) reached a speed of 4104 mph in 1962, with Joseph Walker as pilot. Such tremendous increases in flight speed did not come easily. Many difficult technical problems, or "barriers," had to be overcome. These problems occurred in all areas: structures (e.g., vibration, flutter, compressibility, etc.), aerodynamics, propulsion, materials, navigation, and control. The so-called "sonic barrier" and "thermal barrier" were also overcome.

During the evolution of the airplane, progress in aeronautics has received its impetus largely from the urgency of military needs. Under the war influence, a great investment in resources was made in the research, design, and construction of progressively superior aircraft. Subsequently, the technology associated with advanced military airplanes was applied to new designs and adaptations for commercial purposes. Military design requirements were best indicated by the slogan "Higher, Faster, and Farther." No sooner was one requirement met than another, more stringent requirement was set, with primarily Government-sponsored research leading the way to continual improvements.

To attain its high levels of performance, aviation has required, perhaps most of all, a team of dedicated, creative, imaginative, and courageous people: scientists, researchers, inventors, designers, fabricators, experimental pilots, etc. Many people, with a great variety of specialized skills and technical disciplines, have contributed to the advancement of aeronautics. Whereas the Wright Flyer was largely the product of two minds, today's sophisticated airplane designs result from the contributions of many men.

Progress in aviation, from its very inception, has probably been best characterized as the product of research, or the application of the "scientific method." This method is the logic, or the examination and reasoning process, by which a particular problem or objective is approached. Stepwise, the process involves the collection of available pertinent knowledge, formulation of new hypotheses or theories, critical investigation and experimentation, and, finally, formulation of acceptable conclusions leading to new or revised laws. With sound engineering judgment, this approach translates into careful, systematic study, isolation of variables to evaluate their individual effects, and

extremely close attention to details. This is the fundamental research philosophy, or method of inquiry, that is threaded through the story of aviation.

BEFORE THE WRIGHT BROTHERS

The first documented description of a practical device for manned flight is traceable back to Leonardo da Vinci, around 1500. This remarkable Renaissance man, far ahead of his time, produced detailed drawings of many flying machines, including a helicopter, and a parachute as well. Unfortunately, these were lost to the world for over 300 years. Leonardo and many who followed him were greatly fascinated by birds. As a result, they expended much effort in the study of ornithopters, or flapping-wing devices. None of these devices was ever successful.

In 1766, the English chemist Henry Cavendish found that hydrogen was lighter than air, and the concept of the balloon was introduced. However, it was with a heated-air system that the Montgolfier brothers made the first successful balloon flight, in France in 1783. Interest in balloons led to the subsequent development of dirigibles. However, with the disasters to the "Shenandoah," in 1925, and to the impressive "Hindenburg," in 1937, the death kenll virtually sounded for lighter-than-air ships.

The real prelude to manned powered flight came with the development of gliders. The champion in this was Germany's Otto Lilienthal. With his gliders, Lilienthal made more than 2000 flights over a 6-year period, traveling on some occasions more than 270 yards. His technique of shifting his body weight effected some measure of stability and control. In 1896, he died in a glider crash, before he could complete previously laid plans for a powered flight using a carbonic-acid-gas motor. A predecessor, Sir George Cayley (1773-1857), was actually the first to assemble in theoretical form the many elements necessary for practical flight. His first model glider (1804) was accepted by some as the original airplane. Cayley concentrated on the aerodynamics: the importance of streamlining, movable tail surfaces, and the stabilizing effect of dihedral. Another

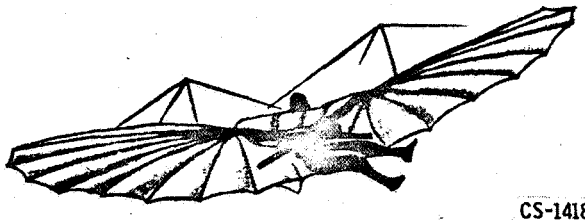

CS-14188

Otto Lilienthal (1894).

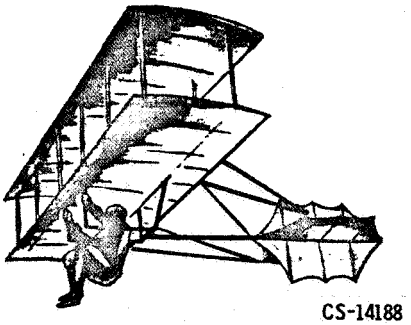

CS-14188

Octave Chanute (1896).

notable contributor among the glider enthusiasts was Octave Chanute, an American civil engineer. He introduced in a biplane glider a method of bracing the wings by struts and diagonal wires.

ERA OF THE WRIGHT BROTHERS

The story of powered flight must certainly include Samuel Pierpont Langley, architect, astronomer, physicist, mathematician, and, in later life, Secretary of the Smithsonian Institution. This esteemed scientist conducted many experiments in aerodynamics (e.g., using his "whirling table" to simulate airspeeds up to 70 mph). In 1896, he built and flew an unmanned, steam-powered model, which he called an "aerodrome," for a distance of 3200 feet. Based on this feat, Langley received a government subsidy to construct a full-size, man-carrying aerodrome. A most remarkable feature of this craft was the engine, built by Langley's assistant, Charles M. Manly. A five-cylinder, four-cycle, radial engine weighing only 125 pounds for 52.4 horsepower, it was far ahead of its time. An enormous publicity buildup preceded Langley's attempt at manned flight, but the aerodrome failed, in October 1903. As an aftermath, Professor Langley was thoroughly discredited in the eyes of the general public. He died heartbroken within a few years.

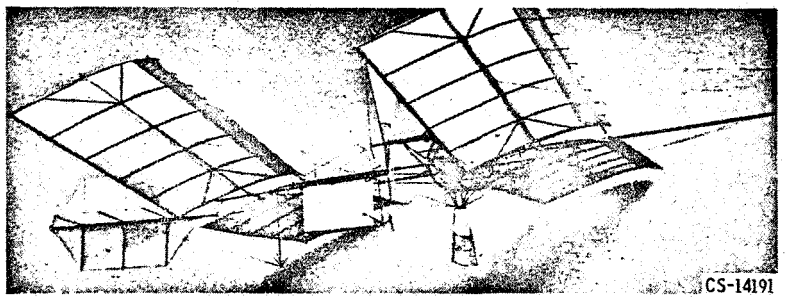

CS-14191

Professor Samuel P. Langley's aerodrome.

During these same several years, the Wright brothers - Orville and Wilbur - had dedicated themselves to the task of achieving manned powered flight. Their approach and concentration of energies differed from all others. They had recognized that the methods of construction for sustaining wings and for suitable powerplants were in such advanced stages that both would be worked out satisfactorily. Unlike other experimenters, however, they felt that the key to success was the development of a proper mechanism for achieving stability and control of the aircraft. Therefore, the Wrights focused their attention on this objective during their many glider and wind-tunnel tests. They had at an early point discovered the most important principle of control - the aileron principle.

The Wrights did not have formal engineering training. They owned and operated a bicycle shop in Dayton, Ohio. However, they were devoted experimentalists in their leisure and read extensively all publications relating to aerodynamics. In their experimentation, they found the existing gas-pressure tables in the literature to be in error and had to generate their own data. The Wrights built their own wind tunnel and studied a great variety of wing shapes in a detailed, systematic manner. They were true practitioners of the scientific method.

On the flat beach of Kitty Hawk, North Carolina, on December 17, 1903, a little more than 2 months after Langley's failure, the Wright brothers achieved the first manned, powered, sustained flight. On the last flight of the day, Wilbur remained aloft for 59 seconds and traveled 852 feet. Their Flyer (fig. 1-1) was a biplane with a wing span of 40 feet, 4 inches, and weighed 605 pounds. Its two propellers were driven by bicycle-type gears and chains connected to the engine shaft. They built their own engine, which produced 12 horsepower and weighed over 200 pounds. They also designed and built aerodynamically efficient propellers. The main feature of their airplane, however, was their system of control: elevator, warpable wings, and movable rudder. The ele-

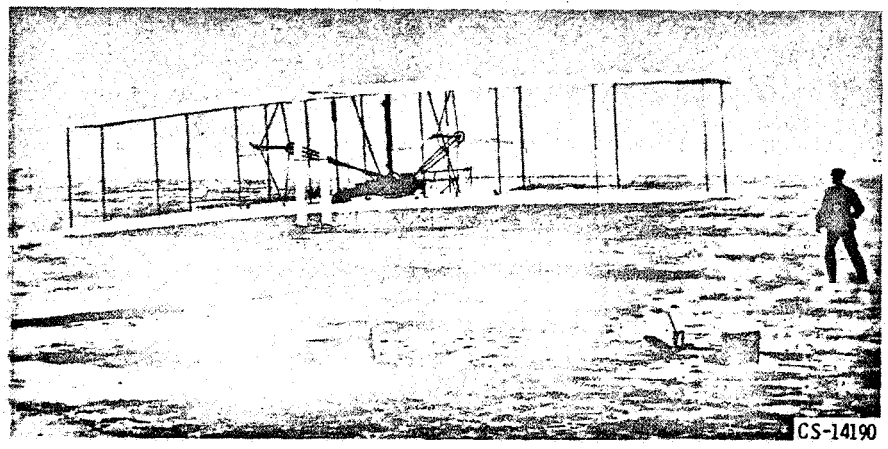

Wright brothers' airplane (1903).

vator, mounted at the front of the airplane, was lever-operated. Wing warping was achieved by means of cables attached to a cradle in which the operator lay. To bank the airplane to the left, for example, the operator swung his hips and the cradle to the left. This tightened the cable attached to the outer strut of the right wing and thereby warped the rear edge of that wing downward. The increased air pressure on the downward-warped wing caused it to rise. At the same time, an auxiliary cable gave the left wing an upward warp, which tended to lower that wing. The rudder was controlled by means of cables that were interconnected with the wing-warping cables, so that rudder movement and wing warping were synchronized. This overall scheme transferred control of the aircraft to the skill of the pilot. In later years, the Wrights' wing-warping method of control was supplanted by ailerons on the outboard portions of the wings.

Invention and achievement did not bring the Wright brothers the sweet taste of success. In the wake of Langley's fiasco, public interest in and reaction to flying were very low. The Wrights, of course, were pressing to capitalize on their invention. However, it was not until December 1907 that the U. S. Government (Army Signal Corps) first advertised for bids for an airplane. The Wrights' bid of $25,000 was accepted. For the remainder of their years, they were to be almost continually caught up in the stress of patent litigations. Glenn H. Curtiss emerged as the chief competitor of the Wrights. Meanwhile, through shows, competitions, and demonstrations, interest in flying caught on in Europe. Technical advancements were gradually incorporated into the airplane, particularly by Curtiss in his applications for the Navy. Elmer Sperry in this period also made significant contributions to aircraft instrumentation.

WORLD WAR I

At the onset of World War I in Europe (1914), France and Germany each had around 1500 aircraft. These initially were used only for reconnaissance. It was not long, however, until aerial dueling occurred with pilots using carbines, muskets, rifles, and even revolvers. Within 5 months of the start of hostilities, the French began mounting machineguns on the upper wings of their light Nieuports (fig. 1-8). By pulling on a lanyard, the pilot could fire the machinegun. Once the magazine was emptied, he had to land, reload, and take off again.

In February 1915, a Frenchman, Roland Garros, devised a way of firing a machinegun, mounted on the engine hood of his plane, straight ahead through the revolving propeller. The blades, fitted with metal plates, deflected about 7 percent of the bullets; the rest passed through unobstructed. This type of installation allowed the pilot to reload the gun in flight. This French technique took a heavy toll of German aircraft.

Before long, the Germans countered with a more lethal invention, by the Dutch air-

plane designer Anthony H. G. Fokker. He devised a forward-firing machinegun synchronized to fire through the propeller without striking the blades. With this invention, German airplanes for a time held mastery of the air. British pilots suffered so many casualties that they referred to themselves as "Fokker fodder." Eventually, of course, the Allies were able to reproduce the weapon for themselves and equalize the odds in combat.

Technological superiority in the design and arming of aircraft passed back and forth across the battlefronts of Europe. Whenever one side brought an improved airplane to the front, the other side strove to equal or surpass it. Fokker's airplanes made rate of climb and maneuverability requisites for combat. Dogfights approximated hand-to-hand combat in the air.

When the United States entered the war, in 1917, it did not have a single airplane fit for combat. The War Production Board was set up to administer the manufacture of aircraft. A patent pool was established to expedite the military program. In this arrangement, prime responsibility resided with the automotive industry. The Board's policy was to build only copies of foreign airplanes and to equip them with American designed motors. The principal airplane built was the DeHavilland 4, shown in figure 1-7. As a contribution to the war effort, the program was a rather dismal failure, with much gross inefficiency in evidence. This particular example of mass production had failed.

American fliers, on the other hand, gave an extremely good accounting of themselves in combat. At the end of the war, Rickenbacker's "Hat-in-the-Ring" squadron led all others, with 69 confirmed victories. Rickenbacker himself (fig. 1-6) had destroyed 26 German airplanes in combat. Many other U. S. heroes of the air emerged from battle.

The importance of the airplane in warfare was a subject of enormous controversy at the close of World War I. Brigadier General Billy Mitchell became the leading proponent and standard-bearer in a bitter campaign for the recognition and establishment of airpower. In 1921, plagued by sharp charges and demands by Mitchell, the military undertook, as an experiment, the aerial bombardment of captured German naval vessels off Chesapeake Bay. This undertaking was to evaluate the very basis of the controversy - the potency of the airplane as a weapon system. At the conclusion of the tests, Mitchell's bombers had sunk a submarine, a destroyer, a cruiser, and the dreadnought "Ostfriesland." His charges and demands became increasingly stronger and eventually forced his courtmartial in 1925 for insubordination. When convicted, Mitchell resigned from the Army. Public sentiment was in Mitchell's favor, but he had almost no support among the military.

LATE '20's AND THE '30's

Upon the close of war in Europe, many fliers returned to civilian life, only to find

generally widespread public apathy toward the airplane. Little opportunity was available to earn a livelihood by flying or to initiate commercial flight ventures. Many took to barnstorming: demonstration and stunt-flying at rural fairs all over the country. The Air Service, spurred by General Mitchell, took to establishing new transcontinental flight records and round-the-world exploits.

The Post Office was operating the airmail service, begun in 1918, with poor equipment and much hazard and hardship to the courageous men who flew. The passage of the Kelly Act by Congress in 1925 transferred the mail routes to private contractors. This provided fledgling air-transport companies the financial means to start expanding into the great airlines they have become today. In October 1925, Henry Ford was successful bidder for one of the first contract airmail routes (Cleveland-Detroit-Chicago) and was the first private operator to carry the mail. Ford put into service the Stout all-metal monoplane, powered by a single Liberty engine. Later, when Stout redesigned his monoplane to be powered by three Wright Whirlwind engines, Ford bought out the Stout organization, and this plane became the famous Ford Trimotor.

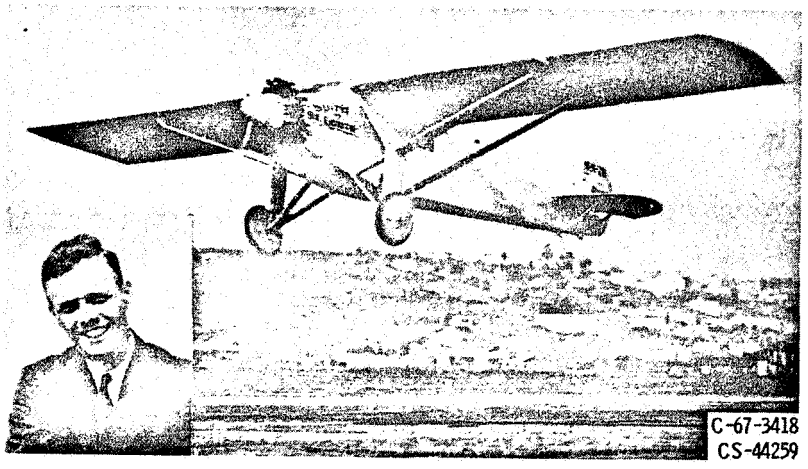

Charles A. Lindbergh and his Ryan monoplane, "Spirit of St. Louis," which he flew solo on a nonstop flight across the Atlantic from New York to Paris in 1927. (Courtesy of Smithsonian Institution.)

In 1927, Charles A. Lindbergh made the first nonstop solo flight across the Atlantic (New York to Paris). In his special Ryan monoplane "Spirit of St. Louis," he traveled 3610 miles in 33 hours, 32 minutes. As a result of his great personal achievement, "Lindy" became a national hero and the subject of public adulation. Aviation was on the upswing.

In 1933, Wiley Post established a record with his solo, round-the-world flight in a Lockheed Vega, the "Winnie Mae." The flight covered 15,596 miles in 7 days, 18 hours, 49.5 minutes. The "Winnie Mae" was powered by a Pratt & Whitney 9-cylinder, 425-

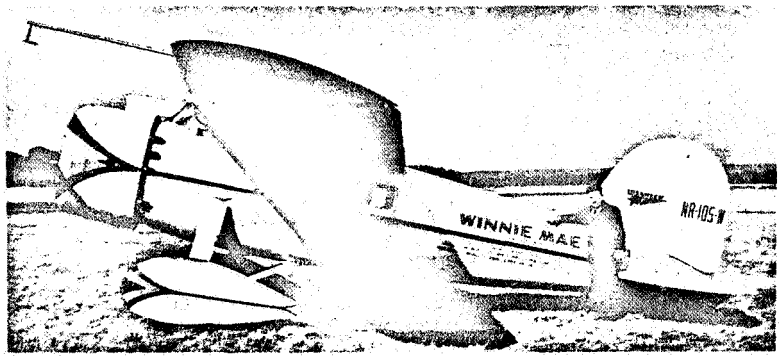

Wiley Post and his Lockheed Vega, "Winnie Mae," which he flew solo on a record-setting, around-the-world trip in 1933. (Photo from J. W. Caler collection.)

horsepower Wasp engine. On this flight, the plane was equipped with an improved version of the Sperry Gyroscope Company's automatic pilot and a radio-directional device that registered on a dial the direction of the station to which the radio was tuned. Post, in an impressive display of pilot stamina, made only 11 stops during the flight.

In 1936, an outstanding milestone in airplane technology was reached when the Douglas DC-3 (fig. 1-37) went into commercial service. This airplane had two 900-horsepower Wright Cyclone engines, weighed 24,000 pounds, and had a useful payload of 9000 pounds - one-third greater than that of any preceding airplane. The DC-3's 185 mph represented a 50-percent increase in cruise speed over that of its predecessors. In retrospect, the DC-3 over the years has been outstandingly profitable and preeminently safe.

During the late 20's and the 30's, the National Air Races were firmly established. The best pilots, including James H. ("Jimmy") Doolittle, Roscoe Turner, Harold Neumann, Jacqueline Cochran, etc., competed annually for the most coveted prizes: the Thompson

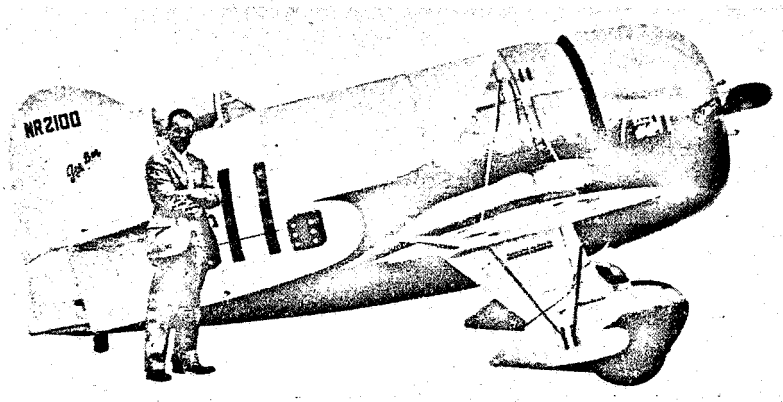

James H. Doolittle and the Granville Gee Bee racer which he flew to victory in the Thompson Trophy Race of 1932. (Photo from J. W. Caler collection.)

Trophy, for the fastest time in a closed-course pylon race, and the Bendix Trophy, for a transcontinental race. Speeds were increasing notably; for example, James H. ("Jimmy") Doolittle won the 10-lap, 100-mile Thompson Trophy Race in 1932 in a special Granville Gee Bee racer with an average speed of 252.68 mph. These races gave impetus to the development of the retractable landing gear, new fuels, and better engines.

During this period, the amazing technological advances of aviation resulted largely from the superb cooperation between the industry and the government research laboratories. The work of the National Advisory Committee for Aeronautics (NACA) was particularly noteworthy.

In aerodynamics, drag was significantly reduced as the monoplane with thick, internally braced, cantilever wings supplanted the biplane, with its interplane struts, and the externally braced monoplane. Between 1929 and 1934, more than 100 wing sections were tested in the wind tunnels of the NACA Langley laboratory. Of these, the famous NACA-23012 airfoil came to be widely used throughout the world. High wing loadings (i.e., high lift per unit area) were attained through the use of wing flaps and leading-edge slots. The guiding principle in increasing aerodynamic efficiency was the reduction of parasitic (or profile) drag. To reduce drag, therefore, NACA turned its attention to the powerplant and developed the NACA cowling in 1929. This device increased the economy of the airplane by more than 10 percent, simply by covering the knobby engine parts to streamline the nacelle and by providing an ingenious ducting system for handling the required cooling air for the enclosed engine.

There were other important developments, such as standardization on the all-metal monocoque, or stressed-skin, construction, which is a single-shell fuselage wherein the skin and stiffeners bear most of the flight loads; improvements in the use of the supercharger to permit higher altitude capabilities; developments in radio for instrument flying and blind landings; and the introduction of the variable-pitch propeller. In the late 30's, aeronautical research facilities in England, France, Germany, and Italy were expanding rapidly, for Europe was getting ready for war.

WORLD WAR II

In September 1938, President Franklin D. Roosevelt set dramatic new U. S. goals for airpower and aircraft production: 10,000 combat airplanes per year. Brigadier General Henry H. ("Hap") Arnold was made Chief of the Army Air Corps. Mass production of military aircraft was to be America's first step against the threat of Fascist aggression. To avoid the costly technological errors of World War I, the U. S. Government selected aircraft manufacturers as the prime contractors, and the automotive industry was drawn into production schemes as subcontractors. This plan resulted in industrial miracles. The annual rate of aircraft production increased steadily and reached its peak in 1944,

when, in that single year, 96, 318 military aircraft were produced.

When World War II began, it fast became obvious that this was to be a war of airpower. For Americans, the Japanese attack on Pearl Harbor was a stunning demonstration of this fact. Thus, the tremendous U. S. production rate of military aircraft became a major factor in deciding the war in favor of the Allies. Throughout the war, many U. S. aircraft were to carry the brunt of battle - among them, notably, the B-17 Flying Fortress (fig. 1-28), B-29 Superfortress (fig. 1-43), P-47 Thunderbolt (fig. 1-35), P-38 Lightning (fig. 1-42), P-39 Airacobra, P-40 Warhawk (fig. 1-27), P-51 Mustang (fig. 1-38), B-24 Liberator (fig. 1-33), B-25 Mitchell (fig. 1-34), and the B-26 Marauder (fig. 1-41).

In its pursuit of the war effort, America took the view that the principal function of the airplane was bombardment. The Boeing B-17 Flying Fortress was first produced in 1939 and established international records for distance and weight carrying. It was not only fast, but was astonishingly sturdy and had a featherlike maneuverability. After a mission, it was not at all unusual to find a B-17 badly shot up but limping safely back to base. In Europe, the results of high-altitude, precision and saturation bombing proved to be the real turning point of the war. The remarkable Norden bombsight ensured success in daylight bombing from altitudes above the flak of antiaircraft fire.

Round-the-clock air attack on Germany was the prime objective of the air war in Europe. The bombing missions needed the support of a long-range fighter escort. But not until July 1943 did the P-47 Thunderbolts attain an escort range of 340 miles, which was inadequate. The P-38 Lightnings in 1944 had an escort range of 585 miles. About the same time, the P-51 Mustangs were delivered. These airplanes were able to speed ahead of the bombers and clear the skies of German aircraft for a distance of 850 miles.

The P-51 Mustang (fig. 1-38), an outstanding combat performer during World War II, was largely a product of NACA research. Early tests in the Langley low-turbulence wind tunnel showed that considerable drag reductions were possible by controlling the pressure distribution over the wing. In 1940, the NACA's Annual Report to President Roosevelt included this one brief paragraph:

> Discovery during the past year of a new principle in airplane-wing design may prove to be of great importance. The transition from laminar to turbulent flow over a wing was so delayed as to reduce the profile drag, or basic air resistance, by approximately two-thirds. It is too early to appraise adequately the significance of this achievement. So far, its application is limited to small airplanes, but there are indications of its ultimate applicability to larger airplanes through continued research. It should increase the range and greatly improve the economy of airplane operation.

This new principle was applied to the wing design of the Mustang airplane. The P-51 was also subjected to other aerodynamic cleanup studies and remedies by NACA. The results are now history. In both speed and range, the P-51 was the foremost propeller-driven fighter of this period.

In the bomber class, the successor to the B-17 was the famous Boeing B-29 Superfortress. First flowin in July 1943, this airplane brought about the defeat of Japan. The

B-29's four engines produced 2200 horsepower each, compared with 1200 in the B-17. Takeoff weight was 140,000 pounds, compared with the 55,000 pounds of the B-17. With a wing span of more than 140 feet and a pressurized cabin, the B-29 could be flown with comfort at 35,000 feet. It had an operational radius of 2300 miles with a 10,000-pound payload. In 1945, of course, it was the B-29 that carried the atomic bomb to Hiroshima and brought about the end of the war.

During the latter stages of the war, the jet airplane began to emerge. Bell Aircraft in 1943 produced the YP-59 Airacomet, the first jet fighter in America. This airplane utilized the turbojet engine researched and developed by Frank Whittle in England. Actually, the Germans had been busy, too, and had put into operation in the preceding year the Messerschmitt-262 jet fighter. For a given thrust level, the turbojet engine is smaller, lighter, and simpler in design than the reciprocating engine. However, it also has a higher fuel consumption. Propulsive efficiency of the jet engine increases with speed, whereas with a propeller, compressibility losses (associated with high-speed airflow over a lifting surface) cause performance to fall off drastically. Introduction of the jet engine thus opened up still higher ranges of aircraft speed.

POST-WORLD WAR II

One of the successors to the B-29 bomber was the Strategic Air Command's B-36, built by Convair (fig. 1-40). This was the largest airplane to enter the Air Force inventory. It had a wing span of 230 feet and a length of 162 feet. Its gross weight on takeoff was 370,000 pounds, compared with 140,000 pounds for the B-29, and its nominal range was 10,000 miles. Early versions of the B-36 were powered by six propeller engines.

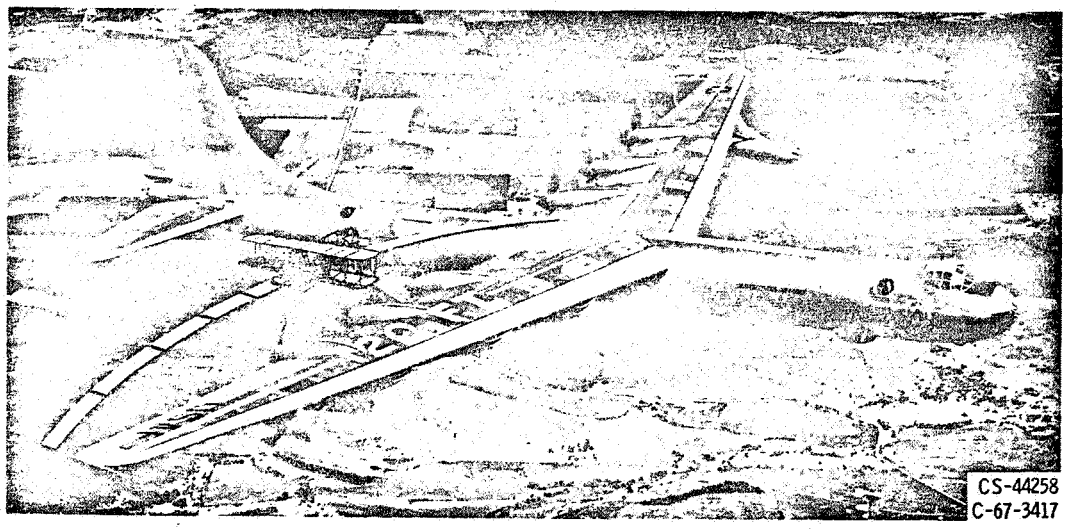

Convair B-36 long-range strategic bomber in contrast to Wright Flyer.

On later versions, four turbojet engines were added. The B-36 was expensive: $3,500,000, compared with $640,000 for the B-29. Its top speed was about 435 mph. For further size comparison, the original Wright Flyer is sketched on the photograph, illustrating again the dramatic evolution of the airplane.

Currently, the primary heavy bomber of the Strategic Air Command is the B-52 Stratofortress (fig. 1-47). The Boeing B-52 is powered by eight jet engines, each with a thrust rating of 17,000 pounds. In 1957, with in-flight refueling, the B-52 flew 24,325 miles in 45 hours, an average of 540 mph. The role of the long-range, high-speed bomber is now being challenged by the application of rocket-powered, guided missiles, such as ICBM's.

The Century series jet fighters are illustrated in figures 1-49 to 1-54. These airplanes are highly sophisticated aerodynamically and are electronically complicated. All generally have transonic or supersonic dash capability. In contrast with World War I fliers, today's combat pilots must be highly trained and are more dependent on systems performance than on individual flying skills. This change is obviously a consequence of the tremendous flight speeds, which preclude human observations and determinations in flight. Electronic systems for navigation, control, weapons firing, etc., must necessarily predominate. One look into the pilot's compartment of a modern jet will quickly corroborate this.

In 1960, Russia announced that a U.S. aircraft had been shot down over Soviet territory as it was attempting a photoreconnaissance mission. The airplane was the Lockheed U-2. This airplane is of interest here because it was designed for a very special and specific purpose. Originally, the U-2 was to be used by NASA for weather research and high-altitude radiation sampling. The design objective was to achieve maximum possible altitude performance within the state of the art. This performance was obtained by using a sailplane-type wing, keeping structural weight and strength low, and using a specially designed high-altitude version of the Pratt & Whitney J-57 engine with low-volatility fuel.

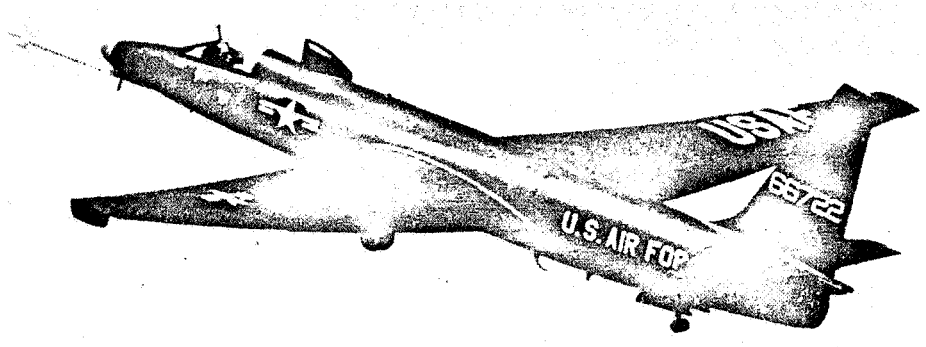

C-67-3414

Lockheed U-2 high-altitude jet aircraft for weather and radiation research and photoreconnaissance missions. (Courtesy of Smithsonian Institution.)

An example of U-2 weight savings is the single main landing gear. Small jettisonable wheels keep wings level during takeoff roll. The U-2 is able to maintain level flight at altitudes above 70,000 feet, with a range of 3000 miles or more. This aircraft illustrates the practical trade-offs and compromises available to the designer to meet particular specifications. Speed, for example, was the uppermost consideration in the Gee Bee racer, shown previously. Therefore, that airplane was practically all engine, and everything else was minimized. In World War II, speed of American airplanes was sacrificed for the weight requirements of electronic navigation packages and personnel armor protection. The aircraft designer must balance all requirements as he searches for an optimum.

The F-111A (fig. 1-59) exemplifies another novel approach. With its variable-geometry wings that can be extended in flight for takeoff, landing, and subsonic speeds and then swept back sharply for supersonic operations, the F-111 is designed as a multipurpose aircraft. It can be used for counter-air missions, interdiction, close air support of ground forces, and reconnaissance. Its design Mach number is about 2.5 (i.e., a speed 2.5 times the speed of sound).

The XB-70 Valkyrie was a large, tail-first (canard), delta-wing aircraft, which was designed as a strategic bomber. This airplane was intended to replace the B-52 Stratofortress in service with the Air Force in the mid-1960's. The original B-70 was designed to travel the entire distance to the target and back (a maximum of about 7600 miles) unrefueled, at Mach 3. In March 1963, the decision was made to build two XB-70A aerodynamic research aircraft. The first flight was made in 1964. Thereafter, the XB-70A was used in a joint research program conducted by NASA and the Air Force. At takeoff,

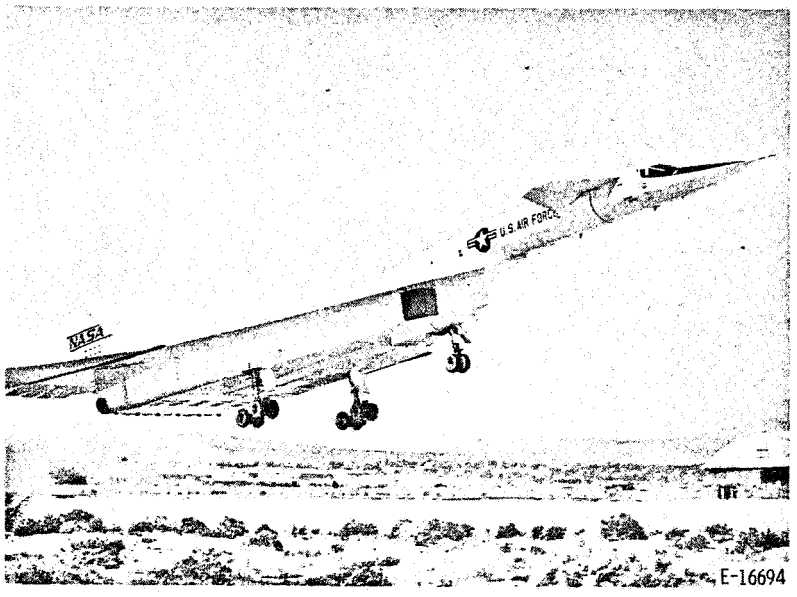

XB-70A research aircraft (Mach 3).

this airplane weighed over 500,000 pounds. The design cruising speed of Mach 3 (approximately 2000 mph) was first attained during the 17th flight, in October 1965. During routine test flights, altitudes of around 70,000 feet were reached. The XB-70A was powered by six General Electric YJ-93-3 turbojet engines (each producing 31,000 pounds of thrust with afterburning) clustered side by side in the rear of the powerplant duct, under the wing trailing edge. The wing span with the tips spread was 105 feet. The length, including the nose probe, was 196 feet. The wings were cantilevered delta wings of very thin cross section. A large, canard foreplane, also with very thin wings was adjustable for trim purposes and was fitted with trailing-edge flaps. North American Aviation was the prime contractor. The XB-70A research program is now finished. Although the B-70 never got into production, results of this research program are expected to feed directly into the planning, design, and operational characteristics of this country's commercial supersonic transport program.

To meet its responsibility - "to supervise and direct the scientific study of the problems of flight, with a view of their practical solution" - NACA/NASA also joined with the Air Force, Navy, and aerospace industry in building and flying a number of advanced, high-speed, research airplanes, including the X-15 (fig. 1-60). The program has been

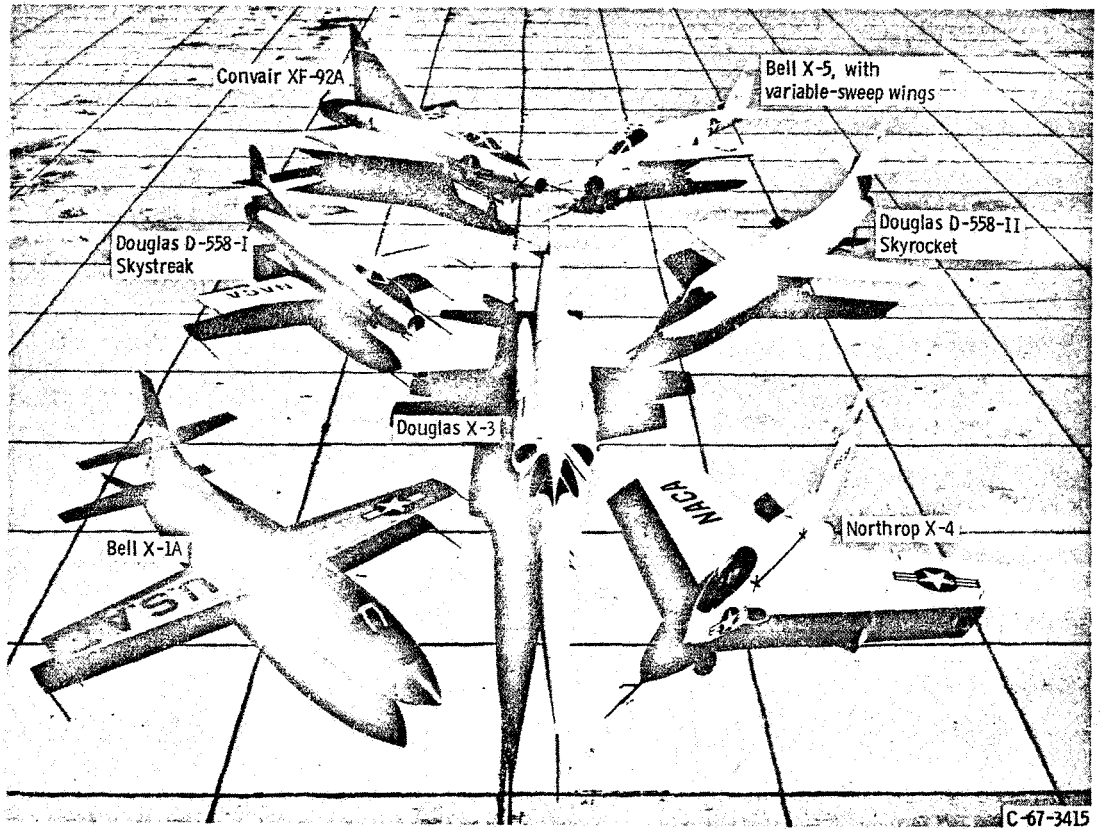

Research airplanes (1956). (Photo courtesy of Smithsonian Institution.)

essentially completed, with tremendous success. The first supersonic flight was achieved by Charles Yeager on October 14, 1947, in the Bell X-1. In 1951, William Bridgeman flew the Douglas D-558-II at Mach 1.89. In 1953, Yeager took the Bell X-1A to Mach 2.5 - 1650 mph. Airplanes flown by service and civilian pilots pushed both speed and altitude records steadily higher. By 1962, test flights of the North American X-15 rocket plane had taken the heat-resistant craft to an altitude of 314,750 feet and a speed of 4104 mph. Each X-15 flight has furnished important design data for high-altitude, hypersonic operational aircraft. The practicability of pilot-controlled reentry into the atmosphere from space has been demonstrated, and a great amount of data on physiological and psychological reactions of man to space flight has been provided.

THE FUTURE

As we look to the future, we can see only further rapid expansion in the field of aeronautics, particularly in the civilian commercial sector. In the immediate offing are the large, subsonic, jumbo jets and the supersonic transports. Both are presently in various stages of research and development.

In the large subsonic airplane category, Boeing has developed its 747 version, already in commercial use, and Lockheed (Marietta, Georgia) is working on the C-5A. By way of illustration, the latter airplane will have a gross takeoff weight of 728,000 pounds, a wing span of 223 feet, and a 65-foot-high tail. The C-5A is being designed to move 110 tons (or up to 900 passengers, on three decks) 3000 miles in 7 hours.

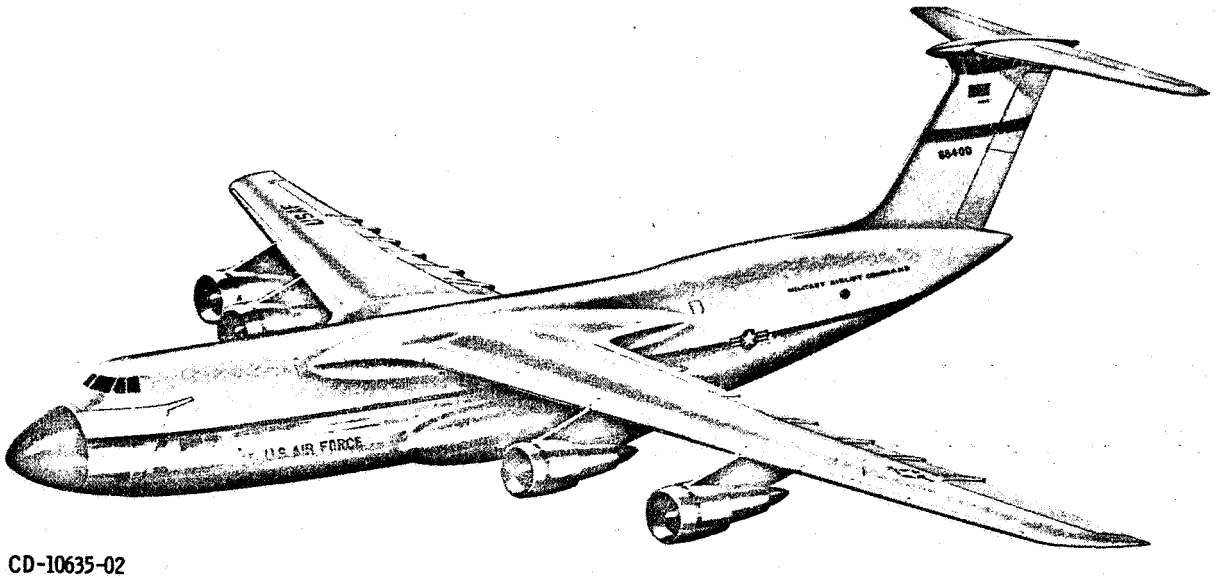

CD-10635-02

Lockheed C-5A subsonic jumbo jet.

Power for this job will be supplied by four TF-39 turbofan jet engines, built by the General Electric Company, each developing 41,000 pounds of thrust. This fan engine is expected to have a specific fuel consumption one-quarter less than that of a standard turbojet. This type of airplane will offer large-scale, economic transportation in both the passenger and cargo markets.

The commercial supersonic transport (SST) also has been an international technological challenge, with the British and the French cooperating to develop the 128-passenger,

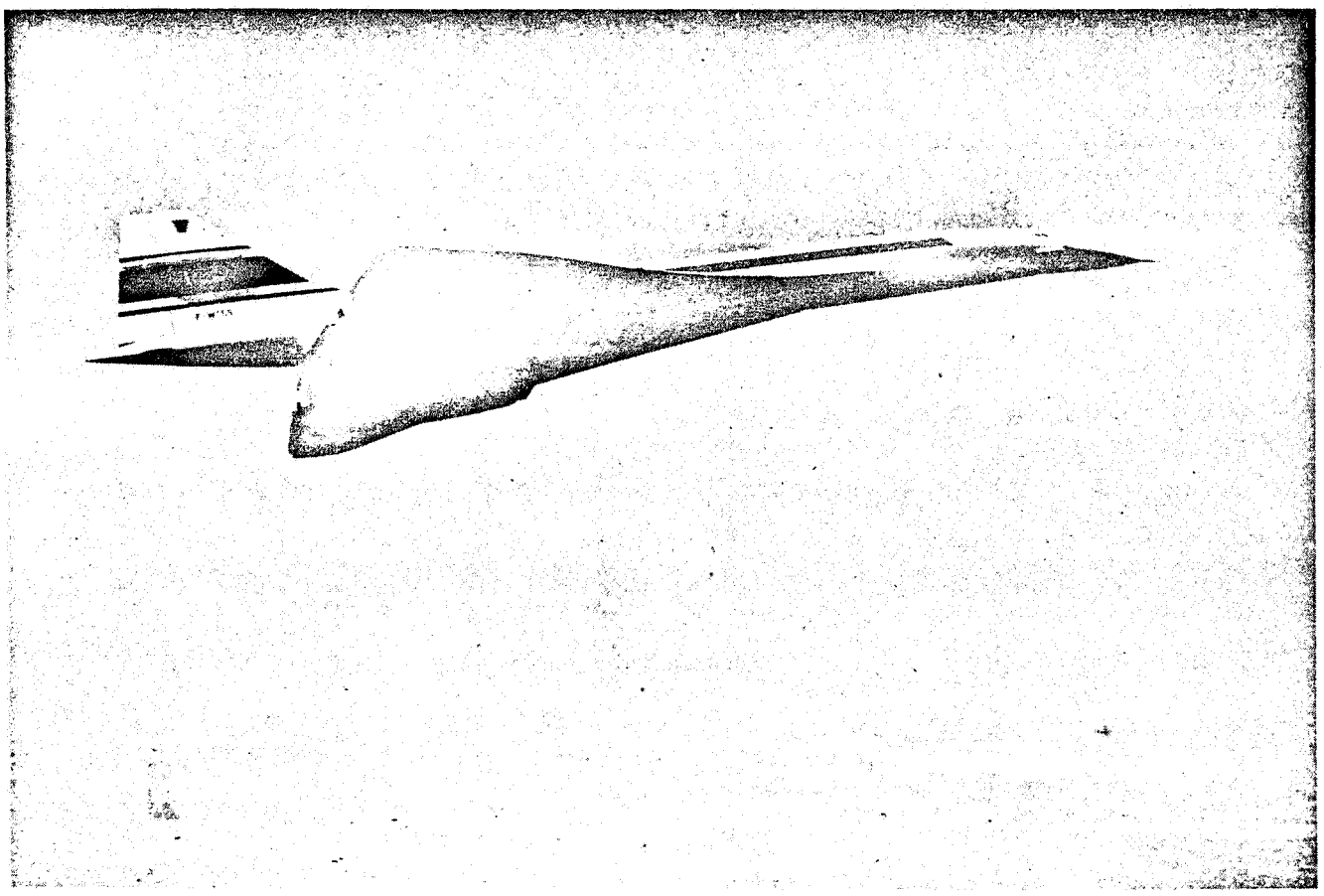

First prototype Concorde 001, a cooperative British-French project.

Mach 2.2 Concorde; the Soviet Union developing a comparable aircraft, the TU-144; and the United States working with the Boeing Company on a larger and faster SST prototype. These various efforts began in the mid-1960's. When commercial supersonic transports become operational, the sonic-boom problem is expected to restrict their use mainly to transoceanic and transpolar flights.

The original Boeing SST design had pivoted, variable-sweep wings. But because pivoted wings, for this type of aircraft, imposed unacceptable weight penalties, the design

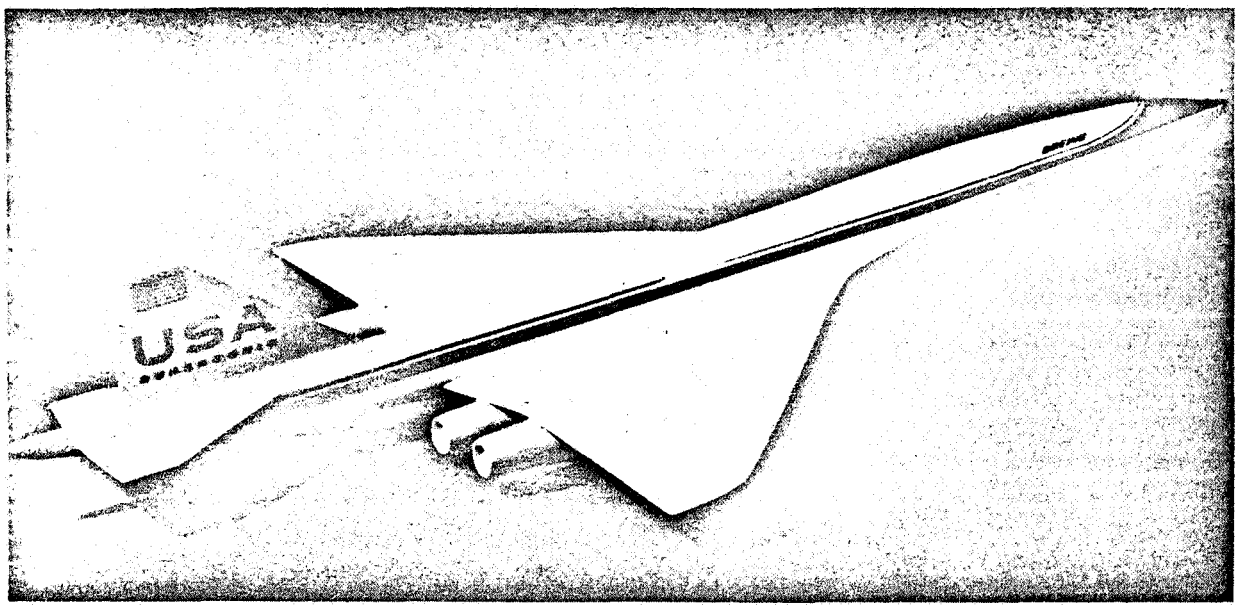

Model of proposed Boeing fixed-wing supersonic transport. (Reprinted from Interavia, January 1969, with their permission.)

was modified to a fixed-wing configuration. This aircraft was designed to carry 250 to 350 passengers at a speed of Mach 2.7 (1800 mph) and at a cruising altitude of 64,000 feet. The estimated range, with 313 passengers, was over 4000 miles. Plans called for building most of the Boeing SST of an alloy of 90 percent titanium, 6 percent aluminum, and 4 percent vanadium. Maximum takeoff weight was set at 750,000 pounds, with propulsion provided by four 67,000-pound-thrust General Electric GE4/J5P turbojet engines mounted under the rear of the wing.

Another general area of special interest to the aeronautics program is V/STOL (Vertical and Short TakeOff and Landing) aircraft. The utility of the helicopter, particularly in the military situation (Vietnam), is unquestionable. Some helicopters are illustrated in figures 1-68 to 1-70. A great variety of other V/STOL configurations are under active study. With tomorrow's mushrooming populations, the megalopolitan areas will have an acute need for short-distance, high-speed transportation. V/STOL aircraft may pose an attractive and practical solution. However, much research and development work remains.

It is appropriate here to quote the late Dr. Hugh L. Dryden:

> Aeronautical technology ... has exploited the power of organized effort, learning to draw on all the resources of science, and to synthesize and integrate the effort of men of many disciplines and skills.

The future looks to be even more promising.

APPENDIX A

AN AVIATION CHRONOLOGY IN BRIEF

1903 Langley's aerodrome, with Charles Manly as pilot, fails in its second attempt to fly and plunges into the Potomac River. Six days later, on December 14, Wilbur Wright travels about 40 feet in 3.5 seconds. On December 17, the Wright Flyer goes 852 feet in 59 seconds at Kitty Hawk, North Carolina. This is the first, manned, powered, airplane flight.

1906 Santos-Dumont (France) makes first airplane flight in Europe. Flight duration, 8 seconds.

1908 Lt. Thomas E. Selfridge is first U.S. military man to fly "heavier-than-air" machine. Glenn Curtiss pilots "June Bug" 1 kilometer before official witnesses. First airplane owned by U.S. Army is Wright biplane. In France, Henri Farman goes up with a passenger (Delagrange) for 150-foot hop - the first passenger-carrying flight.

1909 Herrig-Curtiss Co., the Wright Co., and the Glenn L. Martin Co. are established. The first airplane flight across the English Channel is made by L. Bleriot in his "Number XI."

1910 A Curtiss biplane, piloted by Eugene Ely, takes off from land and flies out to a platform on the cruiser "Pennsylvania." This act forms basis for concept of a naval aircraft carrier. Shortly afterward, Captain I. Chambers, USN, develops compressed-air catapult for launch from shipboard.

1911 Curtiss is recognized for his invention and successful demonstration of the hydroplane - the Triad - a seaplane equipped with retractable wheels for ground landing. First airplane is delivered to the American Navy. First airmail in U.S. is carried aloft by Earle Ovington on Long Island.

1912 The first fighter plane is single-seat Farnborough B.S. 1, designed by deHavilland.

1913 Elmer A. Sperry demonstrates his gyroscopic stabilizer to the Navy. Sikorsky designs first multiengined airplane, the four-engined biplane "Bolshe."

1914 Elmer A. Sperry develops optical-type drift indicator and gyroscopic compass. Lawrence Sperry develops automatic pilot.

1915 The NACA is established by act of Congress. The first fighter is equipped with a fixed, forward-firing machinegun; this is Anthony Fokker's Eindecker Scout. The gun is synchronized to fire through the whirling propeller. Junkers designs

first cantilever-wing, low-wing, all-metal airplane - the J-1 monoplane.

1916 World altitude record of 16, 500 feet is set by V. Carlstrom in a twin-engined JN Curtiss.

1917 U.S. declares war on Germany. McCook Field, Dayton, Ohio, is established as the Air Service Experimental Base.

1918 Army begins regular airmail service between Washington, D. C., and New York City. First Navy Curtiss-1 (NC-1) flying boat is successfully flown.

1919 Leak-proof tanks, free parachute back-pack, reversible- and variable-pitch propellers, syphon gasoline pump, and fins and floats for emergency water landings are developed. The turbocompressor, or supercharger, is developed by Dr. Sanford Moss of General Electric. Lieutenant Commander A. C. Read and five-man crew fly a Curtiss NC-4 Navy flying boat in the first airplane crossing of the Atlantic (New York to Lisbon via Newfoundland and the Azores). First nonstop crossing by Captain Alcock and Lieutenant Whitten-Brown in a Vickers Vimy from Newfoundland to Ireland in approximately 16 hours.

1921 As an outgrowth of charges by Brigadier General William ("Billy") Mitchell, the military undertakes experimental aerial bombardment of captured German vessels in Chesapeake Bay. Submarine, destroyer, cruiser, and dreadnought "Ostfriesland" are sunk in these tests.

1922 Wing-type radiator is developed by Curtiss. World speed record of 222.96 mph is set by Billy Mitchell in Curtiss racer. Berliner helicopter rises vertically to 12 feet and hovers successfully. DeBothezat helicopter is successfully test-flown for 1 minute, 42 seconds.

1923 First refueling in midair between two airplanes. World speed record is set at 266.6 mph in Curtiss racer.

1924 First aerial circumnavigation of the globe - four Army Douglas biplanes leave Seattle, and two return after covering 26, 345 miles in an elapsed time of 175 days.

1925 Oleo landing gear is tested for Navy on NB-1 airplane. Ford Motor Company takes over the Stout Metal Airplane Company and begins producing the Ford Tri-motor, an all-metal monoplane designed by William A. Stout. Billy Mitchell is court-martialed and found guilty of insubordination. Cleveland opens its $1, 000, 000 municipal airport, which covers 1000 acres.

1926 Pratt & Whitney Aircraft Company produces its first engine, a nine-cylinder, radial, air-cooled engine, developing 400 horsepower at 1800 revolutions per minute. Lieutenant Commander Richard E. Byrd and Floyd Bennett fly over the North Pole in a trimotored Fokker.

1927 Lindbergh makes first, nonstop, solo flight across Atlantic (New York to Paris) in Ryan monoplane "Spirit of St. Louis" - 3610 miles in 33 hours, 32 minutes.

1928 Frank Whittle, a young, English air cadet, publishes a paper predicting application of jet propulsion to high-speed aircraft.

1929 James H. Doolittle makes first, public demonstration of instrument flying. Major Spaatz, with a crew of four, sets refueling endurance record in Fokker Army transport "Question Mark" - 150 hours, 40 minutes, 15 seconds. NACA cowling is developed.

1932 Doolittle wins the 100-mile Thompson Trophy Race in a Gee Bee racer with an average speed of 252.68 mph. New developments are a mechanism for controlling pitch of propeller and a liquidometer for displaying the condition of all fuel tanks on the airplane.

1933 Westbound transcontinental record of 11 hours, 30 minutes, established by Colonel Roscoe Turner in Wasp-powered, Wedell-Williams monoplane (Bendix Trophy Race, New York to Los Angeles). Wiley Post in a Lockheed Vega, the "Winnie Mae," sets record for solo round-the-world flight (15,596 miles in 7 days, 18 hours, 49.5 minutes). James R. Wedell breaks speed record for landplanes with 305.33 mph. Boeing builds 75 Model 247-D, all-metal transports for airlines and a fleet of P-26-A pursuit planes for Army. Retractable landing gears and a new radio compass are introduced.

1935 Howard Hughes sets new landplane speed record of 352.388 mph in his "Special." Douglas Aircraft produces first of famous DC-3 transports. Device for elimination of propeller ice is introduced.

1936 Pratt & Whitney develops new 1160-horsepower, 14-cylinder, twin-row, Wasp engine. Whittle begins experiments on gas-turbine engine.

1937 Hughes flies from Los Angeles to New York in 7 hours, 28 minutes, 25 seconds for average of 327.5 mph. Dirigible "Hindenburg," filled with hydrogen, crashes and burns, marking the beginning of the end for rigid-airship transportation.

1938 First production Supermarine Spitfire fighter (low-wing, single-seater) is completed in England.

1939 B-17 Flying Fortress goes into production. Bell Aircraft builds P-39 Airacobra for Army. Heinkel He 178 (first jet plane) is flown successfully in Germany.

1940 Puncture-proof gasoline tanks are tested at Wright Field. Boeing 307-B Stratoliner, first supercharged, pressurized-cabin airplane, is introduced.

1941 First successful true "flying wing," developed by Northrop, is announced by the Army. Jet-powered Gloster plane, powered by a Whittle-I jet engine, is built and flown on May 14. The 650-pound Whittle engine produces more thrust than a comparable Rolls-Royce reciprocating engine that weighs 1650 pounds.

1942 Doolittle leads his B-25 Mitchell bombers in raid against Japanese mainland after taking off from carrier "Hornet." First operational military jet, the Messerschmitt-262, is tested in Germany. First flight of Bell YP-59 Airacomet, first jet fighter in America.

1943 Water injection is used for power augmentation in fighters.

1944 U. S. Army Air Force peaks at 2, 383, 000 men and 64, 591 planes. Germany puts first rocket-propelled airplane into operation, the Messerschmitt-163 Komet.

1945 B-29 drops atomic bomb on Hiroshima, Japan.

1947 Mantz wins Bendix classic (2045 miles in P-51 Mustang at average speed of 460. 4 mph). Allison announces production of its new liquid-cooled, V-1710-G6 engine rated at 2250 horsepower. Allison also introduces new jet engine rated at 7500 horsepower at 600 mph. Lockheed P-80R sets speed mark at 623. 3 mph. Douglas D-558-I Skystreak flies 650. 6 mph. First, manned, supersonic flight (Mach 1. 06, or approx 670 mph) is achieved by Charles Yeager in rocket-powered Bell X-1. A separate Air Force is established as a coequal partner with the Army and Navy - the realization of Billy Mitchell's dream.

1948 Wright Aeronautical announces new 18-cylinder, air-cooled engine (R3350-26-W Cyclone), rated at 2700 horsepower. F-86 Sabrejet flown at 674 mph by Major R. L. Johnson. Vickers Viscount (with turboprop engines) enters airline service.

1949 Douglas D-558-II Skyrocket hits speed of 710 mph at 26, 000 feet.

1951 D-558-II Skyrocket flown 1238 mph at 79, 494 feet.

1952 Convair XF2Y-1 Sea Dart, first combat-type airplane equipped with hydroskis, makes its debut in San Diego. With the Air Force and NACA, Bell investigates variable-sweep wings on the X-5.

1954 Boeing-707 is tested: speed, 550 mph; range, 3500 miles; capacity, 150 passengers.

1959 First flight of North American X-15, built for hypersonic flight, eventually to approach Mach 7.

1962 X-15A, with Joseph Walker as pilot, reaches 4104 mph. Major Robert M. White climbs to 314,750 feet altitude in the X-15A.

1963 Lieutenant Colonel Robert A. Rushworth attains Mach 6.06 in the X-15A, causing craft's skin temperatures to rise above 1300° F. The B-58 Hustler makes the longest supersonic flight in history (nonstop from Tokyo to London in 8 hours, 35 minutes, for an average speed of 938 mph).

1964 First test flight of the F-111A (TFX) variable-sweep-wing, tactical fighter, designed for maximum speed of Mach 2.5. The Lockheed A-11, or USAF YF-12A, a Mach 3 prototype fighter, is announced. (This plane was first flown secretly in 1963.)

1965 Design cruising speed of Mach 3 is attained for the first time by the XB-70A Valkyrie strategic bomber (North American) on its 17th flight, October 14.

APPENDIX B

AIRPLANE COMPONENTS AND TERMINOLOGY

The components of an airplane and the terminology used are defined in the following sketches:

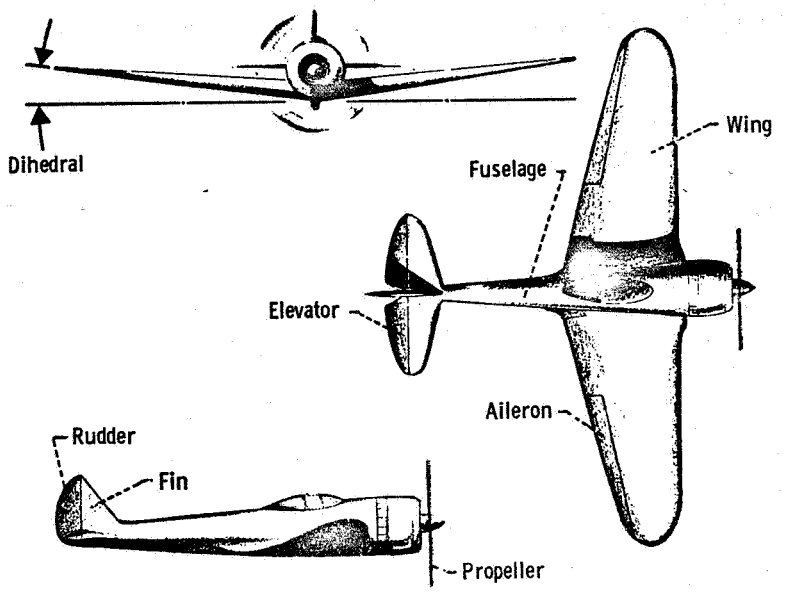

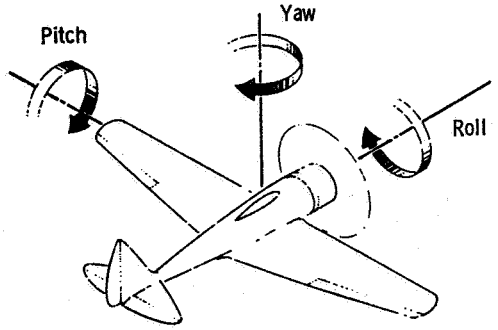

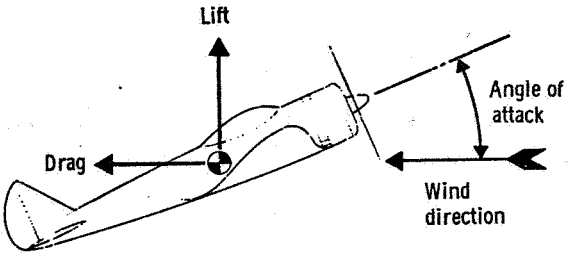

BIBLIOGRAPHY

Anon.: The American Heritage History of FLIGHT. American Heritage Publ. Co., Inc., 1962.

Dryden, Hugh L.: Aerodynamics - Theory, Experiment, Application. Aeron. Eng. Rev., vol. 12, no. 12, Dec. 1953, pp. 88-95.

Dryden, Hugh L.: A Half Century of Aeronautical Research. Proc. Am. Philosophical Soc., vol. 98, no. 2, Apr. 15, 1954, pp. 115-120.

Gray, George W.: Frontiers of Flight, The Story of NACA Research. Alfred A. Knopf Publ., 1948.

Morris, Lloyd; and Smith, Kendall: Ceiling Unlimited. The Macmillan Company, 1953.

Shrader, Welman A.: Fifty Years of Flight. Eaton Manufacturing Co., 1953.

Stever, H. Guyford; Haggerty, James J.; and the Editors of Life: Flight. Time, Inc., New York, 1965

USAF Photo Package No. 1, Rev. May 1965.

USAF Photo Package No. 2, reissued 1967, Historical Aircraft Photos.

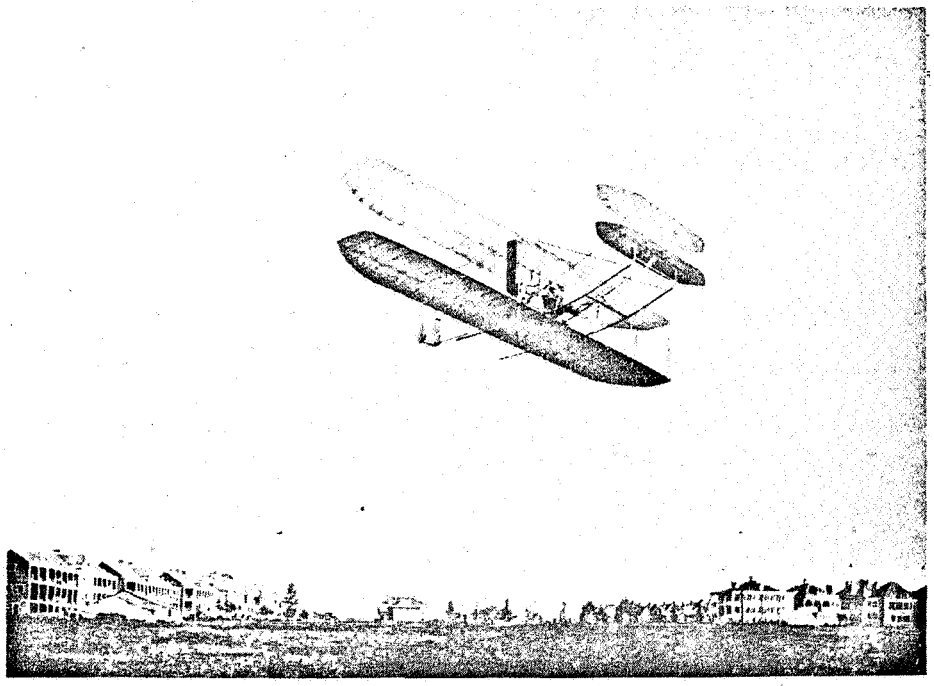

Figure 1-1. - Orville Wright circles Fort Myer, Va., during tests conducted for the War Department, in 1908. During these tests, he made the world's first flight of longer than 1 hour.

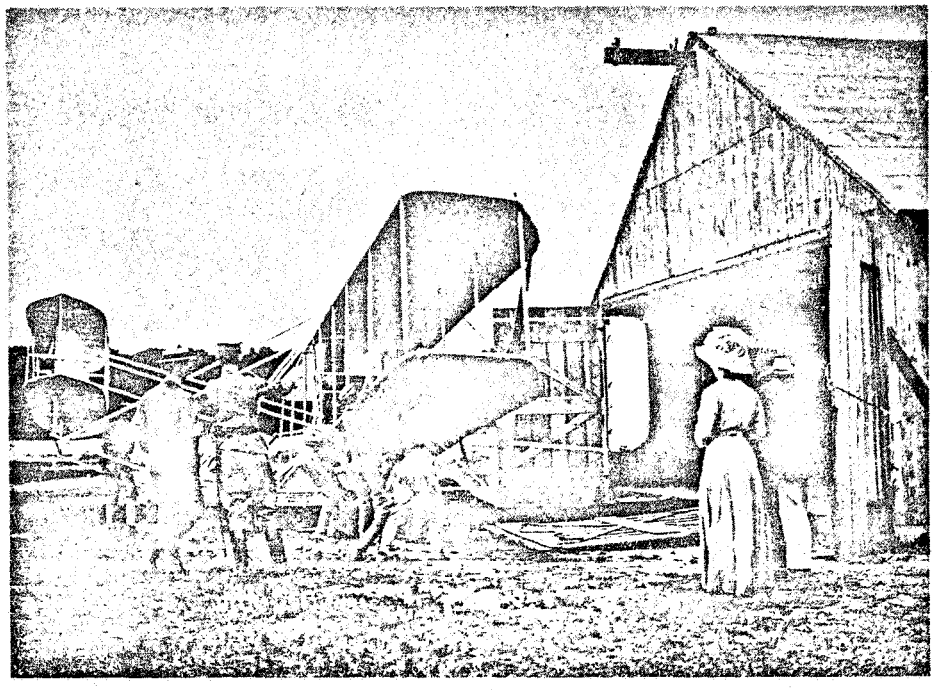

Figure 1-2. - Wilbur Wright's Flyer is moved into a "hangar" while curious military and civilian spectators watch.

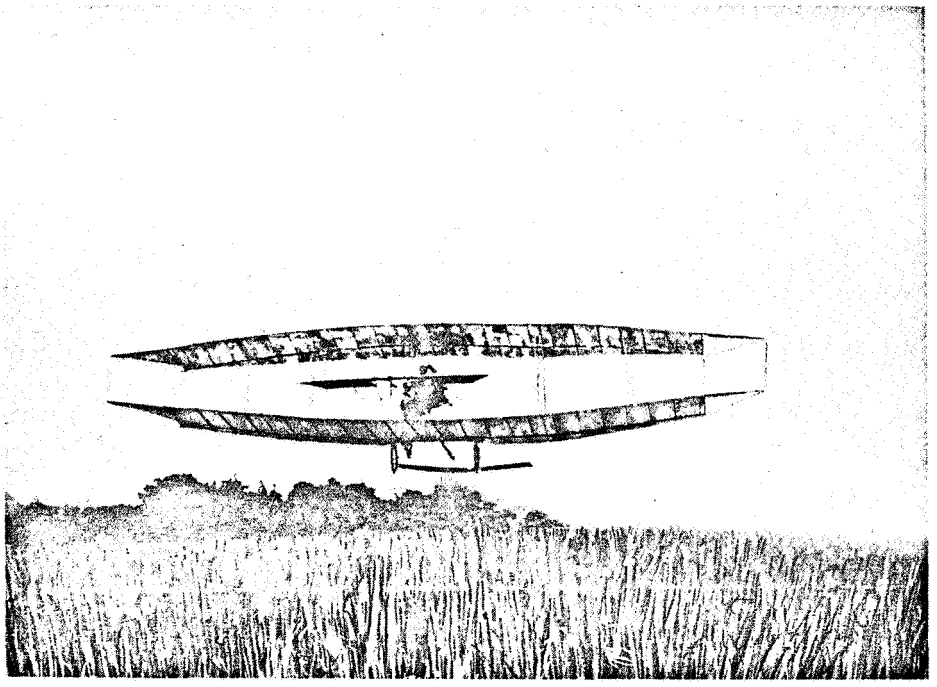

Figure 1-3. - Glenn Curtiss scored a dusty triumph when his "June Bug" made a 6000-foot flight in 1908.

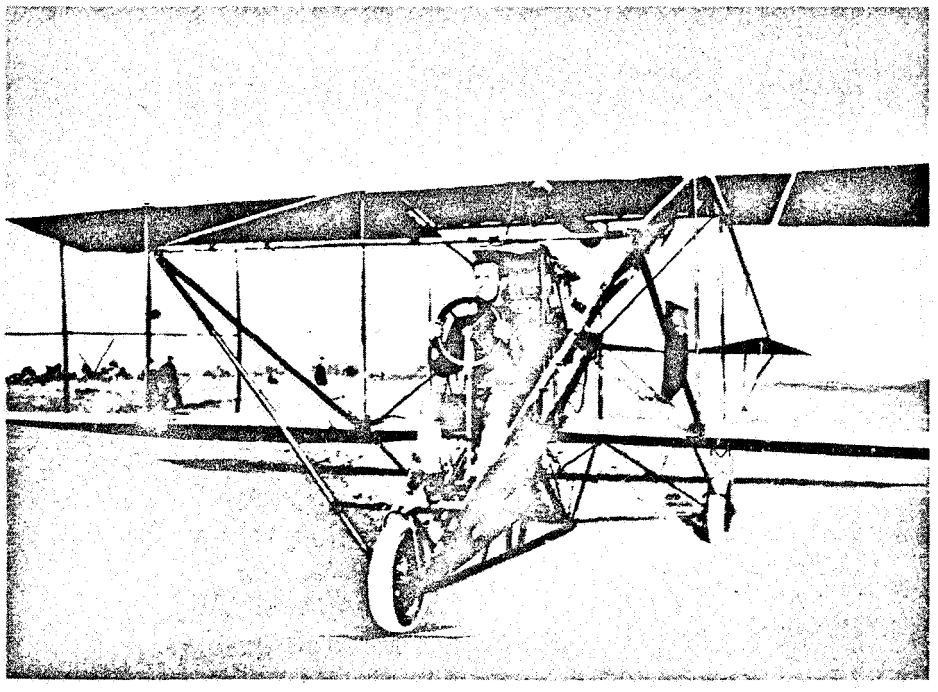

Figure 1-4. - Early U. S. aviator prepares for a flight in a Curtiss military airplane in 1913. Powered by a four-cylinder engine mounted behind the pilot, these pusher-type airplanes proved too dangerous and were not accepted by the War Department after 1914.

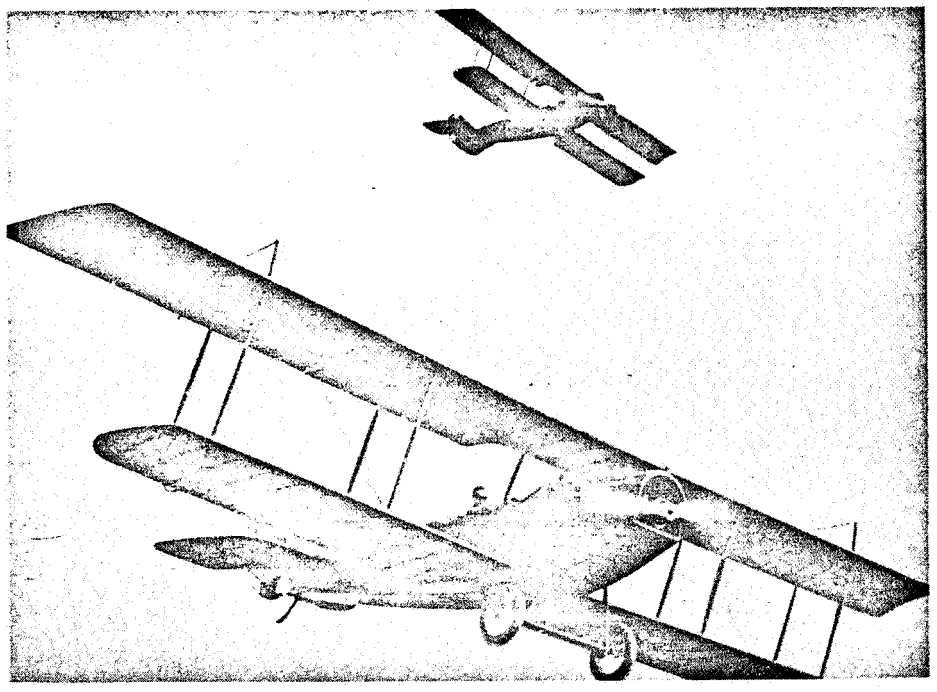

Figure 1-5. - World War I Curtiss JN-4's in formation. Although thousands of these airplanes were built during the war years, none took part in the air battles over France and Germany. Affectionately known as the "Jenny," this plane, flown by a generation of pilots, was the mainstay of the early barnstorming era.

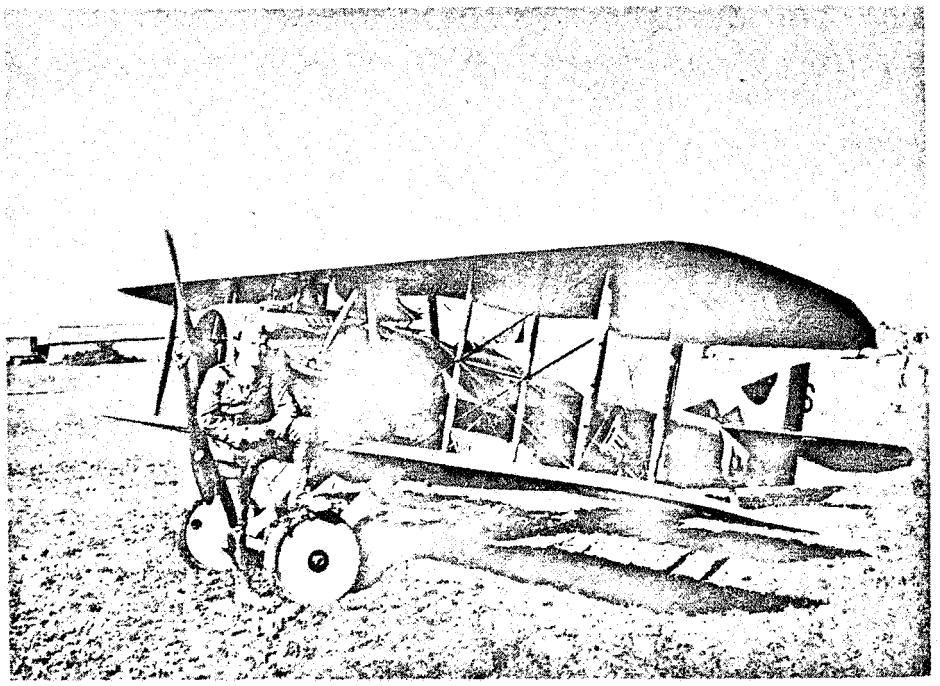

Figure 1-6. - U. S. ace of aces, Captain Eddie Rickenbacker, with his famous "Hat-in-the-Ring" Spad 13 of World War I fame. The Spad, one of the finest fighting machines developed during World War I, was the favorite airplane of American pilots. Built by the French, 893 of these machines were purchased by the United States.

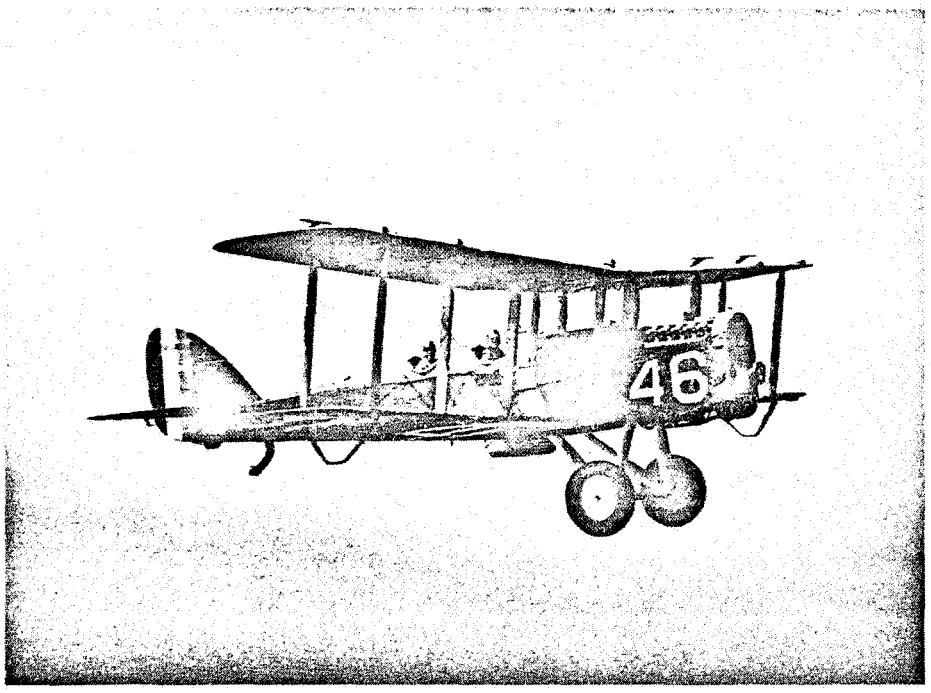

Figure 1-7. - The DeHavilland 4-B, post-war American modification of British-designed DeHavilland 4, which had been produced in the United States for use during World War I. American pilots used the original DeHavilland 4 for observation and bombing missions during 1918.

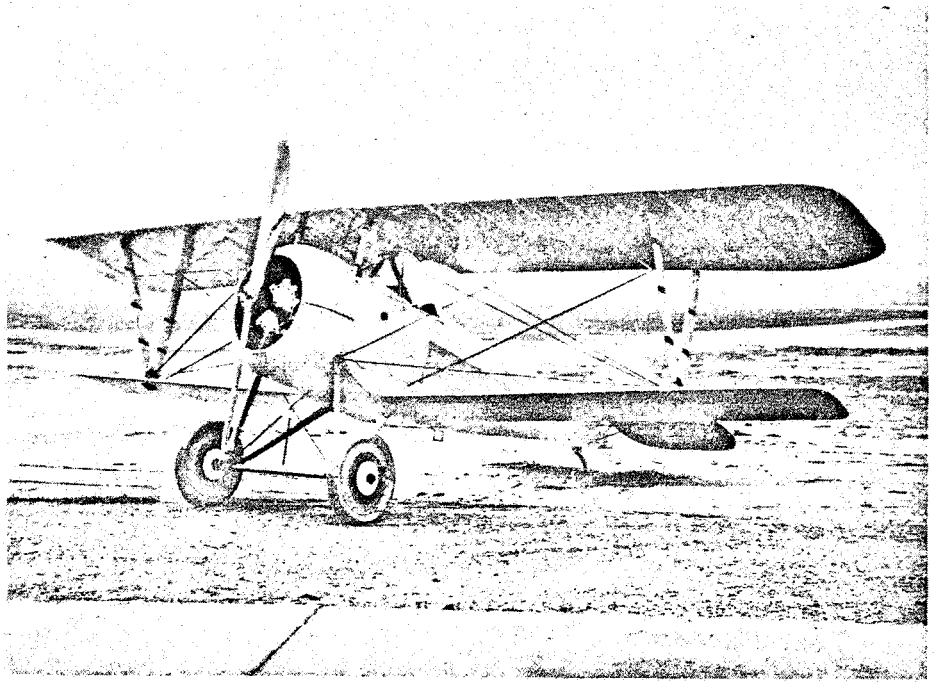

Figure 1-8. - The Nieuport 27, built by the French, was flown by many American pilots during World War I. Although it had the uncomfortable habit of shedding fabric from its top wing, many top-ranking aces built up their scores in this highly maneuverable little pursuit airplane. This was the plane that Captain Eddie Rickenbacker used in starting his string of victories.

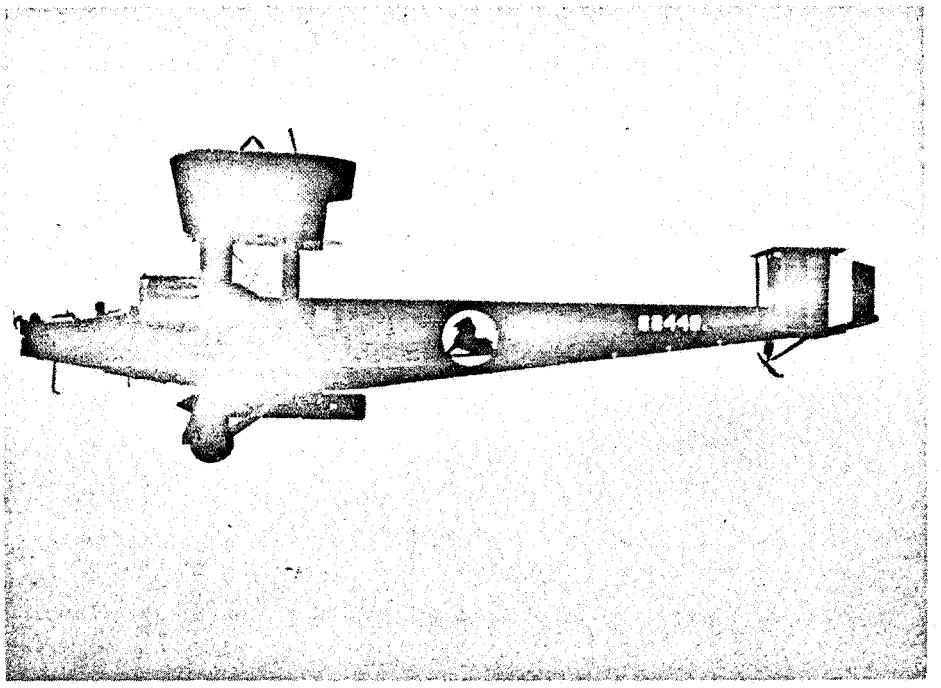

Figure 1-9. - Handley-Page bombers of British design were manufactured in the United States during World War I. With a gross weight of more than 14,000 pounds, this twin-engined aircraft was truly a "heavy" of its time. Air Marshall Hugh M. Trenchard organized British-built heavies like these into an independent Strategic Bombardment Force for attacks against the German homeland.

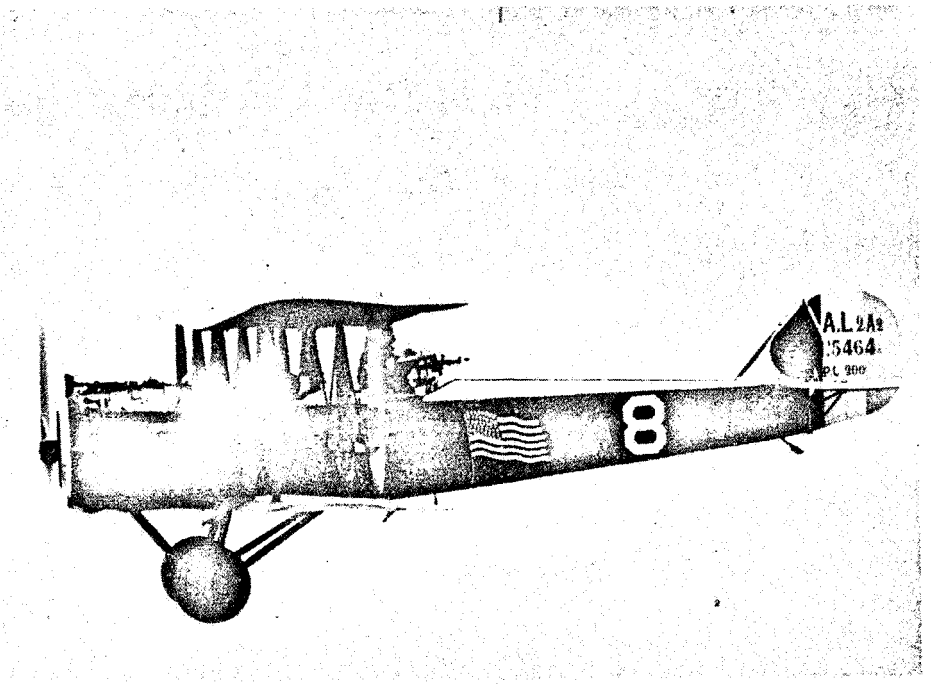

Figure 1-10. - The Salmson 2 A. 2 was a French-designed, two-place observation plane used by the American Expeditionary forces in World War I. The United States procured 705 of these planes for use in 10 A. E. F. Air Service observation squadrons serving in France. Powered by a 750-horsepower engine, the Salmson had a top speed of 116 miles per hour.

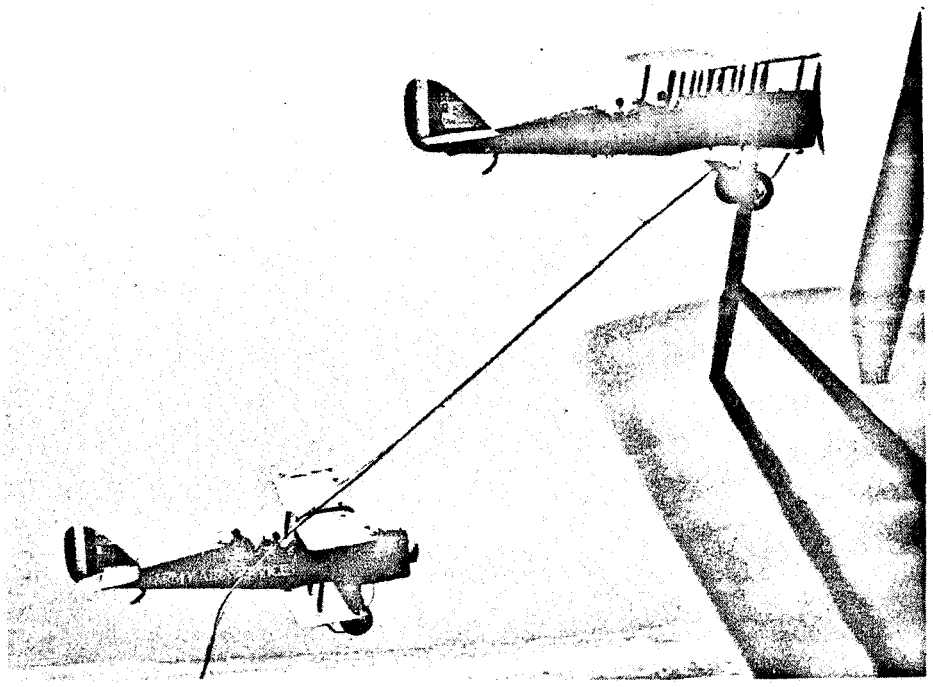

Figure 1-11. - Refueling tests using DeHavilland 4-B's were conducted by military aviators in 1923. These tests set the pattern for techniques that were to be so important in the development of aviation. As crude as the equipment was, an endurance record of 37 hours and 15 minutes was established by these pioneering pilots.

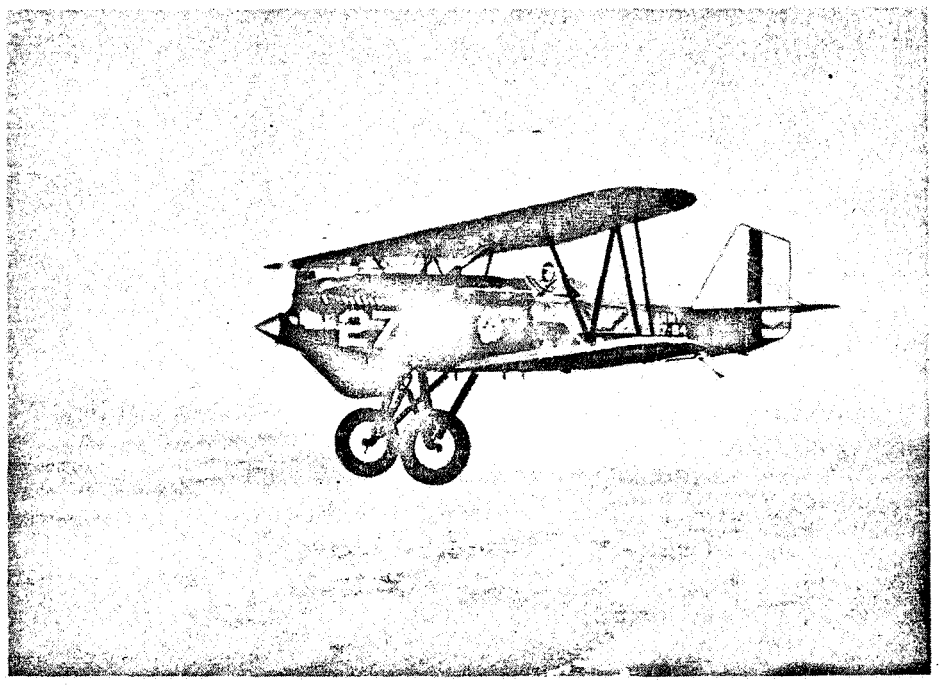

Figure 1-12. - The Curtiss Hawk P-1 flew from New York to San Francisco in 1924. The 2670-mile flight, made in 21 hours and 48 minutes, included five stops. This Hawk biplane was refined from the P-1 through the P-6.

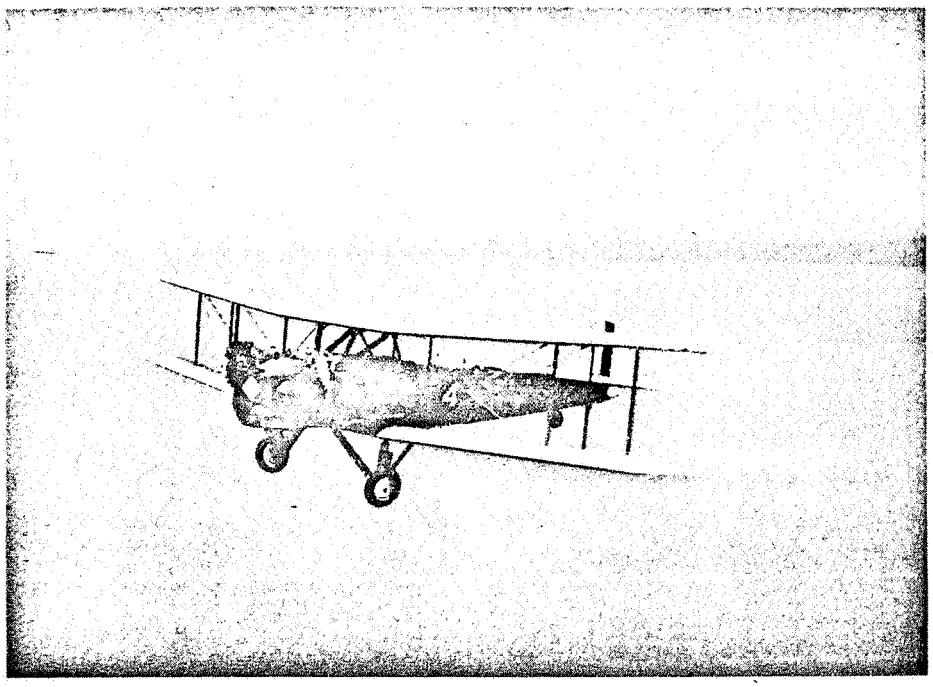

Figure 1-13. - The Keystone B-3, first of the "B" category bombers. Delivered to the newly established Army Air Corps, it had a 74-foot, 8-inch wing span and a gross weight of more than 12,950 pounds. The B-3 was powered by two 525-horsepower, air-cooled radial engines and had a crew of five.

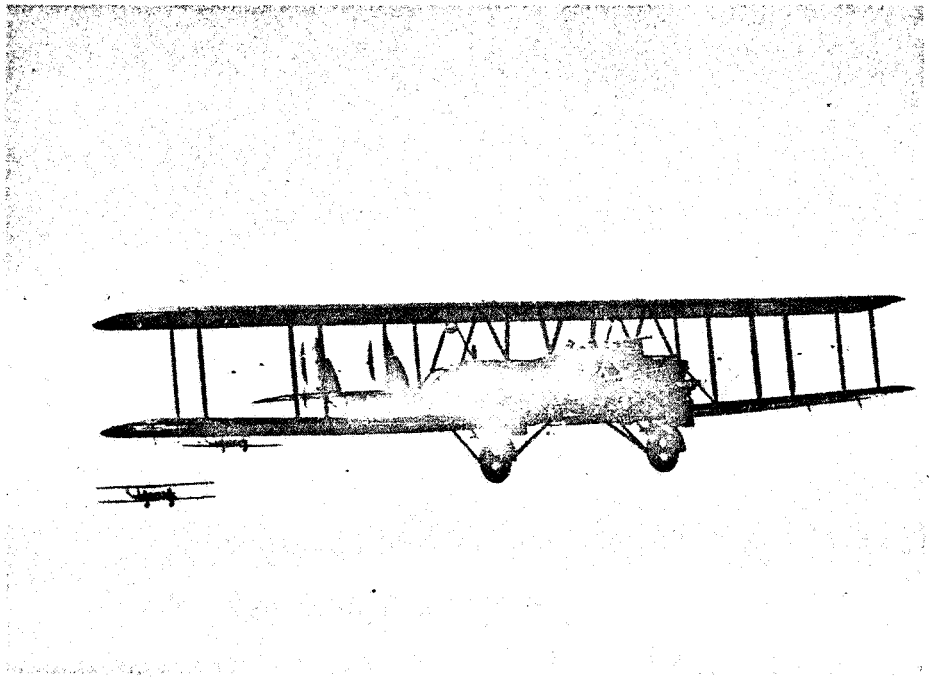

Figure 1-14. - "Mosquitoes to kill elephants" was said of General Billy Mitchell's Martin MB-2 bombers when he sent them against battleships. During tests conducted in 1921 and 1923, three war-prize German warships and two obsolete U. S. battleships were sunk by these aircraft.

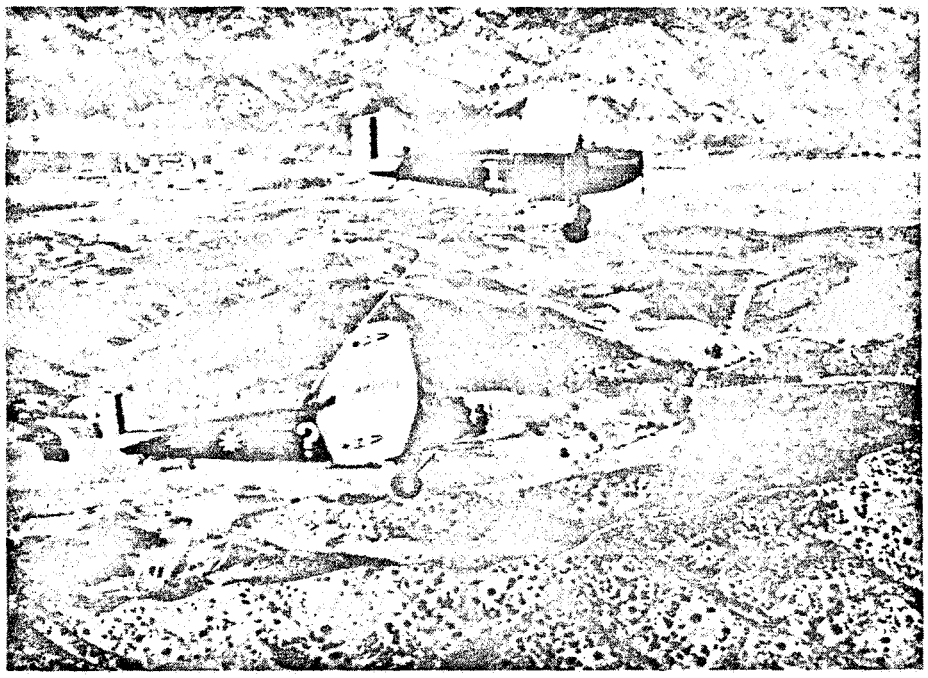

Figure 1-15. - The "Question Mark," a Fokker C-2, supplied more information on refueling techniques when it set an endurance record of almost 151 hours in 1929. Forty-three times during the historic flight the refueling plane hovered less than 20 feet over the appropriately named "Question Mark," passing down food, supplies, and more than 5000 gallons of gas.

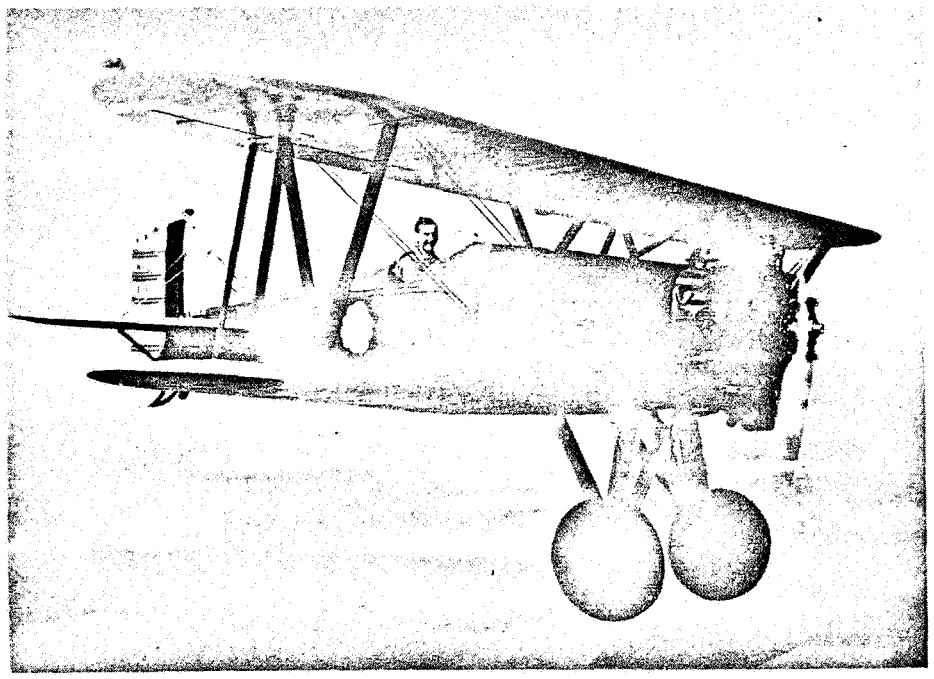

Figure 1-16. - The Boeing P-12 series pursuit aircraft was one of the finest biplane fighter aircraft ever designed. It was a highly maneuverable, sensitive plane. Grossing only 2700 pounds, this little pursuit aircraft, with its 450-horsepower engine and a skilled pilot at the controls, could loop on takeoff, a feat that attested to its outstanding design.

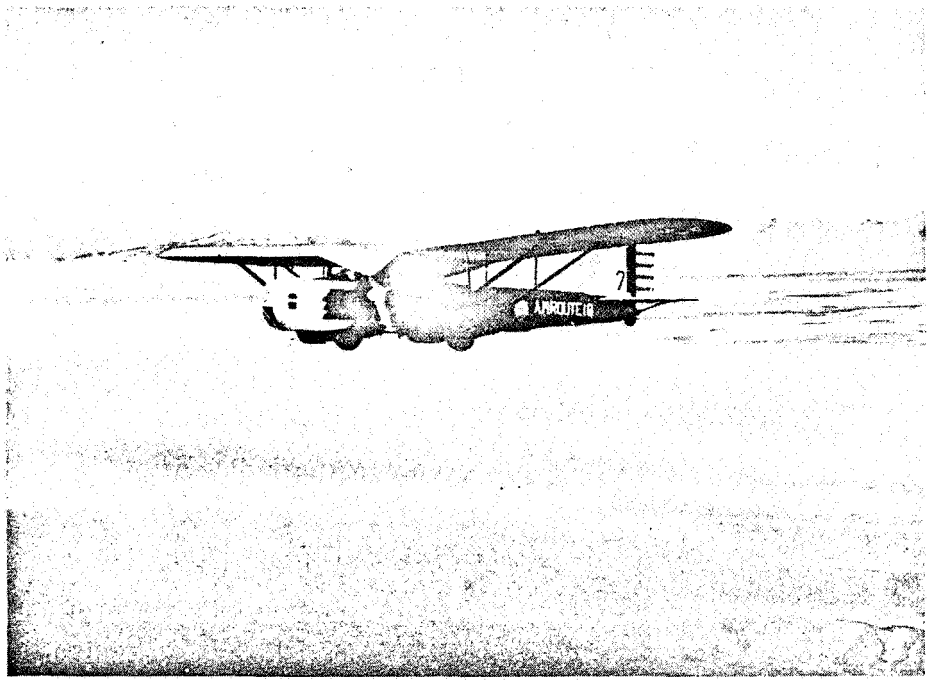

Figure 1-17. - The Douglas B-7, a transitional product of new bomber theories, still had the struts that typified the age of the biplane. Designed as a fast day-bomber, it had fabric-covered wings, an all-metal fuselage, metal control surfaces, and hydraulically operated, retractable landing gear. The B-7 flew mail over the Salt Lake City - Oakland route in early 1934 when the War Department was directed to take over all domestic airmail flights.

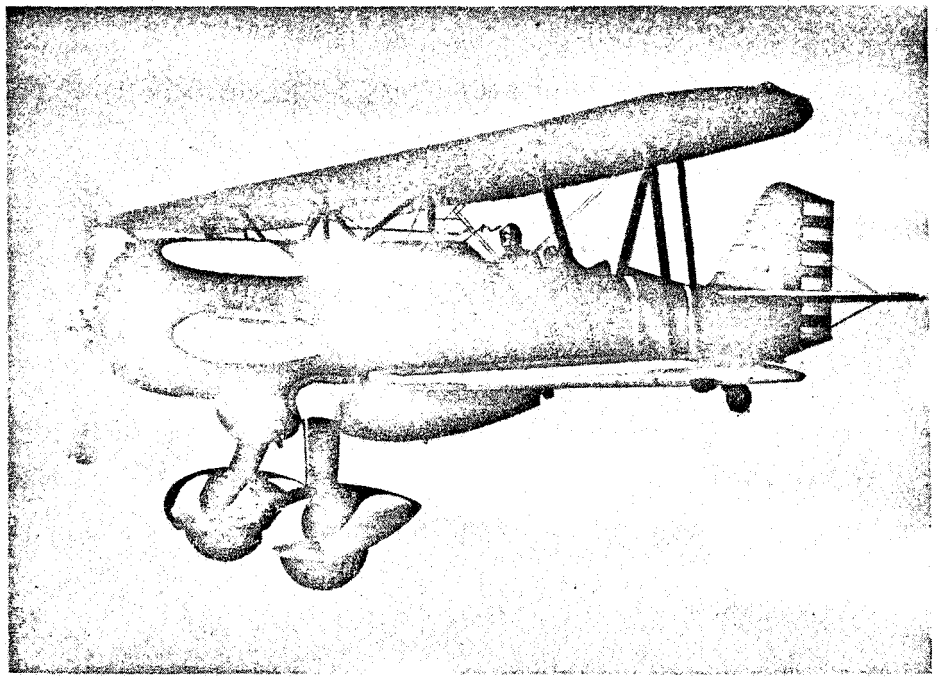

Figure 1-18. - The Curtiss P-6E was the most famous of the Hawk series of pursuit planes. One of the most beautiful biplane fighters ever built for the Air Corps, it was highly maneuverable and armed with two synchronized machineguns. Powered by a 600-horsepower liquid-cooled Curtiss engine turning a three-bladed propeller, this little fighter had a top speed of 197 miles per hour. A later model, the P-6F, was the first military aircraft to exceed 200 miles per hour in level flight.

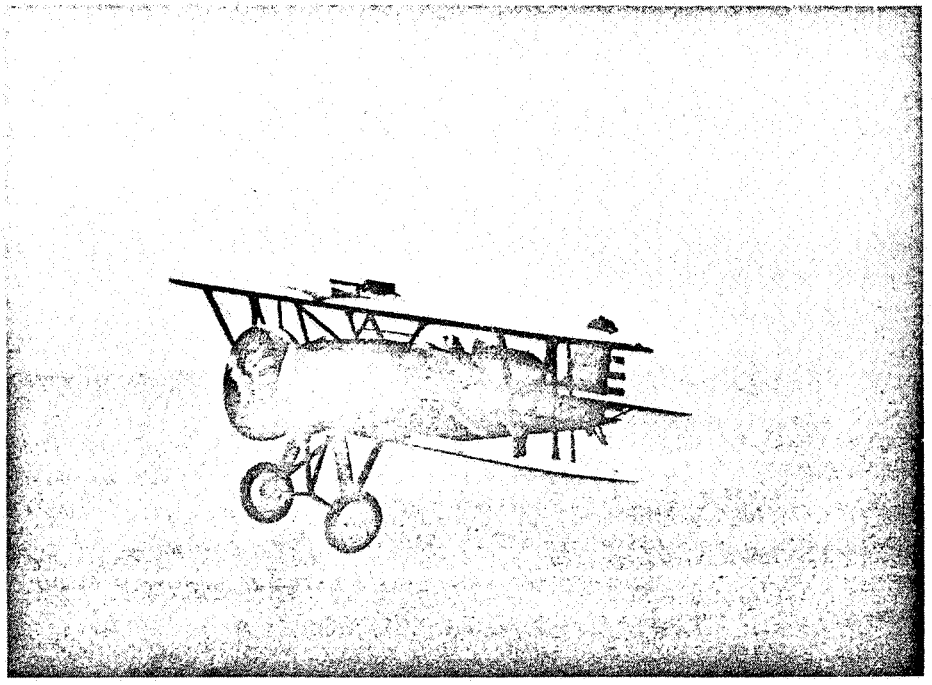

Figure 1-19. - The P-12E by Boeing was the first production-built Air Corps pursuit plane with an all-metal, monocoque fuselage. The P-12's had a long service life, serving with frontline squadrons from 1929 to 1936. In all, 366 of this series were produced; 110 of them were E models.

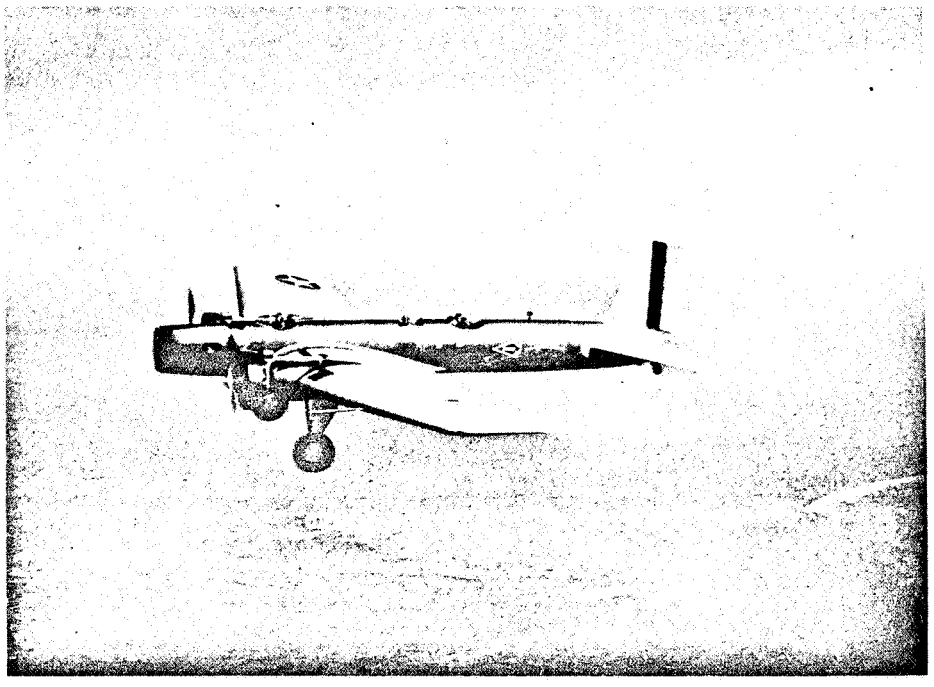

Figure 1-20. - A new aerodynamic concept was introduced when Boeing Aircraft Company produced the B-9, a low-wing, all-metal monoplane, in the 1930's. Earlier bomber aircraft, generally designed for multipurpose use, could not be as effective as one planned for a specific mission.

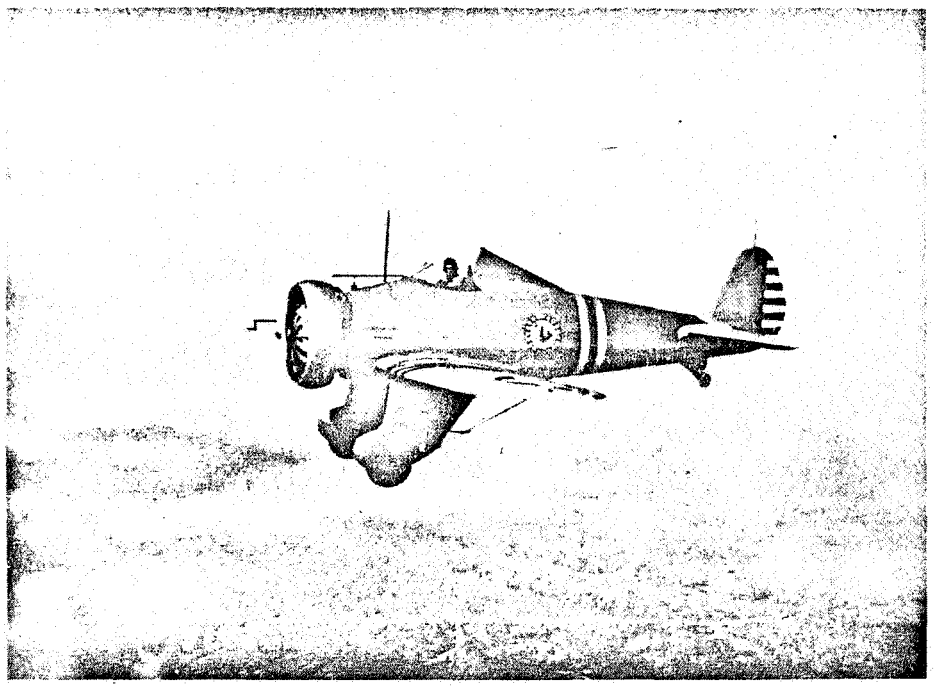

Figure 1-21. - The Boeing P-26 Peashooter, designed to meet the increasing performance of the new bombers, was the first all-metal, low-wing fighter delivered in numbers. During this period, many thought the pursuit ship obsolete. Bombers were becoming so much faster that it was difficult for fighters to keep up with them.

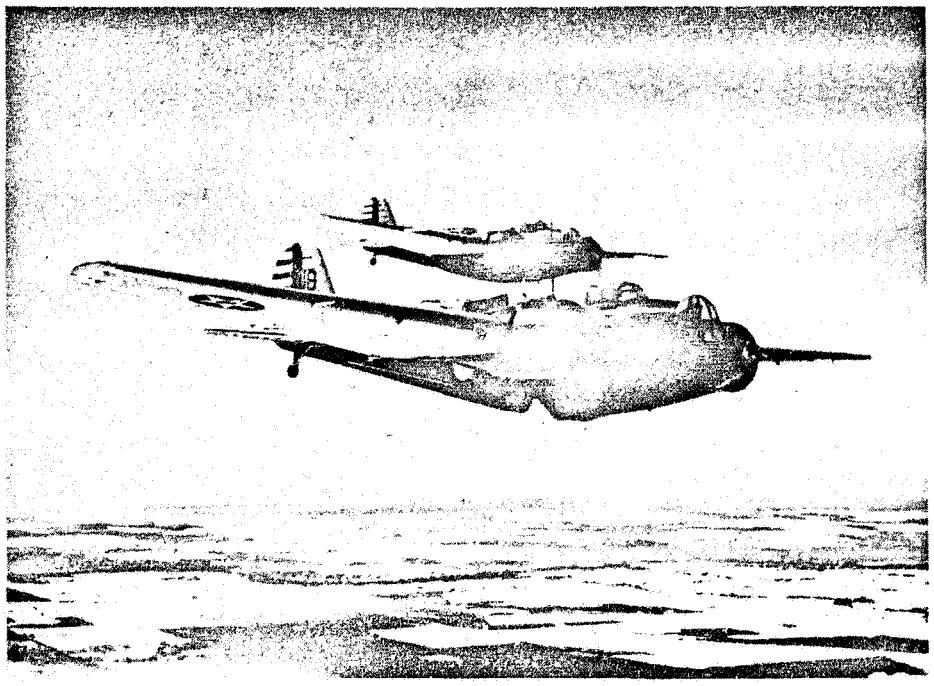

Figure 1-22. - A new generation of bombers was realized with the production of the Martin B-10. Featuring enclosed cockpits, a power-operated turret, retractable landing gear, and newly designed engine cowlings, it had a top speed of 212 miles per hour.

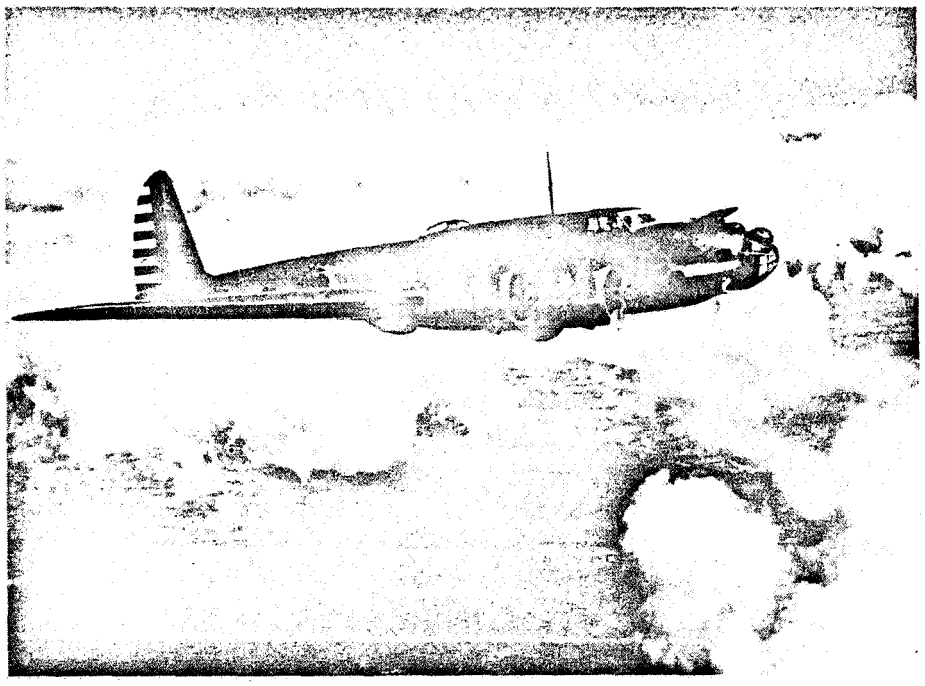

Figure 1-23. - In August 1934, Boeing began construction of the XB-17. First flown in July 1935, it led the way to one of the world's most famous series of bomber airplanes. Flying characteristics of this plane were outstanding for the time, establishing performance records that far outclassed most airplanes of the era. Accepted by the military in January 1937 as the YB-17 Flying Fortress, it had a top speed of 256 miles per hour, service ceiling of 30,600 feet, and a maximum range of 3320 miles.

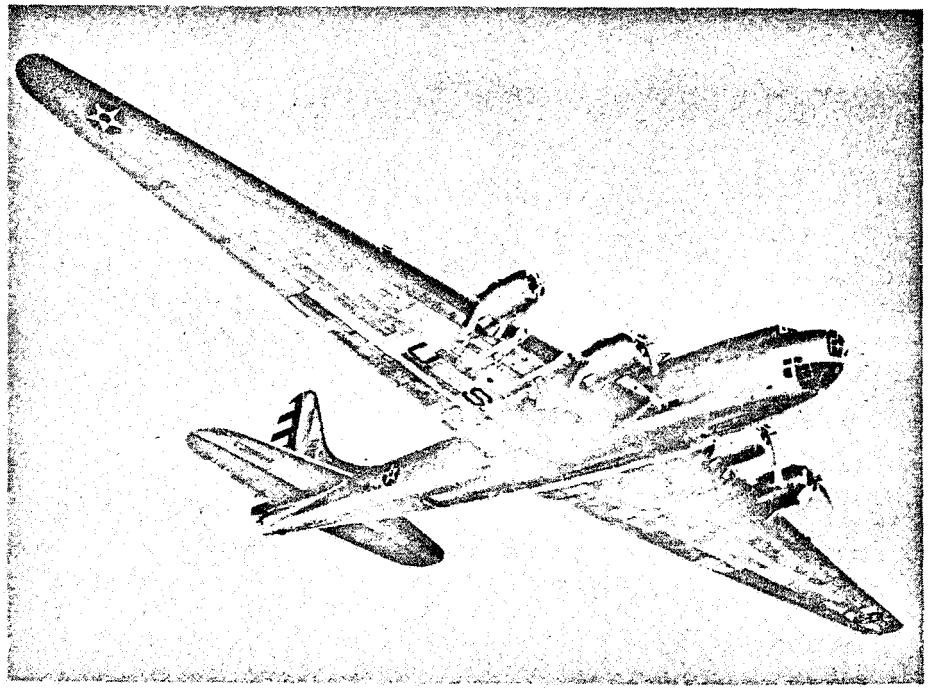

Figure 1-24. - The Douglas XB-19, conceived in 1935, first flew in 1941. The culmination of $6\frac{1}{2}$ years of engineering, this giant aircraft dwarfed all others of the time. It had a wing span of 212 feet, a 132-foot, 4-inch fuselage, 8-foot main tires, and a rudder 42 feet high. It had a range of 7710 miles with a fuel load of 10,400 gallons.

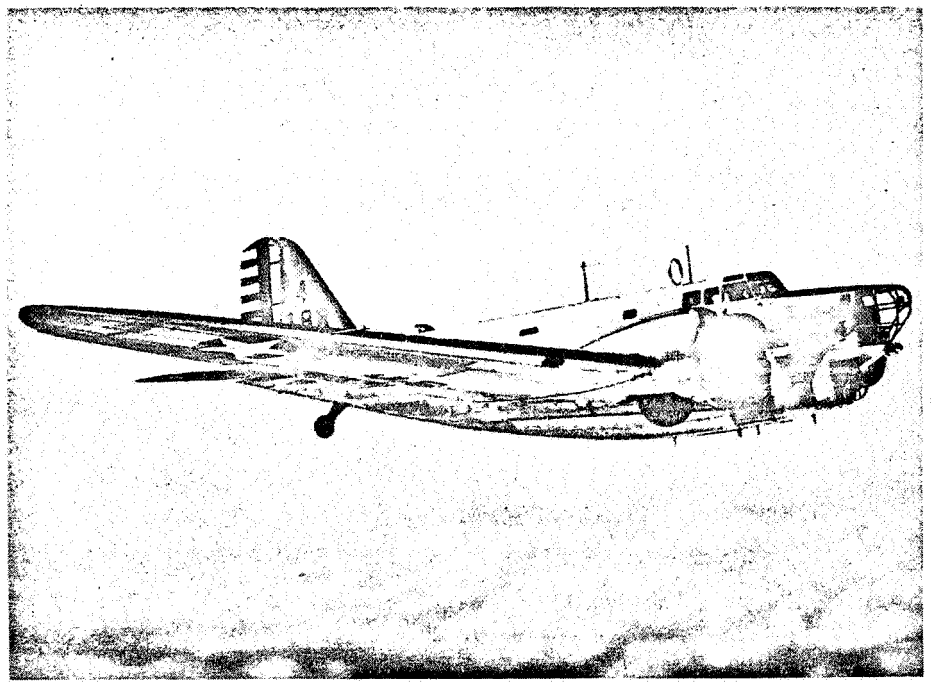

Figure 1-25. - Air Corps bomber competition of 1936 resulted in Douglas Aircraft Company getting an order for 177 B-18 Bolos. Quite similar in appearance to the famed DC-3 commercial airliner just coming off Douglas production lines, the Bolo was a very reliable airplane with good performance.

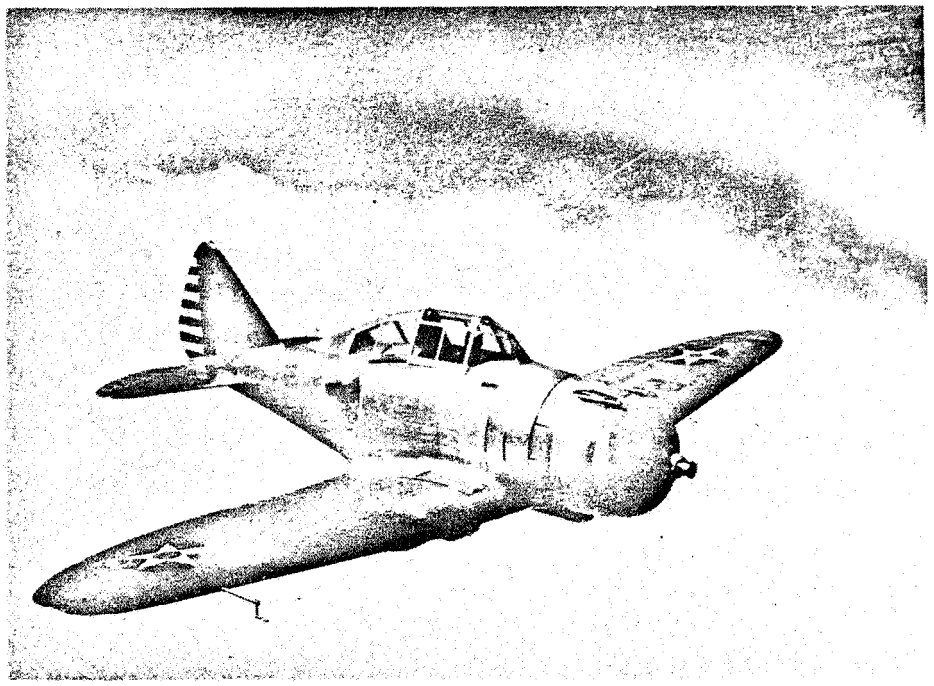

Figure 1-26. - The P-35 of Major Alexander DeSeversky's aircraft company (1936), a forerunner of future fighters, proved to be a wonderful airplane to fly. Almost 50 miles per hour faster than the P-26, its armament still did not make it the fighting machine pilots needed to keep up with bomber development.

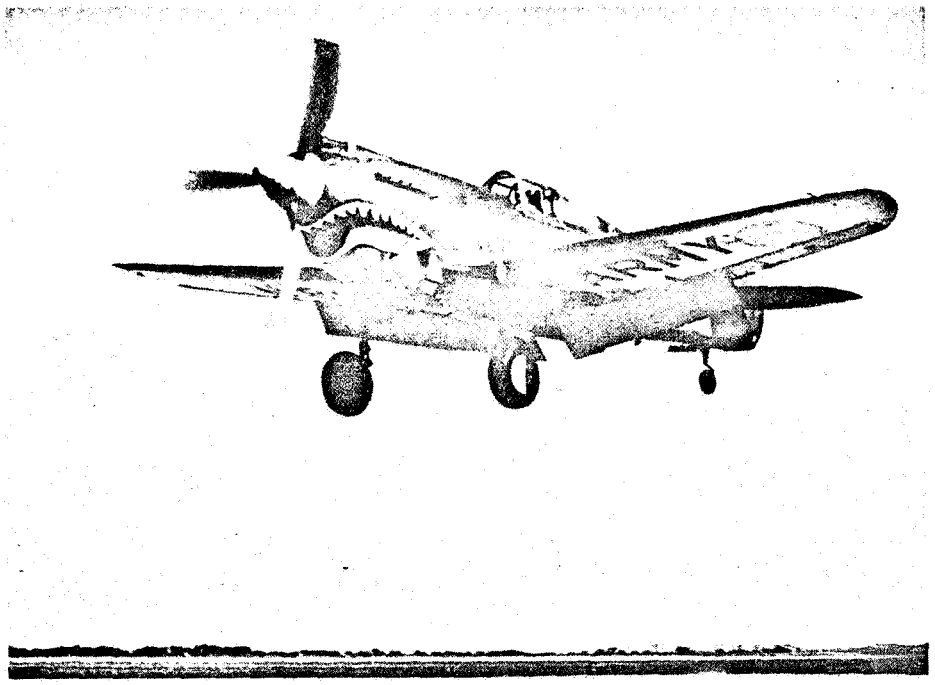

Figure 1-27. - Hawk, Tomahawk, Kittyhawk, Warhawk were the official names given to the Curtiss P-40. Praised, abused, called excellent and inferior, this much-discussed World War II fighter saw action on every fighting front in the world. Always less maneuverable and slower than first-line German and Japanese adversaries, it proved far more rugged.

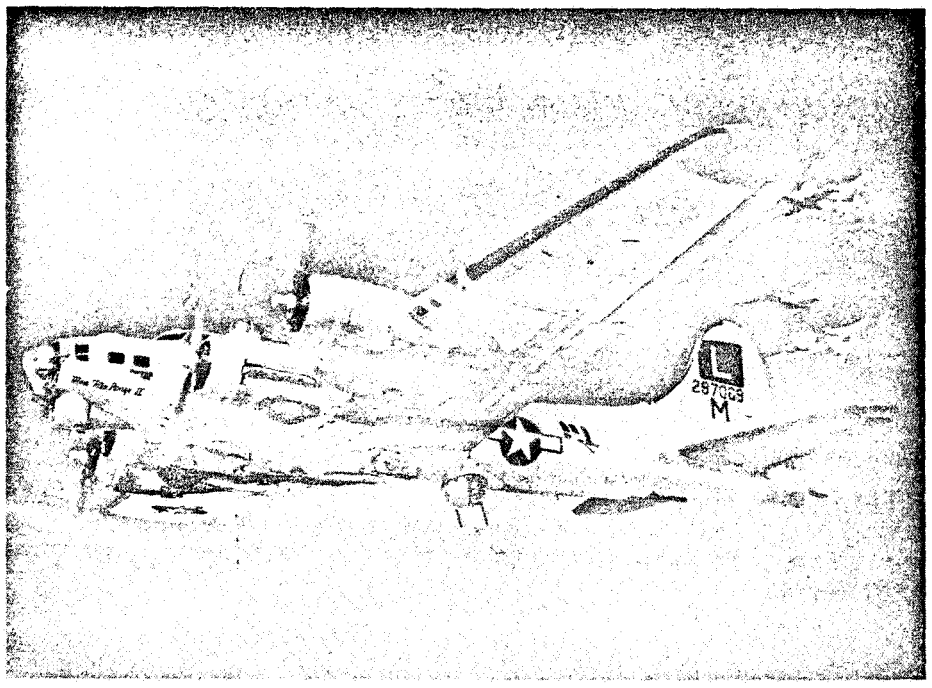

Figure 1-28. - The World War II Flying Fortress (B-17), scourge of the skies over embattled Europe, no longer had the thin, graceful lines of its 1936 sister. Redesigned to take the war to the enemy, the slim rudder had given way to a broad dorsal fin that enclosed twin stinger 50-caliber machineguns in the tail. Top and belly turrets bulged from the fuselage, showing their ugly gun snouts. Airmen gunners stood at open side hatches with their 50's bearing on anything that came their way.

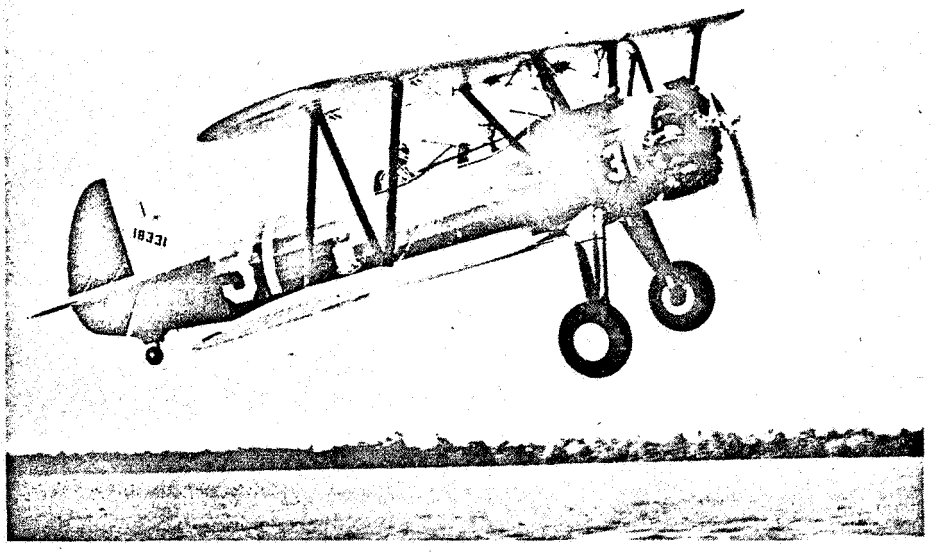

Figure 1-29. - The Stearman PT-17 Kaydet was used for primary flight training prior to and during World War II by both the Air Force and the Navy. Equipped with a 220-horsepower engine, the two-place biplane had a top speed of 135 miles per hour.

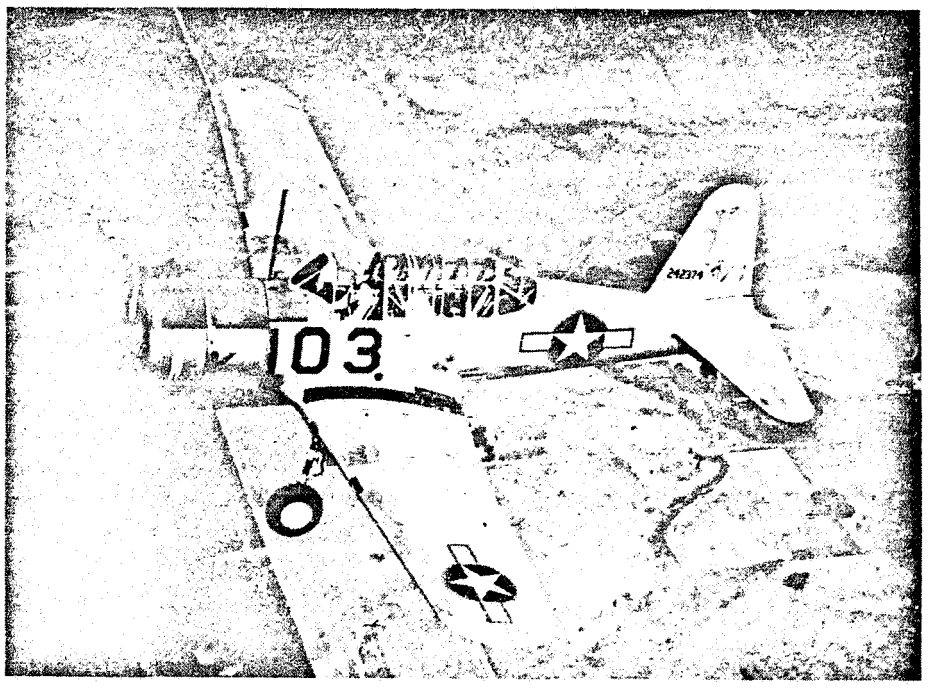

Figure 1-30. - The Vultee "Vibrator" (BT-13) was familiar to thousands of fledgling pilots going through basic flying training in the 1940's. The BT-13 was a heavier airplane than those flown in primary training, and its higher horsepower and pronounced torque provided trainees with the feel for the combat planes to come.

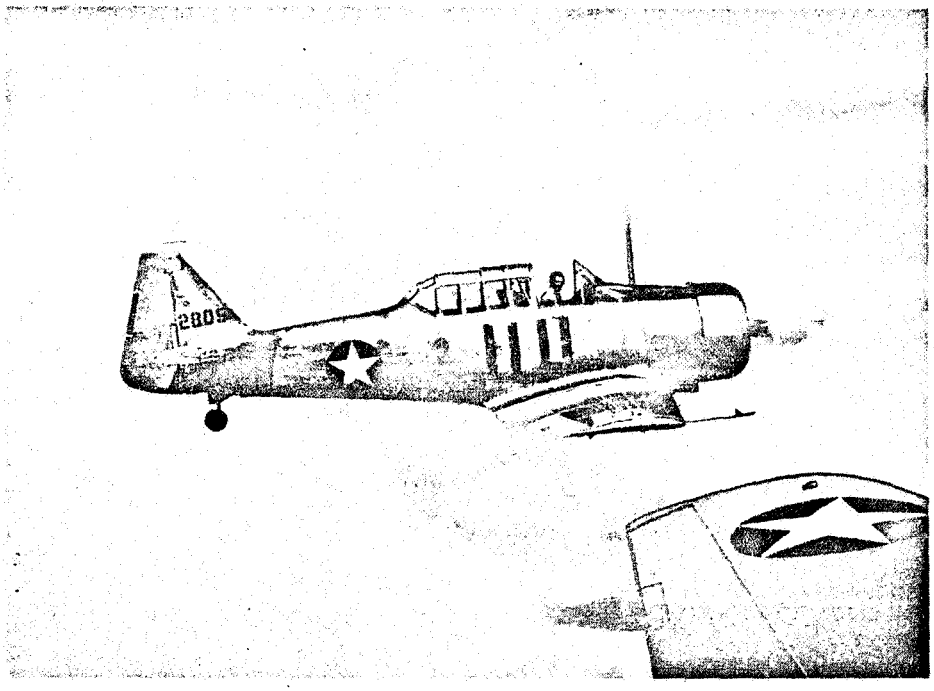

Figure 1-31. - Flown by more military pilots, worldwide, than any other aircraft, the North American AT-6 Texan had an unusually long service life. Produced as an advanced trainer in 1938, it was used in U. S. Air Force pilot schools until September 1956.

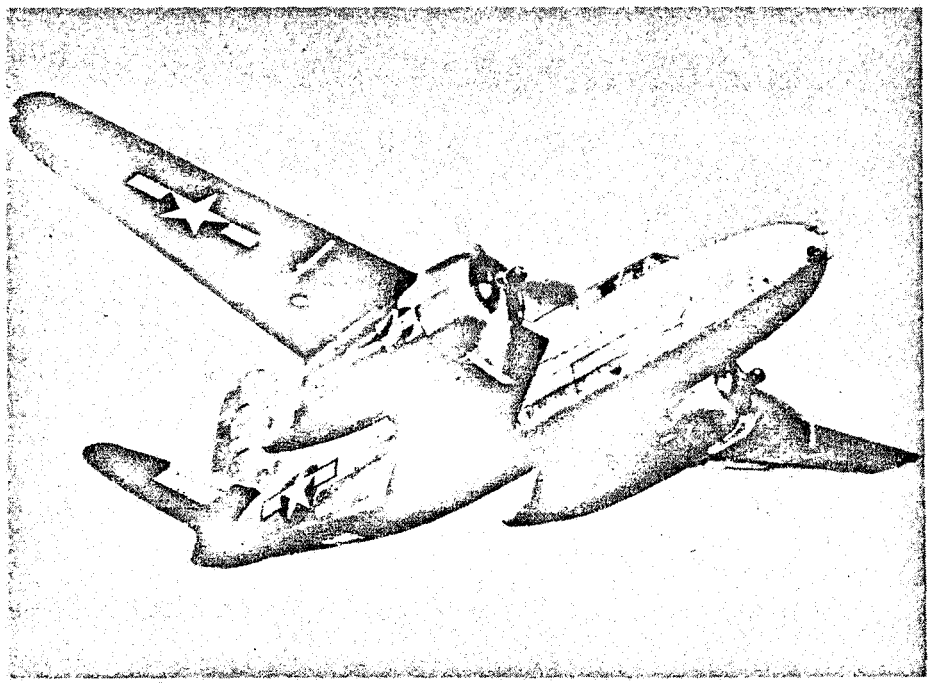

Figure 1-32. - The Douglas A-20 was developed from a bomber designed for the French in 1937 and first flown in 1938. Designated the Havoc by the Americans, early production models were delivered to the British, who renamed it the Boston.

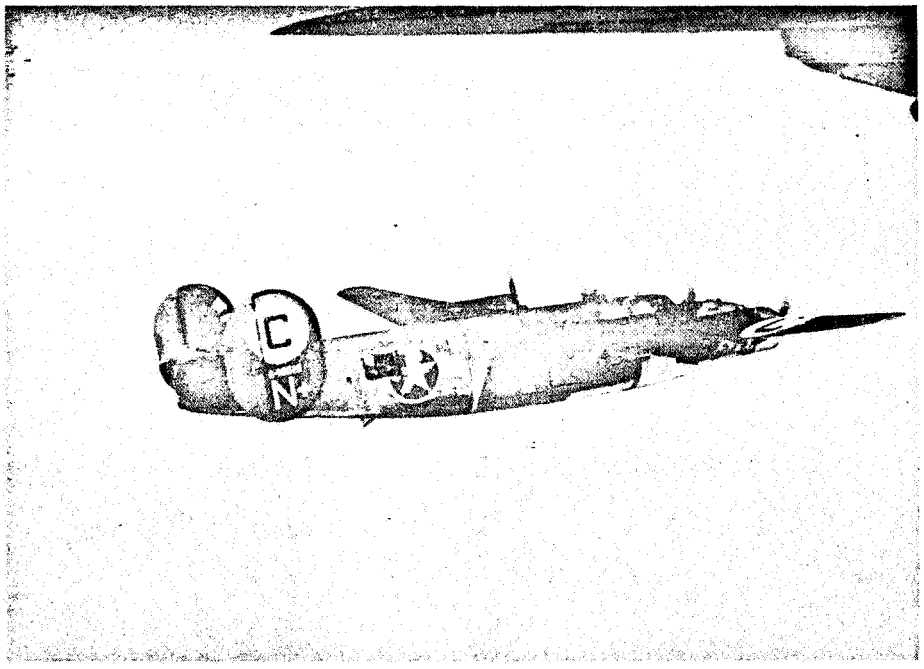

Figure 1-33. - The Convair B-24 Liberator is probably best remembered for its service in early raids on Nazi oil refineries at Ploesti, Rumania. Losses during the August 1, 1943, raid on Ploesti were extremely high. Of the 163 Liberators that reached the target, 54 were lost, and 144 airmen were killed or missing.

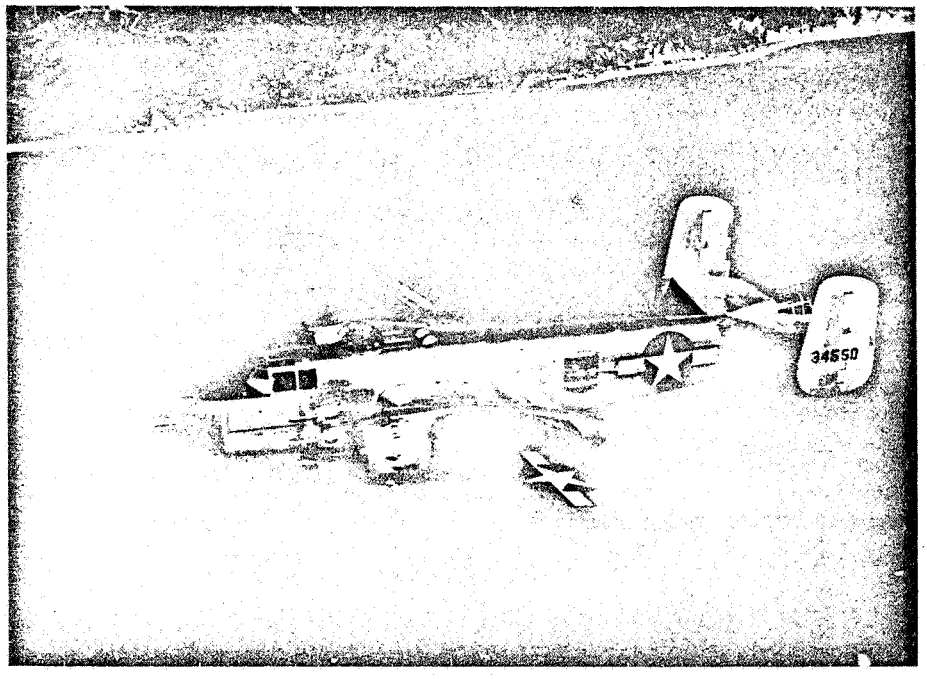

Figure 1-34. - The North American B-25 Mitchell bomber, named after General Billy Mitchell, saw combat in most World War II theaters. The most famous exploit of this versatile plane was unquestionably the carrier-based attack planned by the Air Corps and led by Lieutenant Colonel Jimmy Doolittle against the Japanese mainland early in the war.

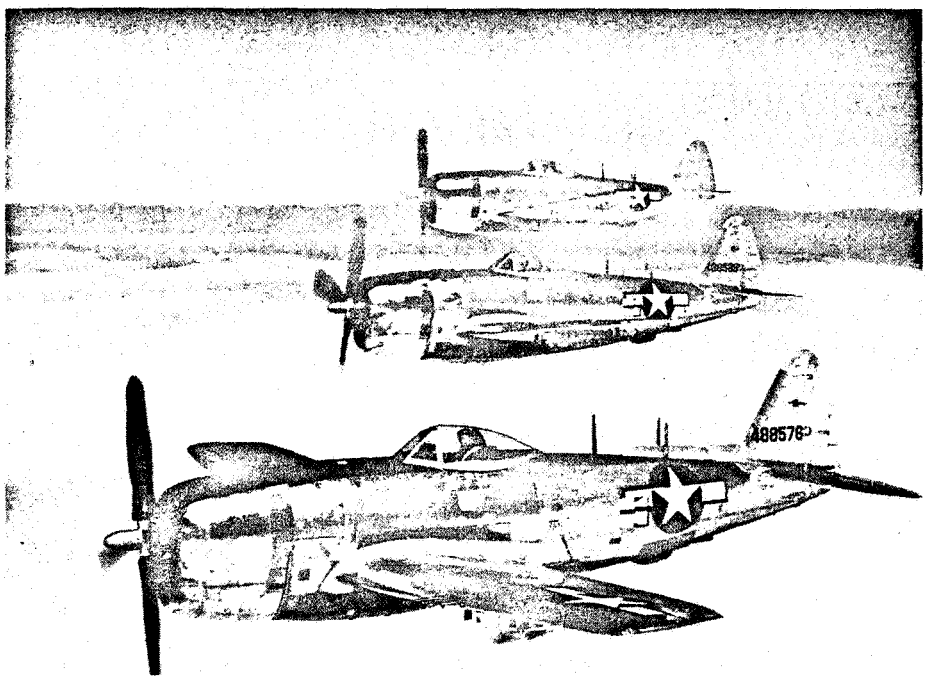

Figure 1-35. - "Juggernaut," or affectionately "Jug," was the name given to the rugged Republic P-47 Thunderbolt by its pilots. Twice as heavy as any single-engine fighter before it, the P-47 was the culmination of years of work by Major Alexander DeSeversky.

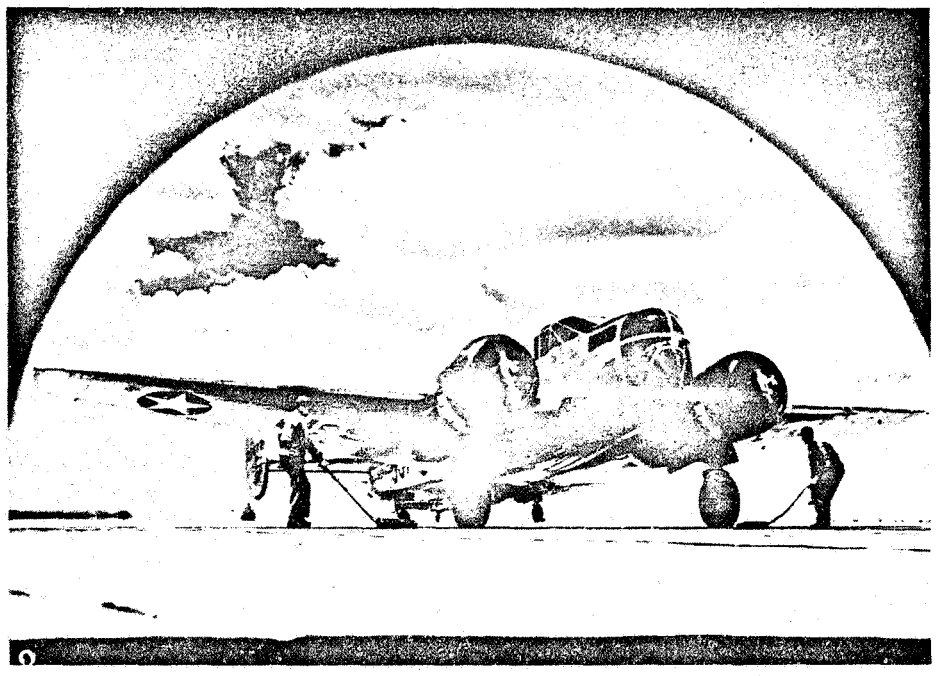

Figure 1-36. - In continuous production since 1937, the twin-tailed, model 18 Beech light commercial transport was adapted to navigator and bombardier training during World War II. As the Plexiglas-nosed Beech AT-11, it was a familiar classroom to the 45,000 World War II bombardier cadet graduates.

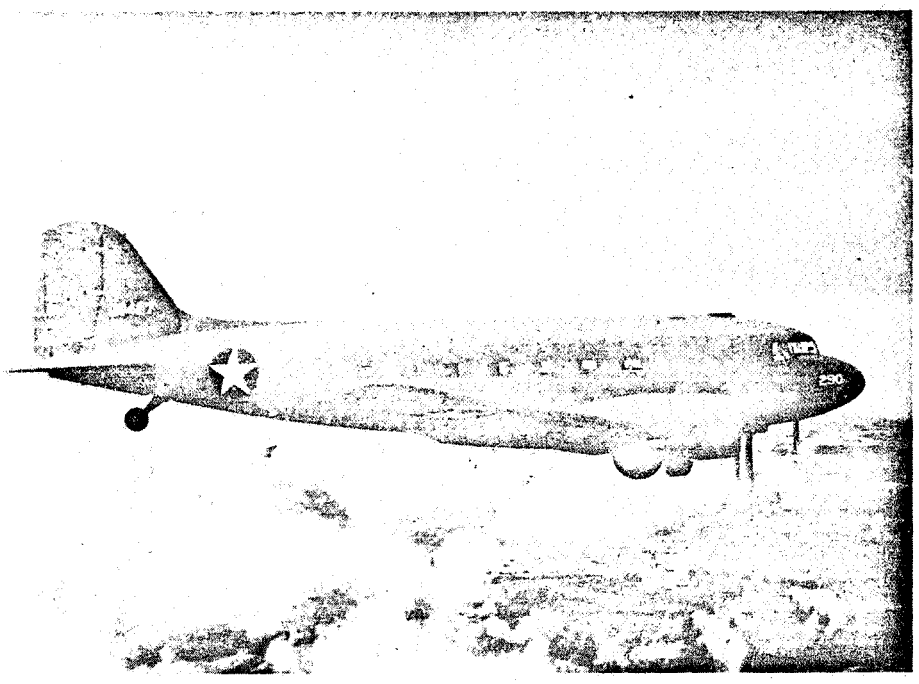

Figure 1-37. - DC-3, C-47, Dakota, and Skytrain were the official names of this world-famous Douglas-built cargo and passenger plane. To her crews, however, this lovable old bird was called the "Gooney." Large airline demands for this model and resultant production improvements led to the DC-3 in June 1936. This is the plane that became the workhorse of the Services during World War II.

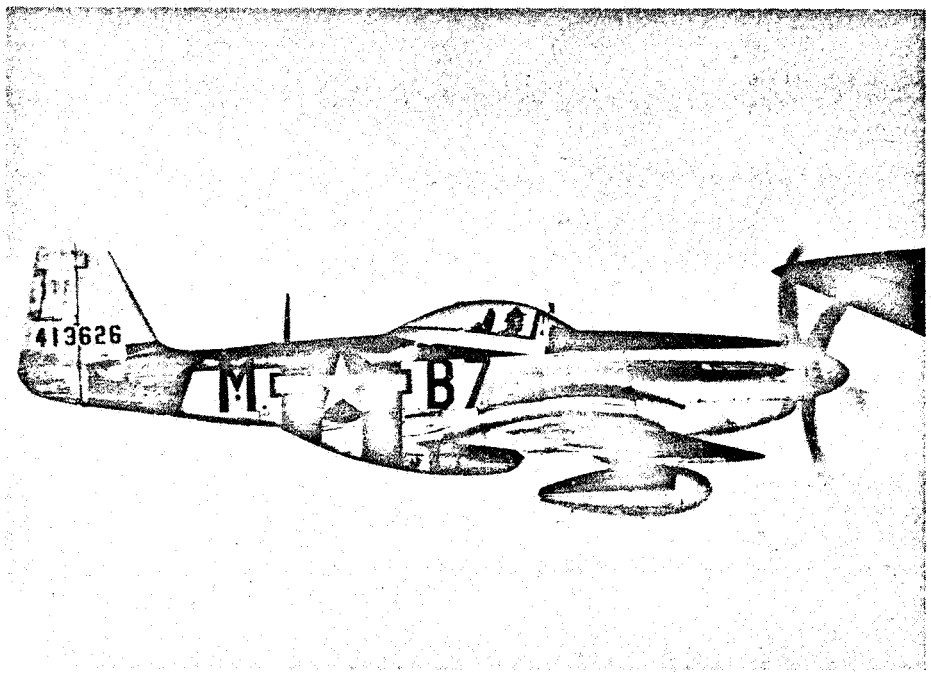

Figure 1-38. - The P-51 Mustang was originally designed for the Royal Air Force in 1940. With a deadline of 120 days for delivery, North American Aviation achieved the almost impossible, by producing the first model in 117 days. Called the best all-around American-built fighter of World War II, it was faster, more maneuverable, and most important, had a greater cruising range than any other fighter in the USAAF.

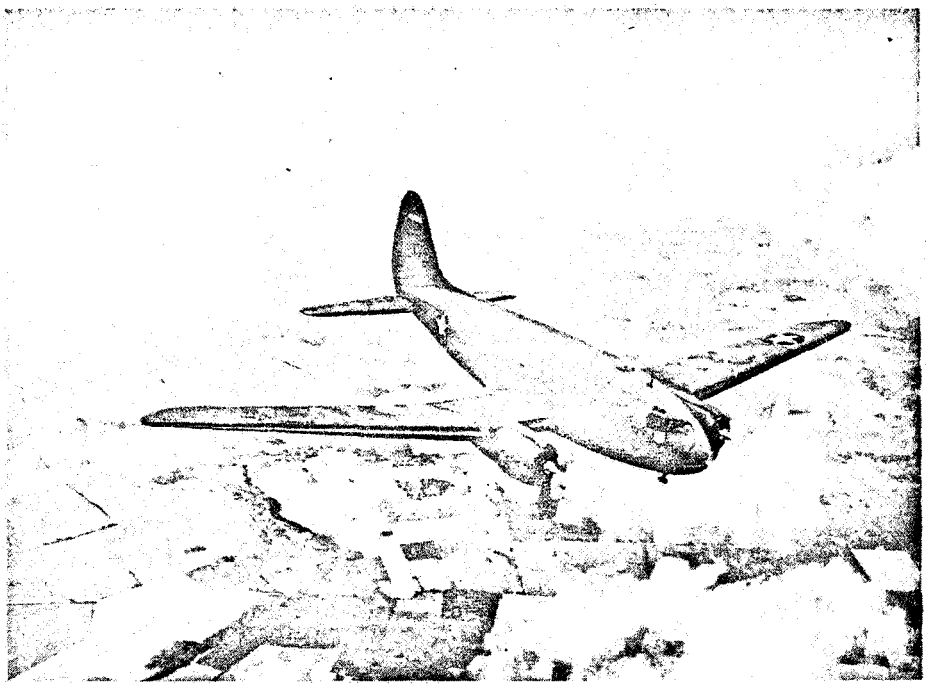

Figure 1-39. - The C-46 Commando, built by the Curtiss-Wright Corporation, first saw action late in World War II. With a capacity of 15,000 pounds, it was the largest twin-engined plane at the time. The Commando served in all theaters as a troop and cargo carrier, flying ambulance, and tow plane for gliders.

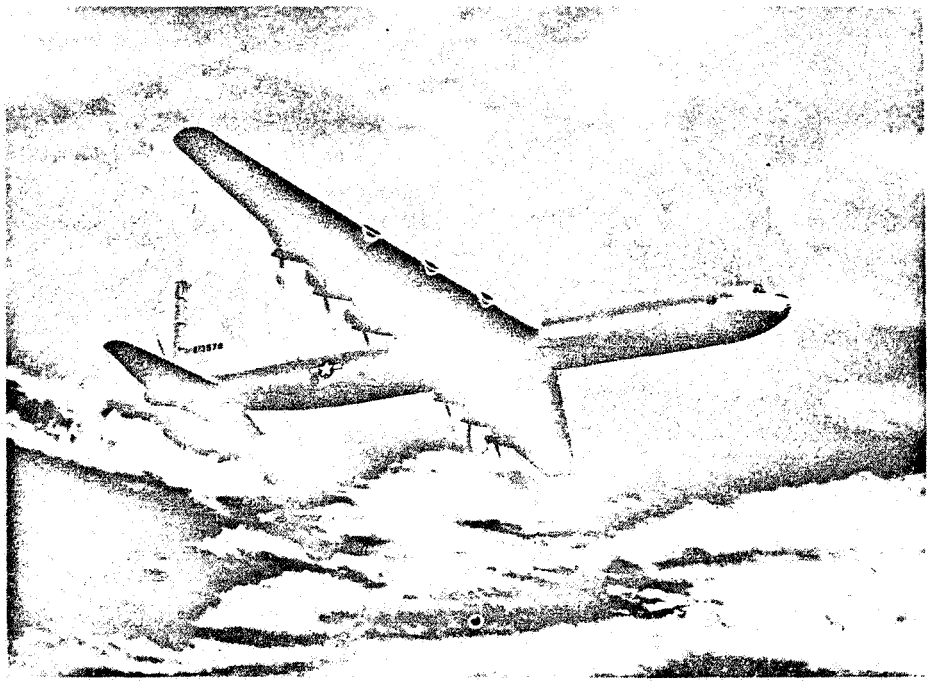

Figure 1-40. - The Consolidated B-36 Peacemaker was the biggest bomber, in size, to enter the Air Force inventory. Development began in 1941. It was not flown, however, until the fall of 1947. The Peacemaker lived up to its name in helping to deter general war for more than 10 years. The B-36 originally was powered by six turbopropeller, pusher engines. The "D" version, introduced in 1949, had four additional turbojet engines paired in pods, one under each wing. This ten-engined version had a top speed of 435 miles per hour, a ceiling of 45,000 feet, and a bomb load of 84,000 pounds.

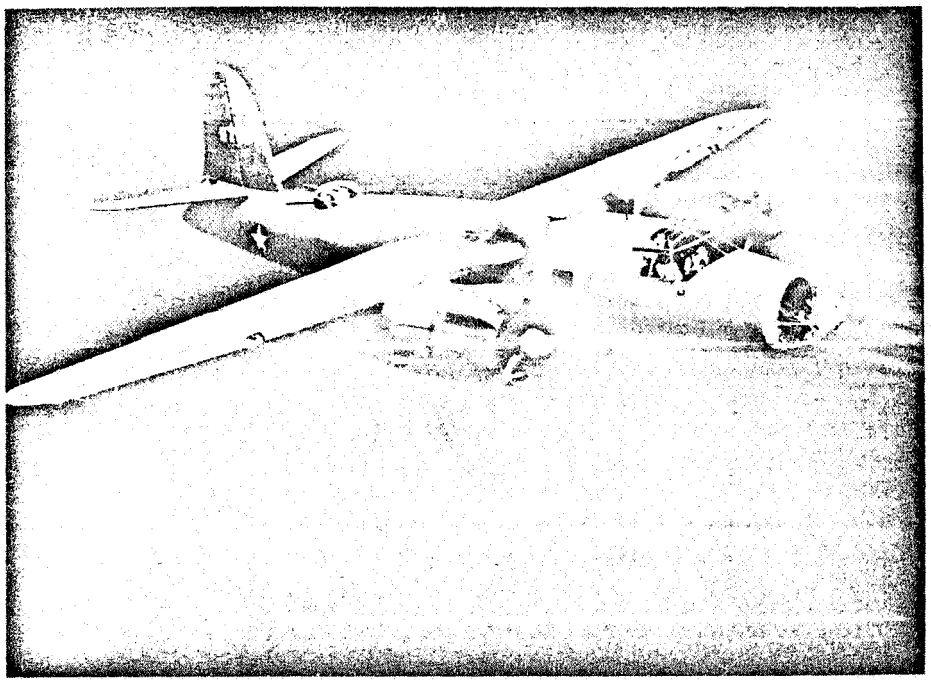

Figure 1-41. - Built by Martin, the B-26 Marauder amassed a creditable combat record in Africa, Europe, and the Pacific during World War II. With its unusually high wing loading and a landing speed of 135 miles per hour, the Marauder was one of the most controversial airplanes of its time.

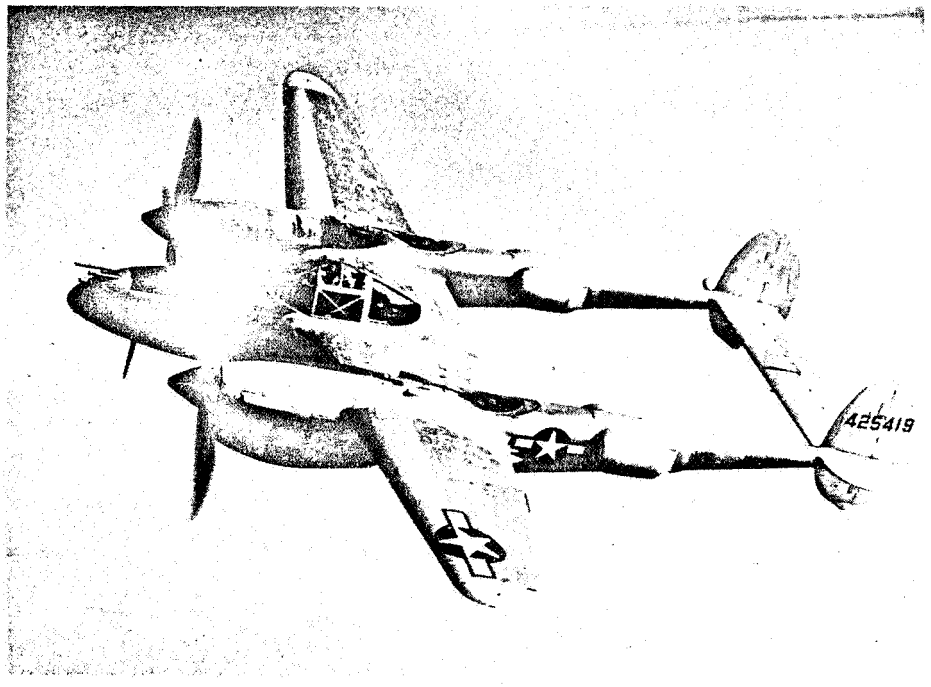

Figure 1-42. - Operational in 1942, the Lockheed P-38 Lightning was designed in 1937 and first flew in 1939. Known as the "Fork-Tailed Devil" by the Germans and Japanese, the Lightning piled up an impressive record in Europe and the Pacific. With hydraulic aileron boost and counterrotating propellers, it was a wonderful airplane to fly. A rapid roll, the ability to dive at extremely high speeds (up to 780 mph), and concentrated firepower made it a formidable adversary.

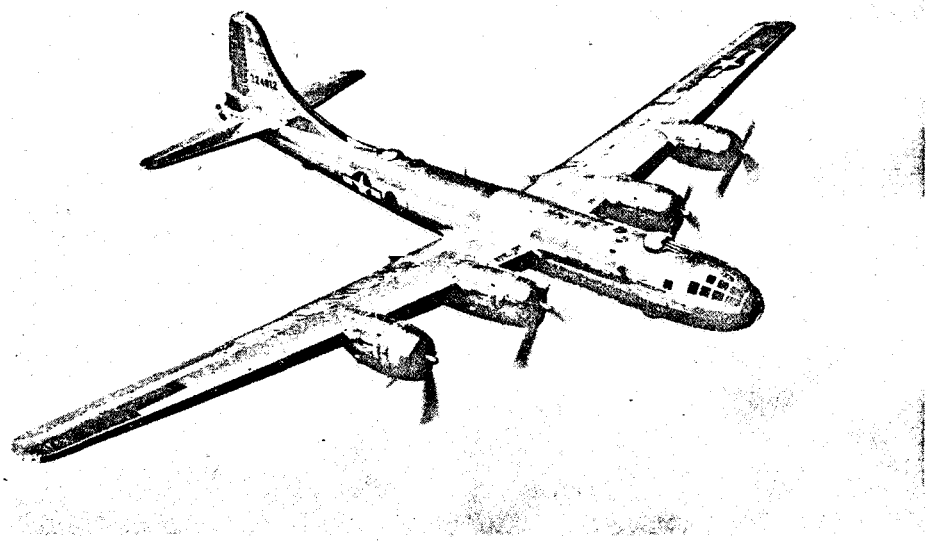

Figure 1-43. - The B-29 Superfortress, built by Boeing, has been called the weapon that won the war in the Pacific. Designed to carry large bomb loads long distances, it made possible the strategic bombardment that brought Japan near to collapse. It was a very sophisticated airplane with a pressurized cabin, highly advanced remote-control gun-firing system, and tremendous bomb capacity.

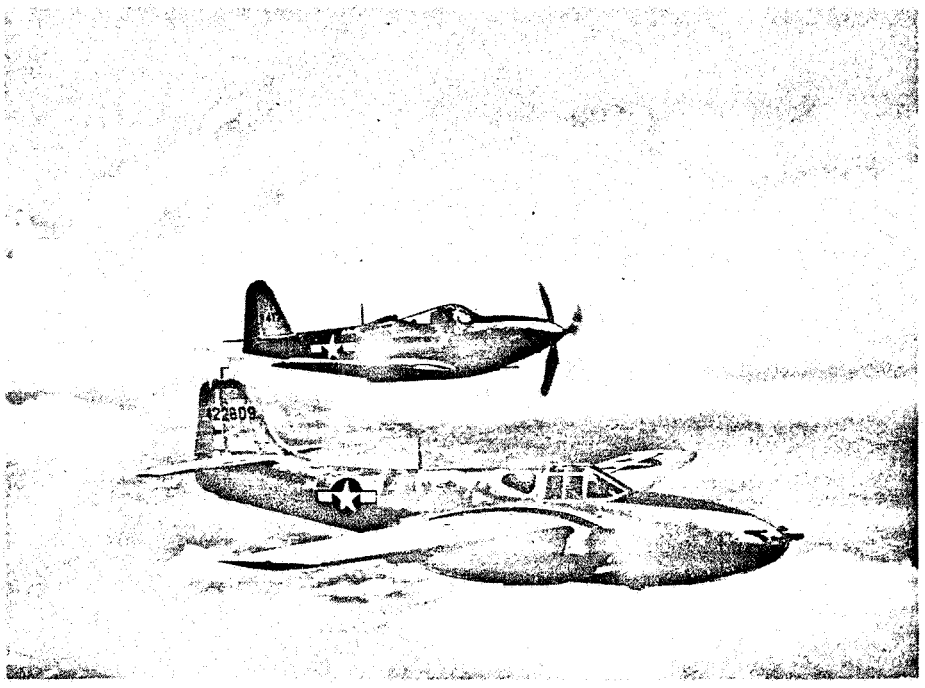

Figure 1-44. - The first jet aircraft produced for the USAAF and flown in October 1942 was the Bell XP-59A Airacomet (bottom). Powered by twin 2000-pound-thrust jets, this airplane was not as fast as the operational fighters of the time. The Bell P-63 Kingcobra (top) was propeller driven and had a 37-millimeter cannon in the nose.

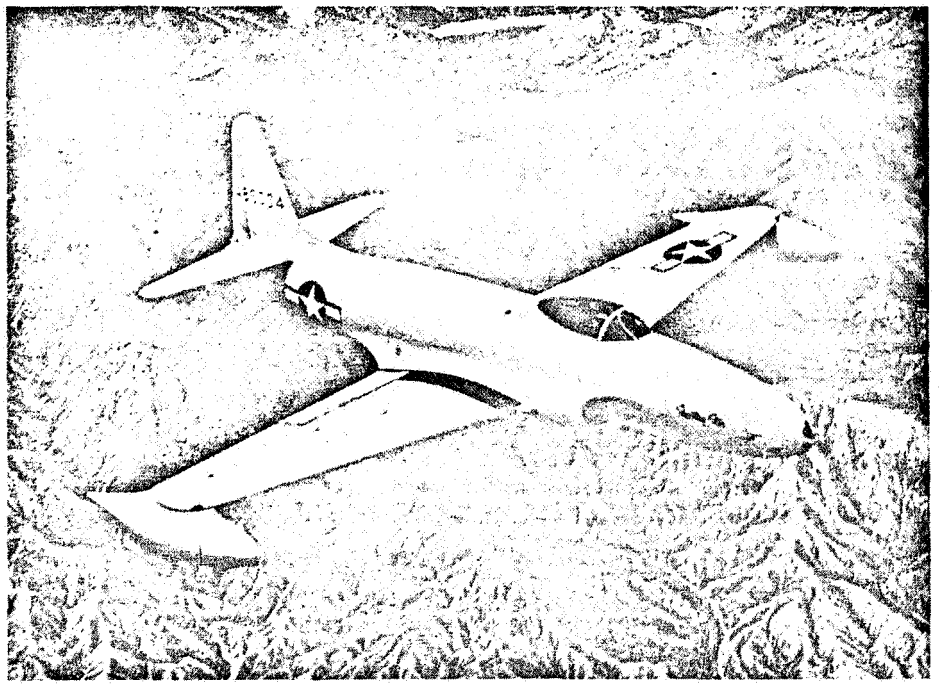

Figure 1-45. - Development of the jet-propelled Lockheed P-80 Shooting Star marked the dawn of the jet age. The Shooting Star, designed as an answer to the enemy jets appearing in the skies over Europe, was built in the record time of 143 days. The prototype of this jet flew on January 8, 1944.

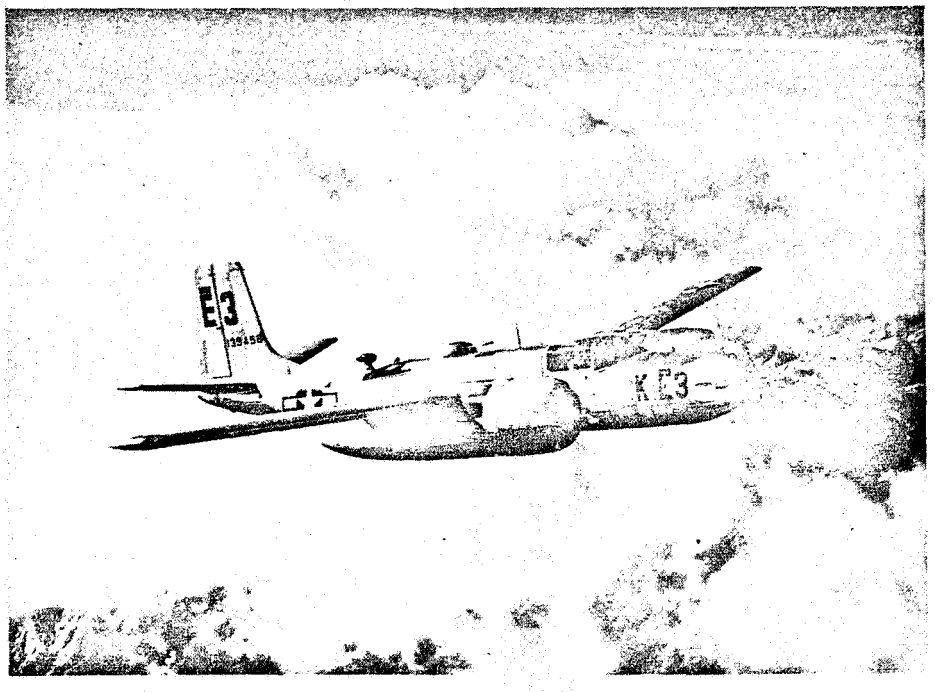

Figure 1-46. - The Douglas B-26 Invader is a tactical light bomber well suited for counter-guerrilla air action. The earliest models of the B-26 (then the A-26) saw service during the Battle of the Bulge in World War II. Extremely versatile, it has a speed of more than 350 miles per hour.

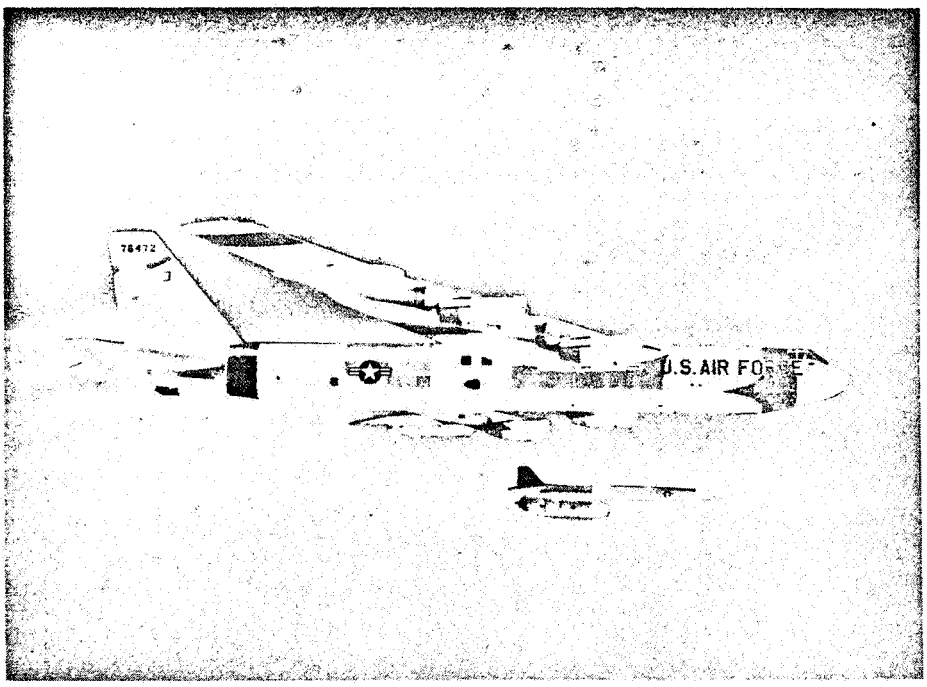

Figure 1-47. - Since 1955, the Boeing B-52 Stratofortress has been the Strategic Air Command's primary heavy bomber. It can carry two Hound Dog air-to-surface guided missiles. In 1957, three B-52's, using in-flight refueling, flew around the world, 24,325 miles, in 45 hours.

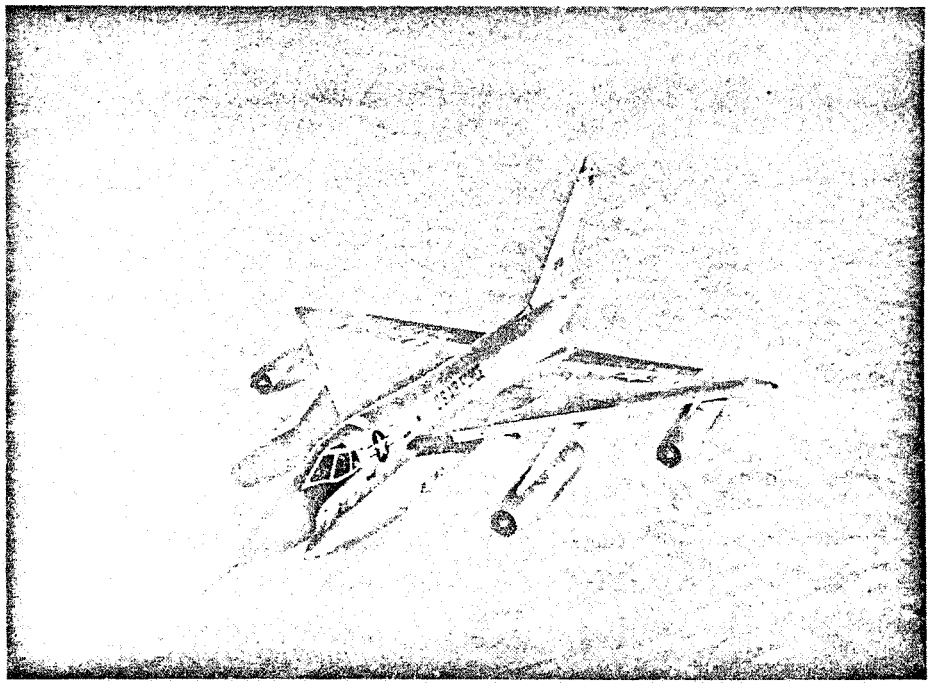

Figure 1-48. - The fastest bomber in the Strategic Air Command, the Convair B-58 Hustler has made the longest supersonic flight in history. In October 1963, a B-58 flew nonstop from Tokyo to London in 8 hours and 35 minutes, averaging 938 miles per hour. It carries its nuclear punch in a pod slung underneath.

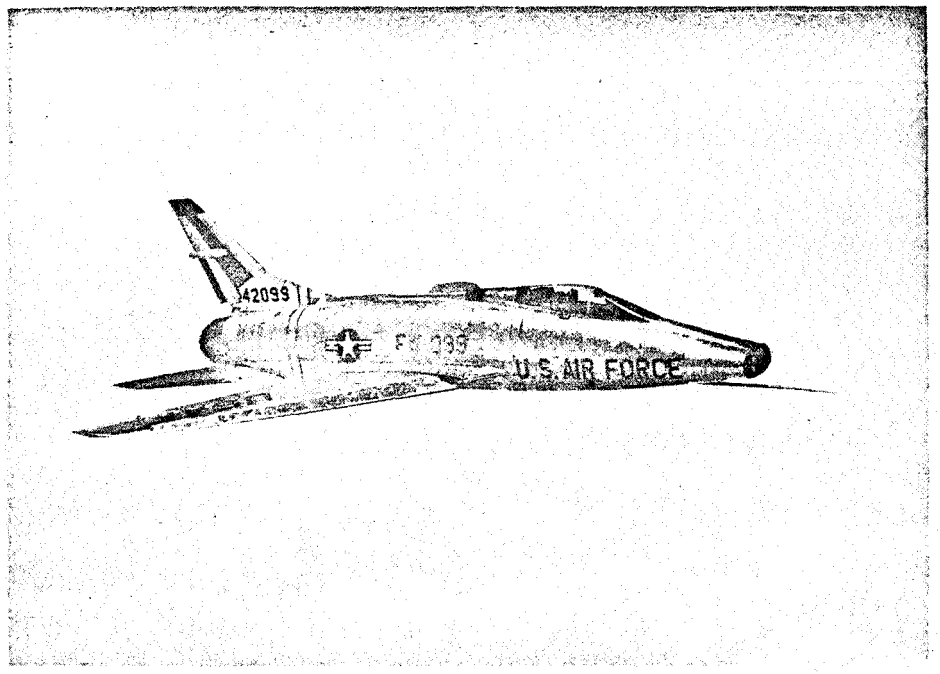

Figure 1-49. - The first USAF aircraft to fly supersonically in level flight, the North American F-100 Supersabre has been the workhorse of tactical air units. The first Supersabre was delivered to the Tactical Air Command in late 1954.

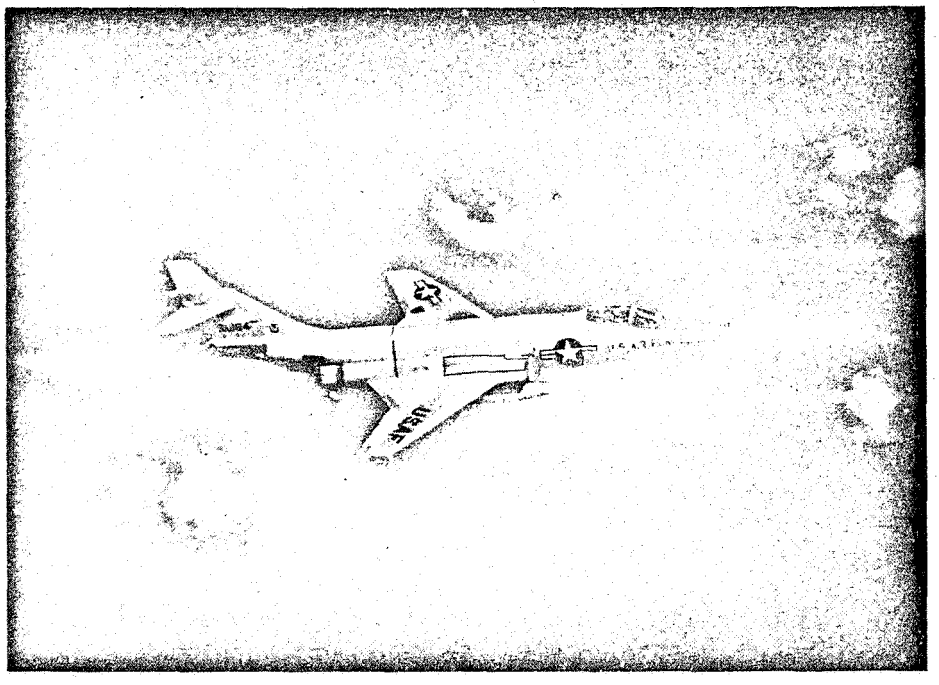

Figure 1-50. - The McDonnell RF-101 Voodoo was the USAF's first supersonic photoreconnaissance aircraft. From 45,000 feet, the Voodoo can photograph an area 217 miles long and 8 miles wide plus an area mosaic of 20,000 square miles.

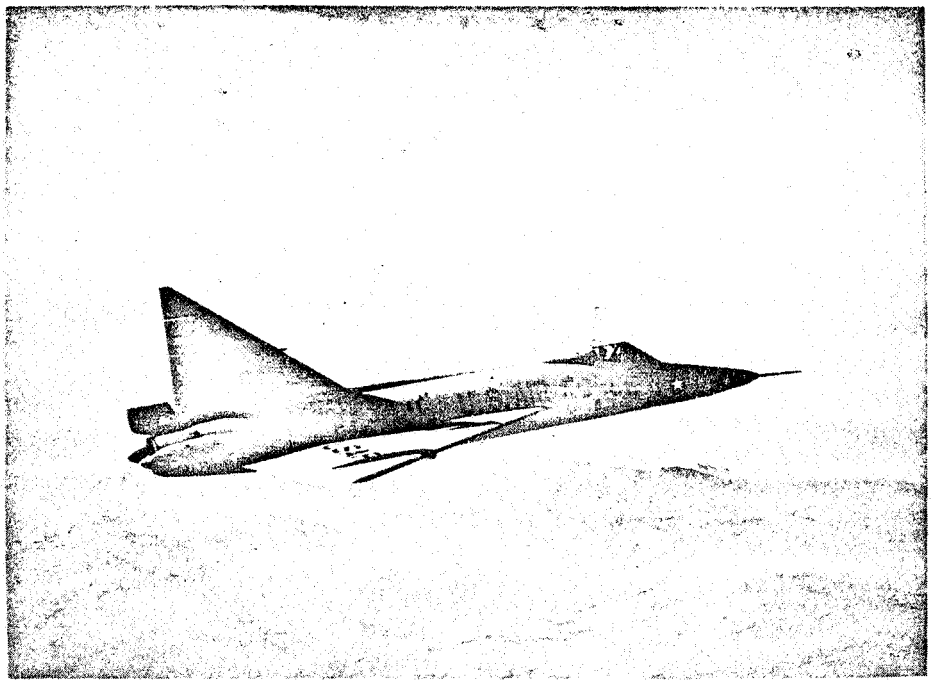

Figure 1-51. - The Convair F-102 Delta Dagger was the world's first supersonic all-weather jet interceptor. Flown first in 1953, it became operational in the Air Defense Command in 1956. It uses electronic "eyes" to locate hostile aircraft by day or night, in good or bad weather.

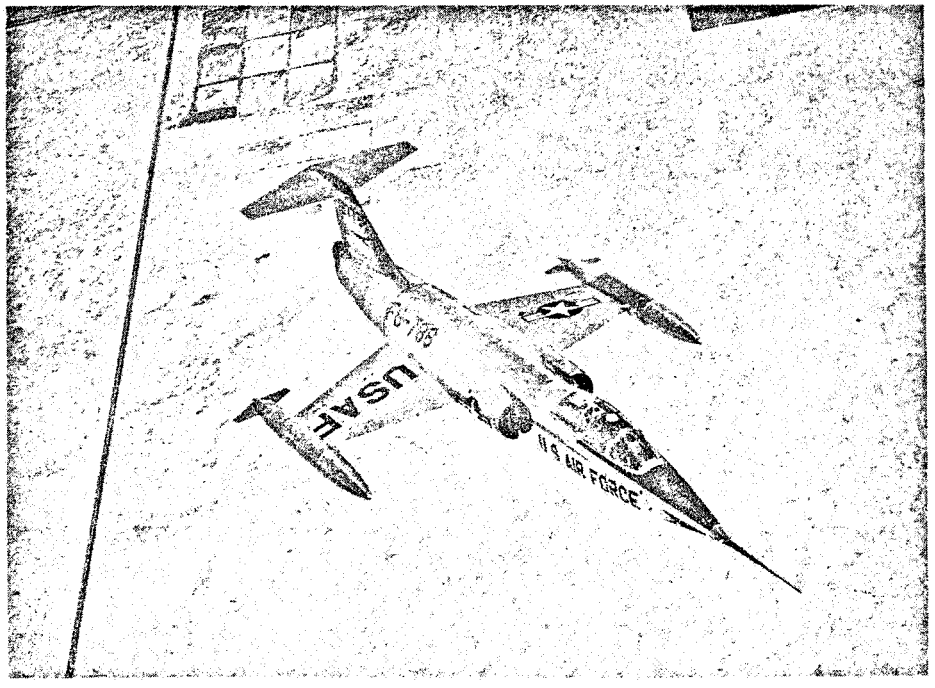

Figure 1-52. - The Lockheed F-104 Starfighter was designed as a supersonic air superiority fighter. It serves either as a tactical fighter or as a day-night interceptor.

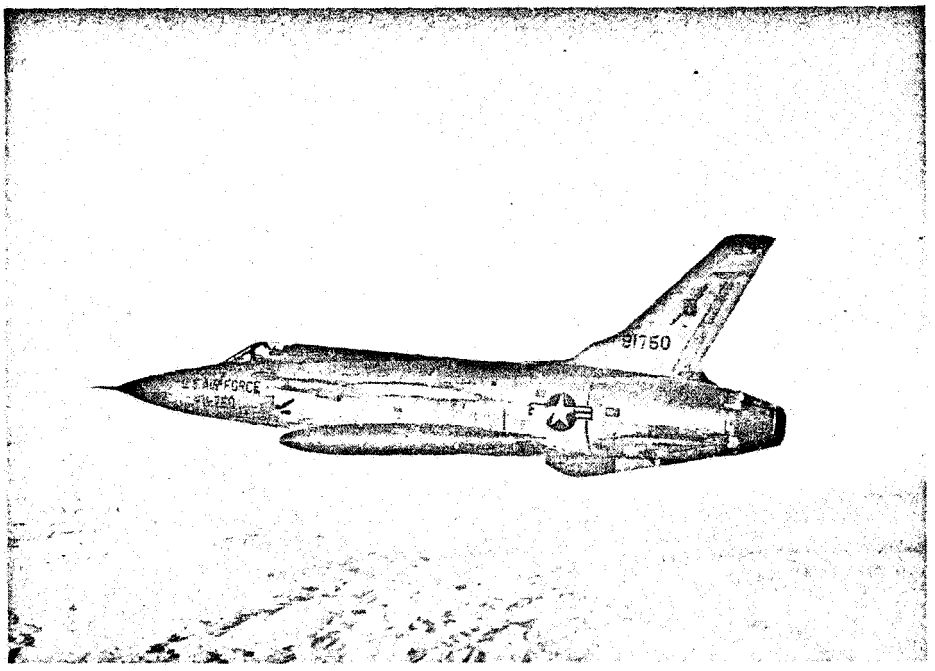

Figure 1-53. - The Republic F-105 Thunderchief is a 1400-mile-per-hour aircraft which can deliver 12,000 pounds of bombs. It also has a nuclear payload capability.

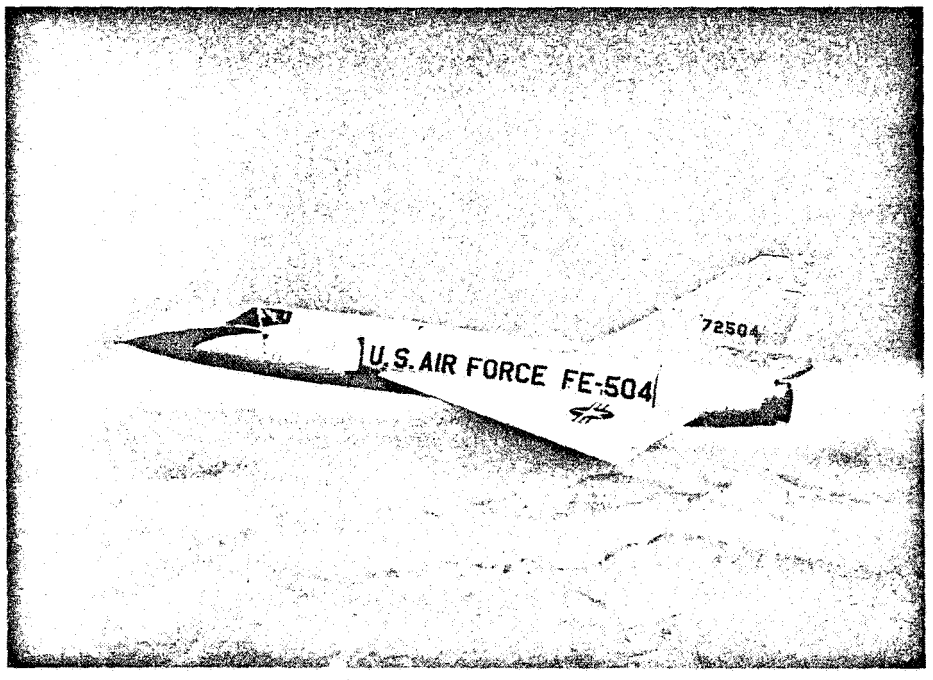

Figure 1-54. - The Convair F-106 Delta Dart's afterburning jet engine can push this all-weather interceptor to speeds of more than 1400 miles per hour and to altitudes above 50,000 feet.

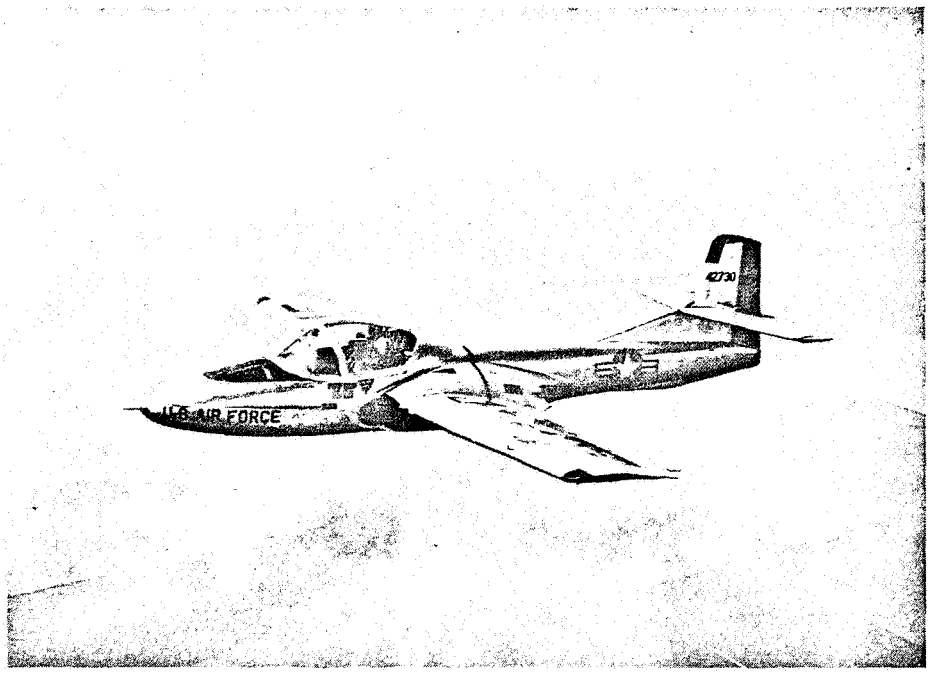

Figure 1-55. - The Cessna T-37 is a 350-mile-per-hour jet trainer.

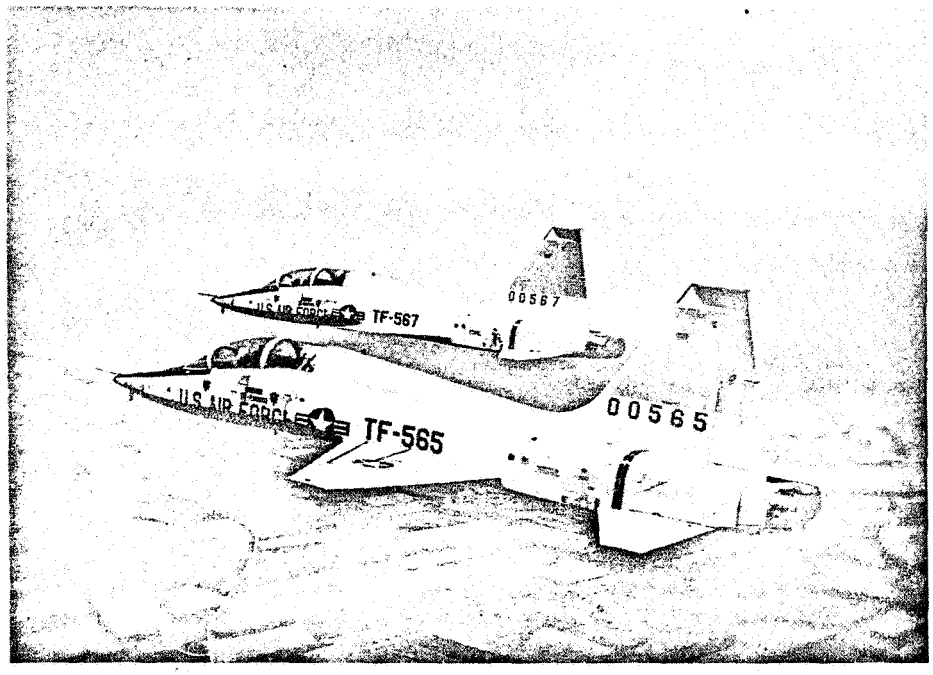

Figure 1-56. - The Northrop T-38 Talon is a basic, two-place, supersonic jet trainer capable of 850 miles per hour with a range beyond 1150 miles.

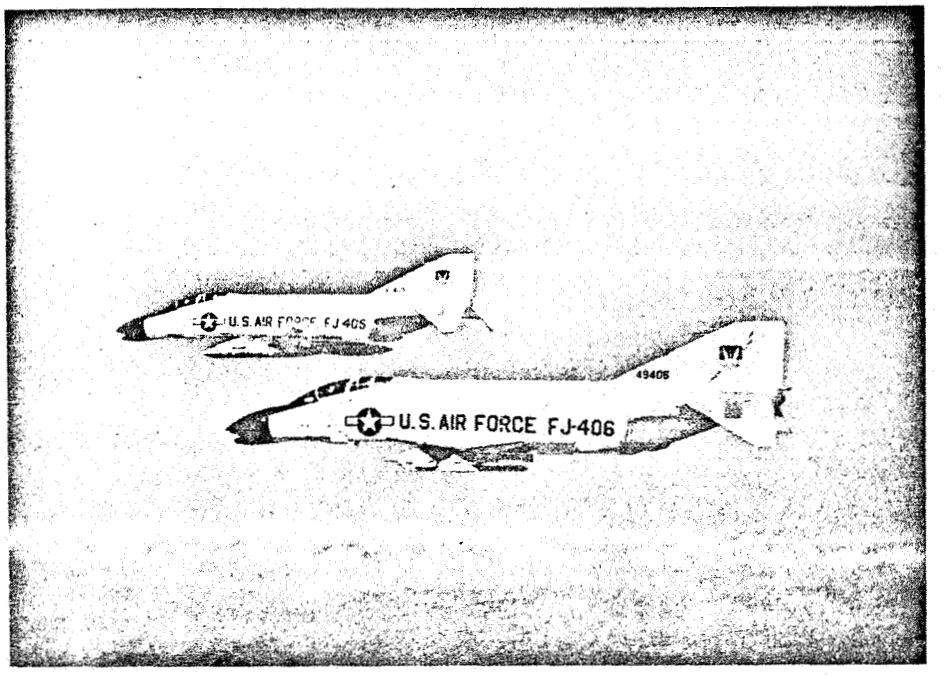

Figure 1-57. - McDonnell F-4C is capable of 1600 miles per hour. It has an all-weather bombing system for use in placing either conventional or nuclear bombs on target.

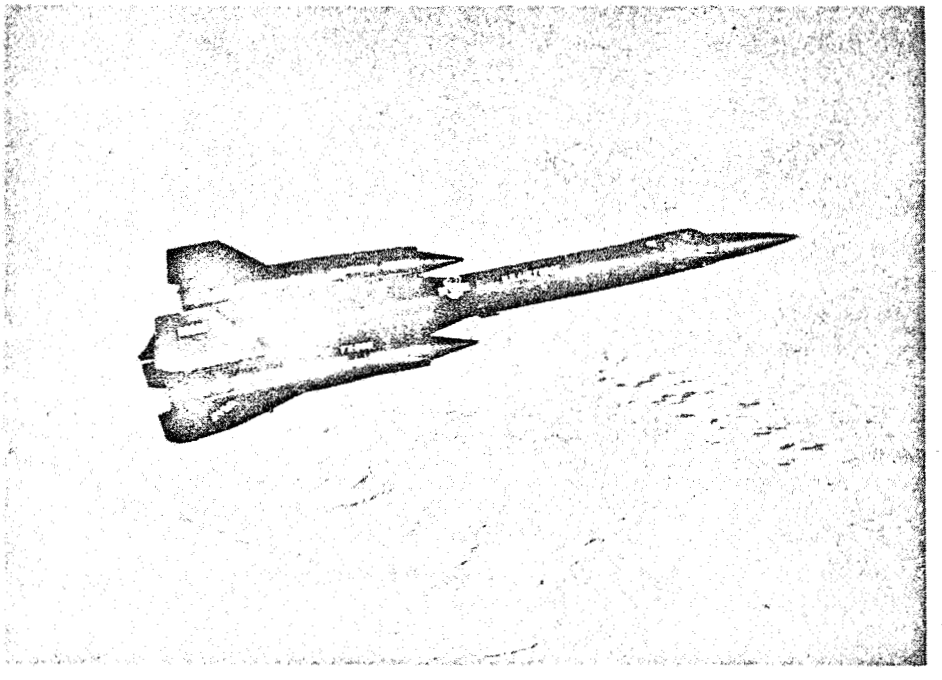

Figure 1-58. - The Lockheed YF-12A has been tested in sustained flight at more than 2000 miles per hour at altitudes above 70,000 feet.

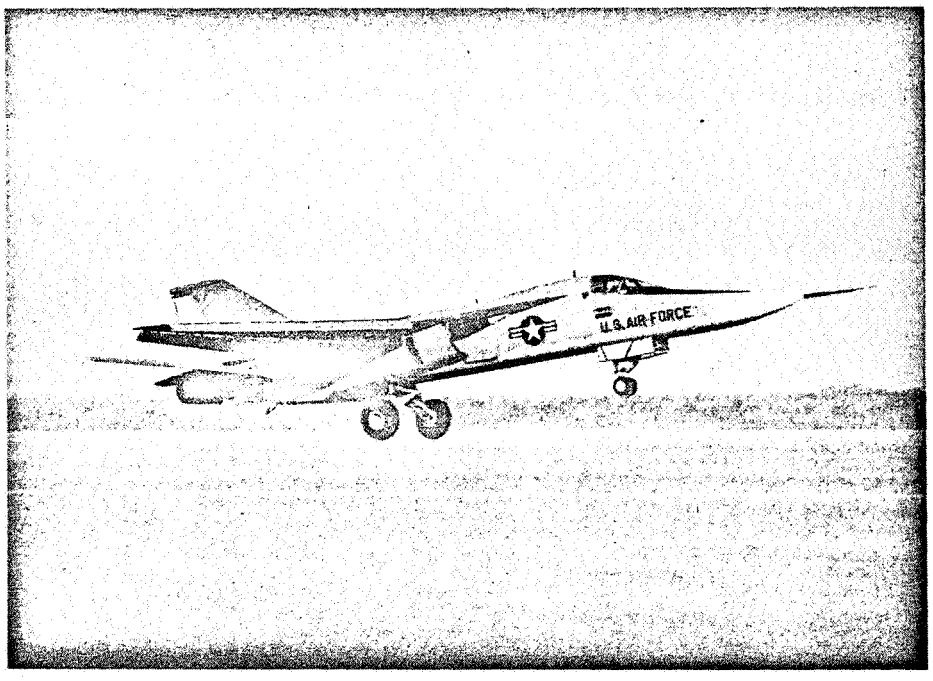

Figure 1-59. - The General Dynamics F-111A is a fighter with wings that can be extended or swept back sharply while in flight. A multipurpose aircraft, it can be used for counter-air, interdiction, close air support of ground forces, and reconnaissance missions.

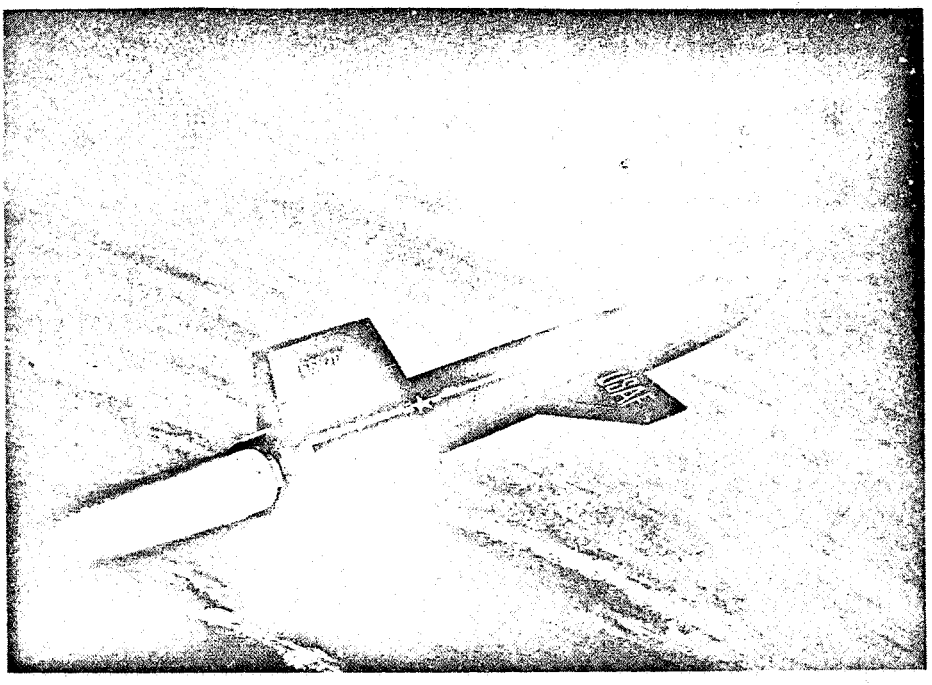

Figure 1-60. - More spacecraft than aircraft, the North American X-15 is the product of an experimental program jointly begun by the USAF, NASA, and the Navy to study aerodynamic, structural, and physical problems encountered during hypersonic flight and reentry.

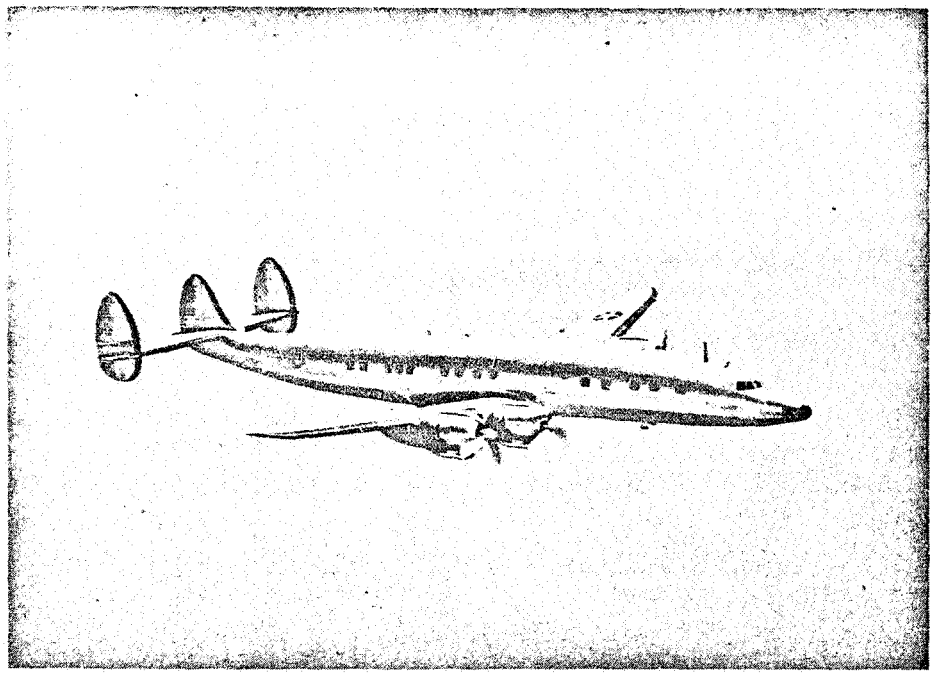

Figure 1-61. - The Lockheed C-121 Super Constellation is a four-engine transport with a cruising speed of about 300 miles per hour. It can fly more than 3500 miles nonstop.

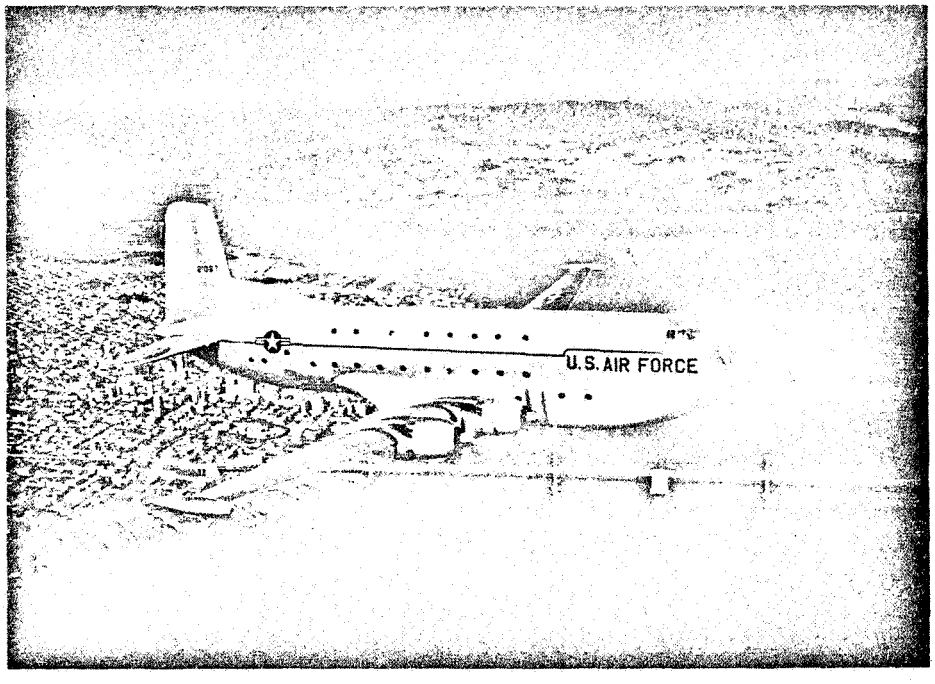

Figure 1-62. - The Douglas C-124 Globemaster can carry 50,000 pounds of cargo for more than 2300 miles.

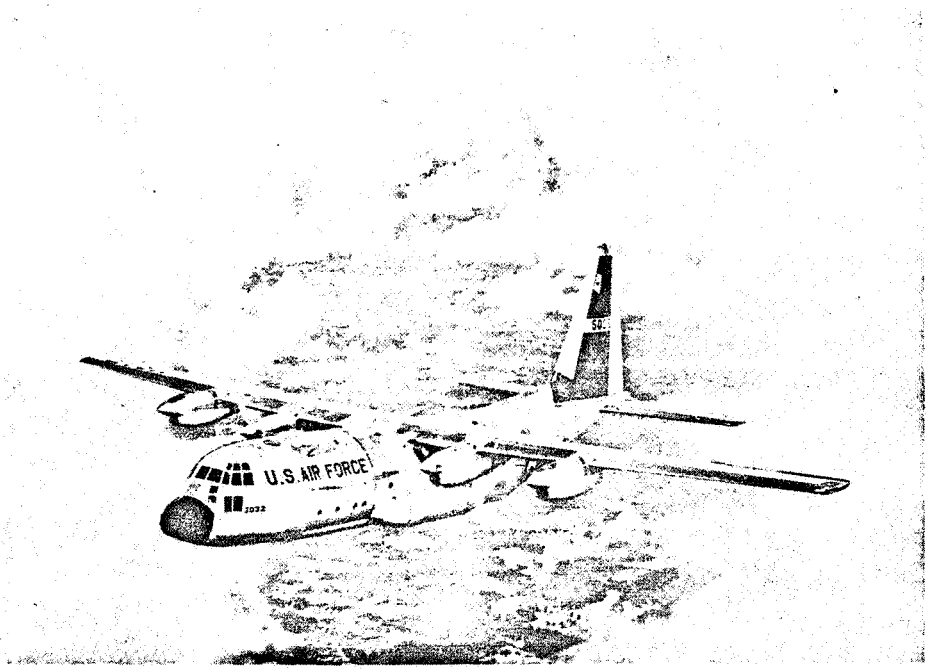

Figure 1-63. - The Lockheed C-130 Hercules has made the difficult military job of aerial resupply routine. It can transport 92 combat troops with full battle gear, 64 fully equipped paratroppers, or 74 litter patients and two medical attendants across the Atlantic nonstop.

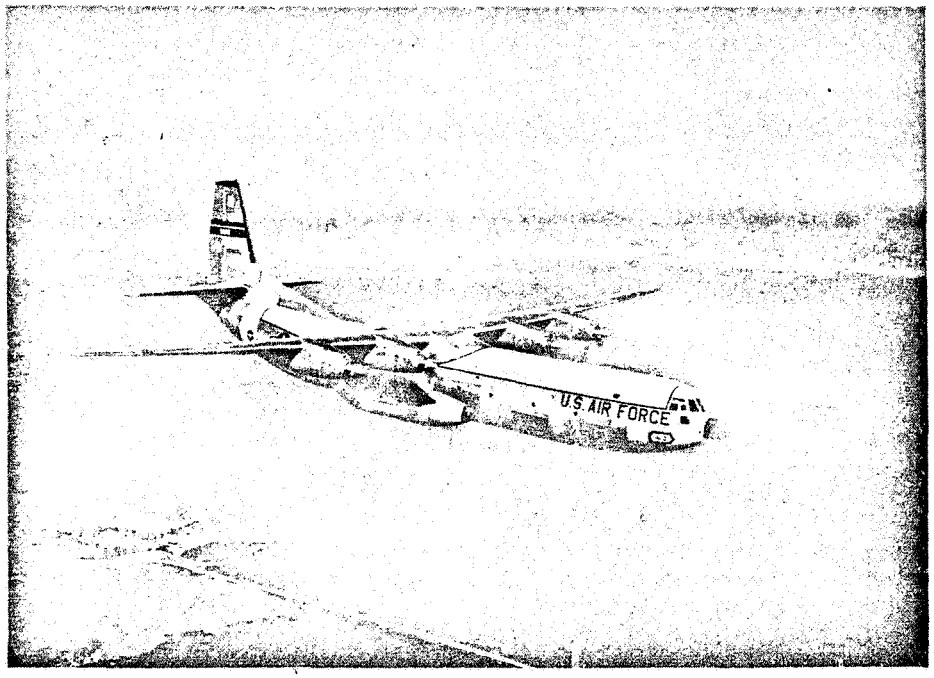

Figure 1-64. - The Douglas C-133 Cargomaster, largest turboprop transport in the USAF inventory, made its first flight in 1956. It can airlift our operational intercontinental ballistic missiles at speeds up to 300 miles per hour.

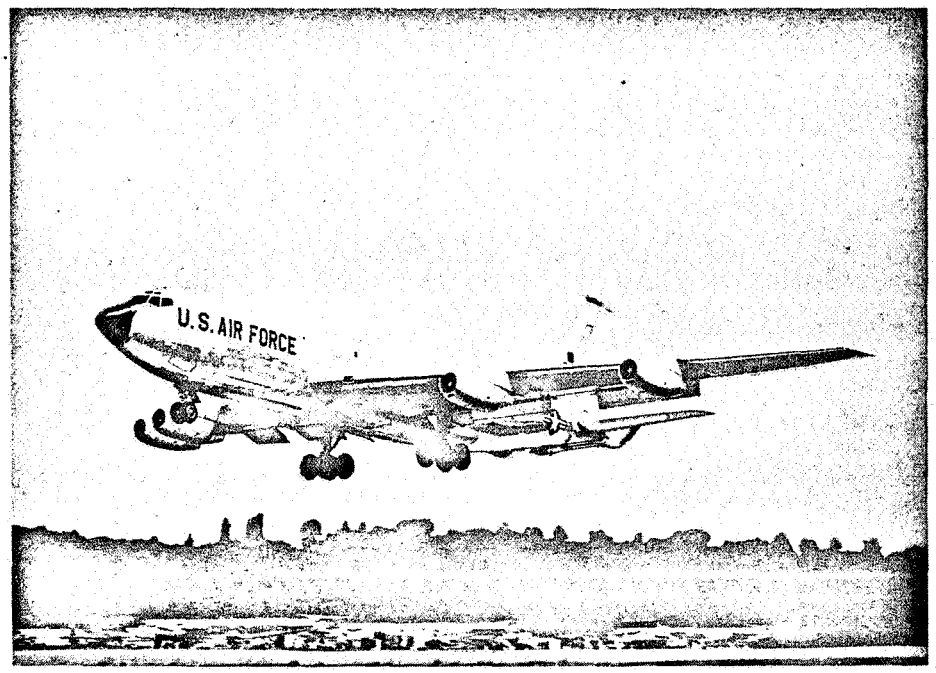

Figure 1-65. - The jet-powered Boeing KC-135 Stratotanker first entered the USAF inventory in 1957. It functions as a "flying filling station" for jet bombers and fighters.

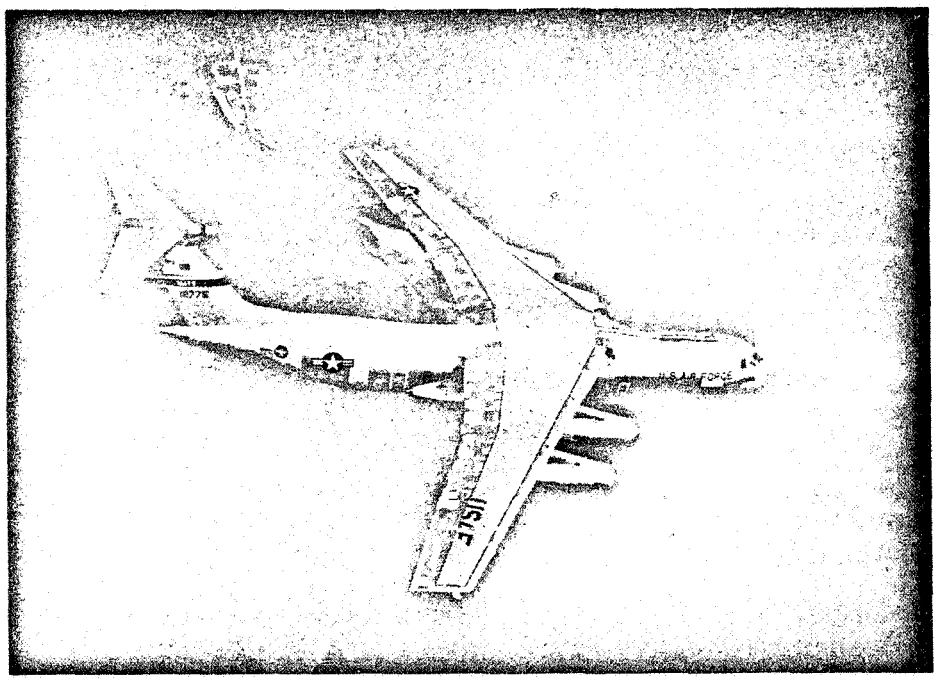

Figure 1-66. - Lockheed C-141A Starlifter has a 6547-cubic-foot cargo compartment with an automated cargo handling system.

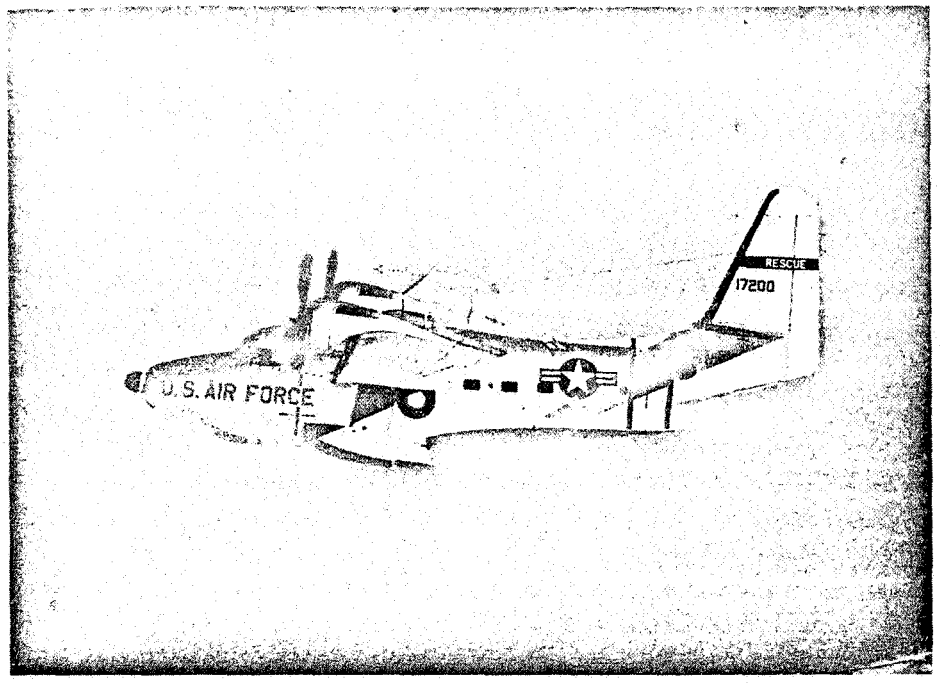

Figure 1-67. - The Grumman HU-16 Albatross is a twin-engined amphibian used by the Air Rescue Service. It first flew in 1947.

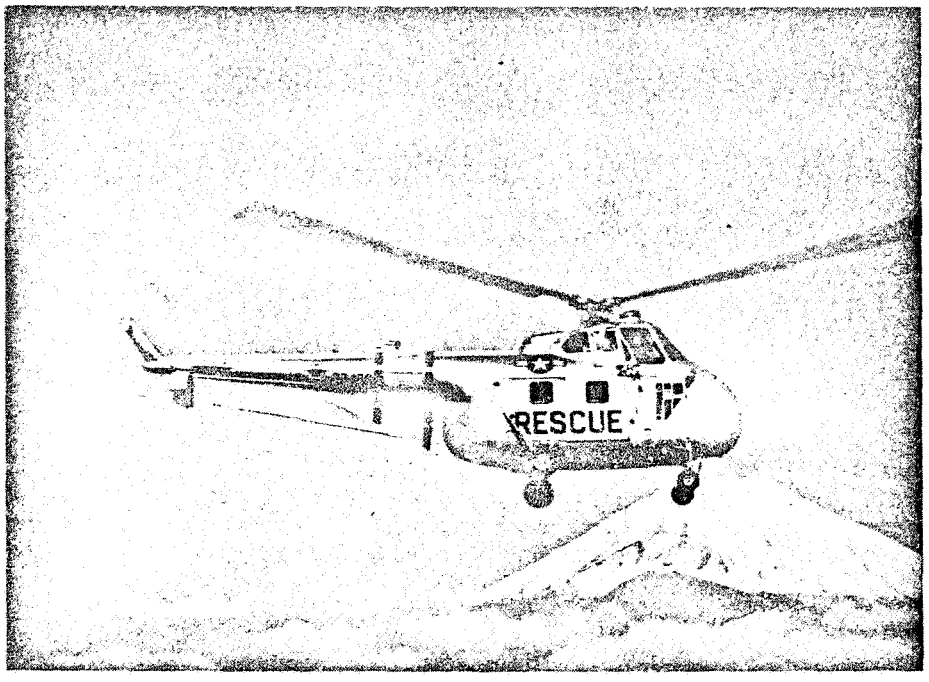

Figure 1-68. - The Sikorsky HH-19 Chickasaw is the original "whirlybird." It can fly at 70-mile-per-hour speeds over distances exceeding 300 miles.

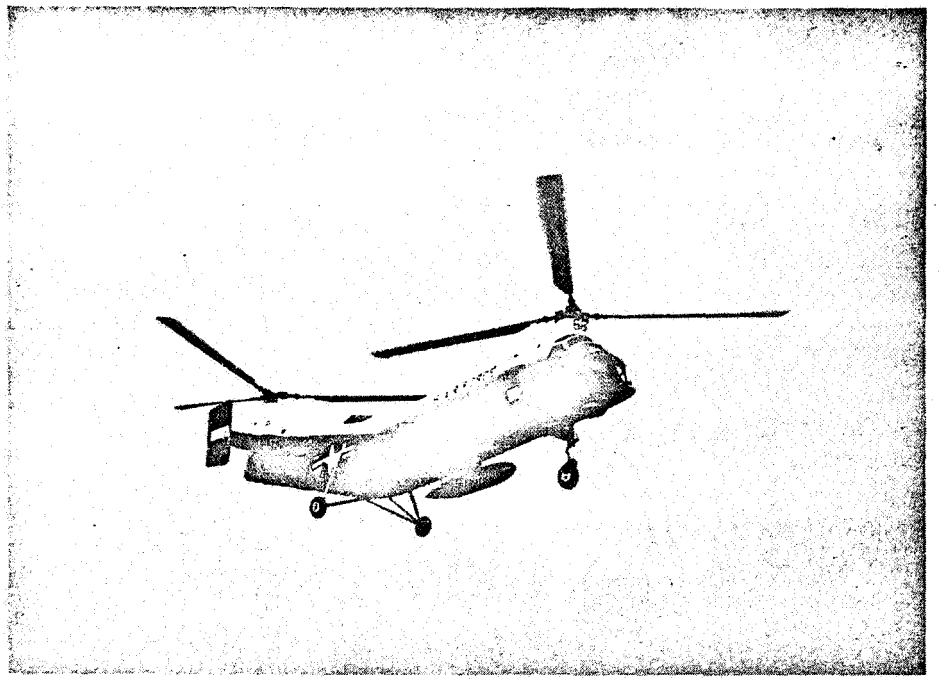

Figure 1-69. - The Vertol CH-21 Workhorse can carry 20 fully equipped troops. It also serves as a flying ambulance able to evacuate 12 litter patients and a medical attendant from locations inaccessible to conventional aircraft.

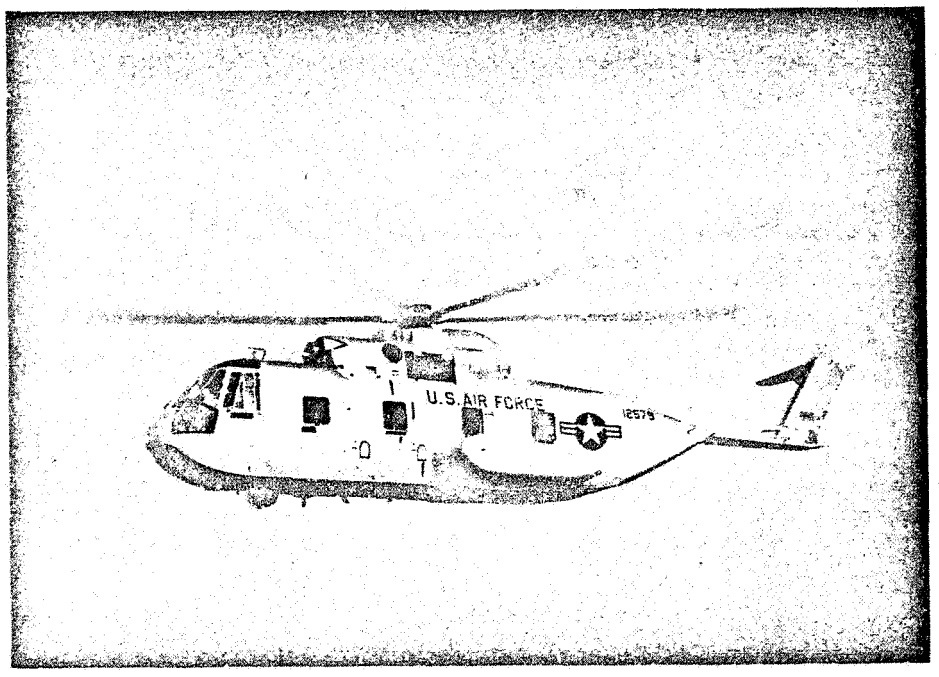

Figure 1-70. - The Sikorsky CH-3C is powered by twin turbine engines and has a hydraulically operated rear loading deck and a 5000 pound payload capacity. It is amphibious.

2. FLUID PROPERTIES PERTAINING TO AERODYNAMICS

Robert W. Graham*

Aeronautics is concerned with the flight of aircraft through the Earth's atmosphere. Aerodynamics, on the other hand, is a technical discipline dealing with the motion of air or any other gaseous fluid and with the forces acting on a body that is in motion relative to such a fluid. Thus, aerodynamics might include the study of air flowing through a jet engine, hot combustion gases flowing through the thrust chamber and nozzle of a rocket engine, air flowing over the outside surfaces of aircraft, and the reentry heating problems of spacecraft.

Some basic characteristics of airflow are discussed in this chapter. The relations of these flow characteristics to the lifting performance of a wing or the thrusting capability of an engine are explained in greater detail in subsequent chapters.

EARTH'S ATMOSPHERE

The discussion of the flow characteristics of air should begin with a brief explanation of the nature and composition of the Earth's atmosphere. Our atmosphere is composed principally of oxygen (21 percent by weight) and nitrogen (78 percent by weight). It also contains measurable quantities of 15 other elements or chemical compounds, including carbon dioxide, neon, hydrogen, methane, and ozone. The sum of all these constituents gives air a molecular weight of 28.964, which applies for the first 60 miles of altitude. This is generally within the range of altitude considered for flight applications. Above 60 miles, the composition of the atmosphere changes abruptly, as shown by the molecular weight distribution in figure 2-1.

Other properties of the atmosphere that are of interest include static temperature, static pressure, and density. These properties also vary with changing altitude. (The adjective "static" is used to modify "temperature" and "pressure" because these properties are measured with an instrument that is not moving with respect to the air.)

Figures 2-2 to 2-4 show the approximate distribution of the static temperature, static pressure, and density, up to an altitude of 200 miles. It is interesting to note that the

*Head, Experimental Section, Fundamental Heat Transfer Branch.

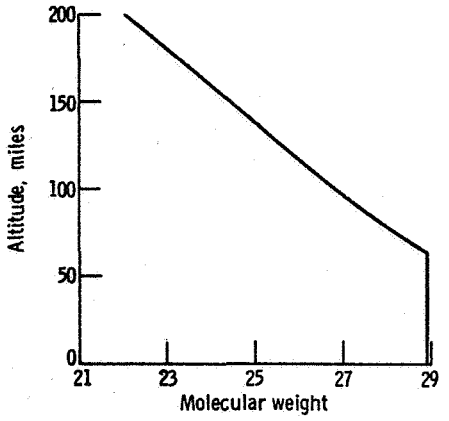

Figure 2-1. - Variation of molecular weight of air with altitude.

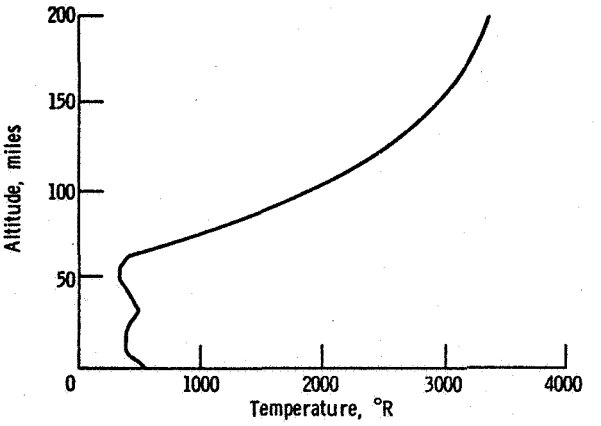

Figure 2-2. - Variation of atmospheric temperature with altitude.

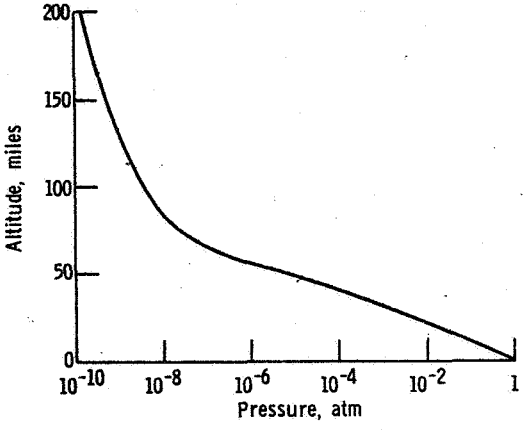

Figure 2-3. - Variation of atmospheric pressure with altitude.

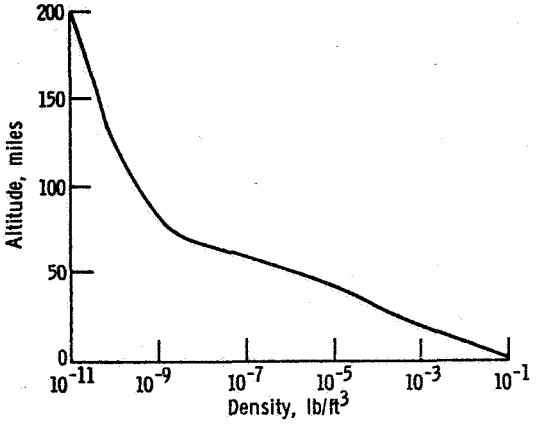

Figure 2-4. - Variation of atmospheric density with altitude.

temperature distribution goes through two reversals in trend before reaching a definite high-altitude trend of a rapidly increasing temperature.

Both density and pressure drop rapidly with increasing altitude in the lower altitudes (less than 60 miles). It appears that the drop in pressure has the greatest effect on the local density. (Density is also dependent upon temperature.)

Any consideration of a flight path over a range of altitude must take into account the rapid changes in the static properties of the atmosphere.

CHARACTERISTICS OF FLUIDS

Although air has its own properties as an atmosphere, it belongs to a general family of materials known as fluids. To be classed as a part of this family, air has to have cer-

tain generic traits of fluids. These traits are important in understanding flight and propulsion in the atmosphere.

Continuum Character

The first characteristic of a fluid is its continuum property. Although the spacing between atoms or molecules may be large, and there may be large voids in the fluid structure, the spacings are close enough so that a disturbance initiated at any point in the fluid is sensed by the neighboring molecules and can be transmitted far beyond the origin of the disturbance.

For instance, when water is being poured into a glass, all of the molecules sense the restraining effect of the glass. Likewise, all of the gas in a balloon senses the wall surrounding it. As a continuum, the fluid easily conforms to the shape of any vessel into which it is placed.

The continuum characteristic of a fluid enables it to transmit pressure and to conduct heat. Pressure and temperature result from the molecular-scale collisions of the fluid.

Compressibility

A simple fluid structure model may be thought of as a series of spheres connected by springlike forces. Such a model is sketched in figure 2-5. For liquids, the flexible bonds between the molecules are strong and stiff. As a result, the spacings between the molecules do not change appreciably. The fluid is said to be incompressible. Gases, on the other hand, have more flexible bonds, which enable the spacing to vary. This variable spacing is called compressibility. Compressibility is an important characteristic of air. For all gases, increased temperature spreads the spacing, and increased pressure tightens

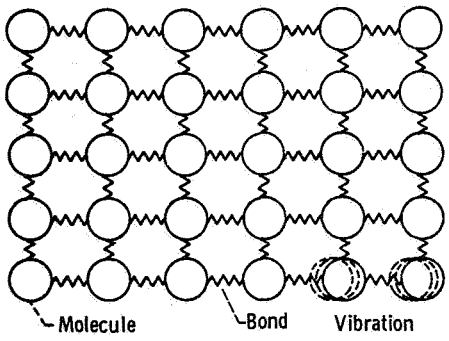

Figure 2-5. - Model of fluid structure.

the spacing. As is probably self-evident, the density of a gas is related to compressibility. For a given gas, the density is directly proportional to pressure and inversely proportional to temperature. This relation is known as the perfect gas law.

$$\rho = \frac{1}{R}\frac{P}{T}$$

where ρ is the density, P is the pressure, R is the gas constant, and T is the absolute temperature.

With a properly used general gas constant, the above simple equation applies to all gases over a broad range of conditions. If, from the preceding equation, the variation of the density of a gas for different temperatures and pressures is known, the compressibility of the gas can be computed. Suppose a gas is initially at density ρ_1 and by external compression it reaches a final density ρ_2. In this compression, the pressure has changed from P_1 to P_2. In equation form the compressibility is

$$\text{Compressibility} = \frac{\left(\dfrac{\text{Change in density}}{\text{Final density}}\right)}{\text{Change in pressure}} = \frac{\left(\dfrac{\rho_2 - \rho_1}{\rho_2}\right)}{P_2 - P_1}$$

Acoustic Velocity

It has been mentioned that a fluid has the capability of transmitting disturbances by its continuum property. The mechanism of transmission is a chain reaction of forced molecular collisions. These collisions produce small, local pressure changes in the fluid. The speed with which the disturbance travels depends on how quickly one molecule can reach an adjacent one. If the molecular spacing is large, the disturbed molecule has a relatively large distance to travel before transmitting its message. However, if the spacing is small, the message travels quickly. We learned earlier that the relative magnitude of the spacing determines the compressibility of the fluid. Thus, in highly compressible fluids (gases) these disturbances travel slower than in nearly incompressible fluids (liquids).

When a person is speaking, his voice is a disturbance to the air around him. The small pressure waves generated by the speaker's voice box are transmitted to the listener by the mechanism described previously. The velocity of transmission is the acoustic velocity. The acoustic velocity is the speed with which all small pressure disturbances travel in a fluid. The term "small" means that the disturbance is small compared with the average pressure of the fluid. Large disturbances, such as detonations, can travel

at velocities exceeding the acoustic velocity. In this case, the disturbance pressure may be many times greater than the original static pressure of the fluid. It has already been explained that the acoustic velocity is affected by the compressibility of the fluid. For small disturbances, the relation of the acoustic velocity to the compressibility and density of the fluid is given by the following equation:

$$\text{Acoustic velocity} \approx \sqrt{\frac{1}{(\text{Density})(\text{Compressibility})}}$$

Viscosity

In discussing the continuum characteristic of a fluid, it was mentioned that a fluid easily conforms to the shape of a surrounding vessel. In fact, this facility to conform to shapes is a distinguishing characteristic of fluids. While the molecules of a fluid arrange themselves easily, they do have a resistance to motion. This resistive force, which acts to prevent the motion of one fluid molecule on top of another, is called viscosity. Figure 2-6 is a diagram illustrating the viscous force between two fluid layers. An important extension of this concept occurs at the interface between a fluid and a solid wall. The resistive force between the fluid molecules and the wall material is known as viscous drag. Its magnitude depends on the fluid viscosity, the smoothness of the wall, and the velocity of the fluid motion (actually the square of the velocity). Viscous drag is very important in any fluid-flow situation, whether it is flow through an engine or flow over a wing.

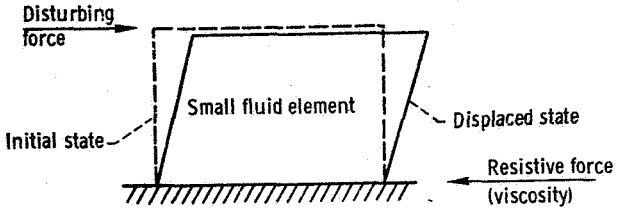

Figure 2-6. - Viscosity of a fluid.

CHARACTERISTICS OF FLUIDS IN MOTION

In the preceding discussion we dealt primarily with the static characteristics of fluids. The following discussion concerns the dynamic characteristics of fluids.

Total Pressure and Temperature

Static pressure and temperature result from random molecular motion. However, when a fluid is in motion, the molecules possess motion in the direction of flow as well as their inherent translational motion. Thus a temperature or pressure probe placed so that its sensing element is facing the flow will sense a higher temperature or pressure. Such measurements are referred to as total measurements, because the energy of directed fluid motion is included. They are indexes of the total energy possessed by a fluid in motion. The difference between total and static measurements is used to compute the velocity of fluid flow.

Mach Number

Mach number is the ratio of the fluid velocity to the local acoustic velocity of the fluid. Since acoustic velocity is inversely proportional to compressibility, Mach number is directly proportional to compressibility. This is the important meaning of Mach number to the aerodynamicist. A high Mach number means that in a flow process the density is subject to considerable change throughout the flow field.

Reynolds Number

Another important number in fluid mechanics is the Reynolds number. In this number, the momentum of the flow (product of density ρ times velocity V) is compared with the coefficient of viscosity μ.

$$Re = \frac{\rho V}{\mu} \cdot d$$

The Reynolds number Re is made dimensionless by the inclusion of a length dimension d. This length dimension can be a characteristic length, such as the flow-path length, the chord of a wing, or the diameter of a duct.

Reynolds number tells whether the momentum or viscous forces dominate the flow. A low Reynolds number signifies that the viscous forces are dominant; a high Reynolds number denotes that the momentum controls the flow and the fluid viscosity is less important.

Perhaps one of the most significant uses of Reynolds number is in the discrimination between laminar and turbulent flows, which are discussed in the following section.

Laminar and Turbulent Flows

At low Reynolds numbers, where viscosity is dominating, the flow of fluids can be described as layers, or lamina, of steady fluid streams which do not appear to mix as the flow progresses down the channel. The flow has the appearance of fluid fibers bundled in the channel. This type of flow is called laminar flow.

At a higher Reynolds number, the flow pattern changes into turbulent flow. The identifiable fluid layers, or fluid fibers, of laminar flow no longer exist. Instead, there is considerable mixing in the flow, through the action of eddies or vortexes. These eddies give the flow a fluctuating, or nonsteady, characteristic, which can be measured. Figure 2-7

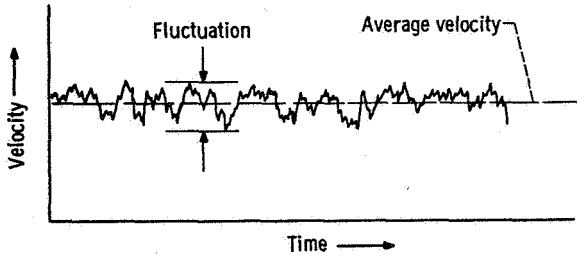

Figure 2-7. - Turbulent-flow velocity trace.

represents an actual velocity measurement of a turbulent flow. A sensitive instrument called a hot wire was placed at a fixed position in a flow channel and the flow was recorded over a time interval. Note from the figure that there is an average velocity, but the instantaneous level fluctuates around this average.

Turbulent flow is the most frequently encountered type in practical applications of flight and propulsion, and it is much more difficult to analyze than laminar flow.

Boundary Layer

In discussing the viscosity of fluids, it was mentioned that a very significant viscous effect occurs at the interface between a solid wall and a fluid. In fact, this frictional effect represents the chief resistance that the flow experiences. This friction is the drag of the airplane or the pressure loss in a pipe or channel.

Most of these frictional effects are absorbed by the fluid in a layer near the wall. The viscous effects in this region can be observed by measuring the local velocity distribution at various positions (distances) away from the wall. A velocity profile, such as shown in figure 2-8, results from such measurements. Note that the velocity decays

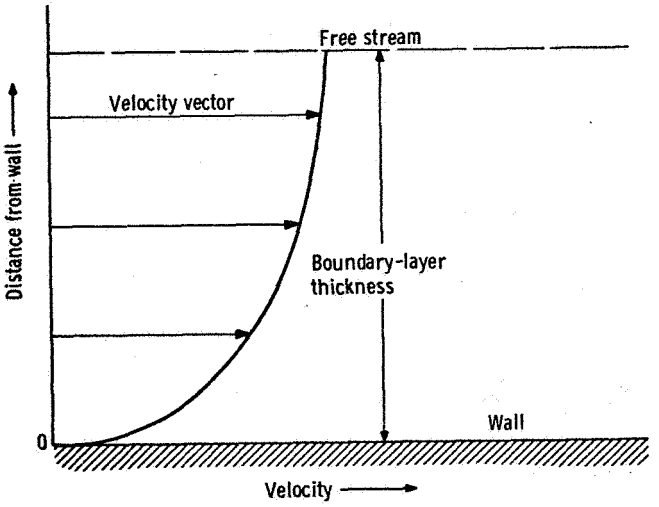

Figure 2-8. - Boundary-layer velocity profile.

to zero velocity at the wall. The thickness over which most of this velocity decay occurs is called a boundary layer. It represents the fluid thickness wherein the viscous qualities of the fluid are dominant. In most analytical procedures the boundary layer and the free stream (flow region outside the boundary layer) are treated separately. Different assumptions are applied in the analyses for each region. The presence of friction makes the boundary layer a very complicated region to analyze.

The boundary layer is also important in studies of heat transfer between the fluid and the wall. In aerodynamic heating, the fluid friction of the boundary layer is converted to heat at the wall. For instance, if all the kinetic energy of relative fluid motion is converted to heat within the boundary layer, an airplane flying at Mach 2 (at 100 000 ft altitude) may experience surface temperatures exceeding 300° F. At higher Mach numbers the heating can be very severe. Reentry vehicles from space missions develop surface temperatures which can vaporize metal. Consequently, cooling techniques, such as the use of ablative shields, are required to protect the vehicle.

BIBLIOGRAPHY

Anon.: U.S. Standard Atmosphere, 1962. NASA, USAF, and U.S. Weather Bureau, Dec. 1962.

Cowling, Thomas G.: Molecules in Motion. Harper & Brothers, 1960.

Zucrow, Maurice J.: Principles of Jet Propulsion and Gas Turbines. John Wiley & Sons, Inc., 1948.

3. DRAG

Richard J. Weber*

When an object moves through the air, the air molecules are moved from their normal positions. When the molecules are disturbed, according to Newton's Third Law of Motion, they in turn react back on the object and exert aerodynamic forces. Sometimes there is a force perpendicular to the direction of motion; this is called lift and is discussed in chapter 4. Invariably, there is an additional force that acts parallel, but opposite, to the direction of motion; this retarding force is called drag.

Since the drag continually tends to slow down an airplane, a forward thrust must be provided by the engine(s) in order to keep flying (fig. 3-1(a)). The larger the thrust that is needed, the more fuel that is consumed. Calculating the drag of an airplane is, therefore, extremely important, since it affects how big the engines must be and how much fuel must be consumed.

Drag is not always undesirable (fig. 3-1(b)). In fact, the same viscous effects which cause friction drag also make it possible to generate lift on a wing. That is, a perfect nonviscous fluid would not cling to or follow the contour of the wing surface. This clinging is called the Coanda effect and is necessary to obtain the flow deflection that results in lift. Hence, the existence of drag is essential to the production of lift. The relation of this Coanda effect to lift is discussed further in chapter 4.

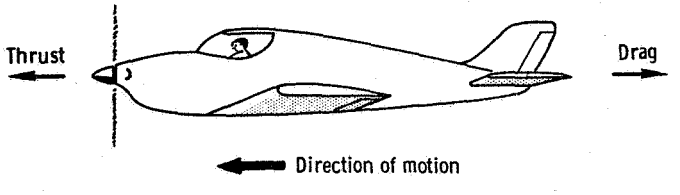

(a) Detrimental drag.

Figure 3-1. - Effects of drag.

*Chief, Mission Analysis Branch.

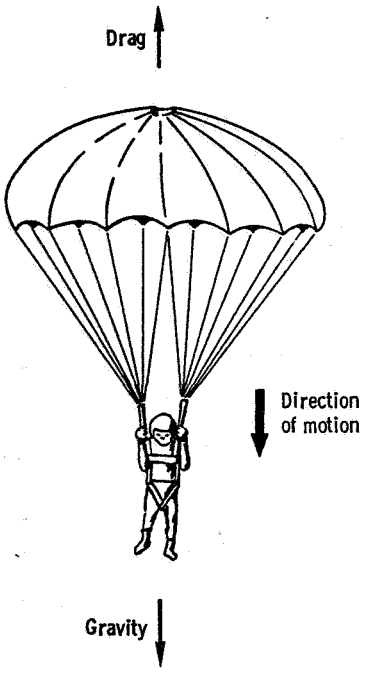

(b) Beneficial drag.

Figure 3-1. - Concluded.

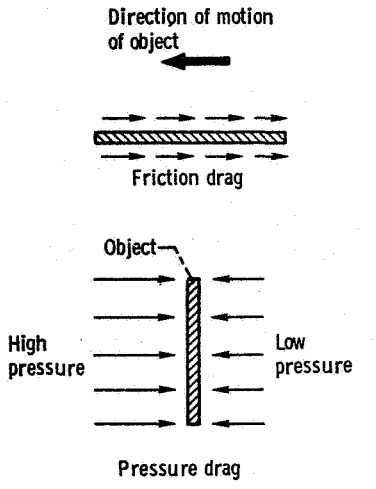

Figure 3-2. - Two kinds of drag on a moving object in a fluid.

It is convenient to classify drag in two different categories - friction drag and pressure drag - depending on how the drag force is exerted on the object (fig. 3-2). Friction drag is due to the stickiness of fluids. Even a smooth, flat plate tends to drag along fluid molecules, and this causes a retarding force. Pressure drag is caused by unequal pushing of the air on the front and back of an object. The pressure drag may be further classified as induced drag, which is related to the amount of lift, and wake drag, which is independent of lift. (Another way of classifying drag is in terms of whether or not it depends on lift. In this system of classification drag due to lift is the induced drag, and profile (or parasite) drag is the sum of friction and wake drags.)

Since induced drag is discussed in chapter 4, only friction and wake drags are discussed herein.

FRICTION DRAG

As an object moves through the atmosphere, molecules of air tend to stick to the surface and be dragged along. To accelerate these molecules, a force is required, and the reaction force on the object is felt as friction drag. The sticking tendency of a fluid is

measured by its viscosity, as already mentioned in chapter 2. Air is not as viscous as liquids such as molasses, but friction drag is, nevertheless, the main type of drag for subsonic airplanes.

Friction drag of a gas is quite different from the solid friction to which we are more accustomed. When an automobile tire pushes against the ground, for example, solid friction produces a force that drives the car. The force is generated locally at the junction between the tire and the ground. It is fairly accurate to consider the force as due to the interlocking of microscopically small bumps on the two surfaces. This is true even if the tire is spinning or skidding relative to the ground, except then the little bumps tend to tear away from the main material.

However, when a solid object is placed in a gas stream, the gaseous friction generates a force not just at the surface of the object but over a finite distance from the surface, called the boundary layer (see chapter 2). At the outer edge of this layer, the gas molecules move at the full velocity of the gas stream; at the inner edge of the layer, the molecules hardly move at all (relative to the object). This gradual change in velocity through the layer causes a sliding or shearing motion that results in a drag force. The boundary layer may be likened to a deck of cards on a table. If the top card is slowly pushed sideways, it slides and moves the next card a little less, which, in turn, moves the next card even less, and so forth, until the bottom card is reached, which sticks to the table.

The magnitude of the friction drag depends on the physical properties of the gas (density and viscosity), the velocity of the gas stream (or of the object moving through the gas), and the surface, or "wetted," area of the object. For laminar boundary layers, which are expected at low values of the Reynolds number (see chapter 2), the friction drag is proportional to the velocity raised to the 1.5 power. For example, doubling the velocity increases the laminar drag by $2^{1.5}$, or 2.83 times.

As the velocity (and hence the Reynolds number) is increased more and more, the flow eventually becomes turbulent, and the friction drag jumps to a value perhaps 4 times higher. In this region the drag is roughly proportional to the velocity squared. Doubling the velocity now increases this new, high drag by 2^2, or 4 times.

Obviously, the friction drag on an airplane can be reduced considerably if the laminar boundary layer can be prevented from becoming turbulent.

PRESSURE DRAG

When any object is standing still in the atmosphere, there is a pressure force (equal to 14.7 lb/in.^{2} at sea level) pushing on it. Because the pressure is the same on all sides of the object, there is no net force in any particular direction. If the object is moving, however, pressure differences can develop.

Theoretically, in subsonic flight through an ideal nonviscous fluid, these pressure differences are nonexistent; that is, if the pressure gets higher on the front (or upstream) side of the object, it should get just as high on the back (or downstream) side. Thus, the net pressure force would be zero. This situation should apply to all objects, regardless of shape. Physically it requires that the flow of air, which divides in front of the object to go around it, should smoothly follow the shape of the object and join together again at the back of the object. In so doing, the pressure would be high at the front, decrease to a low value at the side, and rise again to the same high value at the back.

In actuality this smooth joining together at the back of the object does not happen; the reason for this is friction. The air in the boundary layer loses energy because of friction and cannot fight its way back to the same high pressure on the back side (just as a roller coaster cannot roll down one hill and then coast up to the same height on the next hill). As a result, a region of low-pressure "dead" air forms behind the object. The main flow of air separates from the object in order to pass around this "dead" space.

The ideal and the actual situations are illustrated in figure 3-3 for the case of a circular cylinder moving from right to left. The figure shows the direction of the air particles as they stream past the cylinder and graphs of the pressures exerted on the surface of the cylinder. In the ideal case the air fills in behind the cylinder just as smoothly as it divided in front. The corresponding pressure distribution is just as smooth. The pressure force is proportional to the area under the curve and is the same on the back side as on the front. No net force is generated.

In the actual case, the flow separates from the back of the cylinder, and the pressure is lower than it should be. The graph area for the front side is higher than for the back, so that there is a net force on the front of the cylinder pushing it backward, or downstream. This force is called the pressure drag and is added to the friction drag described

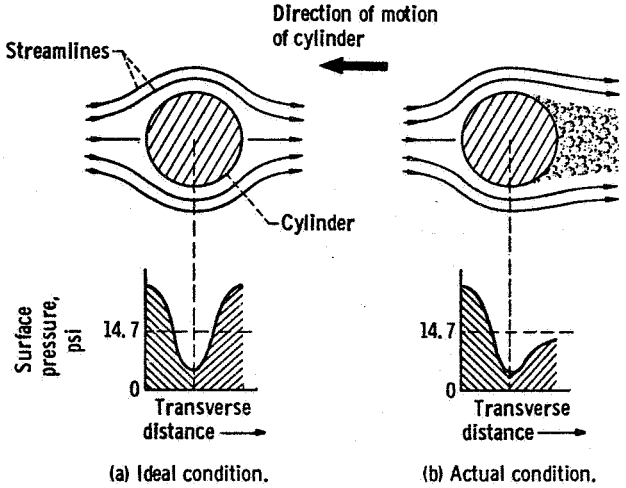

Figure 3-3. - Pressure drag on a circular cylinder.

earlier. (In subsonic flow, the pressure drag is really caused by the friction drag. In supersonic flow, however, the pressure drag becomes even larger and is caused by shock waves. This is discussed in chapter 11.)

For blunt shapes, the pressure drag can be very high. For example, the pressure drag on a cylinder is between 30 and 120 times (depending on Reynolds number) as high as the direct friction drag. Therefore, streamlining is an important consideration in aircraft design.

INTERFERENCE DRAG

Up to this point, we have discussed the drag of simple shapes (spheres, cylinders, flat plates, etc.) with nothing else near them. A complete airplane, of course, is not one of these simple shapes. However, in order to simplify the design and analysis of a new type of airplane, it is convenient to consider the airplane as being composed of many smaller, simpler shapes that are put together. Experimental and theoretical data have been accumulated on the drag of common simple shapes, such as wings or streamlined fuselages. The drag of the complete airplane can then be estimated by adding up the drags of the individual pieces. When this is done, it is usually discovered that the actual drag of the airplane is greater than the sum of the individual drags. This extra increment of drag is called interference drag. It exists because the individual drags are measured for isolated components. However, when the components are combined in an airplane, each one sets up disturbances in the airstream that affect the flow over the other components. These disturbances usually (not always) result in an increase in total drag.

As an example, suppose a small step is to be put on the side of a fighter airplane to help the pilot climb into the cockpit. When the step is tested by itself in a wind tunnel, it has a drag of 1 pound. However, if the step is installed on the plane in the corner between the wing and the fuselage, its drag is 6 pounds. The drag due to intereference in this case is 5 pounds.

COMPRESSIBILITY DRAG

The preceding discussion is based on flight at fairly slow speeds (no more than a few hundred miles per hour). At these speeds the air can be considered to be incompressible; that is, the changes in velocity and pressure of the air flowing around the airplane do not change the density of the air. At higher speeds, density changes start to become important. The primary effects arise at flight speeds approaching the speed of sound. The reason for this is that as the airstream flows around the outside of the airplane, it is

forced to travel a longer, more circuitous path than if the airplane were not present. The longer path requires the air to move momentarily at a higher velocity than the flight speed, or the free-stream velocity. (The free stream is that stream of air flowing past the aircraft which is not affected by the aircraft.) Thus, as the flight speed approaches the speed of sound, the velocity of the airflow over the surfaces of the aircraft may become supersonic and form shock waves, which cause major increases in drag. This sudden drag rise is the reason why most airplanes (such as current passenger planes) do not fly faster than about 550 miles per hour. As more powerful jet engines are developed, however, it becomes more feasible to fly faster despite the high drag. Also, different shapes can be used to partly avoid the drag rise. As a result, military airplanes can now fly supersonically, and even commercial supersonic transports are being developed. The drag rise due to the presence of shock waves (i.e., compressibility drag) is a different type of pressure drag. Its characteristics are discussed in chapter 11.

METHODS OF DRAG REDUCTION

The following discussion concerns some of the various methods that can be used to

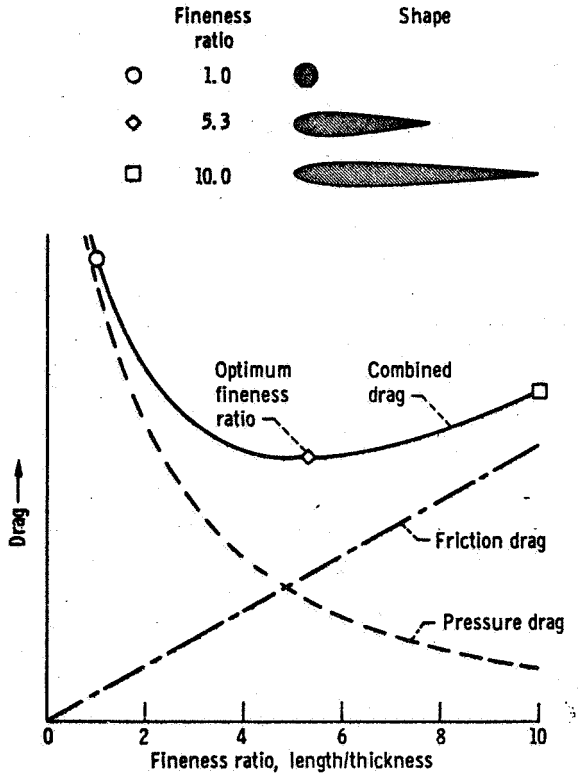

Figure 3-4. - Effect of streamlining.

reduce drag. It should be noted that at subsonic flight speeds all drag-reduction methods involve some form of boundary-layer control.

Because the pressure drag on a blunt shape can be intolerably high, it is necessary to shape the various parts of an airplane in the proper fashion to minimize drag. This is called streamlining, and its purpose is to enable the air to flow as smoothly as possible around the various parts of the airplane without separating on the back side. Generally this requires the use of well-rounded edges and long, slender shapes. (The relation between shape and airflow is discussed in more detail in chapter 4.)

The effectiveness of streamlining is shown in figure 3-4. For a constant thickness, as the length is increased, the pressure drag decreases. The process cannot be carried to extremes, however. More length increases the surface area of the object, which increases the friction drag. When the two drags are added together, it is found that there is an optimum fineness ratio (length divided by thickness) that yields minimum combined drag.

We might also include in the term "streamlining" the avoidance of abrupt bumps and roughness (such as protruding rivet heads). Each little rough spot contributes a bit of pressure drag. Since there could be many rivets and other protrusions on an airplane, the total increase in drag would be appreciable if roughness were not controlled. Even dirt and mud can cause noticeable penalties. The following table shows how small roughness affected the measured profile drag on one particular wing:

Surface condition	Relative drag
Smooth and polished	1.00
Common service condition (with rivets, joints, camouflage paint)	1.32
Service condition with thin mud	1.94
Service condition with heavy mud	2.78

Another reason for streamlining is that it is sometimes possible to control the pressure distribution around an object in such a fashion that the boundary layer is prevented or delayed from becoming turbulent. The corresponding reduction in friction drag can be very worthwhile. (Chapter 1 mentioned the application of this technique to the wings of the P-51 "Mustang" airplane of World War II.)

A method of reducing friction drag that is now being tried on some airplanes is the removal of some of the boundary layer before it can become turbulent. Figure 3-5 shows how this works. The top of the figure shows the cross section of an ordinary wing. The boundary layer always starts out thin and laminar. However, as distance from the leading

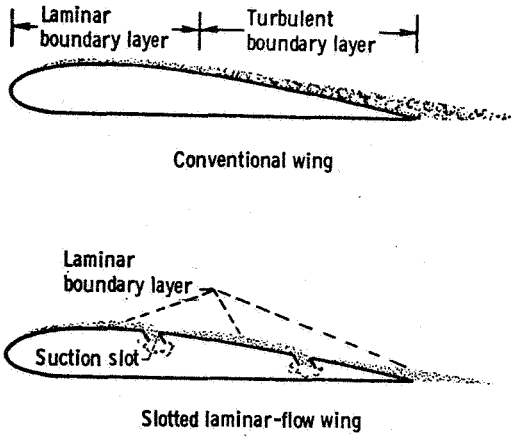

Figure 3-5. - Boundary-layer control by means of suction slots.

edge increases, the boundary layer gradually thickens. At some thickness the layer becomes unstable and the smooth flow breaks down and becomes turbulent. (A more general measure of boundary layer was introduced in chapter 2 in terms of the Reynolds number, which varies directly with distance.) To prevent this transition from laminar to turbulent flow, suction slots may be placed in the wings, as shown in the lower part of figure 3-5. The thick boundary layer is sucked away through the slot by means of a pump, so that the flow behind the slot starts all over again as if it were at the front of the wing. The slots are located at such intervals that the boundary layer is never long enough to become turbulent.

The friction drag on this slotted type of wing can be much lower than on the conventional wing. Some of the drawbacks are the power and weight needed to operate the pump and the tendency of the slots to become clogged with dirt.

An interesting method of drag reduction is the use of vortex generators, which are placed on the upper surfaces of the wings of some airplanes. Each generator is actually a little wing, only 1 or 2 inches long, sticking out into the airstream. Despite the previous statements about the importance of streamlining and avoiding roughness, the use of vortex generators actually reduces the total drag of the wing. The reason they work is that they mix some of the high-energy free-stream air into the low-energy boundary layer. (The behavior and effects of vortexes are explained in chapter 4.) The energized boundary layer is then more capable of following the wing surfaces near the trailing edge, so that separation is delayed or prevented. This prevention of separation is effective both in decreasing drag and increasing lift, especially at high angles of attack. Vortex generators cause some increase in friction drag, but this is outweighed by the greater reduction in pressure drag.

Other methods of controlling the boundary layer include the addition of high-energy air by blowing through reverse scoops and the use of mechanical means (discussed in

chapter 4) to turn the airflow. Most of these methods impose some penalties in the forms of increased complexity and weight.

SAMPLE CALCULATIONS OF DRAG EFFECTS

Detrimental Drag

For a better understanding of the detrimental effects of drag, it is helpful to calculate the effect of drag on the performance of an actual airplane. Because data happened to be available (ref. 1), let us consider the Messerschmitt Me-109. This was a small, propeller-driven fighter used by the Germans in World War II. Its weight was 6700 pounds, and it had a top speed of 380 miles per hour with a 1200 horsepower engine. The total drag at maximum speed was 1140 pounds. This was distributed among the various parts of the airplane as follows:

Aircraft component	Percent of total drag
Wing (including surface roughness)	38
Fuselage (with roughness and canopy)	14
Tail surfaces (including roughness)	7
Engine and radiator installation	23
Extras (such as guns and tail wheel)	11
Induced drag	7

(These values are taken from reference 1, which is probably the best source of information on all aspects of the subject of drag.) Another way of breaking down the total drag of this airplane is on the basis of friction and pressure drags:

Type of drag	Percent of total drag
Skin-friction drag (smooth, turbulent)	33
Pressure drag due to surface roughness and imperfections	15
Pressure drag due to exposed parts (mostly engine)	33
Interference drag	6
Compressibility drag	6
Induced drag	7

These percentages show that the Me-109 was actually a very poor aerodynamic design. The unavoidable portions of the drag are the friction drag (33 percent) and the induced drag (7 percent). Very good design could get rid of practically all of the remaining drag. Compared with a well-streamlined airplane, the Me-109 had an aerodynamic efficiency of only 33+7 = 40 percent.

It is interesting to consider what would happen to the top speed if the efficiency were raised from 40 to 100 percent (i.e., if the efficiency were increased by a factor of 2.5). If the speed were not changed, the engine power required to overcome drag would decrease by the same factor; that is, only 480 of the available 1200 horsepower would be used. The speed of the airplane could now be increased until the power requirement increased by the factor of 2.5 and the full 1200 horsepower would again be utilized. Most of the drag would be turbulent skin friction, which, as has been mentioned previously, is proportional to the velocity squared. The power required to propel an airplane is proportional to the product of drag times velocity, hence to velocity cubed. This is equivalent to saying that the cube root of the power is proportional to the velocity. For our particular example then, if the power were to increase by a factor of 2.5, the speed could increase by a factor of $\sqrt[3]{2.5} = 1.36$. Thus, the new top speed would be $380 \times 1.36 = 516$ miles per hour.

Beneficial Drag

In a few situations, drag is useful. In some types of boats (with the old square-rigged or the modern spinnaker sails), drag is used for propulsion. Drag brakes are sometimes used on airplanes to slow them down. Parachutes also produce deceleration through drag.

The usefulness of the drag of a parachute can be illustrated by a comparison of the terminal velocities of a falling man with and without a parachute. Terminal velocity refers to the speed at which the drag force that retards the fall is equal to the gravitational pull downwards. This is then the maximum falling speed that can be reached.

As a first step, it is convenient to introduce the concept of aerodynamic coefficients. This is a way of expressing aerodynamic forces in nondimensional form, namely

$$C = \frac{F}{\frac{1}{2}\rho V^2 A}$$

where

C coefficient of force

F actual force

ρ air density

V velocity

A some reference area

Since this chapter is concerned with drag forces, the drag coefficient C_D is defined as

$$C_D = \frac{\text{Drag}}{\frac{1}{2}\rho V^2 A}$$

The usefulness of this concept is that C_D tends to be nearly constant when changes are encountered in air density, velocity, or size of the object.

In the example of a falling man the upward drag force is set equal to the downward weight W; thus

$$\text{Drag} = W$$

By using the definition of drag coefficient, the equation can be rewritten to obtain

$$\frac{1}{2}\rho V^2 A C_D = W$$

or

$$V_t = \sqrt{\frac{2W}{\rho A C_D}}$$

where V_t is the terminal velocity. A man-shaped object has a drag coefficient of about 1.0. An average value for the frontal area of a 180-pound man is about 5 square feet. Substituting these values in the equation (where $\rho = 0.0024$ slug/ft^3 at sea level) yields

$$V_t = \sqrt{\frac{2 \times 180}{0.0024 \times 5 \times 1}} = 173 \text{ feet per second} = 118 \text{ miles per hour}$$

For comparison, a typical parachute has a drag coefficient of 1.6 and an area of 490 square feet. Substituting these values into the equation gives

$$V_t = \sqrt{\frac{2 \times 180}{0.0024 \times 490 \times 1.6}} = 14 \text{ feet per second}$$

REFERENCE

1. Hoerner, Sighard F.: Fluid-Dynamic Drag. Second ed., Midland Park, N.J., 1958.

4. AIRFOIL AND WING THEORY

Roger W. Luidens*

Herein we will concern ourselves with the wing or airfoil: its purpose, its working principles in terms of fundamental physical laws, and the design devices that can be used to give certain desired performance characteristics.

FORCES ON AN AIRPLANE

The function of a wing is best seen by examining the forces on an airplane in horizontal, unaccelerated flight (fig. 4-1). The airplane is pulled vertically downward by the attraction of gravity. This force is the weight W. If the airplane were unsupported, it would fall to the Earth. The purpose of the wing is to provide an upward lift L to support the airplane weight. In the process of providing lift, the wing also causes a drag D in the horizontal, downstream direction. This drag, as well as other drags, must be overcome by the engine thrust T.

An airplane designed for long-range cruising requires a highly efficient wing. The wing efficiency is measured by how much drag it produces while providing the lift to sup-

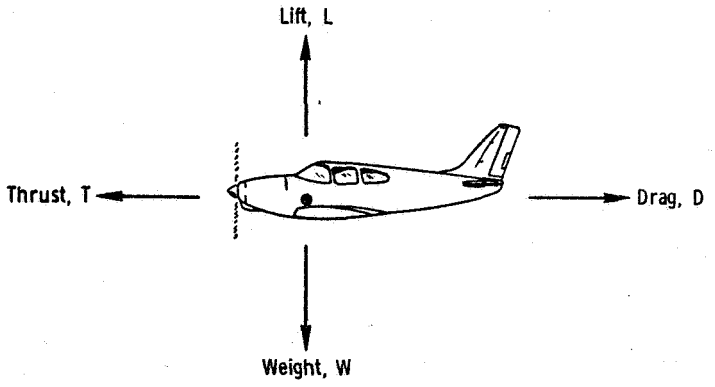

Figure 4-1. - Forces on an airplane.

*Chief, STOL Propulsion Branch.

port the airplane. This is expressed as the lift-to-drag ratio L/D. Thus, a high L/D indicates high efficiency.

For reasons of safety and ease of flying, slow takeoff and landing speeds are desirable. This requires a wing that provides adequate lift at slow speed. In the jargon of the aerodynamicist, this is a "high-lift" wing.

AIRPLANE FLIGHT TESTS VERSUS WIND-TUNNEL TESTS

To observe and study the airflow over a wing, it is obviously not practical to move alongside the airplane while it is in flight. It is more convenient to place the airplane in a wind tunnel, where it is held stationary while air is blown past it. It is important to understand that these two situations are equivalent. This is perhaps most easily rationalized by considering the example of a slow-flying airplane being observed by a man standing on the ground. If the airplane is flying at a speed of 30 miles per hour in still air, it passes the observer at a speed of 30 miles per hour. In other words, the airplane is moving at 30 miles per hour with respect to both the ground and the air. However, if this same airplane is flying against a 30-mile-per-hour headwind, then it is flying at 30 miles per hour through (with respect to) the air, but it is standing still with respect to the ground. In this case, the person on the ground can observe the airplane much more easily. If sidewalls were placed around the airplane and the 30-mile-per-hour headwind were continued, the airplane would be, in effect, in a wind tunnel. In considering the airflow, the important thing is the motion of the air relative to the airplane (or vice versa) and not the motion of the airplane relative to the ground. Thus, from the standpoint of aerodynamics, the wind-tunnel forces are the same as the flight forces. The remainder of the discussion, therefore, is based on the assumption of a stationary airplane with air moving past it.

BASIC PRINCIPLES OF LIFT

Wing lift is frequently explained in terms of Bernoulli's law (see chapter 5). In our analysis of the flow over a wing, however, we can utilize Newton's laws of motion to obtain a physical representation of the principles of lift.

Newton's Laws of Motion

Newton's Third Law of Motion states that for every action there is an equal and oppo-

site reaction. A familiar example of this law is the firing of a gun. Consider a single-shot pistol mounted on a theoretically weightless and frictionless roller skate, as shown in figure 4-2. (In this example, aerodynamic drag is also neglected.) When the gun is fired, the bullet, which has a mass m_1, leaves the gun with a velocity v_1. (The bullet mass, in slugs, is its weight at the Earth's surface, in pounds, divided by the acceleration due to gravity at the Earth's surface, in feet per second per second.) At the same

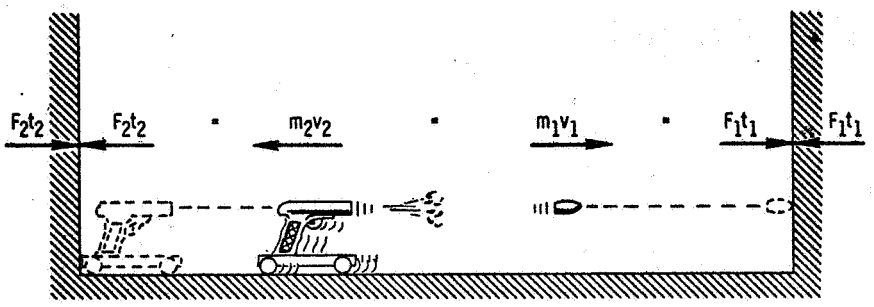

Figure 4-2. - Illustration of Newton's laws of motion.

time, the gun is "kicked" in the opposite direction. If the mass of the gun is m_2, it moves backward at a velocity v_2. The momentum of the bullet is m_1v_1, and the reaction momentum of the gun is m_2v_2; according to Newton's law, these two momentums are equal. The bullet will hit the wall on the right with a force F_1 that exists for a short time t_1. The gun will hit the wall on the left with a different force F_2 that exists for a different time t_2. The kick that is received and counteracted by each wall is the product of the respective force and the length of time that the force exists. Therefore, the kick from the bullet that is received and counteracted by the right wall is F_1t_1, and the kick from the gun at the left wall is F_2t_2. This is the kick that a person feels in his hand if he is holding the gun when it is fired.

Newton's Second Law of Motion states that the rate of change of momentum of a body is proportional to the force acting on the body. This law can be represented by the equation $F = mv/t$, or $Ft = mv$ (where mv is the momentum). Newton's First Law of Motion states that if a body in motion is not acted upon by an external force, its momentum remains constant. Thus, the application of Newton's laws of motion to the example of the gun shows that the kick of the gun against the left wall equals the momentum of the gun, which equals the momentum of the bullet, which equals the kick of the bullet against the right wall.

$$F_2t_2 = m_2v_2 = m_1v_1 = F_1t_1 \tag{1}$$

For the next example, a machinegun is used instead of the single-shot pistol. The bullets from this gun are fired into a bullet trap that is mounted to a wall by means of a spring-and-shock-absorber assembly, as shown in figure 4-3. (Springs and shock absorbers on a car are used to smooth out the many "kicks" from the road into an average force that is equal to and counteracts the weight of the car.) The bullet trap, by virtue of its mounting, converts the kicks from the individual bullets into an average force F that is

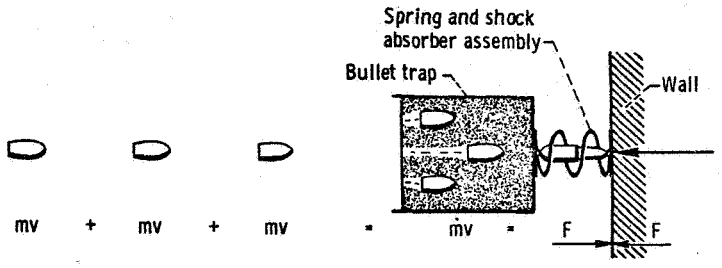

Figure 4-3. - Converting individual impulses to an average force.

received and counteracted by the wall. "Average force" in this context means a force that exists continuously in time and does not vary in magnitude. By this definition of average force, the total, or continuous, kick at the wall over a long period of time t must be Ft. The total "action" from a large number of bullets in the same length of time is the number of bullets n times the action per bullet. Equating the total action with the continuous kick, by Newton's laws of motion, yields

$$nmv = Ft \tag{2}$$

But the number of bullets n is equal to the number of bullets per second $\dot{n}$ times the time t. Therefore, equation (2) can be written as

$$t\dot{n}mv = Ft \tag{3}$$

Since t occurs on both sides of the equation, it can be cancelled from both sides. Also, the number of bullets per second $\dot{n}$ times the mass per bullet is just the mass flow per second $\dot{m}$. The average force on the wall from a stream of machinegun bullets is then the mass of bullets per second (the mass flow rate) times their velocity.

$$F = \dot{m}v \tag{4}$$

Figure 4-4 illustrates a series of examples, each of which gives the same average

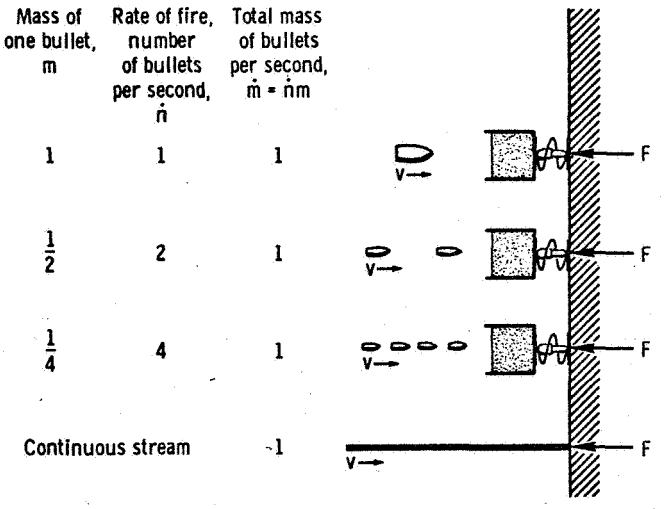

Figure 4-4. - Various mass flow systems producing same average force.

force F on the wall. As the number of bullets per second ṅ is increased, the mass m of each bullet is correspondingly decreased to maintain the same mass flow rate ṁ (see columns at left of fig. 4-4). The limit is a continuous flow of mass (similar to water out of a hose). For the example with the bullets, a bullet trap, spring, and shock absorber are needed to obtain the average force. However, this equipment would not be needed if the example were one of a continuous stream of mass.

Equation (4) is a general law that results from Newton's laws of motion. It is important to note that the force F acts along the same line as v.

Air Flow

Aerodynamics concerns the flow of air rather than bullets. Therefore, the next step towards understanding the lift of a wing is the application of equation (4) to a stream of air.

To determine the force of a stream of air by equation (4), the mass flow rate per unit time, ṁ, must first be known. If the airstream is flowing through a tube, as shown in

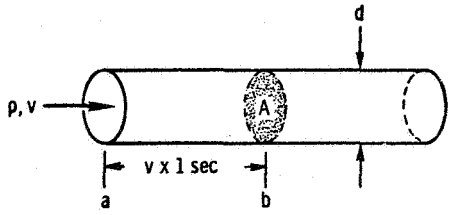

Figure 4-5. - Airstream in a tube.

figure 4-5, the mass flow rate is the mass flow past any point in the tube during some unit period of time, such as 1 second. Consider a particle of air that is at point a when timing is begun. At the end of 1 second, that particle of air is at some point b downstream from a. The distance between points a and b is determined by multiplying the flow velocity v by 1 second. Thus, the volume of air that passes point a during 1 second is obtained by multiplying the cross-sectional area of the tube A by the flow velocity of the air v by 1 second. The mass of this air (which is the mass flow rate per unit time, $\dot{m}$) is the density ρ multiplied by the volume flow per unit time, vA.

$$\dot{m} = \rho v A \tag{5}$$

For a sample calculation of mass flow rate, consider a tube being held out the window of a moving car so that the longitudinal axis of the tube coincides with the direction in which the car is traveling. The air density is obtained from a table of air density versus altitude above sea level. The velocity v of the air in the tube is the car velocity, obtained from the speedometer. The cross-sectional area of the tube is obtained by measuring the tube diameter d and then using the equation

$$A = \frac{\pi d^2}{4} \tag{6}$$

The preceding example of airflow in a straight tube was used only to determine the mass flow rate; there was no force, or lift, on the tube. However, airflow through a bent tube does produce a force on the tube.

Assume that the downstream end of the horizontal tube of the preceding example is bent downward at an angle β, as shown in figure 4-6. The upward force, or lift, L produced by the bent airstream can be calculated by equation (4). The mass flow rate $\dot{m}$ has already been calculated by equation (5). The lift is caused by the flow velocity that is parallel but opposite in direction to the direction of the lift; this velocity is designated v_L. The flow exiting from the end of the bent tube has a velocity v and an angle β with

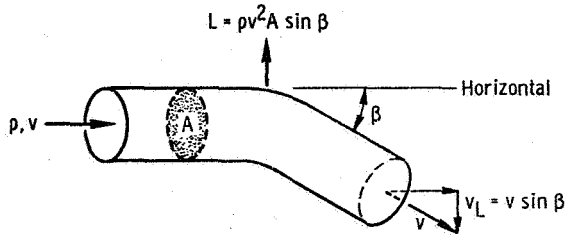

Figure 4-6. - Bent airstream generates lift.

respect to the horizontal plane. The vertical downward component of this velocity is $v \sin \beta$. Therefore, from equations (4) and (5), the lift L is given by

$$L = \dot{m}v_L = (\rho vA)(v \sin \beta) = \rho v^2 A \sin \beta \tag{7}$$

For those who are unfamiliar with trigonometry, a brief explanation of trigonometric functions should be useful at this point. Trigonometry is the mathematical study of the relations between component parts of triangles. In any triangle, if three of the parts (angles and sides) are known, including at least one side, the other three parts can be

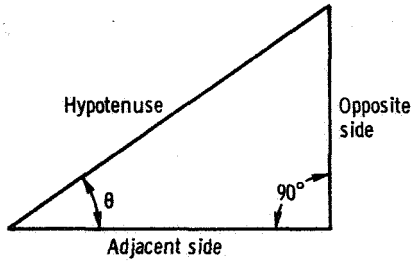

Figure 4-7. - Right-angled triangle as it applies to definitions of trigonometric functions.

determined by using trigonometric functions. These functions are simply ratios of sides of a right-angled triangle, shown in figure 4-7. The most commonly used functions (sine, cosine, and tangent) are defined as follows:

$$\sin \theta = \frac{\text{Side opposite } \theta}{\text{Hypotenuse}}$$

$$\cos \theta = \frac{\text{Side adjacent to } \theta}{\text{Hypotenuse}}$$

$$\tan \theta = \frac{\text{Side opposite } \theta}{\text{Side adjacent to } \theta}$$

where the hypotenuse is the side opposite the right angle (90^o). These functions depend only on the angle θ, because if this angle and the right angle are maintained constant, an increase in any side of the triangle requires a proportionate increase in the other sides. Because all sides of the triangle increase or decrease proportionately, the ratios of sides (i. e., the functions) remain constant. Therefore, the trigonometric functions vary only when the angle θ is varied.

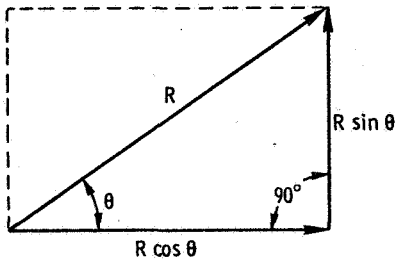

Figure 4-8. - Vector relations.

Trigonometric functions are useful in vector considerations. (A vector is any quantity that has both magnitude and direction, such as force, velocity, acceleration, and displacement.) In many problems it is useful to replace a single vector by two or more vectors equivalent to it, or vice versa. The equivalent two or more vectors are called components of the original vector, which, conversely, is called the resultant of the components. For example, a vector R (resultant) along the hypotenuse at an angle θ from the adjacent side is equivalent to, or can be resolved into, a component R cos θ along the side adjacent to θ and a component R sin θ along the side opposite θ, as shown in figure 4-8. The vectors are represented by arrows. The length of the arrow is proportional to the magnitude of the vector, and the direction of the arrow is the direction of the vector. It should be noted that the resultant vector R represents the diagonal, and the component vectors represent two adjacent sides of a rectangle. These two component vectors may be drawn so as to form any one of the four corners (right angles) of the rectangle. However, the component vectors must have the correct directions; that is, the arrows representing the component vectors must point away from the tail and/or toward the head of the arrow representing the resultant vector.

Velocity is a vector because it has magnitude (speed) and direction. Therefore, the velocity v of the airstream bent downward at an angle β from the horizontal, as shown in figure 4-6, can be resolved into a horizontal component v cos β in the direction of the original flow and a vertical downward component v sin β.

Lift on a Wing

A first approximation of the lift on a wing can be obtained by relating the airflow over a wing to the airstream in a tube (fig. 4-9). In the figure, the wing is shown by the solid lines. For illustrative purposes, let us assume that the effective stream tube of air affected by the wing is a tube with a diameter that is equal to the wingspan b. Therefore, in equation (7),

$$A = \frac{\pi b^2}{4}$$

Substituting this term into equation (7) yields the following equation for wing lift:

$$L = \rho v^2 \frac{\pi b^2}{4} \sin \beta \tag{8}$$

For small angles of attack, the angle β at which the flow is bent in the imaginary tube is just the wing angle of attack α.

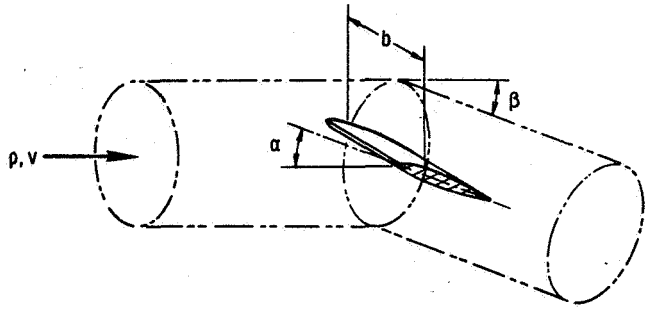

Figure 4-9. - Imaginary stream tube of air affected by wing.

It must be emphasized that equation (8) provides only an approximation of the lift; however, the equation does take into account most of the factors affecting lift. A more precise analysis of wing lift would show that equation (8) should be multiplied by the term $4/\left[2 + (b^2/S)\right]$, where b^2/S is the aspect ratio of the wing, which is discussed later in this chapter.

Coanda Effect

In the preceding development of the wing-lift theory, it was implied that separate particles, such as bullets, would lead to the same result as a continuous fluid, such as water or air. In the examples of the bullets and the flow in a tube, this was true. But, in other instances, fluids do have different properties from those of particles.

The theory of the preceding section that the flow over a wing can be approximated by the flow in a tube is dependent on a fluid property called the Coanda effect. This effect is best illustrated by the following simple experiment. If sand is poured on the upper right side of a cylinder, as shown in figure 4-10(a), the grains of sand bounce to the right. If water is poured on the upper right side of the cylinder (fig. 4-10(b)), the water

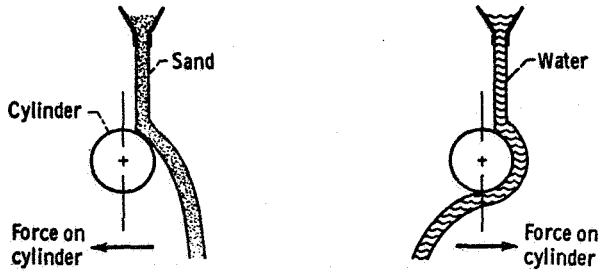

(a) Solid particles.

(b) Fluid. (Example of Coanda effect.)

Figure 4-10. - Difference between paths of solid particles and fluid around a curved surface.

clings to the surface of the cylinder, so that it leaves the cylinder at the lower side and flows toward the left. This tendency of fluids to cling to surfaces over which they flow is the Coanda effect. The grains of sand, obviously, do not cling to the surface. Because of the Coanda effect, the airflow over a wing tends to cling to the surface of the wing and is, therefore, turned by the wing. It should be noted that this tendency of a fluid to cling to a surface is limited; that is, the fluid eventually breaks away from the surface, as shown in figure 4-10(b).

If equation (7) were applied to the two examples of figure 4-10, the sand would produce a component of force to the left on the cylinder because the grains of sand bounce to the right; the water would produce a component of force to the right on the cylinder because the water leaves the cylinder to the left.

HIGH LIFT

The preceding discussion dealt with the basic principles of lift. These principles will now be applied to the problem of generating high lift.

One of the principal requirements for high lift is at landing, because it permits a slower landing, which is easier and safer. (An airplane also requires high lift for improved maneuverability at high altitudes.) At landing, the lift still should be only equal to the airplane weight. Therefore, to the aerodynamicist the term "high lift" signifies the ability of an aircraft to fly slowly or to change direction rapidly at high altitude. From equation (8) it is obvious that if the lift L is too high (i.e., greater than the airplane weight), it can be reduced by decreasing the velocity v. Thus, achieving a high lift at a specified velocity is equivalent to achieving a lower velocity at a specified lift. For landing, flight at low velocity with the lift equal to the airplane weight is desirable. The present discussion considers the subject of lift from the standpoint of the aerodynamicist; that is, the discussion concerns high lift at a specified velocity.

The variables that affect lift are contained in equation (8). For the purpose of this

discussion, let us assume that three of these variables are fixed. The air density ρ is determined by the altitude of the airport at which the airplane is landing or by the altitude at which the airplane is maneuvering. The velocity v is assumed to be some specified value. The wingspan b is determined by the configuration of the airplane. Even if these three variables are fixed, high lift can still be obtained by means of flow turning.

Equation (8) includes the term $\sin \beta$, where β is the angle through which the flow is turned. According to equation (8), the lift should increase as the flow-turn angle β is increased up to the limit of 90°, where $\sin \beta$ reaches its maximum value of 1. In practice, for small angles of less than 15°, the flow-turn angle β (and the lift) can be increased by merely increasing the angle of attack α (fig. 4-11(a)). As the angle of attack is increased up to 15°, the airflow remains attached to the surface of the wing (Coanda effect) and is turned by it (fig. 4-11(b)); thus, the flow-turn angle β is the same as the angle of attack α. However, if the angle of attack is increased above 15°, the lift does not increase any more; instead, it drops a little and then remains fairly constant for higher angles of attack. The reason for this is that when the angle of attack is greater than 15°, the airflow separates from the upper surface of the wing and is no longer turned by it (fig. 4-11(c)). In this case, the flow-turn angle β is no longer the same as the angle of attack α. This condition of flow separation, which is analogous to the water breaking away from the surface of the cylinder in figure 4-10(b), is called wing stall. (In a liquid, such as water, this separation phenomenon is referred to as cavitation.)

Obviously, the principle of turning the airflow through a large angle to obtain high lift is difficult to put into practice because of the problem of getting the flow to turn. Some attempted solutions to this problem are the so-called "high-lift devices" discussed in the next section.

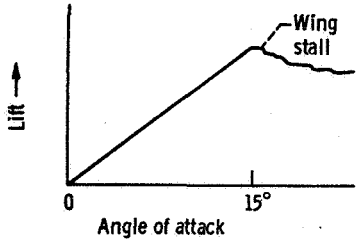

(a) Lift as function of angle of attack.

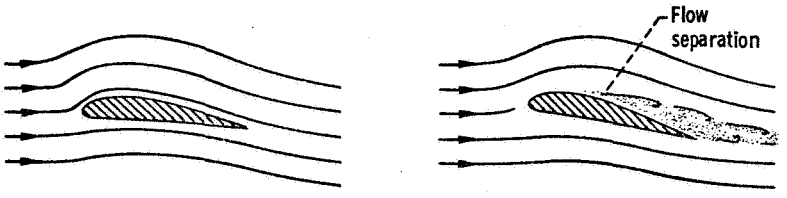

(b) Angle of attack less than 15°. Attached airflow; complete flow turning.

(c) Angle of attack greater than 15°. Separated airflow; partial flow turning.

Figure 4-11. - Effect of angle of attack on lift and airflow.

HIGH-LIFT DEVICES

The high-lift devices used to improve flow turning are actually antistall or antiseparation devices. A measure of the success of such a device in preventing flow separation, or in turning the flow, is the maximum lift produced by the wing to which the device is applied. The maximum lift is expressed as a dimensionless coefficient $C_{L, max}$. The various devices are compared in terms of this parameter.

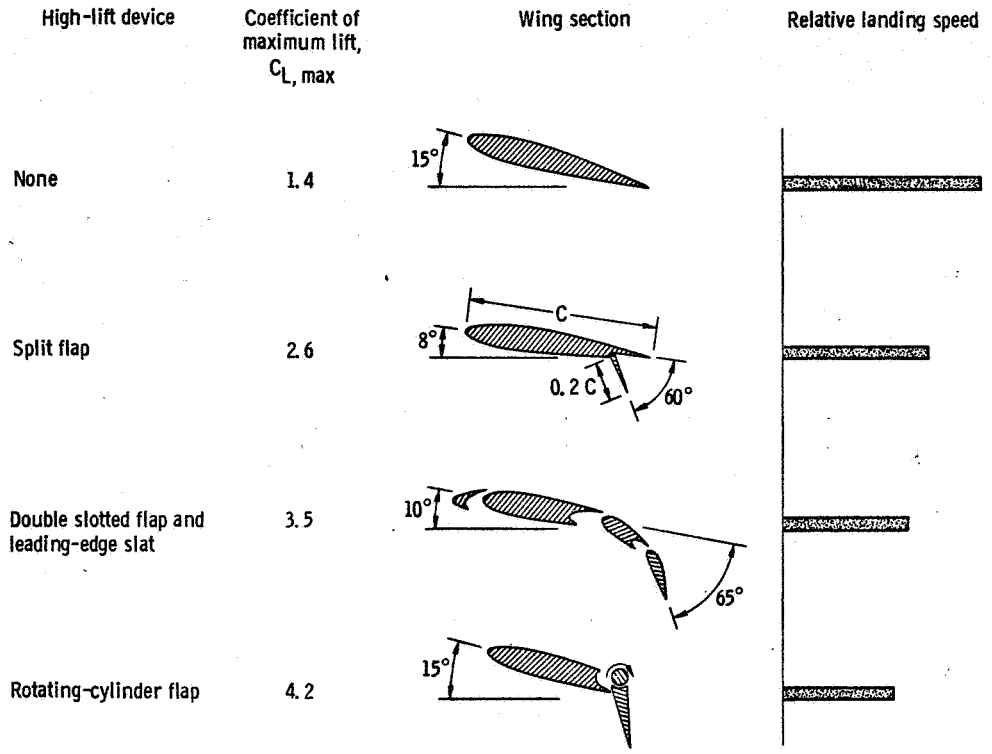

Figure 4-12. - High-lift devices.

Wing stall can occur abruptly, as when the flow separates from the leading edge, or it can occur gradually, as when the flow separation spreads forward from the trailing edge. Therefore, there are leading-edge and trailing-edge high-lift devices. Figure 4-12 shows several types of high-lift devices and their effectiveness in terms of $C_{L, max}$. The $C_{L, max}$ increases from approximately 1.4 for a plain wing to approximately 4.2 for a wing with a rotating-cylinder flap.

The effect of a rotating cylinder, one of the high-lift devices, is illustrated in figure 4-13. Because of the Coanda effect, the flow of water is turned a certain amount even if the cylinder is stationary (fig. 4-13(a)). If the cylinder is rotating in the direction of flow, the attachment is increased and the flow is turned through a greater angle (fig. 4-13(b)). This is exactly the way a rotating cylinder works when it is applied to the wing

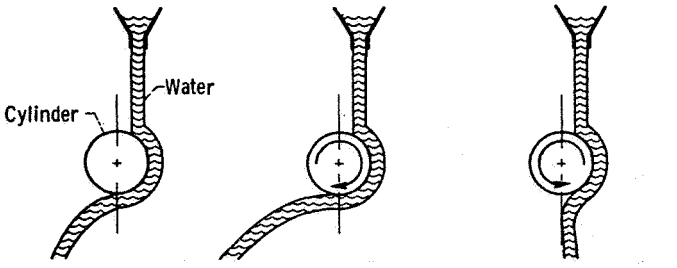

(a) Stationary cylinder.

(b) Cylinder rotating in direction of flow. Increased flow attachment.

(c) Cylinder rotating counter to direction of flow. Decreased flow attachment.

Figure 4-13. - Effect of rotating cylinder on flow attachment.

of an airplane. Of course, if the cylinder is rotating counter to the direction of flow, separation occurs sooner and the flow is turned less (fig. 4-13(c)).

DRAG AND EFFICIENCY

The preceding discussion of high lift did not deal with the subject of wing drag. To learn why a wing of finite span causes drag and to understand wing efficiency, the flow around a wing must be examined in more detail than was done in the preceding discussion.

Local Flow Over a Finite Wing

When a wing is producing lift, the pressures on the bottom of the wing are higher than those on the top. Any fluid tends to flow from an area of high pressure to one of low pressure. Therefore, the air tends to flow from the bottom to the top of the wing, as indicated by the upward arrows at the leading and trailing edges in figure 4-14. To understand what actually happens to this upward flow of air, it is helpful to consider again the example of water flowing around a cylinder, as shown in figure 4-15. The flow readily

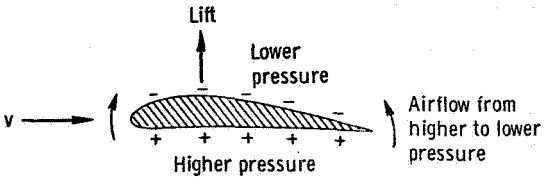

Figure 4-14. - Pressures on lifting wing.

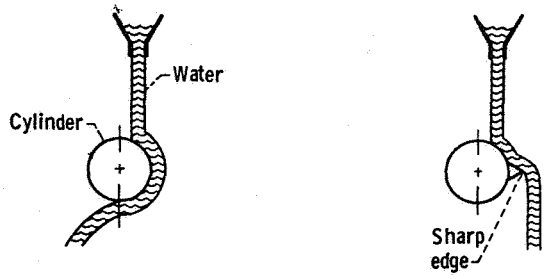

(a) Flow around well-rounded surface.

(b) Flow over sharp edge.

Figure 4-15. - Effect of sharp edge on flow attachment.

follows a smooth, well-rounded surface (fig. 4-15(a)), but it cannot follow the surface around a sharp corner or over a sharp edge (fig. 4-15(b)). Therefore, the leading edge is made round and the trailing edge sharp, so that air from the bottom of the wing will flow up around the leading edge but not around the trailing edge (fig. 4-16). This upward flow around the leading edge causes the streamlines ahead of the wing to rise up to meet the wing, as shown in figure 4-16. The overall effect of the wing-section shape is that it turns the airflow so that the air leaves the wing in a downward direction; thus, the wing produces a lifting force.

The higher pressures on the bottom of a lifting wing also cause air to flow up around the wingtips, as shown in figure 4-17. In this case, the airflow pivots up and around the wingtip in a circular pattern (viewed from the front), with the tip of the wing in the center of the circle. This is called a vortex flow.

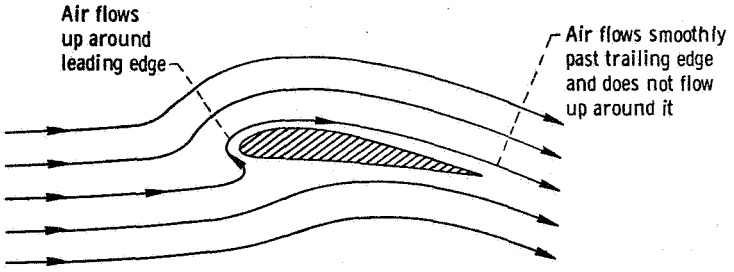

Figure 4-16. - Flow induced by pressures on lifting wing.

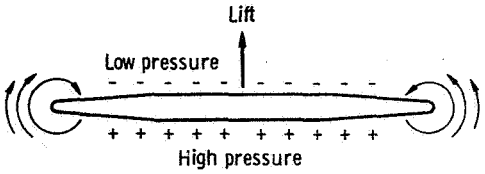

Figure 4-17. - Front view of lifting wing showing vortex flows around wing tips.

Vortex Flow

There are many common examples of vortexes: tornadoes hurricanes, dust devils, water spouts, the flow down the bathtub drain, the flow around a canoe paddle during a stroke, smoke rings, the flow around the tips of a lifting airplane wing. The twist in the exhaust flow from a moving car, especially a car with twin exhausts, looks much like the pattern shown in figure 4-17.

Vortex flow is characterized by velocities that are higher at the center than at the outer edges of the vortex (fig. 4-18). A simple experiment for observing the wingtip vortex and the velocity distribution in a vortex is shown in figure 4-19. At the tip of a wing, three paddle wheels of different diameters are mounted on an axis that is alined with the free-stream direction. Each paddle wheel is free to rotate independently of the others. The paddle blades are alined with the free stream direction, so that if there were no disturbance to the free-stream flow, the blades would remain alined with the flow and the paddle wheels would not rotate. However, in their position behind the wingtip, the paddle blades will tend to aline themselves with the local flow, which is changed from the free-

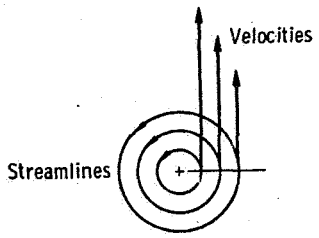

Figure 4-18. - Velocity distribution in a vortex.

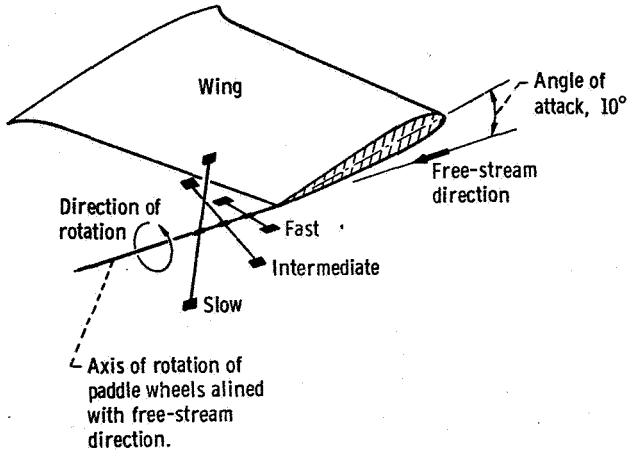

Figure 4-19. - Experiment illustrating wingtip vortex flow.

stream direction by the effect of the wing at its angle of attack. The movement of the paddle blades in alining themselves with the local flow causes the paddle wheels to rotate. Therefore, the rotation of the paddle wheels is an indication of the vorticity of the local flow downstream of the wingtip. This experiment will also show that the smallest-diameter paddle wheel rotates the fastest and the largest-diameter wheel rotates the slowest. This is consistent with the previous description of the velocity distribution in a vortex (fig. 4-18). This experiment can be performed with a model wing mounted to the side of an automobile so that the forward motion of the automobile generates the free-stream velocity relative to the wing.

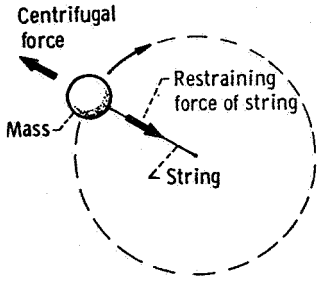

Figure 4-20. - Centrifugal force.

Centrifugal force, illustrated in figure 4-20, is a familiar phenomenon which acts on any body, or mass, that is being constrained to travel along a curved path. The air in a vortex has mass and is, therefore, subject to centrifugal force. However, a force that is caused by the pressure variation in a vortex prevents the air from being thrown out of the vortex by the centrifugal force. The pressures in a vortex are low at the center and high at the outside. This pressure variation creates an inward force (air tends to flow from high to low pressure) that counteracts the centrifugal force. Thus, the force due to the pressure variation serves the same purpose as does the string in the example of figure 4-20.

Since a vortex has low pressure in the center, the end of the vortex cannot be open to the higher-pressure outside air, because this higher-pressure air tends to flow into the center and break up the vortex by eliminating the pressure force which counters the centrifugal force. Thus, as shown in figure 4-21, vortexes are closed loops (such as a smoke ring), or they terminate at the fluid boundary (as a tornado terminates on the ground).

The vortexes from the wingtips extend rearward and join a lateral vortex that is shed from the trailing edge of the wing when the wing speed is changed, as when the speed is increased at takeoff. These joined vortexes and the wing form a closed-loop pattern similar to that of a smoke ring.

The direction of the wingtip vortex flow (fig. 4-22) is such that these vortexes exert

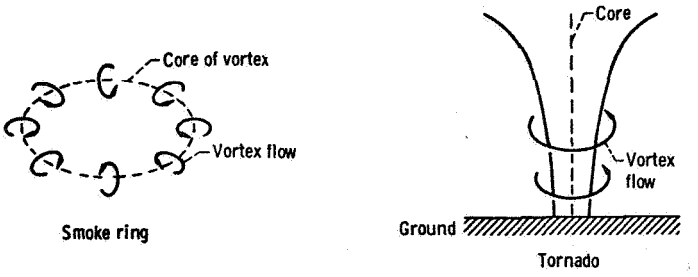

Figure 4-21. - Vortexes are closed loops or terminate at the boundary of the fluid.

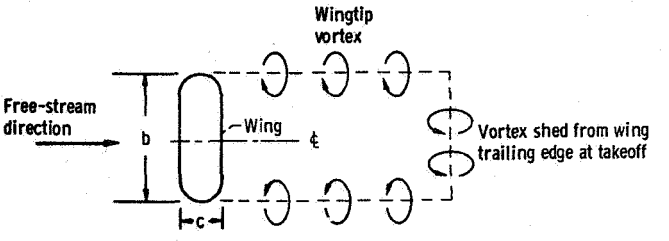

Figure 4-22. - Top view of wing and vortex pattern.

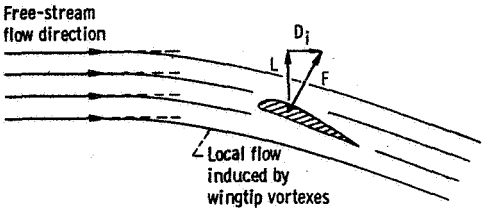

Figure 4-23. - Effect of wingtip vortexes.

a downward force on the local airflow about the wing, as shown in figure 4-23. It has already been explained and shown (figs. 4-18 and 4-19) that the velocity is greatest near the center of a vortex. Therefore, the downward flow (and force) of a wingtip vortex is greatest at the center of the vortex. To minimize the downward effect of the wingtip vortexes on the local airflow about the wing, the vortexes should be moved as far apart as possible; that is, the wingspan b should be large in comparison with the wing chord c. The ratio of the wingspan to the mean aerodynamic chord $\bar{c}$ (or the ratio of wingspan squared to wing area S) is called the wing aspect ratio AR.

$$AR = \frac{b}{\bar{c}} = \frac{b^2}{S} \tag{9}$$

Induced Drag

As shown in figure 4-23, the downward influence of the wingtip vortexes extends even ahead of the wing, so the wing operates in a downflow. Even though the force F on the wing is perpendicular to the local flow, this force now has a component parallel to the free-stream direction; this component is the induced drag D_i. The induced drag is proportional to the lift L. The downflow at the wing, which is related to the wing aspect ratio AR, is also proportional to the lift L. The drag due to lift, or induced drag, is actually given by the following equation:

$$D_i = \frac{L^2}{\pi\, AR}$$

The induced drag is only one of the drags on an airplane; other drags are discussed in chapter 3.

The previous description of flow, illustrated in figure 4-16, seems to conflict with the present description, illustrated in figure 4-23. Actually, both descriptions are correct. The two flows exist simultaneously and are superimposed on each other as shown in figure 4-24.

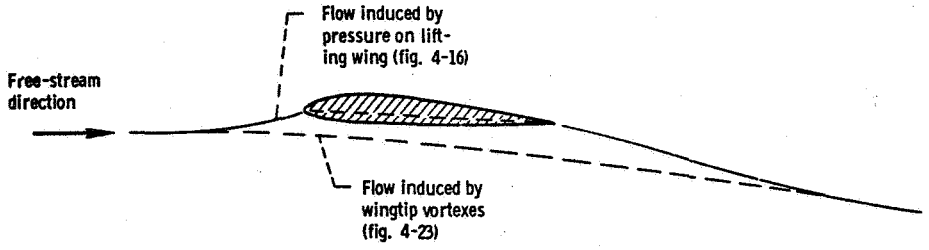

Figure 4-24. - Airflow about lifting finite wing.

Lift-To-Drag Ratio

The aerodynamic efficiency of a wing (or airplane) is measured by its lift-to-drag ratio L/D; that is, the efficiency is measured by how much drag a wing causes while providing a specified lift. At the subsonic speeds being considered in the present discussion, the wing aspect ratio has a most important effect on wing efficiency, as shown in figure 4-25(a). In general, a high wing aspect ratio leads to a high airplane lift-to-drag ratio. What aspect ratio is selected depends on the design objective. (Plan views of various design configurations are shown in fig. 4-25(b).) The four-place light airplane indicated in the figure is designed for a range of about 1000 miles and to be cheap. The commercial

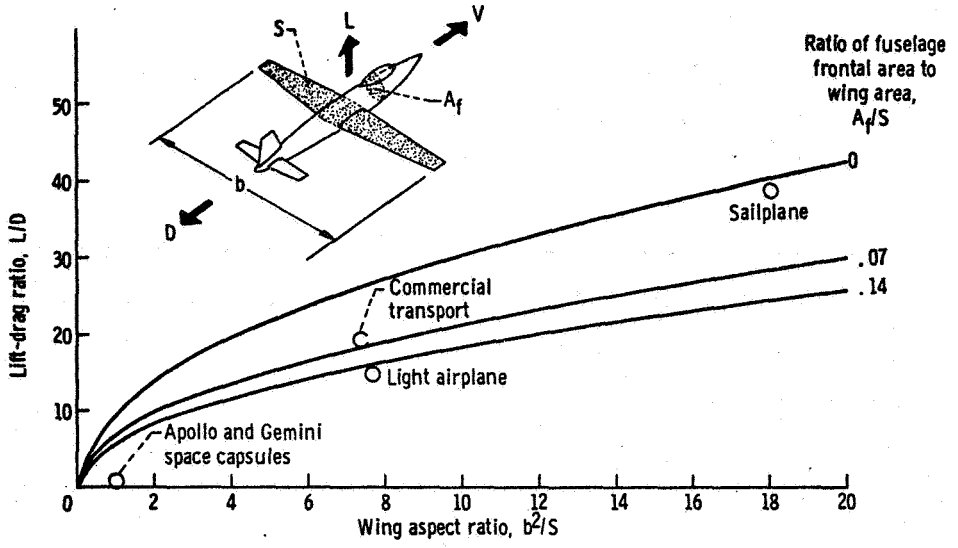

(a) Effect of wing aspect ratio and fuselage size on aircraft lift-drag ratio.

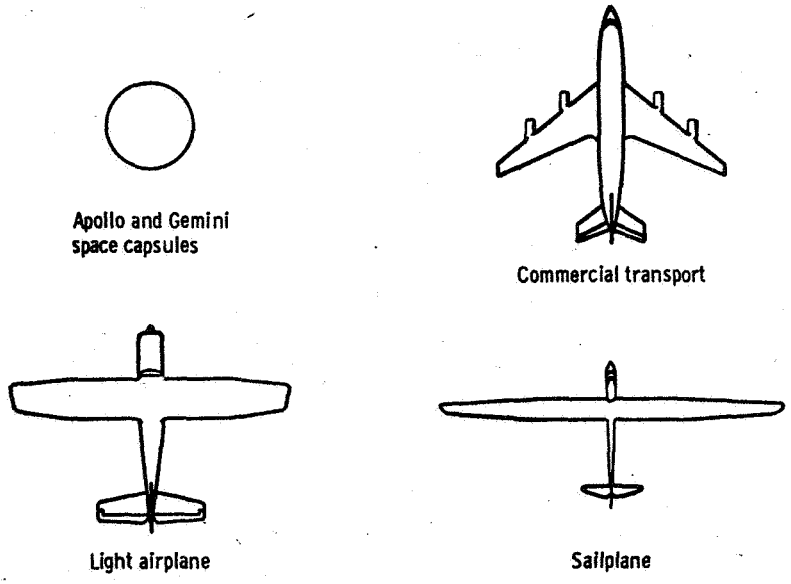

(b) Aircraft plan views.

Figure 4-25. - Aircraft lift-drag ratios.

transport is designed for a range of about 3000 miles and to make money for the airlines. The sailplane is designed to glide a long distance. The Apollo and Gemini space capsules (which travel in the atmosphere at hypersonic and supersonic speeds, as well as at subsonic speeds) are designed aerodynamically to provide only limited control over the landing accuracy on return from orbit (i.e., ability to land in a target area with a diameter of perhaps 50 miles).

aerodynamic center. A point in a cross section of an airfoil, on the aerodynamic chord, about which the pitching moment remains practically constant with nearly all changes in angle of attack. This point is usually located a distance of approximately 25 percent of the mean aerodynamic chord back from the leading edge. This is the point where lift can be considered to be concentrated.

angle of attack. The angle between the chord line and the free-stream direction (fig. 4-26(a)).

aspect ratio. The ratio of the square of the span of an airfoil to the total airfoil area, or the ratio of the span to the mean geometric chord.

camber. The curvature of the mean line, or centerline, of an airfoil profile (section) relative to the chord line.

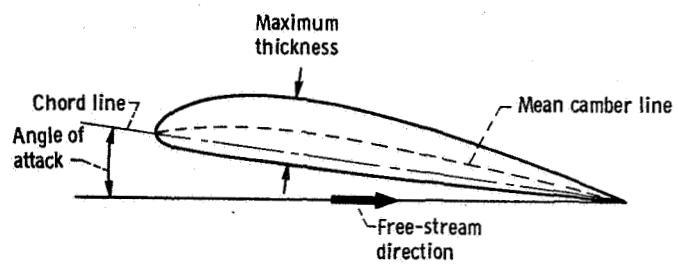

(a) Wing cross section.

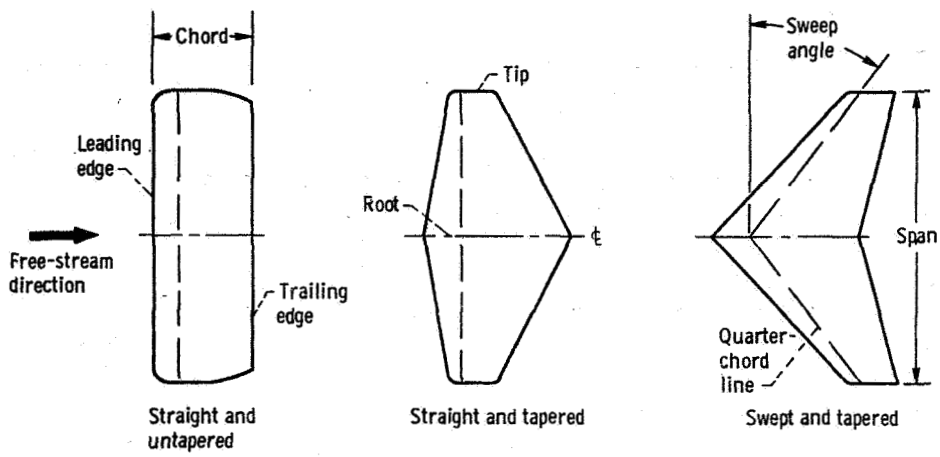

(b) Wing planforms.

Figure 4-26. - Airfoil and wing terminology.

chord. The straight line joining the leading and trailing edges of an airfoil or joining the ends of the mean line (or mean camber line) of an airfoil profile. The length of that part of the chord line intercepted by the extremities of the leading and trailing edges of an airfoil section (fig. 4-26(b)).

chord line. A straight line through the centers of curvature of the leading and trailing edges of an airfoil section. This line is generally used as a reference line from which the ordinates and angles of an airfoil are measured (fig. 4-26(a)).

free stream. The stream of fluid outside the region affected by a body in the fluid.

leading edge. The forward edge of an airfoil or wing. The edge that normally meets the air first (fig. 4-26(b)).

maximum thickness. The maximum dimension of an airfoil or wing measured perpendicular to the chord line and usually occurring at the quarter-chord line (fig. 4-26(a)).

mean aerodynamic chord. Approximately the same as the mean geometric chord.

mean camber line. The mean line, or centerline, of an airfoil profile; that is, the line midway between the upper and lower surfaces of an airfoil (fig. 4-26(a)).

mean geometric chord. The average chord length of an airfoil, obtained by dividing the planform area of the airfoil by the span.

moment. A tendency to cause rotation about a point or axis, as of an airplane about its center of gravity; the measure of this tendency, equal to the product of the force and the perpendicular distance between the point or axis of rotation and the line of action of the force.

pitching moment. A moment about a lateral axis of an airfoil or aircraft.

planform area. The area within the outline of an object as viewed from the top. With respect to an airfoil or a wing, it is the area within the outline of the projection of the airfoil or wing on the plane of its chords (fig. 4-26(b)).

quarter-chord line. The line through the quarter-chord points of an airfoil (fig. 4-26(b)).

quarter-chord point. The point on the chord line at one quarter of the chord length behind the leading edge.

root. The base or inner end of an airfoil, wing, or blade (fig. 4-26(b)).

span. The dimension of an airfoil or a wing from tip to tip, measured in a straight line (fig. 4-26(b)).

sweep. The slant (forward or rearward) of a wing or airfoil, or of a reference line in an airfoil, with respect to a plane that is perpendicular to the longitudinal axis of the aircraft (fig. 4-26(b)).

sweep angle. The angle between a reference line, usually the quarter-chord line, of an airfoil or wing and a plane that is perpendicular to the longitudinal axis of the aircraft (fig. 4-26(b)).

sweepback. The backward slant from root to tip of an airfoil or wing, or of some reference line of an airfoil (fig. 4-26(b)).

taper. A gradual reduction, from root to tip, of either the chord length or thickness of an airfoil or wing (fig. 4-26(b)).

taper ratio. The ratio of the tip chord length of an airfoil to the root chord length.

tip. The outermost extremity of an airfoil or wing (fig. 4-26(b)).

trailing edge. The rear edge of an airfoil or wing. The edge over which the airflow normally passes last (fig. 4-26(b)).

twist. A variation of the angle of attack of an airfoil from root to tip.

washout. A permanent twist (or warp) given a wing such that the angle of attack decreases from the root to the tip of an airfoil.

5. PROPELLER THEORY

Earle O. Boyer*

An aircraft propeller may be considered as an engine-driven screw. The blades of the propeller correspond to the threads of a screw. As a propeller rotates, the blades "bite," or slice, into the air in a manner similar to the way the threads of a wood screw, for example, slice into the wood. (Some European engineers and aerodynamicists call an aircraft propeller an "airscrew.") Thus, in its rotation, the propeller reacts with the surrounding fluid to produce an axial force, or thrust.

This chapter concerns specifically the aircraft propeller, but the basic principles discussed herein are also applicable to rotors and fans. This discussion is intended to provide merely some basic understanding of the theory and principles of a propeller rather than to provide a comprehensive knowledge of the subject. (Technical expressions pertaining to propellers are defined in the GLOSSARY at the end of this chapter.)

It is important to realize that even in this age of jet aircraft, rockets, nuclear power, and space exploration the propeller still serves a vital function in both civilian and military aviation. The reason for this is that currently the piston engine and propeller are a more efficient and more economical power plant than the jet engine for low flying speeds. That is, at low speeds the piston engine uses less fuel than the jet engine to develop a given thrust. Also, the piston engine is currently cheaper than the jet engine. Therefore, the piston engine and propeller are commonly used to power small private airplanes, agricultural airplanes, military spotter airplanes, and bush-flying airplanes. Propellers are proving useful, too, in the field of V/STOL aircraft (see chapter 10).

PRINCIPLES OF PROPELLER THRUST

Let us now concern ourselves with some of the basic principles by which a propeller actually produces thrust. In this discussion, aerodynamic lift and propeller thrust are explained in terms of Bernoulli's law. (In chapter 4, lift was explained in terms of Newton's laws of motion.)

*Aerospace Engineer and Pilot, Aircraft Operations Branch.

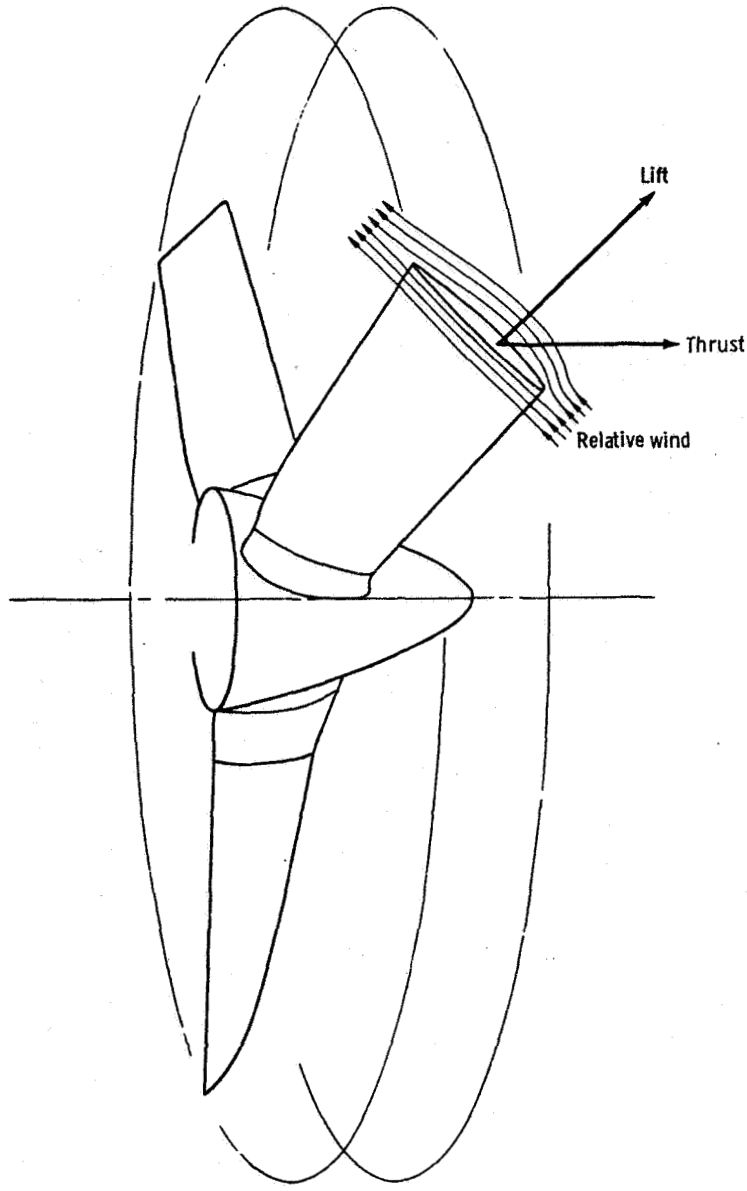

Figure 5-1. - Propeller blade considered as an airfoil rotating in the vertical plane.

A propeller blade is an airfoil (similar to a wing) set to rotate in the vertical plane (fig. 5-1). Thus, the blade may be considered as "lifting" the airplane forward, as the wing lifts it upward. Figure 5-2 shows the basic forces (lift and drag) generated by an airfoil. The upward lift that is generated is the net result of the pressure distribution over the airfoil (fig. 5-3(a)). One of the factors governing the pressure pattern over an airfoil is the velocity of the air flowing over the surface (fig. 5-3(b)).

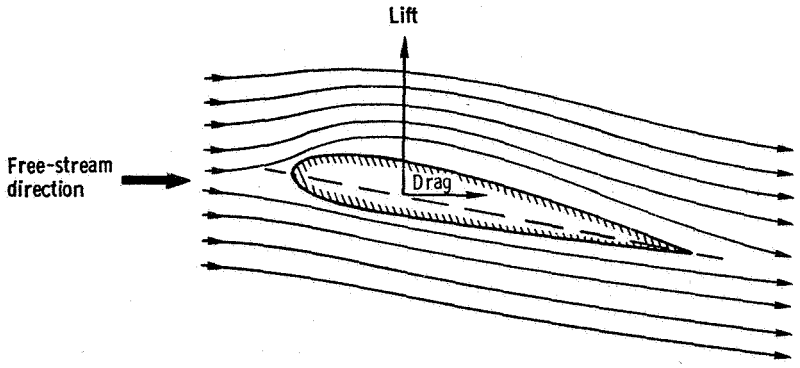

Figure 5-2. - Basic forces generated by an airfoil in an airstream.

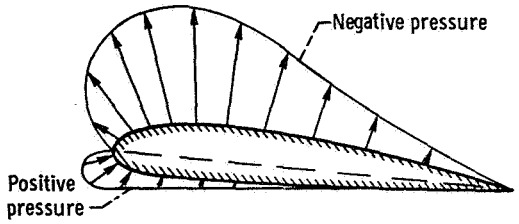

(a) Pressure distribution.

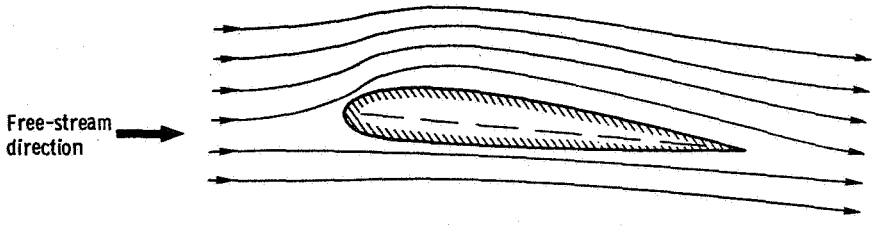

(b) Airflow.

Figure 5-3. - Interrelation of pressure distribution and local airflow velocity over an airfoil.

Bernoulli's Law

The relation between velocity and pressure is given in Bernoulli's law, which states that in a flow of incompressible fluid the sum of the static pressure and the dynamic pressure along a streamline is constant if gravity and frictional effects are disregarded. (For calculations involving low subsonic flow velocities, air may be considered to be incompressible.) The equation for Bernoulli's law is

$$P = p + \frac{1}{2}\rho V^2 = \text{Constant}$$

where P is the total pressure, p is the static pressure, and $\frac{1}{2}\rho V^2$ is the dynamic-pressure term, wherein ρ is the fluid density and V is the flow velocity. From Bernoulli's law it follows that where there is a velocity increase (dynamic-pressure increase) in a fluid flow, there must be a corresponding pressure decrease (i.e., a static-pressure decrease). Figure 5-4 illustrates Bernoulli's law as it applies to airflow within

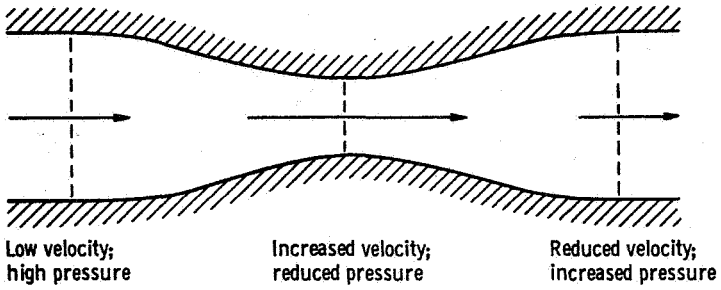

Figure 5-4. - Bernoulli's law applied to airflow within a venturi.

a venturi. At the venturi inlet, the velocity is relatively low and the static pressure is relatively high. In the throat region of the venturi, where the velocity increases, the pressure decreases in accordance with Bernoulli's law. (The principle of flow acceleration in a venturi is discussed in chapters 6 and 7.) Finally, at the venturi exit the velocity decreases and, therefore, the pressure increases.

Perhaps Bernoulli's law is more easily understood if it is considered as representing a special form of the principle of the conservation of energy, illustrated in figure 5-5. The total mechanical energy of the rolling ball shown in this figure corresponds to the total pressure of the fluid flow of Bernoulli's law, the potential energy corresponds to the static pressure, and the kinetic energy corresponds to the dynamic pressure. Thus, the total mechanical energy of the ball is the sum of its potential energy and its kinetic

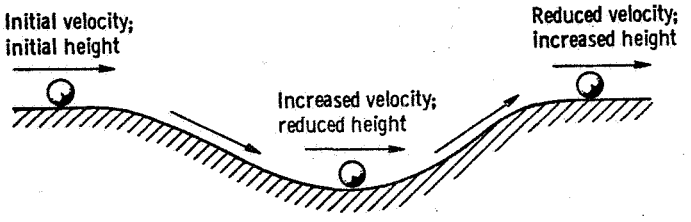

Figure 5-5. - Principle of conservation of energy. (Velocity represents kinetic energy; height represents potential energy.)

energy. If the ball is assumed to roll without friction, the total mechanical energy remains constant (conservation of energy) regardless of the relative magnitudes of the potential and kinetic energies.

As the ball rolls along a level surface at a constant velocity, the potential and kinetic energies are both constant. When the ball starts to roll down a slope, the velocity and kinetic energy begin to increase, and the height and potential energy begin to decrease. At the bottom of the slope, the velocity and kinetic energy are maximum, and the height and potential energy are minimum (or zero). The bottom of the slope of this example corresponds to the venturi throat of the previous discussion, where the flow velocity (dynamic pressure) is maximum and the static pressure is minimum. As the ball rolls up the next slope, the velocity (kinetic energy) decreases, and the height (potential energy) increases. Throughout these changes in the potential and kinetic energies, the total mechanical energy of the ball remains constant, just as the total pressure of the fluid flow in Bernoulli's law remains constant.

Airflow Over Airfoil Surfaces

Of course, Bernoulli's law alone does not explain the lift of an airfoil. Because of the profile of an airfoil and the angle of attack, the air that flows over the top surface of an airfoil must follow a longer, more indirect path (see fig. 5-3(b)) than does the air that flows along the bottom surface. (On a propeller blade, the "top" surface is the upstream face, or camber face, and the "bottom" surface is the downstream face, or thrust face.) The air that flows along the longer path must speed up so that behind the airfoil it can rejoin the stream of air flowing along the shorter path. Therefore, according to Bernoulli's law, the pressure on the top surface of the airfoil becomes lower than the pressure on the bottom surface. This pressure difference is the basis of the lift of an airfoil (or the thrust of a propeller blade). In fact, the lift of an airfoil is directly proportional to the dynamic pressure of the airflow, which is a function of the velocity $\left(\text{dynamic pressure} = \frac{1}{2}(\text{density})(\text{velocity})^2\right)$.

The velocity of the local airflow relative to the surface, particularly the top surface, of an airfoil (therefore, the lift or thrust of the airfoil) depends on the profile, or shape, of the airfoil, the angle of attack, and the velocity with which the airfoil meets the airstream (i.e., the relative-wind velocity).

Airfoil Profile and Angle of Attack

The profile and the angle of attack of an airfoil determine how much the air flowing

over the top surface of the airfoil must detour from the path of the air flowing along the bottom surface. The extent of this detour, in turn, determines the increase in the velocity of the local airflow along the top surface over the velocity of the local airflow along the bottom surface.

The effective profile of a wing can be changed during flight by the use of certain types of flaps. The profile of a propeller blade, however, cannot be changed during operation.

The angle of attack of an airfoil is the acute angle between the chord line of the airfoil and the direction of the relative wind. On most aircraft the wing is mounted immovably to the fuselage. Therefore, the wing angle of attack of an aircraft in flight is normally changed by changing the pitch attitude of the aircraft. (On some aircraft the leading edge of the wing can be raised and lowered to change the wing angle of incidence and, therefore, the wing angle of attack. The wing angle of incidence is the acute angle between the wing chord line and the longitudinal axis of the aircraft.) The angle of attack of a propeller blade can be changed by changing the rotational speed (rpm) of the propeller, the forward velocity of the aircraft, or the pitch of the propeller blade.

Relative Wind

For a simplified analysis of a wing, the velocity of the relative wind may be assumed to be the forward velocity V of the aircraft (fig. 5-6(a)). For a more precise analysis,

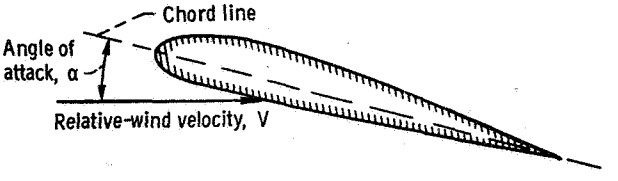

(a) Induced flow (downwash) velocity not included.

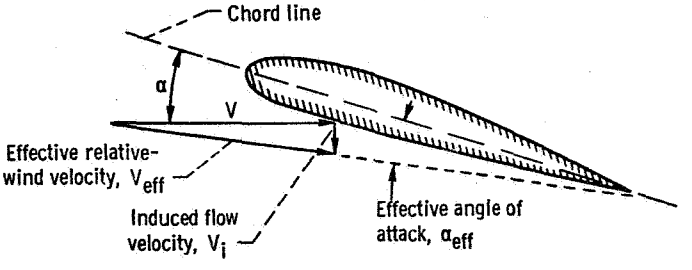

(b) Induced flow (downwash) velocity included.

Figure 5-6. - Relative wind velocity for a wing.

however, the velocity of the induced flow (downwash) due to the tip vortex (discussed in chapter 4) must also be considered. Thus, the actual effective relative-wind velocity V_{eff} (fig. 5-6(b)) is the resultant of the forward velocity V and the induced-flow velocity V_i. (The resolution of vector quantities, such as velocities, is discussed in chapter 4.)

The relative wind of a propeller blade is more complex than that of a wing, because a propeller has rotational motion as well as forward motion. For a simplified analysis, the relative-wind velocity at any segment of a propeller blade (fig. 5-7(a)) may be assumed to be the resultant velocity V_R of the forward velocity V and the linear velocity $2\pi rn$ due to rotation. (In the term for the velocity due to rotation, r is the radius from the axis of rotation to the blade segment, and n is the rotational speed.) For a more precise analysis of a propeller blade, just as for a wing, the induced-flow velocity must be taken into account. Therefore, the actual effective relative-wind velocity V_{eff} (fig. 5-7(b)) for any segment of a propeller blade is the resultant of the forward velocity V, the linear velocity due to rotation $2\pi rn$, and the induced-flow velocity V_i.

The linear velocity $2\pi rn$ in the plane of rotation is much less at the blade root than

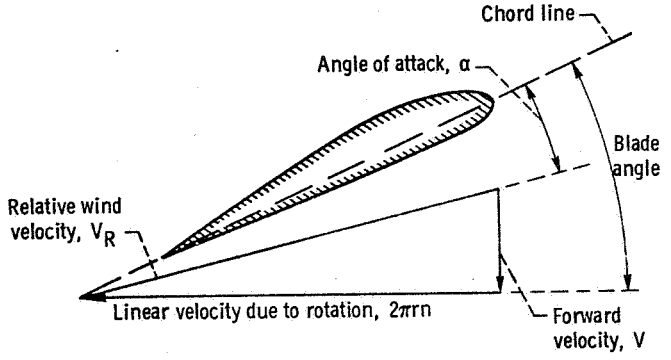

(a) Induced flow velocity not included.

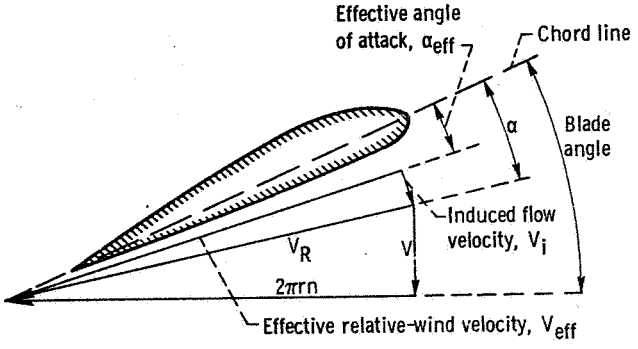

(b) Induced flow velocity included.

Figure 5-7. - Relative-wind velocity for a propeller blade.

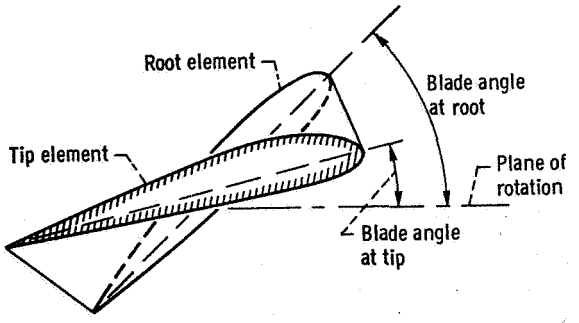

Figure 5-8. - Blade twist.

at the blade tip. Therefore, the relative wind at the root sections is almost parallel to the axis of rotation, while at the tip it is nearly perpendicular to this axis. To obtain an efficient angle of attack at all points along the blade, the blade is twisted (fig. 5-8) so that the blade angle at the root is large, while at the tip the angle is quite small.

The rotational speed of a propeller (and therefore the relative wind) is normally limited by the blade-tip speed's approaching the speed of sound. As this limit is approached, high tip losses occur. Tip loss is the loss of lift at the tip of an airfoil because of the tip vortex (discussed in chapter 4). Also, when the blade tip approaches sonic velocity, shock waves can cause severe vibrations, which, in turn, can damage or destroy the propeller. (The cause and the effects of shock waves are discussed in chapter 11.)

Lift and Drag - Thrust and Torque

On an aircraft wing, the relative wind produces a force vector R which can be resolved into components perpendicular and parallel to the relative wind (fig. 5-9); the perpendicular component is lift, and the parallel component is drag. On a propeller blade, the force vector R produced by the relative wind is resolved into components perpendi-

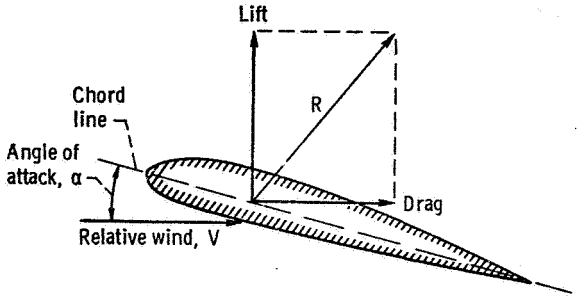

Figure 5-9. - Resolution of the total aerodynamic force acting on a wing into lift and drag components.

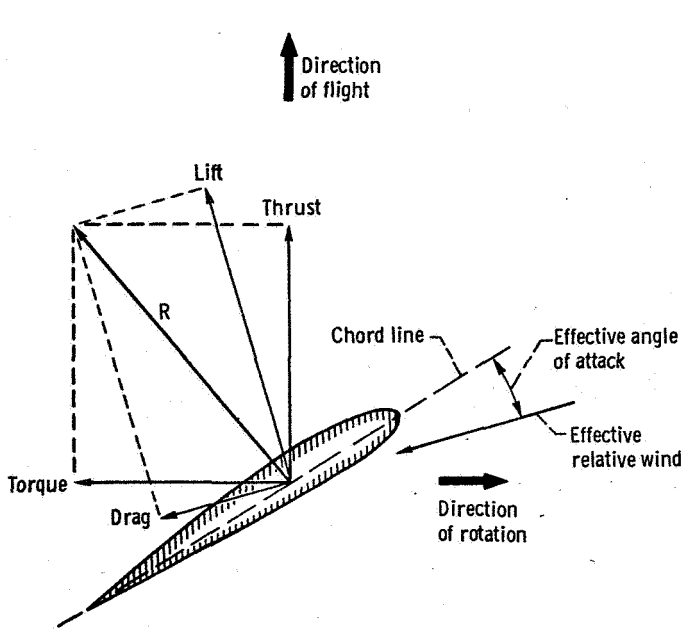

Figure 5-10. - Resolution of the total aerodynamic force acting on a propeller blade into thrust and torque components.

cular and parallel to the plane of rotation (fig. 5-10); the perpendicular component is thrust, which propels the aircraft forward, and the parallel component is torque, which counteracts the engine torque. (Note that fig. 5-10 also shows the lift and drag for the propeller blade.)

Aerodynamic Efficiency

The efficiency of a wing is measured by its lift-to-drag ratio (discussed in chapter 4). It was explained earlier that lift is a function of the angle of attack. However, drag is also a function of the angle of attack. (Drag increases with increasing angle of attack.) Therefore, the most efficient angle of attack for a given wing is that angle which provides the maximum lift-to-drag ratio. Since the effect of the relative wind on a propeller blade is resolved into thrust and torque components, the efficiency of a propeller is measured by the ratio of the thrust power produced by the propeller to the torque power supplied by the engine. Thus, the most efficient angle of attack for a given propeller blade is the angle at which this ratio is maximum.

At a constant rotational speed (rpm), the most efficient, or desirable, angle of attack can be maintained by varying the blade pitch to compensate for the effects of variations in the forward velocity. However, variations in the forward velocity (and in the angle of attack) affect not only the efficiency of the propeller but also the load on the engine. That is, a change in the angle of attack causes a change in the engine torque power required to

turn the propeller. This variation in the load, in turn, causes a variation in the rpm. It is usually desirable to operate an aircraft engine at some specific rpm that will provide the required power at a satisfactory rate of fuel consumption with a safe margin of engine reliability. Therefore, the blade pitch of a controllable-pitch propeller is normally varied to maintain a specific rpm for most efficient engine operation rather than to maintain a specific angle of attack for most efficient propeller operation. However, a propeller is always matched to the engine to provide maximum thrust from the available engine power. Thus, by varying the blade pitch it is possible to maintain an efficient engine speed, without seriously degrading the aerodynamic efficiency of the propeller as its angle of attack is changed.

THEORETICAL PERFORMANCE OF A PROPELLER

So far, we have explained the principles by which a propeller blade or blade segment produces thrust. Now we shall briefly consider the three commonly used theories for calculating the total thrust of the entire propeller.

Momentum Theory

A propeller produces thrust by slicing into the air and accelerating it rearward in a long slipstream. As the propeller forces the air mass rearward, a reaction force (thrust) is produced in the forward direction, in accordance with Newton's laws of motion. The more air the propeller pushes back each second, the greater is the thrust.

The momentum theory assumes that a rotating propeller is composed of an infinite number of blades and can, therefore, be replaced physically by an actuator disk. This actuator disk is assumed to be capable of producing a uniform change in velocity (in the axial direction) of the air stream passing through it, without any air losses at the periphery of the disk (i.e., at the blade tips). Furthermore, the air being accelerated through the disk is assumed to be a perfect, incompressible, nonviscous fluid. The airstream flowing through the disk is assumed to be irrotational. Thus, the energy of the flow in front of and behind the disk (but not through the disk itself) is considered constant, with no energy lost because of rotation.

As the air stream approaches the face of the disk, the velocity increases from the original free-stream velocity, and the pressure decreases from the original free-stream pressure. The velocity continues to increase as the flow passes through the disk. However, the pressure at the disk suddenly increases by twice the amount that it had decreased in front of the disk. Thus, as the flow leaves the disk, the pressure is higher

than the free-stream pressure. Downstream of the disk, the pressure decreases again to the free stream value, while the velocity increases. According to the momentum theory, one-half the velocity increase occurs in front of the disk and one-half behind the disk. (Note that Bernoulli's law does not hold for flow through the disk, but it does hold for the flow in front of and behind the disk.)

The momentum theory is useful for illustrating the type of flow produced by a propeller, and it can be used to calculate the maximum theoretical thrust of a propeller. However, this theory is of limited use in propeller design work, because it does not account for energy lost in slip-stream rotation, profile drag losses, losses due to nonuniform thrust along the blade, blade-interference losses, and losses due to increased drag and changes in flow at speeds where air becomes compressible.

Blade-Element Theory

The blade-element theory for calculating the performance of a propeller is more accurate than the momentum theory, because it takes into account the rotational speed, blade twist, blade airfoil section, and number of blades.

This theory considers any element of a propeller blade as a small wing and assumes that each element acts independent of the other elements. This theory further assumes that the induced-flow velocity for each, or any, element is the same as for a wing of a given aspect ratio (usually 6).

First, the thrust and torque for individual elements (with the assumed induced flow velocity) are calculated. Then, these thrust and torque values obtained for individual elements are summed (added together) to obtain the total thrust and the total torque for the entire propeller.

Although the blade-element theory is useful for preliminary claculations, it is still not sufficiently precise, because it merely assumes a certain induced-flow velocity and it ignores tip losses and blade interference losses.

Vortex Theory

In principle, the vortex theory is very similar to the blade-element theory. However, with the vortex theory the induced-flow velocity for each blade element is actually calculated, rather than assumed to be the same as produced by a wing of aspect ratio 6.

The calculated thrust and torque values obtained with the vortex theory closely approximate the actual values, even though this theory also ignores tip losses and blade-interference losses. More exact theories, which account for these losses, have been developed, but these theories are beyond the scope of this chapter.

TYPES OF PROPELLERS

A propeller is commonly classified according to its means of pitch control, its configuration, or its location on the engine. These general bases for classification result in many specific types of propellers. The following are just a few of these types.

The fixed-pitch propeller is one that has a certain built-in blade pitch, or blade angle, which cannot be changed. The principal advantages of this type of propeller are simple construction (usually a single piece of wood or aluminum), low weight, and low cost. The main disadvantage of this type is that it is designed to provide maximum efficiency at only one specific operating condition.

The adjustable-pitch propeller is one whose blade angle may be varied only while the propeller is at rest. Thus, this propeller may be adjusted (on the ground) to provide maximum efficiency at any one specific operating condition.

A controllable-pitch propeller is one whose blade angle may be changed by remote control from the cockpit while the propeller is rotating. This enables the pilot to select the most efficient blade angles for the various operating conditions during the flight. In the simplest versions of this type of propeller, the blade angle is changed by mechanical means, such as a simple lever arrangement. In the more elaborate versions, the blade angle is changed by electrical and/or hydraulic means.

An automatic propeller is one that incorporates a control mechanism which automatically adjusts the blade angle for maximum efficiency for the varying operating conditions during flight. Various electrical, hydraulic, and mechanical devices are used to change the blade angle, or pitch angle, but all these devices depend on a centrifugal governor for primary control. The governor senses any changes in the engine speed and causes the pitch-changing mechanism to change the blade angle accordingly.

A feathering propeller is a controllable-pitch propeller whose blades can be rotated about their root-to-tip axes so that the blade chords can be oriented approximately parallel to the thrust axis or to the direction of airflow (blade angle approximately 90°). Feather-

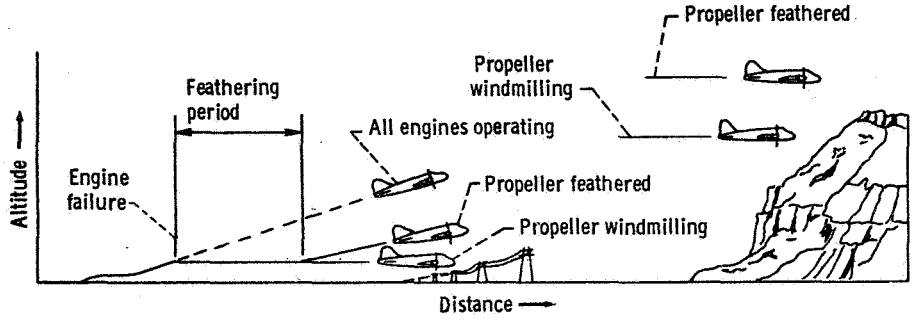

Figure 5-11. - Effect of propeller feathering on performance of multiengine aircraft with one engine inoperative.

ing the propeller of an inoperative engine prevents the propeller from windmilling and minimizes its drag. Thus, on a multiengine aircraft, feathering the propeller helps the aircraft to maintain a specific flight condition with the remaining operative engines (fig. 5-11) and reduces the asymmetric thrust.

A reversible-pitch propeller is a controllable-pitch propeller whose pitch, or blade angle, can be changed (during rotation) from positive to negative values so as to provide reverse thrust. This reverse thrust is used primarily to slow down the aircraft during the landing roll, thereby reducing the landing roll and the brake wear. Reverse thrust can also be used during a dive to prevent the airplane from exceeding the maximum speed that its structure can withstand safely.

A contrarotating propeller consists of two propellers mounted on concentric shafts, having a common drive, and rotating in opposite directions. A contrarotating propeller can absorb (and convert to thrust) more engine power than can a single propeller. Therefore, contrarotating propellers are used on engines that produce more power than can be absorbed by single propellers. The contrarotating propeller also provides some aerodynamic advantages over the single propeller. The slipstream from a single propeller rotates. This rotating slipstream strikes the surfaces of the aircraft from various angles and thereby increases the drag. Furthermore, the rotation of the propeller in one direction causes the airplane to tend to rotate in the opposite direction (torque reaction), thereby creating a control problem. With a contrarotating propeller both of these problems are eliminated, because the slipstream flows in a straight line and the torque reaction is neutralized. The main disadvantages of the contrarotating propeller are increased weight and complexity.

GLOSSARY

airfoil. An aerodynamic surface (such as an airplane wing or a propeller blade) designed to provide a useful reaction force when in motion relative to the surrounding air.

airfoil section. A cross section of an airfoil taken perpendicular to the span axis or root-to-tip axis of the airfoil. Also, the form or shape of an airfoil section.

angle of attack. The acute angle between the airfoil-section chord line and the relative wind velocity, measured in a plane perpendicular to the span axis or the root-to-tip axis of the airfoil.

blade (propeller). The thrust-producing and major torque-absorbing component of a propeller. It may be constructed integrally with a propeller hub, or it may be assembled in a propeller hub.

blade angle. The acute angle between the blade airfoil-section chord line and the plane of rotation.

blade axis. The root-to-tip axis about which the individual blade may rotate to change pitch.

blade element. A segment of a blade between two blade sections that are an infinitesimal distance apart.

blade root. That portion of the blade nearest the hub.

blade tip. The outermost extremity of the blade; the portion of the blade farthest from the hub.

chord. The straight line joining the leading and trailing edges of an airfoil; the length of that part of the chord line intercepted by the extremities of the leading and trailing edges of an airfoil section.

chord line. A straight line through the centers of curvature of the leading and trailing edges of an airfoil section. This line is generally used as the reference line from which the angles of the airfoil are measured.

disk area. The area of a circle having the same diameter as a given propeller.

induced flow. Flow drawn into a propeller disk by the vortex system of the propeller; the downwash on the top surface of an airfoil produced by the tip vortex.

thrust (propeller). That component of the total aerodynamic force acting on a propeller which is parallel to the axis of rotation. Positive thrust is in the direction of flight.

tip loss. A loss of lift or thrust at the tip of an airfoil due to the tip vortex.

tip speed. The linear speed of the blade tip of a propeller.

windmilling. The forced rotation of a propeller by the action of air flow through the disc area, which occurs when engine power is cut off suddenly.

BIBLIOGRAPHY

Anon.: Aircraft Propeller Handbook. Bull. ANC-9, Departments of Air Force, Navy, and Commerce, 1956.

Cargnino, Lawrence T.; and Karvinen, Clifford H.: Aircraft Propulsion Powerplants. Third ed., Educational Publishers, Inc., 1962.

Glauert, Hermann: The Elements of Aerofoil and Airscrew Theory. Second ed., Cambridge University Press, 1948.

Hurt, H. H., Jr.: Aerodynamics for Naval Aviators. Office of the Chief of Naval Operations, Aviation Training Division, 1960.

Jones, Bradley: Elements of Practical Aerodynamics. Third ed., John Wiley & Sons, Inc., 1942.

Nikolsky, Alexander A.: Helicopter Analysis. John Wiley & Sons, Inc., 1951.

6. AIRCRAFT PROPULSION

Robert W. Koenig*

The development of aircraft propulsion and the attendant technological advances have been a result of the interaction between economic and military needs. The history of aircraft propulsion began in the 15th century when screw propellers were first envisioned by Leonardo da Vinci. However, the actual need for a propeller did not arise until an engine was devised to drive it. The first successful mechanical flight of a piloted airplane (Wilbur and Orville Wright - 1903) used a screw propeller with a reciprocating engine for power. This type of system still serves well when flight speeds of less than approximately 350 miles per hour are suitable. When man sought to fly at higher speeds (originally for military reasons), a lighter and smaller power plant became essential. The jet engine answered this need. The world's first jet-propelled airplane was flown by the Germans in 1939. It is interesting to note that there was no incentive for developing a jet engine until the art of airplane design had advanced enough to make high-speed flight practical. As a matter of fact, the jet is not particularly attractive for low-speed flight. The propeller provided an essential first step without which we almost certainly would not have developed airplanes at all.

The first successful aircraft propulsion device was a steam engine designed by Henry Gifford; this engine powered a propeller for a dirigible balloon in 1851. Many different propulsion schemes have been used since then, but this chapter concerns only current aircraft propulsion systems and those of the near future. The engines considered are for use only in the atmosphere. They use the oxygen from this atmosphere (air) to combine with fuel for combustion. These engines are classified as airbreathing engines. Experimental aircraft exist that use rocket engines for propulsion (e.g., the X-15). Such an engine carries its own oxygen supply. However, this type of engine will not be considered herein.

INTERNAL-COMBUSTION, RECIPROCATING ENGINE

Four-Stroke Cycle of Operation

The reciprocating engine was originally the primary power source used to drive a

*Aerospace Engineer, Mission Analysis Branch.

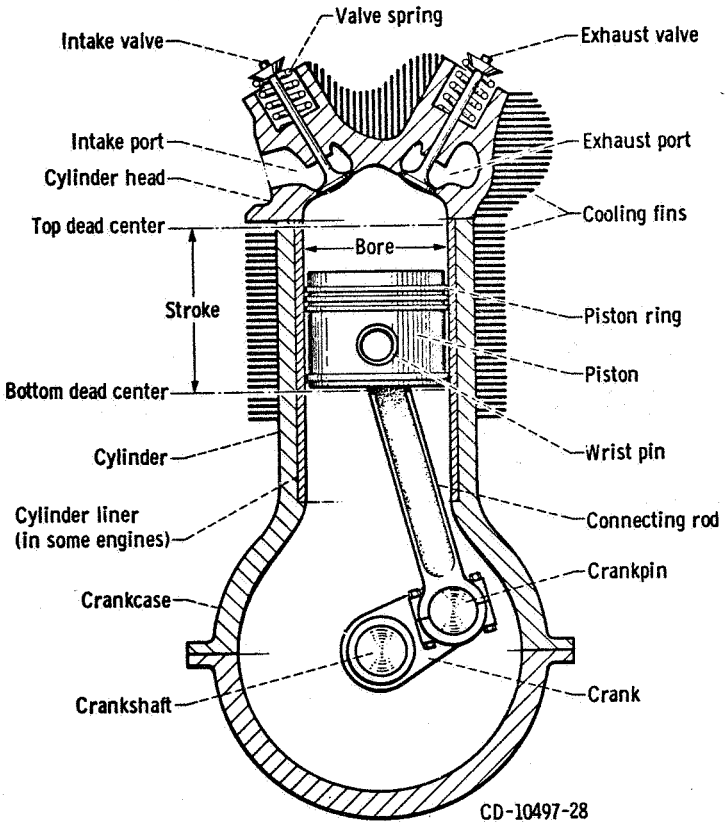

Figure 6-1. - Nomenclature of air-cooled, internal-combustion, reciprocating engine.

propeller. An internal-combustion, reciprocating engine has one or more cylinders in which the combustion of fuel takes place. Some of the principal parts and nomenclature of an air-cooled engine are shown in figure 6-1.

In general, a machine of any kind performing its function repeats over and over again a series of operations. The order in which these operations are performed is fixed, and all parts of the machine return to their original positions at the end of each series. One complete series of this kind is called a cycle.

Most reciprocating engines operate on what is known as a four-stroke cycle; that is, each cylinder requires four strokes of its piston, or two revolutions of the crankshaft, to complete the normal series of operations. There is also a two-stroke cycle, which is normally associated with smaller engines. This cycle is discussed later in the chapter, in the section on model-airplane engines.

The first four-stroke cycle, internal-combustion engine was built by Dr. N. A. Otto, a German, in 1876. Thus, the four-stroke cycle is also called the Otto cycle.

Figure 6-2 illustrates the four strokes (intake, compression, power, and exhaust) of the Otto cycle. The volume swept by the piston during one stroke is called the displacement volume of the cylinder. The volume remaining above the piston at top dead center is called the clearance volume.

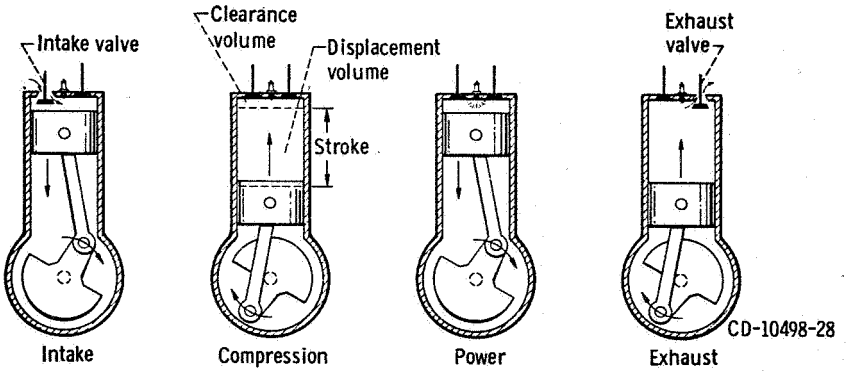

Figure 6-2. - Four-stroke cycle of operation of internal-combustion engine.

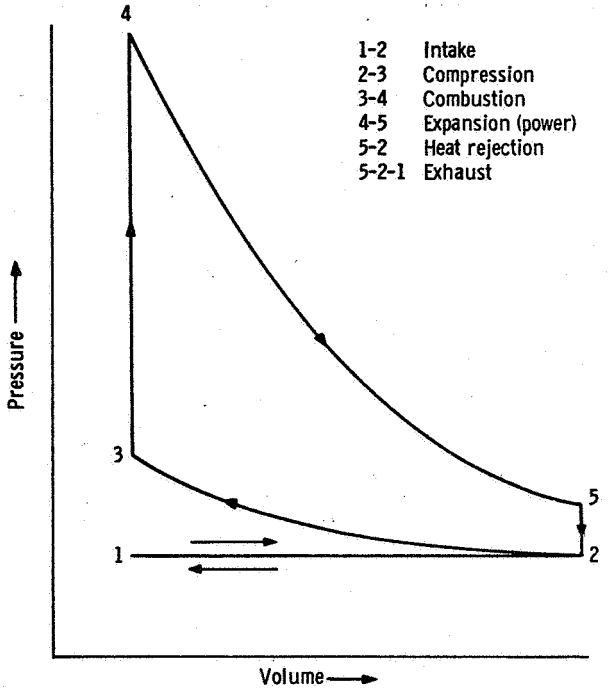

Figure 6-3. - Idealized pressure-volume diagram for cylinder of four-stroke-cycle (Otto cycle) engine.

Figure 6-3 shows a typical pressure-volume diagram for the gas in the cylinder of a four-stroke-cycle engine. The cycle starts with the intake stroke, when the piston is at top dead center (point 1 in fig. 6-3). The intake valve is open, the exhaust valve is closed, and the motion of the piston toward the bottom of the cylinder draws a mixture of fuel and air into the cylinder (line 1-2 in fig. 6-3). When the piston approaches the bottom, the intake valve closes.

The compression stroke (line 2-3) takes place with both valves closed while the piston returns to top dead center. During this stroke, the pressure in the cylinder rises

approximately 150 pounds per square inch. Just before the end of the compression stroke, the mixture is ignited by a spark from a spark plug, or by some other method, and combustion starts. Combustion (line 3-4) takes place very quickly, and the temperature may rise from 500° F to 3500° or 4000° F. The pressure in the cylinder also rises approximately 600 pounds per square inch.

The next stroke is called the power, or expansion, stroke (line 4-5 in fig. 6-3). The valves are still closed, and the hot, high-pressure gas drives the piston to bottom dead center. As some of the energy of the expanding gas is transferred to the piston, the gas becomes cooler, so the temperature in the cylinder at the end of the stroke may be about 2500° F and the pressure about 75 pounds per square inch (point 5 in fig. 6-3). The more the gases are allowed to expand, the more energy is transferred to the piston face and the less heat is rejected (line 5-2). The heat rejected refers to the wasted thermal energy that is removed by the cooling system or blown out the exhaust. In other words, with more expansion, less heat is rejected, and the engine cycle becomes more efficient. The extent of this expansion is approximated by the compression ratio:

$$\text{Compression ratio} = \frac{\text{(Clearance volume)} + \text{(Displacement volume)}}{\text{(Clearance volume)}}$$

This ratio is extremely important because of its effect on engine performance.

Near the bottom of the expansion stroke, the exhaust valve opens, and the piston sweeps the exhaust gas out through the open exhaust valve (line 5-2-1 in fig. 6-3). Then, a new cycle starts (point 1 in fig. 6-3).

Positive work is done by the engine only during the power stroke of the cycle. The energy required to keep the shaft turning during the intake, compression, and exhaust strokes is supplied in the form of momentum by a flywheel, or other mass, connected to the engine crankshaft. In a multicylinder engine, the power strokes are timed to overlap, so that the engine produces a steadier flow of power and a smaller flywheel can be used.

Efficiency Calculations

It is common practice in engineering to establish a figure of merit for a device by comparing its actual performance with the performance it would have under some arbitrary set of ideal conditions. The ratio of actual performance to ideal performance is called the efficiency of the device.

For internal combustion engines, one of the most important efficiencies is the thermal efficiency η_t. This efficiency is the ratio of the useful work done by the engine in a given time interval to the total chemical energy contained in the fuel that is burned during the same time interval.

$$\eta_t = \frac{\text{Work output}}{\text{Fuel-energy input}} \tag{1}$$

$$= \frac{W}{e_c \times w_f} \tag{2}$$

where

W work

e_c chemical energy per pound of fuel

w_f pounds of fuel

The output and input may be measured over any convenient interval such as 1 cycle or 1 minute. Both output and input energies must be expressed in the same kind of units, since η_t is a number without units.

Power Calculations

Power is the rate of doing work. It is generally useless to do a certain amount of work unless it can be done within a reasonable length of time. When work is done at a rate of 33 000 foot-pounds per minute, the quantity of power being produced is known as 1 horsepower. Therefore,

$$hp = \frac{W/min}{33\ 000} \tag{3}$$

From equation (2),

$$W = w_f \times e_c \times \eta_t \times J \tag{4}$$

where J is the mechanical equivalent of heat (a conversion factor) and has a value of 778 foot-pounds per Btu. Then,

$$hp = \frac{(w_f/min)\ J \times e_c \times \eta_t}{33\ 000} \tag{5}$$

The power of an engine depends on the rate at which chemical energy is supplied to the engine (Btu/min) and on the efficiency (η_t) with which the chemical energy supplied is

converted into work output.

The power of an engine can be calculated by first determining the mean effective pressure within a cylinder. This mean effective pressure, in turn, can be determined from the pressure-volume diagram, as will be explained later.

The effective pressure acting against the piston face (top of piston) at any instant during the power stroke is the difference between the downward pressure on the piston face and the upward pressure on the bottom of the piston. This effective pressure varies throughout the power stroke. The average of this effective pressure is called the mean effective pressure (mep).

Work, which is the transfer of energy, is produced when the point of application of a force moves along the line of action of the force. The quantity of work is the product of the force F and the linear displacement L of its point of application in the line of action.

$$W = F \times L \tag{6}$$

The force F is the force (lb) on the piston face. This force is the product of the mean effective pressure mep (lb/in.^{2}) and the area of the piston face A_p (in.^{2}).

$$F = \text{mep} \times A_p \tag{7}$$

The distance L in the work equation is the distance (in.) that the piston travels in the cylinder during one full stroke. Therefore, the work produced in one cylinder during one cycle is given by the equation

$$W = \text{mep} \times A_p \times L \qquad \text{(in.-lb)} \tag{8}$$

But the product of the piston-face area A_p and the stroke L is the displacement volume V_d of the cylinder.

$$V_d = A_p \times L \tag{9}$$

Therefore,

$$W = \text{mep} \times V_d \qquad \text{(in.-lb)} \tag{10}$$

or

$$\text{mep} = \frac{W}{V_d} \tag{11}$$

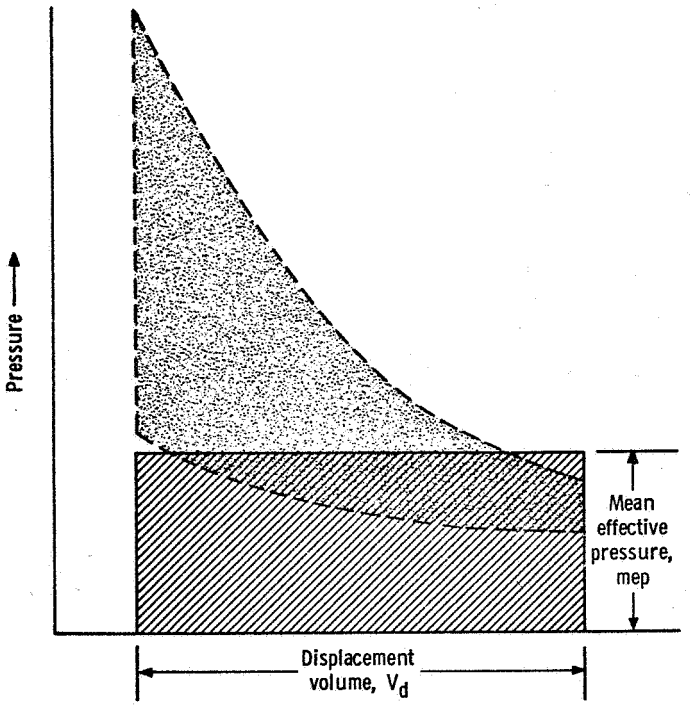

Figure 6-4. - Relation of mean effective pressure to pressure-volume diagram. (Area of rectangle is equal to area within pressure-volume diagram.)

Figure 6-4 illustrates the relation of the mean effective pressure to the pressure-volume diagram. The rectangle in the figure is a simplification of the pressure-volume diagram. The area of the rectangle is the same as the area enclosed within 2-3-4-5-2 in figure 6-3, and the length of the base of the rectangle (displacement volume) is equal to the line 1-2 in figure 6-3. Therefore, the height of the rectangle is the average pressure, or the mean effective pressure.

It has already been shown that the work produced in an engine cylinder during one cycle is the product of the mean effective pressure and the displacement volume. Thus, the area of the rectangle (mep $\times$ V_d) or the area of the pressure-volume diagram represents the work of the cylinder. The mean effective pressure, therefore, can be determined by dividing the area of the pressure-volume diagram by the displacement volume.

As shown in figure 6-5, the pressure-volume diagram of an actual engine cycle is somewhat different from that of the ideal Otto cycle. For the ideal cycle, the work of the cylinder is represented by the area within the dashed line 2-3-4-5-2 in figure 6-5. For an actual cycle, the net useful work is represented by the net positive area of the pressure-volume diagram. The net positive area is the positive area within the solid line 2-3-4-5-2 minus the negative area within the solid line 1-2-1. The positive area represents the total work produced in the cylinder. The negative area represents the work required to draw the fuel-and-air mixture into the cylinder (intake) and to discharge

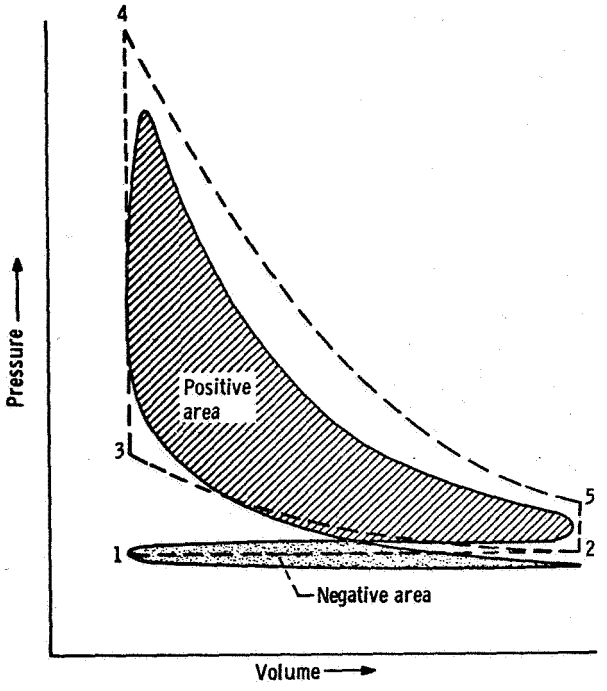

Figure 6-5. - Comparison of pressure-volume diagrams of ideal and actual Otto cycles. (Positive area of diagram of actual cycle represents total work produced in cylinder; negative area represents work expended in drawing fuel-air mixture into cylinder and in discharging exhaust gases from cylinder.)

the products of combustion from the cylinder (exhaust). Thus, for an actual cycle, the mean effective pressure is obtained by dividing the net positive area of the pressure-volume diagram by the displacement volume.

The equation for horsepower was presented earlier in this chapter.

$$hp = \frac{W/min}{33\ 000} \tag{3}$$

From equation (10), the total work produced by the engine W_E in 1 minute is

$$\frac{W_E}{min} = mep \times V_d \times cpm \times n \tag{12}$$

where cpm is the number of cycles per minute, and n is the number of cylinders. The horsepower of the engine hp_E is then given by the equation

$$hp_E = \frac{mep \times V_d \times cpm \times n}{33\ 000 \times 12} \tag{13}$$

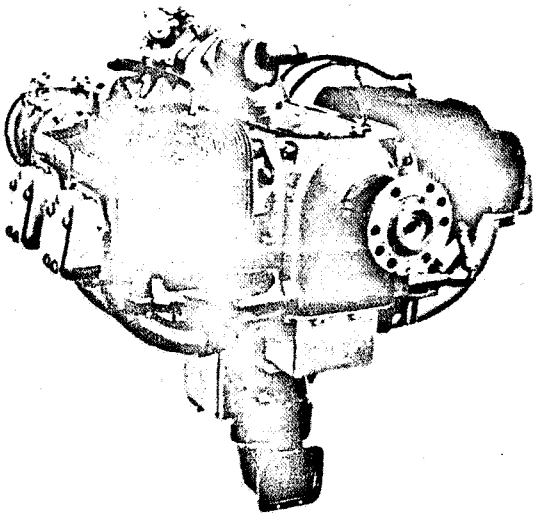

(a) Opposed-cylinder engine (4 cylinders, air cooled).

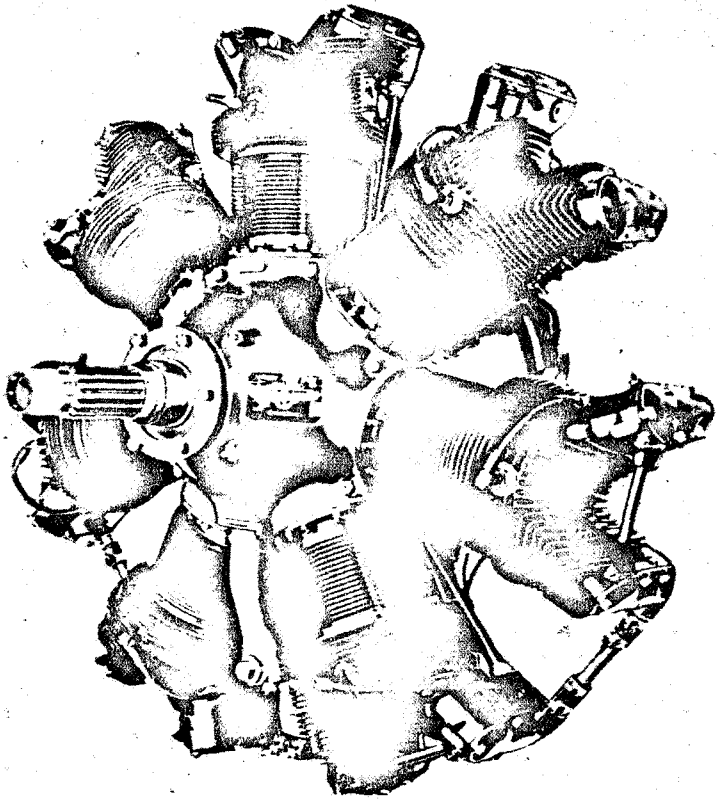

(b) Radial engine (7 cylinders, air cooled).

Figure 6-6. - Reciprocating engines.

where 12 is the factor for converting the denominator from foot-pounds to inch-pounds. This conversion is necessary because the numerator is in inch-pounds (see eqs. (8) and (10)).

Engine Types

Reciprocating engines are commonly classified according to their cylinder arrangements. An in-line engine has its cylinders arranged in a straight line parallel to the crankshaft. Such a line, or row, of cylinders is called a bank. A V-engine has two, a Y-engine has three, and an X-engine has four banks of cylinders so arranged that they resemble, in an end view of the engine, the respective letter. An opposed-cylinder engine (fig. 6-6(a)) has two banks of cylinders on opposite sides (180° apart) of the crankshaft. In this configuration, the axes of the cylinders are usually in the horizontal plane. A radial engine (fig. 6-6(b)) has its cylinders arranged radially around the crankshaft, like the spokes of a wheel. The radial engine is the most popular reciprocating engine for aircraft, because it has a relatively short, stiff crankshaft and a compact crankcase. The frontal area of the radial engine is relatively large, however. Small in-line engines are usually air-cooled, and large in-line engines are usually water-cooled. Radial engines are almost always air-cooled.

JET ENGINES

Gas-Turbine Engines

A gas-turbine engine is essentially a compressor-combustor-turbine combination which provides a net useful shaft-torque output and/or a useful supply of hot, high-pressure exhaust gases. The method used to harness the shaft torque and/or the energy of the exhaust gases to provide thrust determines whether the gas-turbine engine is a turbojet, turbofan, or turboprop engine.

Brayton cycle of operation. - The gas-turbine engine operates on a thermodynamic cycle known as the Brayton cycle. In the ideal Brayton cycle, air is compressed, heated at constant pressure, expanded, and finally cooled at constant pressure. Actually, the cooling phase is an open part of the cycle; that is, the hot air is exhausted, and a fresh charge of cool air is drawn in to be compressed.

Figure 6-7 is an idealized pressure-volume diagram of a gas-turbine engine. This figure illustrates the Brayton cycle of operation and the interrelation of the compressor work and the turbine work of the engine. In the ideal cycle, air enters the compressor at atmospheric pressure (line 1-2 in fig. 6-7), is compressed (line 2-3), and is discharged into the combustor (line 3-4). The area within 1-2-3-4-1 represents the work consumed in the compression (i.e., the work required to drive the compressor). In the combustor,

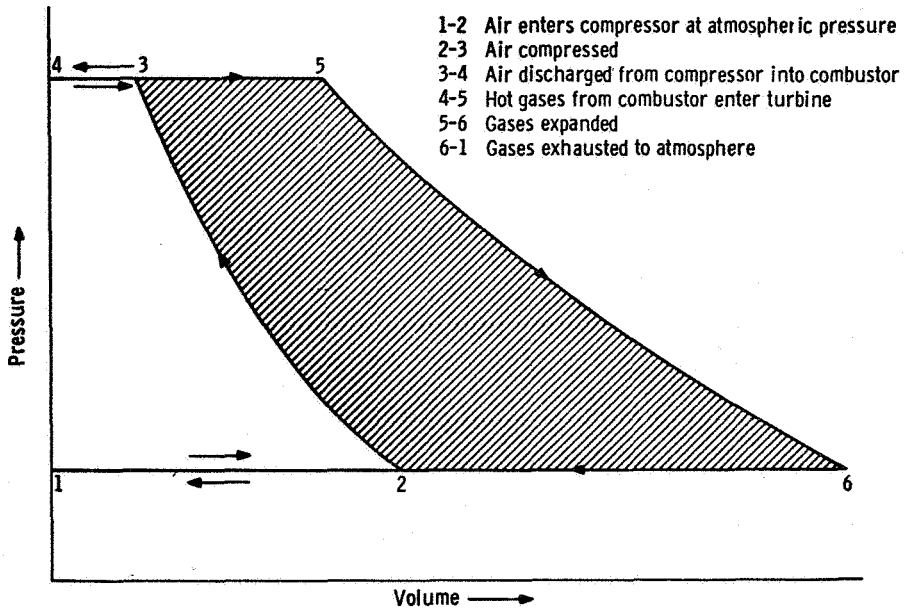

Figure 6-7. - Idealized pressure-volume diagram for Brayton cycle of operation of gas-turbine engine. (Shaded area represents net useful work output of engine.)

the air is mixed with fuel, and the mixture is burned at constant pressure. During this constant-pressure heating, the original volume of air entering the combustor (line 3-4) becomes a larger volume of hot combustion gases that enters the turbine (line 4-5). This increase in volume of the working gas during combustion enables an ideal turbine to produce more work than an ideal compressor consumes. Next, the hot combustion gases are expanded (line 5-6) to ambient pressure. The gases may be nearly fully expanded in the turbine to produce shaft power, or they may be partially expanded in the turbine, to produce some shaft power, and partially in an exhaust nozzle to produce a high-velocity exhaust stream. After expansion, the gases are exhausted to the atmosphere (line 6-1) at ambient pressure. This total cycle of operation is continuous, so that fresh air is continuously entering the engine while exhaust gases are continuously being discharged.

The total work produced by the engine is represented by the area 4-5-6-1-4 in figure 6-7. The work required by the compressor is represented by the area 1-2-3-4-1. Therefore, the net useful work output of the engine is represented by the area 2-3-5-6-2.

A schematic diagram of a basic gas-turbine engine is shown in figure 6-8(a). The compressor is essentially a gas pump and is generally classified as either a centrifugal-flow or an axial-flow compressor. The present discussion concerns only axial-flow compressors. The axial-flow compressor is made up of a multiplicity of stages. Each stage consists of a rotating element (rotor) and a stationary element (stator). Each element is circular and has blades mounted radially on its periphery. The gas flows through these stages in a generally axial direction, and the pressure of the gas rises in each stage.

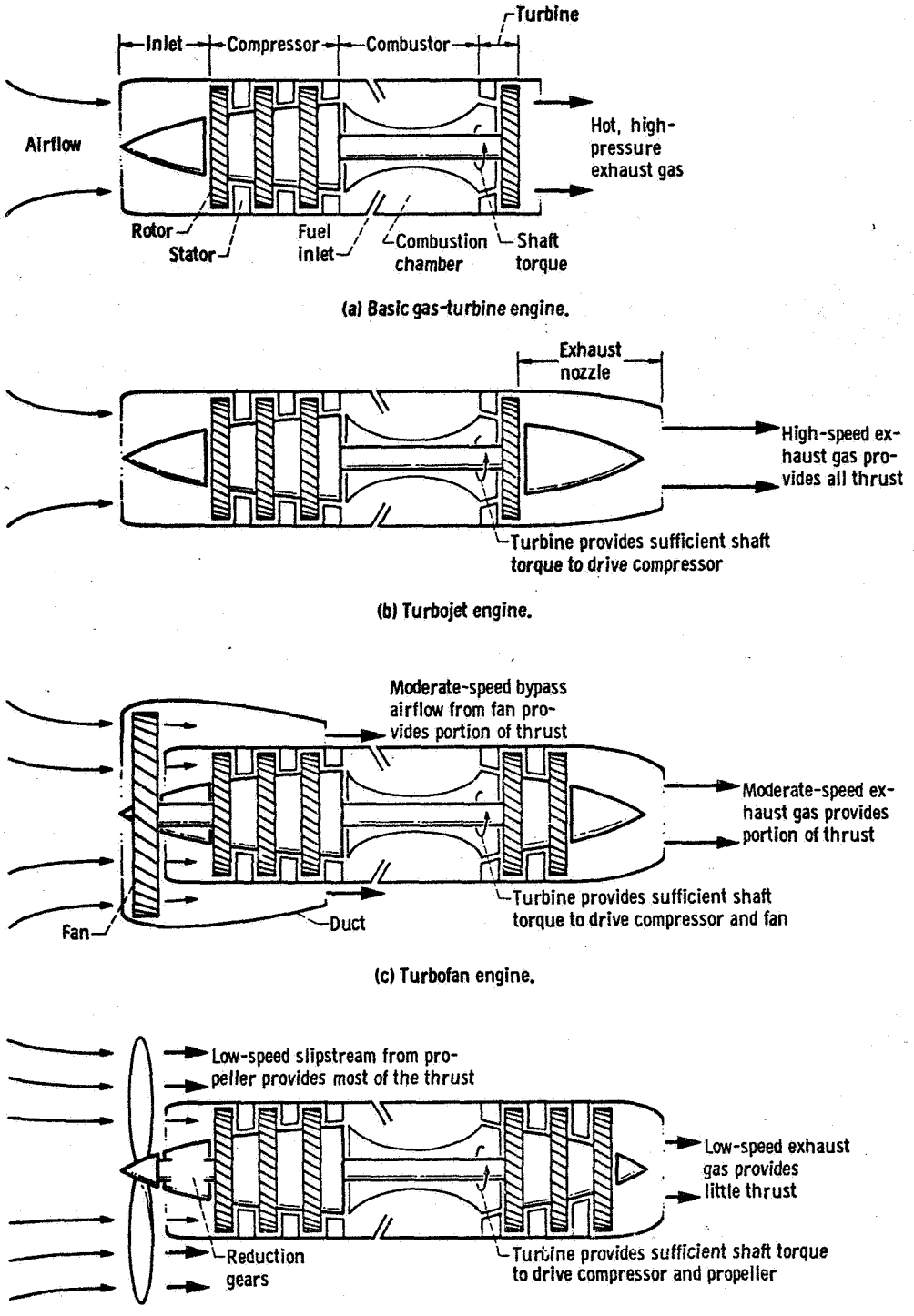

Figure 6-8. - Schematic diagrams of gas-turbine engines.

The rotor blades increase both the velocity and the pressure of the gas. The stator blades reduce the velocity of the gas and thereby convert its kinetic energy into pressure. The high-pressure gas from the compressor is mixed with fuel (kerosene or gasoline) and burned in the combustor. The high-pressure, high-temperature gas is then expanded through the turbine, which drives the compressor and provides a net useful shaft power. In certain types of gas turbine engine, the gas is further expanded through a nozzle to provide a high-velocity exhaust stream.

Turbojet engine. - In a turbojet engine, shown schematically in figure 6-8(b), the gases are partially expanded in the turbine only to provide sufficient shaft power to drive the compressor and accessories. The turbojet engine achieves its thrust by expanding and accelerating the hot gas in a nozzle (i.e., by imparting high momentum to a fluid).

Turbofan engine. - The turbofan (or bypass) engine (fig. 6-8(c)) is a turbojet that has a fan as an additional compressor, along with a duct for the cold air which bypasses the basic gas-turbine engine. To drive the fan, an additional turbine is required, wherein the gas from the combustor is further expanded. Thus, lower velocity exists in the nozzle, since the gas has less available energy to be converted to velocity. However, the large fan enables the engine to draw in more air. Thus, the turbofan engine produces thrust by a combination of high airflow and moderate exhaust velocities.

Turbopropeller engine. - The turbopropeller engine (fig. 6-8(d)) has a propeller driven by a substantially enlarged turbine by means of gears. Nearly all the available gas energy is used in the turbine to drive the propeller. The airflow that the propeller accelerates produces nearly all the thrust for this engine type, with very little nozzle expansion occurring for additional thrust.

Obviously, all these engines are adaptations of the basic gas-turbine engine. Some examples of these various types of gas-turbine engines are shown in figure 6-9.

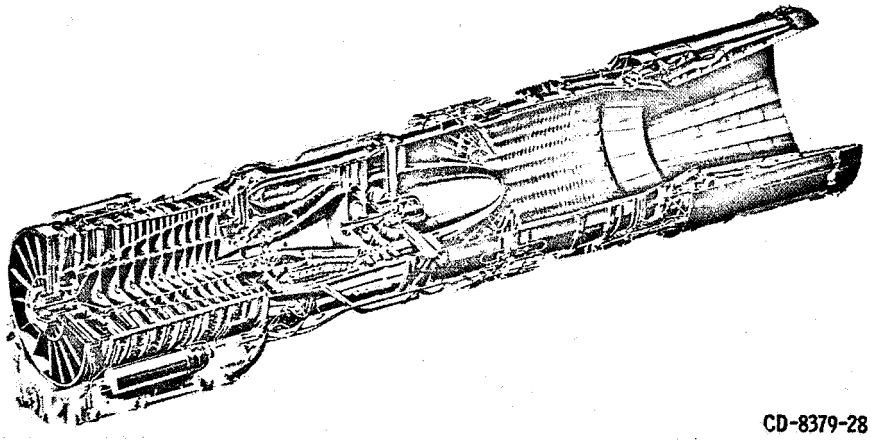

CD-8379-28

(a) Turbojet engine with afterburner. (General Electric YJ93-GE3.)

Figure 6-9. - Cutaway views of typical gas-turbine engines.

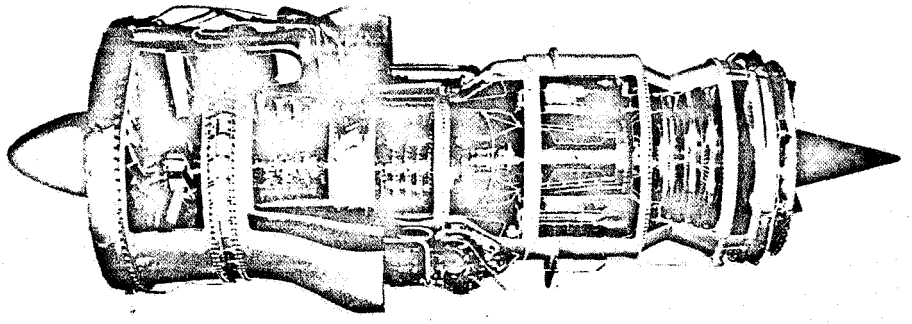

(b) Turbofan engine with forward fan. (Pratt & Whitney JT3D-3B.)

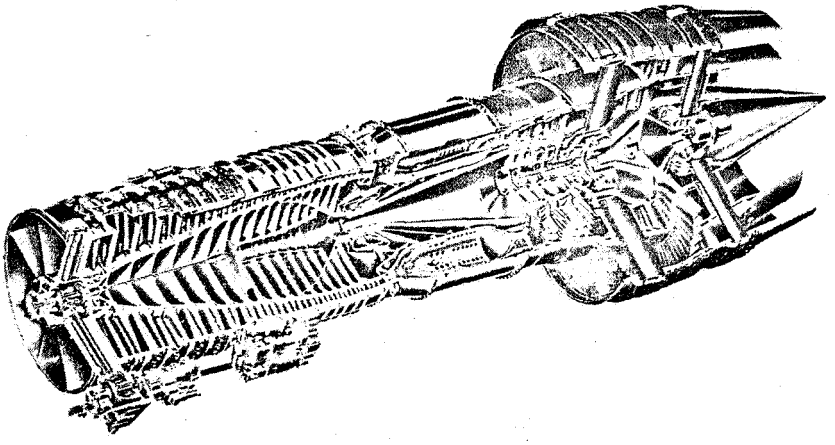

(c) Turbofan engine with aft fan. (General Electric CJ805-23B.)

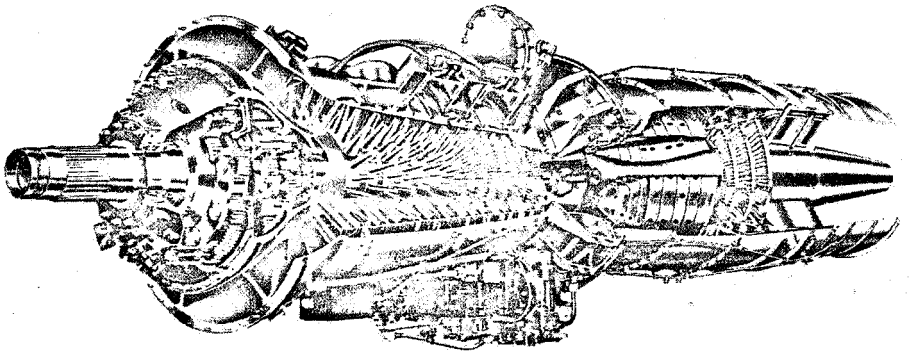

(d) Turbopropeller engine. (Pratt & Whitney T34-P-9W.)

Figure 6-9. - Concluded.

Ramjet Engines

The ramjet (fig. 6-10) is the simplest of all airbreathing engines; it consists of a diffuser, a combustion chamber, and an exhaust nozzle. In the diffuser, the pressure rises as the incoming air is decelerated from flight speed to a relatively low speed (Mach 0.1 to 0.3) before it enters the combustion chamber. The air entering the diffuser is compressed by the ramming action caused by the engine's high forward speed. The air is then mixed with fuel and burned in the combustion chamber. The hot combustion gases are then expelled through the nozzle. Since the incoming air is decelerated to such a low speed, a ramjet can operate at subsonic speeds, but it cannot operate under static conditions (i.e., it cannot develop takeoff thrust). The increased pressure rise occurring in the diffuser at increased flight speeds renders the ramjet more suitable for supersonic flight.

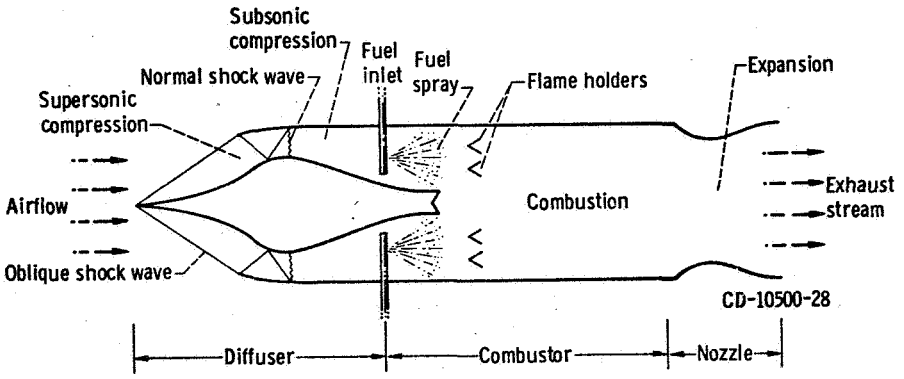

(a) Schematic diagram.

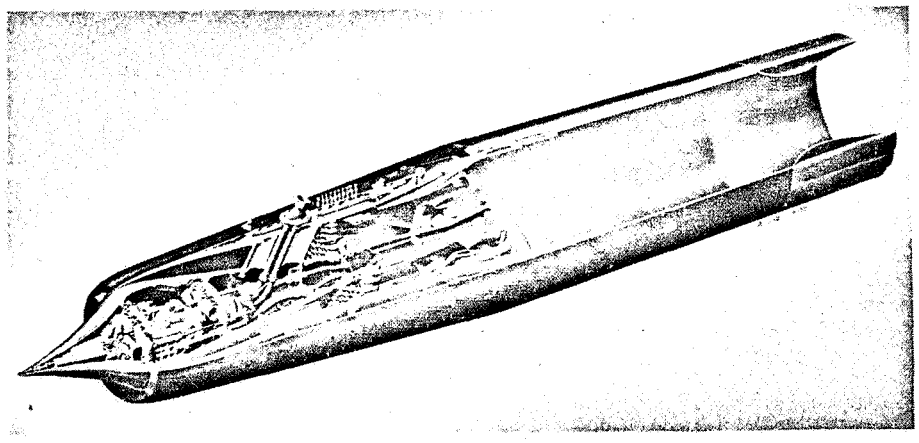

(b) Cutaway view. (Courtesy of Marquardt Corp.)

Figure 6-10. - Ramjet engine.

Another type of ramjet engine currently being considered is the supersonic-combustion ramjet. This type of engine does not diffuse and decelerate the air to subsonic speeds. Therefore, the pressure losses resulting from the deceleration of the air in the inlet are not as great in this engine as in the previously discussed ramjet. The supersonic-combustion ramjet, which is still very much in a research status, is usually associated with flight speeds between Mach 6 and 25. Because of aerodynamic heating associated with very high speeds in the atmosphere, the major limitation of this type of engine is the temperature limit of its structure.

AIRCRAFT PROPULSION TECHNIQUES OF THE FUTURE

Aircraft propulsion technology is advancing continually. Engines are being developed to meet the need for aircraft capable of flying faster, farther, and higher. Schemes will be developed to use more efficiently the gas energy in gas-turbine engines.

Already being considered are aircraft engines that use a nuclear reactor to heat the compressed air, thereby enabling the range to be unlimited by fuel requirements. High-energy fuels such as natural gas (methane) or hydrogen may be used in future generations of engines. Continuing research in all areas of aircraft propulsion for applications ranging from small aircraft to hypersonic transports makes the future of aircraft propulsion promising and exciting.

MODEL AIRPLANE ENGINES

Two-Stroke Cycle of Operation

A four-stroke-cycle engine is seldom used in a model airplane. The cost of manufacturing such an engine for model use is prohibitive, primarily because of the intricate, spring-loaded, cam-operated valves that would be required. The two-stroke cycle engine is much simpler in operation, has fewer parts, and is cheaper and easier to manufacture. In fact, the only moving parts are the piston, the connecting rod, and the crankshaft. Each cycle consists of an intake-compression stroke and a power-exhaust stroke. The intake of fuel and the expulsion of the exhaust gases are controlled by ports, or openings, in the cylinder walls, which are covered and uncovered by the moving piston.

A typical two-stroke-cycle engine (of any size) operates as shown in figure 6-11. On the intake-compression stroke, the upward travel of the piston has a double effect.

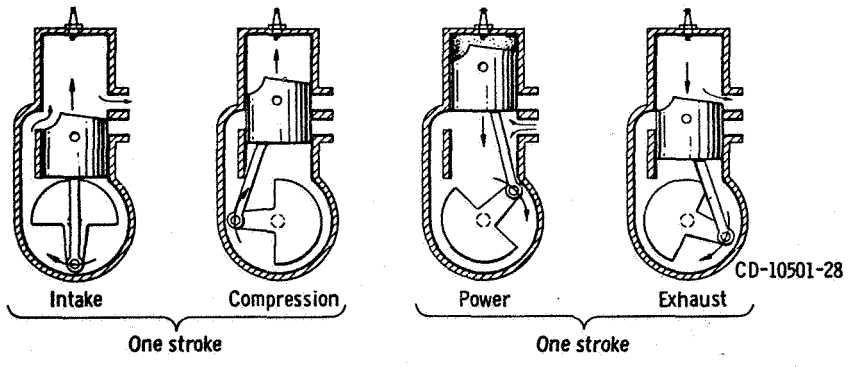

Figure 6-11. - Two-stroke cycle of operation of internal-combustion engine.

First, by creating a partial vacuum in the crankcase, the mixture (fuel and air) is sucked into the crankcase through a special port. Second, vaporized fuel mixture previously forced upward through the bypass passage to the space above the piston is now greatly compressed and ignited. During the resulting power stroke the downward-moving piston uncovers the exhaust port to allow exhaust gases to blow out, and it uncovers the intake port at the upper end of the bypass to allow fresh fuel mixture to push its way into the

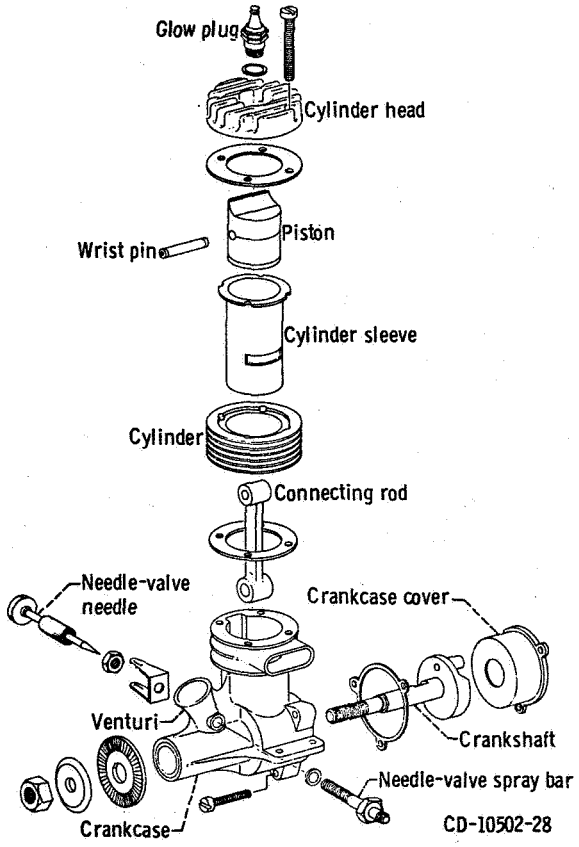

Figure 6-12. - Model-airplane engine.

cylinder. Then, as the piston moves upward again, it covers the exhaust port opening and the bypass intake port, thereby trapping the fuel charge in the combustion chamber. It is interesting to note that vaporized fuel mixture actually fills the crankcase of the two-stroke-cycle engine.

Even though most model airplane engines are of the two-stroke-cycle type, considerable differences may be found between engines of different manufacturers and even between different engines of the same manufacturer. These differences may or may not be obvious and/or significant. Figure 6-12 shows an exploded view of a typical model engine and its nomenclature.

Fuel Systems

One way of classifying model-airplane engines is according to the method used to introduce the fuel mixture into the cylinder. In the two-stroke cycle, for the downward-moving piston to drive the vaporized fuel mixture up through the bypass into the combustion chamber, the crankcase must be sealed. Yet, for the mixture to get into the crankcase in the first place, an opening must be provided. Thus, some means is necessary to close off this opening or port when the piston travels downward and to open it when the piston moves upward.

The simplest and most popular porting system is the shaft valve. This system is characterized by the location of the venturi, or air intake, at the lower front of the cylinder. The crankshaft is bored out from the rear, so that it is hollow, or tubular, for most of its length. At the point where the axis of the venturi crosses the crankshaft, there is a hole through the wall of the crankshaft to the central bore. This hole is radially positioned so that it coincides with the venturi opening at precisely the right time during each cycle to allow the fuel and air mixture to pass from the venturi through the crankshaft into the crankcase. Furthermore, the size of this hole in the wall of the crankshaft determines how long during each revolution of the crankshaft, or each cycle, the mixture can enter the crankcase.

The second most popular intake porting method is the rear rotary valve. In this system, the venturi attaches to the rear crankcase cover and extends outward to the rear, usually in a horizontal position. Inside the crankcase, an accurately machined disk of metal faces up snugly to the smooth inside face of the rear crankcase cover plate. This disk is rotated by an extension of the crankshaft. Cut through the disk is an elongated, arc-shaped opening concentric with the circumference of the disk. The placement and length of this slot as it passes over the opening from the venturi are designed to allow the vaporized fuel mixture to enter the engine at the proper time. The slot determines when and how long the fuel may enter the crankcase during each cycle.

A highly efficient porting system, but one that imposes very exacting design and manufacturing requirements, is the reed-valve system. In this design a thin strip of appropriate metal covers and uncovers an intake port in the rear crankcase cover plate in response to variations in crankcase pressure during each cycle.

Regardless of what method is used to introduce the mixture into the cylinder, a carburetion system is needed to supply the correct amount of the proper mixture of fuel and air to the cylinder. The typical model airplane engine has a very simple carburetor consisting of a venturi and a needle valve, which extends across the throat (i. e., the narrowest portion) of the venturi.

A venturi is a convergent-divergent (wasp-waisted) passage in which the pressure energy of the airstream entering the wide end of the passage is converted into kinetic energy by the acceleration of the airstream through the narrow part of the passage. The model-airplane engine venturi is designed, in length and cross section, to supply the proper amount of air to the engine and to provide maximum acceleration of the air as it passes the needle valve.

In the model-airplane engine, the action of the piston creates a vacuum in the crankcase. Because of this vacuum, air from outside the engine is drawn into the crankcase through the venturi. In other words, the higher pressure outside the engine pushes air into the crankcase. The air enters the wide end of the venturi at some particular flow rate. (Flow rate is the quantity of air passing a given point in the passage per unit of time.) If the pressure difference between the outside and inside of the crankcase remains constant, the pressure will continue to push air into and through the venturi at a constant flow rate. As the cross-sectional area of the converging passage becomes smaller, fewer molecules of air can pass through the reduced area simultaneously. (This holds true only at subsonic velocities, where air is considered to be incompressible.) Therefore, each molecule passing through the constriction must speed up to allow the same number of molecules that enter the wide end of the venturi per unit of time to pass through the constricted part in the same unit of time.

According to Bernoulli's law (see chapter 5), as the velocity of the airflow in the throat of the venturi increases, the pressure decreases. This reduced pressure, as well as the vacuum in the crankcase, causes fuel to be drawn out of the needle valve and mixed with the air in the venturi.

The needle valve is used to set the fuel flow to obtain the desired air-fuel mixture ratio. The needle valve is basically a tube with a tapering rod that fits inside it. The tube (called the spray bar) is mounted across the throat of the venturi. One or two holes are drilled in the wall of the spray bar where it crosses the venturi throat. The fuel line from the tank is connected to one end of the spray bar, and the tapering rod (called the needle, or pin) is inserted in the other end. The end of the spray bar and a portion of the needle are threaded to provide a means of adjusting the position of the needle in the

spray bar. As the needle is screwed inward or outward, a different portion (thicker or thinner) of the tapered needle is located over the hole in the wall of the spray bar. Thus, the obstruction in the path of the fuel is varied.

The venturi-and-needle-valve combination is simple and highly effective, but, since it lacks the float-and-valve system of more elaborate carburetors, it cannot compensate for the changing fuel requirements of the engine during operation. Normally, the needle valve is set before the plane takes off and the setting cannot be changed during flight. However, an engine may be equipped with a pivoted butterfly valve to alter the amount of air entering through the venturi, a double needle valve to alter the amount of fuel entering the crankcase, and a pivoted cover over the exhaust to alter the back pressure in the cylinder. These three devices are usually interconnected to operate simultaneously, and they provide at least two distinct power settings, for high-speed and low-speed operation.

Ignition Systems

Model-airplane engines may be classified according to their ignition systems. Three systems are commonly used to ignite the fuel charge in the cylinder.

The most popular system is the glow-plug system, which has the advantages of simplicity and lightness. The glow plug is similar in appearance to a spark plug, but instead of having two electrodes, it has a small filament. This filament is heated from an outside source (the booster battery) while the engine is being started. Once the engine is running properly, the booster leads are removed, and the glow plug maintains sufficient heat to continue igniting the fuel under compression. The fuel is specially blended to ensure easy ignition and to provide proper lubrication.

Less popular is the spark ignition system, which uses an ordinary spark plug, together with a spark coil, condenser, batteries, switch, and wiring, all of which must be carried inside the plane. A set of contacts, or points, is contained in a housing, usually at the front of the engine, on the shaft. These points make and break contact by means of a cam on the shaft, which separates the points when the lobe, or bump, of the cam comes by once every revolution. By means of a spark coil and condenser, a high-tension current is shot to the spark plug when the points separate. (The collapse of the magnetic field when the points separate produces a high-voltage inductive "kick".) Inside the combustion chamber, an intense spark jumps across the narrow gap formed by the two electrodes of the plug and ignites the fuel charge. This system uses a mixture of gasoline (usually white gas) and SAE No. 70 oil, mixed either two or three parts gasoline to one of oil.

One advantage of this spark ignition system is that the spark may be advanced or retarded to govern the engine speed. Another advantage is the relatively low cost of the fuel. A disadvantage is that the weight of all the extra gear requires a plane large enough

to carry the extra load, and it handicaps the performance of the plane. For this reason, the spark ignition system is used only on relatively large engines.

The third ignition system is compression ignition, or the diesel system. In this case, a special fuel ignites by itself when quickly and greatly compressed. Such a fuel consists of ether, oil, and kerosene, usually in equal parts However, there are many mixture variations, such as 50 percent ether and 50 percent diesel truck fuel. Compressing the fuel mixture to the point of ignition requires a much higher compression ratio than is required with other ignition systems. Therefore, a diesel engine must be stronger and is usually heavier than an equivalent glow-plug or spark-ignition engine. This extra weight is a handicap in a model airplane. In a diesel engine, the compression ratio required for starting is often different from that required for continuous running. Even while the engine is running, the compression ratio must sometimes be varied because of fuel mixture, excessive fuel introduced into the engine by choking or priming, temperature, etc. The compression ratio in a model diesel engine is varied by means of an adjustable contrapiston that fits inside the cylinder at the cylinder head. A T-shaped lever that is connected to the contrapiston extends out through the cylinder head. By turning the lever the contrapiston can be screwed further into or out of the cylinder. This way the volume of the cylinder is decreased or increased, and the compression ratio is increased or decreased. Normally, the contrapiston is adjusted until the particular fuel mixture ignites easily for starting, and then it is readjusted, if necessary, for high-speed running.

Controls

As discussed in the preceding sections, all model engines are equipped with some control devices that affect the performance. The glow-plug engine has a needle valve that controls the fuel and air mixture and, thereby, the speed. The needle valve can be adjusted while the engine is operating, but normally it cannot be adjusted in flight. However, some glow-plug engines are equipped with special venturis, needle valves, and exhausts that can be adjusted during flight for high-speed and low-speed operation. These devices were discussed earlier. The ignition timing of the glow-plug engine cannot be adjusted, because the filament of the plug glows continuously during operation. However, a minor degree of control over the timing is possible by selecting a plug that glows strongly, for early ignition, or a plug that glows weakly, for late ignition. Similar results can be achieved by choosing a fuel that ignites more easily or less easily. Obviously, adjustments cannot be made by these indirect means of control while the engine is operating.

The spark-ignition model engine has the same fuel-mixture control (needle valve) as does the glow-plug engine, but its ignition timing can also be advanced or retarded to suit

the operating requirement. With this system the ignition timing can be adjusted while the engine is operating.

The diesel model engine has a needle valve for control of the fuel mixture. The ignition timing of the diesel engine is controlled by means of the adjustable contrapiston, which was described earlier. This contrapiston can be adjusted while the engine is operating, but it cannot be adjusted in flight.

Displacement Volume

In addition to being classified according to its intake porting and its ignition system, a model airplane engine may also be classified according to its size. The size is based on piston displacement, which is the volume displaced by the piston in a cylinder in a single stroke. The displacement volume is the product of the piston travel, or stroke, and the cross-sectional area of the cylinder. The engine classes based on size are given in the following table:

Class	Displacement, $in.^3$
$\frac{1}{2}$A	0.000 to 0.050
A	.051 to .200
B	.201 to .300
C	.301 to .650

BIBLIOGRAPHY

Anon.: Aviation Week and Space Technology, vol. 86, no. 10, Mar. 6, 1967, pp. 191-196.

Durham, Franklin P.: Aircraft Jet Powerplants. Prentice-Hall, Inc., 1951.

Hesse, Walter J.; and Mumford, Nicholas V. S., Jr.: Jet Propulsion for Aerospace Applications. Pitman Publishing Corp., 1964.

Rogowski, Augustus R.: Elements of Internal Combustion Engines. McGraw-Hill Book Co., Inc., 1953.

Wilkinson, Paul H.: Aircraft Engines of the World 1964/1965. Paul H. Wilkinson, Washington, D.C.

7. GAS-TURBINE JET ENGINES

Jack B. Esgar*

Within the last 15 years, the jet engine has almost completely replaced the reciprocating (piston) engine as a power plant for high-performance, high-speed aircraft. The two main reaons for this change are (1) the propeller used with reciprocating engines becomes inefficient as the velocity of the propeller tip relative to the airstream exceeds sonic velocity, and (2) the power output for a given engine weight for turbine engines is much greater than for reciprocating engines. As a practical limitation, propeller-driven airplanes are limited to flight Mach numbers of about 0.6 (450 mph) or less. Maximum efficient cruise speeds for propeller-driven aircraft are of the order of 300 miles per hour. Commercial jet aircraft cruise efficiently at speeds in excess of 600 miles per hour, and some military aircraft cruise at about 2000 miles per hour. The U.S. supersonic transport, now under development, will be powered by gas-turbine jet engines and will cruise at almost 1800 miles per hour. The main purpose of the jet engine, therefore, is to enable aircraft to fly efficiently at the high speeds demanded by both military and civilian aviation.

Through the development of the modern airplane powered by jet engines, practically any place in the United States is within 4 hours' flying time, and Europe is only 8 hours away by commercial transportation. It is even possible for the traveler to leave the United States in the morning and land in the Orient before sundown. When supersonic transports become operational, these flying times will be cut by as much as two-thirds.

The term "jet engine" is a generic term that can refer to a wide variety of power plants, including turbojet and turbofan engines for powering conventional aircraft, rocket engines for launching space vehicles, and ramjet engines for powering future hypersonic aircraft. In this chapter, however, the term "jet engine" refers to gas-turbine jet engines, such as turbojets and turbofans. Some of the principles discussed, however, are equally applicable to other types of jet engines.

*Assistant Chief, Airbreathing Engines Division.

THRUST AND POWER COMPARISONS BETWEEN RECIPROCATING AND JET ENGINES

Conventionally, a reciprocating engine is rated by the horsepower it delivers at the propeller shaft, and a jet engine is rated by the amount of jet thrust it generates. For a 100-percent efficient conversion, horsepower and thrust can be related by the following equation:

$$\text{Horsepower} = \frac{(\text{Thrust})(\text{Flight speed})}{550}$$

where the thrust is in pounds, the flight speed is in feet per second, and 550 is the factor for converting foot-pounds per second to horsepower. At constant altitude and subsonic velocity, a gas-turbine jet engine develops nearly constant thrust over a wide range of velocities. It can be seen from the above equation that the faster an airplane flies, the more horsepower a jet engine will develop. A reciprocating engine, on the other hand, develops essentially constant power for a given altitude over a range of flight velocities. Thus, the thrust from a reciprocating engine is high at low velocities, but decreases as velocity increases. According to the equation, the thrust of a reciprocating engine should be infinite at zero velocity. Actually, the thrust is limited by the propeller. A conventional aircraft propeller has a thrust limit of approximately 3.5 pounds of thrust per horsepower.

Figure 7-1 presents a comparison of thrust and horsepower outputs of three actual engines (R-4360, JT8D, and GE4), for speeds up to 600 miles per hour at sea level.

The R-4360 is a radial, reciprocating engine built by Pratt & Whitney Aircraft. It is the largest and most powerful aircraft reciprocating engine built. The maximum power at the propeller shaft is 3500 horsepower. The engine weighs approximately 3500 pounds.

The JT8D is a turbofan jet engine used extensively in commercial aircraft such as the Boeing 727 and 737 and the McDonnell Douglas DC-9. The engine, built by Pratt & Whitney Aircraft, has a maximum thrust of 14 000 pounds and weighs approximately 3100 pounds.

The GE4 is a turbojet engine under development by the General Electric Company to power the U.S. supersonic transport. It will have a maximum thrust of about 67 000 pounds and will weigh about 11 000 pounds. At cruise altitude of 65 000 feet and cruise speed of about 1800 miles per hour, the thrust will be reduced to about 15 000 pounds as a result of the rarified air at that altitude.

The R-4360 and the JT8D are approximately the same weight (actually the JT8D is lighter) but the jet engine has greater thrust at all flight speeds and is able to fly at higher speeds. At 300 miles per hour the thrust of the R-4360 has dropped to about one-third of that of the JT8D. The horsepower per pound of engine weight developed by the recipro-

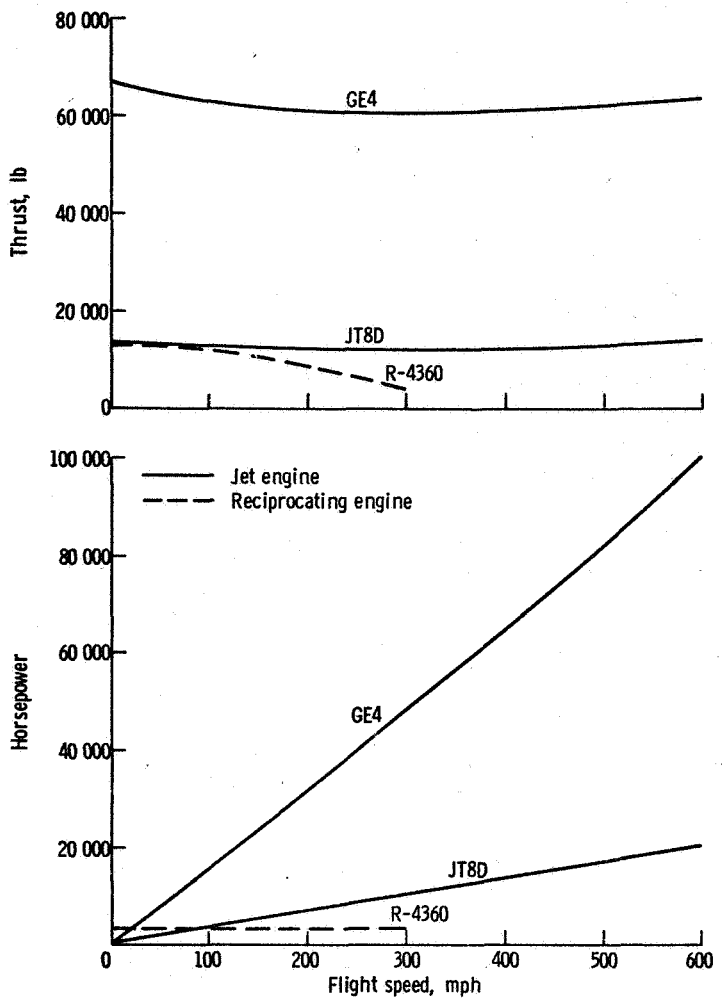

Figure 7-1. - Thrust and horsepower comparisons of reciprocating and jet aircraft engines at sea level.

cating engine remains constant at about 1 horsepower per pound at all flight speeds, but at 600 miles per hour the JT8D jet engine develops almost 7 horsepower per pound. The bigger and more powerful GE4 jet engine develops over 9 horsepower per pound at 600 miles per hour at sea level.

All engines have some limiting flight speed. The practical speed limit for the reciprocating engine is between 300 and 400 miles per hour, because of the low propeller efficiency at high speeds and the steady loss in thrust as speed increases. Jet engines such as the JT8D are primarily subsonic engines. This subsonic limit is imposed by the temperature of the air entering the engine. The GE4, on the other hand, is designed for higher temperatures by using higher temperature materials and cooling in strategic areas. At flight speeds of Mach 2.7 (approximately 1800 mph), at which the U.S. supersonic transport will cruise, the air entering the engine will be approximately 500^{o} F as a result of air compression in the inlet.

At this flight speed and at high altitude, the engine thrust of the GE4 will be approximately the same as that of the JT8D flying subsonically at sea level, but because of the high supersonic cruise velocity, the GE4 will develop about $3\frac{1}{2}$ times as much power as the JT8D does subsonically.

JET-ENGINE THRUST

The thrust of the jet engine is similar to that produced by a toy balloon when it is blown up and released so that the air can escape. Many people think that this thrust results from the escaping air pushing on the air outside of the balloon. This is not a true explanation. The thrust would also occur in a vacuum. To understand the mechanism of this thrust consider figure 7-2. Figure 7-2(a) shows an inflated balloon with the opening

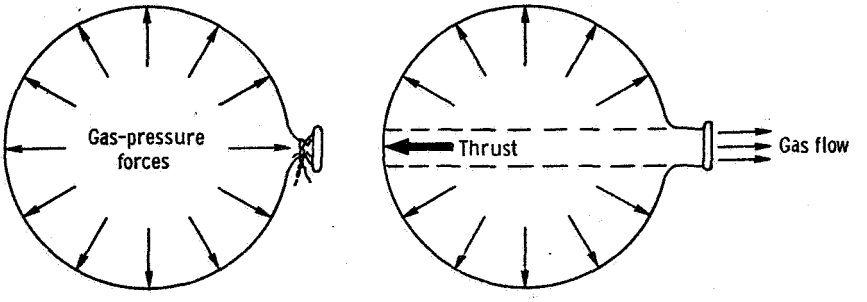

(a) Pressure forces inside balloon in equilibrium - no thrust developed.

(b) Pressure forces inside balloon not in equilibrium - thrust developed from pressure forces acting on unbalanced area inside balloon.

Figure 7-2. - Jet thrust from toy balloon.

tied shut. On the inside of the balloon the gas pressure forces act equally in all directions. As a result, the balloon is in equilibrium; that is, there are no forces causing the balloon to move. Figure 7-2(b) shows the inflated balloon with an opening through which the gas can escape. Now, unequal pressures are acting on the inside of the balloon. At the balloon opening there is no surface for the pressure to act against, but directly opposite the opening the pressure is pushing against the inside of the balloon. As a result, the balloon is accelerated in the direction shown.

In the example of the toy balloon, the thrust is equal to the product of the pressure difference between the inside and outside of the balloon and the net unbalanced area inside the balloon against which the internal pressure acts. This thrust is also equal to the change in momentum per unit time of the gas as it leaves the balloon. Momentum per unit time is the product of mass flow rate (weight flow rate divided by a gravitational constant g) and the velocity. Since the initial velocity of the gas inside the balloon is zero,

the change in momentum per unit time in this case is equal to the momentum per unit time of the gas leaving the balloon. Therefore, the thrust can be expressed by the equation

$$F = \frac{\dot{w}}{g} V_{exhaust}$$

where

F	thrust, lb
$\dot{w}$	weight flow rate of gas, lb/sec
g	gravitational constant, ft/sec^2
$V_{exhaust}$	exhaust velocity of gas, ft/sec

The operation of a jet engine is not quite as simple as that of a toy balloon, because the jet engine is a continuous-flow device that requires many internal components. But the basic principle of thrust generation is the same.

For example, the thrust of the jet engine is equal to the change in momentum per unit time between the inlet and the exhaust.

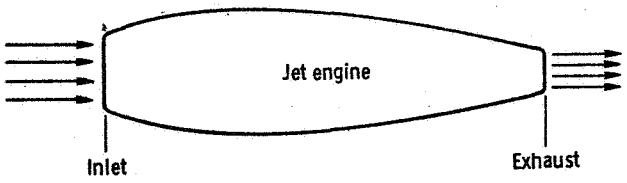

$$F_{engine} = \frac{\dot{w}_{exhaust}}{g} V_{exhaust} - \frac{\dot{w}_{inlet}}{g} V_{inlet}$$

where

$$\dot{w}_{exhaust} = \dot{w}_{fuel} + \dot{w}_{inlet}$$

For the balloon, which is more representative of a rocket, the term for the inlet momentum per unit time $\left[(w_{inlet}/g)V_{inlet}\right]$ is, of course, equal to zero.

A jet engine must pump a large quantity of air through the engine and exhaust it from the jet nozzle at as high a velocity as possible. The velocity of a jet is determined by the pressure drop of the gas as it expands through a nozzle and by the temperature level of the

gas. Therefore a jet engine must be capable of pumping the air entering the engine to a high pressure, heating it to a high temperature, and then expanding it through an exhaust nozzle to a high velocity. Five major engine components are required to generate this high-temperature, high-velocity exhaust-gas stream to produce thrust in the jet engine. These components are the engine inlet, the compressor, the combustor, the turbine, and the exhaust nozzle. For some applications, additional components, such as a fan or an afterburner, are added to provide greater thrust.

FUNCTIONS OF ENGINE COMPONENTS

Figure 7-3 shows cutaway and exploded views of a turbojet engine. Figure 7-4 illustrates schematically the main components of turbojet engines for subsonic and supersonic flight.

The inlet collects ram air and directs it towards the engine compressor. A certain amount of air compression occurs in the inlet. For subsonic flight, this compression is low, but it can become quite high at supersonic flight.

The engine compressor, which can be considered similar to a series of fans mounted on a single shaft, further compresses the air to pressures of from 4 to about 25 times the pressure at the compressor entrance. The amount of air compression in the compressor is dependent primarily on the engine design, but it is also influenced by engine speed and flight conditions.

After the air leaves the compressor, energy must be added to it in the combustor. The combustor in some ways resembles a blowtorch. Fuel is burned in the air stream to increase the temperature to a level of from 1500° to 2500° F, depending on the engine design. At 1500° F, metal glows with a bright yellow color, and at 2500° F, many metals melt. It is, therefore, obvious that special materials are required in the hot portion of the engine. For combustor outlet temperatures above 1800° F, sophisticated cooling methods are required for engine parts downstream of the combustor.

The purpose of the turbine is to supply power to drive the compressor. As shown in figure 7-4, the compressor and turbine are mounted on a single shaft or assembly. The turbine is similar in operation to the windmills used in the Western prairies or in Holland to pump water. The hot gases passing through the turbine rotate the turbine wheel, which in turn rotates the compressor.

After leaving the turbine, the hot gases are expanded through the exhaust nozzle to a high velocity to create engine thrust. In the case of the supersonic-flight engine, shown in figure 7-4(b), it is often desirable to increase the thrust level of the engine by further increasing the temperature, and consequently the velocity, of the exhaust gases. The temperature level of the gases leaving the combustor must not exceed the temperature that the turbine blading can withstand. Therefore, to obtain higher exhaust-gas tempera-

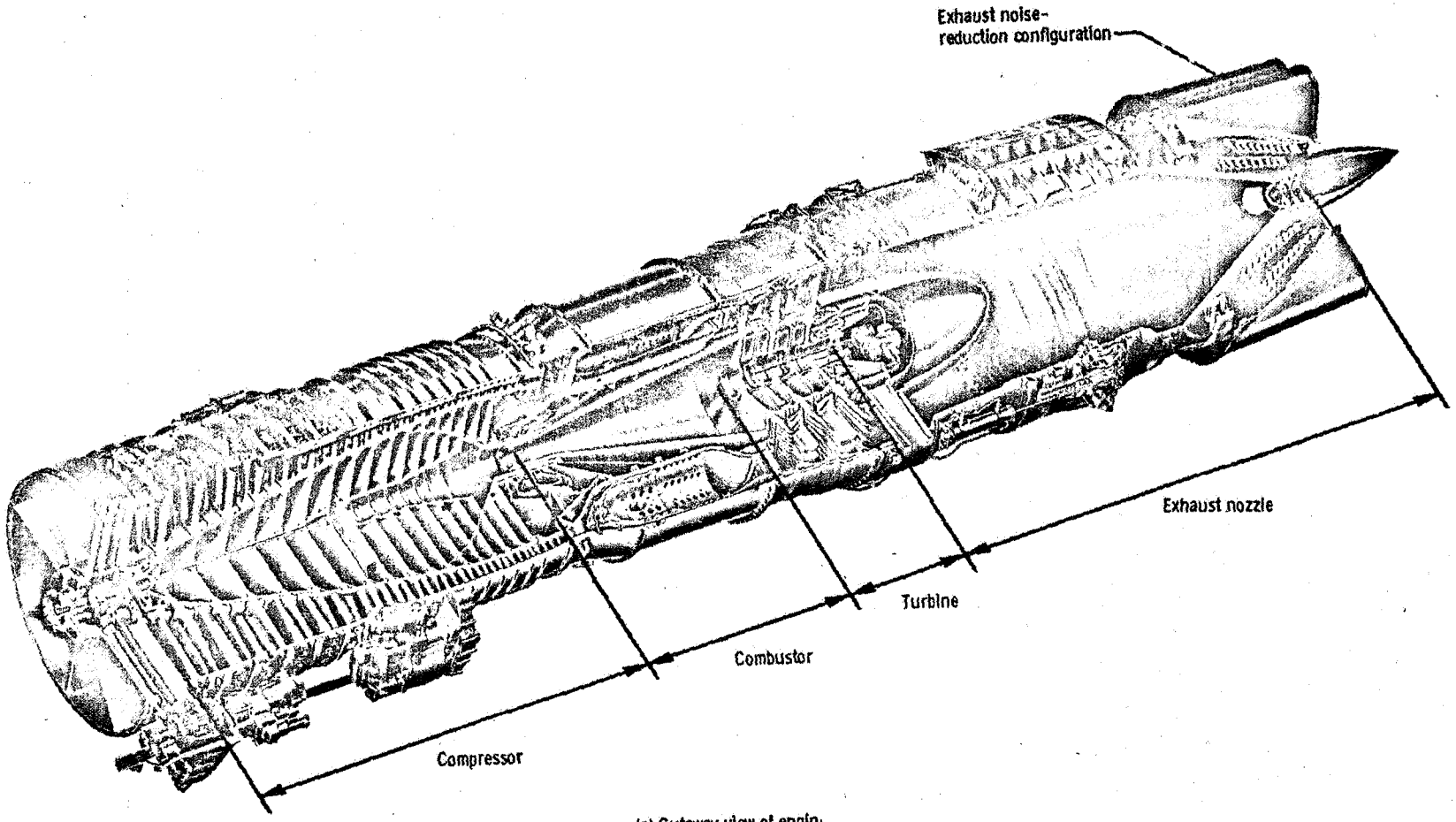

(a) Cutaway view of engine.

Figure 7-3. - General Electric CJ 805-3B turbojet engine.

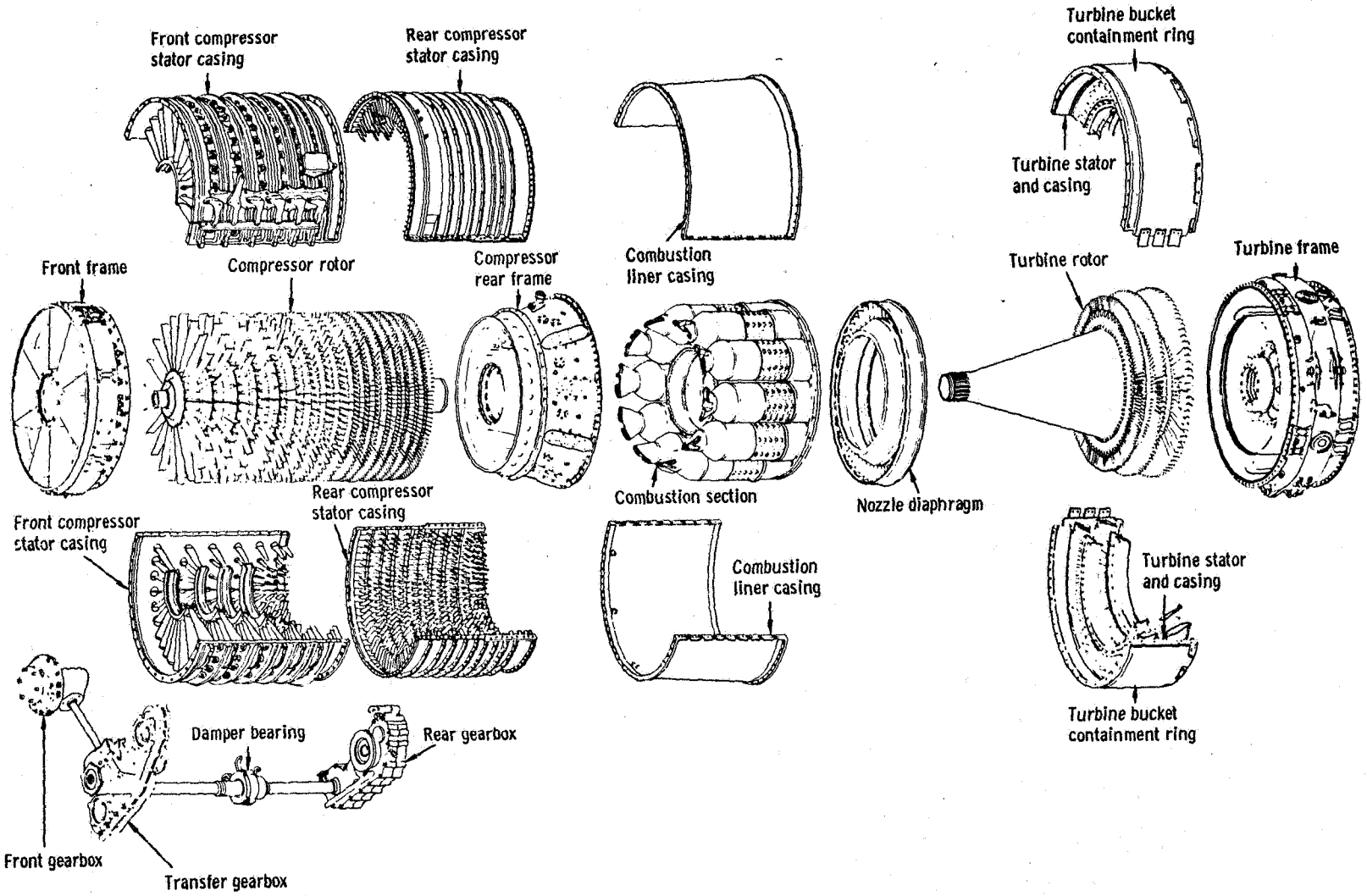

(b) Exploded view of components.

Figure 7-3. - Concluded.

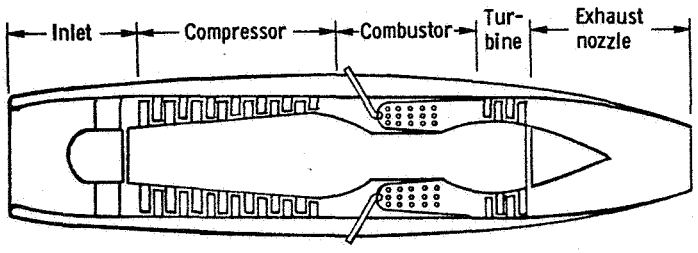

(a) Subsonic-flight engine.

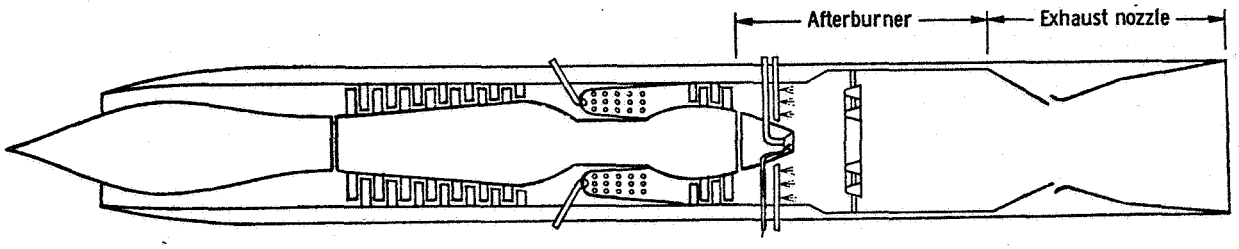

(b) Supersonic-flight engine.

Figure 7-4. - Schematic illustrations of turbojet engines.

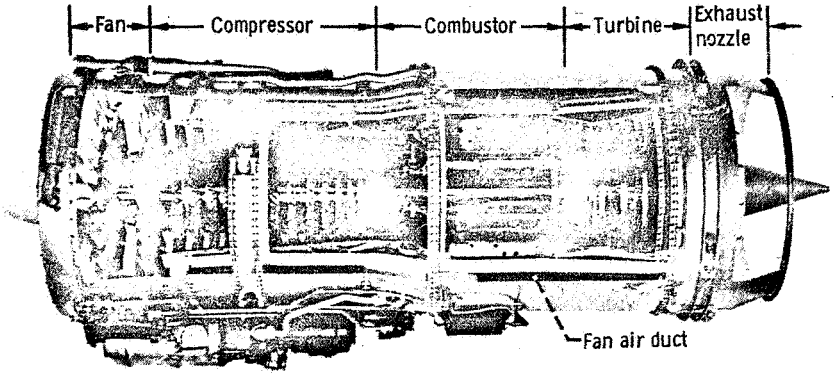

Figure 7-5. - Pratt & Whitney JT8D-1 turbofan engine.

tures, it is necessary to use an afterburner. Fuel is burned in the afterburner in a manner somewhat similar to that in the combustor, and the gas temperature level is raised to as high as 3800° F. This temperature is near the maximum attainable by burning kerosene-type fuels in air. Afterburners are used in military aircraft primarily to obtain bursts of power for relatively short periods of time during takeoff, to achieve high accelerations, or to achieve supersonic flight. For supersonic-cruise aircraft the afterburners are required for takeoff and for accelerating through the transonic speed range (near Mach number of 1.0). Afterburning temperature during cruise is usually lower

than required for takeoff and transonic acceleration.

Turbofan engines, such as shown in figure 7-5, are used in aircraft that are designed to cruise at subsonic speeds. In this type of jet engine, part of the fan airflow bypasses the "core" engine, which consists of the compressor, combustor, and turbine. The amount of air that is bypassed may vary from about one-half to eight times the airflow through the core engine, depending on the engine design.

A turbofan engine has a reduced jet velocity because the average temperature of the jet is reduced - the lower jet velocity improves engine efficiency. Thrust per pound of airflow is also reduced as jet velocity decreases. A turbofan engine compensates for this lower thrust per pound of airflow by having an increased airflow, relative to that of a turbojet, from the bypass air. The net effect is improved efficiency for a turbofan engine with equal or greater thrust for a given core-engine size.

The various engine components that have been mentioned above will now be discussed in greater detail.

ENGINE INLET

Some people do not consider the inlet as part of the jet engine. They consider the front face of the compressor as being the front of the engine. Actually, in terms of an overall powerplant system, the inlet is an important component of the jet engine. In fact, in a supersonic-flight engine most of the air compression occurs within the inlet. Because of the importance of the inlet, and because it is often less well understood than other engine components, we will discuss this component in somewhat greater detail than the others.

During flight, the airplane is moving at a high velocity relative to the ambient air. At high flight speeds (above 300 mph) the air going into the compressor must flow at a velocity slower than the airplane speed in order to maintain efficient compressor operation. As a result, the air must be slowed down in the inlet. As the air slows down, the pressure increases. (The phenomenon was examined in the discussion of drag in chapter 3.) What actually happens in the inlet is that the energy of the air molecules is converted from velocity (or kinetic) energy to pressure (or potential) energy. (The principle of this energy conversion is stated in Bernoulli's law, which is discussed in chapter 5.) The efficiency of an inlet is measured by how much of the total kinetic energy it converts to pressure energy. The amount of pressure that can be generated within an inlet becomes quite high at high flight speeds, as shown in figure 7-6. If all the velocity energy of the air at a flight Mach number of 3 (about 2000 mph) were converted to pressure energy, the pressure would be increased across the inlet by a factor of 37. This pressure rise would be greater than the pressure rise across compressors of current turbojet engines.

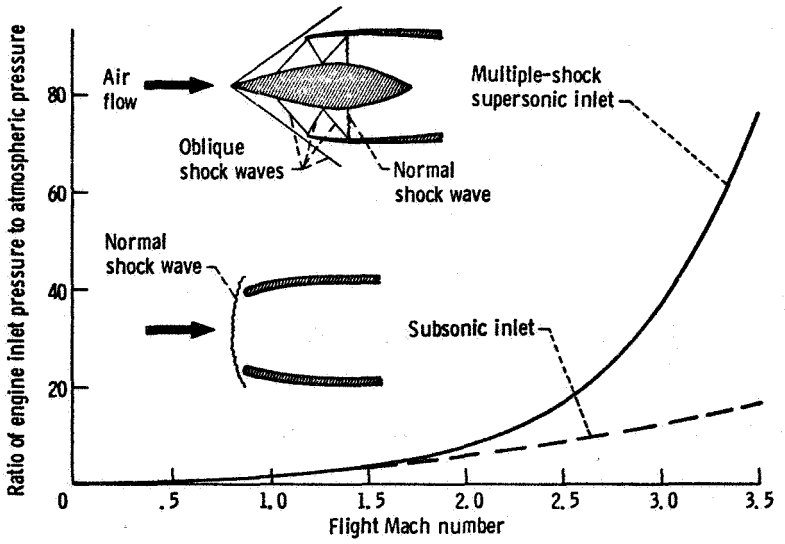

Figure 7-6. - Air compression in engine inlets.

Diffusion and Acceleration

An inlet is basically a diffuser. Therefore, a brief explanation of the diffusion and acceleration processes in subsonic and supersonic flow may be helpful at this point. A diffuser (or inlet) decreases the flow velocity and increases the pressure. A nozzle increases the flow velocity and decreases the pressure. In subsonic flow, a diverging channel acts as a diffuser, and a converging channel acts as a nozzle. In supersonic flow, a converging channel acts as a diffuser, and a diverging channel acts as a nozzle. To understand how diffusers and nozzles work, let us start out by considering a venturi (fig. 7-7) similar to that in the carburetor of an automobile. In the venturi, with subsonic flow at the inlet, the air velocity must increase as the air flows through a converging channel (nozzle section in fig. 7-7) to the throat. The driving force required to accelerate the air molecules is a reduced pressure in the direction of flow (downstream). The

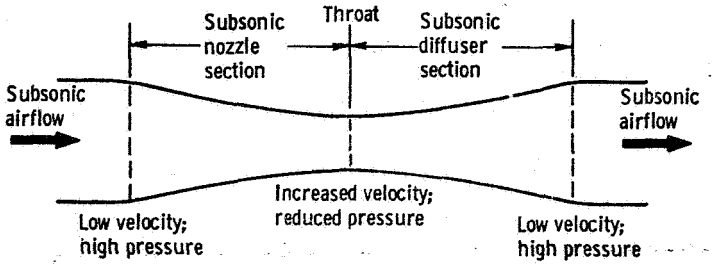

Figure 7-7. - Venturi. (Accelerates subsonic flow to higher subsonic velocities and thereby reduces pressure. Maximum velocity and minimum pressure occur at throat.)

maximum velocity occurs at the venturi throat, where the cross-sectional area is a minimum.

The diffuser section of the venturi acts in a manner opposite to that of the nozzle section. As the cross-sectional area of the passage expands, or diverges, the flow velocity decreases and the pressure increases. The velocity and pressure at the exit of the diffuser section can be almost the same as at the venturi inlet (nozzle-section inlet).

By reducing the pressure at the exit of the diffuser section of the venturi, the pressure is further reduced at the venturi throat, and the velocity increases until, finally, sonic velocity is obtained at the throat. Pressure waves are propagated at the speed of sound; therefore, once sonic velocity is obtained at the throat, pressure waves generated in the diffuser-section exit can no longer be propagated upstream through the throat. As a result, the pressure at the throat cannot be further lowered by reducing pressure in the diffuser section, and the throat velocity cannot be increased above sonic velocity.

The preceding discussion has shown that with subsonic flow a diffuser is a divergent channel, that the diffuser acts in a manner opposite to a subsonic nozzle, that the maximum velocity possible in a convergent nozzle is the velocity of sound, and that this maximum velocity occurs at the minimum cross-sectional area (throat). Obviously, supersonic flow cannot be obtained in a nozzle by further decreasing the flow area. If this were done, a new throat would be formed and sonic velocity would occur at the new throat. Keeping the downstream channel area the same as the throat would keep the flow

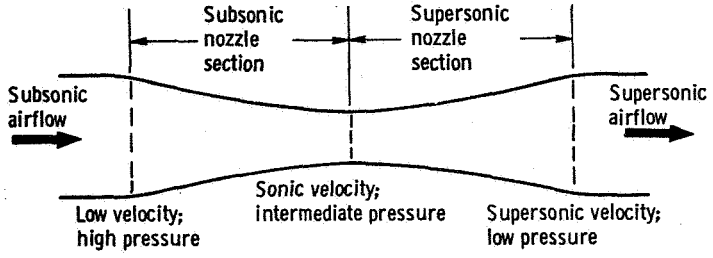

Figure 7-8. - Supersonic nozzle. (Accelerates subsonic flow to supersonic velocities if exit pressure is lowered sufficiently.)

near sonic. Therefore, if supersonic flow is to be obtained, the only approach possible is to increase the flow area downstream of the throat. The resulting nozzle configuration for supersonic flow (fig. 7-8) is similar to a venturi. With this configuration, supersonic flow can be obtained downstream of the throat if the exit pressure of the convergent-divergent nozzle is reduced to a value of about one-half of the inlet pressure, or less.

As pointed out in the discussion of the venturi, a diffuser acts in a manner opposite to a nozzle. Therefore, if we want to reduce the velocity of a supersonic airstream, and also obtain an increase in pressure, the supersonic diffuser (fig. 7-9) would first have a

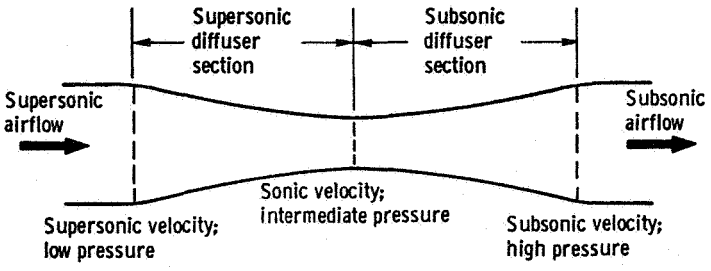

Figure 7-9. - Supersonic diffuser. (Decelerates supersonic flow to subsonic velocities and thereby generates high pressure.)

convergent section to decrease the supersonic velocity to sonic at the throat, and then the diffuser would have a divergent section to further decrease the air velocity subsonically. (Note that the diffuser configuration is also similar to venturi.)

A diffuser with a fixed geometry, as illustrated in figure 7-9, is a schematic, simplified illustration. Variable geometry or an air bleed is required to get a supersonic diffuser with large internal compression "started" or to get it to operate over a range of inlet Mach numbers (or over a range of flight speeds). The ratio of the throat area to the diffuser inlet area must be different for each inlet Mach number, otherwise a normal shock wave (described in the next section) will not stabilize in the diffuser throat. The flow velocity drops from supersonic to subsonic across this shock wave. If the normal shock wave is located in the supersonic region of the diffuser, where the flow has not yet been decelerated to near sonic velocity, large pressure losses may result. In order to "start" a supersonic diffuser with internal area contraction or to get the normal shock wave located at the throat requires that either (1) the diffuser geometry be variable to open up the throat area at low inlet Mach numbers to get the normal shock wave properly located, and then to decrease the throat area as the inlet Mach number increases, or (2) some air be bled out of the diffuser ahead of the throat at the lower inlet Mach numbers (this approach simulates a change in flow area). Additional and more detailed information on flow in inlets is presented in chapter 11.

Subsonic and Supersonic Inlets

At subsonic speeds the function of the inlet is not so much to compress the air as it is to reduce drag by streamlining the nacelle and to direct the inlet air to the compressor face. Inlets for subsonic and supersonic flight are quite different. This difference can be seen in the schematics of the two inlets shown in figure 7-6. The subsonic inlet concept is simple. The inlet is a divergent channel with entrance lips that are rounded to provide an efficient flow field at subsonic speeds. In contrast, the supersonic inlet lips

are sharp, and the inlet is a relatively complicated device.

The supersonic inlet must be capable of efficient operation at both subsonic and supersonic flight speeds. Let us first consider its operation at supersonic flight speed. The airflow channel must first be converged in a manner similar to that described for supersonic diffusers. Part of this convergence and supersonic flow deceleration can be accomplished external to the inlet lips through the use of shock (or compression) waves generated by a contoured centerbody that projects out ahead of the inlet lips, and part of the convergence is inside the inlet. (See multiple-shock inlet in fig. 7-6.) Shock waves and their characteristics are described in chapter 11. As air is decelerated from supersonic to sonic or subsonic velocity, shock waves are formed. A shock wave is a pressure wave across which there is a discontinuity (sudden change) in pressure and velocity. Shock waves can be either efficient or inefficient methods of converting velocity energy to pressure energy. An oblique shock wave, which forms at an angle to the local airflow direction, results in only a relatively small air-velocity reduction. The flow behind the shock wave remains supersonic, but at a reduced Mach number. Oblique shock waves are efficient converters of velocity to pressure, and they can be generated on centerbody surfaces with small successive inclinations to the airflow direction, as shown in figure 7-6.

A normal shock wave at high supersonic speeds is a particularly inefficient method of converting velocity to pressure. A normal shock is one which has its shock front perpendicular to the direction of flow. The air decelerates very abrubtly from supersonic to subsonic velocity as it passes through a normal shock wave.

In a well-designed inlet the supersonic airflow is first slowed down through a series of oblique shock waves until the supersonic Mach number is near 1, and then a normal shock occurs near the inlet throat. The inlet then has a divergent section for deceleration of the subsonic airflow downstream of the throat and the normal shock wave. The subsonic airflow is then decelerated to a Mach number of about 0.4 (about 300 mph) at the compressor face.

Figure 7-6 also illustrates why it is necessary to use the complicated supersonic inlet configurations when flying at high supersonic speeds. The figure shows both the ideal compression (if there were no pressure losses) from a multiple-shock supersonic inlet and the compression from a subsonic inlet that provides only a normal shock at the inlet entrance. Up to a flight Mach number of about 1.5, the two inlets are equally satisfactory. But at Mach 3, for example, the pressure recovered from the supersonic inlet is over three times as high as that recovered from a subsonic inlet.

During subsonic flight with a supersonic inlet, the inlet geometry must be changed for efficient operation. By collapsing the centerbody or moving it backward, the amount of flow contraction in the supersonic inlet is reduced, and this permits the inlet to be used at subsonic speeds. Intermediate centerbody positions are usually required at supersonic flight velocities below the maximum velocity for which the inlet is designed.

Matching of Inlet Airflow Capacity to Engine Airflow Requirement

Another problem that is encountered with supersonic inlets results from the airflow supply characteristics of the inlet being different from the engine requirements. The inlet size is usually chosen so that it will supply the proper amount of air to the engine at a selected flight Mach number. Figure 7-10 illustrates an example in which the inlet and engine airflow characteristics are matched at a Mach number of 3. The quantity of air entering the inlet at this Mach number is exactly the amount of air that would be contained

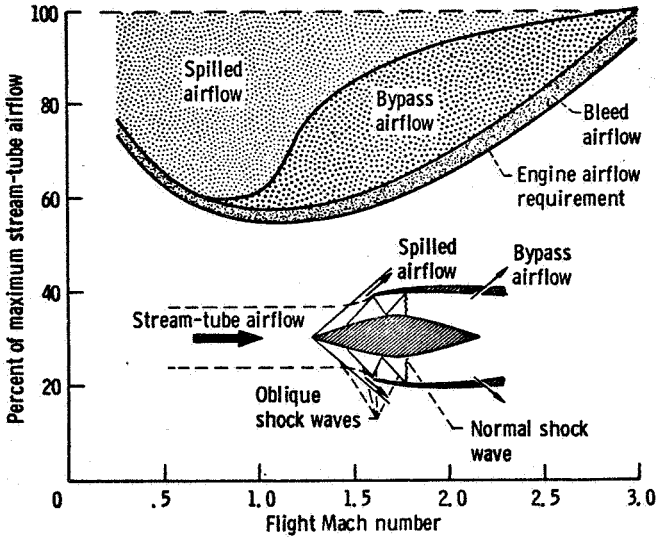

Figure 7-10. - Matching of inlet airflow to engine airflow requirements.

within a "stream tube" of the same diameter as the engine inlet. A stream tube is an imaginary tube of free-stream air containing the air that will pass through the engine. The maximum stream-tube airflow, referred to in the ordinate of figure 7-10, is the airflow that would occur if the stream-tube diameter were equal to the engine inlet diameter. When the diameter of the stream tube of air required by the engine is less than the inlet diameter, air from in front of the inlet must be spilled by shock deflection over the inlet lips, and air is bypassed out of the inlet as illustrated in figure 7-10. This spilled and bypassed air causes increased drag on the engine installation and is undesirable. Part of the research conducted on inlets and on engines is to provide methods of reducing and minimizing these drags in order to improve overall airplane performance. The bleed airflow is air that is bled from the throat region of the inlet to prevent separation of the boundary layer from the walls of the inlet and the centerbody. Bleed ports are located both in the walls of the inlet and in the surface of the centerbody.

COMPRESSOR

As stated previously, the purpose of the compressor is to compress the air leaving the engine inlet to a pressure that is from 4 to about 25 times as high as the pressure at the exit of the engine inlet. The pressure rise is dependent upon many things, including the purpose for which the engine is designed and the flight operating conditions. Modern engines are being designed for much higher pressures than were the engines of a few years ago.

Most engines utilize the axial-flow compressor, such as illustrated in figures 7-3, 7-4, and 7-5. A compressor of this type consists of many stages of rotating and stationary rows of airfoil-shaped blades. From the compressor inlet to the compressor exit the blades become progressively shorter (fig. 7-3), because a smaller flow area is required as the air becomes compressed. Compression of this air requires that work be done on it. This work raises both the pressure and the temperature of the air. The power required to drive the compressor is supplied by the turbine, which will be described later.

The manner in which the air is compressed can be explained with the help of figure 7-11. This figure shows three rows of compressor blades: the inlet guide vanes, the rotor blades, and the stator blades. The inlet guide vanes are used only at the entrance to the compressor. The purpose of these vanes is to turn the air to a favorable entrance angle before it enters the first compressor rotor. In some engines the inlet guide vanes

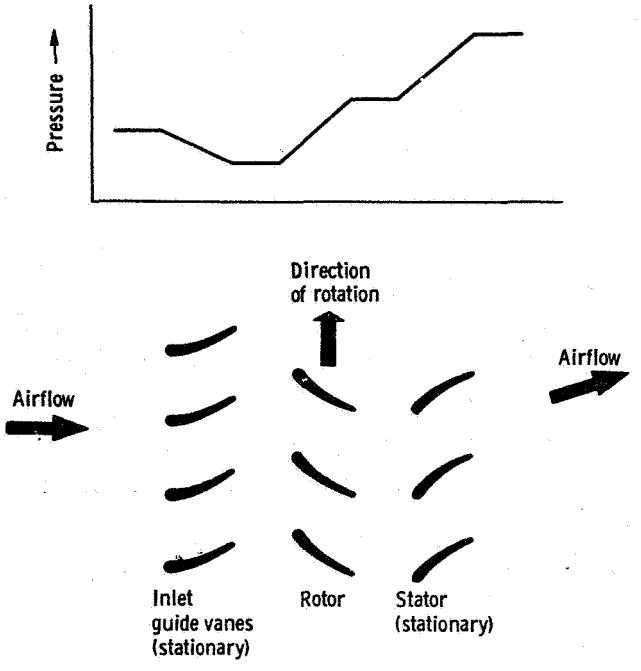

Figure 7-11. - Compressor operation.

are omitted. Each compressor stage consists of a rotor followed by a stat-r. The num-
ber of compressor stages in an engine may vary from about 7 to 20.

Even though the absolute air velocity entering the rotor has a Mach nu- ber of about
0.4, the high rotative speed of the rotor causes the air velocity relative to he rotor to
have a Mach number of 1 or higher. The kinetic energy associated with th- se high en-
trance velocities is converted into a pressure rise across each stage of the compressor
in two ways. First, the rotor blades move faster than the air entering the otor. The
blades push on the air, piling it up on the leading side of the blade, causing an increase
in pressure similar to that experienced by a person holding his hand out the window of a
car traveling at high speed. Second, the absolute air velocity is increased across the
rotor-blade passage as the air is accelerated in the direction of rotation of he rotor.
This high-velocity air then enters the compressor stator, which acts as a d- ffuser, because
the flow channel between adjacent blades increases, or diverges (see fig. 7 -11). During
the diffusion process in the stator, the air is slowed down, and the air velo- ity (kinetic)
energy is converted to pressure (potential) energy. In addition to being slo- ed by the
stator, the air is also turned by it. Thus, the air enters the rotor at the pr oper angle
(direction) and the proper Mach number (velocity).

The amount of compression that occurs in each compressor stage is re- atively small.
The pressure may increase by only 15 to 30 percent across each stage. Bu- when many
stages are combined, the total pressure rise becomes high, and the pressu- e leaving the
compressor may be 25 times as high as the pressure entering the compress or.

In some engines, called turbofan engines, part of the air entering the fa- n is bypassed
around the main portion of the engine while the remainder of the air passes through the
engine compressor. A turbofan engine is shown in figure 7-5. The fan is j- st like the
compressor, except that it is larger in diameter and has fewer stages. The fan usually
has only one to three stages and therefore provides only a modest pressure rise. The
pressure ratio across the fan is generally less than 3. In some engines, the - fan bypass
air mixes with the turbine exhaust gases in the exhaust nozzle. In other eng- ines, the fan
bypass air is discharged from the engine immediately downstream of the fan.

TURBINE

The turbine is mounted on the same shaft as the compressor; therefore , the rotative
speeds of the compressor and turbine are identical. As previously stated, t- ne turbine
supplies the power to drive the compressor, and in most cases the power re- quired is
very high. The turbine power in a small engine for business jet airplanes is - of the order
of 6000 horsepower, while for the largest engine now under development the turbine power
is 130 000 horsepower.

Whereas there is an increase in the pressure and temperature of the air across the compressor, there is a reduction in the pressure and temperature of the gases across the turbine. To ensure that the pressure drop across the turbine will be less than the pressure rise across the compressor (in order to have enough power to drive the compressor and have pressure left for creating thrust in the exhaust nozzle), it is necessary to add energy to the air leaving the compressor. This energy addition is provided in the combustor in the form of thermal energy. The combustor heats the air entering the turbine to temperatures ranging from about 1500° F to well over 2000° F, depending upon the engine design. The combustor will be discussed later.

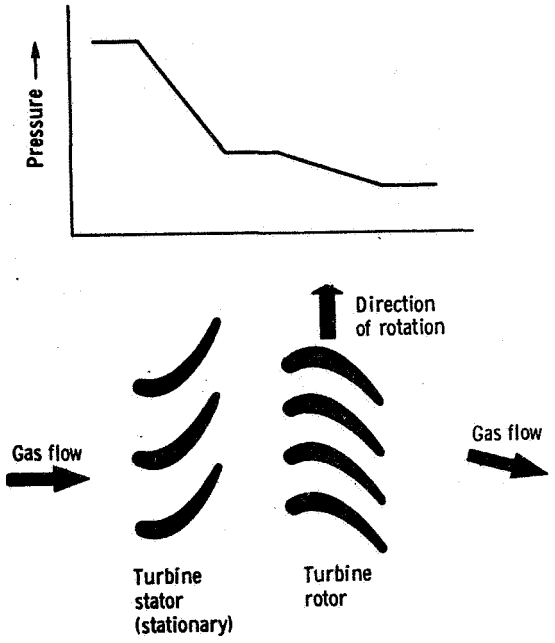

Figure 7-12. - Turbine operation.

The operation of the turbine is illustrated in figure 7-12. The gas leaving the combustor enters the turbine stator at a Mach number of about 0.4 or less. The stator turns the gas to provide a favorable entrance angle to the rotor blades. Furthermore, adjacent stator blades provide converging passages (see fig. 7-12) in which the gas velocity is increased to about Mach 1 at the exit of the stator. The gas pressure decreases in the stator as the velocity increases (a conversion of potential energy to kinetic energy). At a gas temperature of 2000° F, the gas velocity at Mach 1 is over 1600 miles per hour. This high-velocity gas then impinges on the turbine rotor blades and forces them to rotate in a manner similar to that of a windmill. The gas leaving the turbine rotor is at a velocity much lower than that entering the rotor. A large portion of the kinetic energy of the gas has, therefore, been transferred to the rotor in the form of mechanical energy to

provide the power to drive the compressor. The turbine is usually made up of several stages of stator and rotor blades. Modern engines have from two to eight turbine stages.

Most of the current gas-turbine engines have turbine-inlet gas temperatures of 1700° F or less. There are high-temperature turbine blade materials available that can withstand these temperatures. For future engines, however, the trend is toward increasing this turbine-inlet gas temperature in order to provide more power, or thrust, with a given engine size. To enable them to operate at these higher temperatures, the turbine blades must be cooled. This cooling is accomplished by ducting some of the air from the compressor through passages within the turbine blades. Since the air from the compressor is at a lower temperature than the hot gases entering the turbine, the turbine blade temperatures can thus be reduced. Research is currently being conducted to develop cooling concepts and blade materials that will permit operation at higher turbine inlet temperatures.

COMBUSTOR

The purpose of the combustor is to add thermal energy (heat) to the air leaving the compressor. Without this added energy, the turbine would be incapable of driving the compressor.

The combustor consists of four different sections, or zones, as shown in figure 7-13. The first section is the diffuser, in which the air velocity leaving the compressor is reduced to a level that permits efficient burning. The second section is the combustion zone. In this zone, a portion of the air (less than half) is mixed with fuel sprayed into the air by the fuel nozzle. This fuel and air mixture is burned, and the temperature of the gas is raised to between 3000° and 4000° F.

Stable combustion is possible only within these temperature limits for the combustion zone. Since this temperature is too high for the turbine to withstand, it must be reduced.

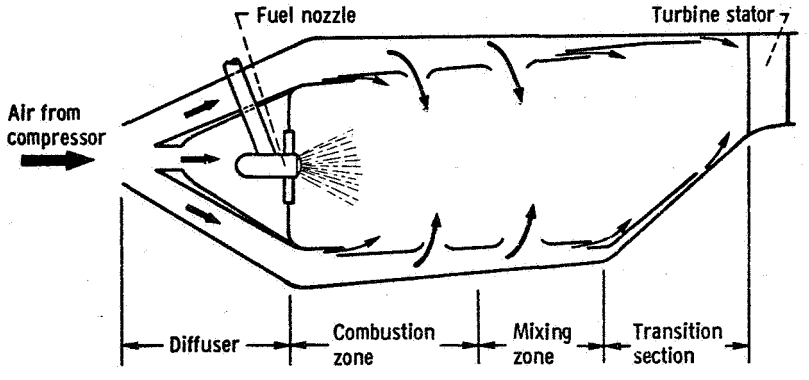

Figure 7-13. - Cross section of annular combustor.

This temperature reduction occurs in the mixing zone of the combustor, where the remaining air (called secondary air), which has been ducted around the combustion zone, mixes with the hot gases from the combustion zone. This secondary air also serves to cool the combustor liner so that it will not become overheated. The secondary air must be very thoroughly mixed with gases from the combustion zone in order to obtain a uniform temperature at the entrance to the turbine.

The last section of the combustor is called the transition section. In this section, the flow area of the combustor is decreased and the gas velocity is increased to provide the proper flow into the entrance of the turbine.

During engine startup, the fuel in the combustion zone is ignited by a spark plug somewhat similar to that used in a car. After the burner is ignited, the electrical energy to the spark plug is cut off because the spark no longer is needed, since the combustion is continuous.

AFTERBURNER

For some engine applications, primarily military and future supersonic transport engines, it is necessary to increase the engine thrust capability by further raising the temperatures of the exhaust gas after the gas leaves the turbine but before it enters the exhaust nozzle. An afterburner (fig. 7-14) is used for this purpose. An alternative to using the afterburner is to build the engine much larger, but a larger engine results in increased weight and, in many cases, increased airplane drag. Therefore, it is more economical to utilize an afterburner when maximum thrust is required, such as at takeoff and during supersonic flight.

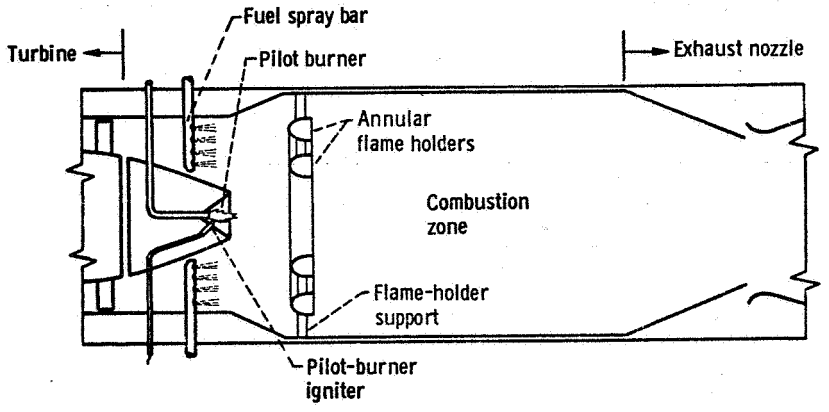

Figure 7-14. - Cross section of afterburner.

The operation of the afterburner is relatively simple and somewhat different from that of the combustor. Burning takes place in a gas stream that has already been heated by the engine combustors and from which some of the oxygen has already been consumed. In some turbofan applications, the fan air is ducted in with the exhaust gases leaving the turbine and this may also be heated in the afterburner. An afterburner nearly always has a pilot burner (shown in fig. 7-14) with an igniter, such as a spark plug, to light the pilot burner. This pilot burner provides an ignition source for the rest of the afterburner. Fuel is sprayed into the main gas stream from fuel spray bars, as illustrated in the figure. A series of flameholders is located a few inches downstream of the spray bars. These flameholders are usually gutter-shaped rings that provide turbulence in the gas stream and provide regions of lower gas velocity, where the burning can take place. Burning cannot take place in high-velocity gas streams at the temperatures encountered in afterburner inlets. Therefore, all of the burning occurs downstream in the turbulent wakes of the flameholders. The temperature of the gas in the afterburner may reach as high as 3800° F, which is far above the melting point of materials used in afterburner or exhaust-nozzle construction. These parts are kept from melting by controlling the temperature profile of the gases leaving the afterburner. The outer annular area of the gas coming into the afterburner does not enter into the combustion process and is not heated to high temperatures. This provides an insulating layer of cooler gas between the afterburner and exhaust-nozzle structures and the hot core gas in the afterburner. In addition, these structures are usually further cooled by ram air or air that is bled from the inlet and that bypasses the engine.

EXHAUST NOZZLE

As discussed earlier, in the section entitled JET-ENGINE THRUST, the thrust from the exhaust nozzle is proportional to the amount of gas flowing through the nozzle and to the exhaust velocity. The purpose of the exhaust nozzle, therefore, is to accelerate the gases leaving the engine to as high a velocity as possible.

The exhaust nozzle for a subsonic engine is much simpler than one for a supersonic engine. For subsonic flight, a fixed-area convergent exhaust nozzle (shown in figs. 7-4(a) and 7-15(a)) can be used. In a subsonic engine, the pressure of the gases within the exhaust nozzle is only high enough to accelerate the gases leaving the nozzle to a speed of about Mach 1 or slightly higher. For this gas pressure, a convergent nozzle is satisfactory.

When an afterburner is used, it is necessary to vary the diameter of the exhaust nozzle. With the afterburner in operation, the gases in the nozzle are heated to a higher temperature and their volume increases; therefore, the exhaust nozzle area must be increased during periods of afterburning.

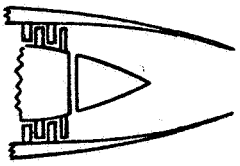

(a) Fixed-area nozzle for subsonic-flight engine.

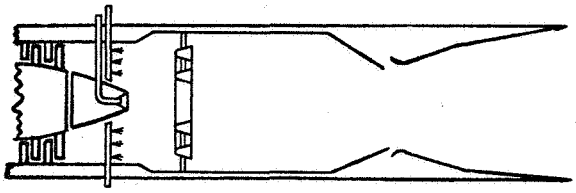

Convergent-divergent configuration for supersonic exhaust velocity

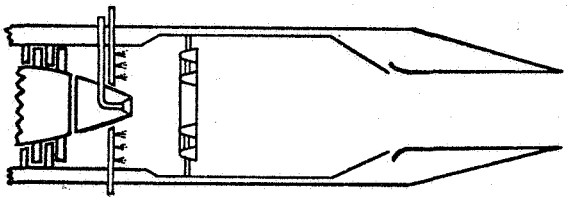

Convergent configuration for sonic exhaust velocity

(b) Afterburner and variable-area nozzle for supersonic-flight engine.

Figure 7-15. - Exhaust-nozzle configurations.

For supersonic flight, the pressure within the exhaust nozzle is much higher than at subsonic flight speeds, because of the added compression that is obtained in the engine inlet. This higher pressure in the exhaust nozzle permits accelerating the gases to velocities much higher than sonic. This acceleration of the gases to supersonic speeds requires both convergent and divergent sections within the exhaust nozzle, as illustrated in figure 7-15(b). The requirement for convergent and divergent passages to obtain supersonic velocities was discussed in the section titled Diffusion and Acceleration.

Since supersonic airplanes must also be able to fly at subsonic speeds, the exhaust nozzle must be variable not only in area but also in shape. Figure 7-15(b) illustrates the variation that must be made in the nozzle configuration between supersonic and subsonic flight.

ENERGY CONVERSION IN JET ENGINE

The discussion thus far has described the operation of the various engine components. It is of interest to consider the entire engine as being made up of a series of energy converters. The more efficiently the components are able to convert between various forms of energy, the more thrust the engine will produce from a given amount of fuel burned. The following energy conversions are performed in the engine:

The inlet converts kinetic energy (velocity) of the entering air to potential energy (pressure) and thermal energy (heat - the air is also heated during the pressure rise). The pressure created acts on portions of the inlet to provide forward thrust, and pressure is also required in the turbine and exhaust nozzle.

The compressor converts mechanical energy (power) to potential energy (pressure) and thermal energy (heat).

The combustor provides most of the thermal energy (heat) to the gas ahead of the turbine by a conversion of the chemical energy in the fuel.

The turbine creates the mechanical energy (power) to drive the compressor by conversion of the potential energy (pressure) and thermal energy (heat) from the gases entering the turbine.

The afterburner converts chemical energy to thermal energy in the gases ahead of the exhaust nozzle.

The exhaust nozzle converts potential energy (pressure) and thermal energy (heat) to kinetic energy (velocity) to produce the remaining thrust output of the engine.

The amount of thrust depends on the size of the engine (the amount of air it can handle), the pressure rise of the air in the engine, the temperature of the exhaust gases, and the efficiency with which all of the engine components can convert energy from one form to another.

8. AIRCRAFT STRUCTURES AND MATERIALS

Robert H. Johns*

We will develop the story of aircraft structures and materials more or less from a historical perspective, beginning with a discussion of wood, piano-wire, and fabric construction, and ending with a brief discussion of supersonic aircraft. Although this includes the entire history of manned powered flight, it has all taken place in the relatively short time since the turn of the century.

Considering only the current inventory of craft for manned flight, the spectrum runs from fabric-covered gliders and small private planes to high-performance military aircraft and huge transports. In addition, there are airships, helicopters, V/STOL craft, and even capsules and lifting bodies for manned space flight and Earth reentry. It is readily apparent that a wide variety of aircraft structural problems can be encountered. They range in complexity from the routine to those requiring highly complex electronic computers for their solution. New problems continue to arise as the state of the art of aircraft design, manufacture, and performance continues to progress at a very rapid pace.

STRUCTURES OF WOOD, PIANO WIRE, AND FABRIC

Obviously, one of the primary considerations in the design of aircraft structures is light weight. This is most apparent when considering gliders. The first successful airplanes were very similar in construction to the gliders of the day. The airplane which the Wright brothers used to make the first successful manned powered flight in 1903 is shown in figure 8-1. The basic materials of construction were wood, piano wire, and fabric. It was most desirable to use the piano wire wherever possible, because it provided the most strength for the least weight. However, the wire could carry only tensile loads; therefore, wood was used to carry compressive and bending loads. The fabric carried no loads but simply served to give the desired shape to various parts of the airplane.

The basic forces which must be considered in designing an airplane are (1) gravity

---

*Head, Structures Analysis Section.

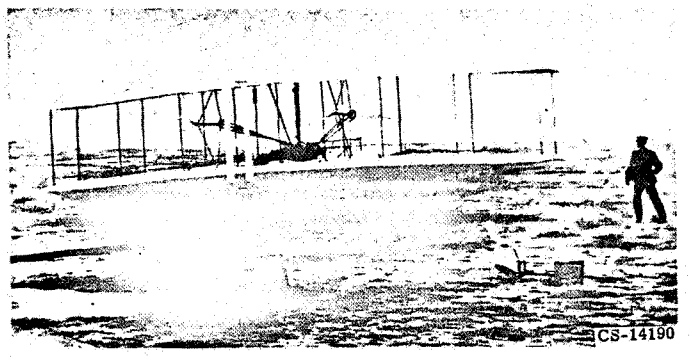

Figure 8-1. - Wright brothers' airplane (1903).

forces, (2) lift forces, (3) drag loads, (4) thrust or propulsive forces, (5) maneuvering loads, and (6) landing loads. In level flight at constant speed, the gravity forces are balanced by the lift forces and the drag forces are equal and opposite to the propulsive thrust.

Wings

Figure 8-2 clearly shows the struts and wires by which loads (forces) were transferred between major components of early airplanes. The earliest airplanes generally had two

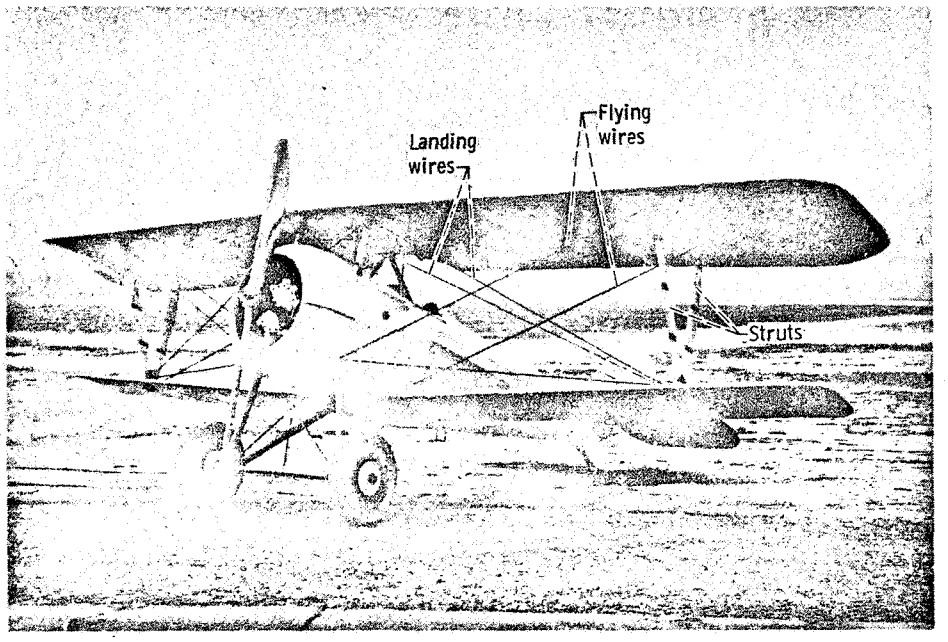

Figure 8-2. - Nieuport 27 biplane.

major lifting surfaces, or wings, and were thus called biplanes. Most of the weight (or gravity force) was in the fuselage, where the engine and passengers were located. The lifting forces, which resist the gravity forces and maintain the airplane aloft, come mainly from the wings. Thus, the lifting forces acting on the wings must be transmitted to the center of gravity (the point through which the resultant of the gravity forces can be assumed to act), which is in the fuselage area. These lifting forces acting on the wings were transmitted to the fuselage through struts and wires between the wing surfaces, as well as through wooden beams, or spars, within the wing cross sections.

When in flight, the lifting forces on the wings are acting upward. The lifting forces on the lower wing are resisted by compressive forces in the outer struts (see fig. 8-2), as well as directly by the fuselage. The compressive loads in the outer struts and the lifting forces on the outer portions of the upper wing are resisted by tensile forces in the flying wires. The lift on the inner portion of the upper wing is transmitted to the fuselage by tensile forces in the inboard, or cabane, struts. Drag forces acting on the wings are transmitted to the fuselage by the spars and internal bracing and wires within the wing cross section.

When the airplane is on the ground or touching down upon landing, the gravity and inertial forces acting on the wings are downward. The inertial forces result from a change in the sinking speed, or the vertical downward component of the velocity of the aircraft. This reduction in the vertical velocity is a negative acceleration, or a deceleration, which produces downward inertial forces throughout the airplane. According to Newton's Second Law of Motion ($F = ma$), the inertial forces are distributed as the product of the local mass and acceleration. The upper wing forces are transmitted in compression through the struts. The forces from the outboard portions of the lower wing and from the outboard struts are resisted by tensile forces in the landing wires; these

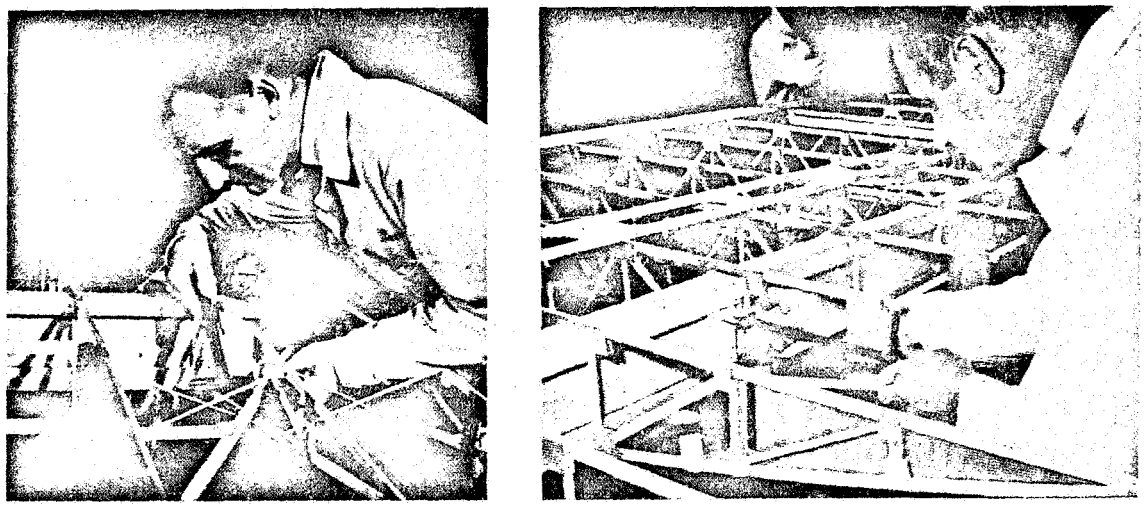

Figure 8-3. - Early wing construction. (Reprinted from Ryan Reporter, July/Aug. 1967, with their permission.)

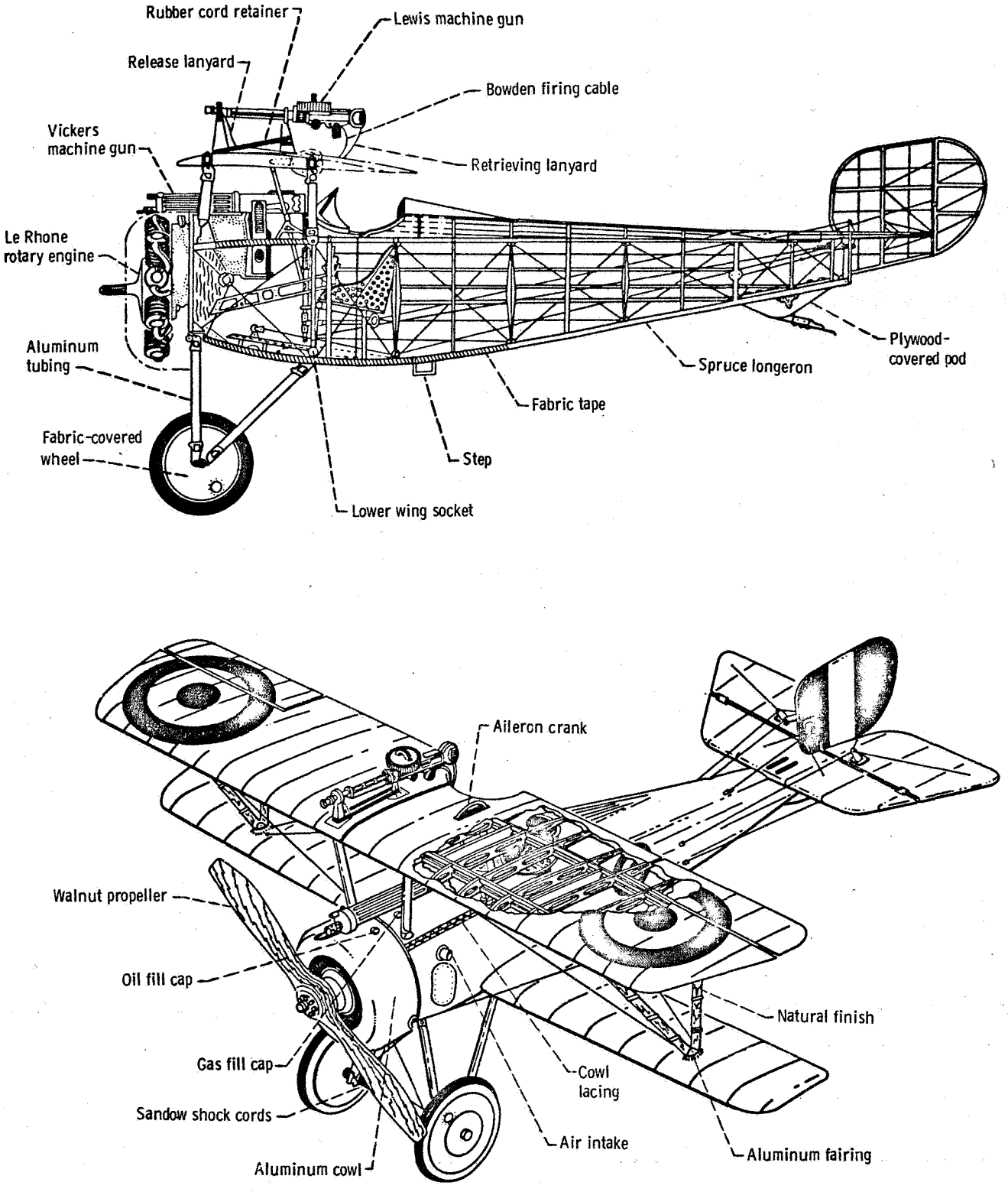

Figure 8-4. - Nieuport 17C. 1 Scout biplane (1915).

tensile forces are transmitted to the fuselage as compression in the inboard struts.

An example of early wing construction is shown in figure 8-3. These photographs were taken during the construction of the "Spirit of St. Louis II," a replica built to commemorate the 40th anniversary of Charles A. Lindbergh's solo flight across the Atlantic in the original "Spirit of St. Louis." The materials used were wood, high-strength wire, and fabric. The photographs show the two main spars and the truss-type structure and wire bracing between the spars.

Fuselage

One example of early fuselage construction is shown in figure 8-4. The structure was basically rectangular in cross section with vertical and horizontal trusses made of wood and wire. The side trusses provided strength and stiffness to carry small lift loads from the tail and to carry forces from the horizontal control surfaces. In addition, loads from the tail skid or wheel were transmitted through the sides. Top and bottom trusses supported loads from the vertical stabilizer and rudder and provided torsional strength and stiffness for the fuselage.

METAL SKIN AND TUBULAR TRUSSES

Metal Structures

As the knowledge of airplane flight loads and structural design progressed, the biplane gradually gave way to the monoplane, such as shown in figure 8-5. Wing construc-

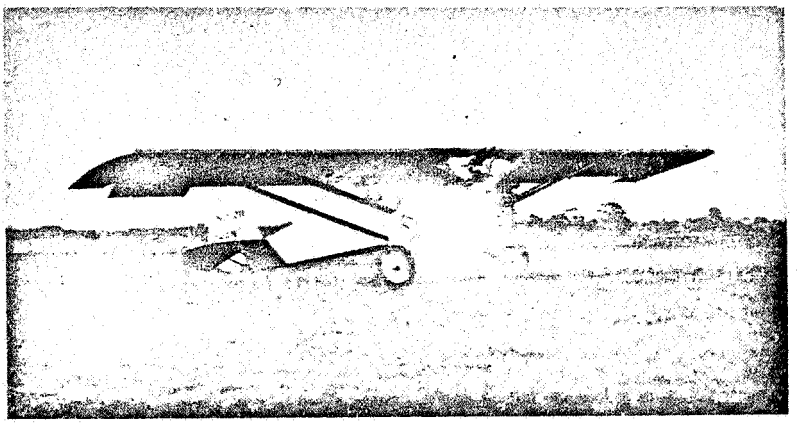

Figure 8-5. - Early high-wing monoplane with semicantilever wing. (Photo from J. W. Caler collection.)

tion had improved sufficiently to permit the outboard portions of the wings to be cantilevered with the lift forces now being carried as bending loads by the structure within the cross section of the wing. This method of support is in marked contrast to carrying the loads through compression struts and tension wires between lifting surfaces and the fuselage. The single wing was more efficient than the double wing. It also eliminated much of the drag associated with the external wires and struts between the two lifting surfaces. However, struts were still necessary to carry the large lifting forces and bending loads near the fuselage.

Eventually, metals began to play a larger role in aircraft construction. An evolutionary change in materials was made in the 1920's when the Ford Trimotor (fig. 8-6)

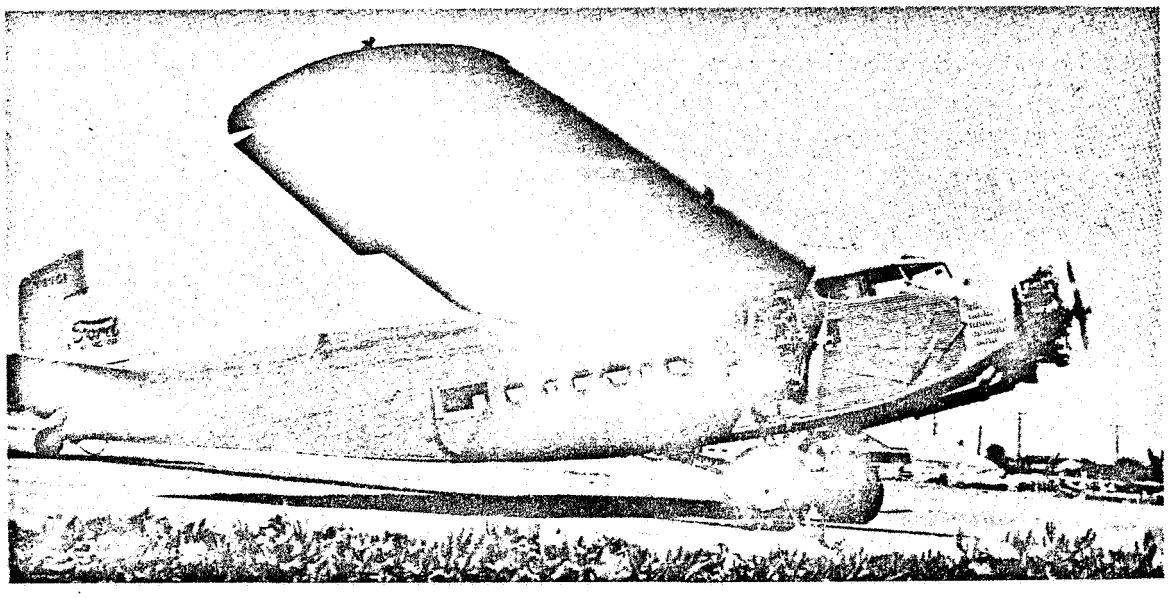

Figure 8-6. - Ford Trimotor, with tubular truss structure and corrugated metal skin. (Courtesy of Island Airlines.)

appeared with a corrugated metal skin covering a metal truss framework. The structure was still not very efficient, however, because most of the loads were carried by relatively heavy welded steel tubing rather than by the skin.

Figure 8-7 shows again details of the construction of the "Spirit of St. Louis II." The many longitudinal stringers apparent in the picture were simply to give aerodynamic shape to the fabric covering. Structural loads were carried by a welded metal truss, which can be seen inside the wooden stringers.

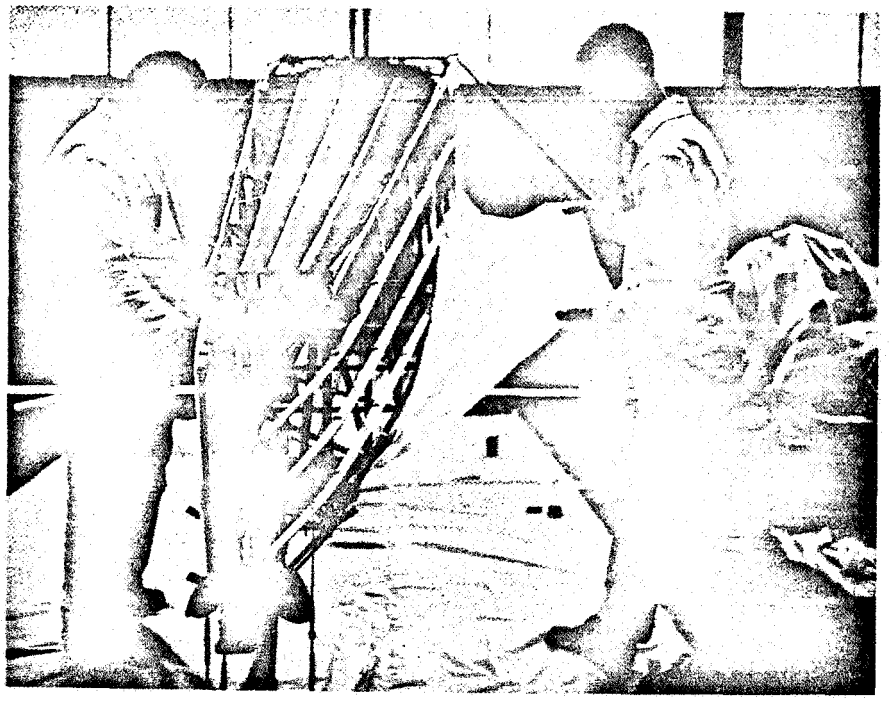

Figure 8-7. - Early fuselage construction. (Reprinted from Ryan Reporter, July/Aug. 1967, with their permission.)

Stressed Skin

The high drag and inefficient load-carrying properties of corrugated metal coverings, the relatively heavy construction of welded tubular trusses, the need for increased compartment space for passengers, and the development of strong aluminum alloys led to the introduction of stressed-skin shell, or "monocoque," structures.

Even prior to World War I, laminated wood (plywood) and metal were being tried in place of the fabric covering on parts of some airplanes. A thin wood fuselage was made by gluing together thin layers of wood on a mold. The smooth wood fuselage was usually stiffened by circular or oval ring frames and longitudinal stiffeners. The wooden shell carried most of the loads and provided a relatively smooth aerodynamic surface with reduced drag. The first such fuselage appeared in France in 1912. This type of construction with a load-carrying shell, or skin, is called "monocoque" after the name of the first model. Literally translated, the word "monocoque" means "single shell."

The use of stressed skin led to the development of thick wing profiles of tapered design, which resulted in a strong cantilever construction with no external bracing (fig. 8-8). The elimination of struts and wires increased the aerodynamic efficiency of the airplane. The thick monoplane wings permitted mounting engines on them and retracting the landing gear into them in flight to reduce the drag further. It also became possible to mount the

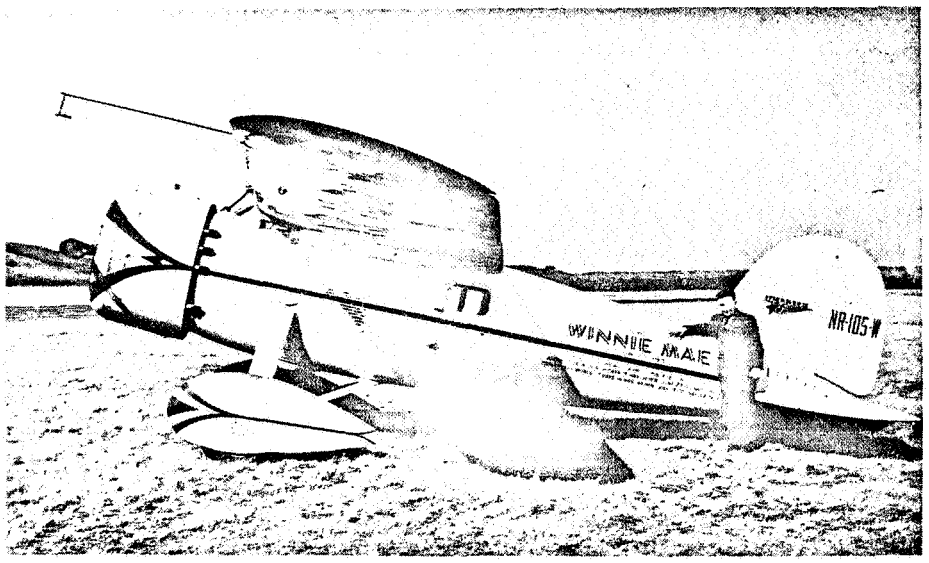

Figure 8-8. - Early monoplane with full-cantilever wing. (Photo from J. W. Caler collection.)

fuel tanks in the wings near the engines and thus free more space in the fuselage for passengers and cargo. The weight of the fuel and engines on the wings counteracted some of the lifting forces and thereby decreased the bending moments at the wing roots. The culmination of these advances was the Douglas DC-3 transport (fig. 8-9), which appeared in the mid-1930's.

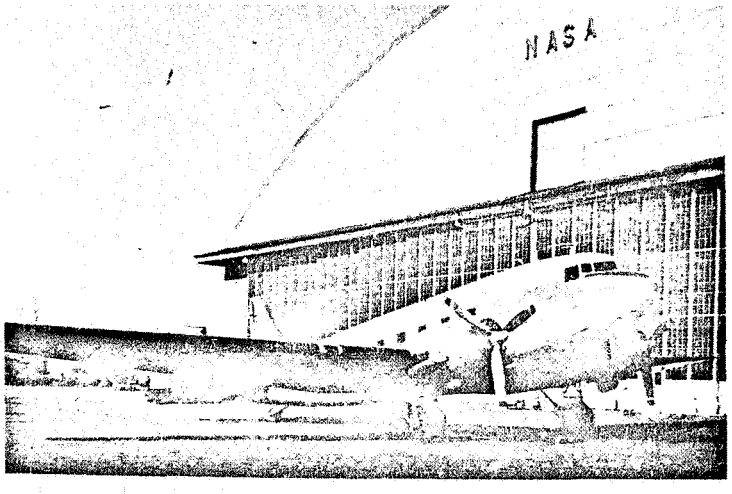

Figure 8-9. - Douglas DC-3 transport.

SEMIMONOCOQUE STRUCTURES

Stiffening

Most elements of today's aircraft structures are made from sheet metal. High-strength thin sheet is very efficient in transmitting tensile loads. However, when called upon to support compressive or shear loads, the thin sheet must be stiffened by ribs, formers, stringers, and longerons to prevent or minimize buckling. If no stiffening members are used, the sheet is designed to carry all the load, and the construction is called "monocoque," or "full monocoque," which means "single shell," as was mentioned previously. A shell thick enough to support all loads would usually be too heavy. Therefore, formers and stringers are used to stiffen the thin skin sufficiently to carry all loads in a lightweight structure. Such stiffened shells are called "semimonocoque" structures.

A typical example of the stiffening used in the semimonocoque structure of an airplane is shown in figure 8-10. This skeletal structure is covered with thin sheet aluminum, which then acts as a stressed skin and is a major load-carrying element of the aircraft. The skin is riveted or spot-welded to the frame. Although not apparent in this illustration, some of the longitudinal structural members are usually much thicker than others. In addition to being stiffeners, they are major load-carrying elements of the primary structure and are called "longerons." Likewise, some of the formers are much heavier than others that serve simply as stiffeners for the skin. They may be closed or nearly closed by webs with reinforced openings in them. Such partitions are called "bulkheads," and may serve to isolate certain parts of the fuselage from others for purposes of pressurization, heating, minimizing noise transmission, fire and smoke protection, or simply to provide surface area on which to mount equipment.

Large concentrated loads, such as those transmitted from the tail surfaces or landing gear, are distributed to the fuselage through fittings on the longerons and bulkheads. Similarly, concentrated loads on the wings, such as engines, rockets, bombs, and droppable fuel tanks, are carried through fittings attached to the main spars in the wings.

Cutouts or access holes must be provided in many areas of the aircraft to permit access to locations within the fuselage. In designing the airframe, the locations and spacing of longerons and bulkheads must be compatible with the locations of major openings such as passenger-access, landing-gear, bomb-bay, and cargo-bay doors. The longerons and bulkheads frequently reinforce the openings and provide alternate load paths for the forces which must be redistributed around the openings. Figure 8-10 illustrates some of these considerations.

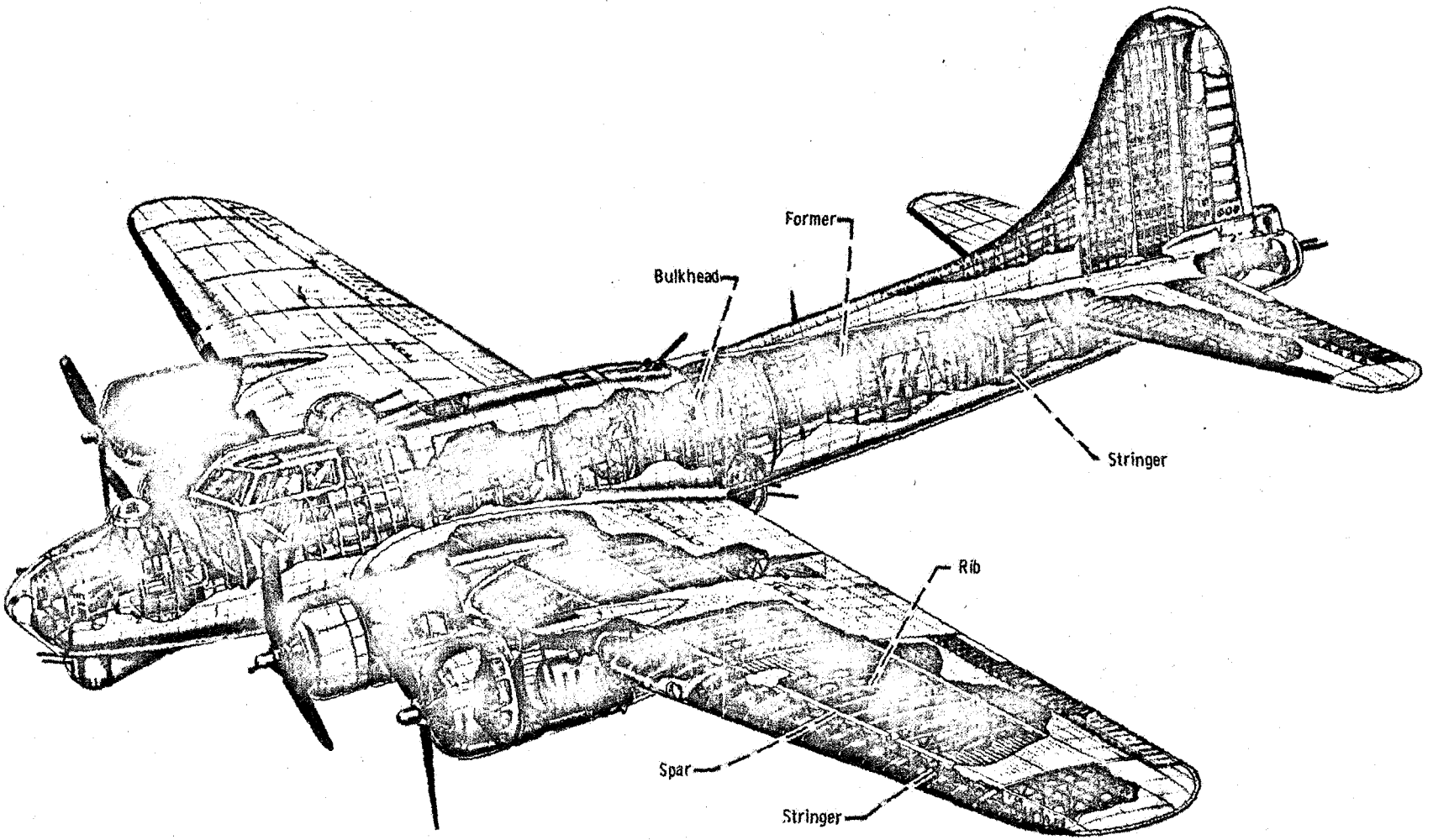

Figure 8-10. - Semimonocoque structure of Boeing B-17G bomber. (Taken from Flying, Jan. 1945, with permission of Aviation Division of Ziff-Davis Publishing Co.)

Pressurized Cabins

Commercial-transport design improved rapidly in the 1930's and 1940's. Along with increased range and altitude capability came the need for passenger-compartment pressurization. Airplanes such as the DC-6 routinely operated at 20 000 feet altitude, where the atmospheric pressure is less than half that at sea level. Passenger comfort and health required that the cabin be pressurized to an equivalent altitude of 7000 or 8000 feet. Thus, the pressure differential across the cabin wall could be as much as 5 to 6 pounds per square inch. Today's commercial jet transports fly at altitudes of about 40 000 feet, with a pressure differential of 8 to 10 pounds per square inch across the cabin wall.

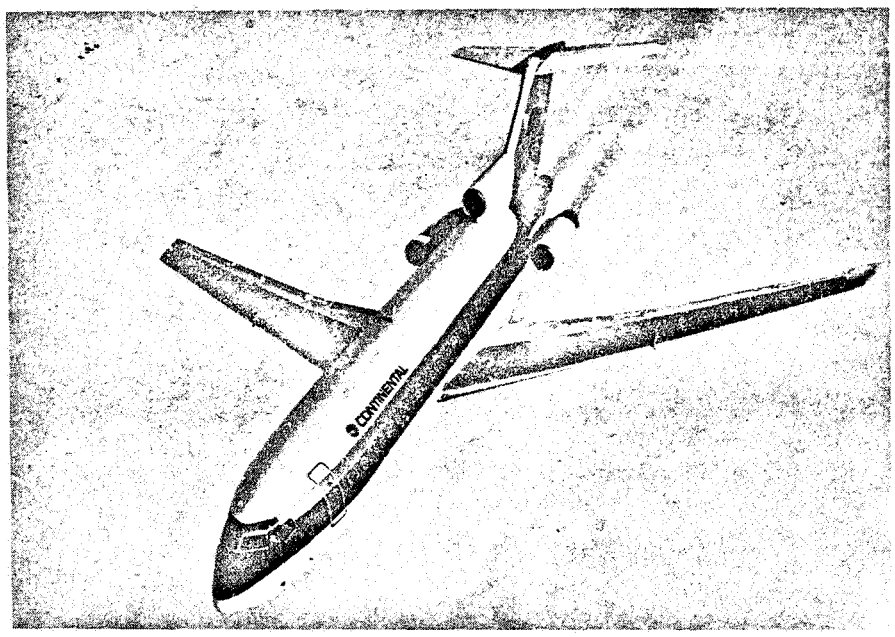

Figure 8-11. - Boeing 727 jet transport. (Reprinted from Aviation Week & Space Technology, Oct. 30, 1967, with their permission.)

Most current commercial jet aircraft are much larger than their predecessors with piston engines. In many respects, these jet aircraft are also quite different in appearance, with swept-back wings, T-shaped tails, and engines mounted directly on the fuselage and at the aft end of the airplane, as shown in figure 8-11. The basic structure, however, is still of aluminum, stressed-skin, semimonocoque construction not unlike the DC-3 of the 1930's.

Thin Wings

Supersonic flight has become possible with the advent of the jet engine. The aerodynamics of such high-speed flight make very thin wings highly desirable. New types of wing structures have been designed to provide the strength and stiffness for such thin wings. Large portions of the outer skin and internal stiffening are machined or forged as an integral structure. This type of construction avoids the forming and riveting together of many smaller pieces and provides a reduction in weight and an increase in the internal volume available for fuel storage. However, the wings of high-performance military aircraft are so thin that some fuel must be carried in the fuselage, and, in many cases, in external droppable tanks under the wings. The trend toward very thin wings has also forced the designer to locate the main landing gear so that it can be retracted into the fuselage rather than into the wings.

MATERIAL AND STRESS CONSIDERATIONS

Ultimate Strength

Until about the 1930's the basic structural requirement was simply that the structure have sufficient strength to support the loads without failing and that it be relatively light. Essentially this meant determining the loads and providing sufficient cross-sectional area so that the stress (load divided by area) did not exceed the ultimate strength of the material.

The most common measure of the ability of a material to provide high strength with minimum weight is its strength-to-density ratio. As the name implies, this is the ratio of the tensile strength of a material to its density (weight per unit volume). The higher the strength and the lower the density of a material, the higher is its strength-to-density ratio and, therefore, its ability to provide minimum-weight structures. However, most high-strength aircraft structural materials, such as aluminum, titanium, magnesium, and stainless steel, have about the same strength-to-density ratio at room temperature. Therefore, other factors usually control the selection of these materials for structural applications. Some of these factors are cost, availability, fabricability, corrosion resistance, fracture toughness (related to impact or notch sensitivity), fatigue strength, service temperature, and creep strength.

Fabricability

Since steel has about the same strength-to-density ratio as aluminum, a logical question is why more steel is not used in airframes. A major reason has to do with minimum gage (thickness) for handling and fabrication. Steel is about three times as strong and three times as dense as aluminum. Consequently, even though they can theoretically carry equal loads with equal weight structure, the steel sheet would be only one-third the thickness of the aluminum. This is undesirable for two reasons. First, the thickness of steel required might be only a few thousandths of an inch. This could produce handling problems during manufacture and increase the manufacturing costs, because such parts can become bent or damaged accidentally more easily than the much thicker aluminum. Also, the possibility of accidentally denting or puncturing the skin of the aircraft is greater.

A second, and more important, reason for using aluminum instead of steel has to do with increased buckling strength to resist compression or shear loads. This will be discussed more thoroughly in the following section on Buckling.

Magnesium has been used in airframe construction but only to a limited extent. It is not normally used, because it is relatively hard to work. Forming magnesium sheet into parts such as channels and angles must be done hot and under controlled conditions. Magnesium is also less corrosion resistant than is aluminum.

Buckling

Less than half of the material in the airframe is selected on the basis of tensile or ultimate strength. Over half of the material is chosen on the basis of buckling considerations. When relatively thin sheets or sections are subjected to compressive or shear stresses, they may buckle or wrinkle at stresses considerably below the yield or ultimate strength of the material. The buckling strength is a function of the geometry of the part, the edge support (or fixity), and the modulus of elasticity (or stiffness) of the material; it is not a function of the tensile strength of the material.

The modulus of elasticity is a material constant relating the deformation to the load on a structural component. Referring to figure 8-12, consider a simple bar with constant cross-sectional area A under the action of a tensile load P. The stress σ, which is a measure of the load intensity on the structure, is defined as the ratio of the load to the cross-sectional area, or

$$\sigma = \frac{P}{A}$$

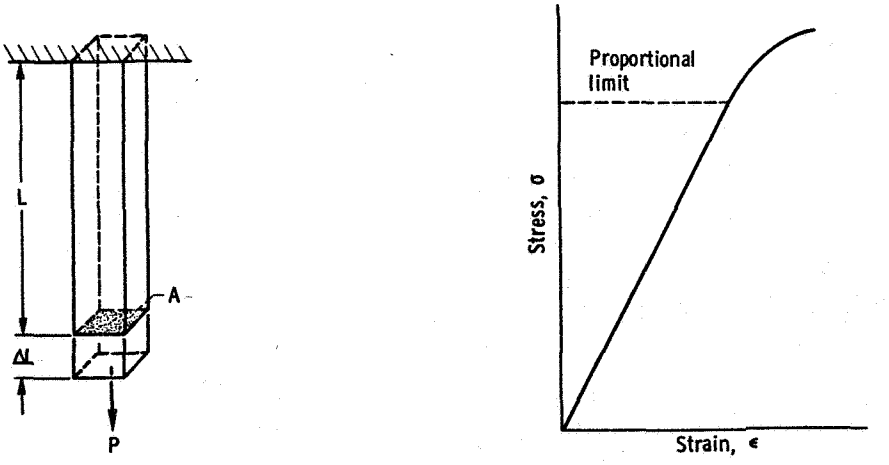

$$\text{Stress} = \frac{\text{Load}}{\text{Area}} \qquad \text{Strain} = \frac{\text{Change in length}}{\text{Original length}} \qquad \text{Modulus of elasticity} = \frac{\text{Stress}}{\text{Strain}}$$

$$\sigma = \frac{P}{A} \qquad \epsilon = \frac{\Delta L}{L} \qquad E = \frac{\sigma}{\epsilon}$$

Figure 8-12. - Stress, strain, and modulus of elasticity.

If the load is measured in pounds and the area in square inches, the units of stress are pounds per square inch (psi).

Any body subjected to a stress also undergoes a deformation. If the bar in figure 8-12 has initial length L, it will lengthen some amount ΔL under the action of the stress σ. The strain ϵ is defined as the ratio of the change in length to the original length, or

$$\epsilon = \frac{\Delta L}{L}$$

As can be seen, the strain is dimensionless and, therefore, has the same value irrespective of the system of units being used.

A typical plot of stress versus strain is shown in figure 8-12. Up to some value of stress called the proportional limit, stress is usually linearly proportional to strain; that is, the ratio of stress to strain is a constant. This constant of proportionality E is called the modulus of elasticity, or "Young's modulus," and is defined by the equation

$$E = \frac{\sigma}{\epsilon}$$

Since strain is dimensionless, the units of the modulus of elasticity E are the same as for stress, namely, pounds per square inch.

As mentioned previously, the buckling strength is a function of the geometry, edge support conditions, and the modulus of elasticity. For a given structural design, the buckling strength (or critical compressive stress σ_{cr}) of the sheet is proportional to the product of the modulus of elasticity and the thickness squared.

$$\sigma_{cr} \propto Et^2$$

As was also mentioned previously, steel and aluminum structures theoretically can be designed to carry the same loads in tension with the same weight. This is because the steel would be only one-third the thickness of the aluminum, since it is about three times as strong Since the density of steel (0.3 lb/in.^{3}) is three times that of aluminum (0.1 lb/in.^{3}), the weights would be the same. However, the modulus of elasticity of steel is also three times that of aluminum (30 000 000 lb/in.^{2} for steel and 10 000 000 lb/in.^{2} for aluminum) Therefore, from the preceding equation, the buckling strength of a steel panel will be only one-third that of an equal weight aluminum panel, because the buckling strength is proportional to thickness squared. (In contrast, the tensile strength is proportional to thickness to the first power.) Consequently, since most of an aircraft structure is designed on the basis of buckling, aluminum airframes are lighter in weight than those designed of steel for subsonic and some supersonic applications. Material selection for supersonic application will be discussed in the section titled THERMAL BARRIER.

Fatigue

Not only must the aircraft structure be designed to carry the maximum load, but it must also be designed to carry the loads repeatedly. A structure may fail if a given load is applied to it many times even though the stresses are low compared with the failure stress which can be obtained under a single cycle of loading. This phenomenon is called metal fatigue. The smaller the maximum stress, the larger will be the number of times the load can be applied without producing a fatigue failure, as shown in figure 8-13. For most materials there is a stress below which an infinitely large number of cycles can be applied without failure. This stress is called the endurance limit or fatigue limit.

One of the primary sources of stress which must be considered in designing against fatigue failure is gust loading. The wings, in particular, may flex many times in response to vertical gust loading during a single flight of the aircraft. Today's jets, flying at 35 000 to 40 000 feet altitude, are above most of the weather and thus are subjected to fewer cycles of gust loading than piston-engine airplanes, which fly at 15 000 to 20 000 feet altitude.

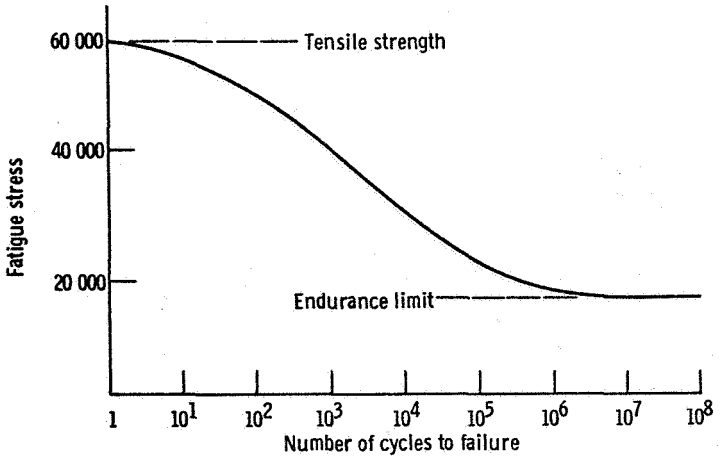

Figure 8-13. - Typical curve of fatigue stress as function of number of cycles to failure.

Pressurization of the passenger compartment produces stresses which are cyclic but occur only once per flight. However, this pressurization was found to be the cause of two disastrous disintegrations at high altitude of the British de Havilland Comet I. This airplane, which was one of the earliest high-altitude jet transports, entered service in 1952. The accidents, which occurred in 1954, were attributed to metal fatigue in the passenger compartment. A test cabin had been statically subjected to twice the expected pressure differential without difficulty. The same cabin was then run through a series of fatigue tests with no failure. However, it was learned later that the high-pressure static test had produced local plastic flow in the material around the windows, which changed the stress pattern produced in the fatigue tests. The fatigue life of the test cabin was thus unknowingly increased beyond that of the production cabins, which were never subjected to such a high-pressure static test.

AEROELASTICITY

The term "aeroelasticity" refers to the mutual interaction between aerodynamic forces and the elastic response of the structure. If the aircraft structure were perfectly rigid, there would be no aeroelastic problems. However, modern aircraft structures are very flexible and therefore must undergo a thorough aeroelastic analysis. This flexibility is vividly illustrated in figure 8-14, which shows the tip of a B-52 wing being deflected upward 22 feet from the undeflected position during a static test of the structure.

Aerodynamic forces produce structural deformations which may, in turn, produce additional aerodynamic forces. Such interactions may be damped out to stable equilibrium, or they may diverge and result in the destruction of the aircraft. One of the most

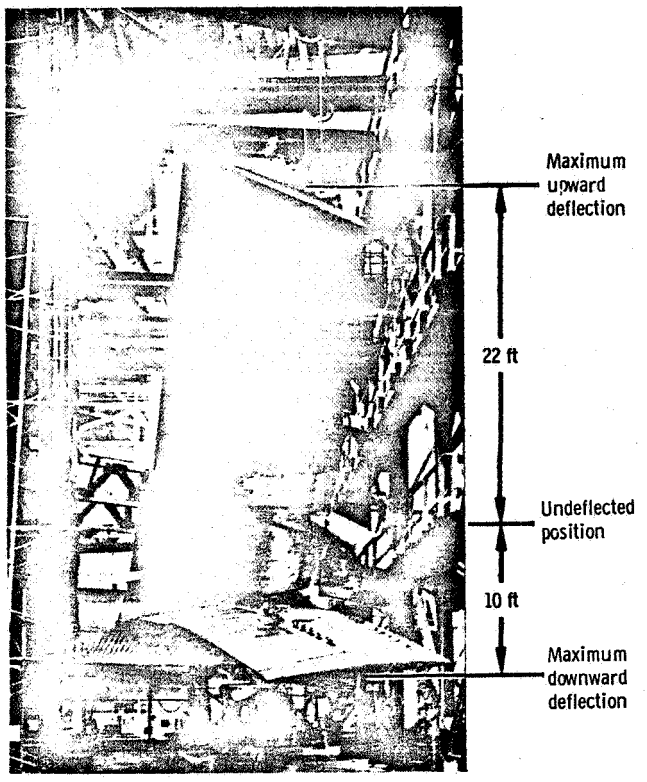

Figure 8-14. - Static test of flexibility of wing of B-52 aircraft. (Taken from "Principles of Aeroelasticity" by Raymond L. Bisplinghoff and Holt Ashley, with permission of John Wiley & Sons, Inc., Pub.)

complex aeroelastic phenomena is called flutter. Flutter is a dynamic instability which occurs at a critical speed called the flutter speed and results from the elasticity of the structure.

A simple example of aerodynamic flutter is the waving motion of a flag. Another example is the behavior of tree leaves, which oscillate as the air load varies between their upper and lower surfaces. Airplane wings, stabilizers, and control surfaces will flutter mildly at certain air speeds but fail violently if the flutter speed is exceeded. It is thus necessary that the flutter speed of all structural components susceptible to this phenomenon be above the maximum flight speed of the aircraft.

Flutter affects aircraft structural design most in requiring high torsional stiffness of the wings. In some instances, wing skin thickness has been dictated by aeroelastic considerations. Mass balancing the control surfaces with respect to the hinge line is also done to minimize flutter.

Another aeroelastic phenomenon which must be considered when designing the aircraft structure is called buffeting. Buffeting is a transient vibration, or shaking, of a structural component, produced by an unsteady airflow with rather powerful impulses. These impulses usually come from wakes or vortexes behind wings, nacelles, or objects

carried under the wings, such as fuel tanks, bombs, or even landing gear. Buffeting can occur at low or high speed and can be mild or catastrophic in nature. Mild buffeting at low speed can be beneficial in that it may warn the pilot that he is at a very high angle of attack attitude and about to stall or lose lift. Severe buffeting can result from interaction between the frequency of the aerodynamic pulses and the natural frequency of a structure, such as a tail surface. This could lead to metal fatigue over a period of time or to sudden collapse of the structure if the stiffness, strength, and damping are insufficient.

THERMAL BARRIER

Just a few years ago, engineers referred to the sonic barrier when discussing technical problems anticipated for future aircraft. As is well known, the term "supersonic" refers to speeds greater than the speed of sound (about 670 miles per hour at sea level; also called Mach 1). Hypersonic speeds are greater than five times the speed of sound, or Mach 5. Today some military aircraft fly at supersonic speeds under cruise conditions. Commercial transports are being built today to fly at almost three times the speed of sound. Obviously, the so-called sonic barrier has been overcome.

Today the thermal barrier appears formidable when considering future airplanes for supersonic and hypersonic flight. The thermal barrier refers to the structural and material problems resulting from very high temperatures being encountered both in the airframe and in the engine. Skin temperatures, especially on the leading edges of wings and tail surfaces, become very high as a result of aerodynamic heating as the air molecules collide with the airframe at very high speed. A typical plot of skin temperature as a function of Mach number is given in figure 8-15.

Aluminum retains most of its strength up to about 300° F and falls off quite rapidly above about 400° F, as shown in figure 8-16. Thus, figures 8-15 and 8-16 show why the

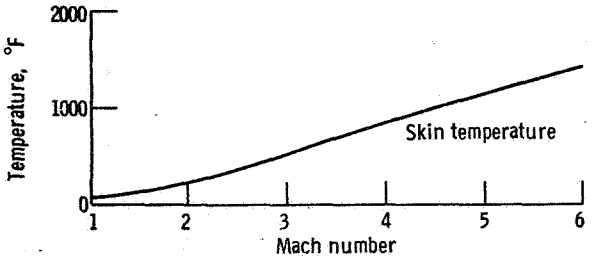

Figure 8-15. - Typical skin temperature as function of Mach number.

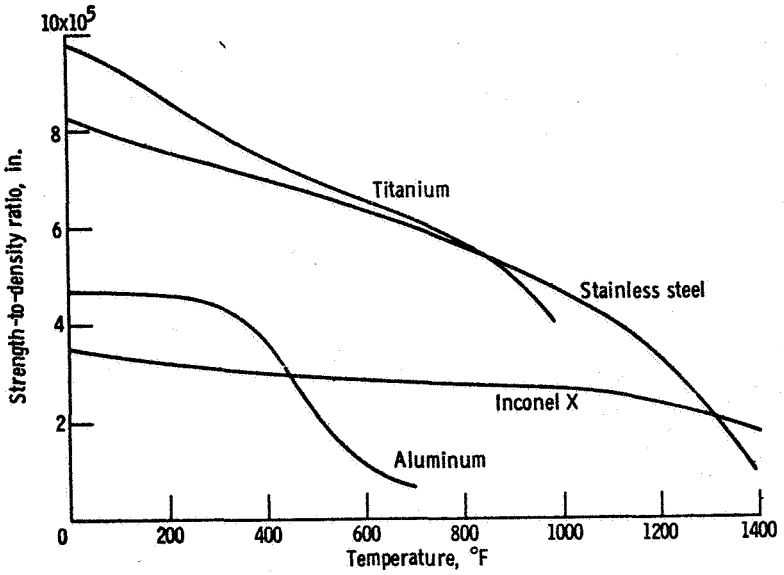

Figure 8-16. - Material strength-to-density ratio as function of temperature.

British-French Concorde, which is an aluminum airplane, is being designed to fly at Mach 2.2. This is about the upper limit of speed and temperature for an aluminum airframe. The United States supersonic transport (SST) will fly at Mach 2.7, or about 1800 miles per hour. The U. S. SST will be built of a titanium alloy to withstand skin temperatures in excess of 500° F.

At speeds in excess of Mach 3, or 2000 miles per hour, skin temperatures exceed 700° or 800° F, which is about the upper limit of usefulness for titanium. Therefore, materials such as stainless steel or Inconel must be used. The experimental X-15 airplane has flown at speeds as high as Mach 6.06 (4104 mph) and up to 354 200 feet (67 miles) altitude. It has an Inconel X skin which has withstood repeated flights that have heated large areas of the structure to a cherry-red 1300° F.

At high temperatures, other problems in addition to those involving material strength are encountered. As discussed earlier, over half of the aircraft structure is critical from the standpoint of buckling strength, which is directly proportional to the modulus of elasticity, or stiffness, of the material. Unfortunately, the modulus of elasticity, and therefore the buckling strength, decreases with increasing temperature. Another problem area involves thermal stresses that are induced because of the differences in temperature and, therefore, the differences in free thermal expansion in adjacent areas of the structure. These thermal stresses must be superimposed on the other stresses when designing the structure.

At high temperatures, materials creep and deform under long-time loading. There is an upper limit on the amount of creep a material can withstand, or the time it can be stressed to a given level; this limit is called the creep-rupture life of the material. Since

the SST is being designed for a life greater than 10 years or 30 000 to 50 000 hours of flying time, creep might be a significant problem. Thermal distortions and creep also affect the aerodynamic properties of the lifting surfaces. These may influence the performance of the airplane, particularly during a maneuver condition.

CONCLUDING REMARKS

This chapter has covered some aspects of the historical development of the modern aircraft structure and the technical advances which permitted its rapid evolution. Some of the ways in which material behavior influences structural design and ways in which aircraft performance may influence material selection have been discussed briefly. Of necessity, the discussion has been general and cursory. Helicopters and V/STOL airplanes were not considered. Lifting bodies for reentry from orbital or space flights and hypersonic airplanes were also omitted from the discussion. As these new types of craft are being developed and tested, aircraft structures and materials are also continually being changed and improved to meet the new requirements.

BIBLIOGRAPHY

Bisplinghoff, R. L.: The Supersonic Transport. Scientific American, vol. 210, no. 6, June 1964, pp. 25-35.

Bisplinghoff, Raymond L.; and Ashley, Holt: Principles of Aeroelasticity. John Wiley & Sons, Inc., 1962.

Bruhn, E. F.: Analysis and Design of Flight Vehicle Structures. Tri-State Offset Co., 1965.

Corning, Gerald: Supersonic and Subsonic Airplane Design. Second ed., Edwards Bros., Inc., 1960.

Heldenfels, Richard R.: Frontiers of Flight Structures. Aeronautics and Astronautics. Nicholas John Hoff and Walter Guido Vincenti, eds., Pergamon Press, 1960, pp. 29-51.

Heldenfels, R. R.: Structural Prospects for Hypersonic Air Vehicles. Aerospace Proceedings 1966. Vol. 1. Joan Bradbrooke, Joan Bruce, and R. R. Dexter, eds., Macmillan and Co., 1967, pp. 561-583.

Hoff, Nicholas J.: Thin Shells in Aerospace Structures. Astronautics and Aeronautics, vol. 5, no. 2, Feb. 1967, pp. 26-45.

Hunsaker, Jerome C.: A Half Century of Aeronautical Development. Proc. Am. Phil. Soc., vol. 98, no. 2, Apr. 1954, pp. 121-130.

Nayler, J. L.; and Ower, E.: Aviation: Its Technical Development. Dufour Editions, 1965.

Stack, John: The Supersonic Transport. Int. Sci. Tech., no. 22, Oct. 1963, pp. 50-54, 56, 58, 61.

9. AIRCRAFT STABILITY AND CONTROL

Clifford C. Crabs*

The stability and control characteristics of an airplane determine its ability to fly smoothly at a constant attitude and air speed, to recover from the effects of atmospheric disturbances, and to respond adequately to the control of the pilot. Stability is the tendency of an object (in our case, an airplane) to remain in a state of equilibrium. An object is in a state of equilibrium when the sum of all the forces and the sum of all the moments acting on it are equal to zero (i.e., when all forces and all moments are in balance). Thus, an object that is in a state of equilibrium experiences no acceleration in any direction. An airplane that is in a steady flight condition (equilibrium) will remain in this condition until the balance of forces or moments is disturbed by some force. Disturbing forces can be caused, for example, by changes in weight, weight distribution, engine thrust, surface shape, surface area, or flight attitude. Such changes may be accidental (e.g., a wind gust disturbing the airplane), or they may be deliberate (e.g., the pilot moving a control surface).

MECHANICAL STABILITY

Mechanical stability is the property that causes an object to develop forces opposing any influence that disturbs the object from its equilibrium position or motion. Mechanical stability has two components: static stability and dynamic stability. Static stability is the property whereby an object that is disturbed from a state of equilibrium develops restoring forces or moments that counteract the disturbance and tend to start the object back towards equilibrium. Dynamic stability is the property whereby the oscillations set up by the restoring forces or moments of a statically stable object that is disturbed from equilibrium are damped. Mechanical stability (both static and dynamic) may be classified as positive, neutral, or negative.

Static Stability

With positive static stability, an object that is disturbed from a state of equilibrium

*Aerospace Engineer and Pilot, Aircraft Operations Branch.

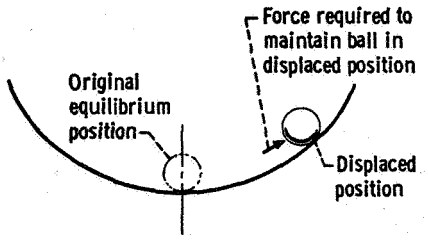

(a) Positive.

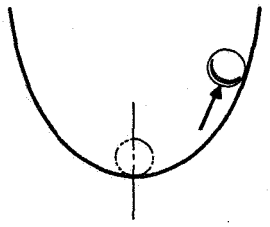

(b) More positive.

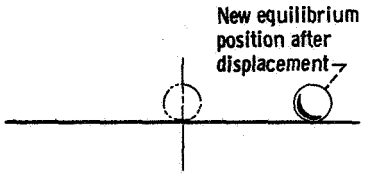

(c) Neutral.

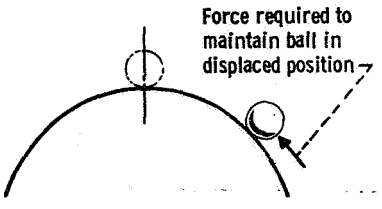

(d) Negative.

Figure 9-1. - Static stability.

tends to return to the original condition. With neutral static stability the object tends to remain in a state of equilibrium, but when the object is disturbed, it may come to rest in a new state of equilibrium. In other words, after the disturbance the object tends neither to return to the original state nor to move further away from it. With negative static stability (static instability), the object is unstable. When the object is disturbed, it tends to continue to move further away from the original state, even after the initial disturbance.

A simple analogy for static stability is a ball resting on various curved and flat surfaces. Figure 9-1(a) illustrates positive static stability. If the ball in this example is displaced from its equilibrium position at the bottom of the curve, it tends to resist the displacement. When the disturbing force is removed and the ball is released in the displaced position, it tends to return to its original equilibrium position at the bottom of the curve.

Figure 9-1(b) illustrates a greater degree of positive static stability. In this example the behavior of the ball is similar to that of the previous example. However, the ball now has a greater tendency to return to its original equilibrium position, because the slope of the curved surface is steeper. Therefore, a greater force is required to displace the ball from its equilibrium position.

Neutral static stability is illustrated in figure 9-1(c). In this example, when the ball is displaced, it has no tendency to return to its original equilibrium position. Therefore, the ball can be displaced by a smaller force than that required to displace the ball with positive stability. When the disturbing force is removed, the ball does not tend to return to its original equilibrium position but assumes equilibrium in the displaced position.

Figure 9-1(d) shows an example of negative static stability (or instability). In this case, the ball is very easily displaced from its equilibrium position. Once the ball is displaced, it continues or tends to continue to move farther away from its equilibrium position, even after the initial disturbance is removed.

The restoring forces or moments developed by an object with positive static stability tend to cause the object to oscillate about its equilibrium position. For example, if the ball in figure 9-1(a) is displaced from its equilibrium position to some point up the slope and is released, it tends to roll back down the slope toward its equilibrium position. If there is no force to slow down the ball, its momentum will cause it to roll through the equilibrium position and up the opposite slope. Then the ball will tend to return down the slope, through the equilibrium position, and back up the original slope. Thus, an oscillation is set up. Dynamic stability concerns the damping (i.e., the displacement-time history) of such oscillations.

Dynamic Stability

An object that has positive static stability also has either positive, neutral, or nega-

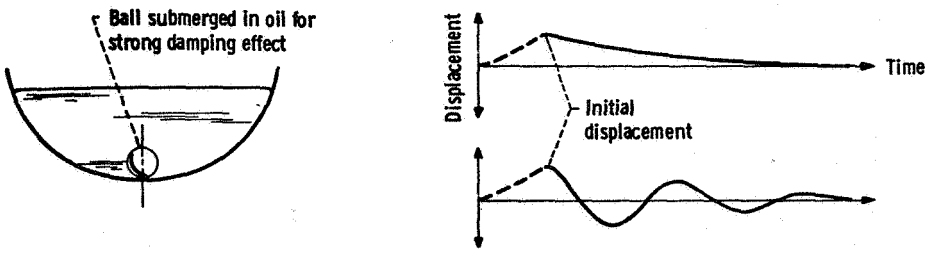

(a) Positive dynamic stability - positive static stability.

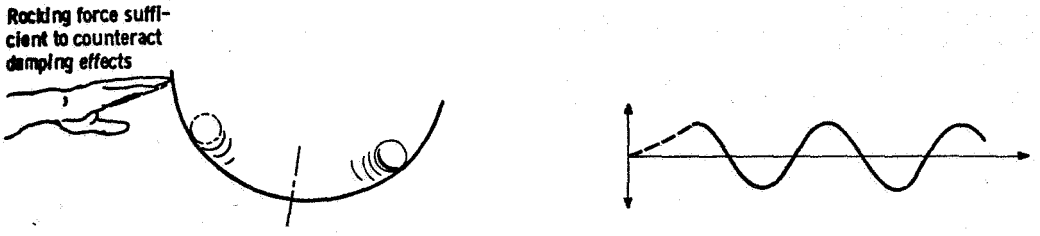

(b) Neutral dynamic stability - positive static stability.

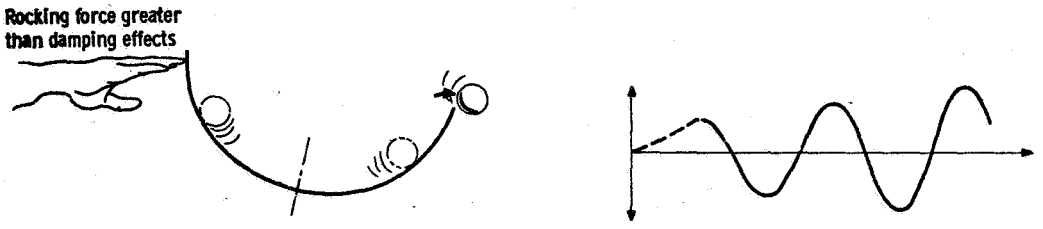

(c) Negative dynamic stability - positive static stability.

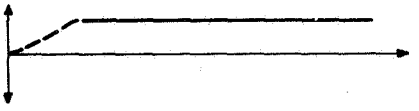

(d) No dynamic stability characteristics - neutral static stability.

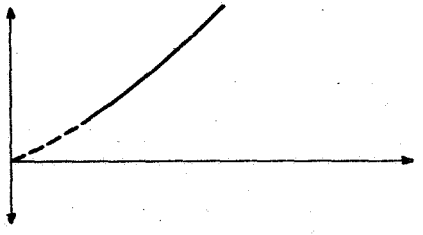

(e) Negative dynamic stability - negative static stability.

Figure 9-2. - Examples and displacement-time histories of dynamic stability and interrelation of static and dynamic stabilities.

tive dynamic stability. When an object with positive dynamic stability is disturbed from a state of equilibrium, the oscillations set up by the restoring forces or moments are damped, and the object gradually returns to its original state of equilibrium. With neutral dynamic stability, the oscillations of the object neither increase nor decrease in magnitude. With negative dynamic stability (dynamic instability), the oscillations of the object increase in magnitude.

Figure 9-2 shows examples of dynamic stability and curves of displacement as a function of time. Positive dynamic stability is illustrated in figure 9-2(a). In this example, the oil provides a damping effect. Thus, if the ball is displaced from its equilibrium position and is released, it returns to, and eventually comes to rest in, its original equilibrium position. The displacement-time curve shows that the ball may return to equilibrium either in a single motion (simple subsidence) or in a series of damped oscillations whose amplitude decreases with time.

Neutral dynamic stability is shown in figure 9-2(b). In this example, either the system is assumed to be frictionless or an outside force is applied to the system (e.g., to rock the concave surface) that is exactly equal to and counteracts the damping forces of the system. Under either of these conditions, the ball rolls the same distance up each slope on every oscillation. The displacement-time curve shows that the amplitude of the oscillations remains constant with time.

Figure 9-2(c) illustrates negative dynamic stability (dynamic instability). In this example, if an outside force is applied to the system that counteracts and exceeds the damping forces, the ball with roll farther up the slope with each oscillation. The displacement-time curve shows the amplitude of the oscillations increasing with time.

With neutral static stability (fig. 9-2(d)), an object does not display any dynamic stability characteristics.

An object with negative static stability (fig. 9-2(e)) has negative dynamic stability.

AERODYNAMIC STABILITY

The aerodynamic stability of an airplane in flight is a form of mechanical stability. An airplane has three components of stability (lateral, longitudinal, and directional), based on its three stability axes (roll, pitch, and yaw), about which it may rotate. These axes (fig. 9-3) are mutually perpendicular and usually intersect at the center of gravity of the airplane. The roll axis is the longitudinal axis about which the airplane rotates when it is inclined laterally (i.e., banked). The pitch axis is the lateral axis about which the airplane rotates when its nose is raised or lowered relative to the tail, as when the airplane is shifted into a climbing or diving attitude. The yaw axis is the normal axis (perpendicular to the plane of the other two axes) about which the airplane rotates when

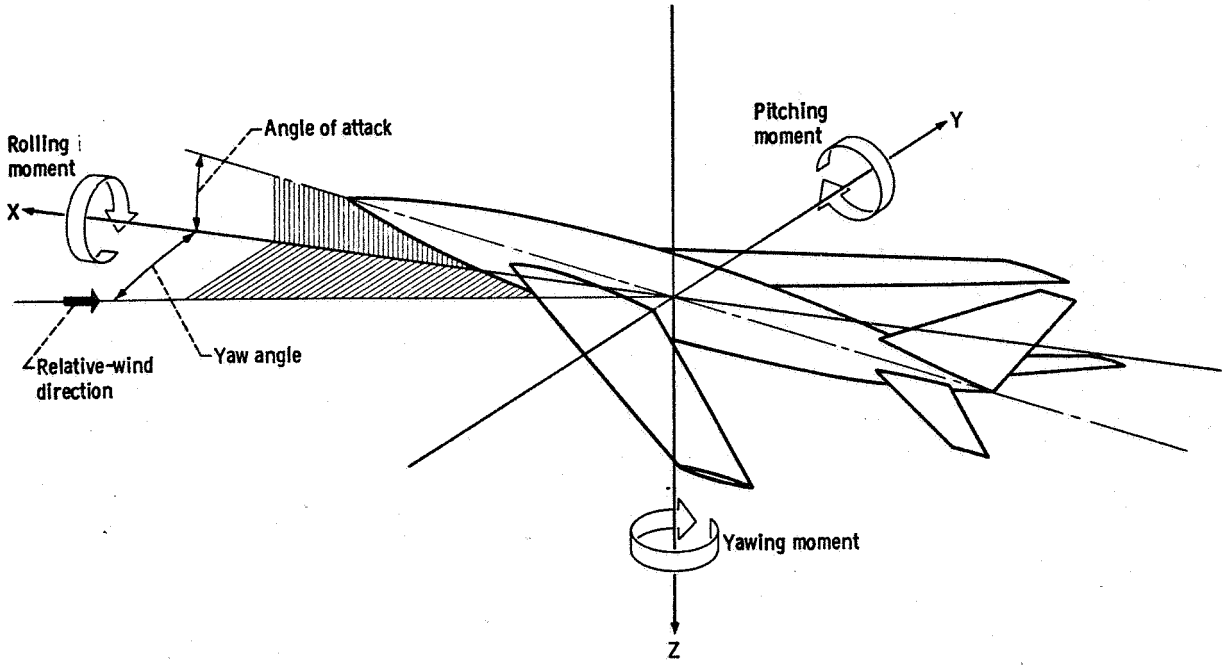

Figure 9-3. - Stability axes. (Arrows indicate conventional positive directions of axes and moments.)

the nose of the airplane is pointed in a new direction to the right or left of the original direction.

An airplane in flight has three degrees of freedom relative to each of its stability axes. (A degree of freedom is one of a limited number of ways in which a point or a body may move or a dynamic system may change.) The three degrees of freedom are angular displacement (rotation) about the axis, linear displacement along the axis, and change of velocity along the axis. Any actual change or displacement of the airplane generally involves a combination of motions and velocity changes relative to all three stability axes.

Of the three previously mentioned components of aerodynamic stability, longitudinal stability pertains to pitching motions, vertical displacements, fore-and-aft displacements, and changes in forward or vertical velocities. Lateral stability refers to rolling motions, lateral displacements (sideslip), and changes in lateral velocity. Directional stability pertains to yawing motions.

Because of its complexity, the overall subject of airplane stability cannot be explained thoroughly in this chapter. Therefore, the following brief and limited discussion is devoted to only static longitudinal stability, and specifically to pitching motions.

Longitudinal Stability

The behavior of an airplane in each component of its stability is similar to the be-

havior of the ball in the preceding examples. Thus, if an airplane with positive static and positive dynamic longitudinal stability is displaced from a level-flight attitude, it returns to and eventually resumes the original attitude. With positive static and neutral dynamic stability, an airplane tends to return to the original attitude but does not resume that attitude. Instead, the airplane overshoots the original attitude and begins an oscillatory pitching motion of constant amplitude. With positive static and negative dynamic stability, an airplane tends to return to the original level-flight attitude, but it begins an oscillatory pitching motion of increasing amplitude.

With neutral static longitudinal stability, an airplane tends to maintain any pitch attitude (climbing or diving attitude) to which it is displaced. When an airplane with negative static longitudinal stability (static longitudinal instability) is displaced from a level-flight attitude, it tends to continue to diverge ever farther from the original attitude.

Effect of Location of Center of Gravity on Stability

One of the factors that affect the static, longitudinal stability of an airplane is the location of the center of gravity relative to the neutral point of the airplane. The neutral point is that point about which the pitching moment of the airplane remains constant, even when the angle of attack of the airplane is changed. In other words, the neutral point is the aerodynamic center of the entire airplane.

When the center of gravity of an airplane is located at the neutral point (fig. 9-4), the airplane possesses neutral, static, longitudinal stability. Figure 9-4(a) shows a neutrally stable, example airplane in an equilibrium, level-flight attitude. The total lift produced by the wing (4800 lb) and the horizontal tail (1200 lb) equals the airplane weight (6000 lb). The nose-up pitching moment produced by the wing (4800 lb × 4 ft = 19 200 lb-ft) is equal to the nose-down pitching moment produced by the tail (1200 lb × 16 ft = 19 200 lb-ft). The center of gravity is located at the neutral point. The wing and the horizontal tail have equal angles of incidence (4°). This condition of equal angles of incidence is called "zero angular difference." Any airplane whose center of gravity is located at the neutral point must have zero angular difference to achieve equilibrium.

The angle of incidence of an airfoil is the angle between the chord of the airfoil and the longitudinal axis of the airplane. The angle of attack of an airfoil is the angle between the chord of the airfoil and the direction of the relative wind at the airfoil. For this example airplane in the level-flight attitude, the relative-wind direction for both the wing and the horizontal tail is assumed to be parallel to the longitudinal axis of the airplane. Therefore, in the level-flight attitude, the incidence angles of the wing and the horizontal tail are also their angles of attack. However, when the example airplane is disturbed

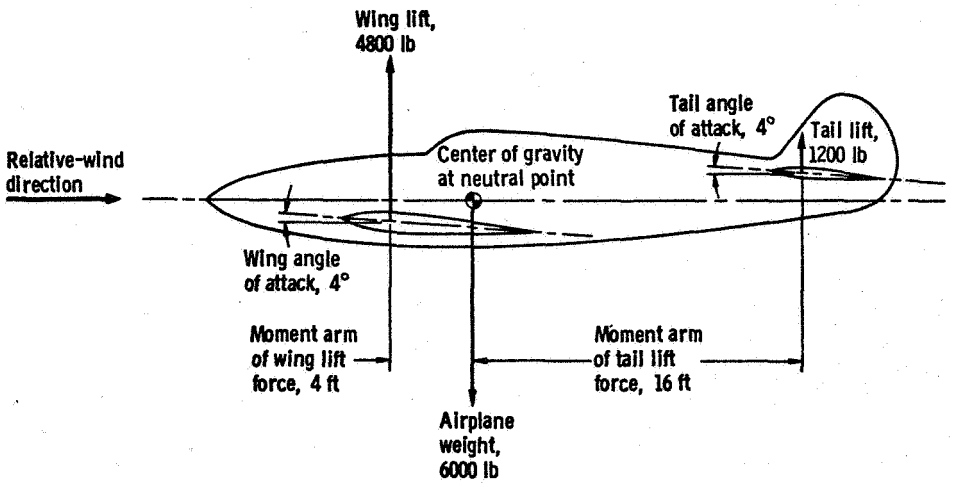

(a) Airplane in initial, equilibrium, level-flight attitude.

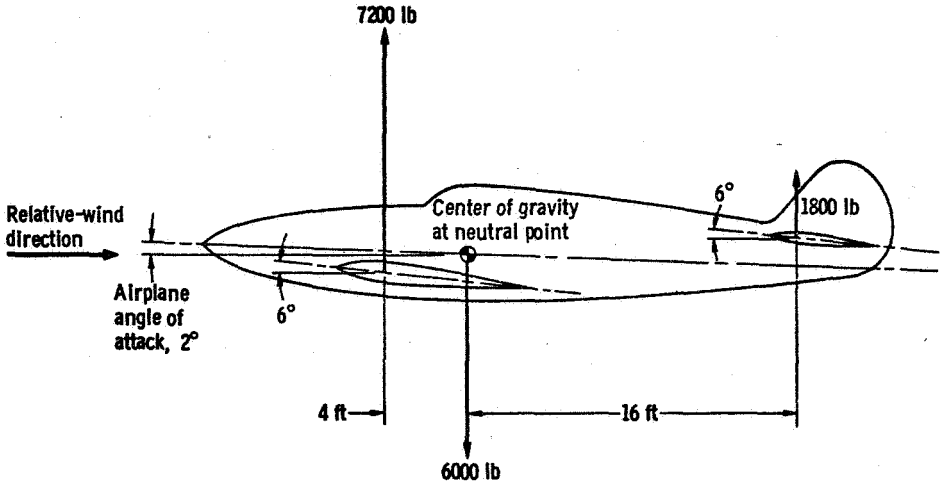

(b) Airplane in displaced, nose-up attitude.

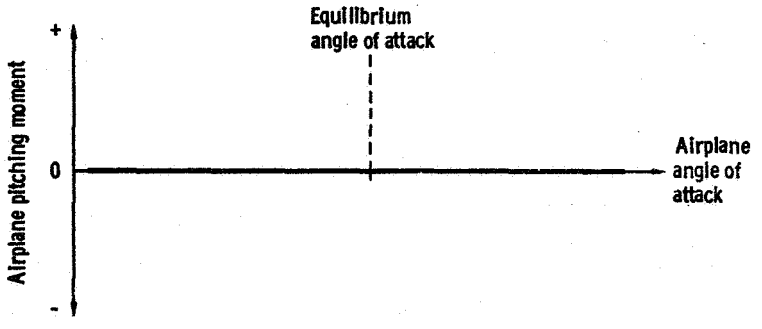

(c) Airplane pitching-moment curve. (Nose-up moment is positive; nose-down moment is negative.)

Figure 9-4. - Forces acting on example airplane with neutral, static, longitudinal stability.

from the level-flight attitude, the angles of attack change, whereas the incidence angles remain unchanged.

When this airplane is pitched upward or downward from its initial, equilibrium, level-flight attitude, it maintains neutral stability. Figure 9-4(b) shows the airplane in a new, upwardly displaced attitude. The airplane angle of attack has been increased by 2^{o}. Therefore, the angles of attack of both the wing and the horizontal tail have increased by 50 percent (from 4^{o} to 6^{o}). Since the lift of an airfoil is a linear function of its angle of attack, the wing lift has increased from 4800 pounds to 7200 pounds, and the tail lift has increased from 1200 pounds to 1800 pounds. However, the nose-up pitching moment produced by the wing (7200 lb × 4 ft = 28 800 lb-ft) is still equal to the nose-down pitching moment produced by the tail (1800 lb × 16 ft = 28 800 lb-ft), so that the resultant pitching moment of the airplane is zero. Therefore, when this airplane is displaced from its initial, equilibrium, level-flight attitude, it tends to remain in the new, displaced attitude. Thus, the airplane displays neutral, static, longitudinal stability.

Figure 9-4(c) shows an example curve of the pitching moment as a function of angle of attack for an airplane with neutral stability. The slope of the curve is zero. This indicates that when the airplane angle of attack is varied, the resultant pitching moment of the airplane remains zero.

If the center of gravity of an airplane is located ahead of the neutral point, the airplane possesses positive, static, longitudinal stability. Figure 9-5(a) shows the example airplane again in an equilibrium, level-flight attitude. The total lift produced by the wing (5400 lb) and the horizontal tail (600 lb) is equal to the airplane weight (6000 lb). The nose-up pitching moment produced by the wing (5400 lb × 2 ft = 10 800 lb-ft) is equal to the nose-down pitching moment produced by the horizontal tail (600 lb × 18 ft = 10 800 lb-ft).

Since the center of gravity has been moved forward of the neutral point, the moment arm of the wing lift force has decreased (from 4 ft to 2 ft), while that of the tail lift force has increased (from 16 ft to 18 ft). Therefore, to achieve equilibrium in the level-flight attitude, the lift force of the wing has been increased (from 4800 lb to 5400 lb), and that of the tail has been decreased (from 1200 lb to 600 lb). These changes in the lift forces have been accomplished by increasing the wing angle of attack and decreasing the tail angle of attack. As mentioned previously, the angles of attack of the wing and tail of this example airplane in the level-flight attitude are assumed to be the same as their incidence angles. So, the incidence angle of the wing has been increased (from 4^{o} to 4.5^{o}), and that of the tail has been decreased (from 4^{o} to 2^{o}). Therefore, the incidence angle of the wing is now greater than that of the tail. This condition is called "positive angular difference." Any airplane whose center of gravity is moved forward of the neutral point, but whose wing and tail surface areas remain unchanged, must have positive angular difference to achieve equilibrium.

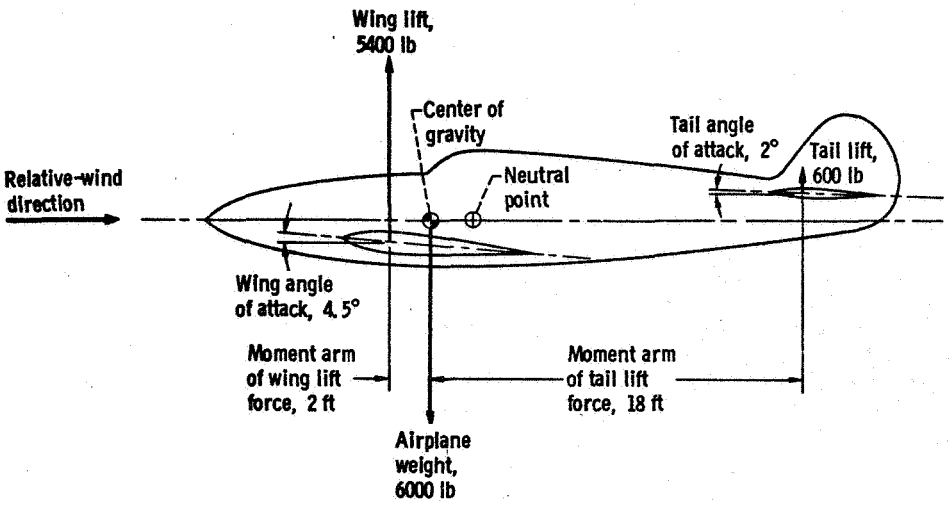

(a) Airplane in initial, equilibrium, level-flight attitude.

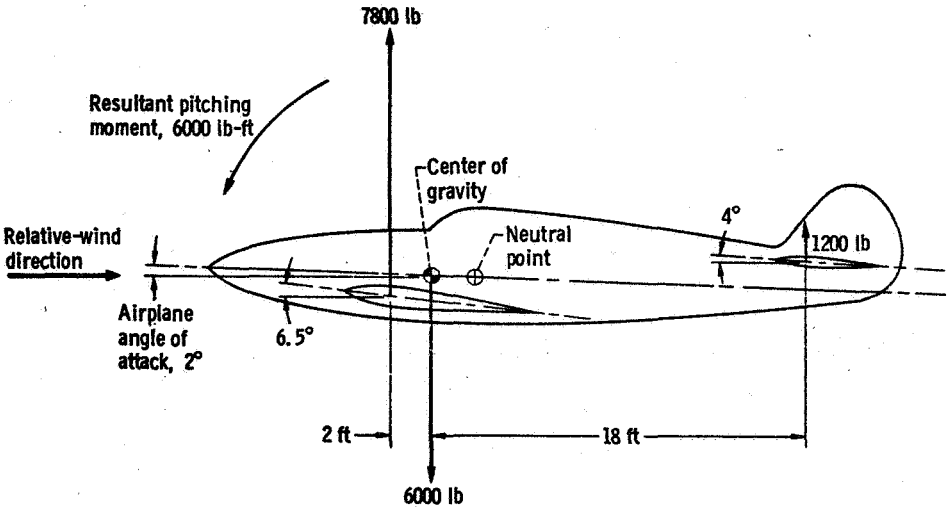

(b) Airplane in displaced, nose-up attitude.

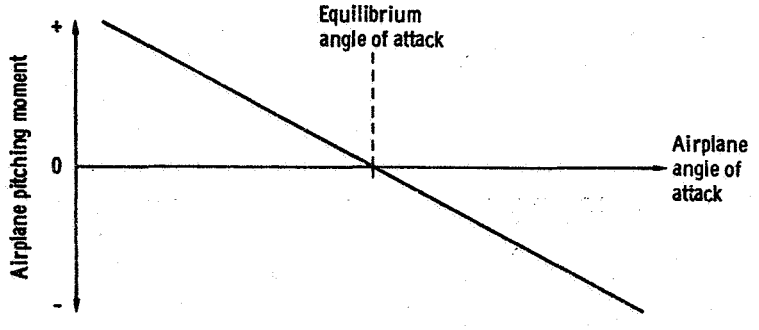

(c) Airplane pitching-moment curve. (Nose-up moment is positive; nose-down moment is negative.)

Figure 9-5. - Forces and resultant pitching moment acting on example airplane with positive, static, longitudinal stability.

When this airplane is pitched upward or downward from its initial, equilibrium, level-flight attitude, it displays positive stability. Figure 9-5(b) shows the airplane in a new, upwardly displaced attitude. The airplane angle of attack has been increased by 2°. Since the wing and the horizontal tail are attached to the fuselage, their angles of attack have also increased by 2°. However, because of the initial, positive angular difference, the wing and tail angles of attack have increased by different percentages. The wing angle of attack has increased by approximately 44.4 percent (from 4.5° to 6.5°), and the tail angle of attack has increased by 100 percent (from 2° to 4°). The lift forces produced by the wing and the horizontal tail have also increased by these percentages. Therefore, the nose-up pitching moment produced by the wing (7800 lb × 2 ft = 15 600 lb-ft) is now less than the nose-down pitching moment produced by the horizontal tail (1200 lb × 18 ft = 21 600 lb-ft). Thus, the airplane has developed a resultant, nose-down pitching moment (6000 lb-ft) that is opposite in direction to the initial, nose-up displacement. This resultant moment tends to return the airplane to its initial, equilibrium attitude. Therefore, this airplane displays positive, static, longitudinal stability.

Figure 9-5(c) shows an example curve of the resultant pitching moment as a function of angle of attack for a stable airplane. For angles of attack smaller than the equilibrium angle of attack (i.e., when the airplane is pitched downward from its equilibrium attitude), the pitching moment is positive (nose-up). At the equilibrium angle of attack, the pitching moment is zero. For angles of attack greater than the equilibrium angle of attack (i.e., when the airplane is pitched upward from its equilibrium attitude), the pitching moment is negative (nose-down). Thus, figure 9-5(c) shows that for a longitudinally stable airplane, the pitching-moment curve has a negative slope. The degree of stability is indicated by the slope, or steepness, of the curve.

When the center of gravity of an airplane is located behind the neutral point, the airplane possesses negative, static, longitudinal stability. Figure 9-6(a) shows the example airplane again in an equilibrium, level-flight attitude. The total lift provided by the wing (4200 lb) and the tail (1800 lb) is equal to the airplane weight (6000 lb). Also, the nose-up pitching moment produced by the wing (4200 lb × 6 ft = 25 200 lb-ft) is equal to the nose-down pitching moment produced by the horizontal tail (1800 lb × 14 ft = 25 200 lb-ft). However, the center of gravity is now located behind the neutral point. For this unstable configuration, the relative lengths of the moment arms of the wing and tail lift forces are such that equilibrium in any specific pitch attitude can be achieved only if the incidence angle of the wing is less than that of the tail. This condition is called "negative angular difference." Any airplane whose center of gravity is moved rearward of the neutral point, but whose wing and tail surface areas remain unchanged, must have negative angular difference to achieve equilibrium. For the example airplane of figure 9-6(a), the wing incidence angle is 3.5°, and the tail incidence angle is 6°. (It should be remembered that for our example airplane in the level-flight attitude, the angles of attack are

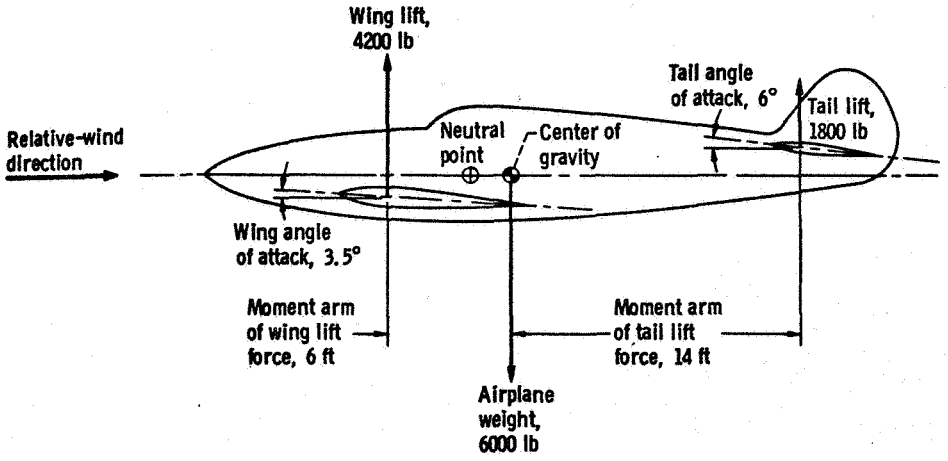

(a) Airplane in initial, equilibrium, level-flight attitude.

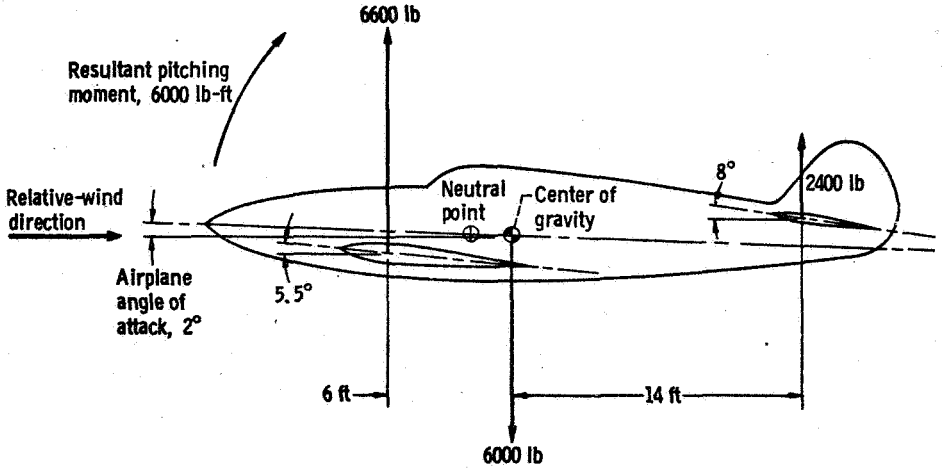

(b) Airplane in displaced, nose-up attitude.

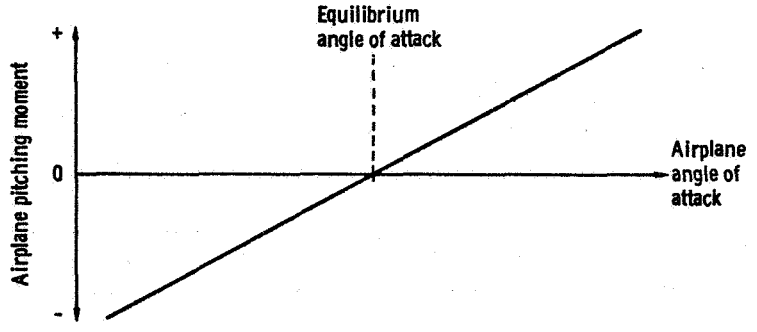

(c) Airplane pitching-moment curve. (Nose-up moment is positive; nose-down moment is negative.)

Figure 9-6. - Forces and resultant pitching moment acting on example airplane with negative, static, longitudinal stability.

assumed to be the same as the incidence angles.)

When this airplane is pitched upward or downward from its equilibrium attitude, it displays negative stability. Figure 9-6(b) shows the example airplane in an upwardly displaced attitude. The airplane angle of attack has been increased by 2°. Thus, the wing angle of attack has increased by approximately 57 percent (from 3.5° to 5.5°), and the tail angle of attack has increased by approximately 33 percent (from 6° to 8°). The wing and tail lift forces have increased by these same percentages. Therefore, the nose-up pitching moment produced by the wing (6600 lb × 6 ft = 39 600 lb-ft) is now greater than the nose-down pitching moment produced by the tail (2400 lb × 14 ft = 33 600 lb-ft). Thus, the airplane has developed a resultant, nose-up pitching moment (6000 lb-ft) in the same direction as the initial, nose-up displacement. This resultant pitching moment tends to cause the airplane to continue to diverge farther from the initial, equilibrium, level-flight attitude. Thus, this airplane displays negative, static, longitudinal stability.

Figure 9-6(c) shows an example curve of the resultant pitching moment as a function of angle of attack for an unstable airplane. For angles of attack smaller than the equilibrium angle of attack (i.e., when the airplane is pitched downward from its equilibrium attitude), the pitching moment is negative (nose-down). At the equilibrium angle of attack, the pitching moment is zero. For angles of attack greater than the equilibrium angle of attack (i.e., when the airplane is pitched upward from its equilibrium attitude), the pitching moment is positive (nose-up). Thus, figure 9-6(c) shows that for a longitudinally unstable airplane, the pitching-moment curve has a positive slope. The degree of instability is indicated by the slope, or steepness, of the curve.

To simplify the preceding discussion of stability, the relative-wind direction was assumed to be the same for the wing and the horizontal tail. However, the horizontal tail of an actual airplane in flight generally operates in the downwash created by the wing. The local airflow past the wing is turned downward by it (see chapter 4), so that the local relative-wind direction at the horizontal tail is different from that at the wing. The downwash from the wing reduces the angle of attack of the tail and thereby affects the longitudinal stability of the airplane. Essentially, the effect of downwash on the horizontal tail necessitates shifting the neutral point (and center of gravity) to a more forward location to maintain the longitudinal stability of the airplane.

Figure 9-7(a) shows the neutrally stable, example airplane in an equilibrium, level-flight attitude, without any downwash. (This is the same example airplane as the one shown in fig. 9-4(a).) The total lift produced by the wing and the horizontal tail equals the airplane weight. The nose-up pitching moment produced by the wing is equal to the nose-down pitching moment produced by the tail. The center of gravity is located at the neutral point. The wing and the horizontal tail have equal angles of incidence (i.e., zero angular difference). Also, in the level-flight attitude, the relative wind direction is again assumed to be parallel to the longitudinal axis of the airplane. Thus, in the level-flight

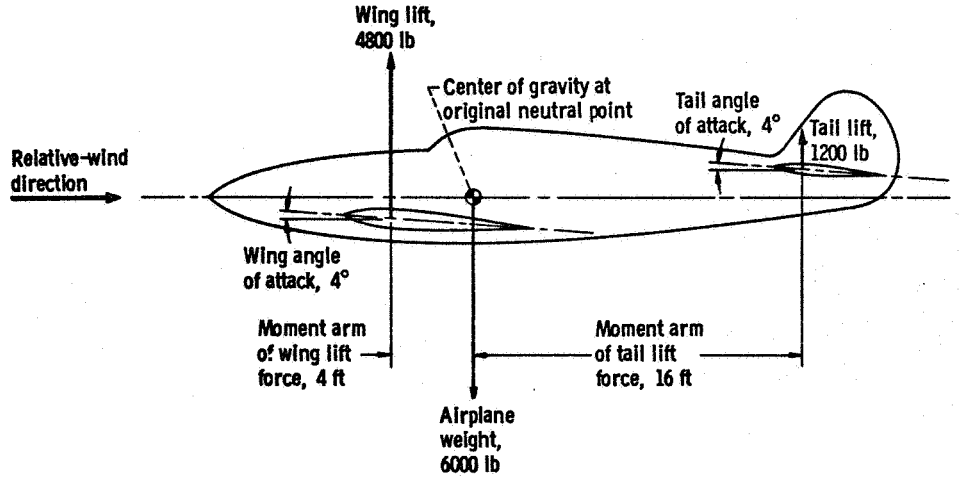

(a) Neutrally stable airplane in equilibrium, level-flight attitude, without downwash.

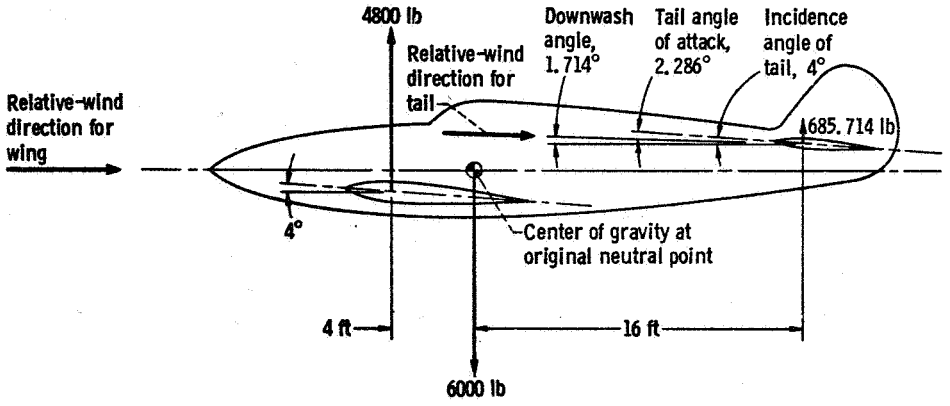

(b) Airplane, with downwash, in level-flight attitude, but no longer in equilibrium nor neutrally stable.

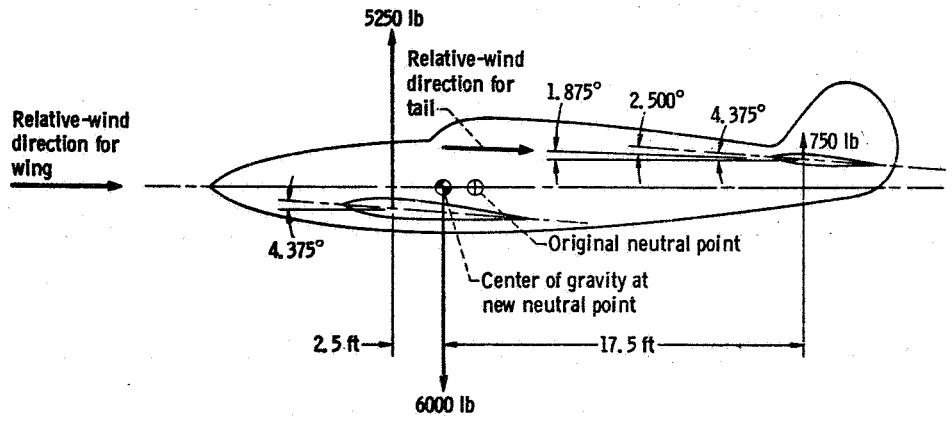

(c) Airplane modified to reachieve neutral stability and equilibrium in level-flight attitude.

Figure 9-7. - Effect of downwash from wing on stability and on location of neutral point of example airplane.

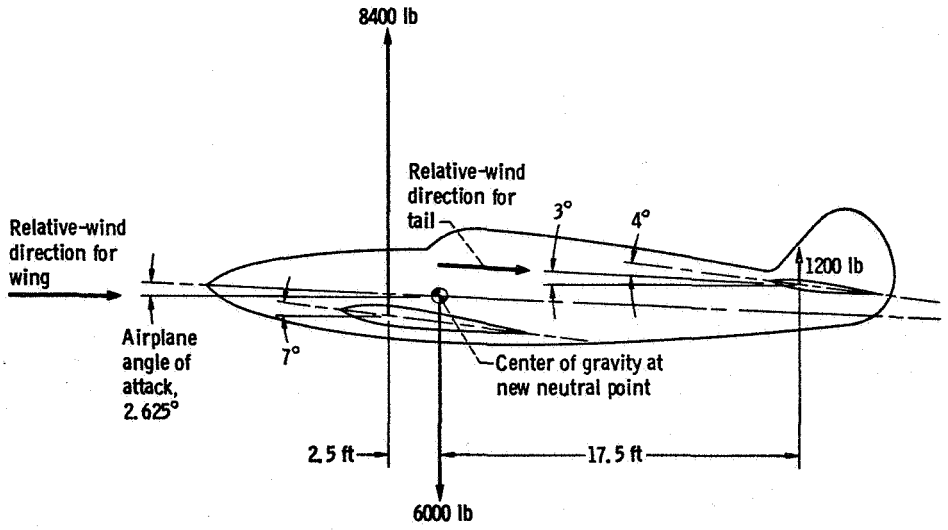

(d) Airplane in displaced, nose-up attitude.

Figure 9-7. - Concluded.

attitude, the incidence angles of the wing and tail are also their angles of attack.

It has been shown previously that if this airplane is pitched upward or downward from its initial, equilibrium, level-flight attitude, it maintains neutral stability.

Figure 9-7(b) shows the same example airplane, still in a level-flight attitude, but with the horizontal tail now operating in the downwash created by the wing. The size of the downwash angle at the horizontal tail depends on the wing angle of attack and the configuration of the airplane. For a given airplane configuration, the ratio of the downwash angle to the wing angle of attack remains fairly constant with changes in the wing angle of attack. The numerical value of this ratio depends on certain design characteristics, such as the horizontal and vertical distances between the wing and the horizontal tail, the surface area of the wing, the aspect ratio of the wing, etc. For the example airplane of figure 9-7(b), the value of the ratio is arbitrarily assumed to be 0.4285. This means that for any given angle of attack, the downwash angle at the horizontal tail is equal to the wing angle of attack multiplied by 0.4285.

To be neutrally stable, an airplane must have zero angular difference, regardless of whether or not the downwash effects are taken into consideration. Therefore, in figure 9-7(b), the incidence angle of the wing is still equal to that of the tail. Since the relative-wind direction for the wing is still parallel to the longitudinal axis of the airplane, the angle of attack of the wing is still the same as its incidence angle (4°). However, the downwash angle at the horizontal tail ($4^{\circ} \times 0.4285 = 1.714^{\circ}$) has reduced the angle of attack of the horizontal tail from 4° to 2.286°. This reduction in the angle of attack has decreased the lift force produced by the tail from 1200 pounds to 685.714

pounds. Therefore, the example airplane is no longer in equilibrium nor neutrally stable. The total lift produced by the wing (4800 lb) and the horizontal tail (685.714 lb) is now less than the airplane weight (6000 lb). The nose-up pitching moment produced by the wing (4800 lb × 4 ft = 19 200 lb-ft) is now greater than the nose-down pitching moment produced by the horizontal tail (685.714 lb × 16 ft = 10 971.424 lb-ft).

This airplane can be restored to a neutrally stable, equilibrium, level-flight condition by first shifting the neutral point and center of gravity forward and then increasing the wing and tail lift forces. First, to restore neutral stability, the neutral point must be moved forward sufficiently to again equalize the nose-up and nose-down pitching moments. For neutral stability, the center of gravity must be located at this new neutral point. Next, to restore equilibrium, the wing and tail lift forces must be increased sufficiently to again equalize the total lift and the airplane weight. These lift forces must be increased by equal percentages at the wing and tail, so as not to destroy the equality of the nose-up and nose-down pitching moments. This change in the lift forces can be accomplished either by increasing equally the wing and tail angles of incidence or by increasing the airplane angle of attack.

Figure 9-7(c) shows the example airplane modified to reachieve neutral stability and equilibrium in the level-flight attitude. The neutral point has been moved forward, so that the nose-up and nose-down pitching moments are again equal. This new neutral point is valid for the wing and tail lift forces (4800 lb and 685.714 lb) shown in figure 9-7(b), as well as for the new lift forces shown in this figure. The center of gravity is now located at this new neutral point.

The wing and tail lift forces have both been increased by 9.375 percent, so that the total lift produced by the wing (5250 lb) and the tail (750 lb) is again equal to the airplane weight (6000 lb). These changes in the lift forces have been accomplished by increasing the incidence angles of both the wing and the tail by 9.375 percent, from 4° to 4.375°. Thus, the wing angle of attack, which, in this example, is assumed to be the same as the wing incidence angle, has also increased by 9.375 percent. This increase in wing angle of attack, in turn, has produced a 9.375-percent increase (from 1.714° to 1.875°) in the downwash angle. Since, in this example, the wing and tail angles of incidence are equal, the tail angle of attack is equal to the wing angle of attack (4.375°) minus the downwash angle (1.875°). Therefore, the tail angle of attack has also increased by 9.375 percent, from 2.286° to 2.500°.

When this airplane is pitched upward or downward from its level-flight attitude, it displays neutral, static, longitudinal stability. Figure 9-7(d) shows the airplane in a new, upwardly displaced attitude. The wing and tail lift forces have both increased, but the nose-up and nose-down pitching moments are still equal. Therefore, the airplane is still neutrally stable.

The preceding examples have shown only the effect of the center-of-gravity location

on the longitudinal stability of an airplane. However, many other factors affect longitudinal, lateral, or directional stability. The following are some of those factors: location and size of stabilizer; location and size of fin; location of wing; wing dihedral; wing sweepback; location of center of pressure; location of aerodynamic center; power loading; wing loading; location of thrust line; location of propeller(s); location of jet-engine inlet(s); location of jet-engine exhaust(s); and flight Mach number.

Effect of Stability on Controllability

Stability in an airplane is always desirable, but not necessarily in the maximum possible degree. Stability has a direct effect on controllability. The controllability of an airplane determines the ease of operating its controls and/or its responsiveness to the controls. Excessive stability reduces maneuverability and renders the airplane stiff, or heavy, to the controls. Too little stability (approaching neutral stability) renders the airplane too sensitive and too responsive to the controls, reduces the control feel received by the pilot, and increases the risk of overcontrol by the pilot. Therefore, the design of any airplane must achieve a satisfactory balance, or compromise, between stability and controllability.

AIRPLANE CONTROL

Control Surfaces

An airplane is controlled by means of various movable surfaces, or airfoils, attached to the wings and tail. When these control surfaces are deflected by the pilot, the aerodynamic forces on the airplane are changed and, therefore, the attitude or direction of the airplane is changed.

The primary control surfaces, shown in figure 9-8, are the elevator, the rudder, and the ailerons. The elevator, which is usually hinged to the rear of the stabilizer, controls pitch. The rudder, which is normally hinged to the rear of the fin, controls yaw. The ailerons, one on each wing, provide roll control. They are located at the trailing edges of the wings and are so connected that when one is deflected upward, the other deflects downward. Simple climbing and diving maneuvers (pitch) can be accomplished by merely deflecting the elevator. But most other maneuvers, including banks (roll) and turns (yaw), require that the pilot coordinate the deflections of two or all three primary control surfaces.

On some airplanes a single control surface serves the combined functions of the ele-

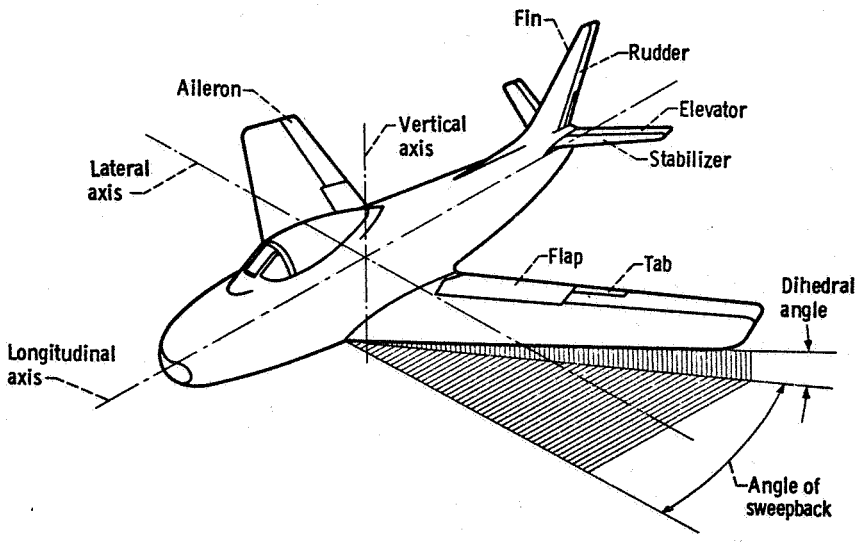

Figure 9-8. - Elements of stability and control.

vator and the ailerons or of the elevator and rudder. Sometimes, an entirely movable horizontal tail surface is used instead of the fixed stabilizer and movable elevator arrangement. Also, an entirely movable vertical tail may be used instead of the fixed fin and movable rudder arrangement.

The secondary control surfaces are tabs, flaps, and spoilers. Tabs are used for balancing and trimming the primary control surfaces, as will be discussed later in the chapter. Flaps have many variations and many uses. Most commonly they are hinged, pivoted, or sliding surfaces located at the rear of the wings and deflected or extended downward to increase the wing lift, especially at takeoff and landing. Spoilers are usually hinged or sliding surfaces mounted on the wings and/or the fuselage. They are used to slow down the airplane by increasing the drag when they are extended.

Hinge Moment of Control Surface

The forces required to move the control surfaces must be of a magnitude tolerable to the pilot. When the pilot deflects a control surface, the pressure distribution resulting from the airflow over the surface creates a moment about the hinge axis. This hinge moment causes the control surface to resist deflection and tend to rotate about its hinge axis back to its undeflected position. Therefore, to maintain the control surface at any given deflection, the pilot must apply, through the controls, an equal and opposite moment to the surface.

The magnitude of the control-surface hinge moment (and, therefore, the magnitude

of the control-stick force required to deflect the surface) increases with the size and speed of the airplane. The stick force increases as the cube of the increase in size and as the square of the increase in speed. For example, if the size of the airplane is doubled, the force required to move a control surface (at any given flight speed) becomes 2^3, or 8, times as great. If the speed of an airplane is doubled, the stick force (for any given airplane size) becomes 2^2, or 4, times as great. Therefore, on large and/or fast airplanes, various techniques are used to reduce the stick force to a reasonable level.

Aerodynamic Balances

One technique for reducing the hinge moment and stick force is to change the pressure distribution about the hinge axis of the control surface by means of some type of aerodynamic balance.

A control surface may have an overhang balance, as shown in figure 9-9(a). For this balance the hinge axis is offset rearward from the leading edge of the control surface. When the control surface is deflected, the pressures on the area ahead of the hinge axis create moments about the hinge axis that are opposite to those produced by the pressures on the area behind the axis. Thus, the net hinge moment of the control surface is reduced.

The horn balance, shown in figure 9-9(b), is similar to the overhang balance, but its balance area is concentrated at one portion of the span of the control surface. When the control surface is deflected, the pressures acting on the balance area (horn area) produce moments that assist the pilot.

The internal balance, shown in figure 9-9(c), consists of an overhang, or balance area, extending forward of the hinge axis of the control surface into a chamber within the contour of the fixed airfoil. The chamber is vented to the ambient upper and lower surface pressures at one chordwise point. Thus, the balancing air pressures are free to act on the enclosed overhang. Within the chamber, the leading edge of the overhang (or balance area) may be sealed by a flexible partition to the forward wall of the chamber. The sealed internal balance is more effective than the unsealed one.

Another type of aerodynamic balance consists of making the trailing edge of the control surface wedge shaped, or beveled, as illustrated in figure 9-9(d). A deflection of the control surface by the pilot causes the bevel on the deflection side of the trailing edge to protrude into the airstream. Then the airstream, which must move faster in going around the bevel, induces a lower pressure on that side of the trailing edge. This tends to pull the control surface in the deflected direction.

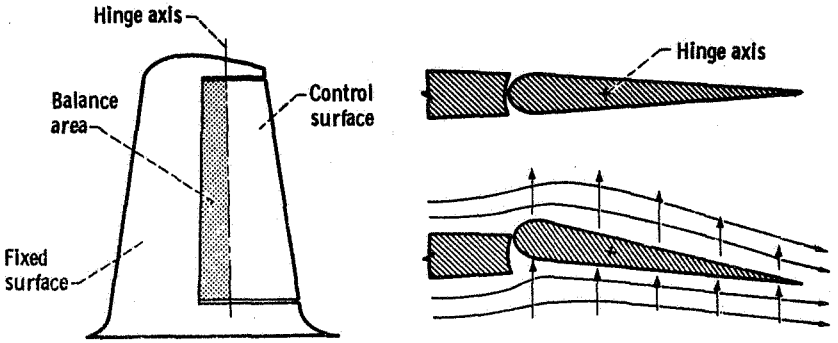

(a) Overhang balance.

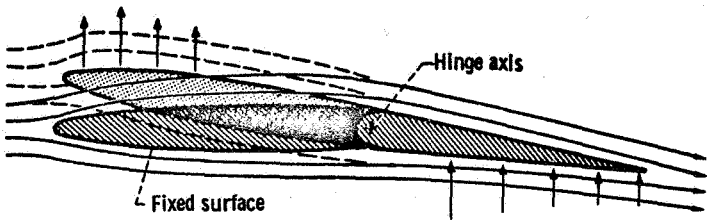

Section A-A

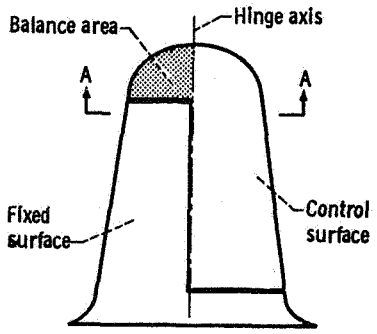

(b) Horn balance.

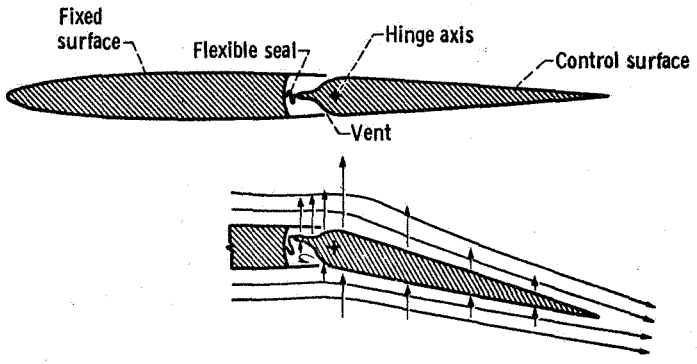

(c) Sealed internal balance.

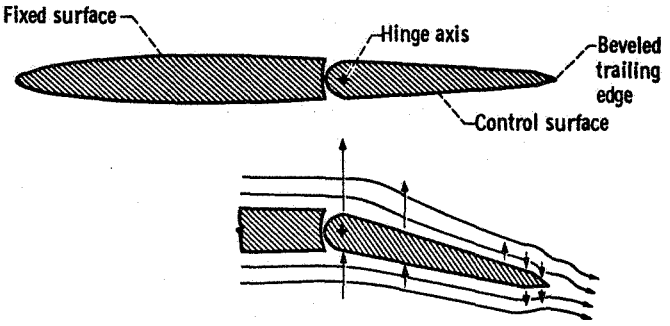

(d) Beveled trailing edge balance.

Figure 9-9. - Aerodynamic balances for control surfaces.

Tabs

A common and effective method of reducing an excessive control-stick force is by the use of a secondary control surface called a tab. This device is a hinged, auxiliary airfoil built into the trailing edge of the control surface. The purpose of the tab is to change the pressure distribution on the control surface near the trailing edge, thereby changing the hinge moment of the control surface. In a strict sense, a tab is really just another form of aerodynamic balance, but the two are commonly treated separately. A tab is extremely versatile, since it can be linked so as to decrease the stick force, trim the airplane, or increase the stick force.

The lagging tab (fig. 9-10(a)) is so linked that when the control surface is deflected by the pilot, the tab deflects in the opposite direction, thereby producing a force which helps to move the control surface. Since the lagging tab is intended merely to help move the control surface, the system must be designed so that the moment produced by the force on the tab is smaller than the hinge moment of the control surface.

The servo tab (fig. 9-10(b)) is linked directly to the cockpit controls. The pilot deflects the tab, which then causes the control surface to be deflected in the opposite direction by the aerodynamic forces acting on the tab. Since the servo tab must provide all the force necessary to move the control surface, the system must be designed so that the moment produced by the force on the tab is larger than the hinge moment of the control surface.

The spring tab (fig. 9-10(c)) is actuated by a spring-loaded mechanism that causes it to supply a fixed percentage of the force required to move the control surface. The action and use of the spring tab are similar to those of the servo tab. However, the springs incorporated in the control system allow the tab to supply only a part, rather than all, of the force required to move the control surface. Some of the stick force is always transmitted through the springs directly to the control surface. As the hinge moment of the control surface increases, the deformation of the springs also increases. This, in turn, causes the linkage to increase the deflection of the tab. The amount of force supplied by the tab depends on the spring rates. Obviously, if the springs are infinitely weak (equivalent to no springs at all), the tab behaves as a servo tab. If the springs are infinitely stiff (equivalent to a rigid rod), the tab does not deflect at all. By preloading the springs, the deflection of the tab can be delayed until a predetermined control force is achieved.

At times it is necessary to hold a control surface in a deflected position to keep the airplane in the desired flight attitude, or trim. Obviously, it would be both inconvenient and tiring for a pilot to apply a constant stick force for long periods of time. Therefore, a trim tab (fig. 9-10(d)) is normally used to keep the control surface deflected. An adjustable linkage allows the pilot to set the tab at the proper angle to reduce the hinge moment of the control surface to zero for any desired flight condition. In other words, the trim

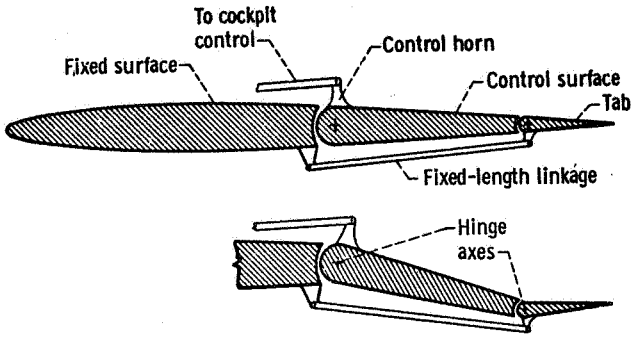

(a) Lagging tab.

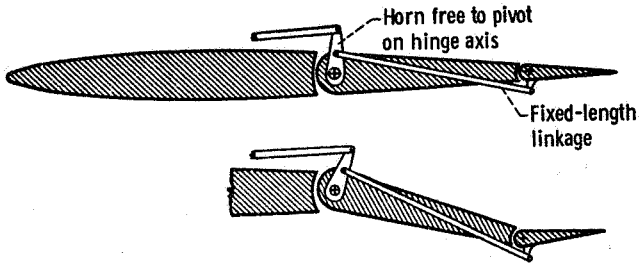

(b) Servo tab.

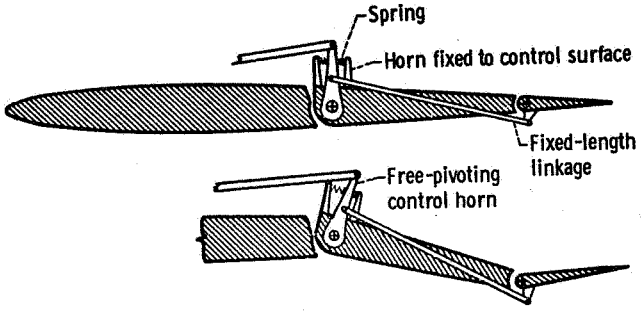

(c) Spring tab.

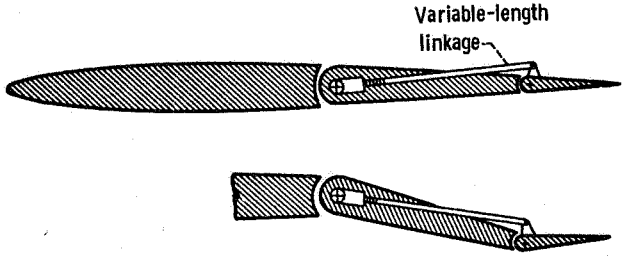

(d) Trim tab.

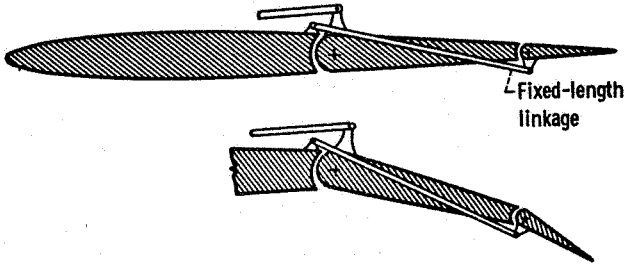

(e) Leading tab.

Figure 9-10. - Tabs used as balances on control surfaces.

tab is set to keep the control surface deflected so that the airplane will maintain the desired flight attitude.

In all these methods of balancing a part of the control force to assist the pilot, there is the danger of providing too much assistance. With too much balancing, a slight movement of the controls may call into play excessively large forces that might overcontrol the airplane. Also, too much balancing reduces the feel that the pilot receives from the controls and thereby impairs his judgement. Thus he may unwittingly overcontrol the airplane. Because of these dangers, the various balancing schemes (including aerodynamic balances) must be designed to leave a sufficient amount of control feel to the pilot. Furthermore, the control feel must be progressive; that is, the control feel must become heavier with increasing deflection of the control surface.

Because of the importance of control feel to the pilot, it is sometimes necessary to increase the stick force. One way to do this is to use a leading tab (fig. 9-10(e)), which serves to increase the hinge moment of the control surface. The leading tab is so linked that when the control surface is deflected the tab deflects in the same direction, thereby adding to the hinge moment.

Mechanical Boost Systems for Control Actuation

On an airplane flying through the transonic speed zone, any type of aerodynamic hinge-moment-reducing device (aerodynamic balance or tab) may perform erratically while mixed subsonic and supersonic flow exists on the control surface. Therefore, on

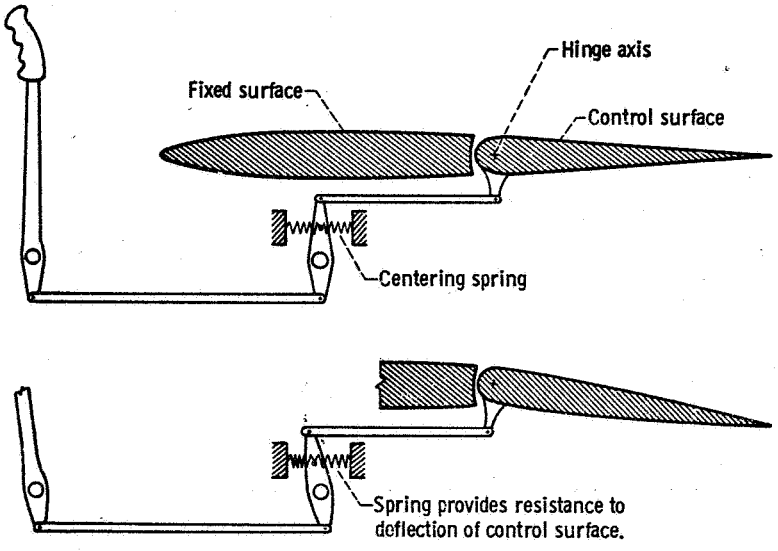

Figure 9-11. - Control stick centering spring used to increase control feel.

some airplanes mechanical systems are used to assist the pilot. Two basic types of mechanical control-actuation systems are in use: the power-boost system and the power-operated system.

In the power-boost system, a mechanical actuator is connected parallel to the direct mechanical linkage between the cockpit and the control surface. Thus the mechanical actuator supplies only part of the force required to move the surface, and the pilot still receives control feel through the direct linkage.

In the power-operated system, the control surface is moved entirely by the mechanical actuator, which, in turn, is controlled by the pilot. With this system, the entire force required to move the control surface is supplied by the mechanical actuator, and none of the hinge moment is fed back to the cockpit controls. Therefore, some sort of artificial feel system must be built into the controls to provide the pilot with the necessary control feel, or resistance. This artificial feel may be provided by a spring system on the controls, as shown in figure 9-11.

BIBLIOGRAPHY

Anon.: Stability and Control Manual. FTC-T1H-64-2004, USAF Aerospace Research Pilot School.

Hurt, H. H., Jr.: Aerodynamics for Naval Aviators. Navweps 00-80T-80, Office of the Chief of Naval Operations, Aviation Training Div., 1960.

Kershner, Wm. K.: The Private Pilot's Flight Manual. Second ed., Iowa State University Press, 1963.

Perkins, Courtland D.; and Hage, Robert E.: Airplane Performance Stability and Control. John Wiley & Sons, Inc., 1949.

Seckel, Edward: Stability and Control of Airplanes and Helicopters. Academic Press, 1964.

10. V/STOL AIRCRAFT

Seymour Lieblein*

Air and ground traffic congestion is a growing problem for commercial aviation. The growth of aviation is creating increased demands on airspace. Some of the major airports are indequate for handling the increased air traffic. Thus, aircraft are spending more and more time on taxiways, waiting to take off, or in holding patterns on the approaches to the airports, waiting to land. The growth of the automotive industry is creating increased congestion on the highways between city centers and airports, between suburban centers and airports, and between cities. Because of these delays in the air and on the ground, the total travel time for the airline passenger is actually increasing.

Air service could be improved and total travel time could be reduced if there were aircraft that could provide short-haul service between city centers, between city centers and major airports, and between major airports. Such aircraft would have to be able to take off and land either vertically or on very short runways and to maneuver (in flight) in confined areas.

Of course, we already have an aircraft that can do this - the helicopter. The usefulness of the helicopter has been demonstrated in military operations, for rescue work in times of disaster, and also for hauling materials and assisting in putting large structures together. However, the helicopter is limited in what it can do - it cannot fly very fast or very far. Therefore, we are looking for something that bridges the gap between the relatively small and slow helicopter and the large, speedy jet transport. This takes us into the realm of the V/STOL's (Vertical/Short Take-Off and Landing), which are aircraft that can take off or land vertically or with a relatively short ground run.

NEED FOR V/STOL AIRCRAFT

V/STOL aircraft can play an important role in both civilian and military aviation. Therefore, aircraft companies and various government agencies, such as the National Aeronautics and Space Administration, the Department of Transportation, the Federal Aviation Agency, the Department of Commerce, and the Department of Defense, are currently conducting studies on civilan and military V/STOL aircraft concepts and applications.

---

*Chief, VTOL Propulsion Branch.

Civilian Applications

The basic motivation for the development of civilian V/STOL aircraft stems from two factors: (1) the expected growth and urbanization of our country's population, and (2) the increased mobility of our population. By the year 2000, our total population is expected to number about 375 million (it is over 200 million now), of which around 33 percent will live in cities of 100 000 people or more. This growth means that our present major metropolitan centers will increase beyond their present large sizes. Projecting this fact into the future, it is not difficult to imagine the situation illustrated in figure 10-1, which shows the merging of cities into large regional complexes. The area shown

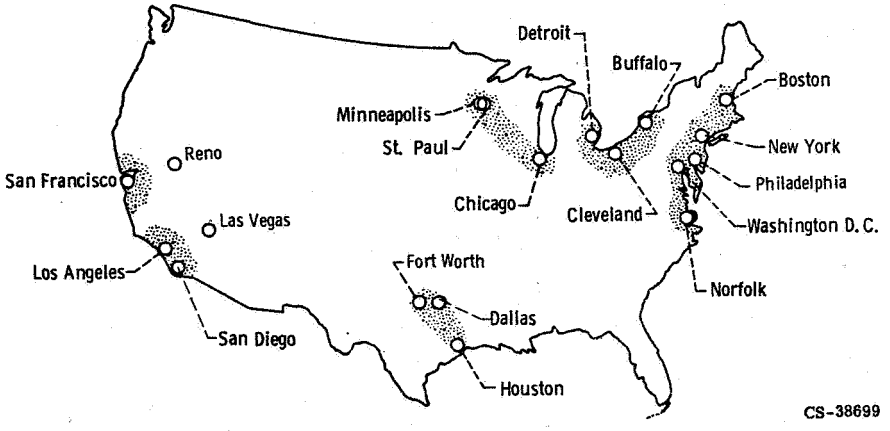

Figure 10-1. - Predicted merging of cities into major metropolitan complexes.

along the Atlantic coast will merge into one large city extending from Boston to Norfolk. Today, this region already is populated by 37 million people. Other regional complexes are shown on the West Coast, on the Gulf Coast, and around the Great Lakes.

We are also becoming a very mobile people. Frequent travel for business or pleasure is increasing substantially. Of course, high-speed ground transportation (auto, bus, rail) will continue to provide much of the population mobility for shorter trips. Today, the number of business trips by ground transportation for distances under 500 miles is 10 times the number by air for the same distances. However, in the future, the available unused land space will be at a premium, and hence the allocation of rights of way for additional freeways and railways will eventually reach a saturation level. Some think we are at that point already. Even today, the percentage of land devoted to roadways and parking areas in cities is very high. For example, 48 percent of the land area in Los Angeles and 38 percent of the land area in Boston is taken up by roadways and parking facilities. Furthermore, air pollution may curtail the expanding use of the auto. Thus, other forms of mass transportation will have to be emphasized in the future.

Today, around our large cities, the effects of increased congestion on the ground and in the air are clearly evident to those who travel. For example, the total travel time (ground and air) between downtown New York City and downtown Washington, D. C., increased from 125 minutes in 1948 to 167 minutes in 1963, despite the fact that airplane flight speeds increased considerably during this period. The increases in travel time result from delays both in the air and on the ground.

Conventional airports must be located on the fringes of cities, because of the need for land and the problem of noise. Thus, as the cities grow larger, the airports will be farther away from the centers of towns, and the ground travel time will increase even more in the future. Also, both the cost and the availability of land limit the number of conventional large airports that are economically feasible. Obviously, then, there is little that can be done to reduce door-to-door trip times with conventional takeoff and landing aircraft.

V/STOL aircraft could solve some of these problems, since their short or vertical takeoff and landing characteristics would enable them to operate from small landing fields (or existing heliports) located closer to the ultimate destinations, and thus reduce the travel time on the ground. Also, such craft could operate at flight speeds approaching those of conventional jets, make their final approaches in the less congested airspace (e.g., at altitudes under 1500 ft), and provide further time savings in the air as well.

The various functions that V/STOL aircraft can provide the civilian community of the near future are shown in figure 10-2, which illustrates anticipated air operations in a seaboard metropolis. First, large transcontinential jets like the Boeing 747 and the

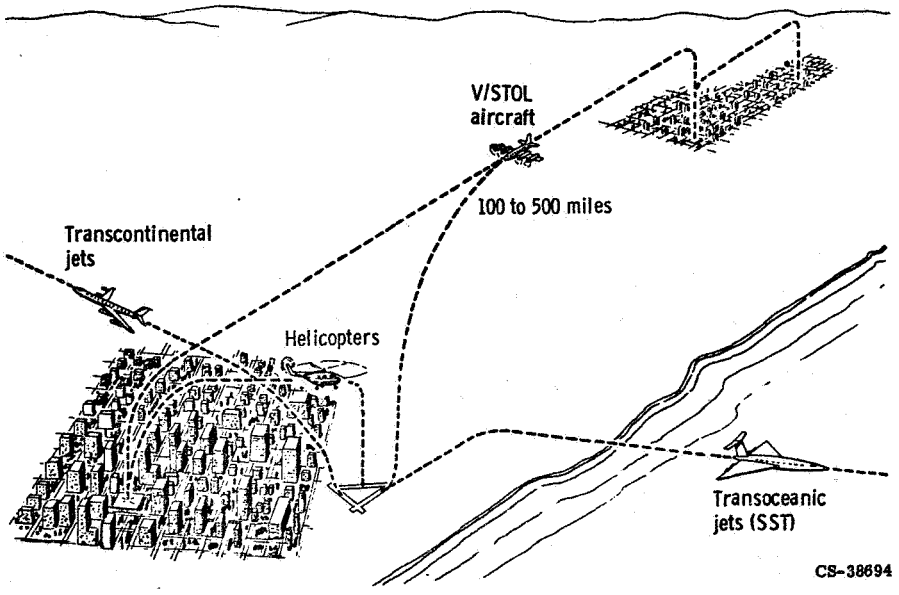

Figure 10-2. - Function of V/STOL aircraft in commercial air service.

Supersonic Transport (SST) will continue to operate from the existing major airfields for these long-range trips. The V/STOL aircraft will provide service for trips from around 100 to 500 miles at speeds approaching those of conventional jets. The V/STOL routes will be between city centers or from city centers to outlying airports as feeder operations for the long-range flights. Also, V/STOL aircraft will provide service between various points within a large city (around-the-town service). In short, the V/STOL aircraft will provide a vital link in a system of speedy, integrated air service that will meet the needs of an expanding, mobile population. As shown in the figure, helicopters will continue to serve for very short trips around town.

At this point, one may ask why helicopters are not used for all VTOL operations. The reason is that current helicopters do not have the speed and range capabilities of the V/STOL aircraft. This is illustrated in figure 10-3, which shows the cruising-speed and

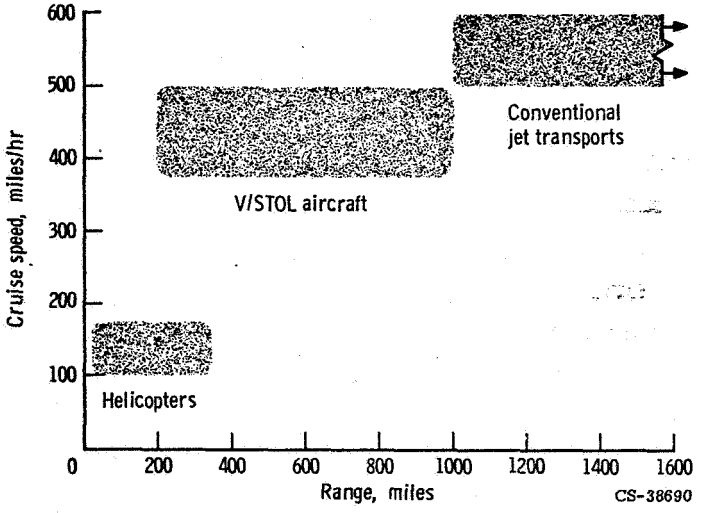

Figure 10-3. - Speed and range capabilities of helicopters, V/STOL aircraft, and conventional jet transports.

range capabilities of the three major types of aircraft: current helicopters, V/STOL aircraft, and conventional jet aircraft. The speed of the current helicopter is restricted by the large drag and performance limitations of the rotor blades, and the low range is due to low fuel capacity. As shown in the figure, the V/STOL aircraft can function over a longer range and at higher cruise speed than the helicopter. Thus, the V/STOL aircraft can bridge the gap between the helicopter and the long-range jet.

Suitable sites for V/STOL airports can be found even in congested cities. Obviously, the selection of an airport site will be governed by considerations of cost, availability of space, and acceptable noise levels. Also, air traffic considerations dictate that the airports within the city use natural flight-approach corridors as much as possible. Hence,

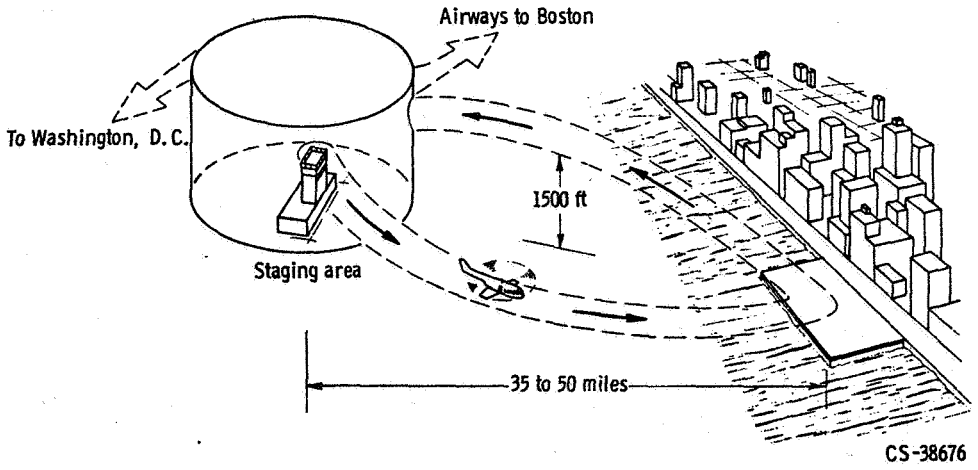

Figure 10-4. - V/STOL air traffic into and out of a large city.

V/STOL airports are expected to be located along rivers, along the shores of large bodies of water, along transportation rights of way, or in "wasteland" areas within the city that are unsuitable for housing or industry. For example, figure 10-4 illustrates a proposed location for an airport along the Hudson River that could serve the mid-Manhattan area of New York. The V/STOL landing pad could be located along the riverfront, with runways no longer than about 1000 feet, and could be built over the roofs of existing waterfront buildings or, better yet, over unused piers. As shown in the figure, the inbound and outbound V/STOL flights would be controlled from a staging area about 35 to 50 miles from the downtown airport. A 1500-foot ceiling would be observed by V/STOL aircraft flying between the staging area and the downtown airport in order to stay below the already congested traffic lanes for conventional aircraft flights.

Airports for V/STOL aircraft should also be located near convenient parking and

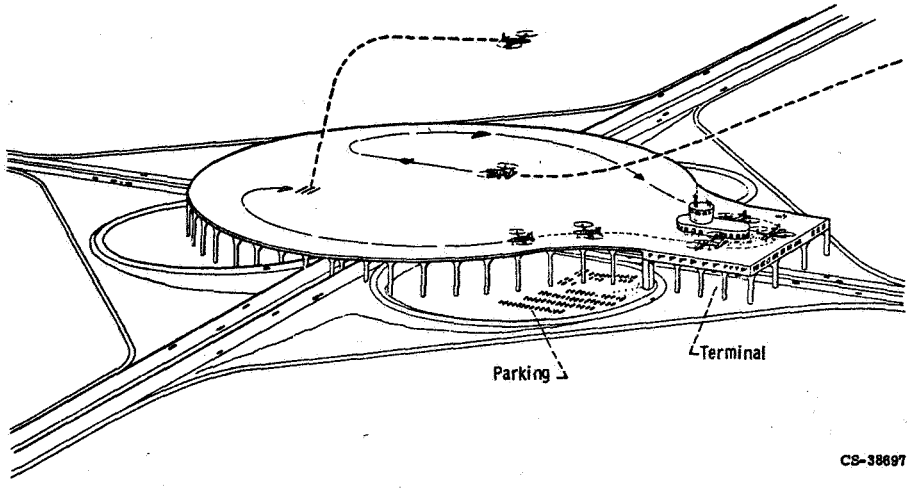

Figure 10-5. - V/STOL airport located over highway cloverleaf.

ground transportation facilities to reduce ground time as well as air time between ultimate destinations. Thus, such airports might be located over large cloverleaf intersections as shown in figure 10-5. The parking areas would be on the ground level under the airport, and the passenger terminal would be immediately beneath the flight deck. The entire airport structure might be about 1500 feet long and about 1000 feet wide. Approach and departure paths would be to and from the central areas of the pad, and the taxiways would be routed along the outer perimeter of the field.

Military Applications

In the past, the major portion of the direct financial support from the Government for the development of V/STOL aircraft has been provided for military applications. The major military uses of V/STOL aircraft are shown in figure 10-6. The foremost application is in the transport function. The long-range transport of supplies and equipment would be provided by heavy transport aircraft such as the Lockheed C-141 (now in service) or the Lockheed C-5A (currently under flight test). The V/STOL transport aircraft would pick up the supplies at the overseas base and deliver them close to the forward area at some remote location. These V/STOL aircraft could use relatively small airstrips that would require minimum preparation. Thus, fast, efficient, large-scale

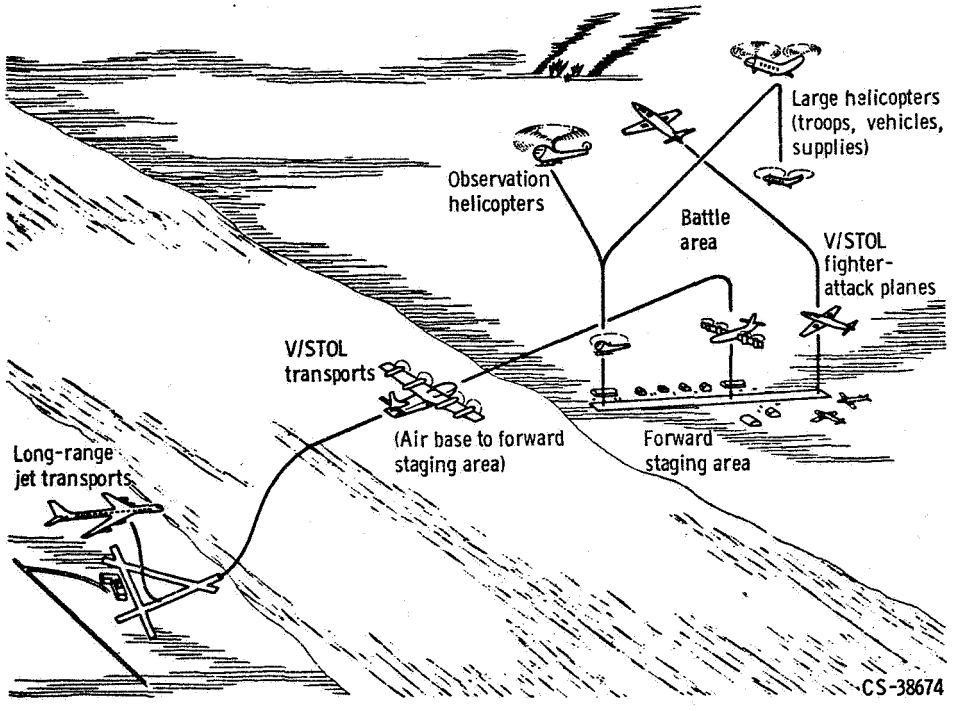

Figure 10-6. - Military functions of V/STOL aircraft.

logistical support (delivery of troops or supplies) could be provided close to the front lines, and this support could keep up with the mobility of the ground forces.

Another military requirement is for V/STOL tactical fighters or ground support aircraft. The operating requirement most critical here is the ability to function from small, unprepared or quickly prepared airstrips. In this way, the fighters can provide maximum support and flexibility and also be sufficiently widely dispersed to make the entire fighter squadron less vulnerable to massive attack and loss of airplanes and runways. In this concept, the V/STOL transport aircraft would provide the necessary supplies for the fighter planes, as well as for the troops. Other important military missions for V/STOL aircraft would be rescue service and antisubmarine warfare.

BASIC CONCEPTS

Figure 10-7 compares the takeoff runs required by three classes of aircraft. A Conventional Take-Off and Landing (CTOL) aircraft is one that requires a long run of about 4000 feet, or more, to take off. A Short Take-Off and Landing (STOL) aircraft is defined as one that requires a takeoff run of 500 to 2000 feet. A Vertical Take-Off and Landing (VTOL) aircraft obviously requires no takeoff run. The combined term V/STOL is used to refer to both VTOL and STOL aircraft as a class, as differentiated from the conventional, or CTOL, aircraft.

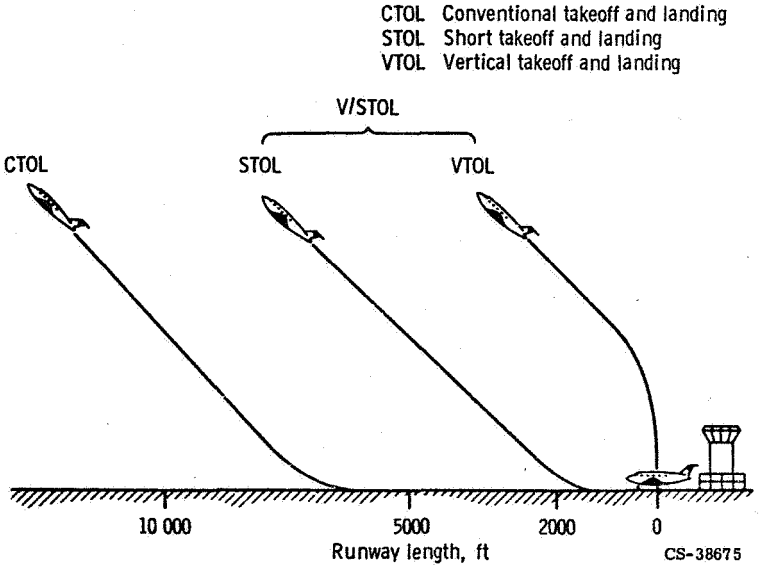

Figure 10-7. - Comparison of takeoff runs of CTOL and V/STOL aircraft.

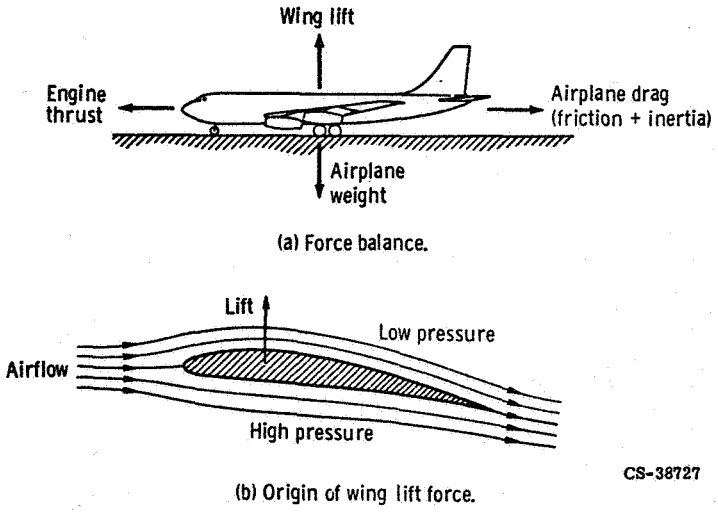

Figure 10-8. - Forces acting on airplane during takeoff run.

Figure 10-8(a) is a quick refresher on the four major forces acting on an airplane as it proceeds down the runway to take off: (1) the airplane weight, which tends to keep it on the ground; (2) the thrust of the engine, which propels the airplane forward; (3) the drag of the airplane, which resists the forward motion; and (4) the upward lift force generated by the wings.

Wing lift is generated because the airflow over the wing creates regions of high and low pressure, as shown in figure 10-8(b). (The principles of lift generation are discussed in chapters 4 and 5.) The pressure difference between the upper and lower surfaces of the wing results in a net upward lift force. This wing lift force is zero at zero flight speed and increases with the square of the forward speed according to the relation

$$L = C_L S \frac{\rho V^2}{2g} \tag{1}$$

where

L lift force, lb

C_L wing lift coefficient determined by the geometry of the wing and its angle of attack

S wing planform area, ft^2

ρ air density, lb/ft^3

V flight velocity, ft/sec

g acceleration due to gravity, 32.2 ft/sec^2

Thus, as the airplane accelerates down the runway, it eventually reaches a forward speed at which the generated wing lift force becomes equal to the airplane weight, and the plane can lift off. Specifically, then, the takeoff condition is

$$L = W \tag{2}$$

where W is the gross weight of the airplane.

STOL Aircraft

From the lift equation we see that the wing lift force can be increased by increasing the lift coefficient. Greater lift coefficients can be obtained if the wings create a greater downward deflection of the air that flows around the wing. Thus, to attain a greater lift coefficient, the wing can be designed with a large flap system, as shown in figure 10-9. The flaps are extended during takeoff to increase the lift coefficient. Thus, the wing lift necessary to balance aircraft weight can then be achieved at a lower forward speed, and consequently, with a shorter runway length. After takeoff, the flaps are retracted to their normal (or cruise) position, as shown by the dotted outline.

However, there is one big problem with such a flap. If we try to deflect the air too much, the air flowing over the upper surface cannot negotiate the curve, so to speak, and separates from the wing surface. (Flow turning and flow separation are discussed in chapter 4.) When this happens, there is a large loss in lift. The boundary layer separates from the surface because the air molecules close to the surface are slowed by friction and form a "dead air" space. The main flow of air must then separate from the surface to

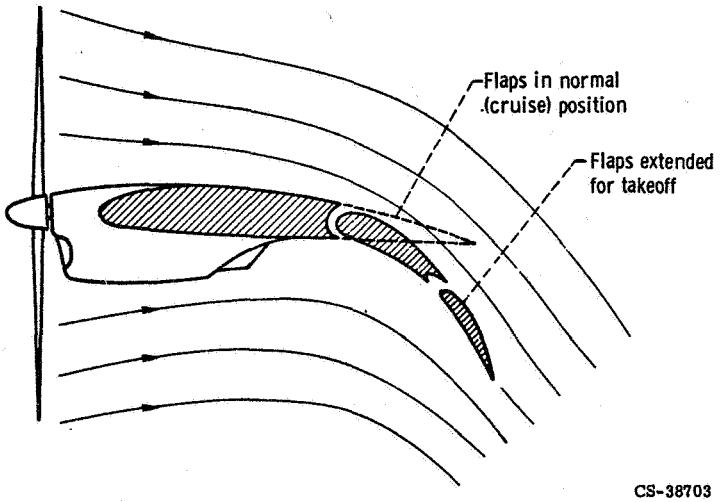

Figure 10-9. - Flaps used to increase lift of STOL aircraft.

pass around this "dead" air. Flow separation can be prevented by adding energy to the boundary layer, so that the molecules will not slow down sufficiently to form a "dead" space.

Some of the ways of energizing the boundary layer for STOL airplanes are shown in figure 10-10.

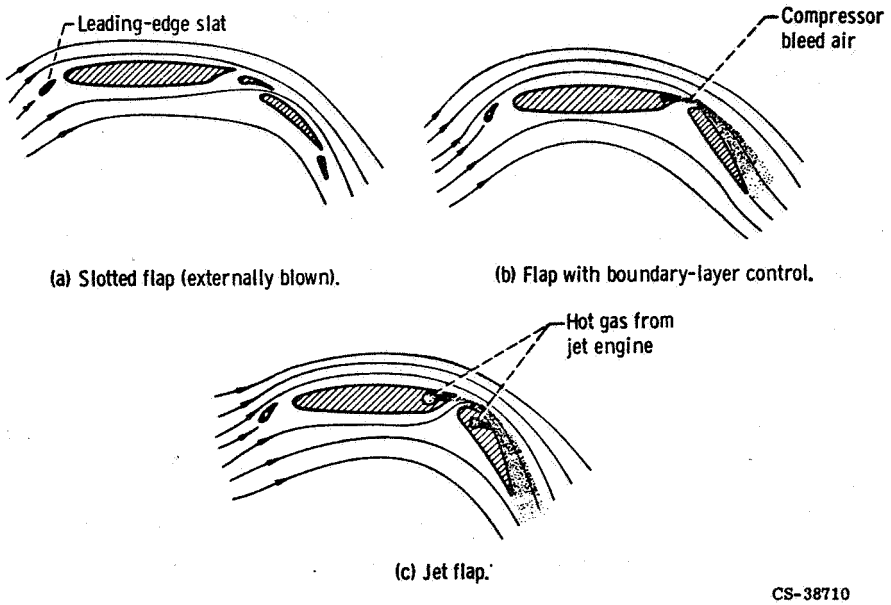

Figure 10-10. - High-lift devices for STOL aircraft.

The wing flap can be slotted, as shown in figure 10-10(a), so that the airflow from the jet engines or propellers can be made to blow through the slots, thus energizing, or speeding up, the boundary layer on the surfaces. High-pressure air can be bled off from the engine compressor and injected along the leading edge of the flap, as shown in figure 10-10(b), thereby energizing the boundary layer. Part of the jet-engine exhaust can be piped through ducts in the wing and flap to blow down as a sheet of jets over the upper surface of the flap, as shown in figure 10-10(c). The large amounts of airflow used in this jet-flap scheme not only energize the boundary layer but also contribute a sizable vertical component of thrust.

All the high-lift schemes shown in figure 10-10 also incorporate leading-edge slats to increase the wing lift coefficient further. The slats increase the lift by increasing the effective curvature of the airfoil.

Another approach that can be used to generate high lift at low forward speeds is to reduce the amount of lift that has to be generated by the wings. This is accomplished either by adding auxiliary engines to provide vertical thrust or by deflecting the exhaust

of the main engines so that there is a vertical downward component of thrust. In this case, the wing lift required for takeoff (total lift = weight) will be

$$L_w = W - T_e \sin \beta \tag{3}$$

where

L_w required wing lift, lb

W gross weight of airplane, lb

T_e engine thrust, lb

β angle of direction of engine exhaust with respect to the horizontal

Thus, the increase in wing lift coefficient C_L required to produce the necessary wing lift at takeoff (eq. (1)) will be reduced compared to the previous cases. For conventional engines with horizontal exhaust, $\beta = 0$, and the lift equation is equation (2).

The use of a vertical thrust component during takeoff is being considered for STOL airplanes, because it can provide for a better design with respect to airplane stability and overall performance than a design which uses only wing lift with very high values of C_L. A vertical thrust component during the takeoff can be obtained by changing the orientation of the axis of the engines or by using deflectors, such as vanes, to deflect the exhausts of the horizontally mounted engines.

VTOL Aircraft

The situation for a vertical takeoff is illustrated in figure 10-11. In a vertical take-

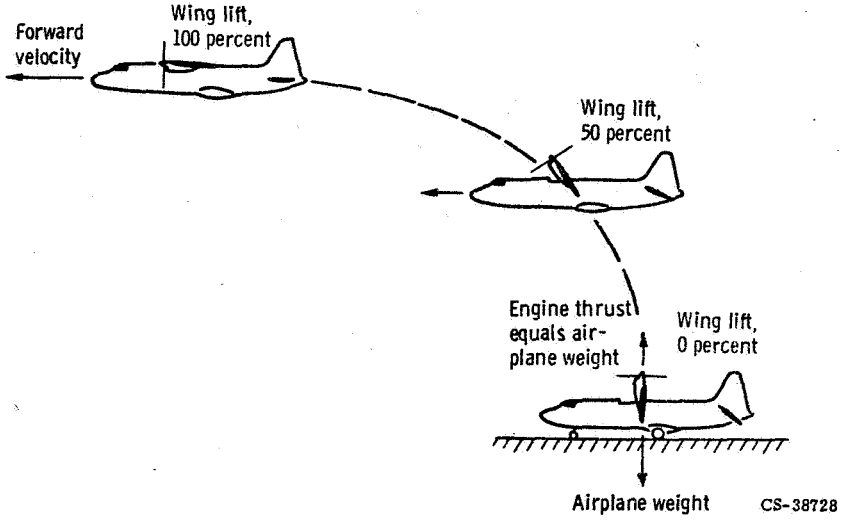

Figure 10-11. - Vertical takeoff.

off, the engine thrust is used directly to generate the entire lifting force, since there is no forward speed to generate wing lift. The figure shows a turboprop airplane in which the wing and engine have been rotated 90° to provide a vertical propeller thrust. (This is just one of several schemes that will be discussed later.) As the airplane rises, the wing is rotated toward the horizontal, so that a forward thrust component is obtained. This causes the airplane to accelerate in the forward direction and start to develop wing lift. After complete transition to the horizontal position, all the thrust is in the forward direction, and the airplane flies away in the normal cruise mode. For vertical landings, the reverse of the process is used.

In addition to differences in takeoff characteristics, VTOL aircraft also differ markedly from CTOL airplanes in the attitude-control devices required for takeoff and landing. To be more explicit here, it may be helpful to review how a CTOL airplane is controlled for maneuvers or for stable flight. The control methods for CTOL airplanes operate on the principle of aerodynamic control; that is, local surfaces are used to deflect the oncoming airstream and thus change the direction of the resultant force vector. Now, to turn a conventional airplane (fig. 10-12) to the left or right, the rudder is deflected left or right; this is called yaw control. To cause the plane to nose up or nose down, the elevators are deflected up or down; this is called pitch control. Finally, to raise one wing and lower the other, the ailerons near the wing tips are deflected in the opposite directions; this is referred to as roll control. (Airplane control is discussed in greater detail in chapter 9.)

Since a VTOL aircraft has no forward flight speed during takeoff or landing, it cannot be controlled during those phases of flight by the methods used on CTOL airplanes. Therefore, some other means of control must be provided for the VTOL aircraft. Two methods of control that can be used are: (1) modulation, or differential variation, of the

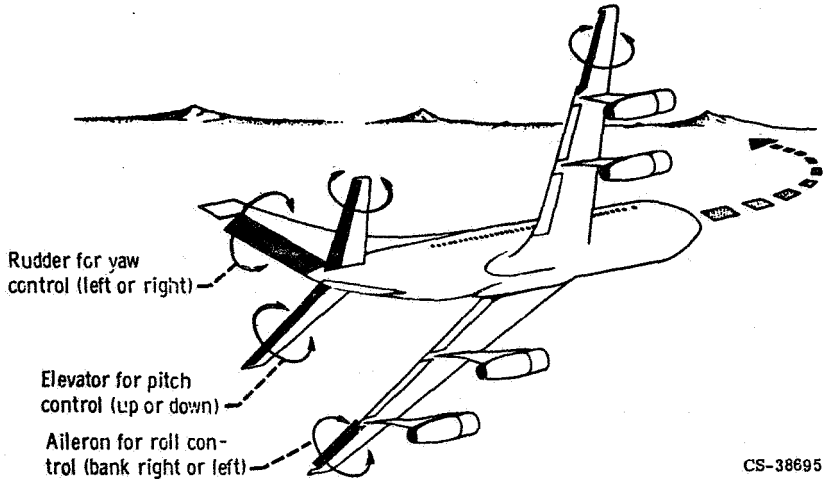

Figure 10-12. - Control methods for CTOL aircraft.

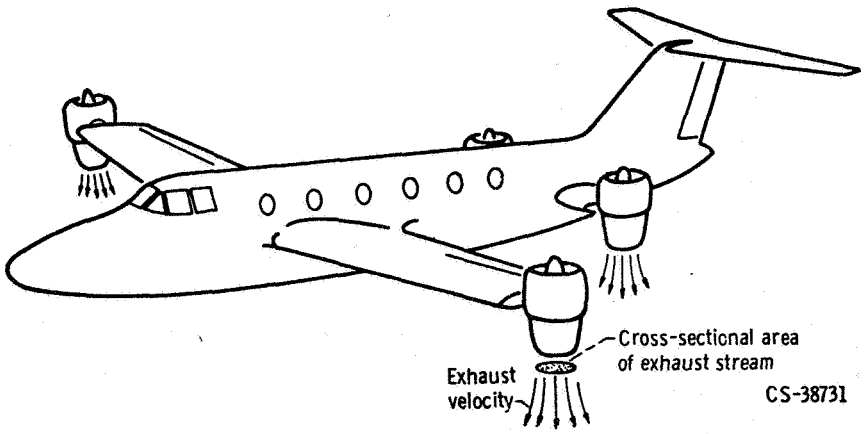

Figure 10-13. - VTOL aircraft control by modulation of the thrust of individual lifting engines.

thrust of the individual lifting engines, or (2) use of auxiliary thrust devices added specifically for control purposes. In some cases a combination of the two methods is used.

The thrust-modulation method of control is illustrated in figure 10-13. This figure shows an example VTOL airplane that has jet lifting engines on the wing tips and on each side of the fuselage near the tail. To nose up or nose down the airplane, the thrust from the two front engines can be varied with respect to the thrust from the two rear engines. Similarly, to roll the airplane from side to side, the thrust on each side of the plane can be varied. Finally, yaw control can be achieved by tilting the wing tip engines in opposite directions laterally.

The use of auxiliary thrust devices for control of a VTOL aircraft is illustrated in figure 10-14, which shows an example tilt-wing airplane. Nose-up and nose-down maneu-

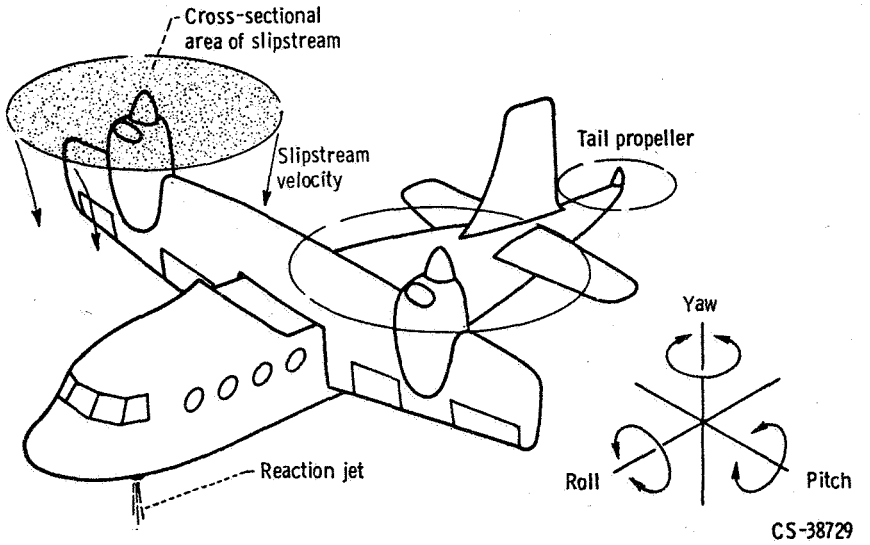

Figure 10-14. - Control of VTOL aircraft by a combination of thrust modulation of the lift engines and auxiliary thrust devices (reaction jet and tail propeller).

vers of the example airplane can be controlled either by the high-velocity jet of air ducted downward under the nose of the airplane, which tends to lift the nose, or by the small propeller in the tail, which tends to lift the tail end. These are called auxiliary control devices because they are not part of the main lifting-engine system, which, in the figure shown, consists of two wing propellers. Reaction jets, such as the one in the nose of the airplane, can also be used on the wing tips for roll and yaw control, but these are not illustrated in this figure.

Figures 10-13 and 10-14 also illustrate some fundamental terms that will be used later in this chapter. Thrust is the propelling force (in pounds) produced by the propulsion system. During vertical takeoff (no forward speed), the thrust equals the air flow rate generated by the propulsion system multiplied by the exhaust velocity of a jet engine or the slipstream velocity of a propeller, rotor, or ducted fan. The exhaust velocity is the velocity at which the exhaust gas is discharged from the jet engine, as indicated by the arrows in figure 10-13. The slipstream velocity is the velocity of the stream of air driven aft or down by the propeller, rotor, or fan, as indicated by the arrows in figure 10-14.

A significant yardstick for comparing the overall performance of various types of V/STOL aircraft propulsion systems, as will be discussed later, is the disk loading. This parameter is obtained by dividing the thrust (lb) of the engine by the cross-sectional area (ft^2) of the exhaust stream or of the slipstream. The cross-sectional area of the exhaust stream is the exit area of the exhaust nozzle of the jet engine, as shown in figure 10-13. The cross-sectional area of the slipstream is the disk area, or swept area, of the propeller or rotor, as shown in figure 10-14, or it is the exit area of the duct surrounding the fan. In general, disk loading and exhaust, or slipstream, velocity are interrelated so that when one is low, the other is also low. Specifically, the disk loading is proportional to the exhaust, or slipstream, velocity squared. This relation between disk loading and velocity squared is derived as follows:

$$\text{Disk loading} = \frac{\text{Thrust}}{\text{Area}}$$

$$\text{Thrust} = \text{Mass} \times \text{Velocity}$$

$$\text{Mass} = \text{Density} \times \text{Area} \times \text{Velocity}$$

Thus,

$$\frac{\text{Thrust}}{\text{Area}} = \frac{\text{Density} \times \text{Area} \times \text{Velocity} \times \text{Velocity}}{\text{Area}}$$

$$= \text{Density} \times (\text{Velocity})^2$$

With density generally constant,

$$\text{Disk loading} \propto (\text{Velocity})^2$$

AIRCRAFT TYPES

Many research V/STOL aircraft have been built and tested in the United States and abroad in the past 15 years, but only one, a British VTOL fighter, has reached operational status. In general, all these aircraft have been different, particularly in the systems used to achieve vertical or short takeoff. Before considering specific V/STOL designs, let us examine the systems used to produce the lift for takeoff or landing.

The four basic devices used to produce thrust for V/STOL aircraft are the rotor, the propeller, the ducted fan, and the jet engine. Table 10-I lists the relative diameter, the

TABLE 10-I. - LIFT-PRODUCING DEVICES FOR VTOL AIRCRAFT

Thrust device		Relative diameter, D	Disk loading, lb/ft^2	Slipstream velocity, mph
Rotor	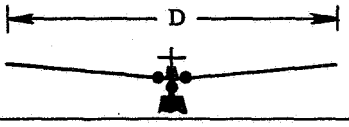	15	6 to 10	40 to 80
Propeller		5	10 to 90	90 to 200
Ducted fan		3	90 to 800	200 to 500
Turbojet		1	900 to 10 000	900 to 1600

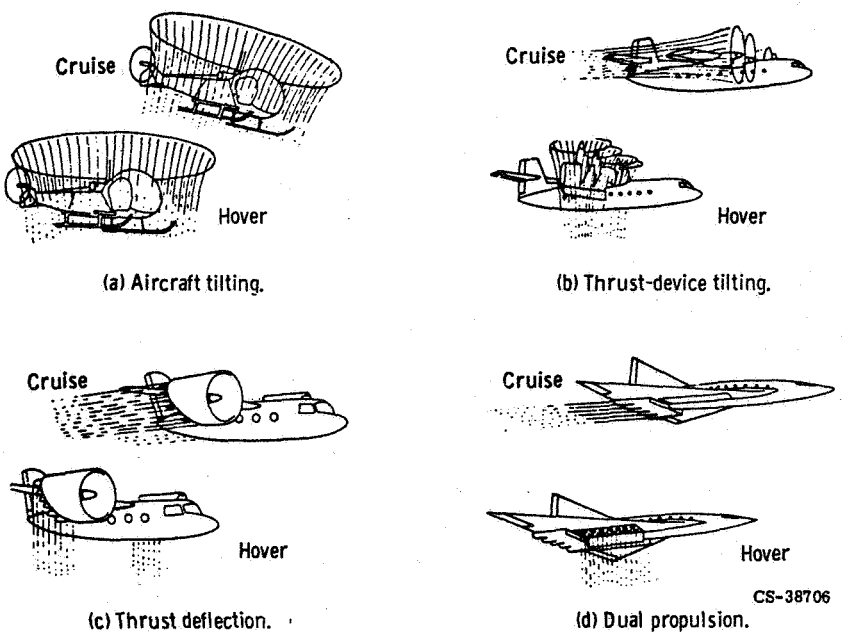

Figure 10-15. - Flight-mode conversion techniques.

typical value of disk loading, and the slipstream velocity of each device.

In addition to these four basic thrust-producing devices, there are four basic methods for directing the thrust in the proper direction for vertical or horizontal flight. These methods, shown in figure 10-15, are aircraft tilting, thrust-device tilting, thrust deflection, and dual propulsion. The figure shows the aircraft in both the hover and cruise mode for each category.

V/STOL aircraft with practically all possible combinations of the thrust-producing devices (table 10-I) and the thrust-directing techniques (fig. 10-15) have been built and flown, with varying degrees of success. Examples of a few of the more successful types will now be given.

Figure 10-16 shows a tilt-rotor VTOL aircraft in the hover and cruise modes. This is the Bell XV-3 convertiplane, which uses two 23-foot-diameter tilting rotors mounted on the wing tips. The rotors can be turned through slightly more than 90^{o} and are driven by shafts and gears from an engine located in the fuselage. Attitude control in hovering flight is the same as for a helicopter. In the event of engine failure in cruise flight, the rotors can be turned to the hover position for an autorotation landing. The aircraft has been flown at speeds up to 180 miles per hour. More modern versions of this aircraft type are being considered for observation, reconnaissance, and rescue missions.

Figure 10-17 shows the Fairey Rotodyne, which was designed by the British as a civilian transport to carry about 60 passengers. This aircraft is a compound helicopter that uses a single 109-foot-diameter rotor for vertical flight and twin propellers for cruise. Two turboshaft engines drive the propellers in cruise and also power auxiliary

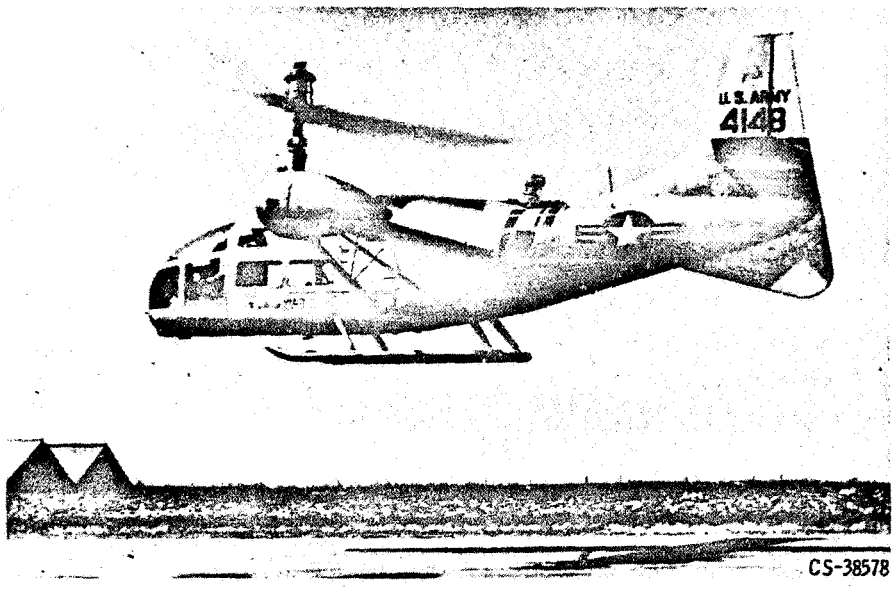

Hovering

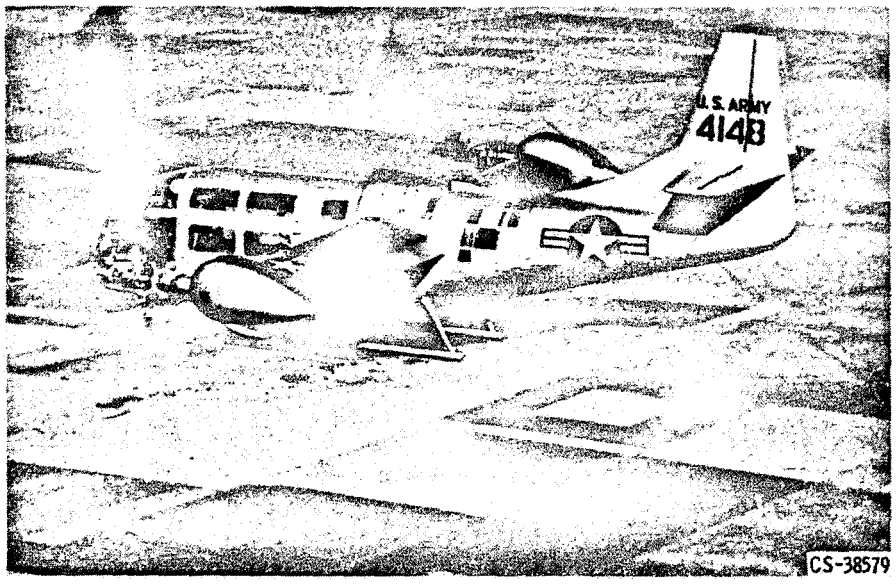

Cruising

Figure 10-16. - Bell XV-3, tilt-rotor convertiplane.

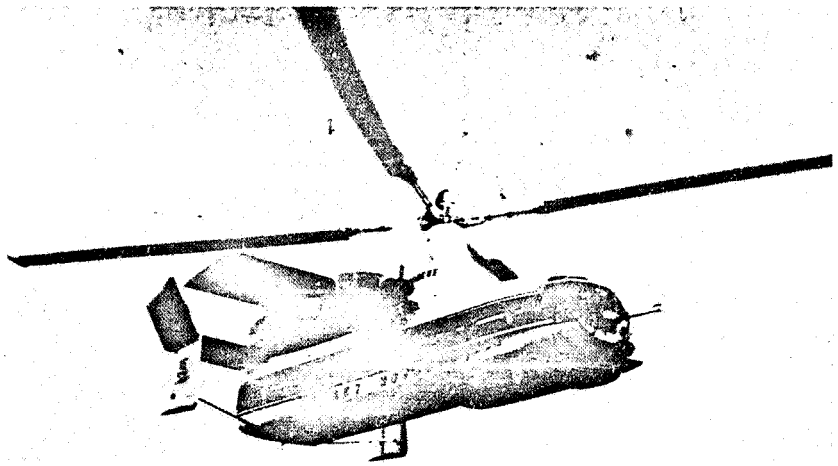

CS-38682

Figure 10-17. - Fairey Rotodyne, compound helicopter.

compressors which provide compressed air to drive the rotor by pressure jets on the rotor tips. During cruise, some of the power is removed from the rotor; that is, the rotor is unloaded. Unloading the rotor reduces the drag and allows a higher cruise speed (in this case, around 200 mph). More recent U.S. designs for this type of aircraft have incorporated concepts in which the rotor is stopped and folded back or stopped and retracted into the fuselage during cruise flight. The purpose of these techniques is to reduce or eliminate the rotor drag and thereby increase the cruise speed capability, in some cases up to 350 miles per hour.

Figure 10-18 illustrates a tilt-wing type of VTOL aircraft. This is the Ling-Temco-Vought XC-142A, which was designed as a military transport. The tilting wing carries four turboshaft engines in separate nacelles. Each engine drives a four-bladed propeller about 16 feet in diameter. The engines and propellers are interconnected by shafts and clutches to provide for symmetrical thrust distribution if one engine fails. The wing is tiltable through 100^{o} from the horizontal, so that the aircraft can hover in a tail wind or fly backwards. The wing is equipped with a large trailing-edge flap and a leading-edge slat, which are programmed (synchronized) with the wing-tilt angle to increase the lift and prevent stall during transition flight. Yaw control during hover is obtained by ailerons in the propeller slipstream. Pitch control is by a horizontal rotor located behind the tail. Roll control is obtained by differential pitch on the propellers. Cruise speed at sea level is about 300 miles per hour, with a range of about 400 nautical miles. At the present time, the XC-142 is being flown to determine the operational suitability of this type of VTOL aircraft for military transport service. Aircraft of this type are also being seriously considered for civilian transport use.

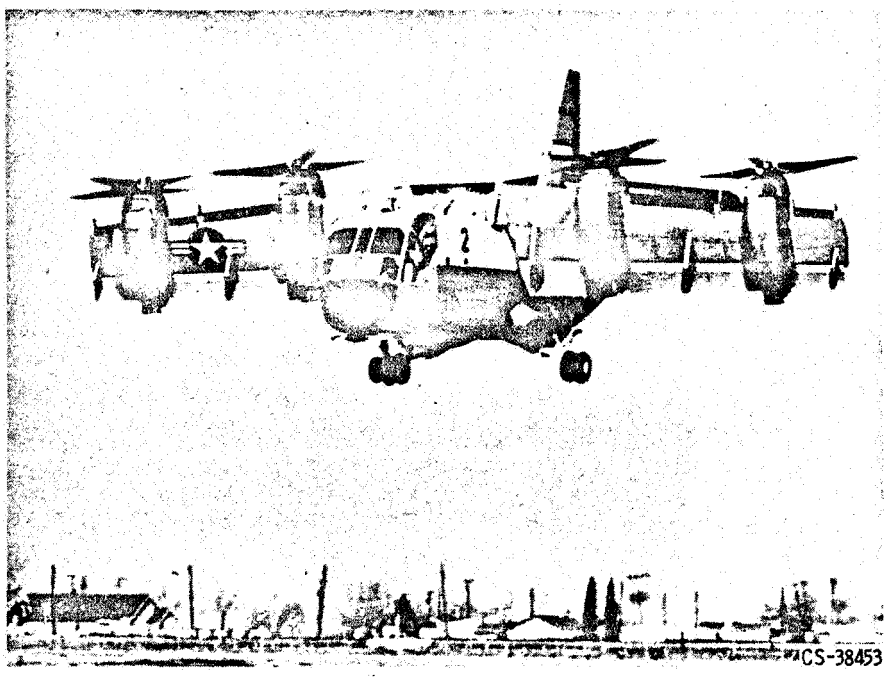

Hovering

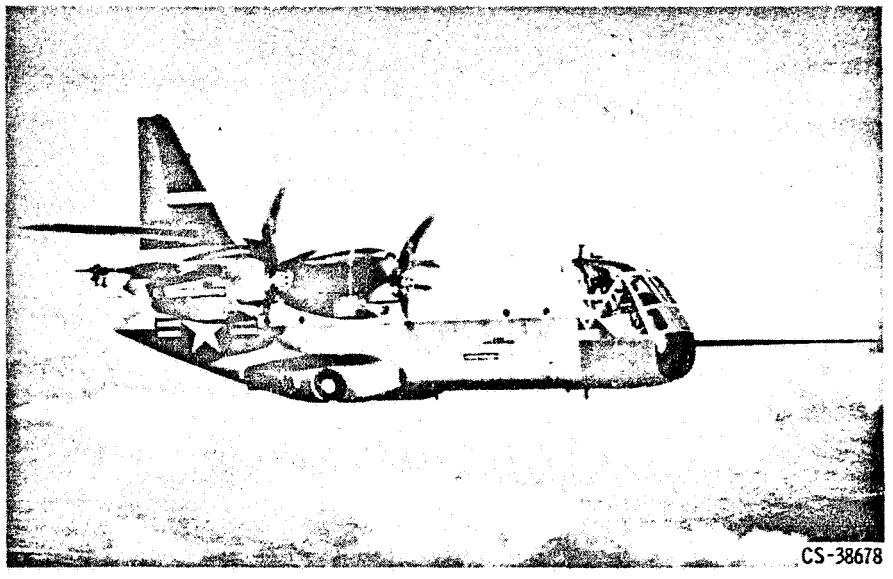

Cruising

Figure 10-18. - Ling-Temco-Vought XC-142A, tilt-wing VTOL aircraft.

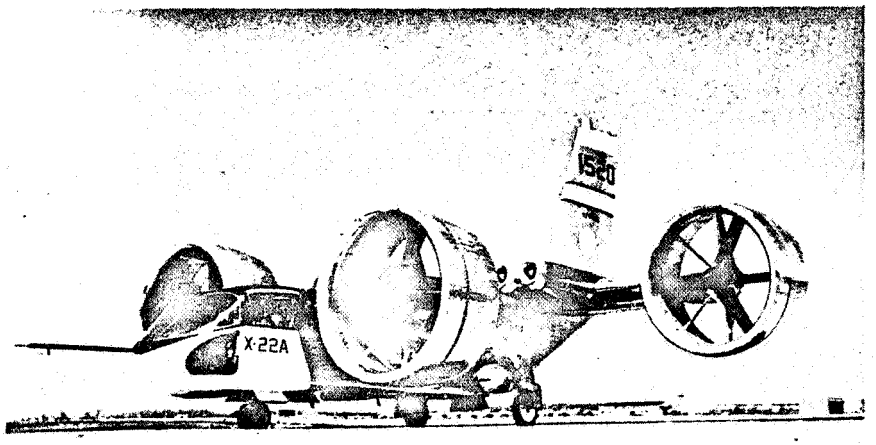

CS-38456

Figure 10-19. - Bell X-22A, tilting-ducted-propeller VTOL aircraft.

Figure 10-19 shows the Bell X-22A. This VTOL aircraft has a propulsion system consisting of four tilting, ducted propellers. It is primarily a research aircraft that is being used to determine the feasibility of this type of VTOL aircraft for military and civilian transport use. Vertical flight is obtained by rotating the ducted propellers to the vertical position. To translate from hovering to cruise flight, the ducts are slowly rotated forward. In cruise flight, lift is supplied by the stubby fore and aft wings and the surfaces of the ducts themselves. Attitude control in both hover and cruise flight is obtained by differential thrust from the propellers and by deflection of the propeller slipstream by movable vanes in the duct exits. Power is provided by four turboshaft engines located on the inboard section of the aft wing. Here again, the engines and propellers are all interconnected. Design cruise speed is 290 miles per hour.

Figure 10-20 shows the EWR-Sud VJ101C, a West Germany fighter aircraft which utilizes a mixed class of VTOL propulsion systems. It has dual propulsion and thrust tilting. The aircraft has six turbojet engines, two for lift only and four for lift and cruise. The lift engines are mounted in the forward part of the fuselage. The four lift-cruise engines are in pairs in tilting pods at the wing tips. This triangular arrangement of the engines allows the use of thrust modulation for pitch and roll control in hovering flight. Yaw control is obtained by tilting the wing-tip pods slightly from the vertical in opposite directions. The aircraft has been flown at speeds slightly over Mach 1.

A transport version using lift engines in fixed pods at the ends of the wings is also being tested by the West Germans. This airplane is called the Dornier Do-31. It has four lift engines in each wing pod and two cruise engines in conventional nacelles under the wings.

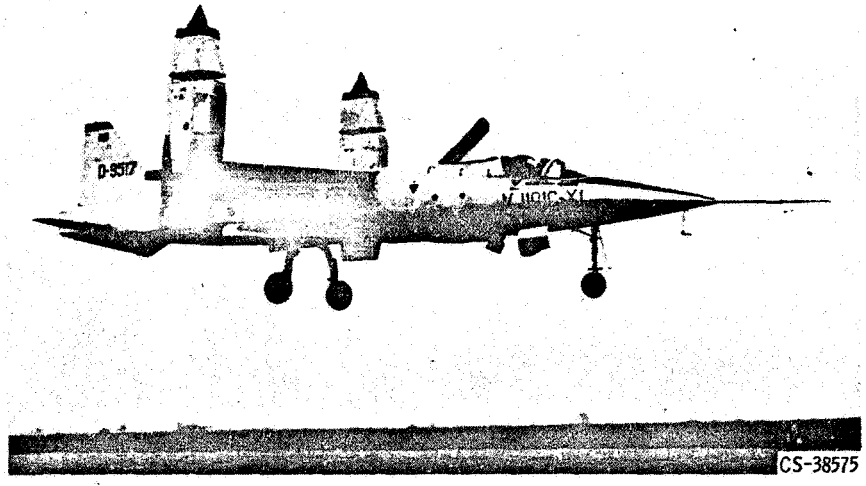

Hovering

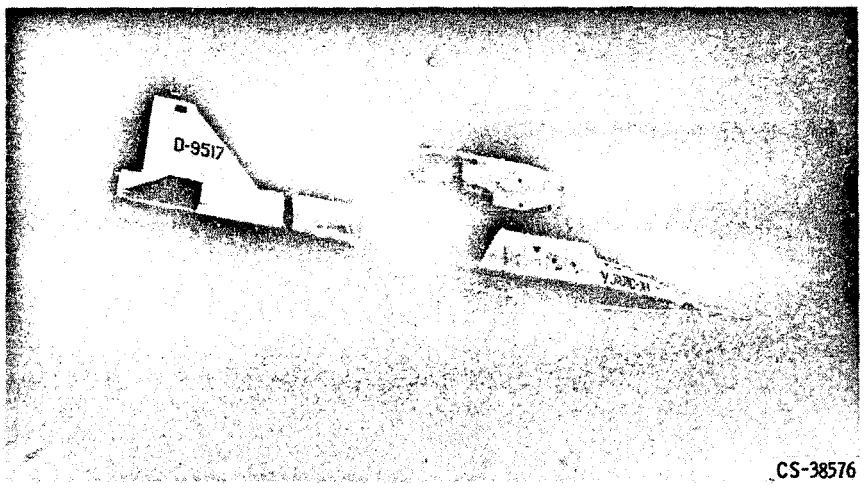

Cruising

Figure 10-20. - EWR-Sud VJ101C, thrust-tilting, dual-propulsion VTOL fighter. (Courtesy of Interavia.)

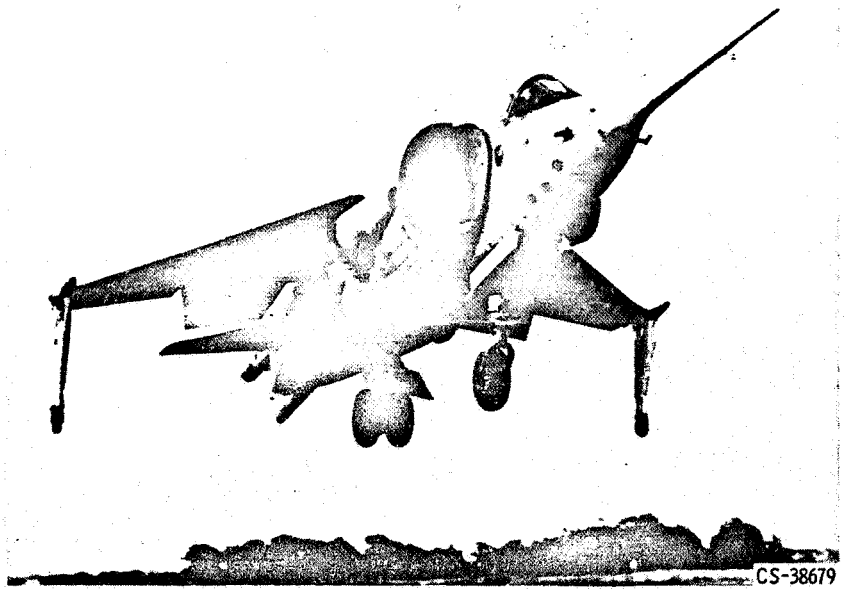

Figure 10-21. - Hawker-Siddeley P1127 Harrier, thrust-deflection type VTOL strike/reconnaissance aircraft.

Figure 10-21 shows the British Hawker-Siddeley P1127 Harrier. This is a thrust-deflection-type VTOL aircraft. A single large turbofan engine is located in the center of the fuselage. The engine discharges its air through two nozzles on each side of the fuselage: one ahead and the other behind the center of gravity. Fan discharge air exhausts through the front nozzles, and the hot gases exhaust through the rear nozzles. All four nozzles are fitted with turning vanes, and the nozzles are rotatable, so that the engine thrust can be directed either downward for vertical flight or rearward for horizontal flight. Attitude control in low-speed flight is by means of reaction jets located at the nose, tail, and wing tips. These reaction jets are fed by compressed air from the engine. The aircraft is designed for transonic flight. The first operational squadron of these strike/reconnaissance aircraft has been formed.

Figure 10-22(a) shows the Dassault Mirage 3V aircraft. This is a French high-speed fighter with VTOL capability. It is a dual-propulsion aircraft with separate engines for lift and for cruise. The layout of the engines in the aircraft is shown in figure 10-22(b). A single cruise engine is located in the tail of the aircraft. Eight turbojet lift engines are located in tandem pairs in the central portion of the fuselage. Air for the lift engines enters the four scoops on the top of the fuselage and exits through doors on the bottom. Attitude control in hover is by reaction jets located at the nose, tail, and under each wing tip. These jets are powered by air from the lift engines.

A more recent dual-propulsion aircraft design was evolved for the proposed V/STOL fighter that was to have been developed jointly by the United States, West Germany, and Great Britain. This aircraft design called for a single cruise engine in the rear, and two

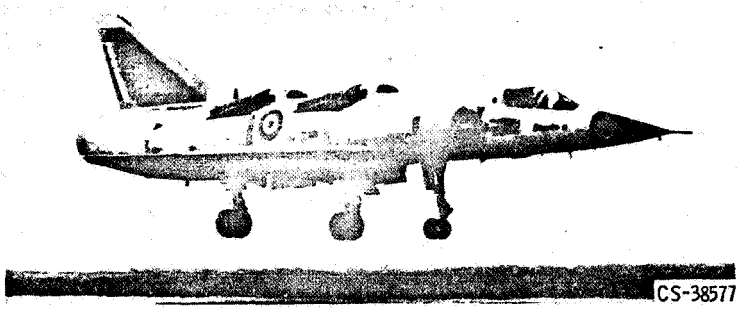

(a) Aircraft in hover mode.

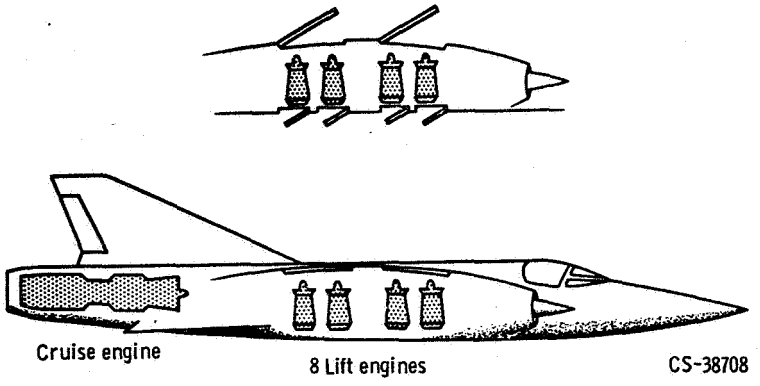

(b) Schematic of dual propulsion system.

Figure 10-22. - Dassault Mirage 3V, dual propulsion VTOL fighter.

direct-lift engines, on each side of the fuselage, that would swing out (like landing gears do) when needed for takeoff or landing. The cruise engine was designed with an exhaust deflector, so that downward thrust could also be obtained from this engine during lift-off. This project, which has just recently been cancelled, was to have been a joint effort in which the U.S. and West Germany were to build the airplane, and the U.S. and Great Britain were to build the engines.

Figure 10-23(a) shows the Ryan XV-5A semi-dual-propulsion VTOL airplane developed for the U.S. Army. A schematic of the propulsion system for this airplane is shown in 10-23(b). Lift thrust is provided by a ducted fan in each wing. These two fans are powered by two turbojet engines located in the top of the fuselage. Cruise thrust is obtained from these same engines. During hover, exhaust gas from the turbojet engine is diverted by a valve to a turbine located on the fan tips, as shown in figure 10-23(c). These tip-turbine fans approximately triple the basic thrust of the jet engines. Each fan is about 5 feet in diameter and is covered during cruise flight by doors on top of the wing and by span-wise louvers underneath the wing. During vertical flight, the doors and louvers are opened fully. In transition, the exit louvers are moved to deflect the airflow backwards. This gives the aircraft a forward acceleration. When minimum speed for

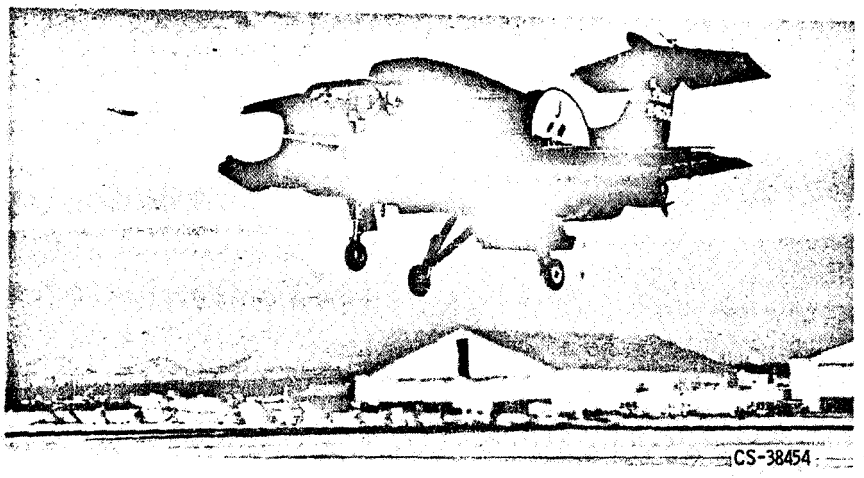

(a) Aircraft in hover mode.

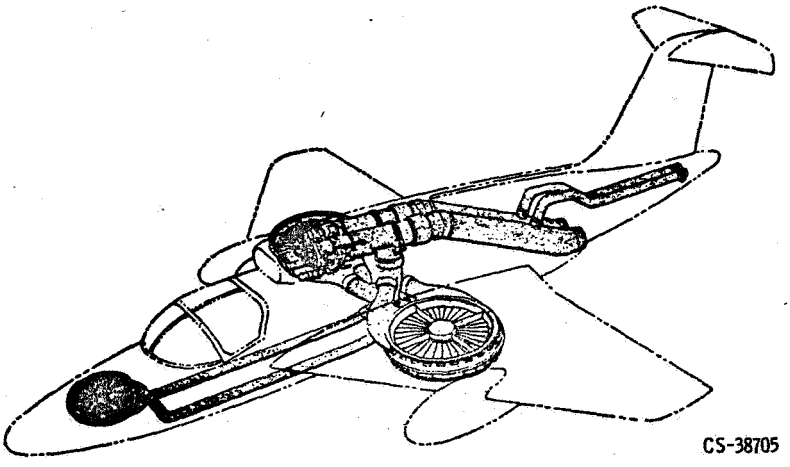

(b) Propulsion-system arrangement.

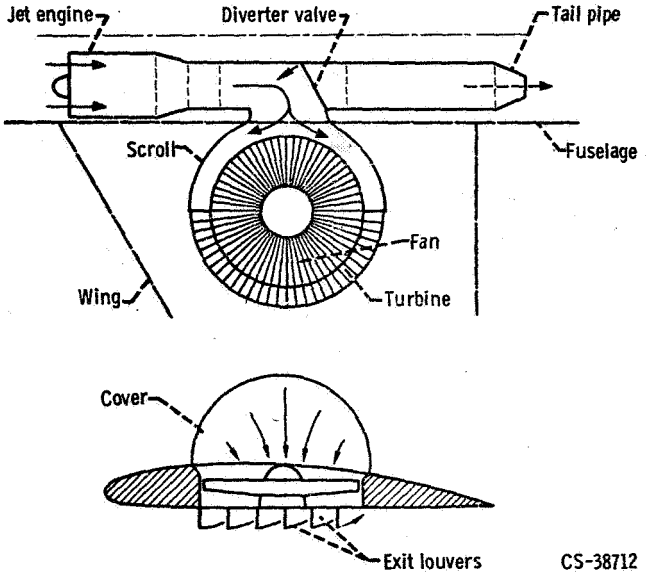

(c) Schematic of propulsion-system elements.

Figure 10-23. - Ryan XV-5A, semi-dual-propulsion VTOL aircraft.

wing-supported flight is reached, the engine exhaust gases are diverted (by means of the valve shown in fig. 10-23(c)) from the fans to conventional jet nozzles under the rear of the fuselage, shown in figure 10-23(b). In hovering, pitch control is obtained by an additional fan in the fuselage nose, and by reaction jets in the tail. Yaw control is by differential movement of the louvers on the fan exits. Roll control is by differential thrust of the wing fans. To provide for symmetrical thrust during an engine failure, the turbojet engines and fan turbines are interconnected. The cruise speed of this airplane is approximately Mach 0.7. The aircraft currently is being flight tested.

TECHNICAL PROBLEMS

In spite of the many V/STOL aircraft that have been and are being designed and built, very few have become operational. One reason for this is that the design and operation of V/STOL aircraft present many problems that have not yet been solved completely satisfactorily. In the following discussion, the principal technical problems pertaining to V/STOL aircraft are summarized briefly and are compared with the problems of CTOL aircraft. The discussion deals primarily with VTOL aircraft, but all items mentioned also apply to STOL aircraft, although to a lesser degree.

Thrust Requirements

One important difference between V/STOL and CTOL aircraft is in their engine propulsion requirements. For conventional jet aircraft, the ratio of engine thrust to aircraft gross weight is about 0.25 to 0.35; that is, a 100 000-pound aircraft would require jet engines that produce around 25 000 to 35 000 pounds of thrust. In contrast, the theoretical minimum basic propulsion thrust for a VTOL aircraft is the thrust required for a vertical takeoff. This means that the ratio of lift thrust to gross weight must be at least 1.0. However, the actual design value of thrust must be even greater than the weight of the aircraft, because of other considerations that will be discussed later. This increased thrust requirement complicates the design of an aircraft. For example, powering a jet airliner such as the Boeing 707 for vertical takeoff would require that it be fitted with at least 12 jet engines instead of four, or that its four engines be doubled in size.

For STOL aircraft, the required thrust-to-weight ratios range between about 0.35 and 0.8, depending on the type of propulsion system and the runway length allowed.

The earlier discussion (in the section titled BASIC CONCEPTS) explained that during takeoff and landing, when the VTOL aircraft has zero or low forward flight speed, the control surfaces do not generate lift or control forces. Therefore, the propulsion system of a VTOL aircraft must also supply control forces to regulate the stability and attitude of the aircraft. (STOL aircraft do not generally require auxiliary control systems.) Some

of the methods by which control forces are obtained were described earlier, in the section titled AIRCRAFT TYPES. For VTOL aircraft, the ratio of required control-thrust power to aircraft weight might range from about 0.1 to 0.2, depending on the configuration. These required values of thrust, just for the control of VTOL aircraft at low speeds, are about half as much as the total propulsive thrust required for today's jet transports. The need for such powerful control systems stems partly from a lack of aircraft stability in hovering near the ground and partly from the requirement that VTOL aircraft be able to maneuver precisely within small or confined areas in turbulent wind conditions. This maneuvering capability demands a rapid control response (approx. 0.1 or 0.2 sec). Therefore, much thrust is needed to meet these control requirements. However, many different control systems are possible, and their exact thrust requirements depend greatly on the total design of the aircraft. Consequently, there is considerable uncertainty among designers concerning the amount of control thrust that is absolutely necessary.

In addition to the control-thrust requirements, the related problems of maintaining sufficient thrust and control in the event of an engine, or thrust-device, failure must also be considered. The thrust problem stems from the fact that during takeoff, landing, or hovering the VTOL aircraft depends entirely on the engine power for lift. Thus, the failure of an engine or thrust device could be disastrous. A brute-force solution to this problem is the use of many thrusters and many engines, where each engine is oversized so that it is capable of producing excess power. Thus, if one engine fails, the others can produce sufficient excess power to compensate for the lost thrust of the failed engine. For example, if jet engines are used to provide thrust directly, the amount of excess thrust that each engine must be capable of producing depends on the number of engines used; as the number of engines increases, the excess thrust capability required from each engine decreases. For a VTOL aircraft, when two engines are used, each engine must be capable of producing 100 percent excess thrust. With four engines, the excess thrust required from each engine is about 34 percent, and with eight engines it is about 15 percent. In comparison, the excess thrust capability required for each engine of a four-engine CTOL aircraft is only about 10 percent.

When one engine fails, increased power can also be obtained from the remaining engines by overspeeding them. However, this procedure is undesirable, because it can severely damage the oversped engines.

The control problem is that the failure of one engine of a multiengine VTOL aircraft could cause the aircraft to flip over, because of the unbalanced thrust. A solution to this problem is to cross-connect all of the engines by either ducting or shafting, depending on the type of propulsion system. For example, figure 10-24 shows the cross-shafting system used on the Ling-Temco-Vought XC-142A, the tilt-wing turboprop aircraft shown in figure 10-18. A clutch located between each propeller and engine automatically disengages the failed engine. The reduced total power is then redistributed through the cross-

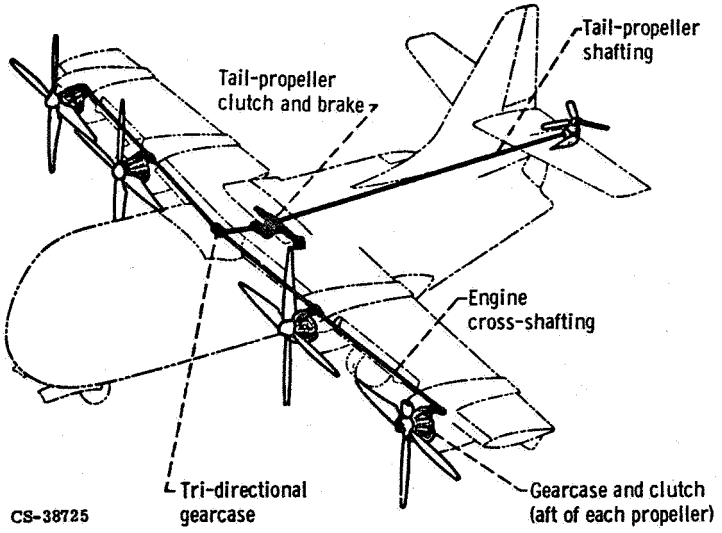

Figure 10-24. - Engines cross-connected for safety in the event of failure of one engine.

shafting system so that equal power is delivered to each of the four main propellers. A reduced power flow also goes to the tail propeller. Obviously, this is a complex arrangement.

The engine- or thruster-failure problem during takeoff or landing is also important for STOL aircraft. However, the tendency of the aircraft to upset because of unbalanced thrust is not as severe, since the STOL airplane is supported completely or mostly by the lift of the wings (lift tends to remain uniformly distributed when an engine fails).

To satisfy the three previously mentioned thrust requirements (lift-off thrust, control thrust, and excess thrust for engine failure) for VTOL aircraft, the ratio of total thrust to aircraft weight must be about 1.15 to 1.3, depending on the overall configuration of the aircraft.

For STOL, as mentioned previously, the required thrust-to-weight ratios are from 0.35 to 0.8. The propulsion system of a V/STOL aircraft will therefore be heavier than for a comparable CTOL plane. For example, for the same size airplane, the propulsion system is only around 6 percent of the total weight for CTOL, but this increases to 12 to 18 percent for STOL, and to 20 to 32 percent for VTOL.

When considered on the basis of the same mission, V/STOL aircraft will certainly be heavier and more costly than comparable CTOL aircraft. In fact, studies indicate that for the same payload (passenger or cargo) capacity, a VTOL transport will be around 50 percent heavier than a CTOL transport and cost about 50 percent more to operate. A breakdown of the relative weights of these two types of aircraft is presented in figure 10-25.

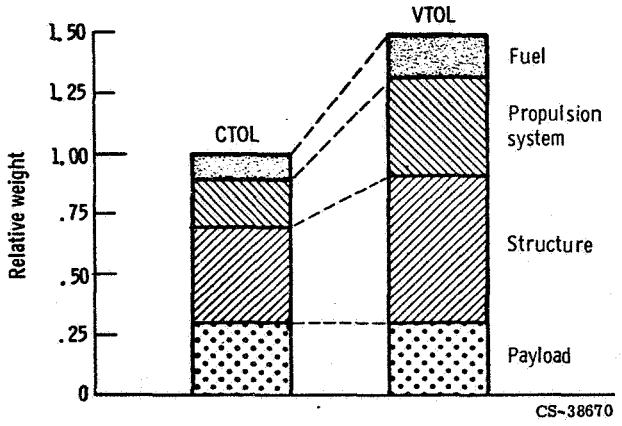

Figure 10-25. - Weight comparison of typical VTOL and CTOL transports with same payload, range, and cruise speed capabilities.

Power Matching

The fact that relatively large amounts of power are required for takeoff with V/STOL aircraft creates a problem for the cruise condition. V/STOL aircraft, especially subsonic configurations, have far more installed power than is necessary to sustain normal cruise flight. For example, if the overall lift-to-drag (L/D) of the airplane in cruise is 10, then the required cruise thrust is only 0.1 of the airplane weight (thrust = drag). However, the installed thrust required for vertical takeoff could be around 1.2 times the airplane weight. Thus, a reduction in thrust to around 8 percent of the takeoff value is required for cruise. Current propulsion systems cannot operate over such a wide range of power output. This is called power mismatch.

Several approaches are taken to ease this "mismatch" problem. In all cases, the powerplants can be designed to give wide ranges of power (e.g., by using variable-geometry components). Using high-bypass-ratio fan engines also helps, since power output falls off rapidly with flight speed for this type of system.

However, these steps may not be sufficient, especially for VTOL. In many cases, it will be necessary to shut down some of the engines during cruise flight, or to use two completely separate systems - one for takeoff and landing, and the other for cruise flight. Examples of this approach to the mismatch problem are the previously discussed EWR-Sud VJ101C aircraft (fig. 10-20) and the Dassault Mirage 3V (fig. 10-22).

Noise

One great obstacle to successful V/STOL operations, especially commercial operations, is noise. The basic reasons for this are that V/STOL operations will bring air-

craft much closer to the populous areas of cities and these aircraft will have far more powerful engines then those used on current CTOL airplanes. It is easy to see, therefore, that aircraft noisiness will be a very important consideration in the evaluation of V/STOL systems.

Aircraft noise is measured in terms of a factor called PNdB, which stands for "perceived noise level in decibels." Noise is basically a succession of pressure waves that are propagated from a generating source (like the aircraft engine). The intensity of the noise (amplitude of the pressure wave) is measured in terms of decibels of the sound pressure with respect to some reference level. Noise is usually propagated over a range of frequencies from about 20 to 10 000 cycles per second. (For rating purposes, sound pressure is usually divided into eight frequency ranges, called octave bands.) Sound of a given intensity can be very annoying if generated at certain frequencies, and less annoying at other frequencies. The perceived noise level of a given sound is numerically equal to the sound pressure level of a reference sound that is judged by listeners to have the same perceived noisiness as the given sound, the reference sound being a band of random noise 1 octave in width centered on 1000 cycles per second.

The PNdB noise rating is an attempt to weigh the sound pressure level (intensity) value to account for the effects of different frequencies. It was originated about 8 years ago from a study of people's reaction to the noise from turbojet and turboprop commercial aircraft operating from the New York City airports. It was found that frequencies in the range from 600 to 4800 cycles per second were most annoying. Thus, the PNdB rating gives relatively more weight to the mid-frequency range of sounds. However, noise prediction is a very complex and difficult procedure, because there are many noise sources and influencing factors involved (such as duration, atmospheric conditions, and the variation in tolerance among different people). Considerable effort is currently underway to improve our ability to rate and predict noisiness and to take these factors into account in a rational manner.

The principal sources of noise in a jet aircraft are the hot gas exhaust from the jet engine and the high-speed rotor blades of the engine compressor. The roar of a jet plane as it takes off is from the exhaust jet, while the whine that is heard when a plane is landing is from the compressor. Propellers and rotors are the principal noisemakers in turboprop planes and helicopters. A rough rule of thumb is that the loudness (intensity) of the noise of an airplane depends on the disk loading (slipstream velocity) of its thrust device, where the higher the disk loading, the louder the noise.

A gross comparison of the predicted noise levels for various types of V/STOL aircraft currently under study is shown in figure 10-26. The figure shows predicted values of PNdB heard at 400 feet either to the side or below a VTOL aircraft of 75 000 pounds gross weight at full power setting. Values are plotted against disk loading, and the various types of thrust devices that were mentioned earlier are located on this scale. Also

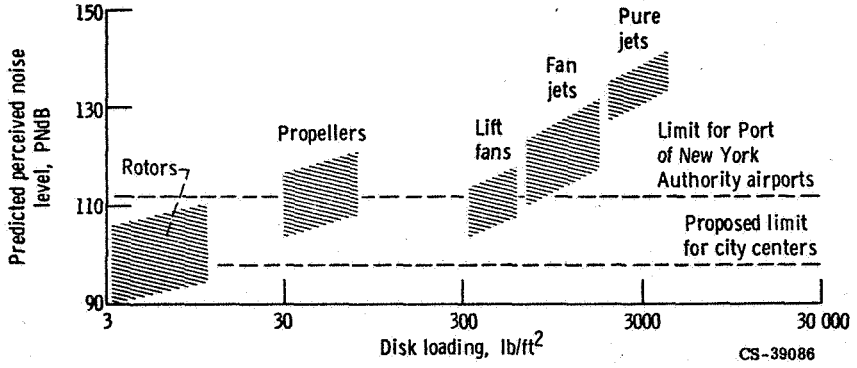

Figure 10-26. - Predicted noise level as function of disk loading for various types of V/STOL thrust devices. Powerplant at full power setting; gross weight of aircraft, 75 000 pounds; distance of aircraft from noise detector, 400 feet. (For comparison purposes, the following are some typical perceived noise levels in decibels: residential area (daytime), 50 to 60; city traffic (daytime), 80 to 90; train at 100 feet, 90 to 100; boiler shop, 125 to 135.)

shown in the figure are two tentative noise limits (indicated by dashed lines). The limit of 112 PNdB is in effect for Port of New York Authority airports (Kennedy, LaGuardia, and Newark). The lower limit of 98 PNdB has been proposed for V/STOL operations from city-center areas. The proposed limit for V/STOL operations is lower because the noise duration would be longer with the slower V/STOL flight speeds near airports and because the airports would be located in or near highly populous areas. The figure indicates that pure jets are completely unacceptable. Fan jets (turbofans), which have drastically reduced slipstream velocities, are a basic improvement, but not enough. With this type of engine the overall PNdB remains high because of the predominant compressor fan noise. In terms of the PNdB, propellers seem to be reasonably good and rotors seem best. However, the character of the noise of these thrust devices is different from that of the jet engines. The noise of rotors, in particular, includes fluctuations (or beats) that can be objectionable. This rotor noise is sometimes referred to as banging. It is quite intense and of relatively low frequency. The PNdB rating as it is now determined does not account for this rotor noise. Therefore, the actual sound of a rotor is worse than is indicated by the noise rating.

Obviously, the noise levels of proposed V/STOL aircraft will have to be reduced, but this will be difficult and expensive.

Downwash Effects

With a VTOL aircraft, high slipstream or exhaust velocities can cause trouble when the discharge from the thrust device is directed downward. Some of the effects of a high-velocity downwash are illustrated in figure 10-27. For example, when a jet-powered

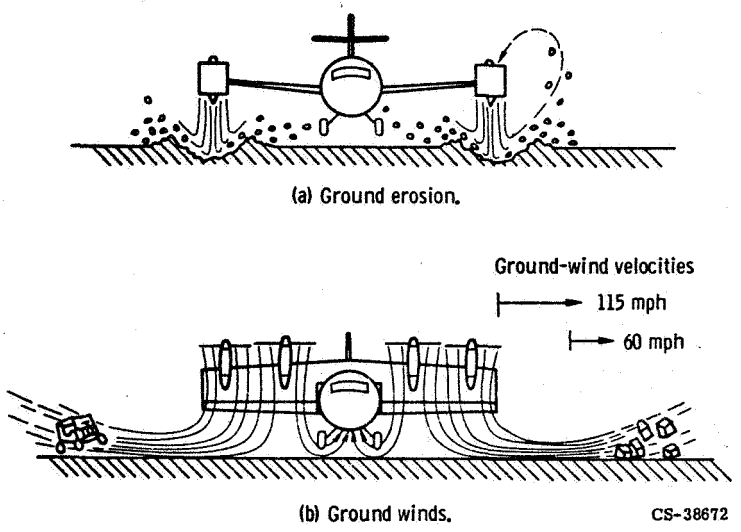

(a) Ground erosion.

(b) Ground winds.

Figure 10-27. - Downwash effects of hovering VTOL aircraft.

aircraft is hovering over unprepared ground (fig. 10-27(a)), the exhaust streams from the jet engines can quickly start blasting sizable holes in the earth. Pieces of debris can be recirculated up and into the engine inlet and also can be thrown up against the landing gear and fuselage. Ground erosion increases with increasing exhaust velocities. Figure 10-27(b) shows a typical turboprop-powered tilt-wing aircraft hovering over a paved runway. The slipstream is turned by the pavement, and the horizontal winds created can be 60 miles per hour even 60 feet away from the aircraft. Such winds can cause damage to objects near the aircraft. The fact that VTOL aircraft are expected to operate from small, confined landing areas makes the ground-wind problem even more serious.

Another aspect of these ground winds is that they can create either positive or negative pressures under the aircraft, depending on the aircraft configuration. With some configurations, the propeller slipstreams or the jet exhaust streams may collide after impinging on the ground surface and flow vertically upward against the bottom of the aircraft (fig. 10-27(b)). This upward flow produces a local positive pressure, or boosting effect.

For airplanes with wings in the normal horizontal position, the high-velocity exhaust of a vertically mounted or deflected jet will drag some of the surrounding air along with it (this phenomenon is called air entrainment). This creates a pronounced airflow toward the jet along the undersurface of the wing or the fuselage. This flow, in turn, reduces the pressures on the surface and results in a negative lift, or downward suction. These positive and negative ground effects contribute to the instability and control problems mentioned earlier.

Another operational problem related to downwash velocity with jet or fan thrusters is that hot exhaust gases may recirculate and enter the drive engines, thereby decreasing

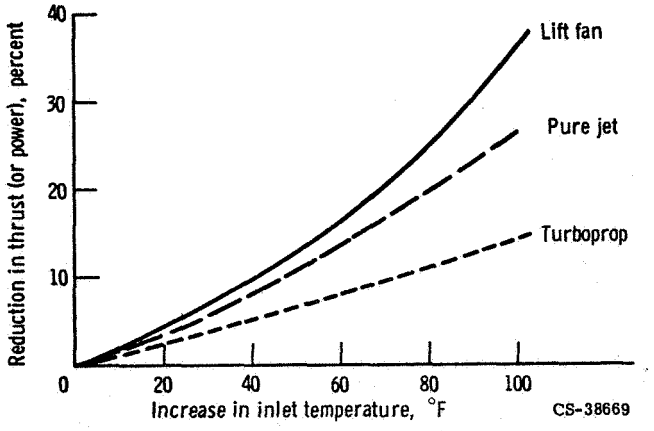

Figure 10-28. - Reduction in engine thrust or power with increase in inlet temperature.

their thrust. Figure 10-28 shows that an inlet temperature increase of only 40° F can cause a 10-percent reduction in thrust in some powerplants. Such a reduction in thrust can seriously affect the performance of a VTOL aircraft. The relative positions of the curves for the three propulsion types shown in the figure are not precise for all engines. They merely show a general trend, based on manufacturers' engine specifications.

Powerplant Selection

A difficult problem confronting V/STOL aircraft designers is the selection of the propulsion system for the aircraft. Of the various propulsion systems (jet, fan, propeller, or rotor) that can be used for V/STOL aircraft, none is clearly far superior to the others. Each system has its advantages and disadvantages. How any given propulsion system compares with other systems depends on the type of aircraft under consideration and the mission it is intended to accomplish. There is an extremely close interrelationship between aircraft configuration and propulsion system, and both have to be considered together when the airplane is designed. This is far more important with V/STOL aircraft than with CTOL aircraft.

However, the principal requirements and desired characteristics of any propulsion system include light weight, small volume, low noise output, low cost, good engine-failure safety, low fuel consumption, small downwash effects, and best match between takeoff and cruise power. Some of these qualities are conflicting by nature. Therefore, any propulsion-system design is a compromise in which some desirable characteristics are sacrificed in order to obtain those characteristics that are essential to the particular application. For example, for a military aircraft, the compromise might be in favor of powerplant performance at the expense of noise and cost. However, for a civilian transport, the compromises may have to be in favor of low noise and low cost.

Recent studies based on current powerplant technology have indicated that VTOL aircraft operation may be up to 50 percent more expensive than CTOL aircraft operation. Most of this cost difference is a result of the relatively greater power requirement of a VTOL aircraft. Considerable effort will therefore be required to improve the characteristics of V/STOL propulsion systems so that they can result in more financially as well as technically attractive aircraft.

NASA PROGRAMS

NASA is strongly interested and actively involved in research on V/STOL aircraft. This phase of aeronautical research is receiving increased emphasis in the three major NASA research centers - Langley, Ames, and Lewis. The Langley and Ames Centers are primarily concerned with overall aircraft aerodynamics and design and with actual flight operations. Their tests are conducted on large-scale airplane models in wind tunnels and on full-size test aircraft.

Here at Lewis the emphasis is on research on propulsion systems and propulsion-airframe integration. Currently, studies are being made of promising propulsion systems for STOL and VTOL aircraft. We are trying to get a better picture of the relative design and performance characteristics of the propulsion systems, as well as their problem areas. The objective is to select systems (powerplants and thrust devices) for further experimental evaluation. Current emphasis is on high-bypass-ratio fans for both STOL and VTOL propulsion. Various design and operating problems are being defined, and means for solving them are being devised. We are also devising and studying various attractive airplane configurations for VTOL and STOL transports.

11. SUPERSONIC AERODYNAMICS

David N. Bowditch*

To introduce supersonic aerodynamics, let us first consider what characterizes supersonic flow. "Supersonic" obviously refers to speeds faster than the speed of sound, or the sonic velocity. A sound wave is a wave with a very small pressure rise across it. When you speak, you form sound waves that travel through the air to someone who senses and interprets the waves as words. These same sound waves speed ahead of a subsonic airplane and start the air moving around its body and wings. However, at supersonic speeds, these sound waves can no longer reach ahead of the airplane and prepare the air to flow smoothly around its parts. The sound waves coalesce to form discrete shock waves with large pressure rises across them. As the aircraft travels faster than the speed of sound, these shock waves are attached to the pointed or sharp (low-angle) surfaces of the aircraft and abruptly deflect, or push, the air around the surfaces of the aircraft. These shock waves, more than any other feature, characterize supersonic flow.

FLOW REGIMES

The characteristics of four flow regimes covering the subsonic through supersonic range are depicted in figure 11-1. In the figure, the point 0 represents the present location of the disturbance, and the points -1, -2, and -3 represent the locations of the disturbance at one, two, and three units of time previously. The circles look like ripples in a pond, caused by a pebble dropped at the disturbance origin. However, in the three-dimensional atmosphere, the circles represent spherical sound waves propagating in all directions at the speed of sound. For zero disturbance-origin velocity, the sound waves form concentric circles about the disturbance (fig. 11-1(a)). When the disturbance-origin velocity V is greater than zero but less than the speed of sound C, the sound waves still propagate ahead of the moving origin (fig. 11-1(b)). However, when the disturbance-origin velocity equals the speed of sound ($V/C = 1$), there is a zone of silence ahead of the disturbance origin that is unaffected by the disturbance (fig. 11-1(c)). At supersonic velocity ($V/C > 1$), the disturbance origin continually outruns the earlier sound waves

*Chief, Propulsion Aerodynamics Branch.

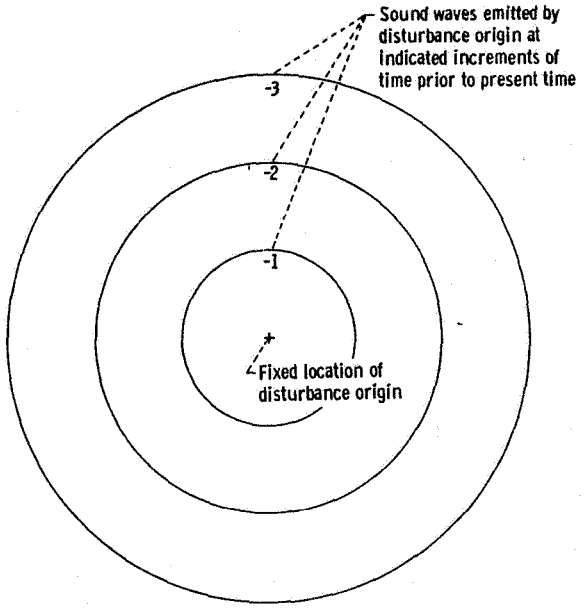

(a) Zero disturbance-origin velocity (V/C = 0).

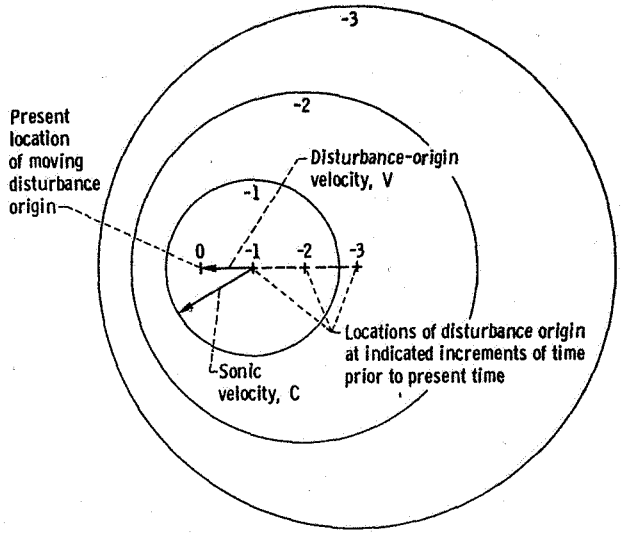

(b) Subsonic disturbance-origin velocity (V/C < 1).

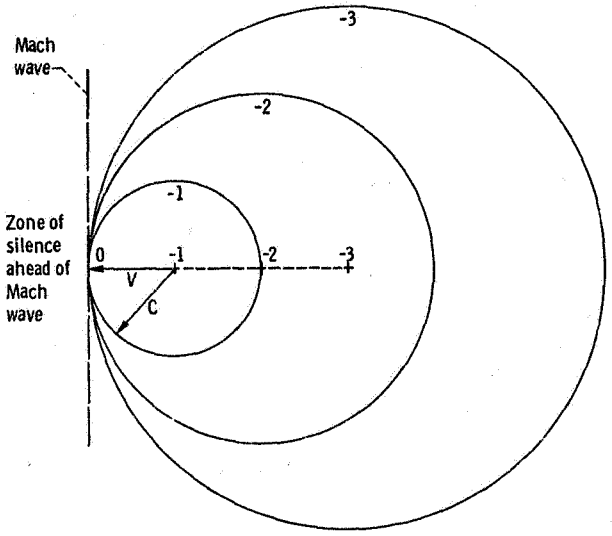

(c) Transonic disturbance-origin velocity (V/C ≈ 1).

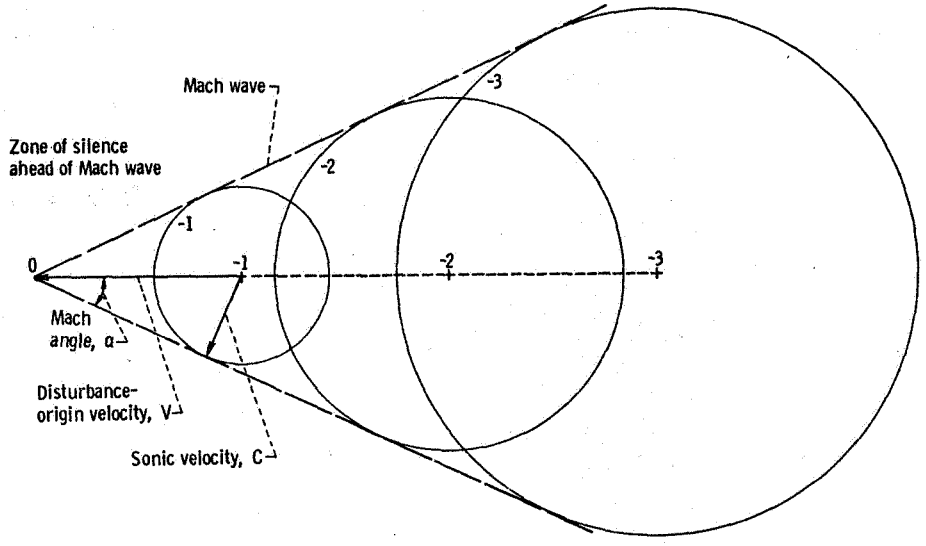

(d) Supersonic disturbance-origin velocity (V/C > 1).

Figure 11-1. - Pressure fields produced by a point disturbance origin moving at various constant velocities.

(fig. 11-1(d)). Thus, the spherical waves propagating from previous points along the path of the origin form a cone behind the moving disturbance origin. The half angle of the cone, called the Mach angle α, is given by the equation

$$\alpha = \text{arc sin } \frac{C}{V} = \text{arc sin } \frac{1}{M}$$

where C is the sonic velocity, V is the disturbance-origin velocity, and M is the Mach number.

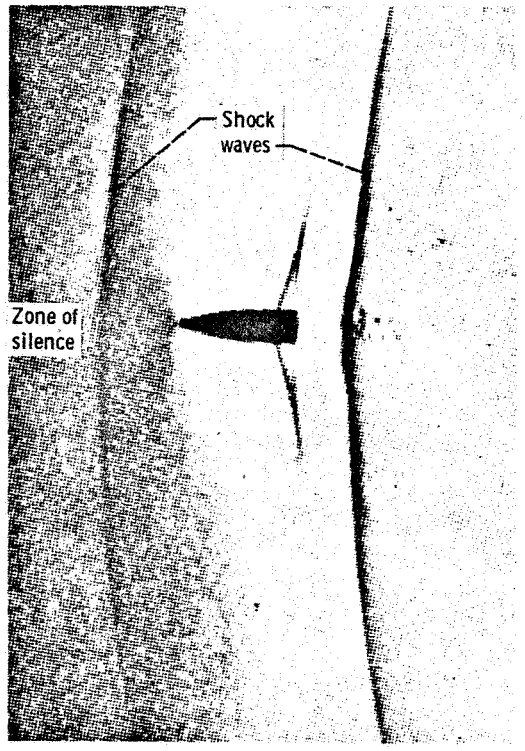

Figure 11-2. - Schlieren photograph of bullet traveling at transonic speed. (From Ackeret and reprinted from "The Dynamics and Thermodynamics of Compressible Fluid Flow," by Ascher H. Shapiro, with permission of the Ronald Press Co.)

Figure 11-2 is a schlieren photograph of a bullet traveling at transonic speed. The shock waves are nearly perpendicular to the direction of the bullet. The "zone of silence," discussed previously, is ahead of the bow wave of the bullet. Figure 11-3 shows two bullets traveling at supersonic speeds through short cylindrical tubes. The tubes restrict the wave travel. As the bullet emerges from the tube (fig. 11-3(a)) or as it passes by a circumferential slot in the tube (fig. 11-3(b)), the spherical nature of the

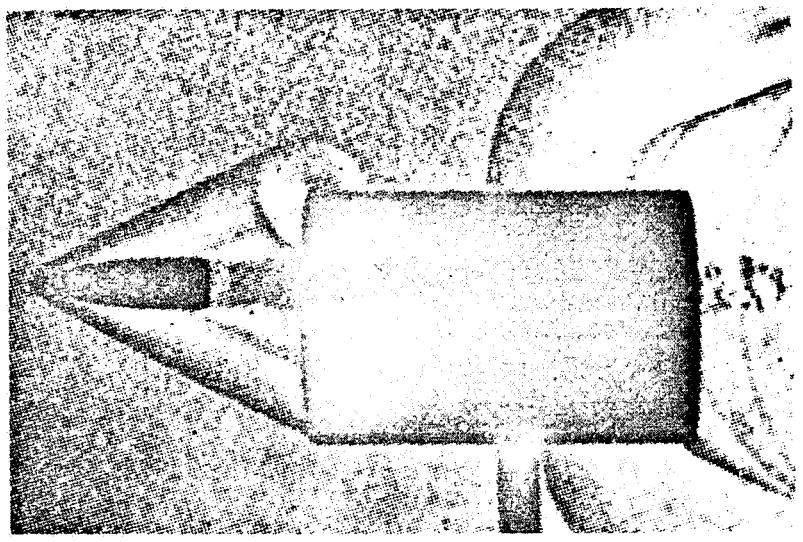

(a) Shadowgraph of bullet passing through single tube.

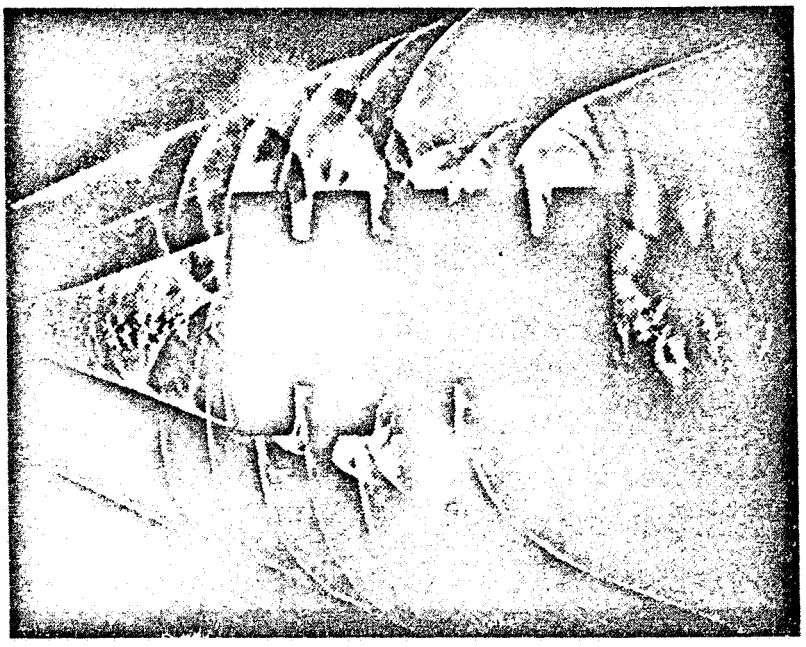

(b) Schlieren photograph of bullet passing through several short tubes in series.

Figure 11-3. - Photographs of supersonic bullets passing through cylindrical tubes, showing Mach cones and spherically spreading wave fronts. (From Ackeret and reprinted from "The Dynamics and Thermodynamics of Compressible Fluid Flow," by Ascher H. Shapiro, with permission of the Ronald Press Co.)

sound wave front is clearly evident. The relatively small Mach angles of the shock waves indicate that these bullets are traveling at high supersonic velocities.

ONE-DIMENSIONAL, ISENTROPIC FLOW

Supersonic flow conditions can be achieved either by accelerating the air past an object to supersonic speeds (as in a wind tunnel) or by moving an object through the air at supersonic speeds. Figure 11-4 is a schlieren photograph of supersonic flow through a

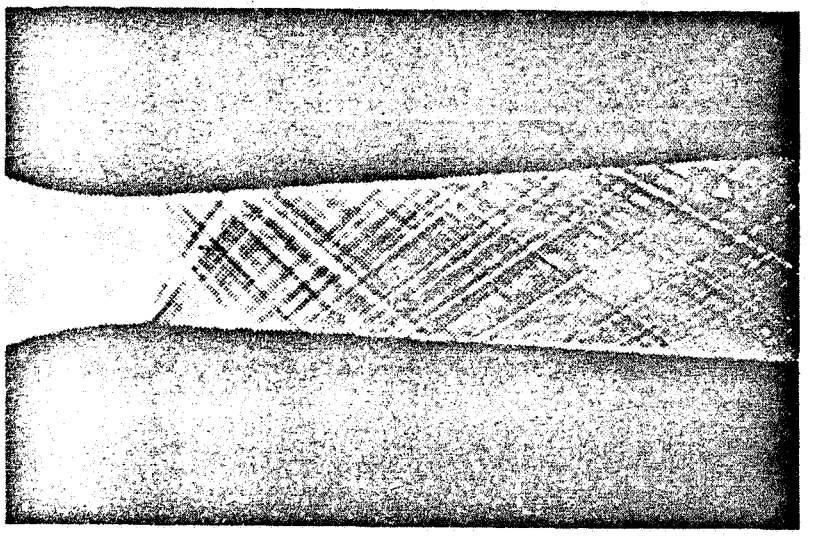

Figure 11-4. - Schlieren photograph of supersonic flow through a nozzle. (From Busemann and reprinted from "The Dynamics and Thermodynamics of Compressible Fluid Flow," by Ascher H. Shapiro, with permission of the Ronald Press Co.)

nozzle. Upstream of the nozzle throat the flow is subsonic. This is indicated by the absence of shock waves. Downstream of the throat the flow is supersonic and attains progressively higher Mach numbers, as indicated by the decreasing angles between the shock waves and the local wall of the nozzle.

The study of flow properties in a nozzle can be simplified by assuming that the flow is one-dimensional and isentropic. These assumptions make it possible to determine the average flow properties at any station in the nozzle. "One-dimensional" means that the flow is assumed to be uniform across the duct at any axial station in the nozzle. The term

"isentropic" specifies two characteristics of the flow: first, there is no heat transfer out of or into the flow (the walls are thermally insulated); second, any conversion of the energy of the random motion of the gas molecules to some other form of energy or work is 100 percent efficient. Pressure and temperature are measures of this random energy.

In order to investigate some of the properties of supersonic flow, we can relate the pressure p, density ρ, temperature T, and flow area A of the gas flowing in a duct to its velocity V, or Mach number M. This requires some basic equations relating the flow properties at any two stations in the duct. The following are the basic relations for the flow properties at any two stations in an isentropic, one-dimensional flow.

Continuity equation (conservation of mass):

$$(\text{Mass flow})_1 = (\text{Mass flow})_2$$

or

$$(\rho VA)_1 = (\rho VA)_2$$

Energy equation (conservation of energy):

$$(\text{Energy flow})_1 = (\text{Energy flow})_2$$

Isentropic relation:

$$\frac{P_1}{P_2} = \left(\frac{\rho_1}{\rho_2}\right)^k$$

Perfect gas relation:

$$p = \rho RT$$

The continuity equation states that the mass flow at station 1 must equal the mass flow at station 2. This assumes that the duct has no leaks. The mass flow is the product of the density ρ, the velocity V, and the local duct area A. Since no energy or work is allowed to leave the duct, the energy equation states that the energy at stations 1 and 2 must be equal. This energy is the sum of the kinetic energy of the flowing gas, which is proportional to ρV^2, and the energy in the random motion of the gas molecules. The energy equation does not state that either the kinetic or the random energies are equal at

stations 1 and 2, but only that their sums are equal at the two stations. Therefore, this permits conversion of random energy into the directed kinetic energy associated with the gas velocity. Since 100-percent conversion efficiency has been assumed, the isentropic relation between pressure and density can be used. The perfect gas relation relates the pressure, density, and temperature of the gas by utilizing a constant R, which is a property of the gas mixture.

For ratios of pressure, temperature, density, and duct area between stations 1 and 2 in terms of Mach number, we calculate the property variations shown in figure 11-5. The pressure, temperature, and density variations with Mach number are presented as ratios of the local values to their values at the point of zero Mach number (i.e., stagnation point). This is accomplished by letting station 1 correspond to a Mach number of zero and presenting the ratios of the local conditions at station 2 to the zero-Mach-number conditions at station 1. Since the duct area is infinite for zero Mach number, the area variation is presented in the form of the ratio of the local duct area A to the area A* at the point in the duct where the flow speed is Mach 1.0. The velocity variation is presented in a similar manner.

Figure 11-5 shows that the cross-sectional area of the duct is minimum at Mach 1.0 (where flow velocity is sonic). This is in agreement with figure 11-4, which showed that the change from subsonic to supersonic flow occurs at the throat. Therefore, achieving supersonic flow in a duct requires that the duct first converge to a minimum area, or throat, and then diverge downstream of the throat. The velocity becomes sonic at Mach 1, and then asymptotically approaches a value of about 2.5 times that speed at very high Mach numbers. This velocity represents all the random molecular energy converted to directed gas velocity. The static pressure is about 50 percent of its stagnation value at Mach 1.0 and drops precipitously thereafter, reaching one-tenth of its stagnation value at Mach 2.1 and one-hundredth at about Mach 3.5. This means that if the stagnation pressure of air entering a nozzle is 15 pounds per square inch, the wall static pressure is only 0.15 pound per square inch at the point in the nozzle where the flow speed is Mach 3.5. It also means that an airplane flying at Mach 3.5 at low altitude, where the atmospheric static pressure is 15 pounds per square inch, could collect air at a stagnation pressure of 1500 pounds per square inch for an engine if the inlet were 100 percent efficient. Figure 11-5 shows that the temperature ratio also drops quickly with Mach number. Thus, if an aircraft is flying at Mach 3.5 through air that has a static temperature of 520° Rankine (60° F), the total temperature of the air striking the surfaces of the aircraft is 1800° R ($520^{\circ} \div 0.29$). If the airplane speed were Mach 6.7, the total temperature would be 5200° R, hotter than the inside of a jet-engine afterburner. This is the heat barrier.

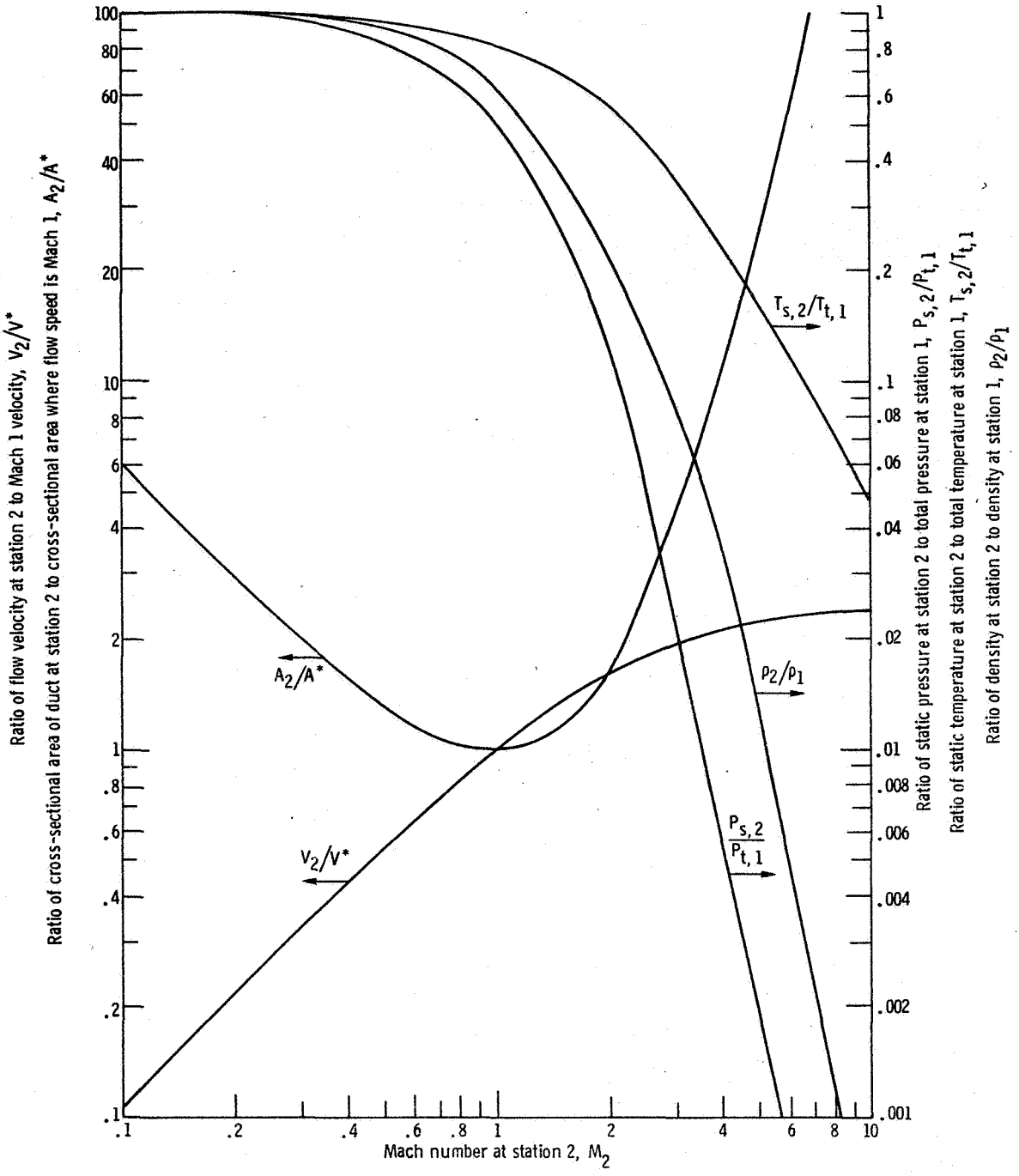

Figure 11-5. - Variation of temperature, density, pressure, area, and velocity ratios with Mach number for isentropic, one-dimensional flow. (Stagnation conditions are assumed to exist at station 1; station 2 is downstream of station 1.)

NORMAL SHOCK WAVE

The following discussion concerns shock waves. The simplest is the normal shock wave (fig. 11-6). Across such a shock wave, the static pressure ratio can be very large. The thickness of a normal shock wave is only about 0.00001 inch. Statistically, this is the average distance an air molecule travels before it collides with another. In supersonic flow, the shock wave produces an abrupt discontinuity in pressure and velocity across it.

The interior detail of the normal shock wave is very complex. To avoid the

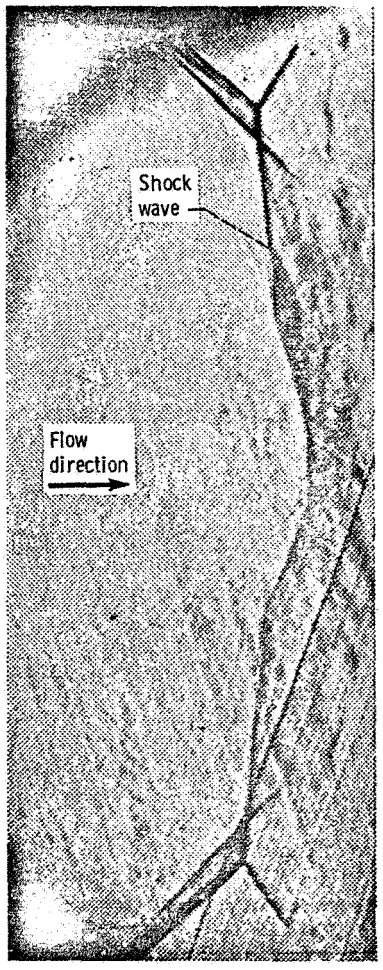

Figure 11-6. - Schlieren photograph of normal shock wave in supersonic wind tunnel. (Courtesy of Massachusetts Institute of Technology Gas Turbine Laboratory.)

necessity of dealing with the complex internal shock processes, the flow is considered at stations a short distance on either side of the shock wave, as shown in the sketch below.

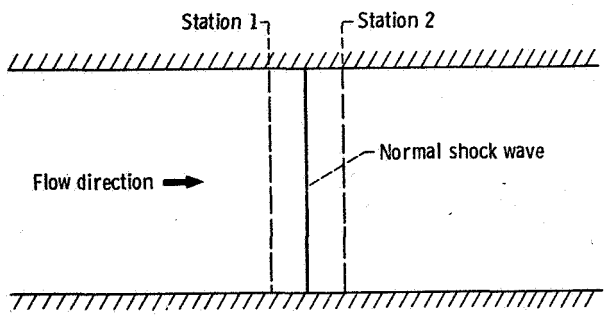

Determining the flow properties across the shock wave again requires some basic relations. The previously discussed continuity equation, energy equation, and perfect gas relation are again applicable. However, the energy-conversion process across the shock wave is no longer 100 percent efficient. Therefore, a new equation is needed to replace the previously used isentropic relation. This necessary new equation is the momentum equation.

$$(\text{Pressure force})_1 + (\text{Momentum flux})_1 = (\text{Pressure force})_2 + (\text{Momentum flux})_2$$

where the momentum flux equals mass flow rate times velocity.

The momentum equation is derived from Newton's Second Law of Motion (Force = Mass × Acceleration). The force is provided by the pressure difference across the shock wave. This force decelerates the flow from a very high velocity upstream of the shock wave to a lower velocity downstream of the shock wave.

Figure 11-7 presents the variation of ratios of pressure, temperature, and other flow parameters across the normal shock wave. Here we see that the downstream Mach number M_2 is always subsonic, becoming smaller as the upstream (initial) Mach number M_1 increases. From the static pressure ratio $P_{s,2}/P_{s,1}$ it can be seen that a normal shock wave with a very small static pressure ratio travels at Mach 1.0. However, increases in pressure ratio increase the speed of the shock wave. A pressure ratio of 10 is required for Mach 3.0, and a pressure ratio of almost 100 is required for Mach 9. The stagnation pressure behind the normal shock $P_{t,2}$ decreases drastically as Mach number is increased. Recovery of this stagnation pressure is one measure of efficiency. Thus, a high-Mach-number normal shock wave has a low stagnation pressure downstream and a corresponding low efficiency. These normal-shock-wave equations hold for a fixed-position normal shock wave terminating supersonic flow in a duct,

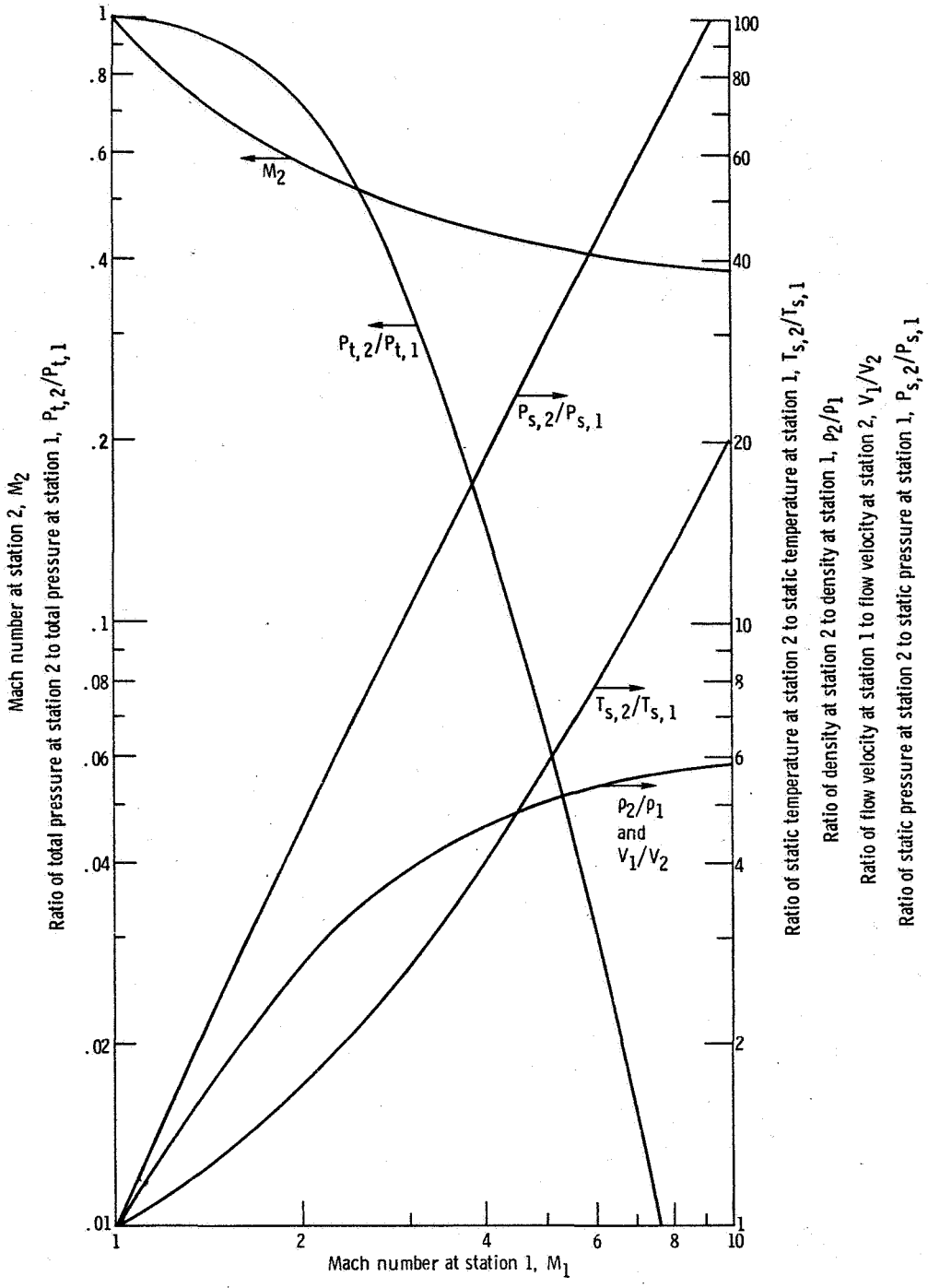

Figure 11-7. - Variation of downstream Mach number and ratios of total pressure, static pressure, static temperature, density, and velocity with upstream Mach number for flow across normal shock wave. (Station 1 is upstream and station 2 is downstream of shock wave.)

for a normal shock wave in front of a supersonic airplane nose, and for a blast wave from an explosion.

OBLIQUE SHOCK WAVE

So far, only flow in one dimension has been considered. This approach permits determining only average conditions and does not consider the details of how the flow travels from one station to another. To do that requires considering at least two dimensions. In the earlier discussion the air was always assumed to be flowing in the same axial direction. In the case of the oblique shock wave, the flow is turned an angle δ from the initial axial direction, as shown in figure 11-8. This then requires considering flow in more than one direction. The pressure rise across an oblique shock wave can be very small for small turning angles or very large for large turning angles and high Mach numbers.

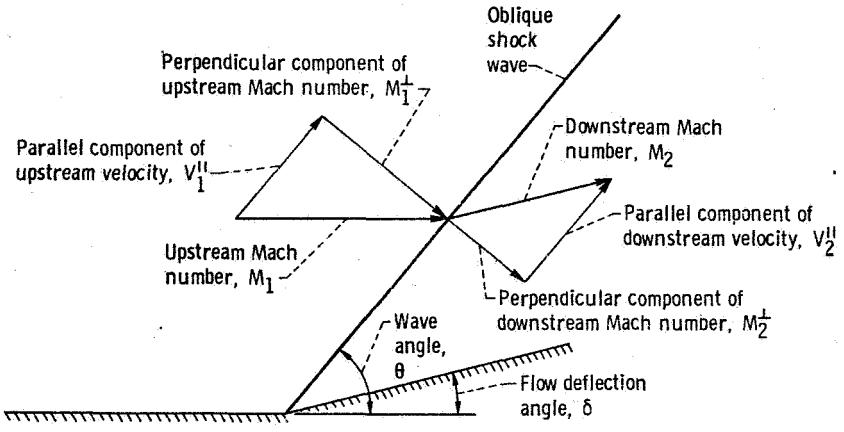

Figure 11-8. - Flow field across two-dimensional oblique shock wave for flow deflection angle of δ degrees.

The pressure force is perpendicular to the wave, so any flow velocity changes must be restricted to this same direction. This means that the velocity $V^{\parallel}$ parallel with the oblique shock is unchanged in traveling across the shock wave. By considering the Mach number component perpendicular to the shock wave, we find that the relation between $M_1^{\perp}$ and $M_2^{\perp}$ is the same as for a normal shock wave. Therefore, if the initial Mach

number M_1 and the wave angle θ are known, it is possible to determine $V^{\parallel}$ and $M_2^{\perp}$, which define the flow deflection angle δ. Normally, the known quantities are M_1 and δ, and tables and graphs are available (ref. 1) to solve the problem without iteration.

Oblique shock waves vary from Mach waves whose normal Mach number is 1 and whose pressure rise is extremely small to waves with large turning angles and large pressure rises. The downstream Mach number M_2 is normally supersonic. Beyond the turning angle δ, where M_2 becomes 1, the oblique shock wave will detach from the turn and move upstream. It is impossible to obtain a low subsonic velocity behind an oblique shock wave. Therefore, the turning angle in an oblique shock wave is limited, and this maximum turning angle increases with Mach number.

PRANDTL-MEYER FLOW

The final type of flow to be considered is two-dimensional isentropic flow, shown in figure 11-9. The changes across shock waves in supersonic flow are very abrupt and

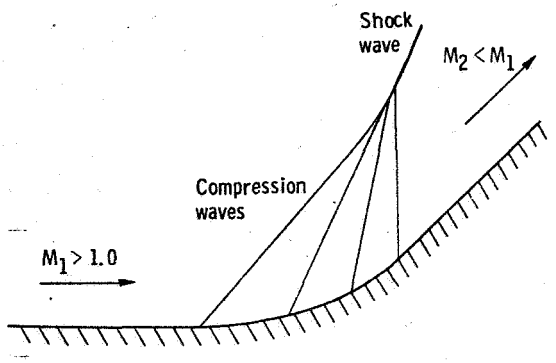

(a) Compression.

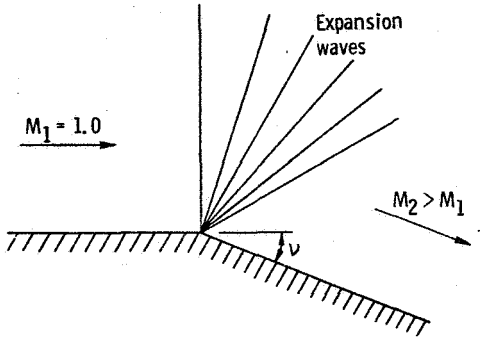

(b) Expansion.

Figure 11-9. - Two-dimensional, isentropic, Prandtl-Meyer flow.

inefficient. However, gradual changes in supersonic flow can be made with 100 percent efficiency by means of a Prandtl-Meyer flow. In this type of flow, an infinite number of extremely weak sound waves are used to compress or expand and turn the flow.

For compression, the wall is turned gradually into the flow (fig. 11-9(a)), thereby creating a series of waves which turn and compress the flow. Wave angles steepen as the Mach number decreases, and the waves eventually coalesce into a single shock wave. For supersonic expansion, the wall is turned away from the flow (fig. 11-9(b)), thereby increasing the flow area in the duct and increasing the supersonic Mach number. As the Mach number increases, the wave angles become lower, and the expansion waves spread out in a fan and never coalesce as they do for a compression. Therefore, most expansions in supersonic flow are 100 percent efficient. For supersonic compression, however, the wall curvature (fig. 11-9(a)) must be carefully designed to prevent the compression waves from coalescing into a strong, highly inefficient shock wave.

For a Prandtl-Meyer expansion of a sonic flow, $M_1 = 1.0$ (fig. 11-9(b)), any specific expansion to an angle ν produces some specific Mach number M_2 downstream of the expansion. The relation between Mach number and the Prandtl-Meyer angle ν is shown in figure 11-10 (where $\nu = 0$ for Mach 1.0).

Since expansion or compression in a Prandtl-Meyer flow is 100 percent efficient, figure 11-10 can be used to determine Mach number or angle for either expansion or compression. Prandtl-Meyer relations can be used to describe and define the stream-

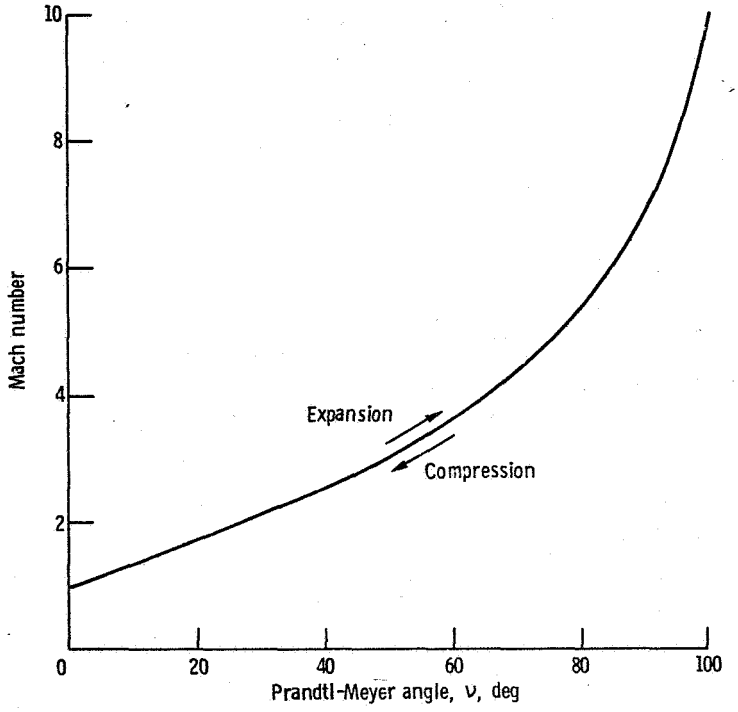

Figure 11-10. - Variation of Mach number with Prandtl-Meyer angle.

lines of flow expanding or turning around a sharp corner. For expansion, the resulting Mach number or the necessary angle can be determined by following the curve upward from the point representing the initial flow conditions to the point representing the final conditions. For compression, the Mach number or the angle can be determined by following the curve downward. For example, if the initial flow is at Mach 2.0 ($\nu = 27^{\circ}$) and the flow is expanded through an angle of 23°, the final Mach number will be 3.0 ($\nu = 27^{\circ} + 23^{\circ} = 50^{\circ}$). If the initial flow is at Mach 2.0 ($\nu = 27^{\circ}$) and the flow is compressed by an angle of 13°, the final Mach number will be 1.5 ($\nu = 27^{\circ} - 13^{\circ} = 14^{\circ}$).

CONCLUDING REMARKS

When the speed of an object is so high that sound waves, or extremely weak pressure waves, can no longer propagate ahead of the object, the flow is supersonic. To deflect the flow around a body at supersonic speeds, shock waves with a finite pressure rise across them are required. These waves can travel faster than sound, and their velocity increases as the pressure ratio across them increases. In general, expansion in supersonic flow is 100 percent efficient. Supersonic compression can be 100 percent efficient if it is done gradually. But the weak compression waves tend to coalesce into strong shock waves, which become inefficient.

REFERENCE

1. Ames Research Staff: Equations, Tables, and Charts for Compressible Flow. NACA Rep. 1135, 1953.

12. SUPERSONIC AIRCRAFT

James F. Dugan, Jr.*

To introduce supersonic aircraft, we will begin with current commercial jet aircraft and consider why they do not fly faster than about Mach 0.8. We will learn that the reason lies in an airflow phenomenon called transonic drag rise. We will see that shock waves, which are normally associated with speeds greater than Mach 1, are the cause of this transonic drag rise.

Next, we will consider an early military supersonic airplane that attempted to overcome the transonic drag rise and almost failed. We will learn that area ruling, or shaping the fuselage to resemble a Coke bottle, actually salvaged the airplane and was responsible for the F-102's going into production. This and other advances in supersonic aerodynamics and advances in high-thrust, low-weight jet engines led first to military airplanes that flew faster than Mach 2 and eventually to an operational reconnaissance airplane that flies faster than Mach 3.

These advances in military supersonic aircraft paved the way for the current effort to bring a commercial supersonic airplane into being. We will consider briefly the supersonic transports of the Russians, the British-French team, and the Americans. Finally, we will consider sonic boom: what it is, why it is such a problem, and how the sonic-boom problem is being handled in the proposed first generation of supersonic transports.

TRANSONIC DRAG RISE

The current subsonic commercial airplanes cruise at about Mach 0.8. Flying faster is attractive to the passenger, since it shortens his travel time. Flying faster is also attractive to the airlines, since it enables them to use their expensive airplanes more effectively and thus make more money. However, the cruise speed is limited to about Mach 0.8 by the sharp increase in airplane drag as Mach 1.0 is approached.

This drag increase is illustrated in figure 12-1, not for a complete airplane, but for a wing with a circular-arc airfoil. However, all wetted surfaces of the aircraft exhibit

*Head, Propulsion Section, Advanced Systems Division.

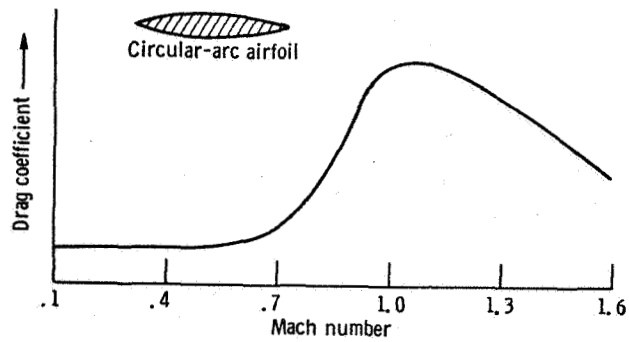

Figure 12-1. - Transonic pressure-drag rise of wing with circular-arc airfoil.

the trend of a high rise in drag as Mach 1.0 is approached. The peak drag occurs at, or just past, Mach 1.0. At higher speeds, drag decreases again, but not to the low levels characteristic of subsonic speed.

These changes in drag near Mach 1 are related to the formation of shock waves. These shock waves are shown in figure 12-2. Consider first the airflow over the wing when the airplane is flying at Mach 0.7. The local speed at the airfoil midspan can reach Mach 1.0, so that standing shock waves form above and below the airfoil and cause an increase in drag. When the airplane flies somewhat faster than Mach 1.0, a bow wave exists upstream of the airfoil leading edge and a pair of oblique shock waves exist at the trailing edge. With such a flow, drag is at maximum. At faster airplane speeds, like Mach 1.3, pairs of oblique shock waves are attached to the leading and trailing edges. Drag is below the maximum value, but still high because of the pressures induced on the wing surface by the oblique shock waves.

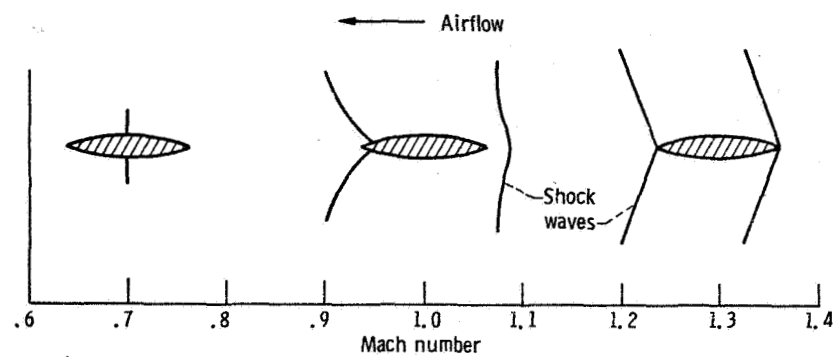

Figure 12-2. - Evolution of shock waves.

AREA RULE

The world's first supersonic all-weather interceptor, the Convair F-102 Delta Dagger, is shown in figure 12-3. In an attempt to meet the U.S. Air Force requirement for a supersonic interceptor, Convair scaled up an earlier configuration with a pure delta-wing planform. Early flight tests showed that even with a high-thrust turbojet engine this aircraft could not achieve supersonic speeds, because of high drag. The whole program was on the verge of being cancelled, but it was rescued by the application of the area-rule theory to the design of the aircraft.

This important theory was developed and verified by Richard Whitcomb, of the NASA Langley Research Center. Simply stated, the rule says that minimum supersonic drag is obtained when the individual airplane components (such as wing, tail, and fuselage) are configured so that a plot of cross-sectional area of the total airplane versus distance along the longitudinal axis of the airplane results in a smooth curve. This usually results in a "Coke-bottle" shape for the fuselage.

When Convair applied this area-rule theory to the F-102, they not only redesigned the fuselage to get the right Coke-bottle shape but also added bulges aft of the wing on each side of the tail pipe to give better area-rule distribution. The bulges can be seen in figure 12-3. These major modifications allowed the airplane to fly supersonically. The F-102 became operational in 1956, and a large number went into service with the U.S. Air Force.

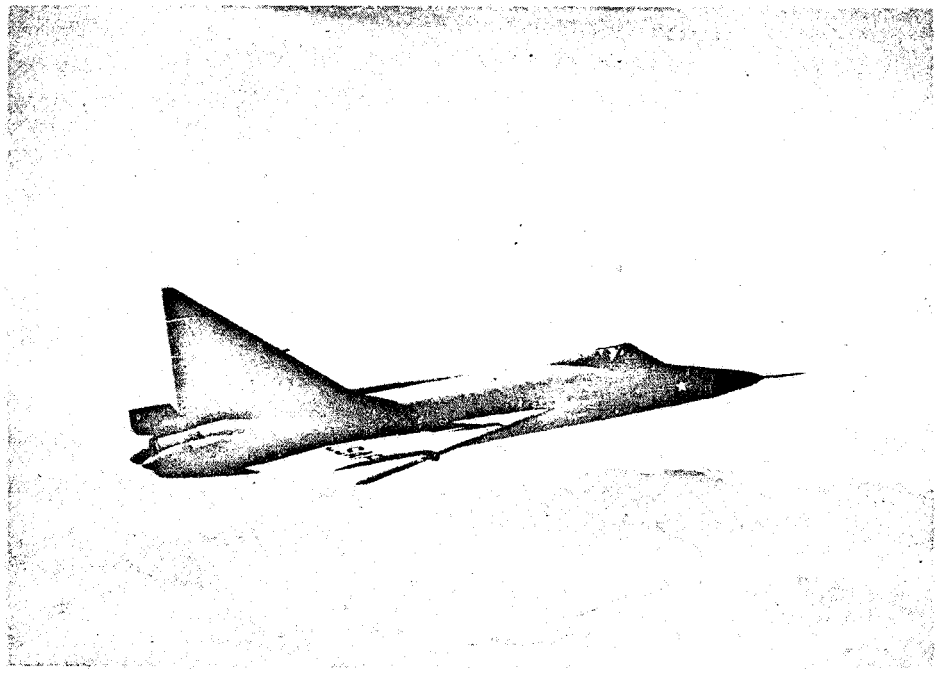

Figure 12-3. - Convair F-102 Delta Dagger interceptor.

The area rule affects the pressure drag (not friction drag) and applies only at transonic and supersonic speeds. The cross-sectional area of the aircraft is obtained from imaginary slices cut through the aircraft, crosswise to its longitudinal axis. These area slices are inclined to the relative-wind direction at an angle equal to the Mach angle, because the wetted surface of the aircraft behaves as if it were subjected to a flow having the magnitude and direction of the velocity component normal to the Mach line. For aircraft speeds only slightly above sonic speed (e.g., Mach 1.2), the Mach angle is approximately 90^{o}; therefore, the cross-sectional slices are taken approximately normal to the relative-wind direction. As the aircraft speed increases, the Mach angle decreases, and the area slices are inclined to the relative-wind direction.

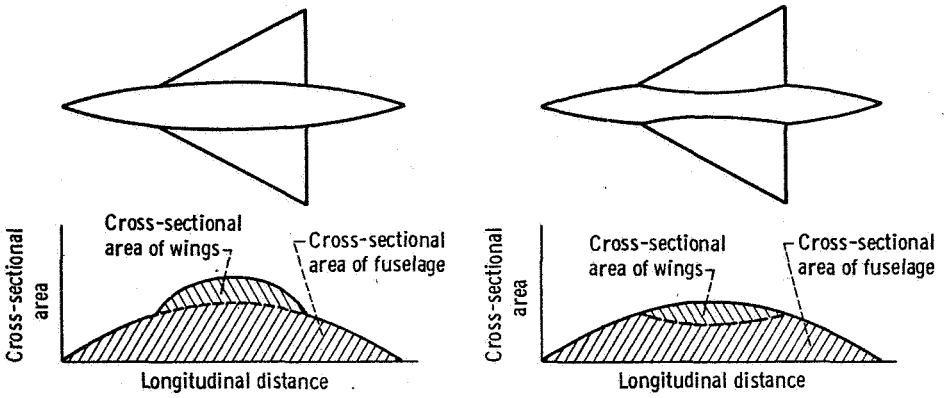

(a) Without area rule. (High transonic and supersonic drag.)

(b) With area rule. (Lower transonic and supersonic drag.)

Figure 12-4. - Application of area rule to aircraft configuration.

Figure 12-4(a) shows a simplified airplane consisting of a streamlined fuselage and a delta wing. If cross-sectional area is plotted against length for this airplane, a bulge appears in the curve. This bulge represents the cross-sectional area of the wing. Since the area variation with length is not a smooth curve, the pressure drag of this airplane at transonic and supersonic speeds is high. Figure 12-4(b) shows a similar airplane, but with a fuselage that is narrowed where the wing is joined to it. The variation of cross-sectional area with length for this airplane is smooth. Therefore, the pressure drag of this airplane at transonic and supersonic speeds is lower than that of the previous example.

Figure 12-5 shows how this reduction in drag comes about. The pressure field produced by supersonic flow over the wing alone is shown in figure 12-5(a). The compressive turning of the supersonic flow by the forward-facing surfaces of the wing produces above-ambient pressures, indicated by "plus" signs. Expansion of the flow over the

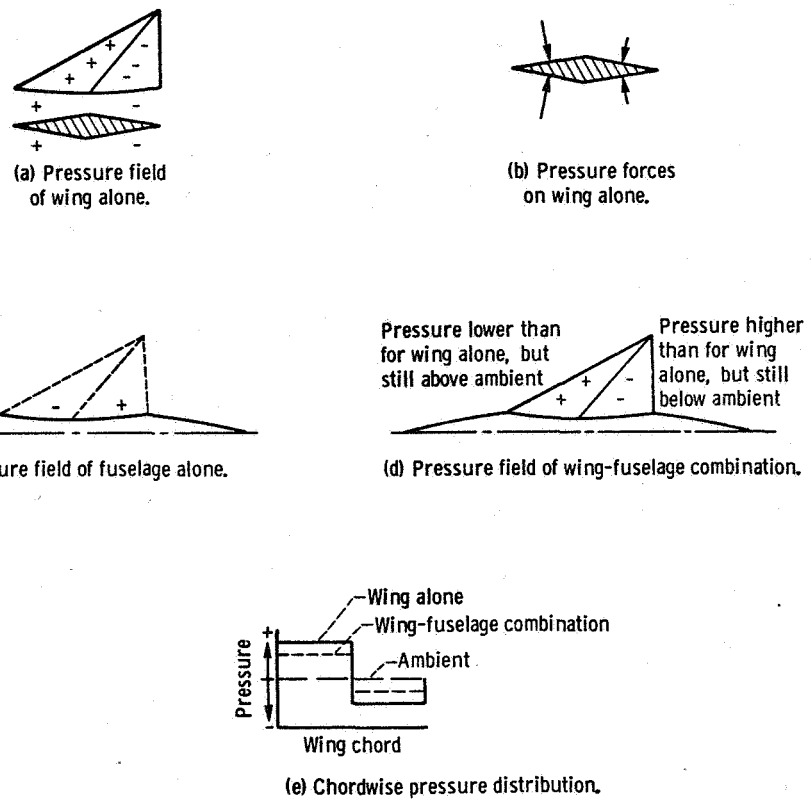

Figure 12-5. - Favorable pressure interference to reduce wing drag.

aft-facing surfaces produces below-ambient pressures, indicated by "minus" signs. (Compression and expansion of supersonic flow are discussed in chapter 11.)

Figure 12-5(b) shows the pressure forces acting on the wing surfaces. When these forces are summed in the lift and drag directions, the resultant lift force is zero, but there is a resultant drag force. Obviously, if the difference between the pressure forces on the forward-facing surfaces and those on the aft-facing surfaces were reduced, the resultant drag would also be reduced.

The indented fuselage alone is shown in figure 12-5(c). At the leading edge of the indentation, the supersonic flow expands around the corner and produces below-ambient pressures (minus signs) over the forward half of the indentation. The compressive turning of the supersonic flow over the rear half of the indentation produces above-ambient pressures (plus signs).

When the wing and fuselage are joined, their pressure fields combine. Thus, for the wing-fuselage combination (fig. 12-5(d)) the pressures on the forward-facing surfaces of the wing are lower and the pressures on the aft-facing surfaces are higher than for the wing alone. The pressure distribution along a wing chord line is shown in figure 12-5(e). The solid curve is for the wing alone and indicates a pressure above ambient (+) acting on the forward-facing wing surfaces and a pressure below ambient (-) on

the aft-facing wing surfaces. The dashed curve in the figure is for the wing-fuselage combination. The low pressures contributed by the forward half of the fuselage indentation have lowered the pressures on the front half of the wing. The high pressures contributed by the rear half of the fuselage indentation have raised the pressures on the rear half of the wing. Therefore, the difference between the pressures on the front half and those on the rear half of the wing is reduced, and the resultant drag force on the wing is also reduced.

In this simplified explanation of the area rule, we have only considered the effect of the rule on the pressure drag of the wing. However, in the design of an actual airplane, the area rule is applied so as to reduce the overall pressure drag of the entire airplane.

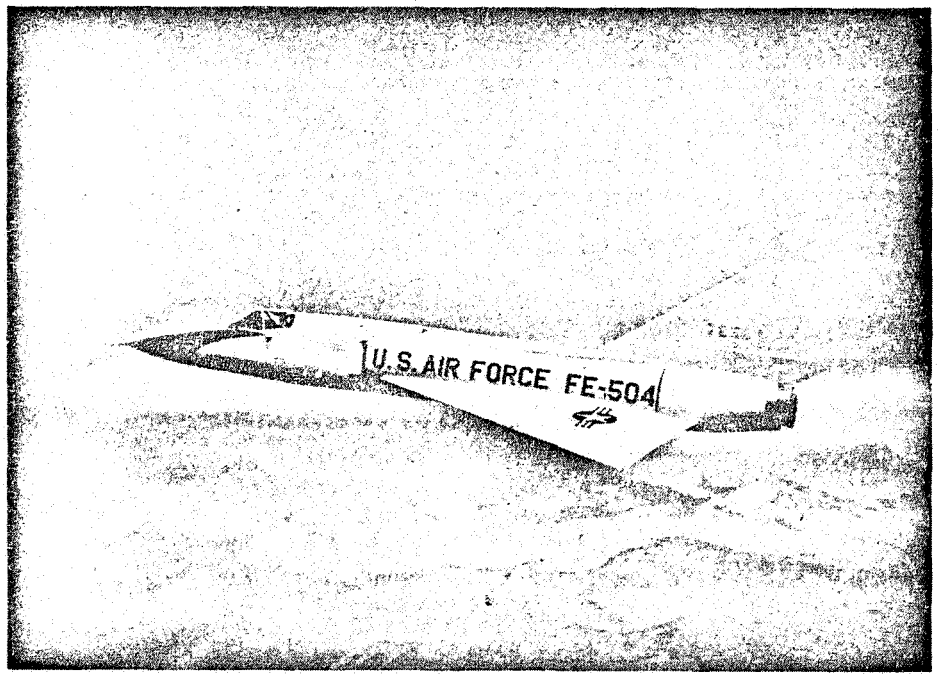

Figure 12-6. - Convair F-106 Delta Dart interceptor.

The Convair F-106 Delta Dart, the successor to the F-102, is shown in figure 12-6. The fuselage of the F-106 is enlarged, and the area rule is incorporated in a much more subtle manner. The prominent bulges on the aft fuselage have disappeared. The engine intakes are much larger than those on the F-102 and are located farther aft, near the wing root. To meet engine airflow requirements efficiently, the intakes must incorporate variable geometry to cover the greater speed range of the airplane. The top speed of the F-106 is Mach 2.3, while that of the F-102 is Mach 1.25. The F-106 became operational in 1959, but today it is still the backbone of the USAF Air Defense Command.

A much publicized and very controversial new airplane is shown in figure 12-7. It was known as the TFX during the time when its future and who was to build it were being hotly debated. It is now known as the F-111 and is built by General Dynamics. Designed for a top speed of Mach 2.5, the F-111 is to be used for a variety of roles, such as tactical strikes, interception, reconnaissance, and strategic bombing. To achieve this

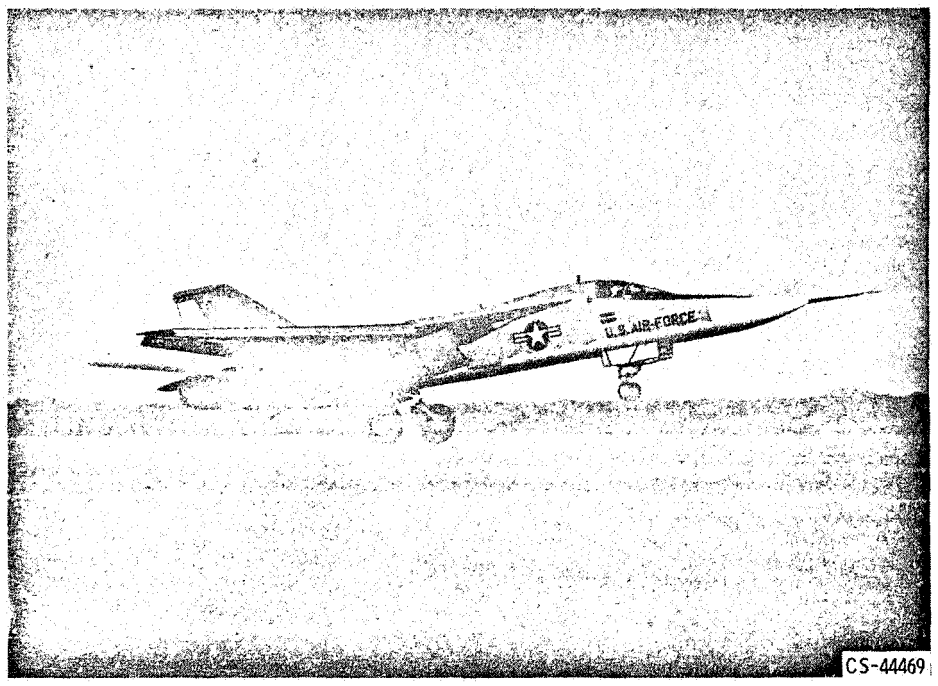

Figure 12-7. - General Dynamics F-111A fighter.

multimission capability, the F-111 makes use of a movable wing, the sweep angle of which can be varied. On supersonic missions, the sweep is great, and the airplane resembles the F-106 of figure 12-6. On subsonic missions and during takeoff and landing, the sweep of the F-111's wing is moderate.

The United States has achieved sustained Mach 3 flight with three airplanes: the North American XB-70, the Lockheed YF-12, and the Lockheed SR-71. The XB-70, shown in figure 12-8, was originally slated for a strategic bombing role. When the airplane is cruising at high Mach numbers, the shock waves arising from the large wedge-shaped engine box beneath the airplane create high pressures, or lifting forces, on the bottom surface of the wing. This was the first airplane designed to exploit the principle of interference, or compression, lift.

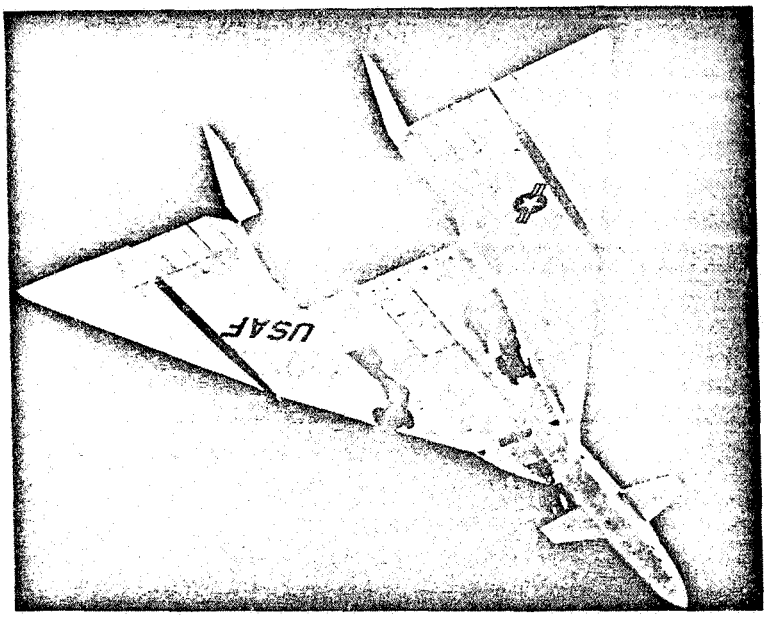

Figure 12-8. - North American XB-70. (Reprinted from Shell Aviation News, No. 318, 1964, *with their permission.*)

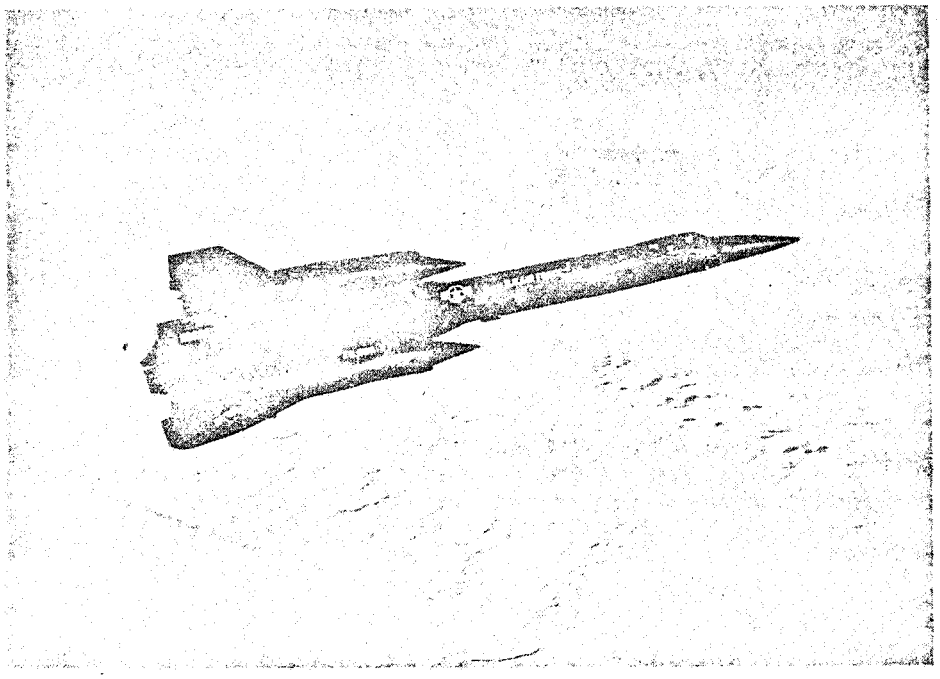

Figure 12-9. - Lockheed YF-12A.

The YF-12A, shown in figure 12-9, is a prototype Mach 3 interceptor. It had the most secret development of any airplane in American history, with the exception of its subsonic predecessor, the U-2. As an advanced experimental jet aircraft, the YF-12 has been tested in sustained flight at more than 2000 miles per hour and at altitudes in excess of 70 000 feet. Its structure is primarily titanium, to withstand the very high environmental temperatures associated with Mach 3 flight.

The SR-71, which resembles the YF-12, is a strategic reconnaissance version of the YF-12. Its nose fairing is different, and the fuselage is longer. The SR-71 has gone into service with the Strategic Air Command. It is equipped with the most advanced observational equipment in the world, which enables it to cover with its reconnaissance "eyes" an area of 60 000 square miles in one hour.

PROPOSED COMMERCIAL AIRCRAFT

Although supersonic airplanes have been in military service for many years, they have not yet been introduced into commercial service. However, three commercial supersonic transports are under development - the Tupolev Tu-144 (Russian), the BAC-Sud Concorde (British-French), and the Boeing supersonic transport (American). Before discussing these airplanes, we will consider why commercial supersonic aircraft are of interest. To the passenger, there is the attraction of much shorter flight times. For example, the supersonic-transport flight time from Chicago to London (4000 statute miles) would be about $2\frac{1}{2}$ hours, as compared to about $8\frac{1}{2}$ hours for the advanced subsonic transports. The airlines and airplane builders are, of course, motivated by the profit potential, which is greatly influenced by currently proven technology in aerodynamics, structures, and propulsion.

Consider first the status of technology in supersonic aerodynamics. Although techniques like the application of the area rule help keep supersonic drag down, the attainable lift-to-drag ratio (aerodynamic efficiency) at supersonic speeds is much lower than that at subsonic speeds, as indicated in figure 12-10. The lift-to-drag ratio is high around Mach 0.8 but drops sharply in the region around Mach 1, because of the onset of shock losses. After the steep drop, the lift-to-drag ratio tends to level off, but continues to decrease gradually as cruise speed increases. This trend is discouraging, but not hopeless, because airplane performance is affected by other factors.

Range is an important consideration in the evaluation of airplane performance. The equation for airplane range is

$$\text{Range} \approx k \frac{L}{D} \frac{M}{sfc} \log \frac{w_g}{w_s + w_p}$$

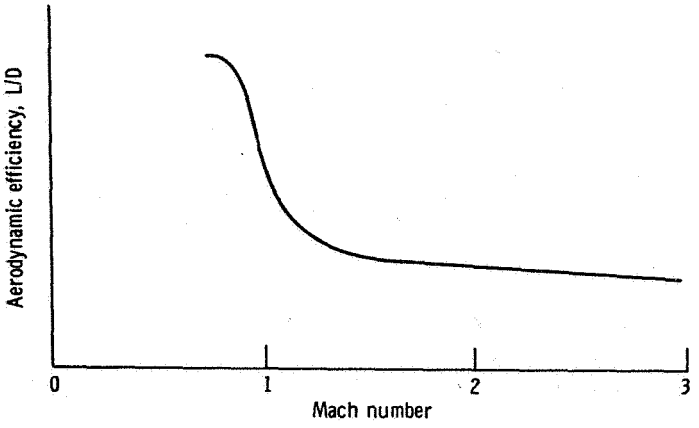

Figure 12-10. - Variation of aerodynamic efficiency with Mach number.

where

k constant

L lift

D drag

M Mach number

sfc specific fuel consumption (amount of fuel used per hour per pound of thrust)

w_g gross weight of airplane

w_s structural weight of airplane

w_p payload weight

The ratio of Mach number to engine specific fuel consumption M/sfc is a measure of engine efficiency. If w_g, w_s, and w_p are fixed, the airplane range will increase as the product of aerodynamic efficiency L/D and engine efficiency M/sfc increases. Fortunately, the efficiency of a gas-turbine engine increases with cruise speed, as shown in figure 12-11. (The curves in fig. 12-11 are intended to show only the general trends of the efficiency variations with Mach number. The curves do not reflect the relative levels, or the relative values, of the three efficiencies.)

The variation of lift-to-drag ratio, or aerodynamic efficiency, with Mach number is repeated in this figure. The overall-efficiency curve represents simply the product of aerodynamic efficiency and engine efficiency. Overall efficiency is high at Mach 0.8, the speed at which current jet transports operate. The efficiency drops at around Mach 1 and then begins to climb. Beyond Mach 2, the overall airplane efficiency is approaching the level attained by current subsonic jets. The choice of a specific cruise Mach number above 2 is largely dependent on the structural materials used for the airframe.

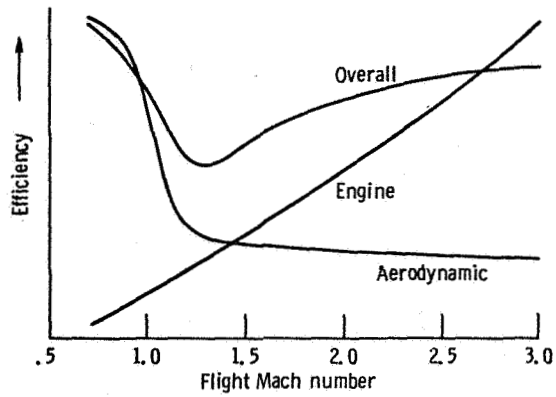

Figure 12-11. - Variation of aerodynamic, engine, and overall efficiencies with flight Mach number. (The curves show only the general trends of the efficiency variations with Mach number and do not reflect the relative levels of the three efficiencies.)

Figure 12-12 shows the variation of structural efficiency with Mach number for titanium and aluminum. The structural efficiency is measured by the ratio of the tensile strength of the material to its density. High ratios result in lightweight structures, which can provide higher airplane performance in terms of longer range or greater payload (in accordance with the range equation). The current subsonic jets that operate at about Mach 0.8 use aluminum as the primary airframe structural material. Aluminum can be used at higher speeds, but somewhat beyond Mach 2 the structural efficiency decreases rapidly to an unacceptably low level. The structural efficiency of titanium is

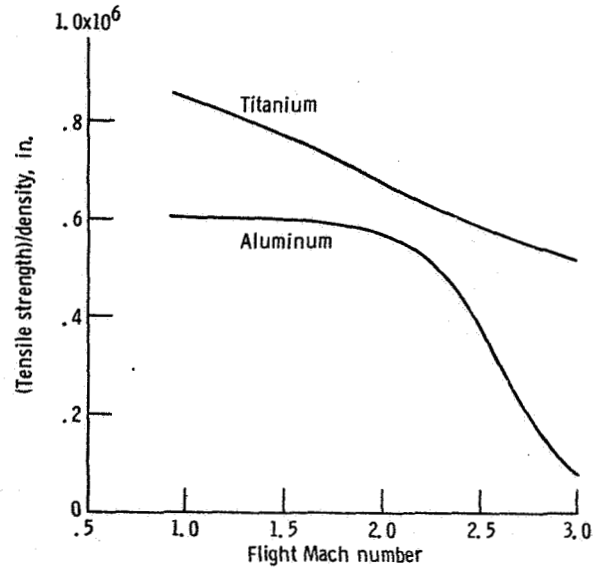

Figure 12-12. - Variation of structural efficiency ((tensile strength)/density) of titanium and aluminum with flight Mach number (speed).

appreciably higher than that of aluminum. Therefore, titanium seems to be a desirable structural material even for subsonic airplanes. However, the technology of using titanium is relatively new.

The Russian supersonic transport (fig. 12-13) is designed for a cruise Mach number of 2.35, and its prime structural material is aluminum. The British-French supersonic transport (fig. 12-14) also uses aluminum as the structural material and is designed for a cruise Mach number of 2.2. The American supersonic transport (fig. 12-15) is being designed for a cruise Mach number of 2.7, and titanium will be used as its prime structural material.

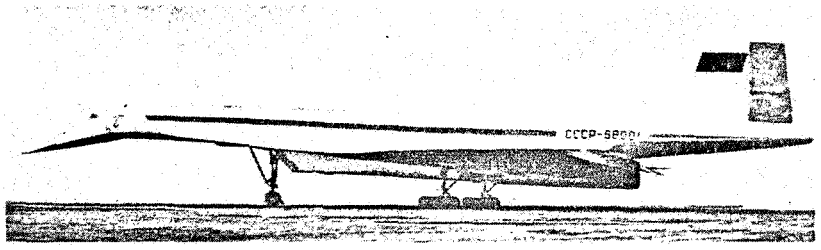

Figure 12-13. - Russian supersonic transport, Tupolev Tu-144. (Reprinted from Life, March 14, 1969, with their permission.)

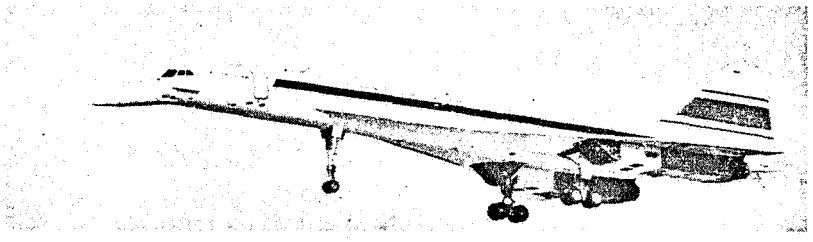

Figure 12-14. - British-French supersonic transport, BAC-Sud Concorde. (Taken from Aviation Week & Space Technology, March 17, 1969, with their permission.)

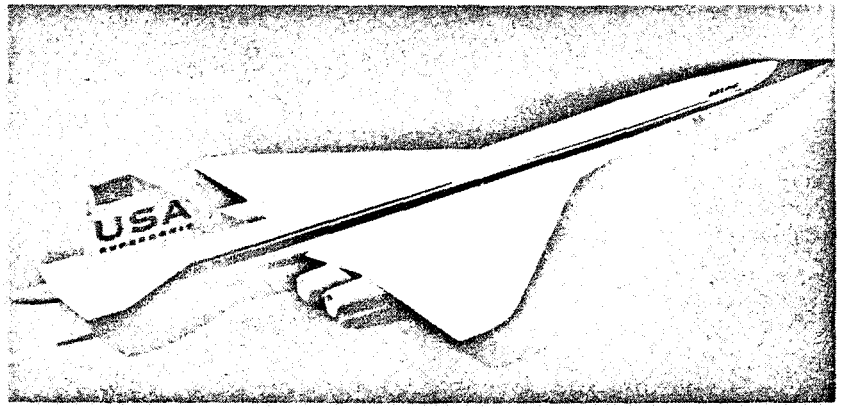

Figure 12-15. - Model of proposed American supersonic transport, Boeing design. (Reprinted from Interavia, January 1969, with their permission.)

SONIC BOOM

Whenever an airplane is flying at supersonic speed, shock waves are attached to the airplane and extend all the way to the Earth's surface, where they are reflected upward toward the sky (fig. 12-16). The variation in air pressure, shown at the bottom of the figure, indicates that there is an abrupt rise in pressure (overpressure) above ambient when the first shock wave passes. Then the pressure decreases to a value below ambient. When the trailing shock wave passes, there is a second abrupt pressure rise back to ambient. Sometimes a double boom can be heard, but generally the wave length and the time increment are so short that only a single boom is heard. The magnitude of the boom is described by quoting the change in pressure or overpressure, in pounds per square foot.

The relation of sonic boom level to probable public reaction is shown in table 12-I. Sonic booms in the range of 0.2 to 1.0 pound per square foot overpressure sound like distant thunder and would probably be acceptable. To achieve such a level of sonic boom, the gross weight of the airplane (and, hence, lift) would have to be low and the altitude for supersonic operation high. Low weight and high altitude both reduce sonic-boom intensity. Estimates based on current airframe and engine technologies indicate that a supersonic transport compatible with a sonic-boom level of 0.8 pound per square foot would have to be so small that it could carry only one or two dozen passengers. The passengers might be satisfied and the people on the ground might not object to the boom,

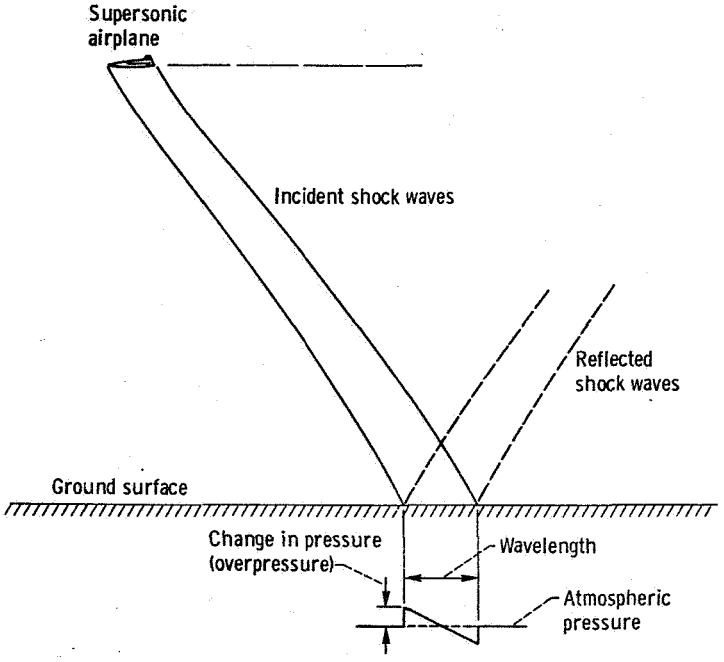

Figure 12-16. - Sonic boom of a supersonic airplane.

TABLE 12-I. - SONIC-BOOM GROUND EFFECTS

Sonic-boom overpressure at ground level, lb/ft^2	Property damage	Comparable sound	Public reaction
0.2 to 1.0	No damage	Distant thunder	Probably acceptable
1.5 to 2.0	No damage to ground structures	Loud thunder	Not acceptable
2.5 to 3.0	Possible damage to windows and plaster	Close-range thunder or explosion	Intolerable

but the airlines would not be able to make any money. Large supersonic airplanes, carrying hundreds of passengers, are required if the airlines are to make a reasonable profit.

The supersonic transports being planned will give rise to sonic booms in the upper range of values. Furthermore, atmospheric conditions, which cannot be controlled, can magnify sonic booms. Therefore, boom levels of 3.0 pounds per square foot and above can be anticipated during a certain number of flights. Booms of this magnitude are intolerable and can damage windows and plaster. Because of this sonic-boom problem, the first generation of supersonic transports is scheduled to service only the prime transoceanic routes. Thus, for the time being, the problem will only be sidestepped rather than solved.

13. MEASUREMENTS IN AERONAUTICAL RESEARCH

Clarence C. Gettelman*

From measurements of pressure, temperature, mass flow rate, and thrust, the performance of an aircraft, an airfoil, an engine, a compressor, or a turbine can be determined. To describe the performance of a wing, compressor or turbine blade, we are interested in the lift and drag under conditions of use. We must also know the velocity or Mach number of an aircraft or air in a wind tunnel. We may want to know the Reynolds number (ratio of the inertia force of the fluid to the viscous force of the fluid). The significances of these and other characteristics are discussed in preceding chapters. Let us examine these characteristics and how they are obtained from measured quantities.

The velocity of a fluid with respect to a body in the fluid is determined by measuring the pressure due to the motion of the fluid. This pressure, designated ΔP, is the difference between the total pressure P_t and the static pressure P_s. (These three pressures are discussed in greater detail in the next section.)

$$\Delta P = P_t - P_s \qquad (\text{lb/ft}^2) \tag{1}$$

For an incompressible fluid, the pressure due to the motion of the fluid is

$$\Delta P = \frac{1}{2}\rho V^2 \tag{2}$$

where

ρ mass density of fluid, w/g, lb-sec^2/ft^4

w specific weight of fluid, lb/ft^3

g acceleration due to gravity, ft/sec^2

V velocity of fluid flow, ft/sec

The mass density ρ for a gas (e.g., air) is a function of static pressure and static temperature according to the equation

*Chief, Instrument Systems Research Branch.

$$\rho = \frac{P_s}{gRT_s} \tag{3}$$

where

R specific gas constant, (ft-lb)/(lb)(^{o}R) (for air, 53.3)

T_s static temperature, ^{o}R

Equations (1) to (3) can be combined and solved for velocity V in terms of measurable quantities (ΔP, P_s, and T_s) and constants (g and R).

$$V = \sqrt{\frac{2\Delta P T_s}{P_s}} \cdot \sqrt{g} \cdot \sqrt{R} \tag{4}$$

For an incompressible fluid, the pressure ΔP due to the motion of the fluid is described by equation (2). For a compressible fluid, ΔP includes the compressibility effects and is described by the equation

$$\Delta P = \frac{1}{2}\rho V^2 \left(1 + \frac{M^2}{4} + \frac{2 - k}{24} M^4 \ldots\right) \tag{5}$$

where

M Mach number (dimensionless)

k $\frac{\text{Specific heat at constant pressure}}{\text{Specific heat at constant volume}}$ (dimensionless)

Air behaves as an incompressible fluid at low subsonic speeds and as a compressible fluid at high sonic and supersonic speeds. For example, at Mach 0.2 (subsonic speed) the compressibility effects increase the ΔP of air only about 1 percent above that of an incompressible fluid. Since the compressibility effects are so small, air may be considered as an incompressible fluid at low subsonic speeds. At Mach 1 (sonic speed), however, the compressibility effects increase the ΔP of air about 25 percent above that of an incompressible fluid. Therefore, at high sonic and supersonic speeds, air must be considered as a compressible fluid.

The preceding discussion has explained how two variables (velocity V and density ρ), which are not measured directly, can be determined from measurements of the pressure due to the motion of the fluid ΔP, the static pressure P_s, and the static temperature T_s

Other variables, such as lift coefficient, drag coefficient, Reynolds number, and Mach number, are also not measured directly but are calculated from measurements of pressure, temperature, force, etc. Some of the devices used to make these measurements are discussed in the following sections.

PRESSURE

Sensing Devices

A moving fluid exhibits three kinds of pressure: static pressure P_s, total pressure P_t, and pressure due to the motion of the fluid ΔP. Before any of these pressures can be measured, some sensing device is required that will isolate and detect only that particular pressure which is to be measured. A pressure-sensing device is basically just a tube that is oriented in such a way that it senses one particular kind of pressure.

Static tube. - Static pressure P_s is the force per unit area that a fluid exerts on a surface that is at rest relative to the fluid. This pressure is due to the random motion of the fluid molecules. The static pressure of a flowing fluid is sensed by means of a static tube (fig. 13-1(a)). The tube is arranged so that the opening is facing perpendicular to the flow direction and is flush with a surface along which the fluid is flowing (i.e., a surface that is parallel with the direction of flow). Thus, the opening of the tube is oriented so that it is not subjected to impact or suction effects from the moving fluid. In effect, then, the static tube is at rest relative to the fluid and, therefore, senses only static pressure.

Pitot tube. - Total pressure P_t is the force per unit area that is exerted on a surface which is placed in the path of the flow (and perpendicular to the flow direction) so that it halts the flow. This pressure is due to both the inherent random motion of the fluid molecules and the ordered motion of the molecules in the direction of flow. Thus, total pressure P_t is the sum of the static pressure P_s and the pressure due to the motion of the fluid. Total pressure is sensed by means of a pitot tube (fig. 13-1(b)). This tube is arranged so that the open end of the tube protrudes into the fluid stream, and the opening faces upstream. Thus, the opening of the tube senses the pressure produced by the impact of the fluid stream against it.

Pitot-static tube. - The pressure due to the motion of the fluid ΔP is the difference between the total pressure P_t and the static pressure P_s. This ΔP is obtained by means of a pitot-static tube (fig. 13-1(c)). This device does not actually sense ΔP. Instead, it simultaneously senses total pressure and static pressure. The difference between these two pressures can then be determined with the use of an appropriate measuring device.

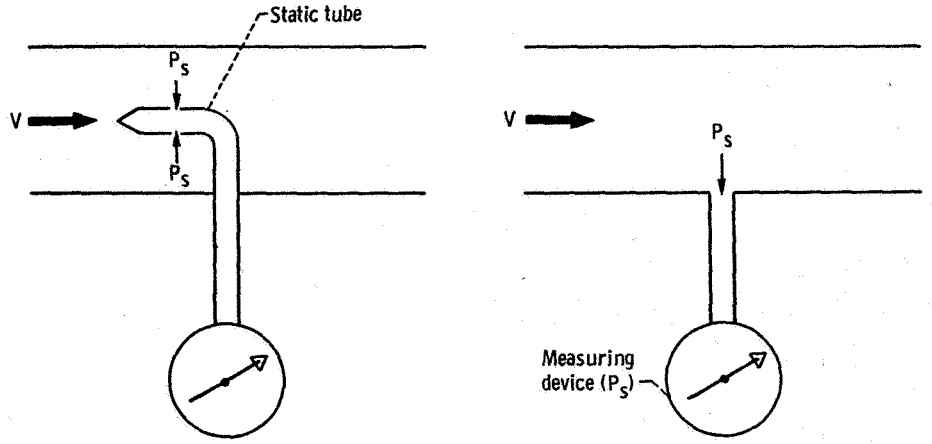

(a) Static tubes.

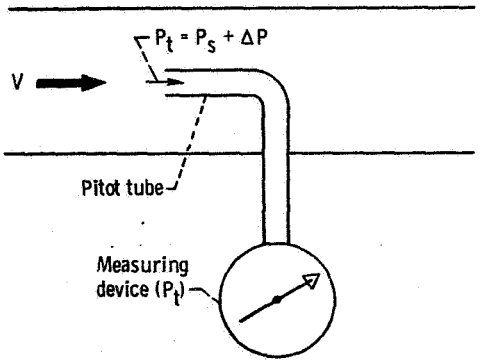

(b) Pitot tube.

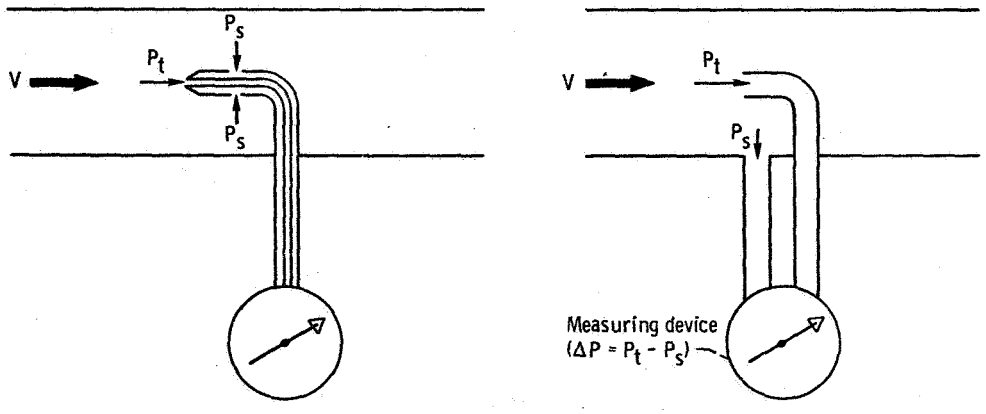

(c) Pitot-static tubes.

Figure 13-1. - Pressure-sensing devices.

Measuring Devices

The pressures of stationary and/or flowing fluids are normally measured with some type of pressure gage, such as a liquid-level manometer or a diaphragm pressure gage. A liquid-level manometer measures pressures of fluids by balancing the pressure against a column (in a tube) of a liquid that does not mix with the fluid whose pressure is being measured. A diaphragm pressure gage balances the pressure of the fluid against the elastic force of a spring or an elastic diaphragm. Both of these types of pressure gage can be designed to measure either differential pressure (i.e., the difference between two pressures) or absolute pressure (i.e., the pressure relative to zero pressure). For measuring the pressures of a flowing fluid, the pressure gage is used in combination with one of the pressure-sensing devices described in the preceding section.

Liquid-level manometer. - Figure 13-2 shows a liquid-level manometer designed to measure differential pressure (e.g., the pressure due to the motion of a fluid, ΔP). The two legs of the U-tube are subjected to two pressures P_1 and P_2. If the two pressures are equal, the liquid level is the same in the two legs of the tube, as shown in figure 13-2(a). If the two pressures are different (e.g., $P_1 > P_2$), the difference between them ($P_1 - P_2$) causes the liquid in the tube to be displaced (fig. 13-2(b)) so that the liquid level is higher in that leg of the tube which has the lower pressure P_2. The height of the liquid column is the vertical distance between the liquid levels in the two legs of the tube. The

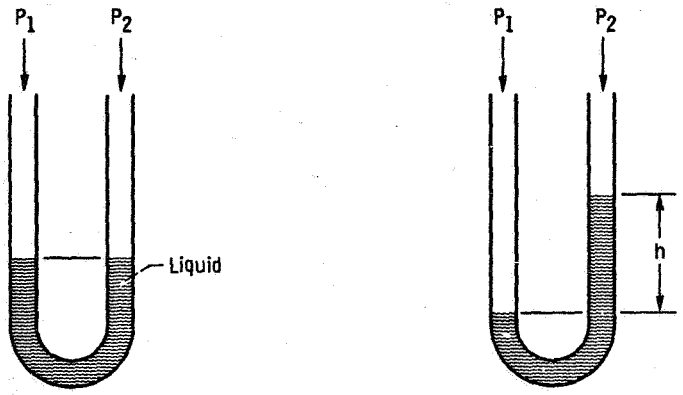

(a) $P_1 = P_2$. (b) $P_1 > P_2$.

Figure 13-2. - Liquid-level manometer for measuring differential pressure.

basic equation for calculating the pressure indicated by a liquid-level manometer is

$$P_m = P_1 - P_2 = wh \tag{6}$$

where

P_m pressure difference indicated by manometer, lb/ft^2

P_1, P_2 pressures in the two legs of the tube

w specific weight of liquid, lb/ft^3

h height of liquid column, ft

Figure 13-3 shows a liquid-level manometer designed to measure absolute pressure (e.g., atmospheric pressure). In this instrument, one leg of the U-tube is sealed and evacuated to zero pressure P_2. Thus, since P_2 is zero, the pressure indicated by the manometer ($P_1 - P_2$) is simply the absolute pressure P_1.

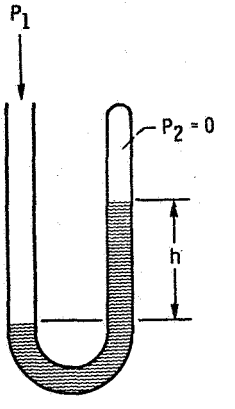

Figure 13-3. - Liquid-level manometer for measuring absolute pressure.

For any given pressure P_m indicated by a manometer, the magnitude of the displacement of the liquid (i.e., the liquid column height) depends on the specific weight of the liquid. The two liquids normally used are water and mercury, and pressure can be expressed as feet (or inches) of water or mercury. The specific weight of water is 62.4 pounds per cubic foot, while that of mercury is 846 pounds per cubic foot. Therefore, a column of water produced by a given P_m is 13.5 times as high as a column of mercury produced by the same P_m. Obviously, the greater the displacement of the liquid per unit of pressure, the easier it is to detect and measure small pressures. Therefore, a manometer that uses water is 13.5 times as sensitive as one that uses mercury.

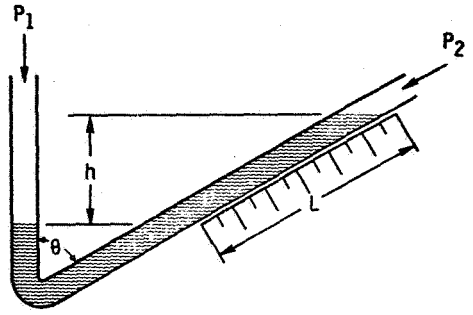

Figure 13-4. - Configuration for increasing sensitivity of liquid-level manometer.

Another method of increasing the sensitivity of a liquid-level manometer is illustrated in figure 13-4. Here the instrument is arranged so that the liquid is displaced at some angle θ relative to the vertical direction. Thus, the length of displacement L along the scale is an amplification of the height of the column h. The relation between h and L is given by the equation

$$h = L \cos \theta \tag{7}$$

Obviously, when θ is zero (i.e., when both legs of U-tube are vertical), cosine θ is 1, and L equals h. But as θ approaches 90°, cosine θ approaches zero, and L becomes larger than h.

Diaphragm pressure gage. - Figure 13-5 shows a diaphragm pressure gage designed to measure differential pressure. This instrument measures pressure by the deflection of an elastic diaphragm or spring element instead of a liquid. When the two pressures P_1 and P_2 are equal, the diaphragm is undeflected (fig. 13-5(a)). When the two pressures are different (e.g., $P_1 > P_2$), the differential pressure ($P_1 - P_2$) causes the diaphragm to deflect (fig. 13-5(b)) towards the chamber that has the lower pressure P_2.

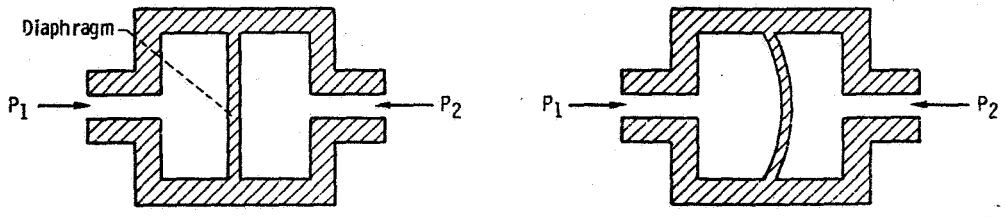

(a) $P_1 = P_2$. (b) $P_1 > P_2$.

Figure 13-5. - Diaphragm pressure gage for measuring differential pressure.

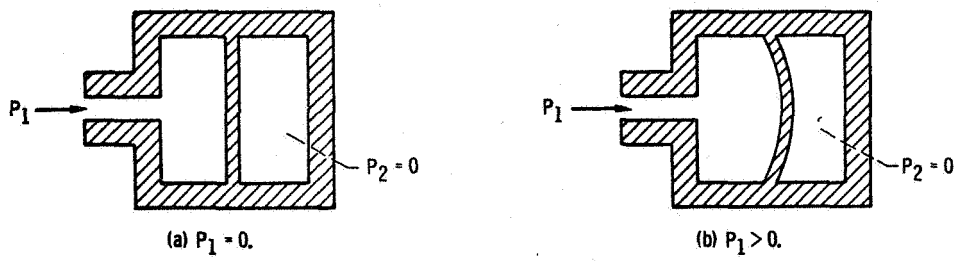

(a) $P_1 = 0$. (b) $P_1 > 0$.

Figure 13-6. - Diaphragm pressure gage for measuring absolute pressure.

Figure 13-6 shows a diaphragm pressure gage designed to measure absolute pressure. In this instrument, one chamber is evacuated to zero pressure P_2 and sealed. Therefore, the pressure indicated by the deflection of the diaphragm $(P_1 - P_2)$ is simply an absolute pressure P_1.

Pressure can be determined from the deflection of the diaphragm of a pressure gage only if the instrument is properly calibrated against a liquid-level manometer or against some other pressure standard, and if the deflection can be measured accurately. Since the total range of deflection of the diaphragm is relatively small, the deflection is difficult to measure accurately by means of a scale. Therefore, the deflection of the diaphragm is commonly measured by means of a strain gage.

Strain Gage

A strain gage is a highly sensitive deflection-measuring device. It is not a pressure-measuring device, but it is used in some pressure gages to measure the deflection of the diaphragm. Then, the pressure that produces the deflection is determined from this measurement. Strain gages have many other applications, some of which are discussed later in this chapter.

A strain gage is basically a thin wire mounted on a surface in such a way that any deflection of the surface either stretches or compresses the wire. A current is passed through the wire and the resistance of the wire is measured to determine the deflection of the surface. The principle of the strain gage is that the resistance R of any given wire is directly proportional to its length L and inversely proportional to its cross-sectional area A.

$$R \propto \frac{L}{A} \tag{8}$$

If the wire is stretched, its length increases and its cross-sectional area decreases;

therefore, the resistance of the wire increases. If the wire is compressed, the effects are the opposite. Thus, the resistance of the wire is a measure of its deformation and of the deflection of the surface on which it is mounted.

Figure 13-7 shows how strain gages can be used to measure the deflection of the diaphragm in a pressure gage. Strain gages are bonded to both sides of the diaphragm. When the pressures P_1 and P_2 are equal and the diaphragm is undeflected (fig. 13-7(a)), the strain gages R_1 and R_2 have equal resistances. When the two pressures are un-

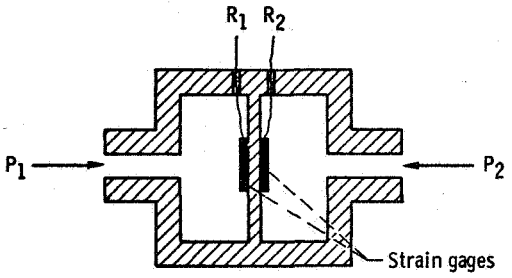

(a) $P_1 = P_2$; $R_1 = R_2$.

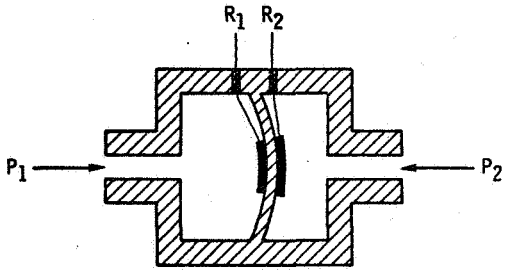

(b) $P_1 > P_2$; $R_1 < R_2$.

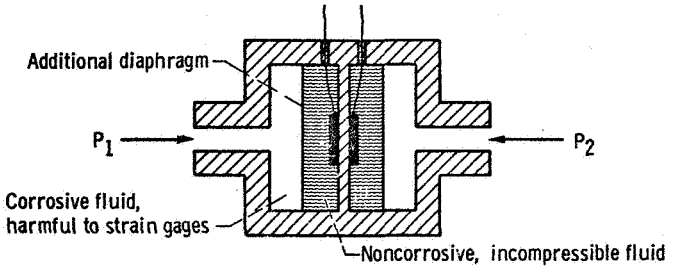

(c) Configuration for protecting strain gages from corrosive fluids.

Figure 13-7. - Use of strain gages to measure deflection of diaphragm of pressure gage.

equal, the deflection of the diaphragm compresses one strain gage and stretches the other (fig. 13-7(b)). The resulting changes in the resistances of the strain gages indicate the extent of the deflection and, therefore, the magnitude of the pressure being measured. For pressure measurements of corrosive fluids, the strain gages can be protected by immersion in an incompressible, noncorrosive fluid contained within additional diaphragms, as shown in figure 13-7(c).

A few examples of commercially available diaphragm pressure gages equipped with strain gages are shown in figure 13-8. Many other pressure-measuring devices are available, and they range in price from about $1 to about $500. The price depends largely on the accuracy of the pressure gage.

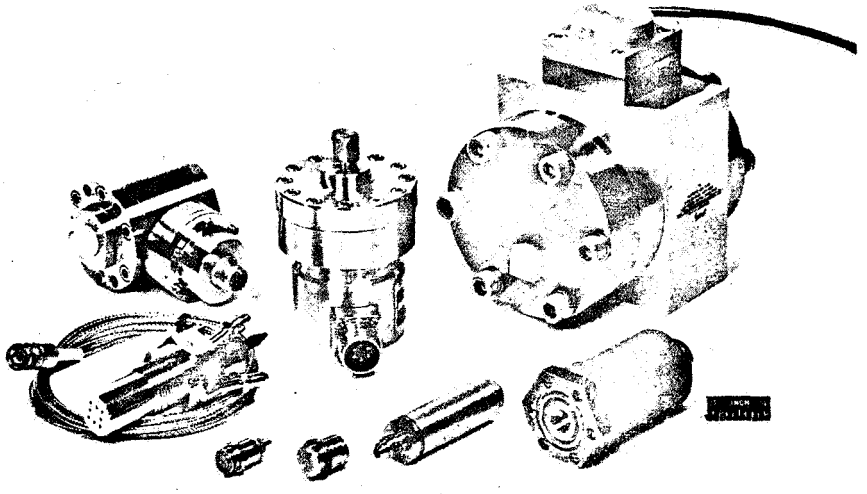

CS-32134

Figure 13-8. - Examples of commercially available diaphragm pressure gages equipped with strain gages.

THRUST

The essential element of most thrust-measuring devices is a spring. When the spring is subjected to a thrust force, the deflection of the spring is a measure of the thrust. A good thrust-measuring spring is one that consistently deflects the same amount each time it is subjected to the same thrust force. Furthermore, the spring must maintain this consistency, or accuracy, over a reasonable range of temperatures.

A schematic diagram of a thrust-measuring spring is shown in figure 13-9. The solid line represents the outline of the spring before it is subjected to a force. When a thrust force F is applied to the spring in the compressive direction, the length of the spring decreases and the width increases, as indicated by the dashed line in the figure.

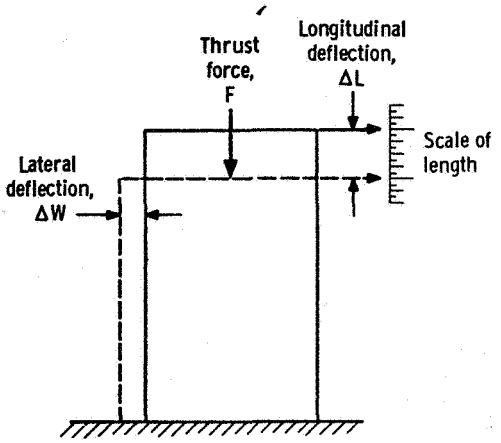

Figure 13-9. - Schematic diagram showing deformation of thrust-measuring spring under compressive load (thrust force).

However, the changes in length and width are not equal. The ratio of the change in width ΔW to the change in length ΔL is a material property known as Poisson's ratio μ.

$$\mu = \frac{\Delta W}{\Delta L} \tag{9}$$

This ratio is constant (within certain limits) for a given material. For most metals, the value of μ is about 0.3. This simply means that when the length of the spring decreases by 10 units, the width increases by 3 units.

For a good-quality spring (determined principally by the material), the longitudinal and lateral deflections are both proportional to the thrust force, even though the deflections are not equal in magnitude. Therefore, the thrust forces can be determined from the deflections (longitudinal and/or lateral) of the spring.

A relatively easy and accurate way to measure the spring deflections is by means of strain gages, which were discussed in the preceding section. Normally, four strain gages are mounted on the spring - two for measuring longitudinal deflections, and two for lateral deflections. The four strain gages are arranged (electrically) in a Wheatstone bridge circuit, as shown in figure 13-10. The resistances R_1, R_2, R_3, and R_4 represent the four strain gages. Longitudinal deflection is indicated by R_1 and R_2, and lateral deflection by R_3 and R_4. Thus, when a force compresses the spring, strain gages R_1 and R_2 shorten and their resistances decrease, while R_3 and R_4 lengthen and their resistances increase. The difference in resistances indicates the extent of the deformation of the spring and, therefore, the magnitude of the force.

Some examples of the many commercially available thrust-measuring devices (thrust cells) for various thrust limits are shown in figure 13-11.

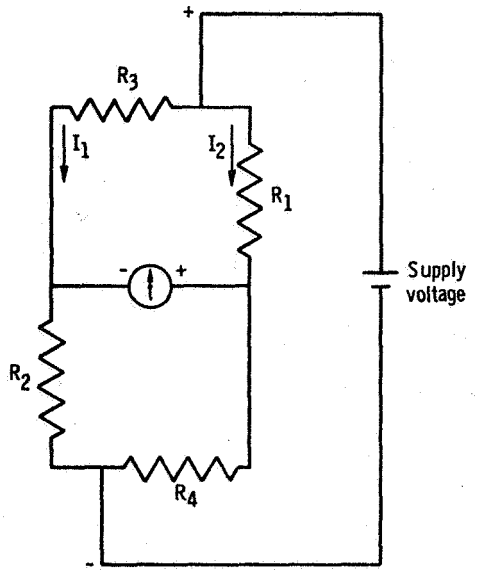

Figure 13-10. - Schematic diagram of Wheatstone bridge circuit arrangement of strain gages used to measure deflection of thrust-measuring spring. (Longitudinal deflections of spring are indicated by resistances of strain gages R_1 and R_2; lateral deflections indicated by R_3 and R_4.)

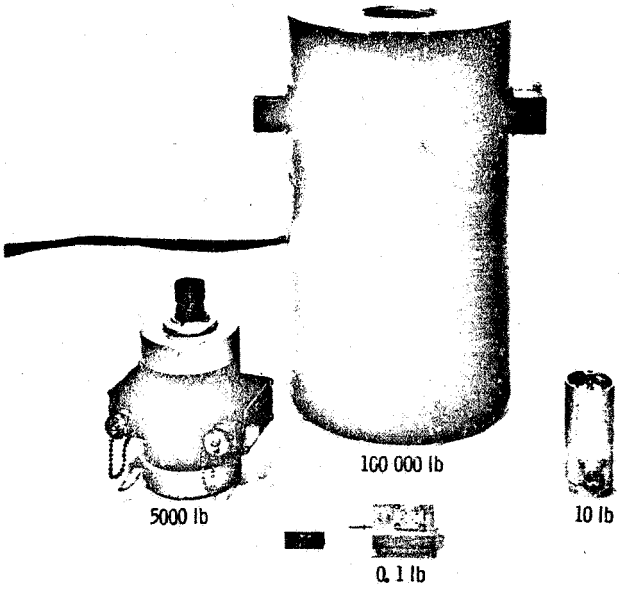

C-69844

Figure 13-11. - Examples of commercially available thrust-measuring devices (thrust cells).

TEMPERATURE

Temperature is a measure of the intensity of heat, and heat is a form of energy resulting from the motions of the molecules or atoms of a substance (fluid or solid).

The temperature of a substance may be sensed by immersing a body (i.e., the sensor) in the substance or by placing it in contact with the substance. The temperature attained by the sensor relative to the temperature of the substance is a function of both the heat transfer from the substance to the sensor and the heat losses from the sensor. Therefore, the temperature of the sensor may not be exactly the same as that of the substance whose temperature is being measured.

If the substance is a flowing fluid, it has a static temperature and a total temperature. Static temperature refers to the heat due to the random motions of the molecules or atoms. Total temperature refers to the heat due to both the random motions of the molecules or atoms and the ordered motion in the direction of flow. Therefore, for static temperature measurements, the sensor must move with the fluid, so that the sensor and the fluid are motionless relative to each other. For total temperature measurements, a stationary sensor is placed in the flow in such a way that the flow is stopped by the sensor. Thus, the kinetic effect of the flow is included in the temperature measurement.

Two devices commonly used to measure temperature are the thermocouple and the resistance thermometer. Of the two, the thermocouple is the simpler device. The resistance thermometer is more complex, larger, more expensive, and more sensitive.

Thermocouple

A thermocouple (fig. 13-12) consists essentially of two electrical conductors of dissimilar metals welded together at one end, with the free ends connected to an electrical measuring instrument. The junction of the two conductors is placed at the point where the temperature T_1 is to be measured. The ends that are connected to the instrument are at a known reference temperature T_2. The difference in temperature between T_1 and T_2 produces an electromotive force. Since T_2 is held constant, the electro-

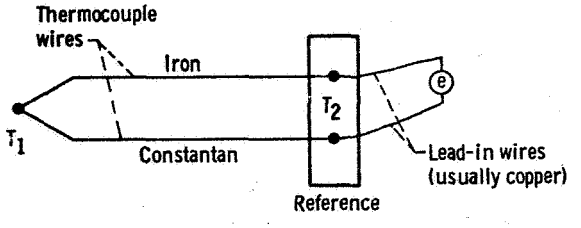

Figure 13-12. - Schematic diagram of thermocouple.

motive force is a function of the temperature T_1. Thus, the voltage e measured by the instrument is an indication of the temperature T_1. The voltage-measuring instrument must be highly sensitive because the voltage produced in the thermocouple is only about 0.00002 volt per degree Fahrenheit.

National Bureau of Standards Circular 561 lists temperature as a function of voltage for the following standard combinations of conductors used in thermocouples:

Chromel - Alumel
Chromel - Constantan
Copper - Constantan
Iron - Constantan
Platinum-13 percent rhodium - platinum

Specific pairs of metals are chosen on the bases of their physical and electrical properties at various temperature levels, as well as on the basis of cost.

Resistance Thermometer

The basis of the resistance thermometer is the fact that the resistance of materials varies with temperature. Thus, if a given piece of material, such as a length of wire, is properly calibrated (resistance as function of temperature), it can be used as a thermometer. The temperature is determined by measuring the resistance of the material.

The material used in the resistance thermometer depends on the temperatures to be measured and the accuracy required. For temperatures above 20° K (temperature of liquid hydrogen), metals are used, because their resistance increases with increasing temperature. The best metal is platinum, because it is obtainable in a highly pure form and because the variation of its resistance with temperature is very nearly linear. Thus, a platinum sensor provides a high degree of accuracy. Where less accuracy is satisfactory, nickel may be used. The metal, in the form of wire, is wound into a compact spiral and is enclosed in a suitable protective housing. Care must be taken to avoid straining the wire, for this would alter its resistance.

The resistance of the wire is measured with a Wheatstone bridge circuit similar to the one used to measure the resistances of the strain gages in a thrust cell (fig. 13-10). In this case, however, three of the resistances are known and fixed, and the fourth resistance is the one that is being measured.

At temperatures below 20° K, the variation of the resistance of metals with temperature becomes so small that the thermometer loses its sensitivity. However, the resistance of materials known as semiconductors, such as carbon or germanium, increases

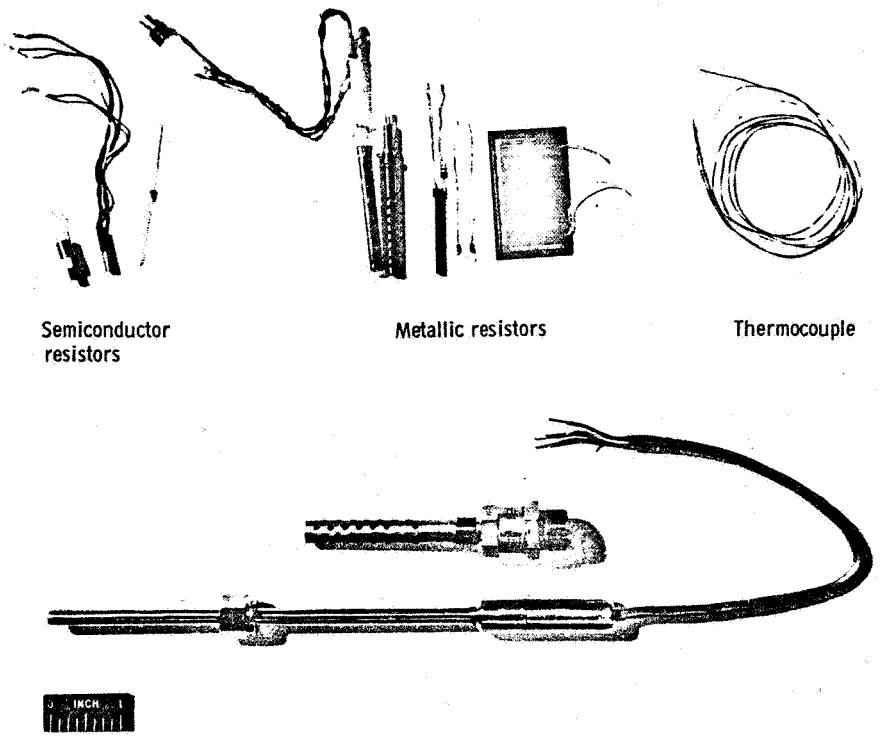

Figure 13-13. - Typical examples of temperature-sensing devices.

as the temperature decreases. Therefore, at temperatures below 20° K, semiconductor materials are used in resistance thermometers.

Some typical examples of temperature-sensing devices are shown in figure 13-13.

VOLUME FLOW RATE

Volume flowmeters, in general, are of two basic types, based on the method by which they measure the flow rate.

One type of flowmeter measures flow rate by repeatedly filling and emptying a known volume and counting the time rate of this action. Various forms of this type of meter are in common use, because they are reliable and relatively inexpensive. Common examples are the nutating-disk meters used to measure water in the home and gasoline at the filling station.

The other basic type of flowmeter determines the volume flow rate from the kinetic energy of the flowing fluid. The discussion at the beginning of this chapter explained how the velocity of a flowing fluid can be determined by equation (4) from certain measurable quantities that include the pressure due to the motion of the fluid. Volume flow rate, in turn, can be determined from the flow velocity by the equation

$$\dot{v} = AV_{ave} \tag{10}$$

where

$\dot{v}$ volume flow rate, ft^3/sec

A cross-sectional area of flow channel, ft^2

V_{ave} average flow velocity, ft/sec

The velocity of a fluid generally varies from a maximum at the center of the flow channel to zero at the walls. Thus, the average flow velocity, required for equation (10), can be obtained from pressure measurements taken at various distances from the walls of the flow channel. This is an accurate but time-consuming process. However, the

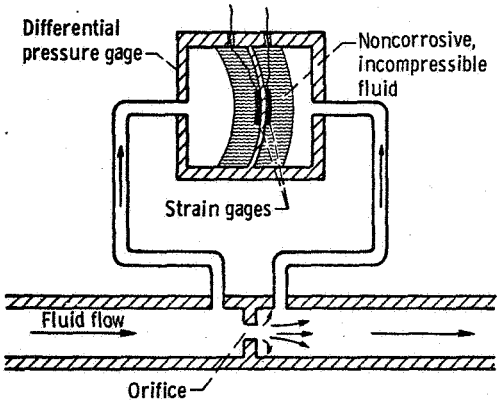

Figure 13-14. - Orifice flowmeter installation.

volume flow rate of an incompressible fluid of known density can be determined from a single pressure measurement. The pressure-measuring arrangement is shown in figure 13-14. A nozzle or orifice is placed in the flow channel, and the difference in static pressure between the upstream and downstream sides is measured with a differential pressure gage. The magnitude of this pressure difference is a function of the flow velocity through the nozzle or orifice. The flow velocity is calculated from this measured pressure differential and is used in the following equation to obtain volume flow rate.

$$\dot{v} = C_d AV \tag{11}$$

where

C_d nozzle or orifice discharge coefficient (dimensionless)

A cross-sectional area of nozzle or orifice, ft^2

V flow velocity, ft/sec

The discharge coefficient C_d is a correction factor that is determined by calibrating the nozzle or orifice. The value of C_d is normally about 0.98 for a nozzle and about 0.6 for an orifice. The coefficient is higher for a nozzle than for an orifice, because the nozzle produces a smoother flow than does the orifice.

Another device which determines volume flow rate from the kinetic energy of the flowing fluid is the turbine flowmeter. In this type of meter, the kinetic energy of the fluid turns a lightly loaded turbine. The load on the turbine is only bearing friction and the small amount of power required to measure the rotational speed of the turbine. The turbine blades are made of magnetic material. As the blades pass a coil-magnet combination, they generate electrical pulses. Thus, the time rate of pulses is a measure of the rotational speed of the turbine. The turbine flowmeter is calibrated (usually with water), and the calibration is expressed as pulses per gallon. Some typical turbine flowmeters, as well as a cutaway view of one, are shown in figure 13-15.

The preceding discussion has described several methods of measuring volume flow rate. In most instances, however, the quantity of primary interest is mass flow rate (lb/sec). The mass flow rate is obtained by multiplying the volume flow rate by the fluid density, which is measured independently.

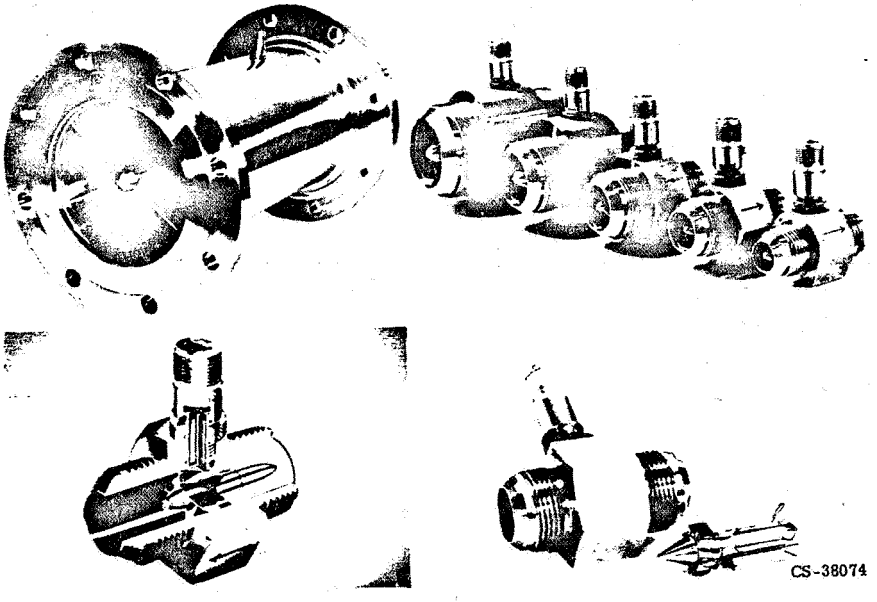

Figure 13-15. - Examples of commercially available turbine flowmeters.

CONCLUDING REMARKS

The measuring devices discussed in this chapter change some measured variable, such as temperature, to an electrical quantity, such as voltage. This is an essential requirement with modern data systems. Very few data are recorded manually. In fact, data should be recorded on a system, such as a digital tape-recording system, which enables the data to be entered in a computer.

BIBLIOGRAPHY

Binder, Raymond C.: Fluid Mechanics. Fourth ed., Prentice-Hall, Inc., 1962.

Cook, Nathan H.; and Rabinowicz, Ernest: Physical Measurement and Analysis. Addison-Wesley Publ. Co., 1963.

Doebelin, Ernest O.: Measurement Systems: Application and Design. McGraw-Hill Book Co., Inc., 1966.

Stout, Melville B.: Basic Electrical Measurements. Prentice-Hall, Inc., 1950.

14. WIND TUNNELS

Leonard E. Stitt*

Wind tunnels are ground facilities for aerodynamic testing of aircraft, missiles, propulsion systems, or their components under simulated flight conditions. The concept of a wind tunnel is rather simple: instead of the object flying through the air at the desired test speed and attitude, it is supported in the test attitude within the wind tunnel, and the air flows past the object at the test speed. The resulting forces of interaction between the object and the airflow are identical in both cases. In a wind tunnel, both the airstream and the attitude of the test model can be controlled by the engineer while all essential information is collected. Obviously, many scale models of a particular configuration can be evaluated in wind-tunnel tests at a relatively small cost, compared to the cost of designing, fabricating, and flight testing a full-scale prototype. Configuration changes can be made rapidly, and a final design can be arrived at that has a reasonable chance of success when the prototype is finally flown. The usefulness of wind tunnels in providing good aerodynamic design information has been demonstrated many times during the past 50 years, both in the United States and abroad.

Wind tunnels have been in use for many years; in fact, they were already in use prior to the first powered flight of the airplane in 1903. An estimated 1000 wind tunnels have been built throughout the world, and about 250 of these have been built in the United States. These wind tunnels range from simple, low-cost, low-speed tunnels used for testing subscale models to highly complex and expensive tunnels used for testing full-scale hardware at supersonic speeds. An example of the latter is the 10- by 10-Foot Supersonic Wind Tunnel at the NASA Lewis Research Center. This tunnel was built in the early 1950's, at a cost of $35 million, to study the aero-thermodynamic problems of propulsion systems.

WIND-TUNNEL DESIGN CONSIDERATIONS

Wind tunnels exist in a wide variety of shapes and sizes depending on cost, speed range, power requirement, purpose, etc. One tunnel design parameter of particular

*Head, Exhaust Systems Section.

TABLE 14-I. - CLASSIFICATION OF WIND TUNNELS ACCORDING TO SPEED OF AIRFLOW IN TEST SECTION

Tunnel class	Free-stream Mach-number[a] range
Low speed	0 to 0.5
High speed	0.5 to 0.9
Transonic	0.7 to 1.4
Supersonic	1.4 to 5.0
Hypersonic	>5.0

[a]Mach number = $\frac{\text{Local stream velocity}}{\text{Local velocity of sound}}$

interest is the velocity of the airflow. In practice, wind tunnels can be classified according to their speed ranges, as shown in table 14-I. Some wind tunnels are restricted to one speed, while others operate over a wide range of speeds. For example, the 8- by 6-Foot Supersonic Wind Tunnel at the Lewis Research Center can operate at speeds ranging from about Mach 0.4 to Mach 2.0. Obviously, such a tunnel is quite useful to the engineer for evaluating a particular configuration over a wide range of flight conditions with only one installation. This versatility must, of course, be weighed against the initial cost and complexity of constructing and operating such a wind tunnel. A few key items that should be considered when designing a wind tunnel are discussed in the following sections.

Wind-Tunnel Types

The two general types of wind tunnels are the open-circuit and the closed-circuit types, shown in figure 14-1.

Open-circuit tunnel. - The open-circuit tunnel (fig. 14-1(a)) is the simpler of the two types and is the one normally used in most schools and universities for demonstration purposes and for laboratory instruction. (An example of this type of tunnel at Lewis is the low-speed tunnel used by the Lewis Aerospace Explorers and described in chapter 17.) Airflow is drawn through the test section by a suitable motor and propeller (or fan) arrangement. An airflow of good quality (low turbulence) is assured in the test area through the use of inlet screens and the proper contouring of the contraction cone. Large contraction ratios are useful in obtaining smooth flow in the test section. Typical contraction ratios (ratio of inlet area to test-section area) range from 7 to 14. The University of Notre Dame has recently used contraction ratios as high as 100 in developing a super-

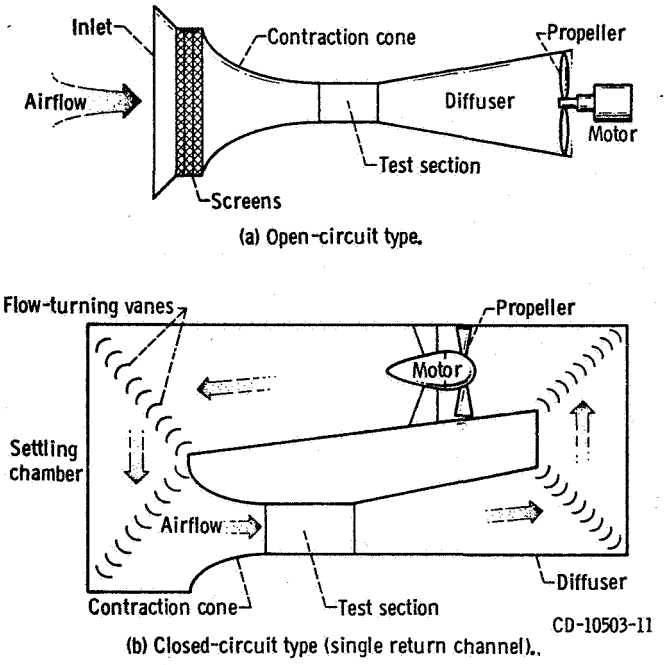

Figure 14-1. - Wind-tunnel types and nomenclature.

sonic smoke tunnel (ref. 1). The test section normally includes windows and appropriate illumination for viewing the model. Downstream of the test section, a diffuser is used to slow the airflow ahead of the propeller to a velocity at which the propeller operates efficiently. The area is increased as rapidly as possible without incurring flow separation from the diffuser walls. Diffuser expansion angles vary from about 6° to 12°, depending on the shape of the cross section. Safety screens can be added downstream of the test section to protect the propeller in case of model failure.

Closed-circuit tunnel. - The closed-circuit tunnel (fig. 14-1(b)) can be more efficient from the standpoint of the power requirement, but it requires more physical space and is more expensive to fabricate than the simple open-circuit tunnel. The closed-circuit tunnel is usually rectangular, and turning vanes are provided to turn the flow efficiently around the 90° bends. The closed-circuit tunnel also features the usual contraction cone and low-expansion-angle diffuser. A settling chamber is also included to reduce the flow turbulence at the entrance to the contraction cone. The test section can be of a variety of cross-sectional shapes, such as square, rectangular, octagonal, circular, elliptical, etc. The test section may be enclosed by walls, or it may be open (no walls) to facilitate access to the test model. A single return channel (fig. 14-1(b)) or two return channels may be used. With two return channels, the test section is normally located in the center between the two parallel channels. A suitable motor and propeller are required for each return channel.

Power Requirement

One of the main parameters that the wind-tunnel designer must consider is the power required to operate the tunnel. This power requirement may be computed by the following equation:

$$BHP = \frac{qAV}{\eta ER550}$$

where

BHP brake horsepower of motor

q dynamic pressure of airflow in test section, lb/ft^2

A cross-sectional area of test section, ft^2

V velocity of airflow in test section, ft/sec

η power transmission efficiency (a measure of power performance of fan-motor combination, relating power input to pumping power)

ER energy ratio of wind tunnel (a measure of aerodynamic efficiency of wind tunnel)

and 550 is the factor for converting foot-pounds per second to horsepower.

For small, open-circuit wind tunnels, the energy ratio usually has a value between 1.5 and 2.5; a highly efficient open-circuit tunnel may have an energy ratio of 3.5. A closed-circuit wind tunnel with an enclosed test section may have an energy ratio between 3 and 7.

Since the dynamic pressure q is equal to $\frac{1}{2}\rho V^2$, the equation for horsepower can be rewritten in the following form:

$$BHP = \frac{1}{2}\frac{\rho AV^3}{\eta ER550}$$

where ρ is the air density in the wind tunnel, in slugs per cubic foot (1 slug = 32.2 $lb\text{-}ft/sec^2$). It is obvious from this equation that the velocity of the airflow is the most influential variable affecting the power requirement of a wind tunnel. Therefore, from a power standpoint, the wind-tunnel designer is faced with a problem. He wants a large test section and a high-speed airflow, but both of these features require high horsepower. Therefore, the general design procedure is to select the desired airflow velocity range and then to determine the largest test-section area that is compatible with the available power.

The following sample calculations for two greatly different wind tunnels show the ef-

fects of tunnel variables on the horsepower requirements.

Tunnel used by Lewis Aerospace Explorers:

$$BHP = \frac{1}{2}\frac{\rho AV^3}{\eta ER550}$$

$$= \frac{1}{2}\frac{(0.002378)(4.16)(75)^3}{(0.75)(2.0)(550)}$$

$$= 2.53$$

10- by 10-Foot Supersonic Wind Tunnel at Lewis:

$$BHP = \frac{1}{2}\frac{\rho AV^3}{\eta ER550}$$

$$= \frac{1}{2}\frac{(0.0001)(100)(3400)^3}{(0.75)(2.0)(550)}$$

$$= 238\ 206$$

This power is supplied by seven electric motors rated at 37 500 horsepower each. This facility (highest-powered wind tunnel in United States) requires about 200 megawatts of electrical power at full load, at a cost of approximately $1400 per hour. Because of the large power requirement, this facility operates primarily at night, when the power requirements of the community are minimum. At night, the electricity required to operate the wind tunnel is readily available at reduced cost from the local electric company.

The availability and cost of electrical power, as well as the initial and operating costs of the tunnel, influence the choice between intermittent and continuous operation.

Intermittent operation. - An intermittent wind tunnel is an open-circuit type that may be either a blowdown tunnel or an indraft tunnel. The blowdown tunnel (fig. 14-2(a)) has a large pressurized tank upstream of the test section. When the tank is opened, the compressed air from it blows through the test section. The indraft tunnel (fig. 14-2(b)) has a large vacuum tank downstream of the test section. When the evacuated tank is opened, its vacuum draws air through the test section.

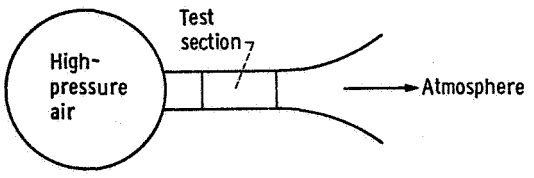

(a) Blowdown tunnel.

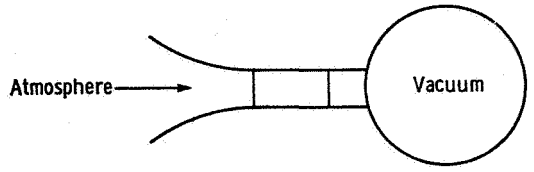

(b) Indraft tunnel.

Figure 14-2. - Intermittent wind tunnels.

The main disadvantage of an intermittent tunnel is that it provides an airflow of only a brief duration before the tank must again be pressurized or evacuated. Therefore, testing time is limited, and special instrumentation must be used to obtain data. Changing model variables during the short test period is also an operational problem. With suitable control systems, the model attitude can be pre-programmed to vary automatically during the test.

Continuous operation. - Continuous operation, which is provided by either open-circuit or closed-circuit tunnels, such as those shown in figure 14-1, is more advantageous from the standpoint of test time. However, it is more costly from a power consideration.

Speed Variability Requirement

One useful feature of a subsonic wind tunnel is that the flow velocity in the test section can be varied by increasing or decreasing the propeller speed within the limits of available power or propeller design. The flow velocity can be increased in this manner until the local flow velocity equals the speed of sound (Mach 1). When this condition occurs, the tunnel is said to be "choked."

The flow velocity achieves Mach 1 at the minimum cross-sectional area (throat) of the tunnel. The only way to obtain a flow velocity greater than Mach 1 is to expand the flow by increasing the flow area downstream of the throat. (The acceleration of an airflow to supersonic velocities is discussed in greater detail in chapters 7 and 11.) The flow Mach number (velocity) downstream of the throat is rigidly determined by the ratio of the local cross-sectional area A to the throat cross-sectional area A^*. This relation between area ratio and Mach number has an important bearing on wind-tunnel design. A supersonic wind tunnel with a fixed area ratio A/A^* can provide only one specific flow

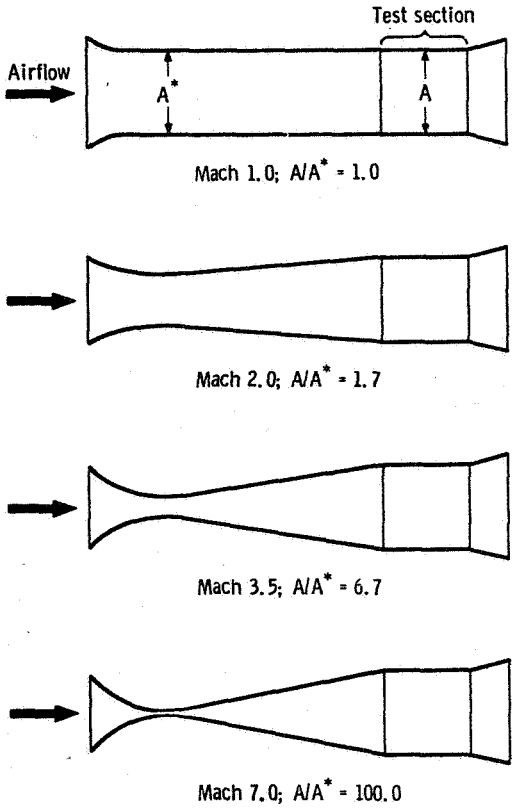

Figure 14-3. - Area variation required for supersonic wind tunnel.

Mach number in the test section. Thus, if the flow Mach number in the test section is to be variable, the tunnel must be equipped with some means of physically varying the area ratio A/A^*. For example, if the cross-sectional area of the test section is fixed, as shown in figure 14-3, the throat area must be increased by a factor of 100 to vary the test-section Mach number from 1.0 to 7.0. The 8- by 6-foot and 10- by 10-foot tunnels at Lewis use flexible nozzles to change both the throat area and the wall contour between the throat and the test section to provide variable Mach number capability. The 1- by 1-Foot Variable Mach Number Wind Tunnel at Lewis features a fixed test-section area and replaceable nozzle "blocks" with various throat areas to provide testing over a range of discrete Mach numbers up to Mach 5.0.

WIND-TUNNEL CALIBRATION

After a wind tunnel has been designed and fabricated, the quality of the airflow in the test section must be determined before the tunnel is used for testing. The flow characteristics that must be determined include the speed and direction of the local flow and the

thickness of the boundary layer along the walls.

The speed of the airflow can be calculated from measurements of the density ρ, the static pressure P_s, and the total pressure P_t of the airflow. These properties, as well as methods of sensing and measuring them and the method of calculating velocity from them, are discussed in chapter 13. For wind-tunnel calibration, these properties are measured with calibration instruments (figs. 14-4 and 14-5) that are adaptions of the basic instruments discussed in chapter 13 and are tailored to the airflow speed range of interest.

Flow angularity, or direction, is usually determined by measuring static pressures or static and total pressures on opposite sides of a symmetrical object that can be alined with the local flow direction or with the wind-tunnel centerline.

In a subsonic wind tunnel, the static and total pressures used to calculate the speed of the airflow usually are determined simultaneously with a pitot-static tube (fig. 14-4(a)).

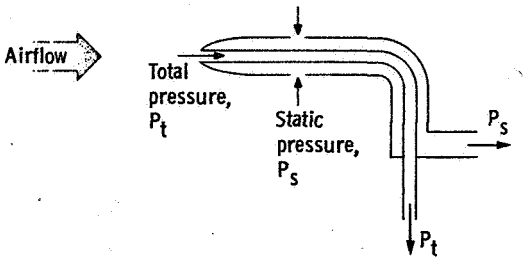

(a) Pitot-static tube, for measuring flow speed.

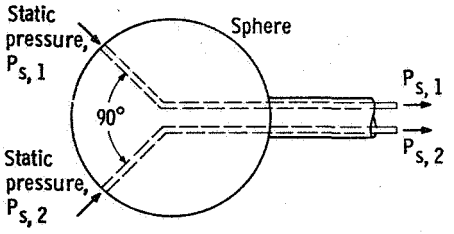

(b) Yawmeter, for measuring flow angularity.

Figure 14-4. - Calibration devices for subsonic wind tunnels.

The pitot tube senses total pressure P_t, and the static tube senses static pressure P_s. Local flow angularity in a subsonic wind tunnel is usually determined with a yawmeter of the type shown in figure 14-4(b). This instrument is basically a sphere with two static-pressure orifices located 90^o apart in its surface. The sphere is pitched in the tunnel until the static pressures at the two orifices are equal, and the angularity of the yawmeter (or flow direction) is then recorded. In this manner, flow angularities in any preselected plane can be measured by proper orientation of the yawmeter.

Both the speed and the direction of the airflow can be determined by means of a cali-

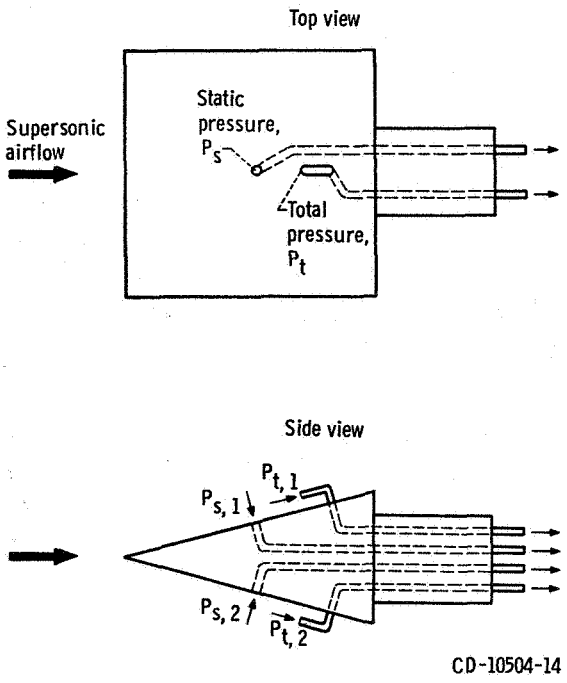

Figure 14-5. - Low-angle calibration wedge for measuring speed and angularity of airflow in supersonic wind tunnel.

bration wedge, shown in figure 14-5. Supersonic wind tunnels are normally calibrated with this type of instrument. The calibration wedge combines the functions of a pitot-static tube and a yawmeter. Measurements of static pressure P_s and total pressure P_t are used to calculate the speed of the airflow. Measurements of the static pressures P_{s_1} and P_{s_2} on opposite sides of the wedge are used to calculate the flow angularity.

The 10- by 10-Foot Supersonic Wind Tunnel was calibrated with a rake (fig. 14-6) consisting of 17 of these wedges. In this manner, a large portion of the cross-sectional area of the tunnel was calibrated at one time. Flow quality along the length of the test section was determined by translating the calibration rake. Flow angularity in perpendicular planes was determined by rotating the wedges 90^{o}. Boundary-layer rakes were also installed at various locations on the tunnel walls to measure the thickness of the boundary layer. The measured boundary-layer thickness in the 10- by 10-Foot Supersonic Wind Tunnel varied from 9 to 12 inches.

At supersonic speeds, shock waves from the forward parts of the test model can reflect from the tunnel walls back onto the rear portions of the model. Calibration bodies, such as cone-cylinder models, can be tested over the complete range of Mach numbers to search for reflected shocks, which can be detected with static-pressure instrumentation. From these calibration results, reflection-free model lengths can be specified. Mach number ranges where reflections are a problem also can be noted and ignored for longer

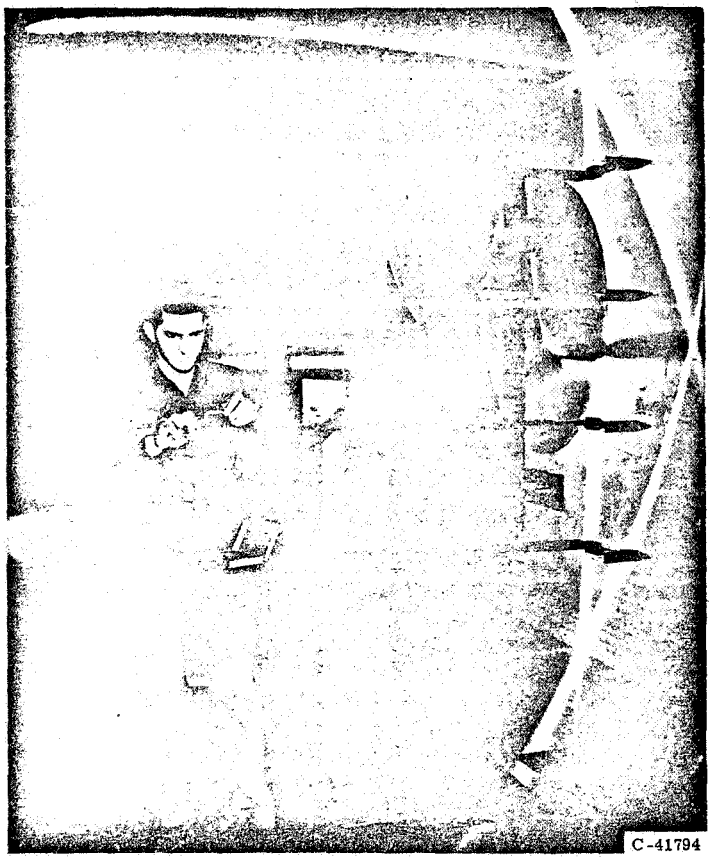

Figure 14-6. - Calibration rake installed in the 10- by 10-Foot Supersonic Wind Tunnel.

models. Calibration bodies of various diameters can also be tested to determine the maximum test-model size that the tunnel can accommodate while still providing interference-free flow over the entire speed range. Limits are then placed on the ratio of model cross-sectional area to tunnel cross-sectional area (or blockage ratio) to obtain good test results. This blockage ratio varies with Mach number and can be as low as 3 percent at transonic speeds and as high as 15 percent at hypersonic speeds.

SUPPORT SYSTEMS

After the test-section flow conditions have been measured, installation of test hardware can begin. Methods of supporting the test article in the stream must be considered carefully, since support systems will interfere with the measurements, and corrections to the results must be kept to a minimum. Various ways are available to support the test models, depending to a great extent on the purpose of the test. A few of the techniques used at Lewis are illustrated in figure 14-7. Sting supports (fig. 14-7(a)) are useful when

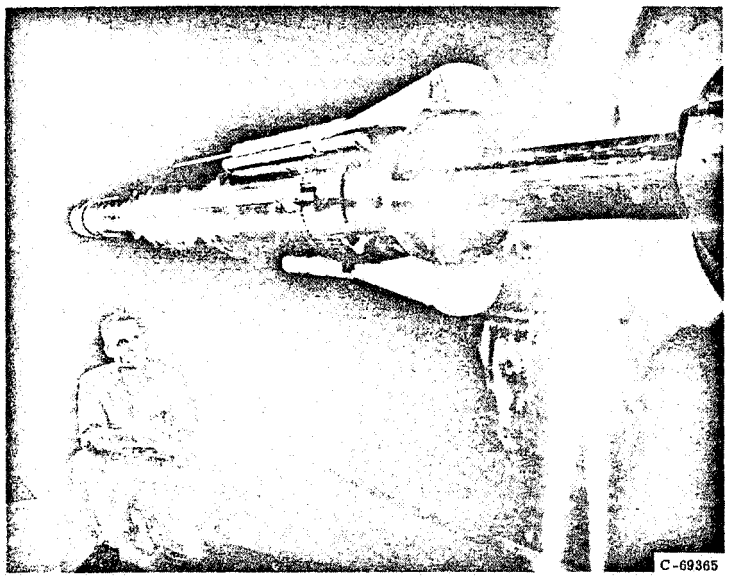

(a) Sting (Atlas/Agena).

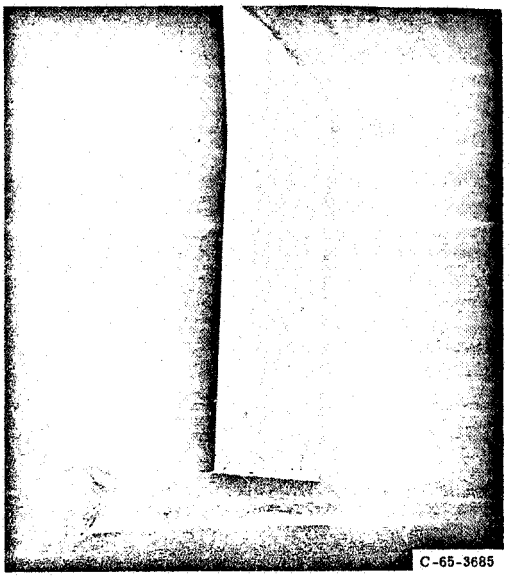

(b) Single strut (Saturn 5).

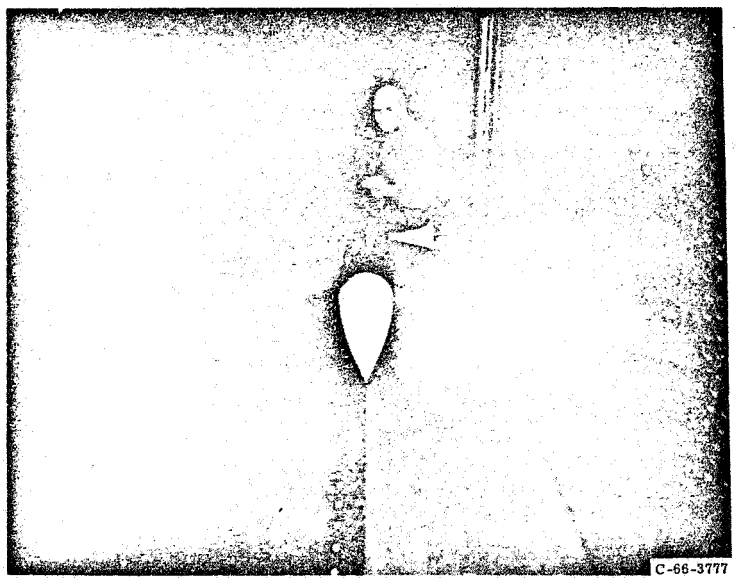

(c) Double strut (jet exit model).

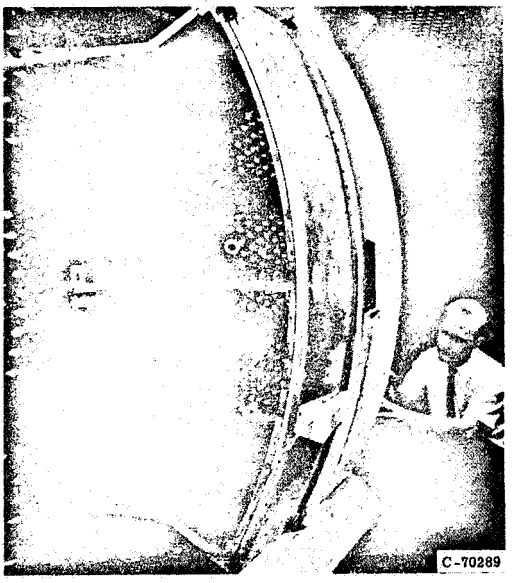

(d) Wall mount (Centaur weather shield).

Figure 14-7. - Typical methods of supporting test object in wind tunnel.

(e) Dynamic mount (Apollo launch escape vehicle).

(f) Wires (decelerator).

Figure 14-7. - Concluded.

external pressure distributions are being measured. Strut supports, either single (fig. 14-7(b)) or double (fig. 14-7(c)), are used when a high-pressure airflow through the test model is required, such as for nozzle tests. With struts, the area downstream of the model remains unobstructed, and the high-pressure airflow (higher pressure than the free-stream airflow) is brought into the model through an air line that can be housed in the normally hollow struts. The struts can also house instrumentation, electrical lines, and fuel lines. Sometimes, test models are mounted directly to the test-section walls (fig. 14-7(d)). Some special test programs require the use of unusual mounting techniques such as those shown in figures 14-7(e) and (f). In some wind tunnels, unsupported, remotely controlled, powered models are tested. Magnetic suspension of test models has also been considered, but this technique presents a problem in obtaining information; telemetering may be one solution to this problem. It should be remembered that support interference effects are one of the main problems facing the wind-tunnel engineer.

TECHNIQUES OF VISUAL OBSERVATION OF FLOW

One of the simplest methods of obtaining information from a wind-tunnel test is by visual observation of the test model during and after the test. Most wind tunnels incorporate windows and appropriate illumination for this purpose. The airflow behavior can be made more clearly visible through the use of smoke, tufts, dye, china clay, etc. For thermal studies, temperature-sensitive paints that change color at various temperature

levels are used. Tests of structural integrity can be run with visual observation only, including a close inspection of the test model after shutdown to determine local damage.

Several optical systems have been developed for observing the flow around test models in supersonic wind tunnels. Two of these optical systems are the schlieren system and the shadowgraph system. Both systems are based on the principle that light rays are refracted (or bent) as they pass through regions of different density. Since strong density gradients (e.g., shock waves) occur in supersonic flow, the flow fields can be viewed by means of these optical systems.

Schlieren System

In the schlieren system (fig. 14-8), light from a point source on one side of the test section is bent by a lens into a beam of parallel rays. This beam is passed through the test section and is then collected by a second lens into an image of the point light source. If a knife edge is introduced at this image point, the intensity of the light being projected on the screen can be reduced. Thus, the image of the test section on the screen can be darkened uniformly to some shade of gray. Then, an object placed in the test section will appear on the screen as a black image (inverted) against a gray background.

When the wind tunnel is in operation, the interaction of the test model and the airflow creates regions of different densities (shock waves, flow separation, boundary layer) in the airflow. Light rays that pass through such regions of different densities are bent (refracted) so that they are no longer parallel to the average (unrefracted) rays in the beam. Therefore, these bent rays do not pass through the point image of the light source. As a result, these rays either completely miss the knife edge and create bright areas (brighter

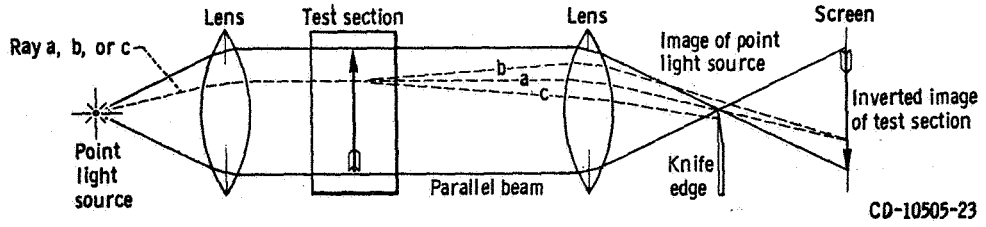

Ray	History
a	Passes through point image of light source; intensity reduced by knife edge; resulting image on screen same shade of gray as background
b	Misses point image of light source; misses knife edge; intensity undiminished; resulting image on screen brighter than background
c	Misses point image of light source; blocked by knife edge; resulting image on screen darker than background

Figure 14-8. - Schematic diagram of schlieren system.

than the background) on the screen, or they are completely blocked by the knife edge and create dark areas (darker than the background) on the screen. Thus, the image on the screen (which can be photographed) shows the locations of regions of different densities around the test model and shows whether these regions have higher or lower than average densities.

Schlieren photographs of a model of a Mach 5.0 air inlet at several free-stream Mach numbers are shown in figure 14-9. These photos indicate the shock positions and how they change with free-stream velocity. The boundary layer along the spike is also visible, since it is a region of low density. Because of the orientation of the knife edge, high-density regions appear as dark areas on the top half of the inlet and as light areas on the bottom half. A schlieren photograph of the flow over a model of the Mariner payload shroud with the Agena second stage is shown in figure 14-10.

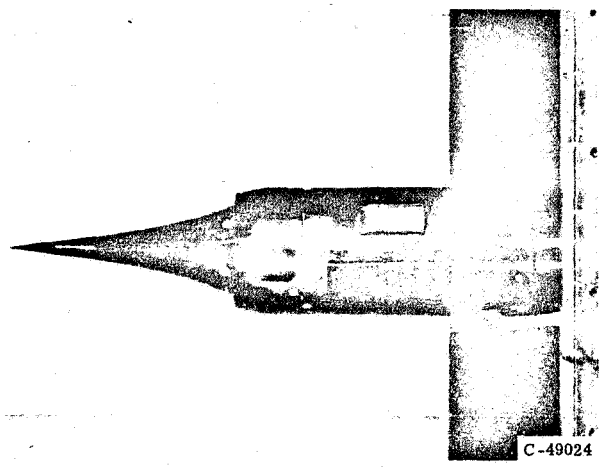

(a) Model of inlet.

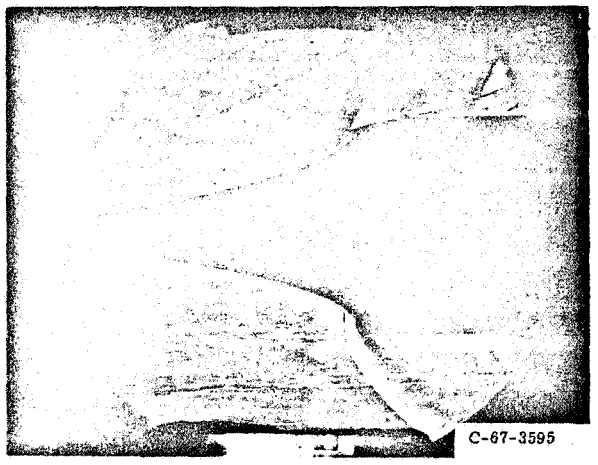

(b) Free-stream Mach number, 2.43.

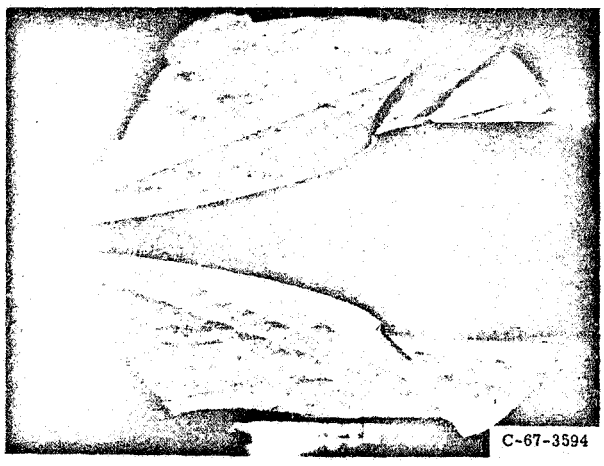

(c) Free-stream Mach number, 3.43.

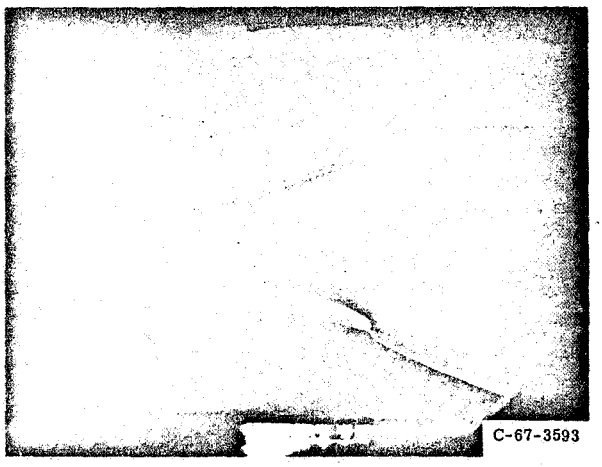

(d) Free-stream Mach number, 4.97.

Figure 14-9. - Schlieren photographs showing shock waves on model of Mach 5 air inlet operating at various free-stream Mach numbers. (Schlieren photographs taken in 1- by 1-Foot Variable Mach Number Wind Tunnel.)

(a) Test model.

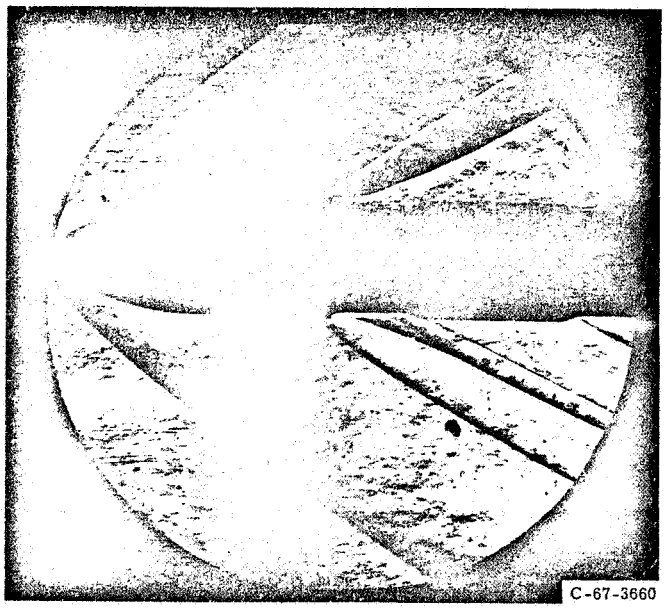

(b) Schlieren photograph (taken in 10- by 10-Foot Supersonic Wind Tunnel).

Figure 14-10. - Schlieren photograph showing shock structure on model of Mariner payload shroud with second-stage Agena. Free-stream Mach number, 2.0; angle of attack, -2°; altitude, 50 000 feet.

Shadowgraph System

In the shadowgraph system (fig. 14-11), light from a point source on one side of the test section is bent by a lens into a beam of parallel rays. As these parallel rays pass through the test section, they are bent by any density gradients that may be present. The light rays are then projected on a screen. The high-density regions of the test section

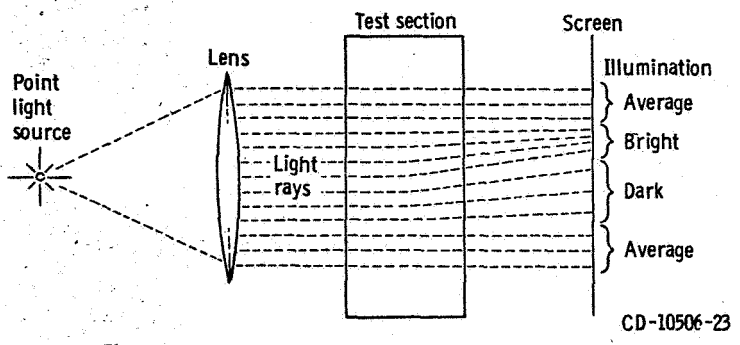

Figure 14-11. - Schematic diagram of shadowgraph system.

appear as dark areas on the screen. Figure 14-12 shows a shadowgraph of the Mach 5.0 isentropic spike air inlet (same inlet as in fig. 14-9) operating at a free-stream Mach number of 1.97. The shadowgraph shows shock waves and regions of local flow separation behind the strong shock wave on the inlet spike.

Schlieren photographs and shadowgraphs can provide both qualitative and quantitative results. For example, not only can the shock waves be observed, but their angles and locations can be accurately measured from the pictures. Usually, flow-field details such as boundary-layer thickness, local pressure variations, and flow velocities must be measured with other instrumentation.

INSTRUMENTATION

In addition to the optical systems described in the preceding section, the engineer can also use a variety of instrumentation to obtain information from wind-tunnel tests. Some of the basic instruments used for steady-state and transient measurements in wind tunnels are described briefly herein. A more thorough discussion of instrumentation is presented in chapter 13.

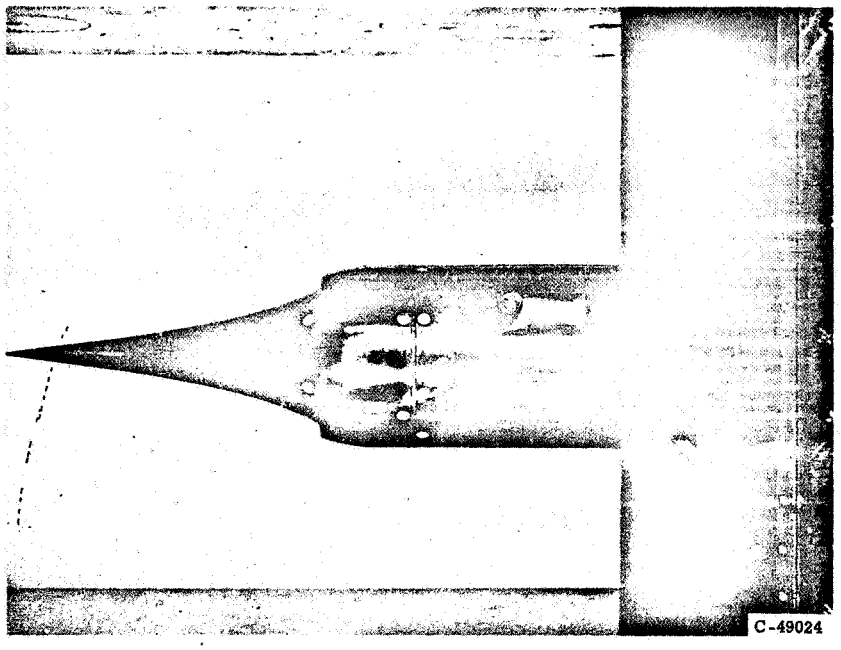

(a) Model inlet.

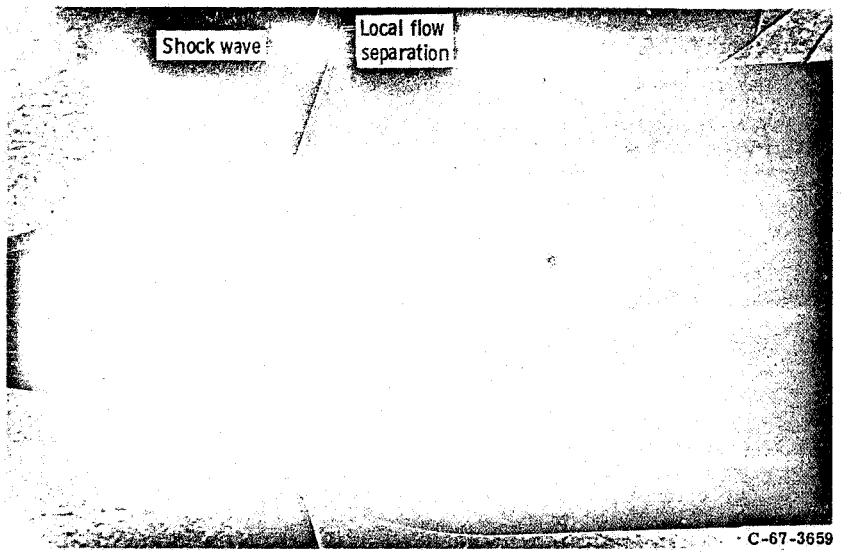

(b) Shadowgraph.

Figure 14-12. - Shadowgraph of model of Mach 5 air inlet operating at Mach 1.97 in the 18- by 18-Inch Supersonic Wind Tunnel.

Steady-State Measurements

Most wind-tunnel data are recorded at various steady-state conditions (i. e., conditions that are not varying with time) of the free-stream flow and test-model attitude. Local flow conditions over the test model are measured with static-pressure orifices and total-pressure, or pitot-pressure, rakes. Small wedges (fig. 14-5) can also be us to provide local Mach number and flow angularity. Temperatures are measured with thermocouples. Forces can be determined by integrating large numbers of static pres· sures or by use of a force balance. Pressure integration is not as accurate as the dire balance reading and requires a large amount of instrumentation. Normal procedure is use a balance for a direct measurement of forces and to supplement these measuremen with general information from static-pressure and pitot-pressure measurements.

Transient Measurements

Sometimes it is desirable or necessary to obtain data under transient conditions (i. e., conditions that are changing with time). For example, it may be necessary to measure the fluctuating pressures in the unsteady flow that exists in regions of flow sep aration or in regions where shock waves interact with the boundary layer. Transient measurements are also required to obtain heat-transfer coefficients in thermal tests. The use of an intermittent wind tunnel (blowdown or indraft) necessitates transient mea: urements, because the airflow in such a tunnel varies with time. Transient measureme in wind-tunnel models can be made with transducers, calorimeters, and accelerometer

REFERENCE AXES

Force balances have been mentioned as one method of directly measuring the force on a test model. The forces or moments acting on an object are measured along or around three mutually perpendicular reference axes. These reference axes may be the wind axes, the body axes, or the stability axes.

Wind-Axis System

Wind-tunnel tests of the external flow and forces on an aerodynamic shape are pri- marily concerned with the wind-axis system (fig. 14-13(a)). Lift, drag, and yaw force: are always measured with respect to the direction of the relative wind. In a wind tunne:

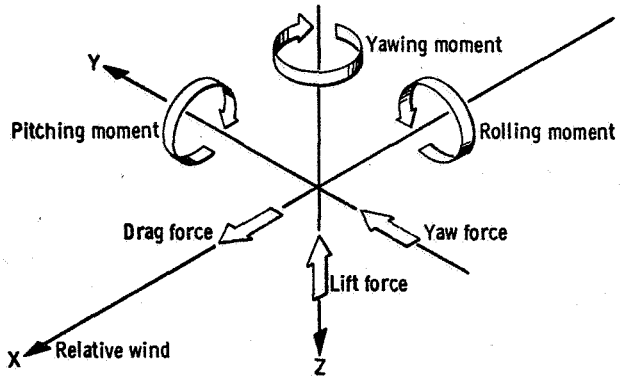

(a) Wind-axis system.

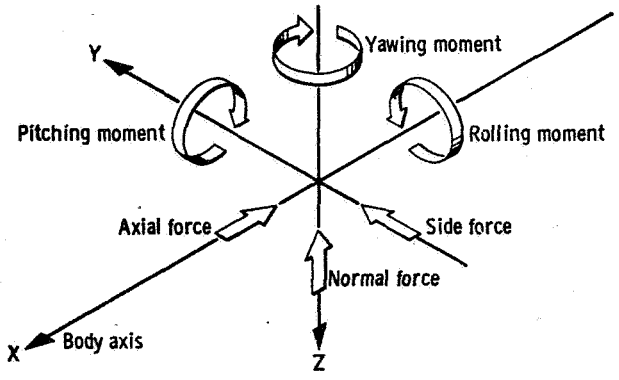

(b) Body-axis system.

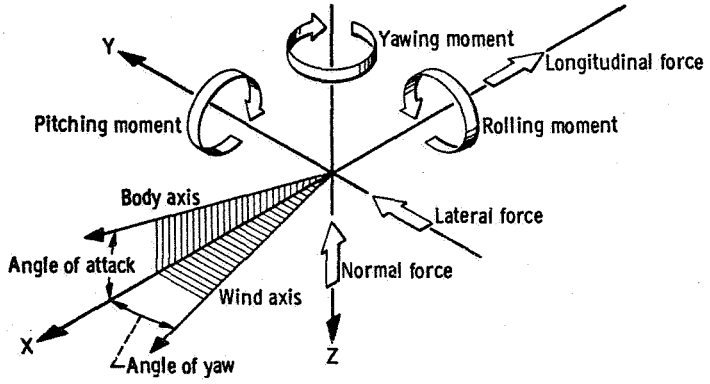

(c) Stability-axis system.

Figure 14-13. - Reference axes for force measurements in wind tunnels. (Arrows indicate positive directions of axes, forces, moments and displacements.)

the relative-wind direction (and the drag axis) is along the axis of the tunnel. The angle that the longitudinal body axis of the test model makes with the relative wind direction is referred to as the "angle of attack" in the pitch plane and the "angle of sideslip" in the yaw plane.

Body-Axis System

The body-axis system (fig. 14-13(b)) is one in which the axes move with the vehicle, and the resulting forces (axial, normal, and side) are measured relative to the longitudinal body axis of the test model. The forces and moments along and around these body axes are measured directly with an internal six-component balance. This axis system is normally used in propulsion tests, since the thrust of a vehicle or a nacelle is usually along the longitudinal body axis. In some propulsion tests, only one component of force is required. For example, for a nacelle mounted rigidly in the wind tunnel at zero angle of attack, the engineer is primarily interested in the single measurement of the resulting axial force (thrust or drag). This force can be measured with a single-component balance.

Stability-Axis System

The stability-axis system (fig. 14-13(c)) is a combination of the previous two systems. In the pitch plane (X - Z), the axes are alined with and perpendicular to the relative-wind direction. In the yaw plane (X - Y), the axes move with the body and are alined with and perpendicular to the longitudinal body axis. No matter which of the three sets of reference axes is used, the measured forces and moments can be easily converted from one system to the other by simple geometrical relations.

WIND-TUNNEL APPLICATIONS

Wind tunnels can be used for a wide variety of tests. The test models can be aircraft and missiles (scale models, full-scale vehicles, or full-scale components), boats, automobiles, bridges, buildings, propulsion systems (reciprocating engines with propellers, turbojets, ramjets, rockets), etc.

Most of the wind-tunnel testing here at the Lewis Research Center concerns the aerodynamics and thermodynamics of propulsion systems. The 8- by 6-foot and 10- by 10-foot wind tunnels were designed specifically for this purpose. These propulsion facilities can operate on two distinct cycles, propulsion or aerodynamic. For propulsion tests, when

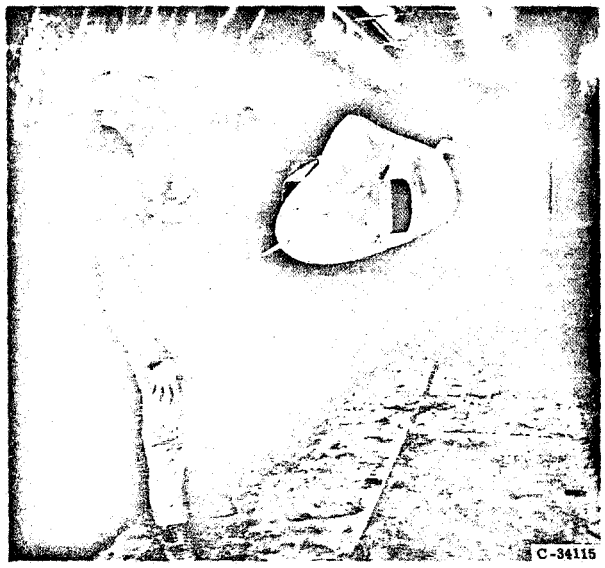

(a) Air inlet (1/4-scale model of F-102 forebody).

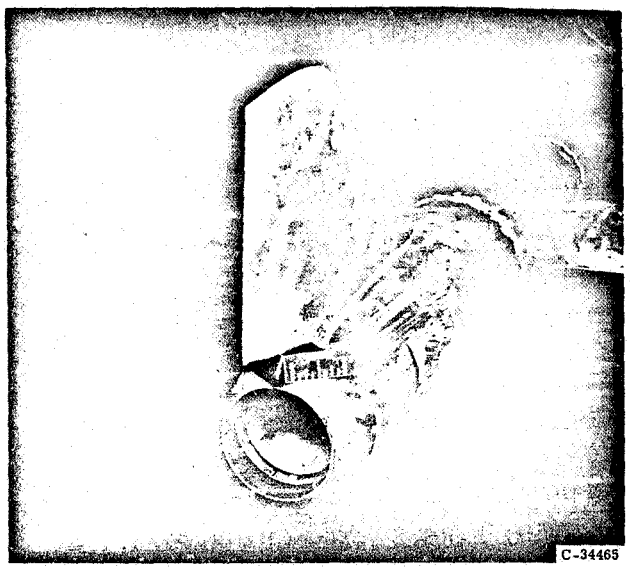

(b) Exhaust nozzle (model of F-104 afterbody).

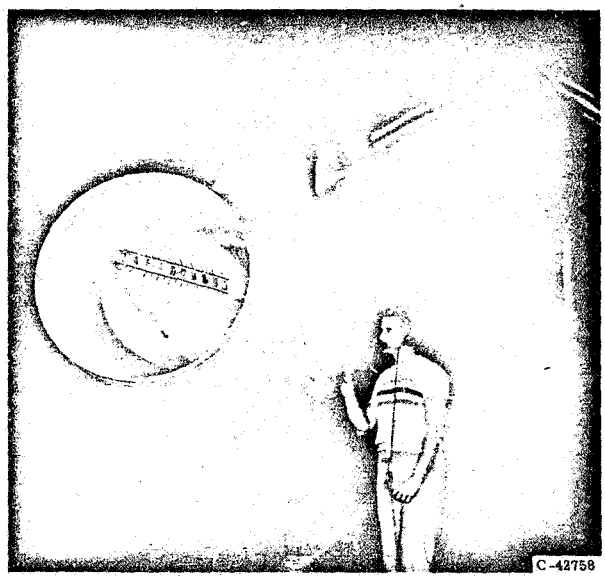

(c) Engine nacelle (full-scale B-58 nacelle, complete with G.E. J79 turbojet engine).

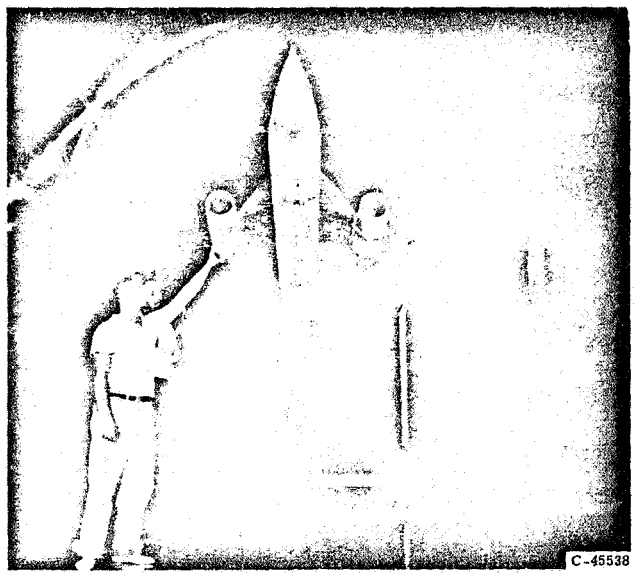

(d) Nacelle - airframe configuration (supersonic airplane model).

Figure 14-14. - Wind-tunnel installations for testing propulsion systems and/or their components.

(a) Saturn C-1, 1/27 scale. (Base-heating measurements.)

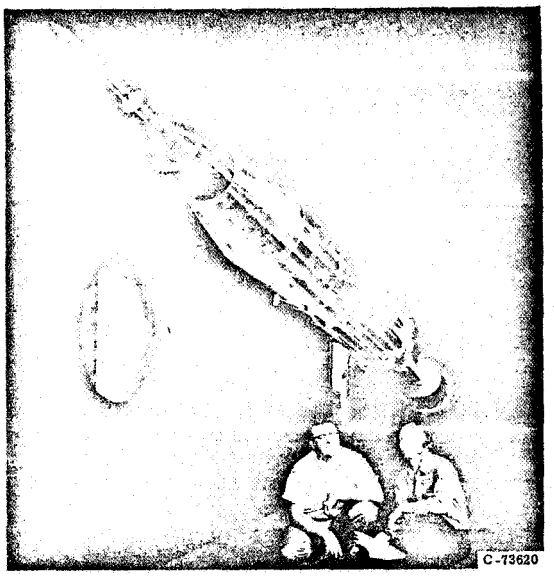

(b) Saturn S-1B, 1/20 scale. (Measurements of fin forces.)

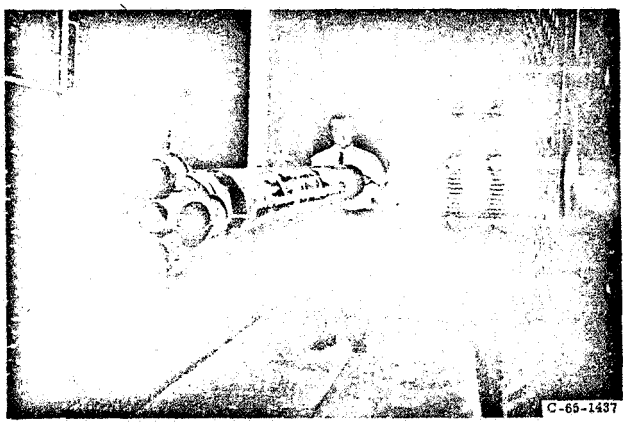

(c) Saturn 5, 1/45 scale. (Base-heating measurements.)

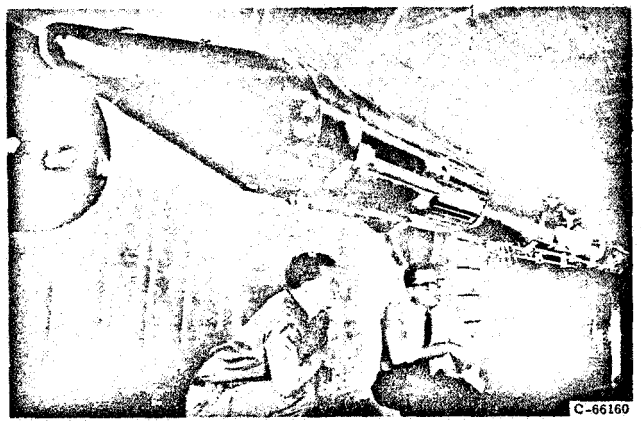

(d) Atlas/Centaur with Surveyor payload shroud, 1/10 scale. (Tests of hydrogen vent.)

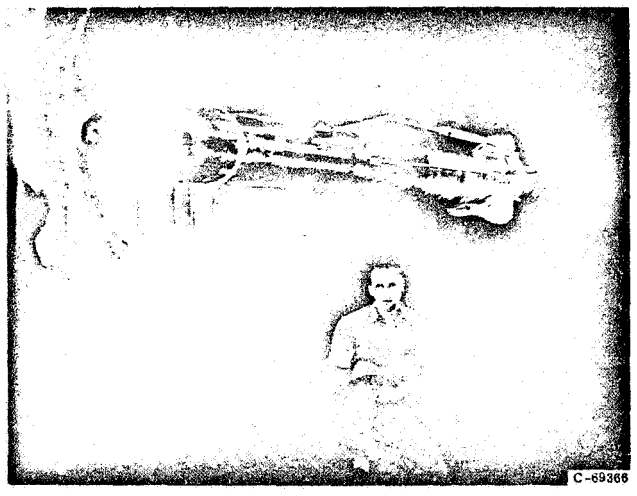

(e) Atlas/Agena with Mariner payload shroud, 1/10 scale. (Measurements of dynamic pressures.)

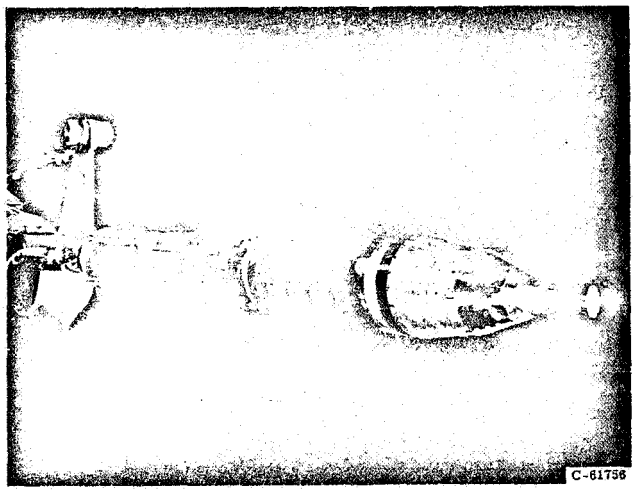

(f) Titan-Gemini, 6-percent scale. (Measurements of aerodynamic forces.)

Figure 14-15. - Wind-tunnel installations of boost vehicles.

operating engines are being studied, the air is brought through the test section once and is discharged back to the atmosphere (open circuit). For aerodynamic tests, the air is allowed to recirculate continuously (closed circuit). These facilities can be operated continuously on the propulsion cycle at supersonic speeds with the use of large air dryers. The expansion process by which supersonic velocities are achieved in the test section causes the air temperature to drop to sub-zero levels. Any moisture present in the airstream would condense in the nozzle and result in nonuniform flow conditions. It is therefore necessary to dry the air before it enters the tunnel, and this function is performed by the air dryer, where many tons of activated alumina act as a desiccant. Running time on the propulsion cycle is limited by the capacity of the dryer beds.

Some examples of the types of tests that have been performed in the Lewis propulsion wind tunnels in the past 15 years are illustrated in figures 14-14 and 14-15. Air-inlet tests have been conducted on most of the existing supersonic fighter planes and bombers, including the F-102 (fig. 14-14(a)), F-104, F-106, F-107, F-111, B-58, B-70, etc. Exhaust-nozzle tests have been conducted for the F-104 (fig. 14-14(b)), B-70, B-58, SST, etc. A complete nacelle for the B-58 bomber (fig. 14-14(c)) was tested at Mach 2.0 in the 10- by 10-Foot Supersonic Wind Tunnel prior to the first supersonic flight of that aircraft. This pod included both the full-scale inlet and the operating J79 turbojet engine. More recent tests have supported the development of the Saturn 1 (figs. 14-15(a) and (b)) and Saturn 5 (fig. 14-15(c)) boost vehicles and the development of the Atlas/Centaur (fig. 14-15(d)) and Atlas/Agena (fig. 14-15(e)) vehicles managed by the Lewis Research Center.

CONCLUDING REMARKS

This chapter has presented a brief discussion of items that should be considered in the design and operation of wind tunnels (e.g., general wind tunnel types, power requirements, methods of supplying power, etc.). Some examples have been presented of typical calibration probes, support systems, visual flow-observation techniques, instrumentation, and models tested in the Lewis Research Center propulsion wind tunnels. It has been demonstrated over the years that wind tunnels can provide useful design information for a large variety of configurations for a modest expenditure of time, money, and manpower. Rigorous testing of subscale and full-scale models in wind tunnels prior to flight has proven to be a logical first step in the orderly development of flight systems.

REFERENCE

1. Goddard, Vincent P.: Development of Supersonic Streamline Visualization. University of Notre Dame, Mar. 1962 (NSF Grant 12488).

BIBLIOGRAPHY

Pope, Alan: Wind-Tunnel Testing. Second ed., John Wiley & Sons, Inc., 1954.

Pope, Alan; and Goin, Kennith L.: High-Speed Wind Tunnel Testing. John Wiley & Sons, Inc., 1965.

Pope, Alan; and Harper, John J.: Low-Speed Wind Tunnel Testing. John Wiley & Sons, Inc., 1966.

15. NAVIGATION

William H. Swann*

Because navigation is a broad and complex subject, a thorough explanation of it in a single chapter is impossible. Therefore, the discussion herein is limited to some of the fundamentals of air navigation. Celestial-navigation methods are not discussed at all.

For the purposes of navigation, the Earth can be considered to be a perfect sphere. This is not truly correct, but it is within the accuracy of the present methods of determining position, and the assumption greatly simplifies the calculations.

INTERSECTION OF A SPHERE WITH A PLANE

If any sphere is cut by a plane, the intersection of the two surfaces is a circle. At one extreme, where the plane is just tangent to the surface of the sphere, the intersection is only a point. As the cutting plane is moved deeper into the sphere, the circle of intersection grows larger. The largest circle is achieved when the cutting plane includes the point center of the sphere and the circle has the same radius as the sphere. Then, regardless of the direction in which the cutting plane is moved away from the center, the circle can only grow smaller. The largest circle that can be formed by this intersection, when the cutting plane contains the center of the sphere, is called a great circle. All the other circles are called small circles. A grid system, consisting of such circles, on the Earth's surface provides a universal method of identifying any point on Earth without reference to landmarks or place names.

Parallels of Latitude

A sphere is a continuous surface, without beginning or end. This is also true of the

*Chief, Aircraft Operations Branch.

Earth, whose only distinctive natural reference line is its axis of rotation, or polar axis. Thus, the poles are distinctive points on Earth, and the polar axis serves as the central axis for one set of reference circles (fig. 15-1). The most important circle of this set is the equator, a great circle halfway between the poles. The plane of the equator is perpendicular to the Earth's polar axis and divides the Earth into a northern and a southern hemisphere. Any small circle whose plane is parallel to the equator is called a parallel of latitude, or simply a parallel. Each parallel is everywhere equidistant from the poles, from the equator, and from every other parallel. Every point on the earth has a parallel passing through it which is designated by its angle to the north or south of the equator, measured from the center of the Earth.

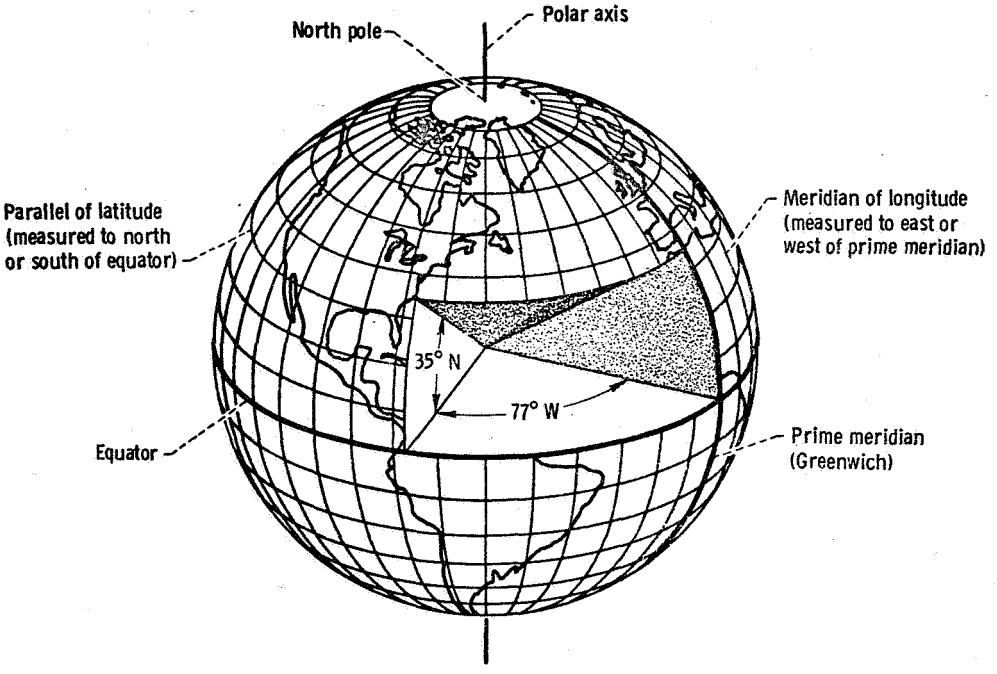

Figure 15-1. - Terrestrial grid system comprised of parallels of latitude and meridians of longitude.

Meridians of Longitude

A great circle passing through the poles is a meridian of longitude, or simply a meridian. Meridians correspond to the north - south streets of a city. Since all merid-

ians are great circles, none of them is distinctive, as is the equator among the parallels. Therefore, one meridian must be selected arbitrarily as a prime, or reference, meridian. In English-speaking countries and many others, the great circle passing through the observatory at Greenwich, England, is used as the prime meridian, and the other meridians are identified by their angular distance to the east or west of Greenwich.

GRID SYSTEM

The parallels and meridians intersect to form a grid system, as shown in figure 15-1. Any point on Earth can be identified by naming the parallel and meridian which pass through it. Thus, the 40° N. parallel and the 75° 10' W. meridian designate the location of Philadelphia. These coordinates are called latitude and longitude. The latitude of a point is its angular distance north or south of the equator and ranges from 0° at the equator to 90° N. and 90° S. at the poles. The longitude of a point is its angular distance east or west of the prime meridian (Greenwich) and ranges from 0° at the prime meridian to 180° E. or 180° W. of the prime meridian.

An important characteristic of a great circle (not necessarily a meridian) is that it marks the shortest distance between two points on the surface of the Earth. Actually, the shortest distance between any two points is along the straight line between them. However, if the two points are located on the surface of a sphere the straight line between them passes beneath the surface. Therefore, the shortest route along the surface of a sphere (e.g., the Earth) between two points is that route which most closely approximates a straight line. Any route between two points on the Earth's surface is curved. The least curved, and shortest route is the one whose radius of curvature is greatest. The maximum radius of curvature is the radius of the Earth (i.e., the radius of a great circle). Therefore, the shortest route between two points is an arc of the great circle that passes through the two points.

CHARTS (MAPS)

Now that we have described a grid system for naming positions on the Earth's surface, we must have some way of making this information available to the navigator. To do this we use a chart, or map. A chart is a diagrammatic representation on a flat surface of a portion of the curved surface of the Earth.

Desirable Characteristics

The Earth is a sphere and cannot be represented on a flat surface without some type of distortion. It can be truly represented only on a sphere, or globe. This is useful for some purposes. For navigation, however, it is inconvenient to carry and store a globe, even in sections. Therefore, navigational charts are always printed on flat sheets of paper. A chart should have the following desirable characteristics:

(1) The scale should be constant over the whole map.

(2) Angles should be accurately drawn.

(3) Great circles should be shown as straight lines.

(4) Rhumb lines (i.e., lines that cross successive meridians at a constant angle) should be shown as straight lines.

(5) Coordinates should be easy to find and easily plotted.

(6) Charts of adjacent areas of the same scale should be easily joined.

(7) Each cardinal direction (north, south, east, and west) should point the same way on every part of the chart.

(8) The chart should be simply and easily constructed.

(9) Equal areas should be shown equal.

Unfortunately, it is impossible to construct a chart which has all these features. In fact, some of them are mutually exclusive. Therefore, it is necessary to select the method of chart construction which fulfills the requirements of the particular mission. We draw our chart by locating the geographic features in a grid of meridians and parallels, known as a graticule. The construction of this grid is the critical part of the chart-making process, for this determines which of the characteristics the particular chart will have.

Projections

The two most common methods of chart construction are the Lambert projection and the Mercator projection.

Lambert projection. - The Lambert conformal conic projection is illustrated in figure 15-2. In this system, the surface features of the Earth are projected from the center point of the Earth onto the surface of a cone that intersects the Earth's surface along two parallels of latitude. The surface of the cone enters the Earth's surface at one parallel and emerges at another. These two parallels are called the standard parallels. The limits of the projection are parallels slightly beyond, or outside, the two standard

parallels. The apex, or tip, of the cone is outside the Earth and on the polar axis. The cone is coaxial with the Earth.

When the cone is unrolled on a plane surface, the resulting graticule shows parallels of latitude as concentric circles centered at the pole nearest the apex of the cone and shows meridians of longitude as straight lines converging on this pole. Thus, the meridians are normal to the parallels (i.e., the meridian is perpendicular to the line that is tangent to the parallel at the point of intersection).

With the Lambert projection, the angles formed at a given point of intersection of a meridian and a parallel are the same on the surface of the cone (or the chart) as on the surface of the Earth. Therefore, any other angles formed by the intersections of any other lines are also the same on both surfaces. Consequently, the Lambert projection is conformal. This means that the features of the Earth's surface retain their shapes on the chart.

The great advantage of a Lambert chart over other charts is that the scale of distance is practically constant over the entire chart (i.e., within the limits of the projection). Thus, the features of the Earth's surface retain their relative sizes on the chart. Actually, the scale is accurate along the standard parallels, is slightly reduced between the two standard parallels, and is slightly increased between the standard parallels and the limits of projection. For example, the standard parallels normally used for a Lambert projection of the United States are 33° and 45° North. Between parallels $30^{\circ}30'$ and $47^{\circ}30'$ North, the maximum error in the scale is only 1/2 percent. The maximum error for the entire chart of the United States is $2\frac{1}{2}$ percent in southern Florida.

Any straight line on a Lambert chart is very nearly a great circle. In the 2572 statute miles between New York City and San Francisco, the great circle and the straight line connecting them on a Lambert chart are only 9.5 miles apart at midcourse; for shorter lines the deviation is even less. Therefore, for practical purposes a straight line on the Lambert chart may be considered a great circle. A rhumb line (i.e., line of constant direction) is shown as a curved line. Between New York City and San Francisco, the rhumb line departs about 170 miles from the straight line.

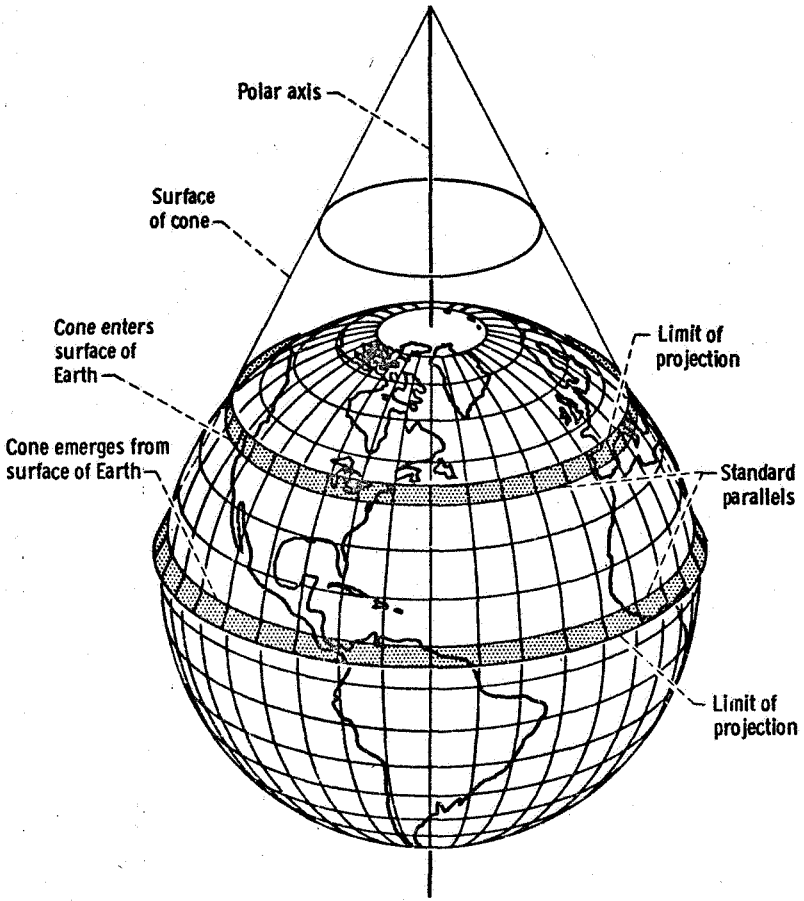
Polar axis
Surface of cone
Cone enters surface of Earth
Cone emerges from surface of Earth
Limit of projection
Standard parallels
Limit of projection

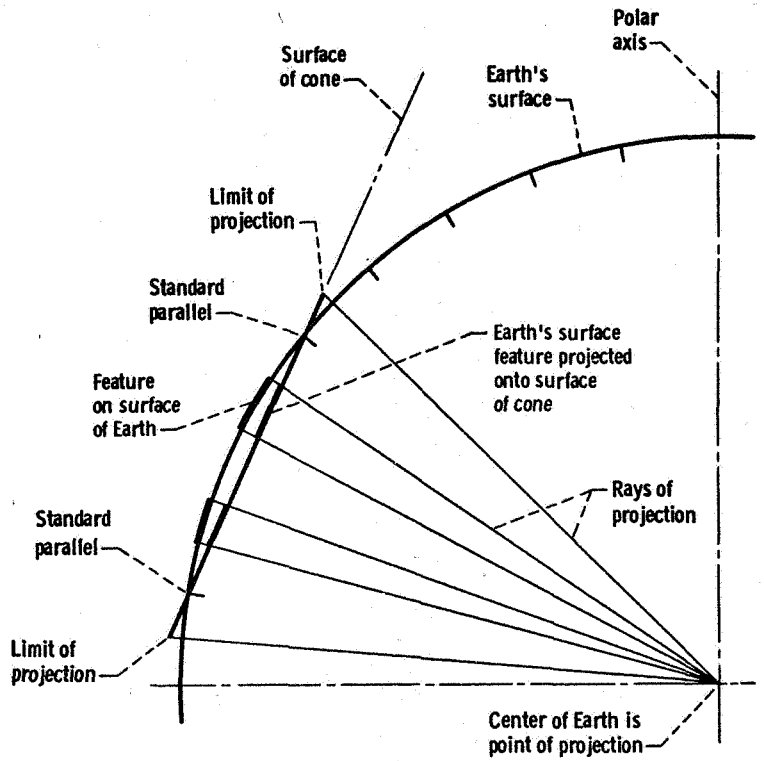
Polar axis
Surface of cone
Earth's surface
Limit of projection
Standard parallel
Earth's surface feature projected onto surface of cone
Feature on surface of Earth
Rays of projection
Standard parallel
Limit of projection
Center of Earth is point of projection

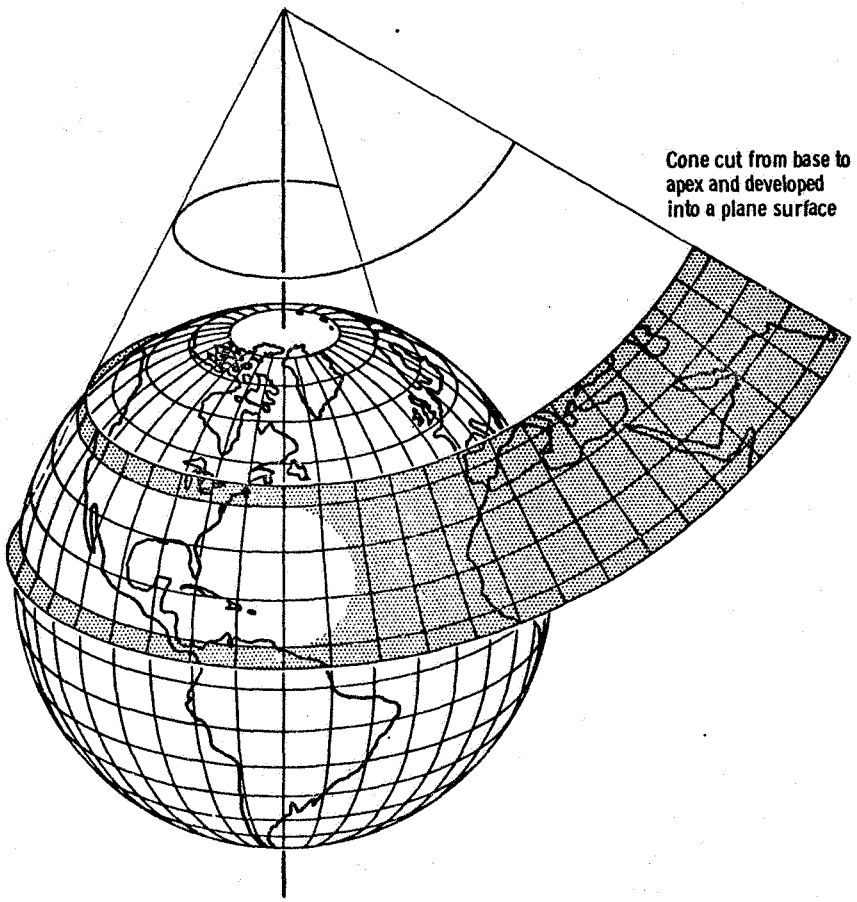

Figure 15-2. - Lambert conformal conic projection.

Mercator projection. - The Mercator conformal projection is basically a modified cylindrical projection. In a cylindrical projection (fig. 15-3), the surface features of the Earth are projected from the center point of the Earth onto the surface of a cylinder that is tangent to the Earth's surface along the equator. When the cylinder is unrolled on a plane surface, the resulting graticule consists of parallels of latitude and meridians of longitude that are straight and perpendicular to each other. The parallels of latitude are parallel and equal in length, and the spacing between them increases with increasing distance north or south of the equator. The meridians of longitude are parallel, equal in length, and equally spaced.

The increasing spacing between parallels of latitude to the north or south of the equator results in increasing distortion, or stretching, in the longitudinal (north-south) direction. With increasing distance to the north or south of the equator, there is also an increasing distortion in the latitudinal (east-west) direction. The reason for this is that in a cylindrical projection the parallels of latitude are equal in length, while on the surface of the Earth (a sphere) they become shorter with increasing distance from the equator. However, the longitudinal and latitudinal distortions are unequal. Therefore, a cylindrical projection changes the shapes, as well as the sizes, of the surface features of the Earth.

In a Mercator projection the graticule is modified (i.e., the spacing of the parallels of latitude is altered) so that at any point on the chart the scale is constant in all directions, and the longitudinal and latitudinal distortions are equal. Thus, small areas of the Earth's surface retain their correct shapes. However, the expanding scale does cause distortion in the shapes of large areas that extend for long distances to the north or south of the equator. The relative sizes of the Earth's surface features on the Mercator chart increase with increasing distance from the equator.

The principal feature of the Mercator chart is that a straight line connecting any two points gives the true direction between them and crosses all meridians at the same angle. Therefore, any such straight line on the map is a rhumb line. This feature is of great value in navigation because aircraft are commonly flown along rhumb lines. A rhumb line is not the shortest distance between two points, but for navigation purposes it represents the easiest and simplest course.

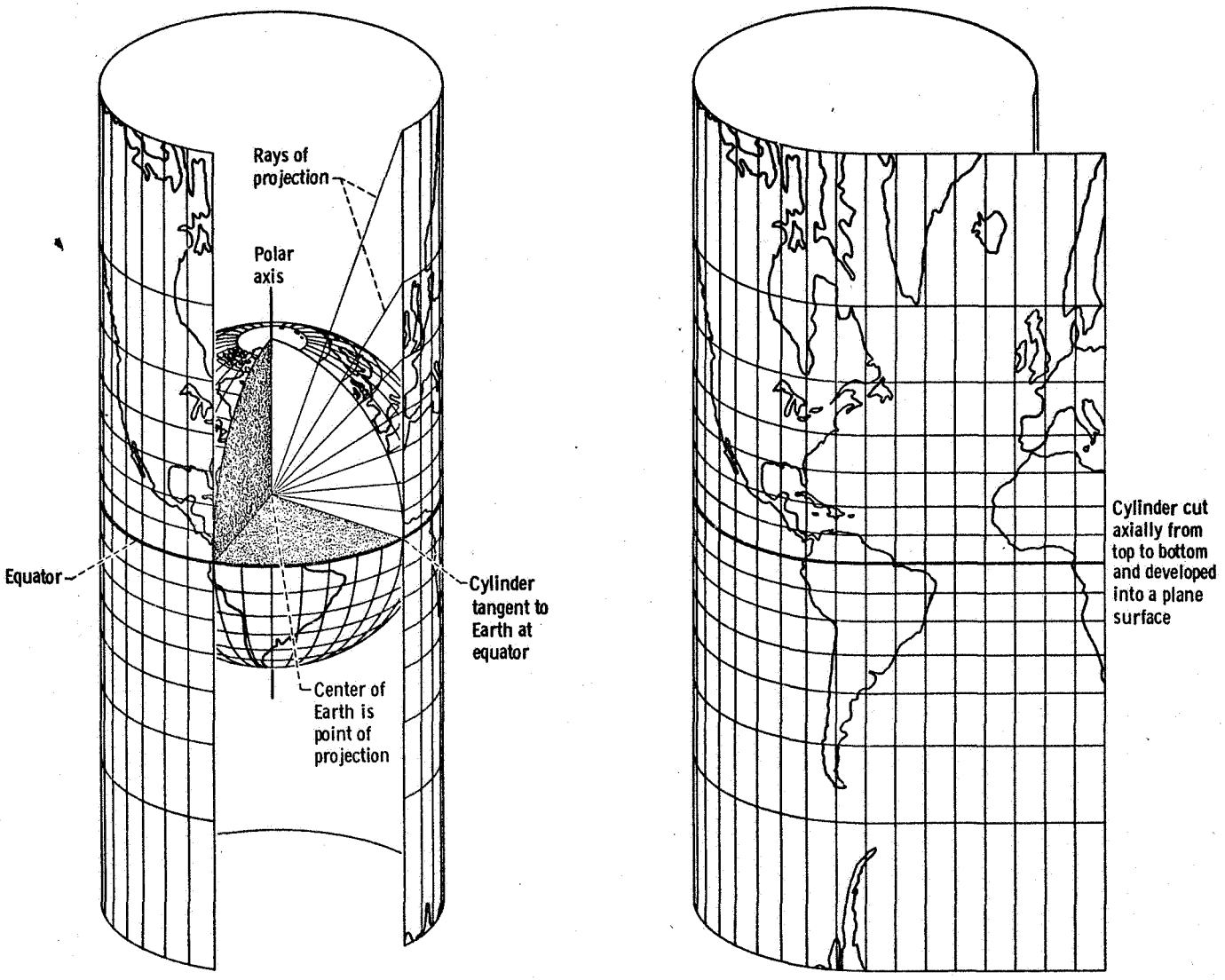

Figure 15-3. - Mercator cylindrical projection.

Scale

The scale of a chart is the ratio of a distance on the chart to the corresponding distance on the surface of the Earth. Charts are made to various scales for different purposes. If a chart is to show a large area of the Earth and not be too large, it must be drawn to a small scale. If it is to show much detail and not be cluttered, it must be drawn to a large scale. For the same size chart, a large-scale chart will show a much smaller area than a small-scale one.

The scale may be expressed by a simple statement, such as "1 inch equals 10 miles." It may be given as the representative fraction, such as "1:500 000" or "1/500 000." This means that 1 inch on the chart represents 500 000 inches (6.85 nautical miles) on the Earth's surface. Scale may be shown graphically on the chart by a graduated line labeled in terms of the distance it represents on the Earth's surface.

Features Shown on Aeronautical Charts

An aeronautical chart does not show all details of the Earth's surface. Instead, it shows and emphasizes those particular features which are useful to the airman. It shows those features which have the most distinctive appearance from the air. Some features are shown out of proportion to their true size for emphasis. For instance, the lines representing roads on sectional and regional charts may appear to be 1/4 mile wide if measured by the scale of the chart. Radio stations are prominently shown, although many are inconspicuous from the air. The following items are usually shown on aeronautical charts:

(1) Man-made features - cities, roads, railroads, etc.
(2) Water - oceans, lakes, rivers, streams, reservoirs, etc.
(3) Relief - difference in elevation of terrain
(4) Aeronautical features - airports, lights, radio facilities, airways, restricted areas, etc.

The symbols representing these various features are standard for any one series of charts but may differ between series.

PLOTTING AND MEASURING COURSES

We will discuss plotting and measuring only with reference to the Lambert chart, as it is the most used in general aviation. Most of the techniques also apply to the Mercator charts.

Distance

A straight line on a Lambert chart is approximately a segment of a great circle. Therefore, a line drawn on the chart between the points of departure and destination represents the shortest distance between them. This length of line can be transferred with a rule or with dividers to the scale on the edge of the chart to find the mileage. Many aeronautical plotters have several of the most common scales, so they may be used to measure distance directly on the chart.

Heading

Since the meridians converge at the poles on the Lambert chart, the angle between a straight line and the meridians varies as the aircraft flies along the route. To avoid the difficulty of flying a varying heading, the angle can be measured at the halfway point between the origin and the destination. This angle gives the constant heading, or rhumb line, which can be followed for the entire trip. For a long trip the rhumb-line course is considerably longer than the great-circle (shortest) course. Therefore, for a long trip the straight line between the origin and destination is divided into several segments. The angle of the rhumb line for each segment is measured at the halfway point of the segment. Thus, a great-circle course is approximated by a series of rhumb lines.

Magnetic Compass

The preceding discussion dealt with direction in terms of angles related to the geographic poles, or true directions. This creates a problem. There is no simple instrument that can be carried on the airplane and can measure angles relative to the geographic poles. The magnetic compass can measure angles and can be carried on an aircraft, but it has certain disadvantages. For example, the Earth's magnetic poles do not coincide with the geographic poles. Thus, even if the magnetic compass could be made to always point exactly at the magnetic pole, a variable correction would still be required. The correction required depends on the location of the compass relative to the magnetic and geographic poles, as shown in figure 15-4. The problem is further complicated by local variations in the Earth's magnetic field. However, for most areas of the Earth's surface these variations are well charted, and the combined effect of the magnetic pole and the local magnetic field is plotted on aeronautical charts as a series of isogonic lines, or lines of equal magnetic variation (fig. 15-5).

Since a compass is affected by all magnetic fields, the aircraft itself also induces

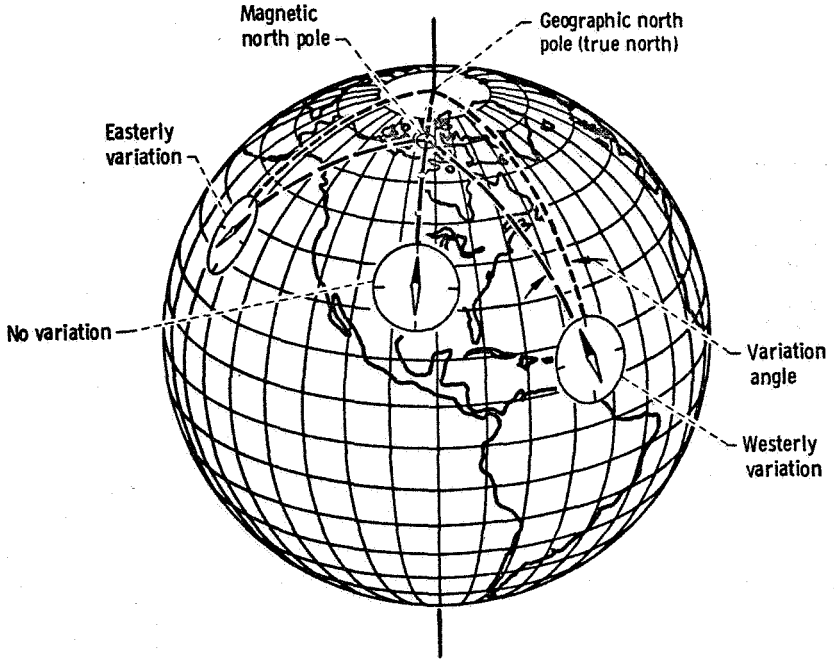

Figure 15-4. - Magnetic variation (declination).

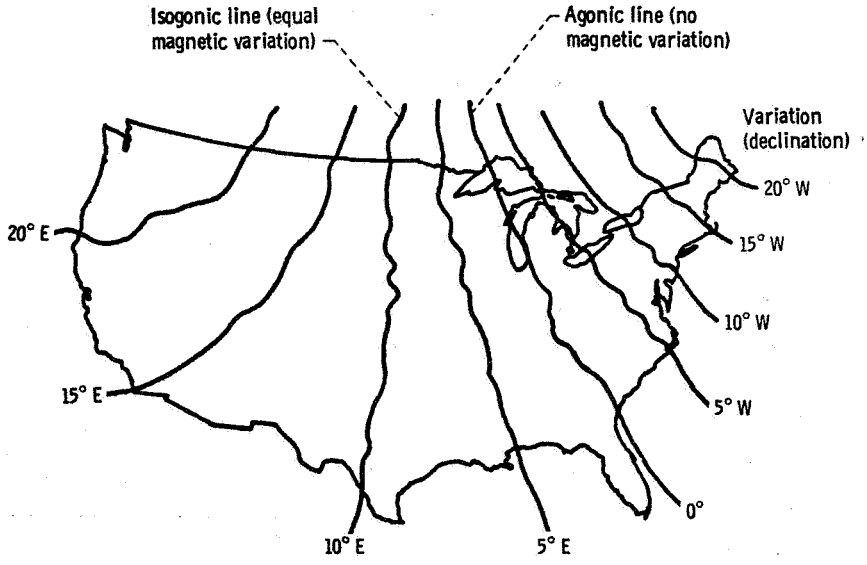

Figure 15-5. - Isogonic chart showing lines of equal magnetic variation (declination).

some error into the magnetic-compass system. The electrical systems of the aircraft create magnetic fields during operation. The ferrous parts of the aircraft also create magnetic fields that affect the compass. Hard landings, lightning strikes, and electrical storms can cause the local magnetic fields of the aircraft to change. Therefore, these magnetic fields must be checked periodically and recorded. The errors caused by local magnetic fields can be reduced by the use of compensating magnets located in or near the compass. But unless these errors are reduced to very small values of 1^{o} or 2^{o}, they should be taken into account when flying. The error due to these local magnetic fields is called "deviation."

Effect of Wind on Flight Path of Aircraft

Any vehicle on the ground, such as an automobile, moves in the direction in which it is headed or steered and is affected very little by wind. An aircraft, however, seldom travels in the exact direction in which it is headed. This is due to the effect of wind on the aircraft.

Wind is the movement of an air mass relative to the Earth's surface. Wind direction is expressed as the direction from which the air mass is moving and is measured clockwise from true north. Wind speed is the rate of motion relative to the Earth's surface.

Consider the effect of the wind on a balloon, which has no motive power of its own. If the balloon is tied to the Earth with a string, the wind blows past it, just as it blows past any fixed object on the Earth. If the balloon is released, it moves with the air mass (wind), just as a bottle floating in a river moves downstream with the current. If the wind is blowing at 20 miles per hour from the west, in 1 hour the balloon will be 20 miles east of the point where it was released.

Any free object in the air moves downwind with the speed of the wind. This is just as true of an aircraft as it is of the balloon. However, the aircraft in flight is also moving forward through the air mass. Therefore, as shown in figure 15-6, the motion of the aircraft relative to the ground is governed by the motion of the aircraft through the air mass and by the motion of the air mass (i.e., the wind) relative to the Earth's surface. Each of these motions is defined by its direction and speed. Therefore, these motions are vectors. (Vector quantities and vector relations are discussed in chapter 4.)

The air vector is defined by the airplane's true heading (i.e., direction in which airplane is pointed) and by its true airspeed (i.e., speed of airplane relative to surrounding air), expressed in nautical miles per hour, or knots. The wind vector is defined by the direction from which it is blowing and by its speed, also expressed in knots. The aircraft's flight path relative to the ground (i.e., the track of the aircraft) and its speed relative to the ground (i.e., its ground speed) define the ground vector. The ground vector

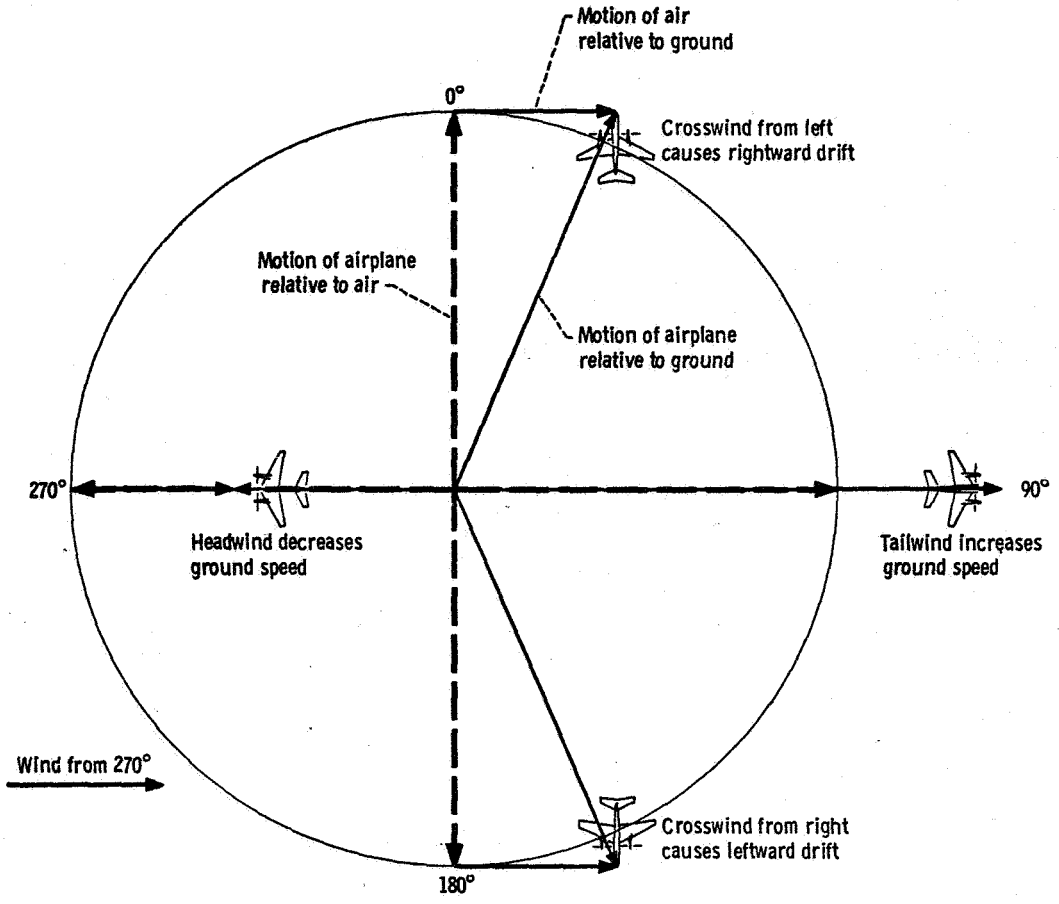

Figure 15-6. - Effect of wind on flight path of aircraft.

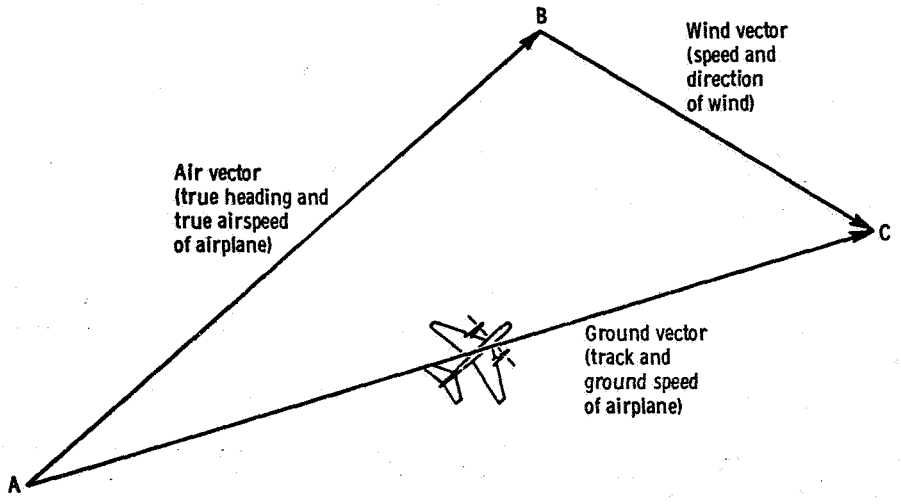

Figure 15-7. - Vector diagram showing relation of air, wind, and ground vectors.

is the resultant of the air and wind vectors and can be determined by means of a vector diagram, as shown in figure 15-7. From a given point (A) a line is drawn in the direction of the true heading of the airplane. The length of this line is drawn proportional to the true airspeed of the airplane. This line (A-B) represents the air vector. From the head (B) of this air vector a line is drawn in the direction in which the air mass is moving. The length of this line is drawn proportional to the wind speed. This line (B-C) represents the wind vector. Finally, a line is drawn between the starting point (A), or tail, of the air vector and the end point (C), or head, of the wind vector. This line (A-C) represents the ground vector. The length of this vector represents the ground speed of the aircraft. The direction of this vector is the direction of the actual flightpath, or track, of the aircraft.

Obviously, a complete vector diagram represents six quantities (direction and speed for each of the three vectors). If any four of these six quantities are known, the remaining two can be determined by drawing a vector diagram. The vectors may be drawn in any sequence. However, the air and wind vectors (i.e., the component vectors) must be drawn head to tail, and the ground vector (i.e., the resultant vector) must be drawn tail

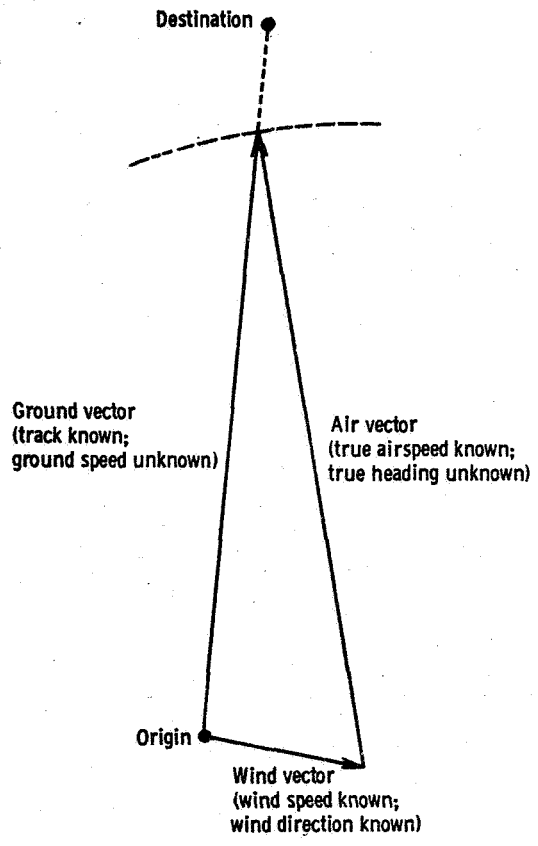

Figure 15-8. - Example vector diagram for common navigational problem of determining ground speed and true heading from known track, true airspeed, wind direction, and wind speed.

to tail with one of the components and head to head with the other.

A common navigational situation is one in which the track (course from origin to destination), the true airspeed, the wind direction, and the wind speed are known. The problem is to determine the ground speed (a ground-vector element) and the true heading (an air-vector element). The following method is used to draw the vector diagram (fig. 15-8). From the origin a line is drawn in the direction of the track that is necessary to arrive at the destination. Also from the origin, the wind vector is drawn. Next, an arc of a circle whose radius is equivalent to the true airspeed and which is centered on the head of the wind vector is drawn to intersect the line representing the track. Finally, a line drawn from the head of the wind vector to this intersection completes the vector diagram. The direction of this line, relative to true North, is the true heading; this is the direction in which the aircraft must be pointed in order to fly the desired track over the ground. The ground speed of the aircraft is represented by the length of the line segment from the origin to the intersection of the track and the arc that marks the airspeed.

NAVIGATION SYSTEMS

The preceding discussion pertained to navigation by visual reference to the Earth's surface or by estimation of the effects of wind on the flight path, called dead reckoning. These methods work well when reference to visible landmarks can be maintained, at least at frequent intervals, but they cannot provide sufficient accuracy for safe operation under conditions of poor weather or for long flights over water. For this type of operation it is necessary to use some navigational aid, or system, that does not require visible landmarks. Some of the currently used navigation systems are discussed briefly in the following sections.

Radio Compass

The radio compass is an instrument that indicates the direction, or relative bearing, of any transmitting station within its frequency range of 100 to 1750 kilohertz (kHz).

The operation of the radio compass is dependent upon the characteristics of a loop antenna. A loop receiving antenna gives maximum reception when the plane of the loop is parallel to, or in line with, the direction of radio wave travel. As the loop is turned from this position, volume gradually decreases, and reaches a minimum when the plane of the loop is perpendicular to the direction of wave travel. The null position (i.e., the position of minimum or zero signal strength) is used for direction finding, as it can be more accurately determined. For a 25^{o} rotation from the maximum signal position,

total signal strength changes less than 10 percent. For the same rotation from the null position, the signal strength changes by 50 percent.

When the loop is rotated to a null position, the radio station being received is located along a line that is perpendicular to the plane of the loop. However, the radio station may be located on either side of the plane of the loop, along this line. Therefore, the loop antenna has a 180° ambiguity. This ambiguity can be eliminated by turning the aircraft briefly to a course perpendicular to the radio beam. When the aircraft is first turned to this new course, the plane of the loop antenna in the null position is parallel to the course. As the aircraft flies along this straight-line course, the antenna must be rotated either clockwise or counterclockwise to maintain it in the null position. Clockwise rotation indicates that the station is to the right of the aircraft, and counterclockwise rotation indicates that it is to the left. Thus, the 180° ambiguity is eliminated, and the aircraft can then be turned back to its original course.

The 180° ambiguity of the loop antenna may also be avoided by connecting the receiver to an additional, omnidirectional antenna. This system (by a process of addition or subtraction of signal voltages from the two antennas) provides a single null, so that the direction to the station is known immediately. This arrangement also allows connection to an automatic servo system which will drive the loop to this single null position and indicate it to the pilot. The Automatic Direction Finder (ADF) is the configuration most used in today's aircraft.

Very-High-Frequency Omnidirectional Radio Range (VOR)

The Very-High-Frequency Omnidirectional Radio Range system, commonly called VHF omnirange, VOR, or omni, is the basic component of the navigation system of the airways in the United States and is coming more into use in other countries. It simplifies the task of navigation and eliminates most of the problems of static and interference found in the low-frequency navigation systems.

The operation of the VOR system is based on the creation of a phase difference between two transmitted signals. One of these signals, called the reference-phase signal, is radiated from the station in a circular, or omnidirectional, pattern. The other signal, called the variable-phase signal, is transmitted as a rotating field. This signal pattern rotates uniformly at 1800 revolutions per minute, which causes the phase of the signal to vary at a constant rate. Therefore, there is a different phase of this signal at each direction from the station. The difference in phase between the reference and variable signals is measured electronically by the aircraft receiver and indicates the direction from the transmitting station to the aircraft. This phase relationship between the two signals is illustrated in figure 15-9.

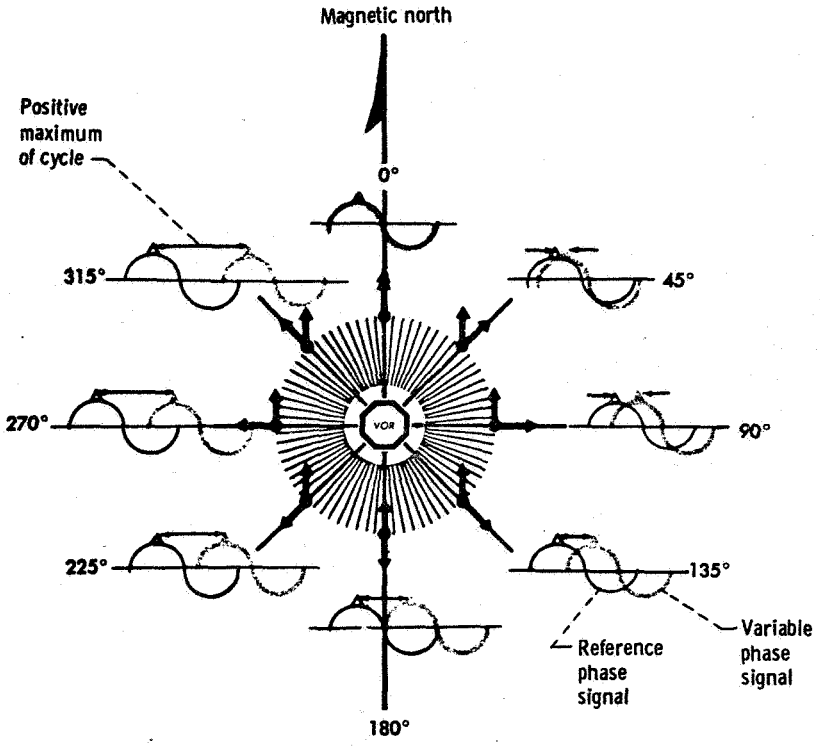

Figure 15-9. - Signal phase angle relation for VOR navigation system. (Signals from VOR station are in phase at magnetic north and vary elsewhere around the station.)

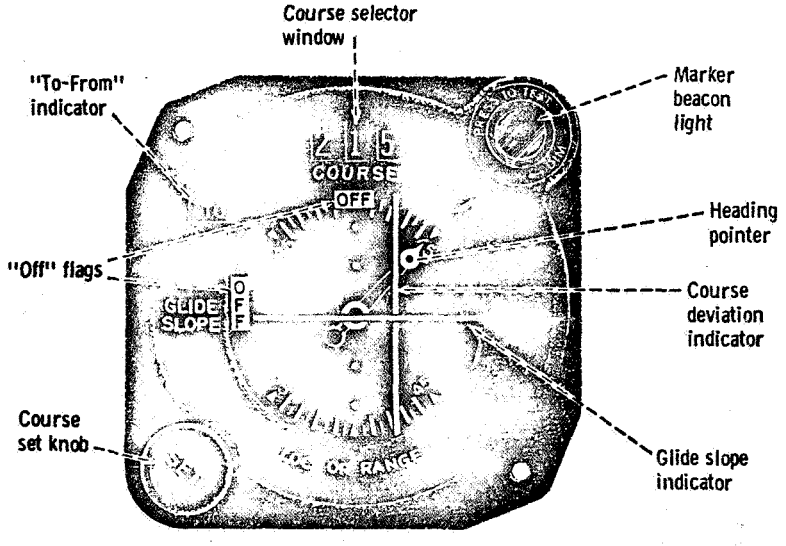

Figure 15-10. - Typical course indicator used with VOR navigation system.

The indicator shown in figure 15-10 is typical of the method of presentation of the VOR information to the pilot. The pilot selects the desired course. The "to-from" indicator shows whether the selected course, if intercepted and flown, will take him to or away from the station. The heading pointer shows the heading of the aircraft relative to the selected course. The deviation indicator (vertical needle) shows the position of the selected course in relation to the position of the aircraft. For simplification, the deviation indicator may be considered to be a portion of the selected course and the heading pointer to be the aircraft. Thus, in the illustration of figure 15-10, the aircraft is to the left of the desired track and is headed toward it at a 45° angle. The glide-slope indicator (horizontal needle) is used when the receiver is tuned to an instrument landing system and functions in the same way as the deviation indicator. When the glide-slope indicator is below the center of the instrument, the desired glide path is below the airplane.

Tactical Air Navigation (Tacan)

The Tactical Air Navigation (Tacan) system was developed in this country for military use. This system, which operates in the UHF range (1000 mHz), provides the pilot with direction information similar to that of the VOR system. In addition, the Tacan system provides the pilot with distance information, so that from a single ground station he can obtain a complete position fix. The primary advantage of this system over the VOR is ease of setting up the ground station. This makes the Tacan system valuable for military use. In the United States, most VOR stations also have Tacan facilities, so that military aircraft equipped only with Tacan may navigate over the civil airways system. Civil aircraft also make use of the distance information obtained from the Tacan signal.

A directional antenna system is rotated at 15 revolutions per second. The aircraft receives a signal that goes from maximum to minimum 15 times per second. As the maximum signal passes through North, a reference pulse is transmitted. The aircraft receiver measures the time between this reference pulse and the maximum signal strength. Secondary lobes on the antenna pattern and auxiliary pulses are superimposed on the basic pattern, as shown in figure 15-11, to provide a fine bearing reference and to give a system accuracy of $\pm 1^{\circ}$. The bearing information is presented to the pilot on an instrument similar to that used in the VOR system.

Distance is determined with Tacan equipment by measuring the elapsed time between the sending of an interrogation pulse by the airborne set and the reception of a reply pulse from the ground unit. These pulses require about 12 microseconds round-trip travel time per nautical mile of distance from the ground station. Since a large number of aircraft may be interrogating the same ground beacon, the airborne set must be able to sort out for measurement only the pulses which are replies to its own interrogations. It does this

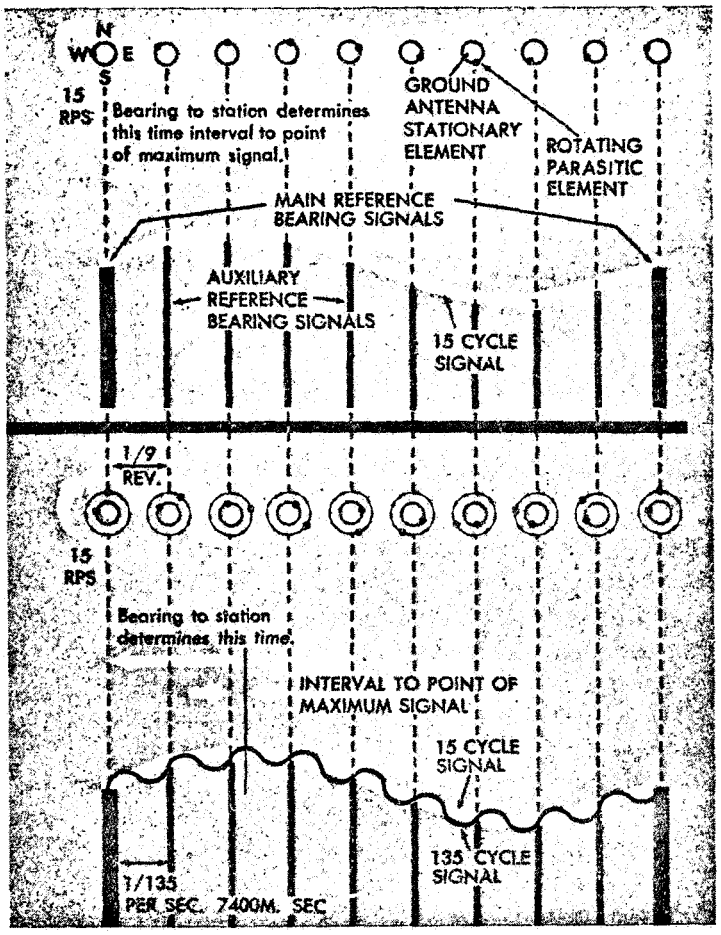

Figure 15-11. - Antenna and signal patterns for combined coarse and fine bearing signals of Tacan navigation system.

by sending its pulses on an irregular, random basis, then sorting out those replies whose pattern is synchronous with the pattern of the interrogations.

The distance measured by the Tacan equipment is the actual, slant range, not the horizontal range, between the aircraft and the ground station. The difference between the slant range and the horizontal range is negligible, except when the aircraft is very close to the station and at high altitude. Obviously, as the aircraft passes directly over the station, the distance indicated by the Tacan equipment is actually the altitude (in nautical miles) of the aircraft relative to the station.

Long-Range Navigation (Loran)

The radio systems previously discussed are basically short-range systems, good for ranges up to about 300 miles, and thus are not applicable to long-range or over-water

navigation. The radio-compass system might be considered an exception to this statement, for it can be used for longer distances under ideal conditions. However, several systems are available which provide equal or better accuracy and greater range. The most popular of these ground-based systems is the Long Range Navigation (Loran) system.

The ground equipment of the Loran system basically consists of pairs of transmitting stations that broadcast pulsed signals. In each pair of stations, one is designated the master station, the other, the slave. The two stations are a known distance apart. The master station transmits a series of pulse signals which are received by both the aircraft and the slave station. Some fixed delay time after it receives each master pulse signal, the slave station transmits a matching pulse signal. The airborne receiver includes a timing device which measures the difference between the arrival times of two matching signals from the two stations. In this time-difference measurement, the time required

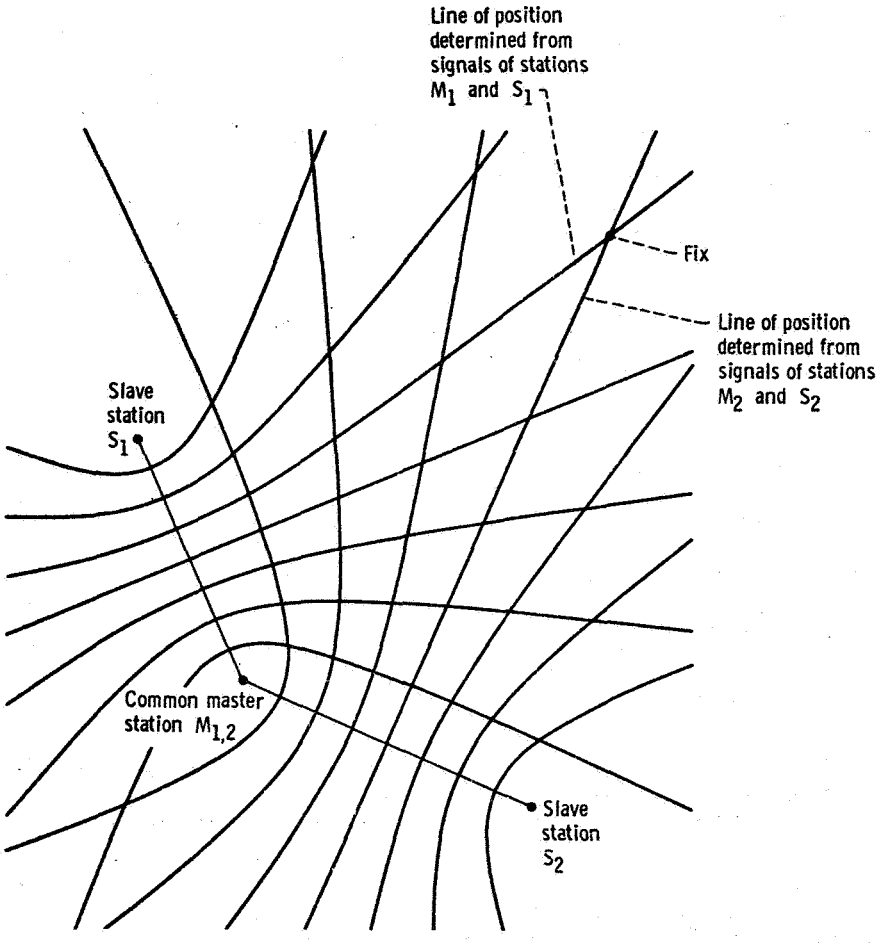

Figure 15-12. - Example Loran chart showing lines of constant time difference for pulsed signals received from paired master and slave stations.

for a master signal to reach the slave station and the fixed time delay of the slave station are both taken into account. Thus, the remaining time difference represents the difference in the distances of the two stations from the aircraft. Special Loran charts, similar to figure 15-12, show series of lines of constant time difference for each pair of stations. Thus, the measured time difference for one pair of stations locates the aircraft along one of these lines. The time differences for two pairs of stations provide a fix (at intersection of lines) of the aircraft's position.

Doppler Navigation

Each of the previously described radio navigational aids or systems requires a source of information (e.g., transmitting stations) separate from the aircraft. Two navigation systems now coming into use on civil aircraft do not require any external information (such as radio signals) once they have been initially set. The two systems are known as Doppler navigation and inertial navigation. However, the Doppler system is not completely passive, as it requires a transmitter aboard the aircraft which sends out pulses to be reflected back from the surface of the Earth. Inertial systems are completely passive and require no signal or information to be radiated outside of the aircraft; therefore, they are of considerable interest for military applications, where detection is a consideration.

In the Doppler system, the normal navigational triangle of velocities is solved by high-accuracy, direct measurement of the aircraft's drift and ground speed. Determination of absolute direction is accomplished by adding heading from the aircraft's heading reference system to the Doppler drift. A suitable navigation computer which accepts the raw data on heading and Doppler drift can convert them to terms of aircraft present position and/or steering and distance information for a predetermined destination.

The Doppler effect works on the principle that a change of frequency occurs between received and transmitted signals when there is relative motion between receiver and transmitter. A simple analogy is that of a stationary observer listening to the whistle sound of a fast-moving express train. As the train approaches him the note of the whistle increases in frequency (and in pitch), reaches a maximum as the engine passes him, then decreases as the train speeds away from him. Similarly, if a moving airborne radar device transmits a beam of radio energy towards the ground, the echo signal received back from the point of reflection changes frequency by an amount proportional to the component of velocity along the beam.

A single-beam airborne antenna would have two disadvantages. First, it would not necessarily measure velocities along the aircraft's track, and second, it would include a vertical component in its measurements if the aircraft deviated at all from level flight.

To overcome the first of these disadvantages, two beams can be radiated, one to each side of the aircraft. Thus, a drift to left or to right during flight causes a greater Doppler shift in either the left or the right antenna, and suitable computation can resolve the difference into a measure of the drift angle. The difference in Doppler shifts can also be used as an error signal to drive the axis of the antenna array into coincidence with the airplane track. In this case, the drift angle is obtained by direct mechanical measurement.

Unwanted vertical components of velocity, the second disadvantage of a single-beam antenna, are eliminated by adding a rearward-directed beam to each forward-directed beam. This system has several advantages. First, the vertical component of velocity is virtually eliminated, since the amount present in the forward-directed beams is equal and opposite to that in the rearward-directed beams. Second, since the Doppler beat frequency is obtained by mixing signals from two beams rather than by single-beam measurement, greater precision of velocity determination is possible. Finally, the necessity for antenna stabilization in the pitching plane is largely eliminated. (Roll errors also affect the Doppler system; but except for special military applications, in which extreme accuracy is required, the expense of roll stabilization of the antenna is seldom justified.)

The Doppler system has certain operating limitations. Over smooth sea surfaces, the signals reflected back to the receiver are sometimes too weak to be usable, particularly if the aircraft is flying at great height. Also, the signal may be lost at certain critical altitudes.

Small residual errors are also present in the system. The principal sources of error in the Doppler radar system alone are antenna misalinement (perhaps 0.2° on the average civil aircraft), variations in the absolute length of a nautical mile with latitude and altitude, and movement of the reflecting surface (e.g., movement of water surfaces due to winds and/or currents). With all these residual errors taken into account, the practical accuracy of most current Doppler radar systems is about 0.5 percent of distance flown along the track and about 0.5° across the track. The above errors relate to only the Doppler radar and do not represent total system error.

Even though it is carefully fabricated, situated, calibrated, and compensated, the gyromagnetic compass is normally the largest single source of error in the complete Doppler system. The gyromagnetic compass can seldom provide an accuracy of better than 1.2° across the track or 2.0 percent of distance flown along the track. Add in a little for computer error in resolution, and total error for the complete system becomes about 0.6 percent along and 2.6 percent across the track.

Inertial Navigation

The inertial navigation system is unique in that the entire system is carried on the aircraft, is completely self-contained, and requires no external information such as radio signals. Essentially, inertial navigation is the process of determining the speed and position of an aircraft from measurements of the accelerations of the aircraft.

Inertial navigation is based on Newton's laws of motion. According to the first law, a body in motion will continue to move at the same speed and in the same direction until it is acted upon by an external force. According to the second law, the force acting on a body is equal to the product of the mass of the body and its acceleration along the line of action of the force.

From these laws, the equations of motion for uniform conditions were developed:

$$s = ut \tag{1}$$

and

$$v = u^2 + 2as \tag{2}$$

where

s distance

u initial velocity

t time

v final velocity

a acceleration

Where velocities and accelerations are constantly varying, these equations are expressed in calculus notation

$$v = a\,dt \tag{3}$$

and

$$s = v\,dt = a\,dt \times dt \tag{4}$$

According to equation (4), distance is equal to the integral of velocity with respect to time. Thus, a mechanized solution based on this equation can average and multiply velocities over infinitesimal periods of time to give an accurate value for distance traveled.

In mechanizing the solution, the first problem is to measure the vehicle accelerations. Thus, the basic components of an inertial navigation system are two accelerometers capable of sensing and measuring aircraft accelerations in the north-south and east-west directions. Several methods can be used for sensing accelerations. Perhaps the simplest is measuring the movement of a spring-restrained mass (Hooke's Law states that the extension of the spring is proportional to the force causing it). However, the basic sensitivity of such a system is not high. Greater sensitivity is usually achieved by using "force balance" instruments, in which the applied acceleration is measured by the force required to rebalance the system against the input acceleration. Such devices are remarkably accurate over a wide range of acceleration values. But if they are to perform their functions usefully and correctly, they must obviously be protected from the pitching, yawing, and rolling motions of the aircraft in which they are mounted. The accelerometers are therefore mounted on a gyro-stabilized, gimbaled platform, which maintains them in a horizontal position with respect to the local surface of the Earth, regardless of any changes in aircraft position and attitude. The gimbaled platform is stabilized by two or three gyroscopes. Such an acceleration-measuring system is capable of measuring the horizontal components of aircraft accelerations without being affected by unwanted vertical components of such accelerations.

But acceleration measurements alone are of little navigational use. The inertial navigation system therefore includes two sets of integrators. The first set integrates the accelerations with time to indicate velocities, and the second set integrates the velocities to indicate distances traveled in the north-south and east-west directions. These distances can then be fed to a navigational computer, tailored to the needs of the user, to produce an automatic, continuous, and accurate display of aircraft position, heading, and distance relative to a predetermined destination or track.

Nothing so useful could be quite that simple; the inertial navigation system is no exception. Gyroscopes need to be corrected for the effects of the Earth's rotation and the aircraft's motion, and this is normally accomplished by feedback from various stages of the inertial navigation system itself. Gyroscope biasing, to reduce errors resulting from mass unbalance and from other causes, is usually performed on the ground at set intervals.

The accelerometers are subject to errors caused by centrifugal forces (since the aircraft is moving around a curved path over the Earth's surface), coriolis forces (caused by the rotation of the Earth), polar compression (because the Earth is an oblate spheroid), and gravity magnitude variation. Therefore, correction terms must be continuously fed back to compensate for these errors.

In addition to all this, the stabilized platform, being a form of pendulum, must be maintained vertical despite horizontal accelerations which would tend to make it lag behind the local vertical by an angle dependent on the magnitude of the acceleration and the

length of the pendulum. This is accomplished by "Schuler tuning"; that is, the platform is made to simulate the behavior of a pendulum whose length is equal to the radius of the Earth. Such a pendulum (i.e., a Schuler pendulum) would always maintain its vertical orientation. The period of such a pendulum is given by

$$T = \frac{R}{g} \tag{5}$$

where

T period of pendulum, sec

R length of pendulum (radius of Earth), ft

g acceleration due to gravity, 32.17 ft/sec^2

If R were equal to the radius of the Earth, the period would be 84.4 minutes. The practical solution is to construct an electromechanical analogue having the same period as the Schuler pendulum. Such an analogue will maintain a vertical orientation relative to the surface of the Earth.

As an example of the sort of precision required, if one of the accelerometers is tilted from the horizontal by as little as $1/60^{\circ}$, the spurious gravity acceleration from this cause alone will introduce a system error of 12 nautical miles at the end of a 1-hour flight. The accelerometers themselves must be sufficiently sensitive and wide-ranging to cope with accelerations varying from perhaps 7 or 8 g to 0.000005 g. If the total navigation system is to be accurate to within 1 nautical mile for 1 hour of flight at 1000 miles per hour, an accelerometer in the system has to be accurate to within less than 0.0003 g.

As regards gyroscope accuracies, it does not seem so long ago that the old aircraft directional gyroscope, with a drift rate of perhaps 10° per hour, was still regarded as a marvelous instrument. Even now the gyroscopes in some gyromagnetic compasses in common use have a free-mode drift rate of more than 5° per hour. However, some currently used gyroscopes have drift rates of only 0.01° per hour; and in the not-too-distant future, gyroscopes with drift rates as low as 0.001° per hour will probably be used.

In spite of gyroscope inaccuracies, the inertial navigation system offers tremendous advantages for both civil and military aircraft. It eliminates the dependence upon the radio wave, transmitted or received, and on celestial and terrestrial references. Inertia navigation measurements (based on Newtonian laws of motion and gravitation) are carried out entirely within the aircraft. The system is therefore available at all times, in all places, regardless of weather, and (of particular importance to the military user) without making any tell-tale transmissions that could be intercepted and possibly jammed.

The accuracies provided by inertial navigation are high compared with the accuracies

of other navigation systems. For example, a maximum error of only 2 nautical miles per hour is well within the state of the art. This error is time dependent only; therefore, the faster the aircraft, the better the performance of the system in terms of accuracy per distance flown, a factor of particular importance for supersonic aircraft.

16. WEATHER SAFETY AND NAVIGATION IN SEVERE STORMS

I. Irving Pinkel*

STORM HAZARDS TO FLIGHT

Severe storms are the principal hazard to flight. The airplane is endangered by the strong, turbulent winds of the storm and by the hail and rain that often accompany it. Here we will describe the nature of these severe storms and some of the techniques for operating safely in storm areas.

An airplane can be lost in severe weather if buffeting from erratic winds places it in flight attitudes from which the pilot cannot recover. The airplane may fall out of control, or the pilot's attempt to restore correct airplane flight may result in a violent airplane maneuver that stresses the airframe to failure. Likewise, hail can damage the aerodynamic surfaces of the airplane sufficiently to require extreme skill to land the airplane safely. Aircraft flying at supersonic speeds (above 700 miles per hour) can receive similar damage from impacting rain droplets at these speeds. Figure 16-1 shows the damage to an airplane that flew through hail. The extensive damage to the leading edge of the wing raises the danger of airflow separation from the top surface of the wing as the aircraft slows for landing. Since the damage to each wing is somewhat different, each wing may generate a different lift, especially at low flight speeds, when the angle of attack is high. This difference in lift between the two sides of the wing may be too great for the pilot to compensate with ailerons and trim tabs, and the airplane may enter an uncontrollable roll on the landing approach. Fortunately, this did not happen to the airplane shown in the figure. It is clear from these considerations that flight through hail and heavy rain showers at high speed must be avoided. In order to do this, the pilot and those who direct his flight from the ground must understand the structure of the storm through which the airplane is flying so that the pilot may pick a safe path.

Severe thunderstorms present the most common flight weather problem. The U. S. Weather Bureau and its successor organization, the Environmental Science Services Administration, have a research center devoted solely to the study of severe storms. Through the work they have done by ground observations and flights through thunder-

*Director, NASA Aerospace Safety Research and Data Institute.

Figure 16-1. - Hail damage to airplane.

storms with instrumented airplanes, they have constructed the picture of the anatomy of the thunderstorm. This information has made it possible for aircraft to fly safely in storm areas.

CHARACTERISTICS OF A THUNDERSTORM

While no two thunderstorms are exactly alike, they all have certain features in common. They have similar modes of development to the violent condition we recognize as a severe storm and have common gross features by which the several stages of the storm's development and dissipation are identified.

The thunderstorm is made up of a series of thunder cells which are often between 5 and 10 miles in horizontal extension but in some instances may exceed 20 miles in horizontal extension. The pilot can recognize the thunderstorm that has reached a dangerous stage in development because its cells, from an airplane, have the appearance shown in figure 16-2. The base of the thunderstorm cloud is usually between 2000 and 10 000 feet from the surface. The tops can have far greater variation in height. They can extend from 15 000 to 60 000 feet. In some rare instances they have been reported at even higher levels. The pilot recognizes that the thunderstorm is fully developed and is, therefore, in a dangerous condition when he observes the prominent anvil cloud at the top

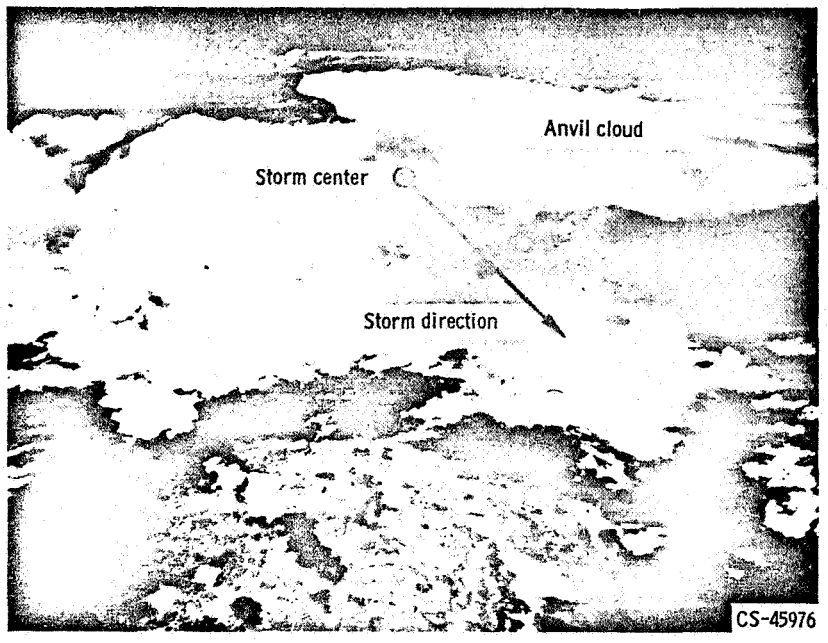

Figure 16-2. - Typical thunderstorm cell viewed from high altitude.

of the thunder cell (fig. 16-2).

By means of ground instrumentation and flights through thunderstorms, the dangerous zones have been mapped as shown in figure 16-3. Here we see a cloud which reaches from 5000 feet to 55 000 feet altitude. The zone of highest winds within the cloud appears as a curved column of air rising upward through the center of the cloud. Its location within the cloud can be roughly estimated from the fact that this rising column produces a bump in the upper perimeter of the cloud. In figure 16-3, this bump appears above

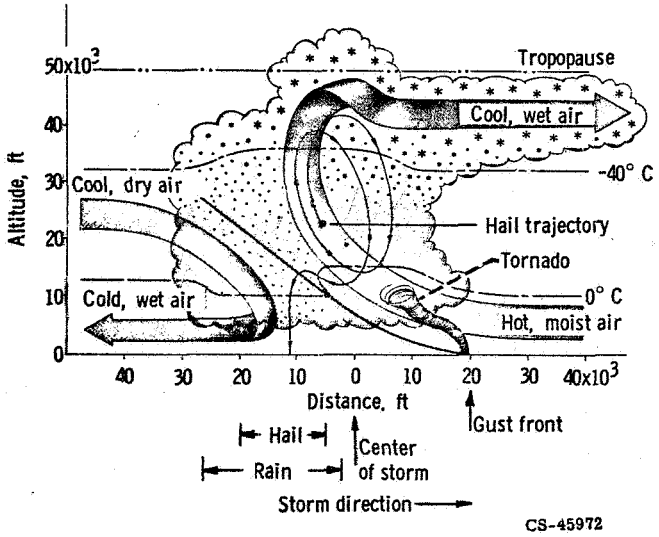

Figure 16-3. - Vertical section through thunderstorm cell showing air currents and areas of precipitation.

the 50 000 foot altitude level. This high-speed column of air originates close to ground level. At this low level, the air is moist and warm enough to have a density less than the cooler air which lies above it. Being less dense than the overlying air, this warm, moist air floats upward through the more dense overlayer. As the air rises, it cools, because it expands in the lower pressures of the higher altitudes. As the air cools, moisture is condensed and the heat of condensation from this moisture warms the air. The net effect is to give the rising air a temperature higher than it would have had if water condensation had not occurred. Because of this warming, the air retains a density less than that of the surrounding air, and so it continues to flow upward. As this air climbs through several thousand feet in this way, it acquires vertical speeds often in excess of 200 miles per hour. An aircraft that flies into such a jet of rising air could be tossed into flight attitudes that would require considerable skill on the part of the pilot to restore it to normal flight attitudes.

When a rising column of air achieves its highest level (immediately under the bump of the upper perimeter of the thunder cell), condensation is stopped. The moisture that condensed as water at lower levels has now frozen to hail in the intense cold of the higher altitudes. Since the velocity of the rising column of air which has blown the water and hail upward is dissipated in the upper altitudes of the thunder cell, the hail falls toward the ground and induces a downward draft of the local air. The falling column of air which moves with the hail is displaced horizontally from the rising vertical column. This displacement is in the direction of the movement of the entire thunder cell. Since the warm, moist air at ground level climbs slantwise through the base of the thunderstorm, the falling hail can drop into this rising column of warm, moist air and be carried aloft for another trip. The condensing moisture in this rising column of air which now carries hail can condense on the hail to add additional layers, and so the hailstone grows. This process of hailstone growth can be repeated as many as a dozen times to produce hailstones the size of golf balls, which eventually fall to the ground.

Clearly, the airplane should avoid the central part of the thunder cell which contains the high upward and downward winds laden with heavy rain and hail. Fortunately, airborne radar gets a very strong signal from rain drops and hail, so that these zones in the thunder cell are clearly visible to the pilot on his radar scope. Thus, an aircraft equipped with radar can fly through thunderstorms with reasonable security. An aircraft not equipped with radar can fly safely through storm areas if it is in radio communication with a ground radar station that can "see" the storm and guide the aircraft through it. An aircraft that is not equipped with radar and not in radio contact with a ground radar station depends on the pilot's judgment and what he can see of the structure of the thunderstorm. Therefore, without the aid of radar, an aircraft should not attempt to fly through thunderstorm areas at night, when the storm is not visible.

Tornadoes may form at the base of the thunder cloud, where some of the warm, moist air enters the cloud. Such a place is marked in figure 16-3. The tornado is visible as a

funnel shaped cloud attached to the cloud base and can, therefore, be avoided by the aircraft during daylight. A tornado can also be detected by radar if the tornado contains debris from the ground or if it contains precipitation.

An important, but less severe, zone of air currents within the thunder cell appears at its trailing edge, where wind-borne, cool, dry air at high altitude enters the thunder cloud and mixes with the cloud droplets. The droplets evaporate in this dry air. The heat required for droplet evaporation is drawn from the air. This cooled air is now more dense than the surrounding air of the cloud and sinks rapidly. This downward stream of air can attain speeds which could upset the inexperienced pilot.

The zones on the ground, relative to the storm cloud, that are subject to precipitation from the storm cloud are shown in figure 16-4. Information like this is useful to the airplane dispatcher, who can determine under what conditions he can dispatch an airplane and the route it should take as it leaves the airport.

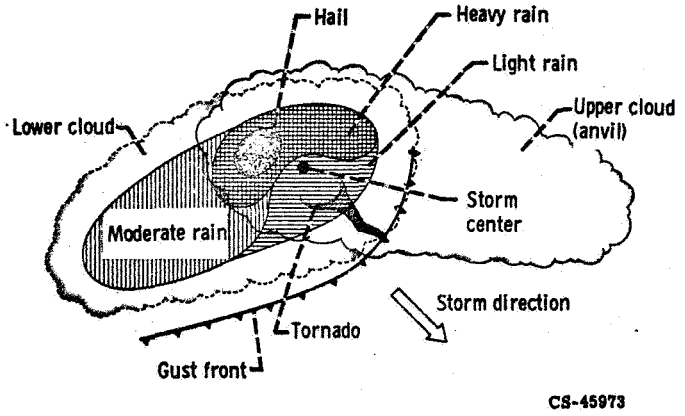

Figure 16-4. - Horizontal section through thunderstorm cell showing areas of precipitation.

In addition to the vertically directed high winds mentioned previously, the thunderstorm contains zones of highly turbulent air, which can buffet the airplane severely. Such buffeting can cause failure of the main airplane structure and the loss of the airplane. These turbulent zones, mapped in figure 16-5, lie adjacent to the strong vertical air currents.

The water droplets which make up many clouds, including those of the thunderstorm, can exist at temperatures below the normal freezing point of water. The zones occupied by these "supercooled" cloud droplets range from the freezing level, marked as 0° C in figure 16-5, to altitudes where the temperature can drop to -20° C. In some rare instances, water droplets are found in the cloud at -40° C.

As an aircraft flies through a cloud, the cloud droplets strike the leading surfaces.

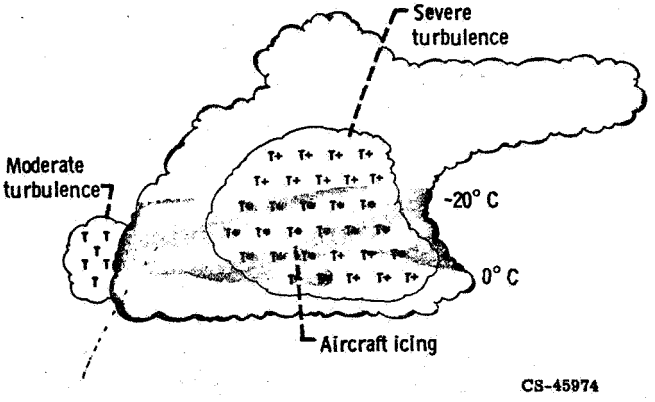

Figure 16-5. - Vertical section through thunderstorm cell showing areas of aircraft icing and turbulence.

When supercooled cloud droplets strike the airplane surface, they freeze. In a few minutes of flight, sizable ice accumulations may form on the aircraft. Such ice formation on the leading edges of wings and tail surfaces can so change the contour of these airplane members as to increase the airplane drag severely and reduce the effectiveness of wings and associated flight control surfaces. High drag slows the airplane and increases the fuel required to complete the flight. Deterioration of the aerodynamic quality of the wing and tail increases the pilot's problem of maintaining proper control. This decline in handling quality of the airplane becomes particularly important on landing, when the airplane moves slowly and is normally sluggish in its response to control movements. Ice accumulations on the aircraft increase the sluggishness to control and thereby increase the likelihood of a crash landing.

Ice is also collected on engine air intakes. The obstruction of the vital airflow to the engine is evident from the engine inlet icing shown in figure 16-6. Should chunks of such massive accumulations of ice break free and be ingested by the engine, the blading within the engine may be damaged.

Aircraft which are certified to fly through icing clouds are protected against ice accumulation by heating those surfaces on which water droplets of the cloud are likely to impinge. However, such icing protection is designed for moderate-to-severe icing conditions and may be inadequate for exceptionally severe icing. An understanding of the structure of the clouds that are most likely to produce severe icing allows the pilot to avoid icing conditions which are beyond the capability of the ice-prevention system of the aircraft. Many years of research flights through icing clouds and cloud-physics studies in NASA and other laboratories have given us a working understanding of this matter. Aircraft seldom get into difficulty now because of icing.

One remaining problem of the severe storm is the lightning hazard that accompanies

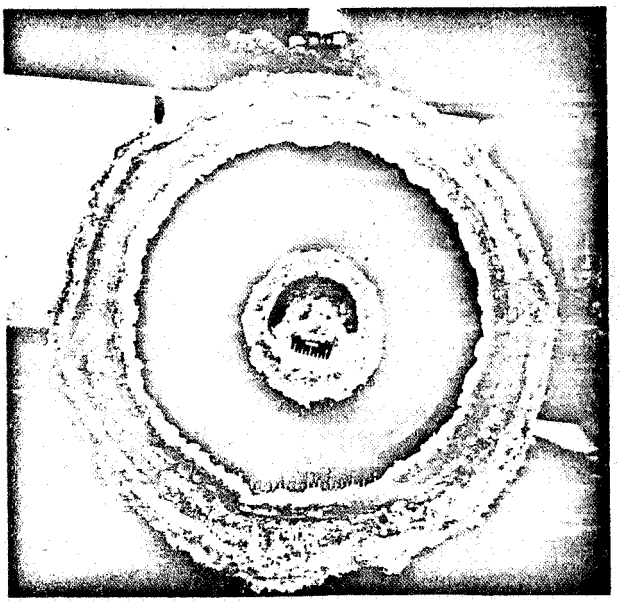

Figure 16-6. - Turbojet-engine inlet icing.

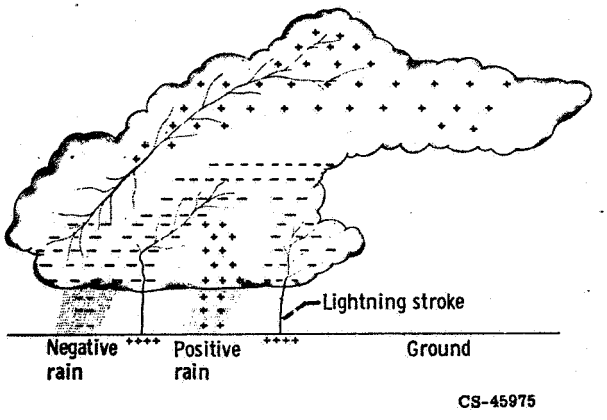

Figure 16-7. - Vertical section through thunderstorm cell showing typical distribution of electrical charges.

it. Figure 16-7 shows a typical distribution of electrical charges within a thunder cell. These charges reside on the rain drops, hail particles, and cloud droplets. In the cloud illustrated in this figure, the positively charged droplets are mostly near the top of the cloud and the negatively charged droplets are near the bottom. While this is generally the case, the opposite often occurs. Lightning, which represents a discharge of electricity from the positive to the negative charges, occurs within the cloud as shown in the figure. Also, the negative charges at the base of the cloud induce the Earth's surface immediately below the cloud to acquire a positive charge. Lightning strikes between the ground and the cloud occur when the potential difference is great enough to form a streak

of ionized air in the space between. The main lightning discharge follows this streak. Ionized air is a good conductor of electricity, whereas normal air is a poor conductor. Aircraft flying beneath the cloud may be struck by the lightning, but ordinarily the damage to the aircraft is modest. The all-metal construction of the aircraft makes it a good conductor of the electricity and it passes the lightning current harmlessly. At the points of the airplane where the strike enters and leaves, small pitting and local burning of the structure is often evident.

However, the lightning may strike the fuel system of the airplane at a location where a combustible atmosphere exists. The probability of ignition of the aircraft fuel is high enough to constitute real danger. Every effort is now being made to ensure that under no conditions will a lightning strike to the airplane ignite the aircraft's fuel, since such ignition is catastrophic.

NAVIGATION THROUGH STORM AREAS

In order to understand how a modern airplane navigates through an area of severe storms, it is useful to review one of the navigation systems most commonly used on commercial and military aircraft. This navigation system, called an omnidirectional radio range (omni), is based on a series of radio stations on the ground which represent the intersection of the airways flown by the aircraft. A flight plan between two airports can be designated by listing the radio stations over which the airplane will fly. Each radio station radiates a signal at a frequency which is distinct from all the others. The airplane tunes its receivers to this frequency. The receiver signal actuates a pointer on an instrument dial which shows the bearing of the radio station with respect to the aircraft. This situation is diagrammed in figure 16-8, which shows the ground-based radio station and five locations of the aircraft with respect to that radio station. The dial pointer in the figure, which corresponds to the dial on the instrument panel in the airplane, shows the compass bearing of the radio station relative to the location of the aircraft. It is obvious from the figure that if the aircraft passes directly over the omni station, the dial pointer reverses itself (i.e., rotates 180°). This reversal of the dial pointer provides the pilot with the exact fix of the aircraft with respect to the ground, because the exact location of the omni station is shown on his maps. When the aircraft is not directly above the omni station, the fix of the aircraft is determined from the bearing of the omni station in conjunction with data from distance-measuring equipment, or DME. (Omni navigation is discussed in more detail in chapter 15.)

A commercial pilot is required to fly along the airways for which he is cleared when he files his flight plan, prior to takeoff. Any deviation from this plan while he is enroute must be approved by the air-traffic controller who monitors his flight from the ground. Such request and approval is accomplished by radio communication.

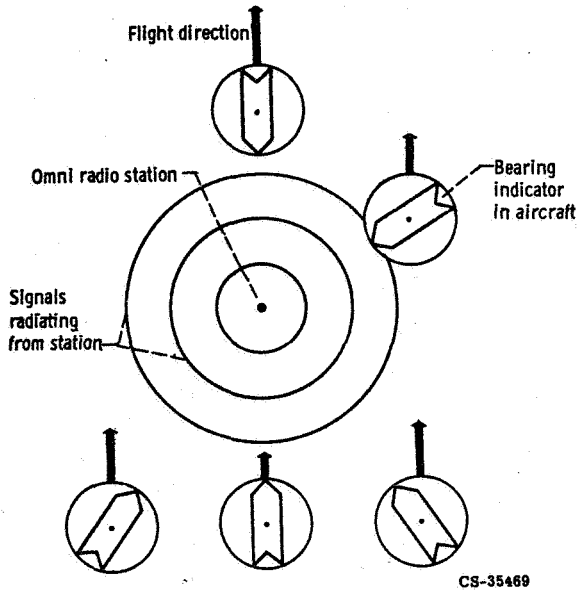

Figure 16-8. - Omnidirectional (omni) radio navigation.

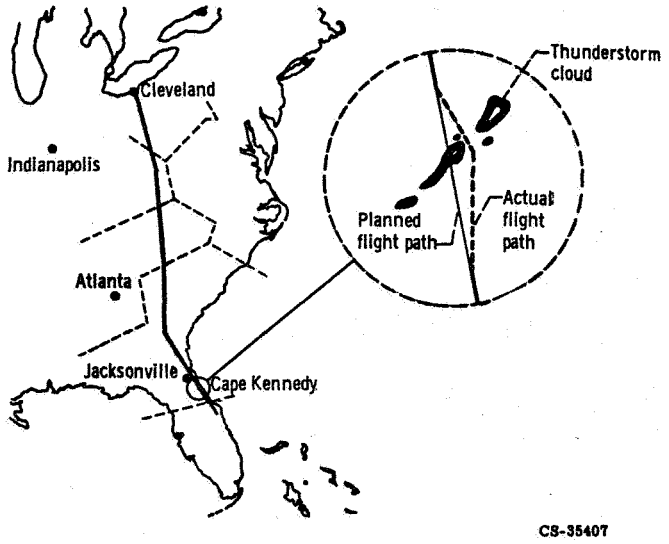

Figure 16-9. - Airway schematic with enroute storm.

Severe weather is one of the principal reasons for requesting deviation of the flight from the prescribed plan. This situation is illustrated in figure 16-9, which shows a typical flight route from Cleveland, Ohio, to Cape Kennedy, Florida. The diagram shows that the aircraft encounters a thunderstorm in its path as it enters Florida. With the consent of the Federal Aviation Administration controller, the aircraft is allowed to deviate from its original plan, shown as a solid line in the figure, and to take the path shown by the dashed line to avoid penetrating the thunderstorm cell in its path.

Most commercial airplanes are equipped with airborne radar systems which display those portions of the clouds that contain rain, snow, or hail. The radar scope on the airplane shows the precipitation pattern within the clouds with respect to the direction of the airplane flight path, as shown in figure 16-10(a), which is a photograph of such a radar scope. The position of the airplane is indicated by the figure of the small airplane at the center of the system of concentric circles marked on the screen. The concentric circles represent fixed, known radial distances from the airplane. In a typical radar display, the radial distance between circles is 10 miles. This radar presentation shows the pilot how he can fly through the storm that lies in his path so as to avoid the precipitation areas, which also mark the zones of high vertical winds and turbulence, as discussed earlier. In the event that the thunderstorm appears as an unbroken line in his path, the pilot can pick his way through the least hazardous portion of the storm by using a setting on the radar which alters his radarscope presentation to show the zones of highest precipitation within the storm ahead. In the radarscope presentation shown in figure 16-10(b), the dark areas within the outlines of the zones of precipitation are the areas of

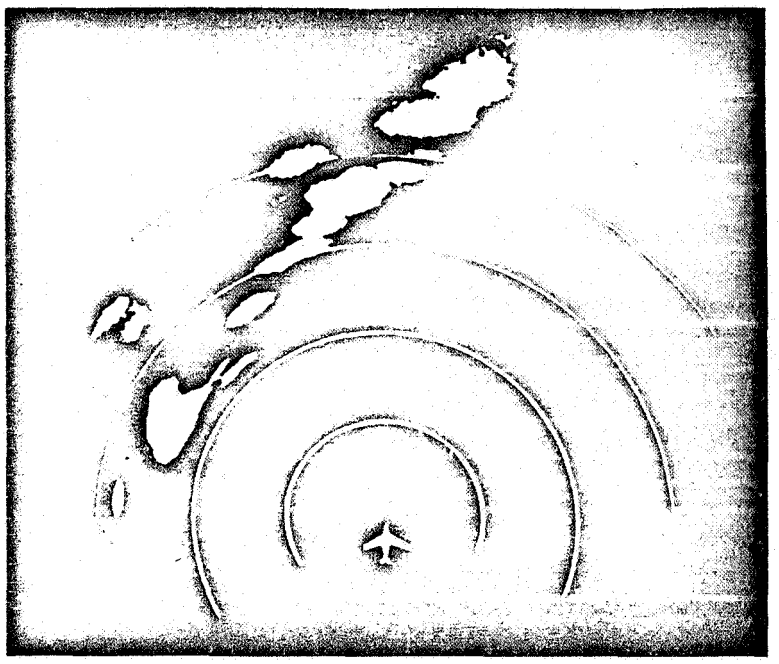

(a) Low-contrast image showing overall areas of precipitation.

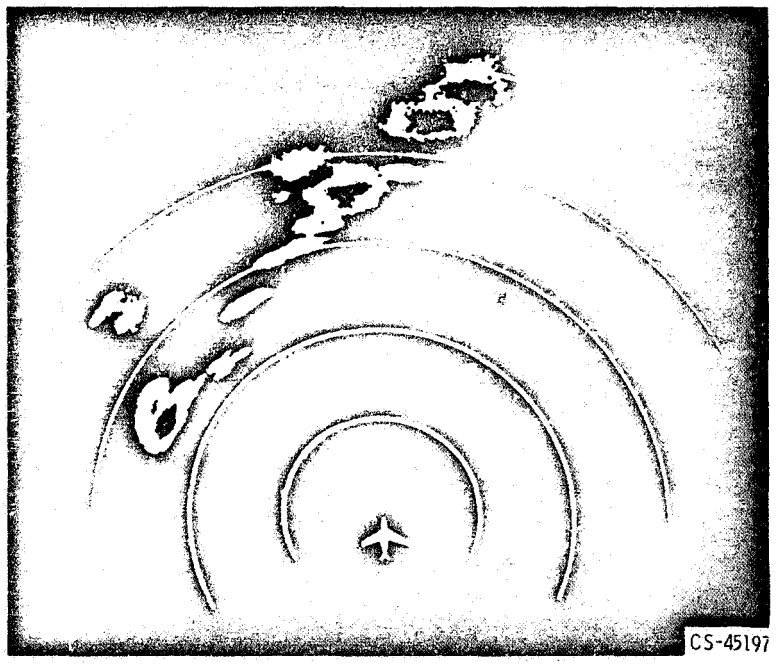

(b) High-contrast image showing zones of most intense precipitation within overall areas of precipitation.

Figure 16-10. - Airborne radarscope presentations of precipitation pattern of storm.

most intense precipitation. The pilot picks his path to avoid these zones and accepts the buffeting he will receive by going through the milder portions of the storm.

CONCLUDING REMARKS

Our knowledge of the Earth's weather and how it influences aircraft flight is progressing rapidly. Instrumentation for navigation and control of aircraft is undergoing a major revolution at this time. Many of the limitations to aircraft flight imposed by the weather should be largely overcome in the next 10 years. After that time, aircraft will be instrumented for detecting turbulent air whether or not associated with storms. These aircraft will be equipped to fly through turbulent air smoothly and, in all probability, to land at airports under conditions of extremely poor to vanishing visibility. Those who have an interest in this subject should review its status periodically, because of the rapid changes which are in progress.

17. PROJECTS IN AERONAUTICS

James F. Connors*

Throughout the Lewis Explorer program in aeronautics, a concerted effort was made to generate a high level of interest and involvement among the participants. Whenever feasible, lectures were augmented by active demonstrations, visual aids, and supplementary films. On occasion, special tours to aeronautical points of interest were arranged. The participants became most directly involved in the program through research assignments, many of which were actual wind-tunnel experiments. The culmination of the program was a full-scale symposium on aeronautics - an excerise in communication - at which the young researchers reported the results of their projects.

DEMONSTRATIONS

The following is a sampling of demonstrations presented in conjunction with the various lectures. Most of these demonstrations can be easily duplicated or approximated by anyone interested in studying basic aerodynamic principles and flow phenomena.

Some demonstrations pertaining to the aerodynamics of an airfoil (chapter 4) are illustrated in figure 17-1. Basic aerodynamic phenomena were demonstrated by means of very simple equipment. For example, the Coanda effect was demonstrated by using a funnel to direct a stream of small, solid particles (shot) and a stream of fluid (water) against the side of a horizontally oriented cylinder (fig. 17-1(b)) and comparing the results. Also, the cylinder was rotated under the water stream to show increases and decreases in the Coanda effect.

For a demonstration of lift (fig. 17-1(c)), a vacuum sweeper was used to provide an airstream. Lift was produced by deflecting this airstream downward either through a bent cylindrical tube or by a curved vane. The lift was evidenced by an upward rotation of the supporting beam about its fulcrum. (Part of the equipment for this demonstration was assembled from a toy erector set.)

In another demonstration (fig. 17-1(d)), visual flow definition was achieved by suspending, or floating, lightweight particles (sawdust) on the surface of water and then

*Director of Technical Services.

moving a flat paddle through the water to show the turbulent wake pattern behind the paddle.

To demonstrate the vortex produced by a wing tip, a simulated wing (a flat board) was mounted on the side of an automobile (fig. 17-1(e)). When the auto was put into motion, the vortex from the simulated wing tip caused a rotation of a spinner that was mounted downstream of the tip.

In conjunction with the discussion of fluid flow through nozzles (chapter 11), a relatively simple water table (fig. 17-2) was used for flow visualization. The water table, based on the physical analogy between water flow and airflow, was used to study streamline patterns for convergent-divergent nozzle geometries under various operating modes. Streamlines can be made visible by placing dye crystals at regular intervals across the upstream end of the water table. Actual pressure distributions along a surface can be derived either from the variation in the distance between streamlines or from the variation in water height along the surface. Water-table studies are much like observing the flow patterns of the vortex that is set up when a bathtub is being drained or of the waves created when a rock is dropped into a calm pond.

EXPERIMENTS

Some basic aerodynamic principles were applied in simple, practical experiments that can be carried out by anyone studying aerodynamics. Many of these experiments were conducted in a moderately small, but fairly sophisticated, low-speed wind tunnel. Details of this particular tunnel, as well as plans and suggestions for constructing a simpler one, are presented in appendix A.

Aerodynamic drag values were obtained in the wind tunnel for a family of cylinders of varying size (1, 3, and 5 in. diam). Each cylinder spanned the tunnel test section. Results are shown in figures 17-3(a), (b), and (c). Flat-plate friction drag (fig. 17-3(d)) was determined as a function of Reynolds number (see definitions in chapter 2). Both laminar and turbulent boundary-layer profiles were obtained. Roughness (or grit) was added to the plate leading edge to ensure early transition to a turbulent layer. Small models of automobiles were used to determine the effect of styling, or configuration, on aerodynamic drag performance (figs. 17-3(e) and (f)). The advantages of streamlined automobile bodies were clearly demonstrated.

Aerodynamic lift was also studied in the wind tunnel for a wide range of airfoil shapes. Both infinite and finite wings were used. Infinite airfoils were those that completely spanned the tunnel and thus had no loss in lift at the ends. For each geometry, the variation in lift coefficient with angle of attack (fig. 17-4(a)) was determined beyond the maximum lift, or stall, point. Smoke (fig. 17-4(b)) and tufts (fig. 17-4(c)) were used

to illustrate the lifting- and stalled-wing conditions. Flaps were added to show that lift could be increased by increasing flap angle (fig. 17-4(d)). Decreasing the wing aspect ratio by shortening the span (fig. 17-4(e)) decreased the slope of the lift-versus-angle-of-attack curve (fig. 17-4(f)) and decreased the maximum attainable lift coefficient. The reason for this effect of the aspect ratio on the lift is that as the aspect ratio decreases, the local loss in lift at the ends becomes a progressively larger percentage of the total wing lift. The end lift loss, or tip effect, was demonstrated by visualization of the vortexes through the use of the tuft grid (fig. 17-4(g)). In effect, the high-pressure air under the wing leaks around to the low-pressure region on top of the wing. At the landing condition, where a specified lift coefficient is required (fig. 17-4(h)), the landing attitude of the aircraft (angle of attack) can be minimized by increasing wing aspect ratio and/or adding a flap.

In wind-tunnel experiments with an aircraft model having variable-sweep wings, the tip vortexes are very graphically illustrated by the tuft patterns at the rear of the test section. Figure 17-5 shows selected frames from a motion picture taken as the model angle of attack and the wing angle of sweep were systematically varied. The aforementioned leakage of air from the bottom to the top of the wing at angle of attack creates a trailing vortical flow behind the tip. It is an important aerodynamic effect in estimating aircraft performance.

An interesting project was called GARAGE, an acronym for Gravity Accelerated Rotational Aerodynamic Gaging Equipment. The project objective was to devise a simple, unique apparatus for effectively measuring lift of various airfoil models, without the obvious complexity and expense of using a wind tunnel.

The apparatus evolved from a rather complicated preliminary design (fig. 17-6(a)) to a relatively simple operational model (fig. 17-6(b)). An airfoil was attached to the extremity of a light, cantilever arm. This arm was connected to a vertical, freely-rotating shaft. A weight was suspended from a fishline that was run through a low-friction pulley and was carefully wound around the vertical shaft. When the weight was allowed to drop, its pull caused the fishline to unwind from the shaft, thereby causing the shaft, with the attached cantilever arm and airfoil, to rotate. The time required for the weight to drop through a measured distance was accurately recorded.

Attached to the outer end of the airfoil was a "whisker." Each time the airfoil made one revolution, the whisker struck a chalked piece of carbon paper mounted on a vertical meter stick. The vertical distance, of lift, of the airfoil was accurately measured at the completion of each run. This vertical rise of the airfoil could be statically calibrated to determine the corresponding lifting forces. The speed of the airfoil is directly proportional to the speed of the falling weight. The speed of the falling weight is a measure of the drag on the airfoil. A stroboscopic (or strobe) light could be used to stop motion and thereby obtain the frequency of rotation and a direct indication of the vertical displace-

ment of the airfoil at that rotational speed. The linear speed of the airfoil could be calculated from the frequency of rotation and the measured length of the cantilever arm supporting the airfoil (i.e., the radius of the circular path of the airfoil). Since drag varies (exponentially) with the square of the velocity, incremental differences in drag could thus be determined for the various airfoil shapes. Some experimentally obtained values of lift and drag with angle of attack are shown in figures 17-6(c) and (d).

Another research project was the design of a model airplane for maximum endurance. The specifications adopted for the project were based on the rules for an actual, worldwide, competitive endurance event, with a significant monetary prize. The specificiations called for a wing area of 1800 square inches, a stabilizer area of 450 square inches, and a gross weight of 11 pounds. The initial concentration of effort was on the powerplant. To this end, a good-quality, 2-cycle, model-aircraft engine was selected. For this engine, a fuel system (fig. 17-7(a)) was designed, fabricated, and assembled for experimental evaluations and modifications. Objectives, of course, were to maximize the amount of fuel and engine performance and, at the same time, to minimize system weight. Engine performance (fig. 17-7(b)) was determined statically and then projected to estimate the performance at a flight speed of 30 feet per second. A 12-inch propeller was used to absorb the load and simulate installation performance. Aerodynamics were investigated to obtain a wing with a high lift-to-drag ratio (L/D). Techniques of lightweight construction were also investigated, and a wing section was fabricated. The resultant aircraft configuration after appropriate weight balancing is shown in figure 17-7(c). The analysis of the overall structure gave the weight distribution shown in table 17-I.

TABLE 17-I. - ESTIMATED WEIGHT BREAKDOWN OF MODEL AIRPLANE DESIGNED FOR WORLD ENDURANCE FLIGHT RECORD

Component	Weight, lb
Wing structure	1.5
Fuselage structure	1.0
Tail structure	.3
Propulsion system	1.2
Control system	1.0
Fuel	6.0
Total aircraft	11.0

To study the aerodynamics of flight, experiments were conducted with small, hand-launched, indoor gliders. Construction details for the glider used and adjustments required for long-duration flight are discussed in appendix B. Two of the most important adjustments for stable flight are the correct location of the center of gravity and the proper "angular difference" between the wing and the horizontal tail. A detailed discussion of these parameters for a hand-launched glider is given in appendix C. (These are also discussed in detail in chapter 9, which deals with aircraft stability and control.)

The gliders were flown (fig. 17-8) to study stability and to determine lift-to-drag ratios and sink rates. The lift-to-drag ratio of an aircraft in steady, gliding flight was shown to be equal to the distance traveled horizontally divided by the attendant decrease in altitude, or, in other words, the glide ratio. This is an aerodynamic phenomenon unrelated to weight. To illustrate this, the weight of the glider was increased by adding clay at the center of gravity, and the experiment was repeated. Although the glide ratio did not change, the gliding speed and its vertical component, the sink rate, were noticeably increased. Also shown was the equality between the power required for level flight and the rate of change of potential energy noted during gliding flight.

TOURS

Tours of places of aeronautical interest constituted an important part of the Lewis Explorer program. The purpose of these tours was to relate the aeronautical studies to the real world of aviation.

During a tour of the hangar of the Lewis Research Center (fig. 17-9), aircraft and their components were described in detail to the group. Aircraft available for inspection were a Convair F-106, a Douglas C-47, a Convair T-29, and an Aerocommander.

A comprehensive tour of various aircraft was accomplished on a visit to the Air Force Museum in Dayton, Ohio. This museum has the world's largest military aeronautical exhibit. It contains over 100 aircraft and missiles, with numerous informative displays of hardware, documents, photographs, and personal memorabilia.

A tour was made of the Air Traffic Control Center at Oberlin, Ohio. This facility is under the jurisdiction of the Federal Aviation Agency (FAA), which, in turn, is under the Department of Transportation. The FAA is responsible for ensuring a safe and orderly flow of civil and military air traffic throughout the nation's airways. The heart of the operation of an Air Traffic Control Center is the radar room (fig. 17-10(a)), where the controller follows the flight of aircraft through his area and is in direct radio contact with the pilots. The controller assigns specific altitudes and clearances to the pilots and provides them with various weather advisories and flight directions. A computer room

(fig. 17-10(b)) provides the latest weather data and airline schedular data for the entire country.

Depending on weather conditions, all aircraft fly by one of two sets of FAA rules - either instrument flight rules (IFR), or visual flight rules (VFR). When the weather is clear, most pilots fly VFR; in bad weather, flights normally are conducted under IFR procedures.

Under VFR, the pilot flies by visual reference to the ground, and he is solely responsible for avoiding other aircraft. His obligation is more than "see and be seen" - it is to "see and avoid." But, when weather and visibility are poor and IFR weather conditions prevail, the responsibility for keeping aircraft separated rests with the air traffic controller. Even in good weather, many pilots, especially those flying high-speed aircraft, elect to fly under IFR in order to take advantage of the separation and the greater protection afforded by FAA's air traffic specialists. All major scheduled airline flights follow this procedure. To guard against possible conflicts in flight paths, all pilots flying under IFR must file flight plans with the FAA.

SYMPOSIUM ON AERONAUTICS

Any program should have a focal point toward which the overall effort is directed. For the Lewis Aerospace Explorer program, the focal point was a full-scale symposium on aeronautics (fig. 17-11). This was, of course, a valuable exercise in communication. Furthermore, it placed schedular deadlines on the various research projects and experiments undertaken by the youths and created a realistic sense of pressure to plan and conduct the experiments efficiently, to complete the projects on schedule, to analyze the results carefully, and to present the results in a professional manner. Except for brief welcoming statements by the Director of the Lewis Research Center and by the Post Adviser, the entire symposium was conducted by the Explorers and was highly successful.

APPENDIX A

WIND TUNNELS

The principal tool for any study of aerodynamics is a wind tunnel. The tunnel used in this Explorer program (fig. 17-12) was constructed by Lewis Technical Services personnel from a 19-horsepower motor, an axial-flow fan, wood, Lucite, and sheet-metal. The test section was 20 inches wide and 30 inches long. Windows were provided on both sides of the test section for viewing the models, and a 10-inch-diameter port was built into the top of the test section for lighting purposes.

Other details of the tunnel and its measuring capabilities are illustrated in figure 17-13. The tunnel flow calibration (fig. 17-13(a)) showed a flat, uniform profile at full power. Top speed was approximately 52 miles per hour. This flow survey was taken along the vertical centerline. Along the walls, the boundary-layer height appeared to be less than 1 inch. By decreasing fan speed and increasing the size of a bypass opening ahead of the motor, the tunnel flow velocity could be varied down to about 18 miles per hour. To ensure minimum disturbance from the fan, a 2-inch-thick honeycomb section was added downstream of the tunnel diffuser and just upstream of the fan.

For flow visualization, smoke was injected so as to follow streamlines in a filamentary fashion through the test section. The smoke generator (fig. 17-13(b)) consisted of a small, electrical strip heater, located within an inclined tube, upon which a light oil was allowed to drip. A small fan blew air across the heater inside the tube to carry the smoke upward through a coiled condenser section into a manifold from which it was injected into the tunnel inlet through a number of orifices. Several layers of fine-mesh screening and a high-contraction-ratio nozzle were used to ensure a low-turbulence inlet flow. Representative smoke pictures are shown in figure 17-13(c).

At the rear of the test section, a grid of nylon tufts (fig. 17-13(d)) was installed as an additional means of flow visualization. As indicated in the representative photos (fig. 17-13(e)), tufts, in this case attached directly to the test model, are light enough to lie back in the direction of the local streamline. Flow separation is evidenced by an obvious randomness in the observed direction of the tufts.

A simplified force-balance system (figs. 17-13(d) and (f)) was used to measure aerodynamic lifts and drags. First, without airflow in the tunnel, the system was balanced (by means of weights in the pans) so that the supporting shaft of the test model was centered in the hole in the test-section window. Then, with airflow in the tunnel, the system was rebalanced by means of additional weights. Since one end of the supporting shaft was held in a ball socket, the values of lift and drag were equivalent to double the weights that were added to rebalance the system.

A person, or group, studying aerodynamics may not have the ability or the means to

construct a sophisticated wind tunnel. However, a simple wind tunnel, powered by an ordinary electric fan, and suitable for elementary investigations and demonstrations of common aerodynamic problems and phenomena, can be constructed by almost anyone from readily available materials.

A typical tunnel of this type (fig. 17-14) consists of a Plexiglas enclosed test chamber of constant cross-sectional area, through which the air stream is drawn by a large, nonoscillating, electric fan. In the inlet of the test chamber, a simple flow straightener, similar in arrangement to the dividing partitions of an egg crate and constructed of heavy bond paper, provides a relatively constant flow distribution across the test section. A simple transition cone between the test section and the fan guard, made of either cloth or cardboard, serves as the diffuser section.

A tunnel with a test chamber 7 inches high and 10 inches wide, a size easily transportable, is capable of handling wing sections or complete models of 7 or 8 inches maximum span.

The tunnel frame should be constructed of an easily worked wood, with the floor and one side made of 1/4-inch-thick plywood. The inlet and outlet sections are of 3/4-inch-thick wood. All mating wood surfaces should be square and smooth to ensure rigidity and an airtight fit. Assembly is made with a waterproof wood glue and small brads and should generally follow the methods presented in figure 17-14.

The top and one side of the test chamber are of a transparent material, preferably Plexiglas, fitted into grooves in the plywood bottom and side panels. Rubber gaskets in the grooves, or small wood battens tacked along the edges of the Plexiglas panels, guard against air leaks.

Heavy bond paper should be used for construction of the flow straightener. Thirteen 1-inch strips, 10 inches long, and nineteen 1-inch strips, 7 inches long, are cut from the paper and are marked off lengthwise at 1/2-inch intervals. The paper strips are then slotted to the center line at 1/2-inch intervals. The 7-inch strips are then assembled on the 10-inch strips, slot into slot, in a manner similar to that used in constructing egg-crate partitions. Glue should be applied at each joint, and extreme care should be exercised to ensure good alinement. When the glue is dry, the structure should be sprayed or painted with thinned shellac or acetone dope for protection against curling of the paper sections. When the flow straightener is being glued into the tunnel inlet, extreme care should be taken to ensure that the eggcrate structure is perpendicular to the floor of the tunnel.

The transition cone, or diffuser, is made of either closely woven, medium-weight fabric or thin cardboard. The pattern to which the material is to be cut is shown in figure 17-14. In cutting the material, allowances should be made for the seam and, in the case of fabric, for a hem around the downstream end of the cone. The seam must be made tight. The upstream end of the cone is glued and tacked tightly around the outlet of

the test chamber. The downstream end of the cone is fastened securely to the fan guard. If the cone is made of fabric, the downstream end can be hemmed and can be secured by drawing it tightly over the fan guard by means of a drawstring in the hem.

Since an extension of the test chamber center line should correspond to the center line of the electric fan, a rigid base should be built up to support the tunnel. No exact dimensions can be given for the height of this base, as dimensions of the fan to be used may vary.

No attempt has been made to specify the methods of mounting models, as the tunnel itself is simple and straightforward and lends itself to a wide latitude of model-mounting systems, either of the rigid or of the "floating" type. A force-balance system, such as the one described earlier, may be used in this tunnel to measure aerodynamic forces on a model.

APPENDIX B

HAND-LAUNCHED, INDOOR GLIDER

Robert G. Spaulding*

The lectures, demonstrations, and experiments in aerodynamics were supplemented with a simple, yet challenging, glider building and flying project. Full-size plans for the small, hand-launched, indoor glider used in this activity are shown in figure 17-15. Details of construction and adjustments are discussed herein.

Although several adjustments are particular to this model, generally speaking, the aerodynamic principles apply to all indoor gliders built for endurance flying. The term "launch phase" refers to the high-speed portion of flight, when the model is thrown vertically to its maximum altitude. "Glide phase" refers to the remainder of the flight. The goal is to make adjustments particular to each phase, thus producing the longest flight time.

This is a basic learning model. From here, follow-on projects employing sweptback or higher-aspect-ratio wings, longer tail moment arms, etc., can be developed, leading to original designs incorporating the best aerodynamic features.

Adjustments

Center of gravity. - The center of gravity (c.g.) is the balance point of the glider. It may be thought of as that point through which all the weight of the glider is acting. The location of the c.g. can be changed by adding or removing weight (clay) at the nose of the model (fig. 17-16). The farther back the c.g. is located, the tighter the circle of flight must be to keep the model from stalling. Therefore, if flying is to be done in a small room, the c.g. must be located relatively far back. For our glider, the c.g. should be located behind the leading edge of the wing by a distance equivalent to 70 to 80 percent of the wing chord.

Stabilizer tilt. - This adjustment (fig. 17-17) affects the diameter and direction of the turning circle during the gliding phase of the flight. Adjustment is made by twisting the tail boom.

A full-scale aircraft normally has its center of gravity located aft of the wing leading edge by a distance of 25 to 30 percent of the wing chord. To turn the aircraft in flight, one or more control surfaces must be deflected into the airstream. This method of turning the aircraft produces high drag.

*Experimental Wood Modelmaker.

For a hand-launched, indoor, endurance glider, the drag must be kept to a minimum. Therefore, the method used to turn a full-size aircraft should not be used to turn the glider. Instead, the glider can be caused to turn by tilting the stabilizer-and-fin assembly. Stabilizer tilt misalines the lift vectors on the wing and stabilizer and gives the glider a natural turn tendency. This is an aerodynamic function and results in a low drag factor. The effectiveness of stabilizer tilt can be increased by moving the center of gravity farther back to increase the load on the stabilizer. Moving the center of gravity rearward necessitates increasing the size of the stabilizer to keep the load factor of the stabilizer the same as that of the wing.

The stabilizer tilt shown in figure 17-17 will place the glider into a leftward gliding circle after a right-handed launch. For a left-handed launch and a rightward gliding circle, the stabilizer must be tilted in the opposite direction.

Angular difference. - Angular difference concerns the angular relation of the wing and the horizontal stabilizer (fig. 17-18). All aircraft must have an angular difference in order to maintain altitude. The amount required for our glider is so small that it should be built without any. Then, the necessary angular difference can be obtained by bending the tail boom.

Wing-tip weight. - Wing-tip weight is used to cause the glider to roll out of the launch phase and into the glide phase in a smooth, efficient manner. Adjustment is made (fig. 17-19) by adding weight (clay), as needed, to the under portion of the appropriate wing tip to cause the glider to roll to the right or left.

Weight on the left wing tip, as shown in figure 17-19, will cause the glider to roll out of the right-banked attitude of a right-handed launch and into a leftward gliding circle. For a left-handed launch and a rightward gliding circle, the weight must be placed on the right wing tip.

Rudder offset. - Rudder offset can be used to compensate for structural misalinement. Adjustment is accomplished by warping the trailing edge of the rudder (fig. 17-20).

Concluding Remarks

This small glider, if carefully constructed and properly adjusted, flies beautifully in small areas. It is hand launched, nearly vertically, in a steep, right bank. The launch adjustments assure proper and efficient flight during the high-speed launch phase. At the top of the climb, if adjustments are proper, the model will roll to the left, flatten out, and glide in tight, left circles. (As mentioned previously, for a left-handed launch and a rightward gliding circle, both the stabilizer-tilt and the wing-tip-weight adjustments must be reversed. That is, the stabilizer must be tilted to the left, and the weight must be placed on the right wing tip.)

Adjustments affect each other. After one adjustment has been successfully completed, other adjustments and readjustments will be necessary. Therefore, all adjustments must be integrated to bring out the best flying characteristics of the glider. Since adjustments create drag, they should be kept to a minimum.

APPENDIX C

EFFECTS OF CENTER-OF-GRAVITY LOCATION AND ANGULAR DIFFERENCE ON FLIGHT CHARACTERISTICS OF HAND-LAUNCHED GLIDER

Fred W. Steffen*

Herein we will explain why the location of the center of gravity (c.g.) and the angular difference between the wing and the tail surfaces affects the flight characteristics of a hand-launched, endurance glider.

The following symbols are used in the discussion and the equations:

A.R.	aspect ratio, b^2/S
b	span
$\bar{c}$	mean chord, S/b
c.g.	center of gravity
d_t	moment arm of tail (measured from c.g. to point 1/4 of $\bar{c}$ aft of leading edge of tail surface)
d_w	moment arm of wing (measured from c.g. to point 1/4 of $\bar{c}$ aft of leading edge of wing)
d_1, d_2	lever arms of weights W_1 and W_2
L	lift force
S	surface area
S_t	tail surface area
S_w	wing surface area
V	velocity of glider relative to air
W_1, W_2	weights on opposite ends of balance beam
α	angle of attack (i.e., angle between surface and air-velocity direction)
α_t	tail angle of attack
α_w	wing angle of attack
$\Delta( )$	small increment in ( )

*Aerospace Engineer, Propulsion Aerodynamics Branch.

The lift forces of the wing L_w and horizontal tail L_t acting through moment arms d_w and d_t about the center of gravity (fig. 17-21) create pitching moments (nose up or nose down). If the sum of the pitching moments about the center of gravity is zero, the glider is trimmed, and $L_w d_w = L_t d_t$. This condition is analogous to that of the balanced beam shown in figure 17-22(a), where $W_1 d_1 = W_2 d_2$. However, a trimmed glider may or may not be stable. A glider is statically stable if restoring pitching moments are created when the glider is rotated in the pitch plane. For example, the balanced beam (fig. 17-22(a)) is trimmed but not stable, because no restoring moments are created if the beam is tilted. In other words, if the beam is tilted, the moment $W_1 d_1$ is still equal to $W_2 d_2$. To make the beam stable, springs may be inserted under each end, as shown in figure 17-22(b). Then, as the beam is tilted, the springs create restoring moments, which tend to restore the beam to its original position.

Figure 17-23 shows a glider with a large amount of clay ballast in the nose, so that the center of gravity is ahead of the wing lift force. For the moment about the center of gravity to be zero, the force from the horizontal tail must be downward (i.e., the tail angle of attack α_t must be negative).

Endurance gliders, however, are usually trimmed with the center of gravity aft of the wing lift force, as shown in figure 17-24. This is done for two reasons: first, the weight of the required clay ballast is reduced, and a reduction in weight causes a reduction in sinking speed; second, both the wing and the tail contribute to the total lift force. Thus, a total lift force equal to the weight can be achieved at a lower gliding velocity V, which, in turn, results in a lower sinking speed. As before, for the glider to be in trim, $L_w d_w$ must be equal to $L_t d_t$ (i.e., the resultant pitching moment must be zero).

For any given location of the center of gravity, the glider can be trimmed at only one wing angle of attack $\alpha_{w,1}$ and one tail angle of attack $\alpha_{t,1}$. Individual adjustments in the wing and tail angles of attack are made by changing the angles of incidence of these surfaces. If the location of the center of gravity is such that the trim angle of incidence of the wing is greater than that of the tail (positive angular difference), the glider is statically stable in the pitch plane. This means that if the glider is pitched upward or downward from its trim attitude (i.e., if the angles of attack of the wing and tail are increased or decreased by some angle $\Delta\alpha$), restoring moments are developed which tend to return the glider to the trim attitude.

To simplify the explanation of how these restoring moments are developed, let us assume that the angles of attack of the wing and tail are equal to their angles of incidence. The lift force from a surface such as a wing or a horizontal tail is directly proportional to its angle of attack. The lift forces per unit area, L/S, for the wing and tail of a glider with positive angular difference are plotted against angle of attack α in figure 17-25(a). Since the angles of attack of the wing and tail are assumed to be equal to their angles of incidence, the trim angle of attack of the wing $\alpha_{w,1}$ is greater than that of the tail $\alpha_{t,1}$. (Although it is not essential to this discussion, the slopes of the two curves are shown to

be different. The slope of each curve is directly proportional to the aspect ratio of the surface. The aspect ratio A.R. is the square of the span b^2 divided by the surface area S. Since the wing usually has a greater aspect ratio than the tail, the curve for the wing has a greater slope than the curve for the tail.) Now if the trim angles of attack of the wing and tail, $\alpha_{w,1}$ and $\alpha_{t,1}$, are increased by $\Delta\alpha$ to $\alpha_{w,2}$ and $\alpha_{t,2}$, the lift per unit area of the tail $(L/S)_t$ is increased by a greater percentage than the lift per unit area of the wing $(L/S)_w$. In the example shown in figure 17-25(a), the tail force per unit area increases 100 percent, while the wing lift force increases by only 50 percent. This excess tail lift causes a nose-down moment which tends to restore the wing and tail angles of attack to their initial values. The glider, therefore, has static stability in pitch.

As the center of gravity is moved farther aft, a center-of-gravity location is reached, where, to achieve zero resultant pitching moment about the center of gravity, the angle of incidence of the tail must be equal to the angle of incidence of the wing (zero angular difference). This position of the center of gravity yields neutral static longitudinal stability and is called the neutral point. This situation is illustrated in figure 17-25(b), which again shows plots of the lift force per unit area L/S as a function of angle of attack α for the wing and tail surfaces. However, here the trim angle of attack of the wing $\alpha_{w,1}$ is equal to that of the tail $\alpha_{t,1}$. Therefore, increasing these angles of attack to $\alpha_{w,2}$ and $\alpha_{t,2}$ by some angle $\Delta\alpha$ produces the same percentage of change in the lift per unit area of the wing $(L/S)_w$ as in that of the tail $(L/S)_t$. Therefore, the resultant moment about the center of gravity remains zero regardless of the angle of attack, and no restoring moments are created. When a glider trimmed in this manner is flown, it often enters an accelerated dive (appears to "run downhill") and crash. For this reason, initial flights should be made with the center of gravity a comfortable distance ahead of the neutral point and with positive angular difference between the wing and the tail.

The location of the neutral point is also modified by the fact that the horizontal tail operates in the downwash of the wing. In other words, the wing acts as a flow straightener for the horizontal tail, so that when the glider is rotated from position 1 to position 2, the $\Delta\alpha_t$ is less than $\Delta\alpha_w$. Although this difference is small for model gliders, it does have the effect of moving the neutral point to a more forward position.

The neutral point for a hand-launched glider can be roughly calculated as follows. First, the percentages of increase in lift per unit area L/S with angle of attack α for both wing and tail are set equal (this is the situation with zero angular difference). In equation form, this can be written as

$$\frac{\Delta\left(\frac{L}{S}\right)_w}{\left(\frac{L}{S}\right)_{w,1}} = \frac{\Delta\left(\frac{L}{S}\right)_t}{\left(\frac{L}{S}\right)_{t,1}}$$

or

$$\frac{\left[\frac{\Delta\left(\frac{L}{S}\right)}{\Delta\alpha}\right]_w \Delta\alpha_w}{\left(\frac{L}{S}\right)_{w,1}} = \frac{\left[\frac{\Delta\left(\frac{L}{S}\right)}{\Delta\alpha}\right]_t \Delta\alpha_t}{\left(\frac{L}{S}\right)_{t,1}}$$

Since the wing and tail are both rigidly attached to the fuselage (and if downwash effects are disregarded),

$$\Delta\alpha_w = \Delta\alpha_t$$

Then,

$$\frac{\left(\frac{L}{S}\right)_{w,1}}{\left(\frac{L}{S}\right)_{t,1}} = \frac{\left[\frac{\Delta\left(\frac{L}{S}\right)}{\Delta\alpha}\right]_w}{\left[\frac{\Delta\left(\frac{L}{S}\right)}{\Delta\alpha}\right]_t}$$

For the resultant moment about the center of gravity to be zero,

$$\left(\frac{L}{S}\right)_{w,1} S_w d_w = \left(\frac{L}{S}\right)_{t,1} S_t d_t$$

Then

$$\frac{d_t}{d_w} = \frac{\left(\frac{L}{S}\right)_{w,1}}{\left(\frac{L}{S}\right)_{t,1}} \frac{S_w}{S_t} = \frac{\left[\frac{\Delta\left(\frac{L}{S}\right)}{\Delta\alpha}\right]_w S_w}{\left[\frac{\Delta\left(\frac{L}{S}\right)}{\Delta\alpha}\right]_t S_t}$$

Now

$$d_{total} = d_w + d_t$$

Therefore

$$d_t = \frac{d_{total}}{1 + \frac{d_w}{d_t}} = \frac{d_{total}}{1 + \frac{\left[\frac{\Delta\left(\frac{L}{S}\right)}{\Delta\alpha}\right]_t S_t}{\left[\frac{\Delta\left(\frac{L}{S}\right)}{\Delta\alpha}\right]_w S_w}}$$

If the aspect ratio of the wing is approximately equal to the aspect ratio of the tail, then

$$\left[\frac{\Delta\left(\frac{L}{S}\right)}{\Delta\alpha}\right]_w \approx \left[\frac{\Delta\left(\frac{L}{S}\right)}{\Delta\alpha}\right]_t$$

and

$$d_t \approx \frac{d_{total}}{1 + \frac{S_t}{S_w}}$$

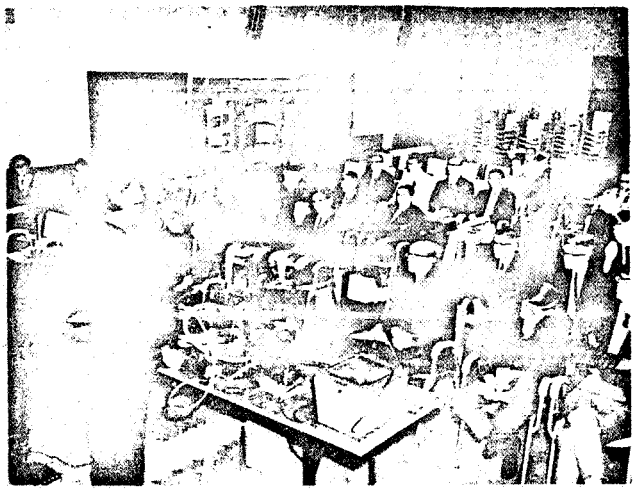

(a) Meeting overview.

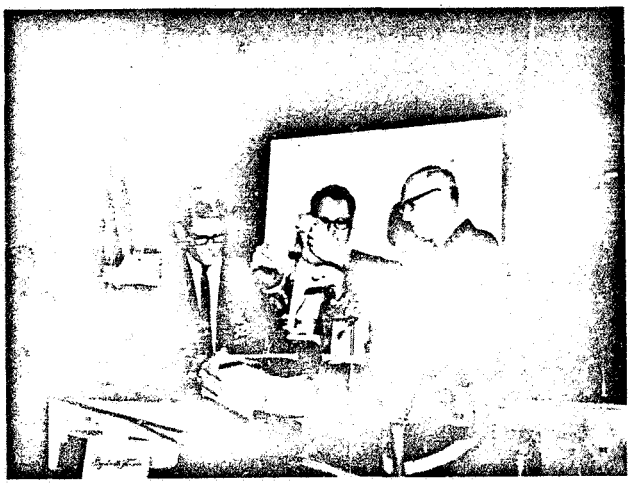

(b) Comparison of fluid flow and particle flow over a curved surface.

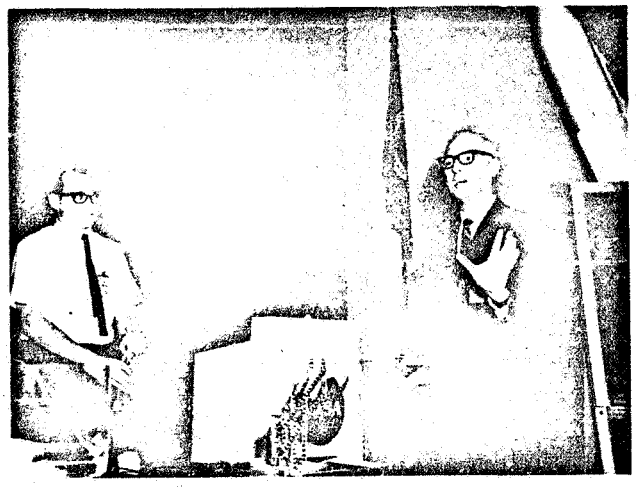

(c) Lift results from the bending of airflow either by passage through a bent tube or by deflection across an inclined surface.

(d) Fluid flow separates and produces a turbulent wake behind a moving blunt-based body.

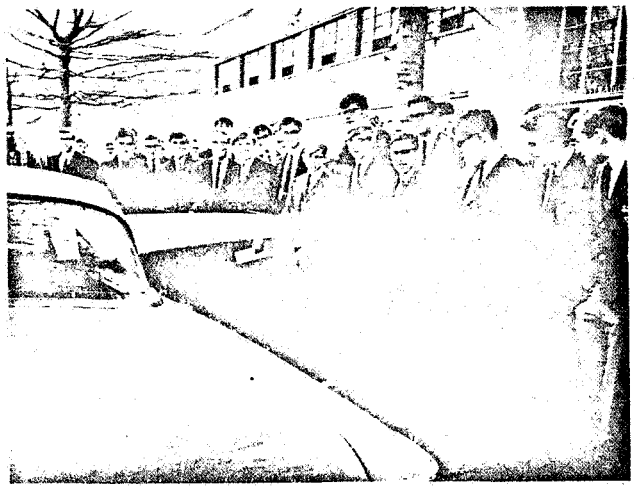

(e) Tip of a finite airfoil produces vortex flow.

Figure 17-1. - Aerodynamics demonstrations.

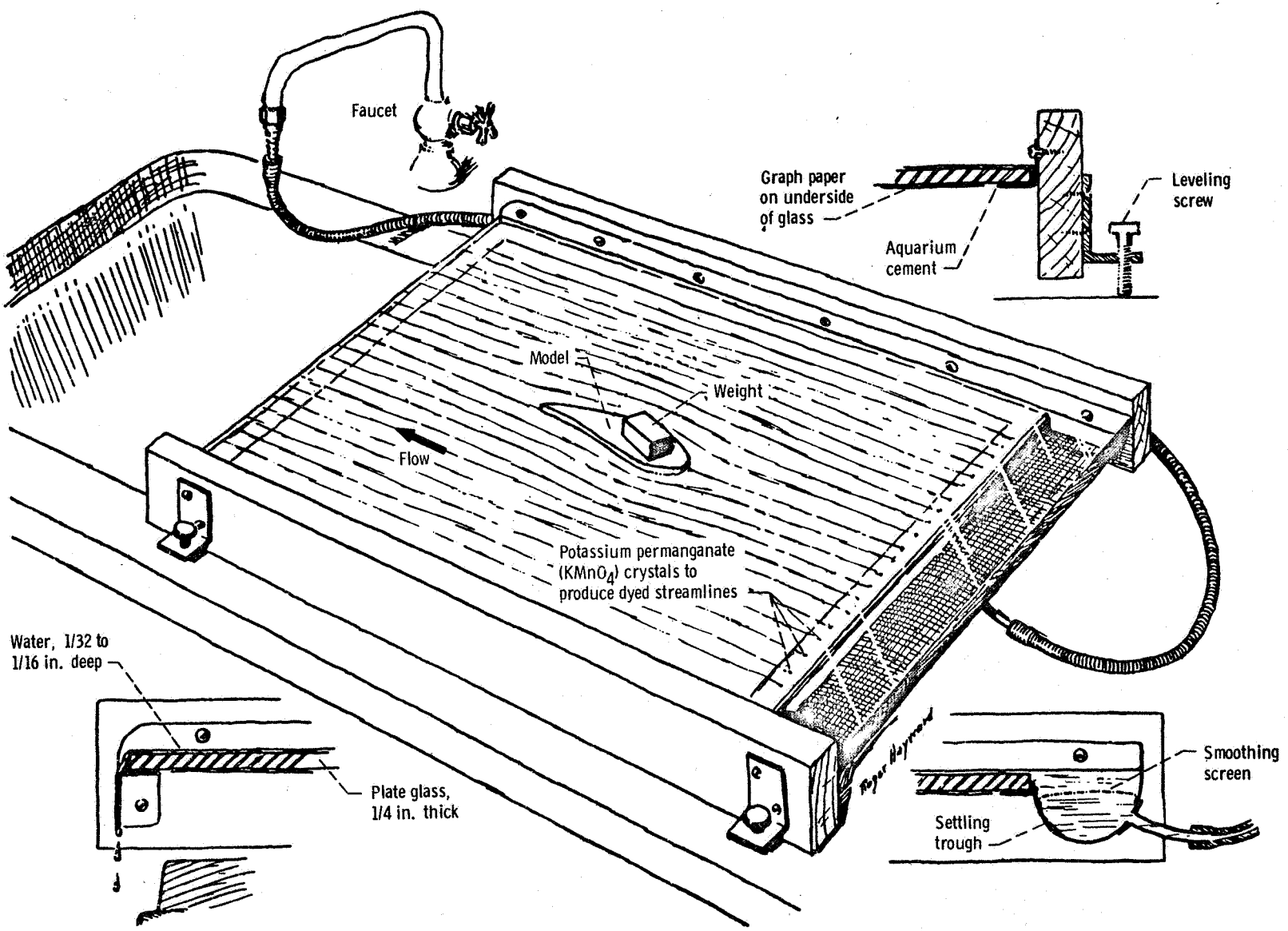

Figure 17-2. - Simple design for a water table. (Courtesy of Scientific American.)

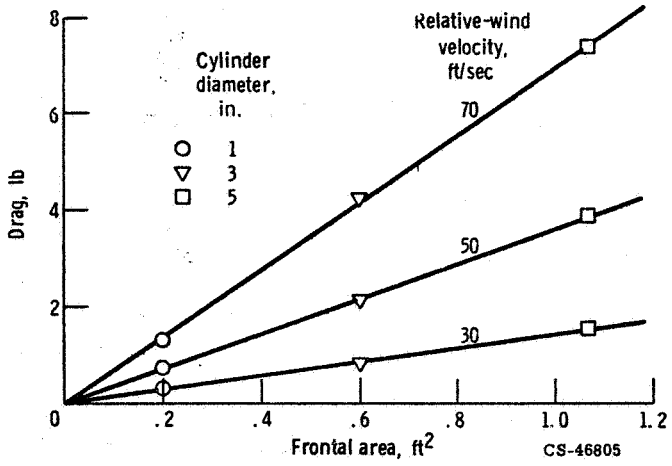

(a) Drag as a function of frontal area for circular cylinders.

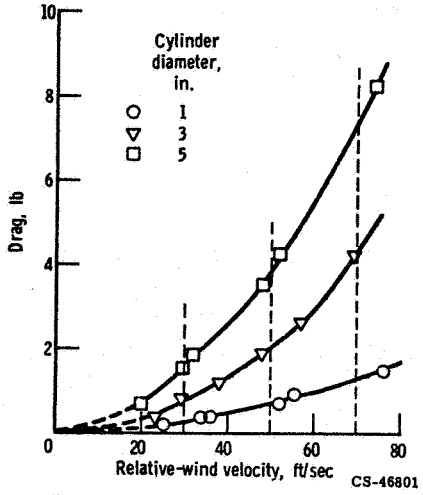

(b) Drag as a function of velocity for circular cylinders.

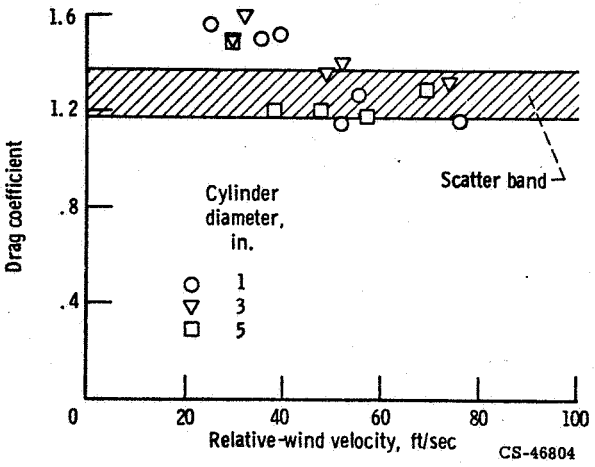

(c) Drag coefficient as a function of velocity for circular cylinders.

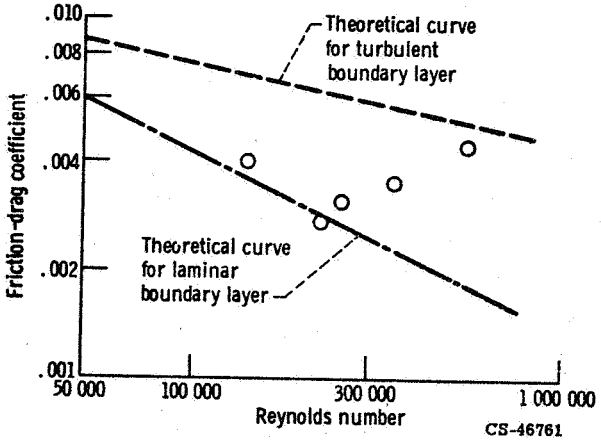

(d) Friction-drag coefficient as a function of Reynolds number for a flat plate.

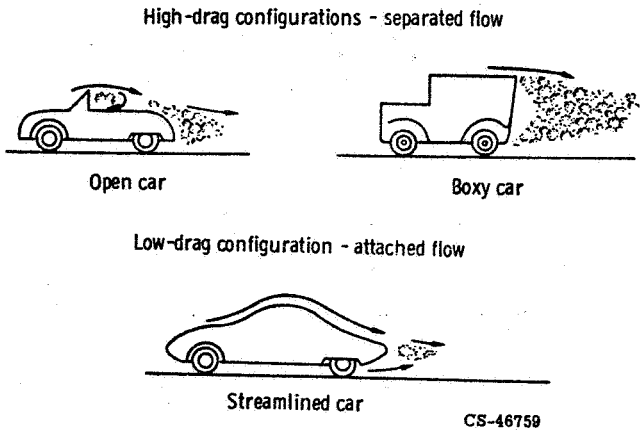

(e) Flow-separation patterns behind automobiles.

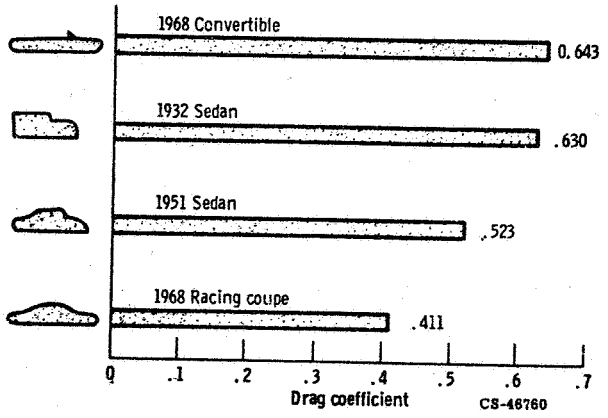

(f) Experimentally obtained drag results for automobiles traveling at 50 miles per hour.

Figure 17-3. - Wind-tunnel studies of drag.

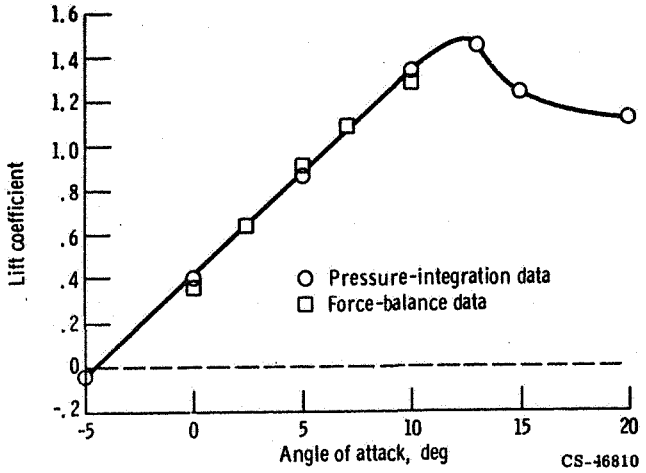

(a) Airfoil lift coefficient as a function of angle of attack.

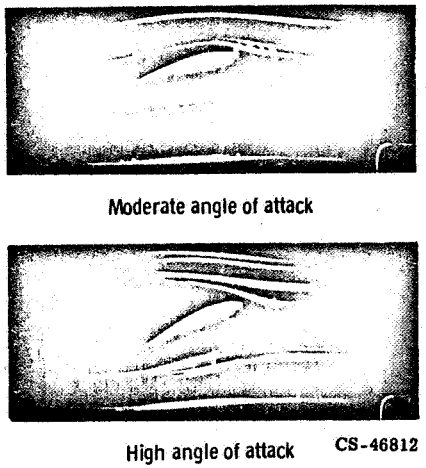

(b) Use of smoke for visualization of airflow pattern over airfoil at moderate and high angles of attack.

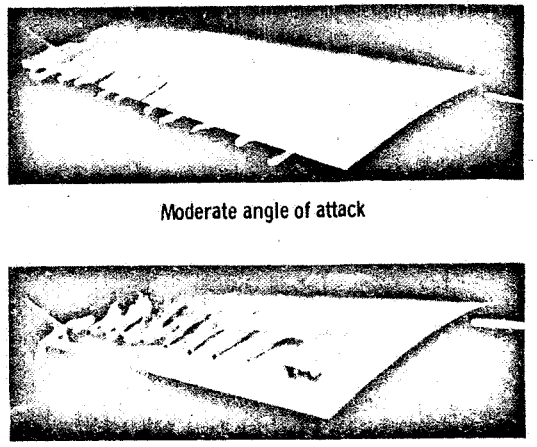

(c) Use of tufts for visualization of airflow pattern over airfoil at moderate and high angles of attack.

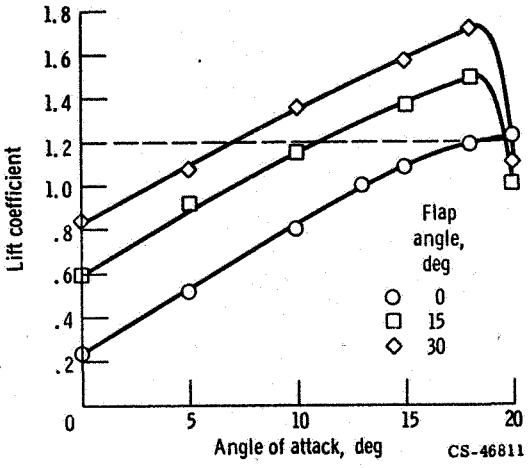

(d) Effect of flap on lift coefficient of airfoil.

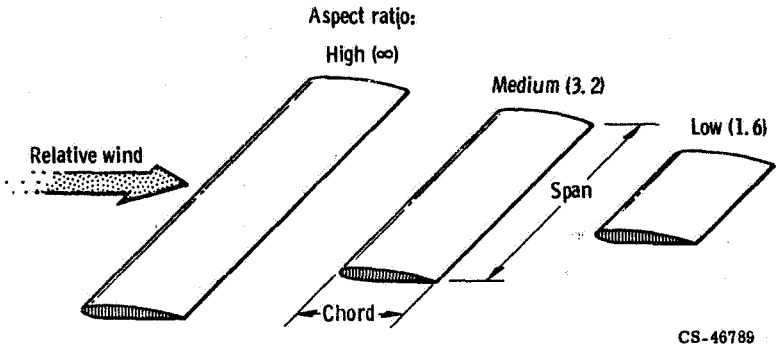

(e) Finite wings with different aspect ratios (span/chord).

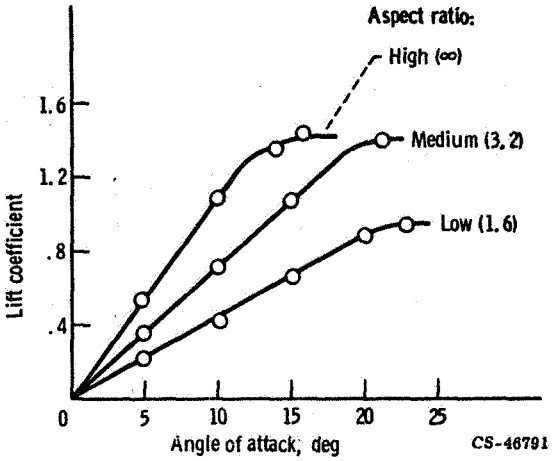

(f) Effect of aspect ratio on lift coefficient of airfoil.

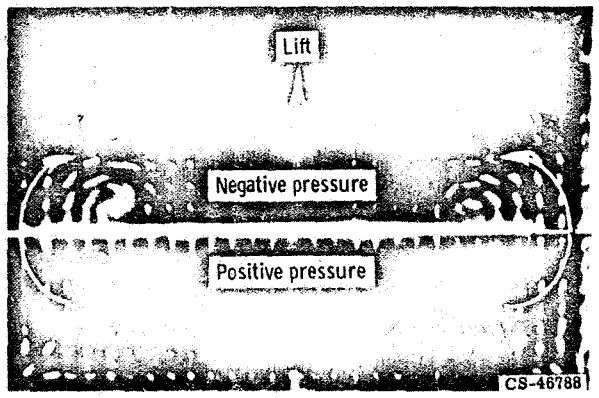

(g) Photograph of tuft pattern showing wing-tip vortexes.

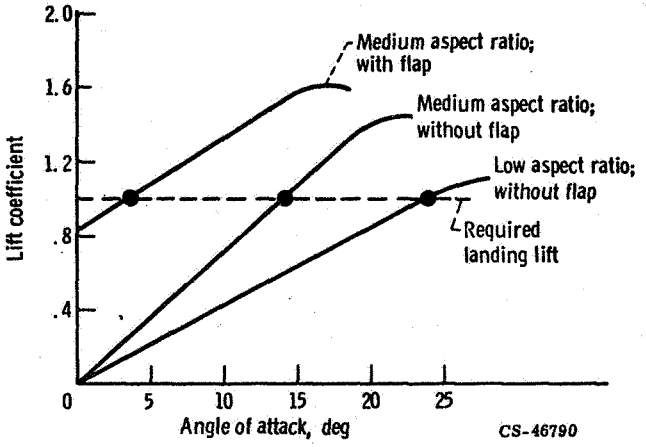

(h) Interrelation of the effects of wing angle of attack, aspect ratio, and flap on the lift coefficient of the wing.

Figure 17-4. - Wind-tunnel studies of lift.

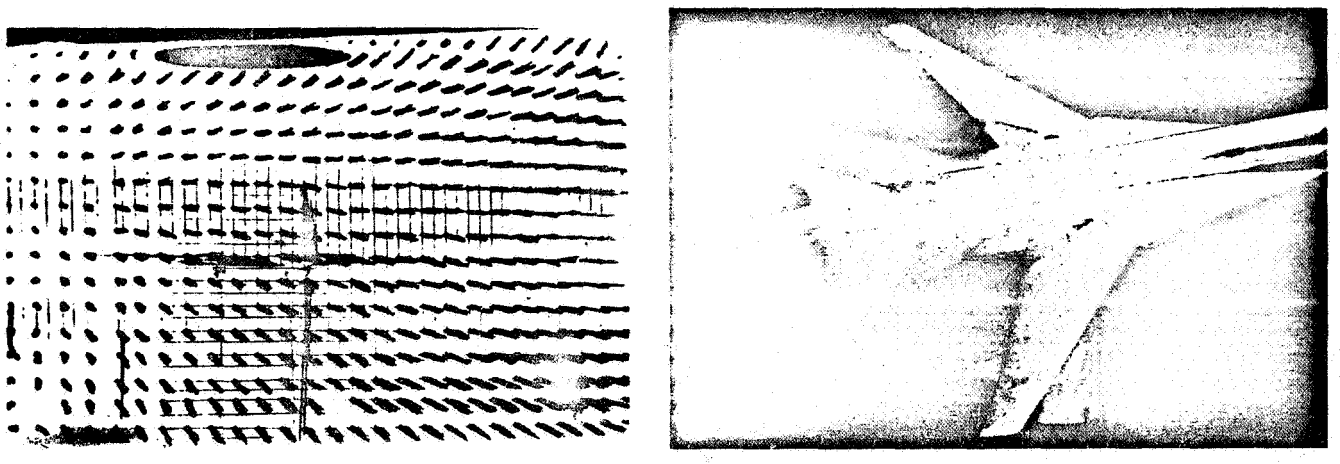

Zero angle of attack

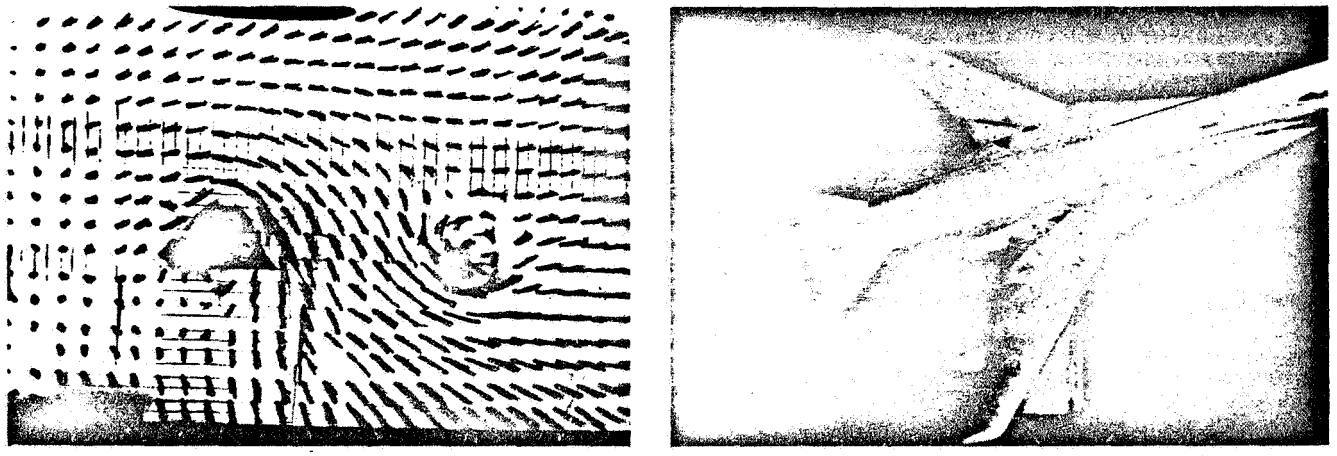

Moderate angle of attack

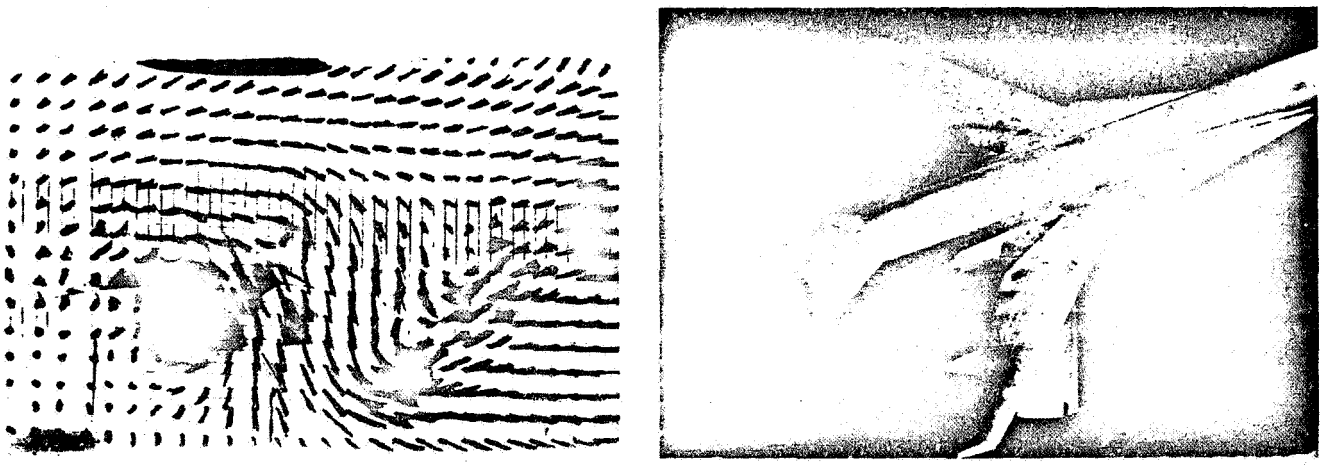

High angle of attack

(a) Wings unswept.

Figure 17-5. - Tuft patterns showing variation of downstream airflow with angle of attack for aircraft model with variable-sweep wing.

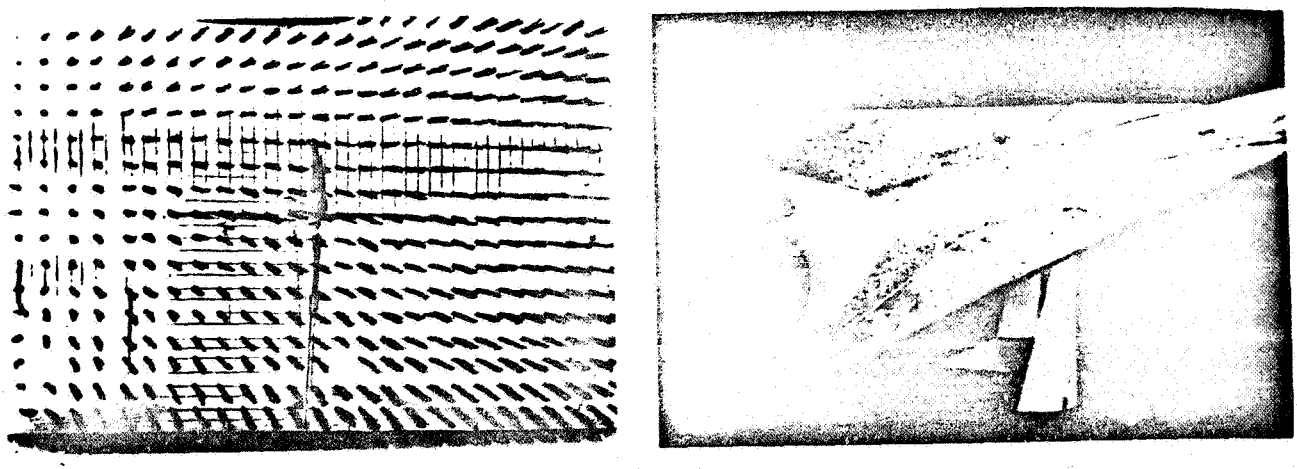

Zero angle of attack

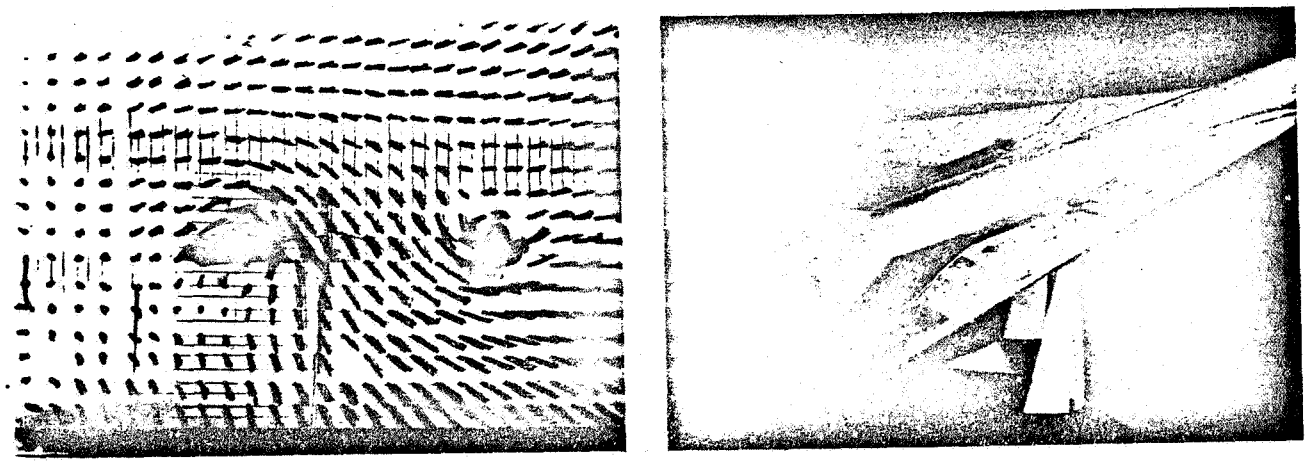

Moderate angle of attack

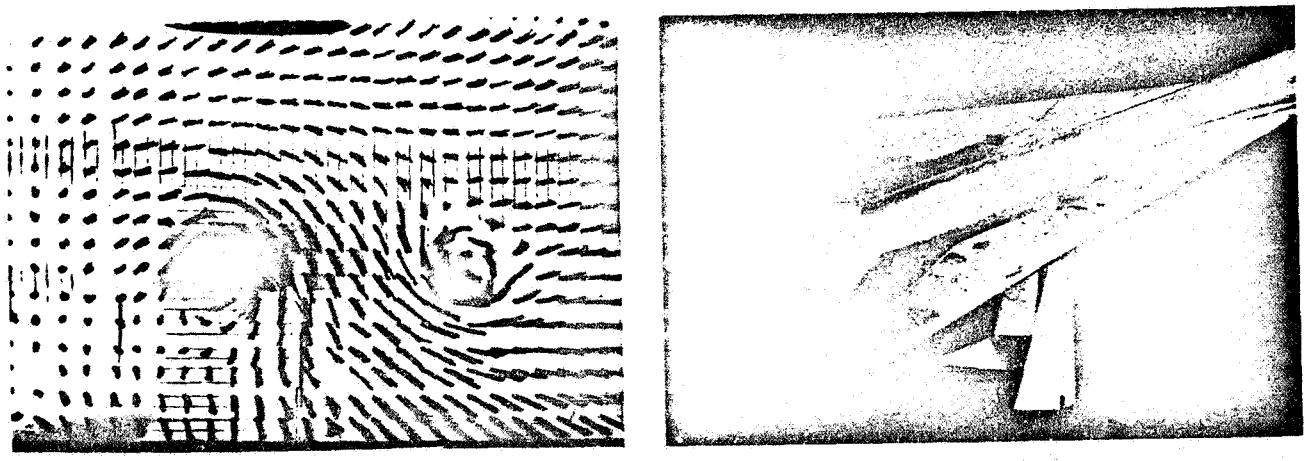

High angle of attack

(b) Wings fully swept.

Figure 17-5. - Concluded.

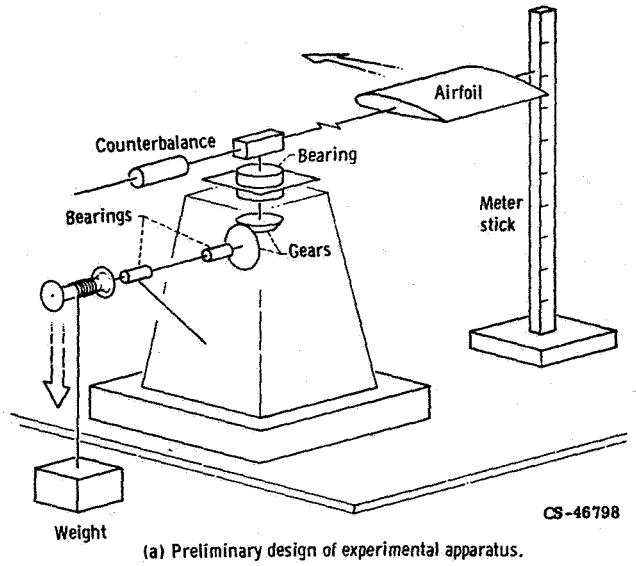

(a) Preliminary design of experimental apparatus.

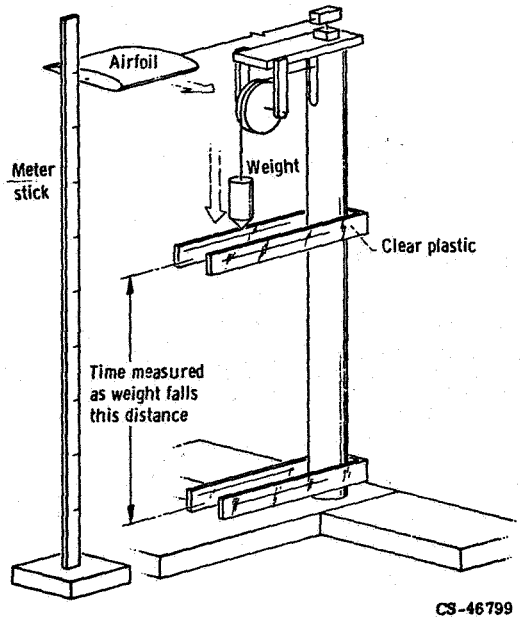

(b) Operational model of experimental apparatus.

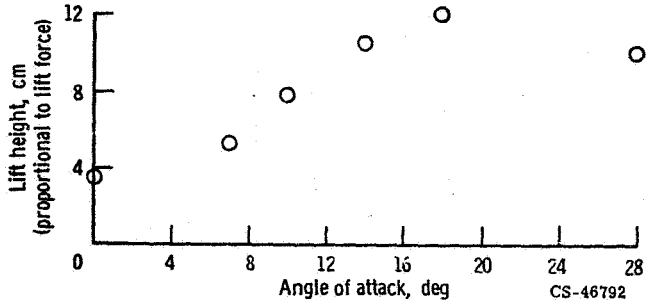

(c) Lift as a function of angle of attack for a plane wing. (Relative-wind velocity, ≈10 mph.)

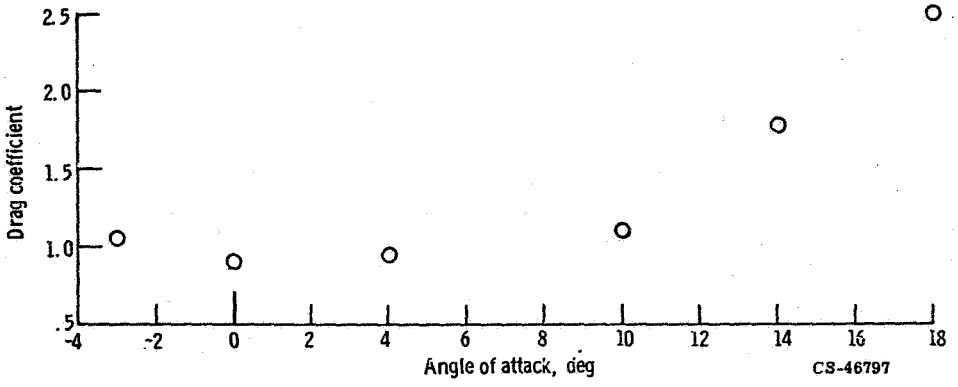

(d) Drag as a function of angle of attack for a plane wing.

Figure 17-6. - Project GARAGE (Gravity Accelerated Rotational Aerodynamic Gaging Equipment).

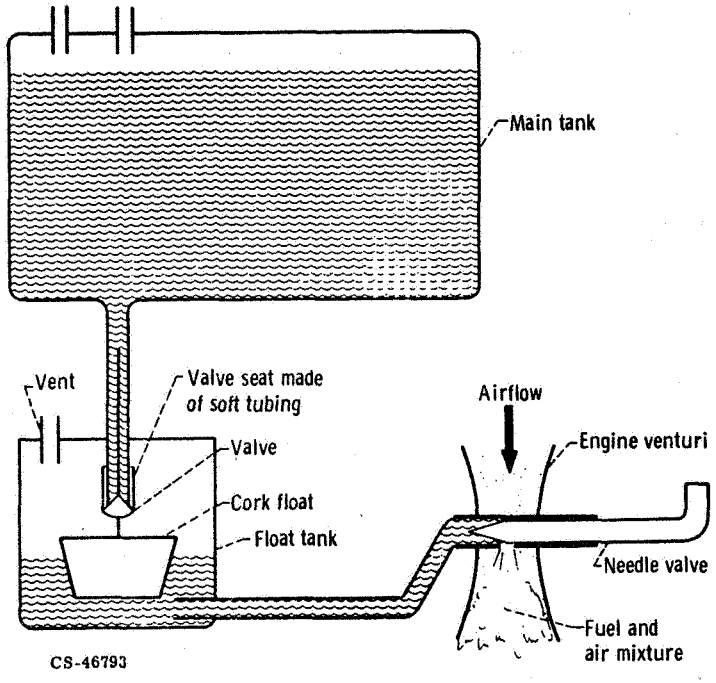

(a) Schematic diagram of fuel storage and metering system.

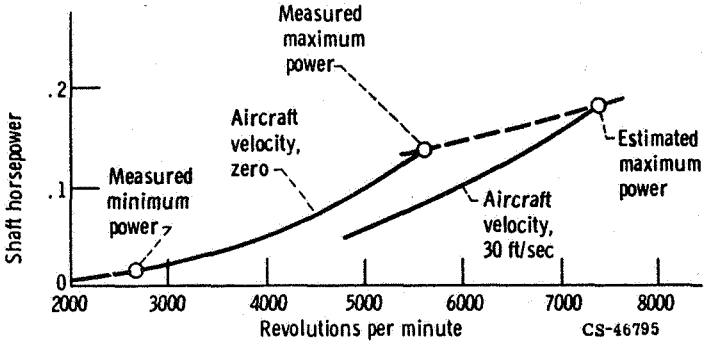

(b) Engine performance with 12-inch-diameter, 6-inch-pitch propeller.

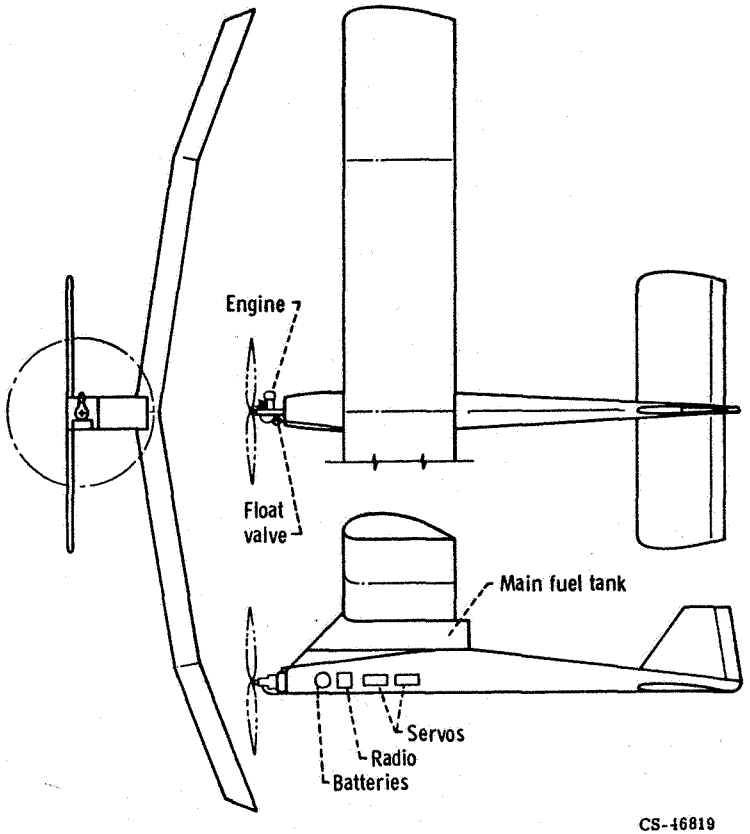

(c) Airplane configuration. (Wing area, 1800 in.^{2}; stabilizer area, 450 in.^{2}; gross weight, 11 lb.)

Figure 17-7. - Radio-controlled model airplane designed as a candidate for world endurance flight.

Figure 17-8. - Use of hand-launched, indoor glider for aerodynamics study.

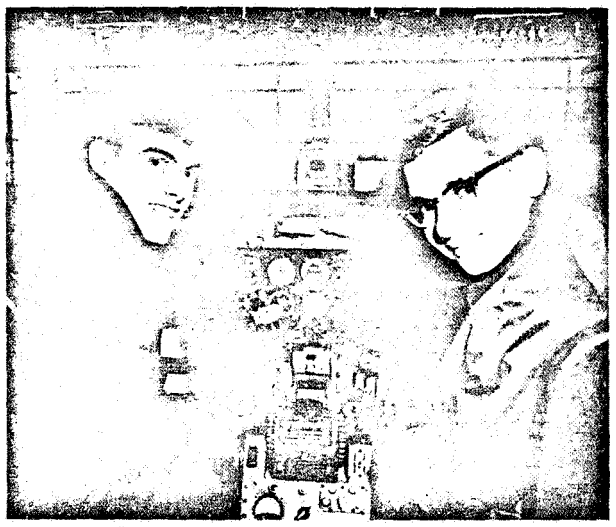

(a) Cockpit checkout.

(b) Landing-gear inspection.

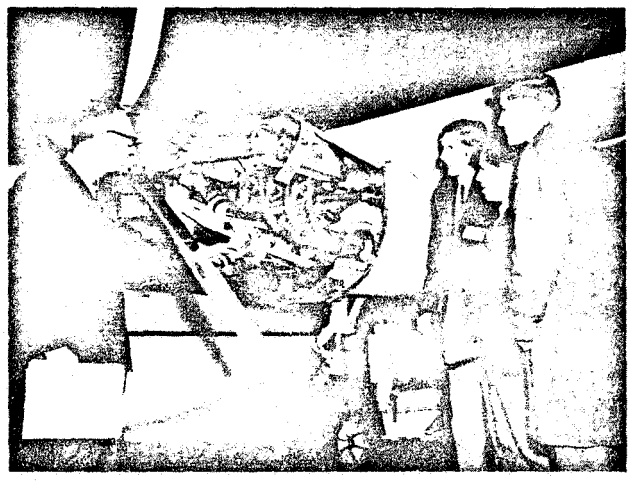

(c) Discussion of engine and propeller.

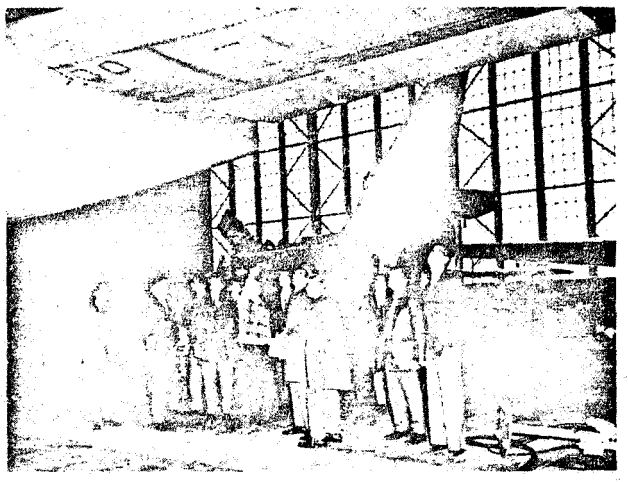

(d) Pointing out control-surface details on the horizontal tail.

Figure 17-9. - Tour of hangar and aircraft.

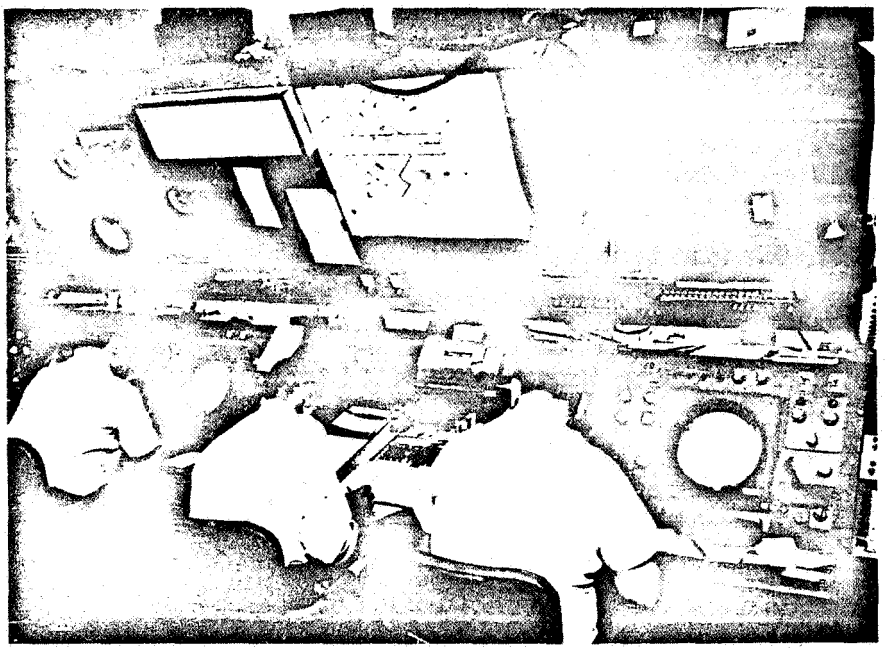

(a) Air traffic control (or radar) room.

(b) Computer room (weather data and airline schedules).

Figure 17-10. - Tour of Air Traffic Control Center.

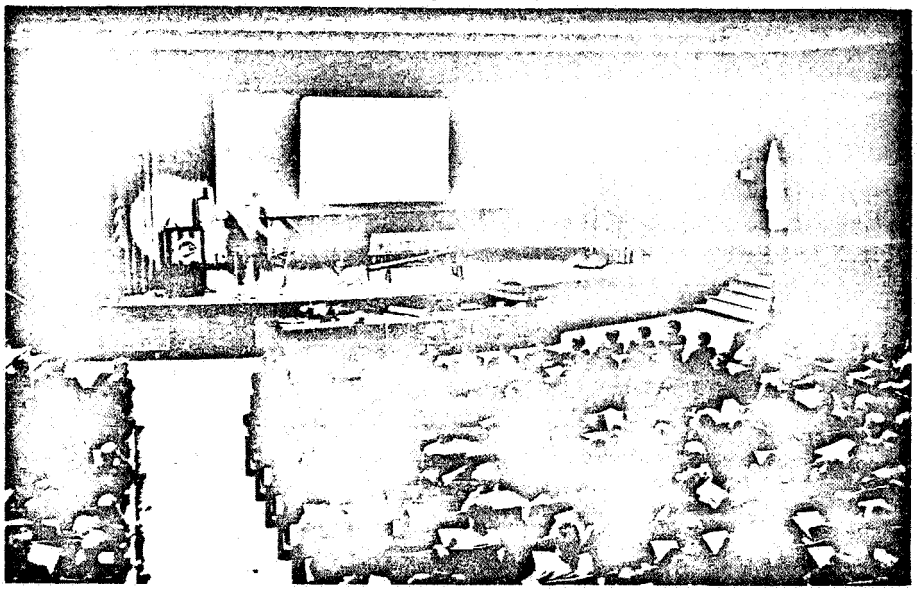

(a) Overview of auditorium.

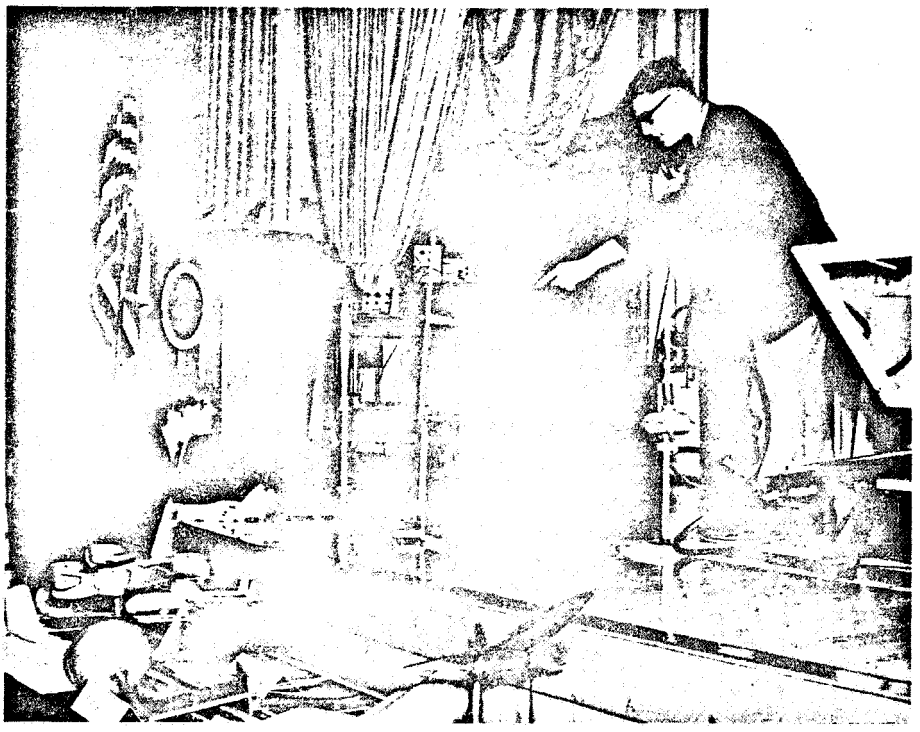

(b) Demonstration of Project GARAGE (aerodynamics experiment).

Figure 17-11. - Aeronautics symposium.

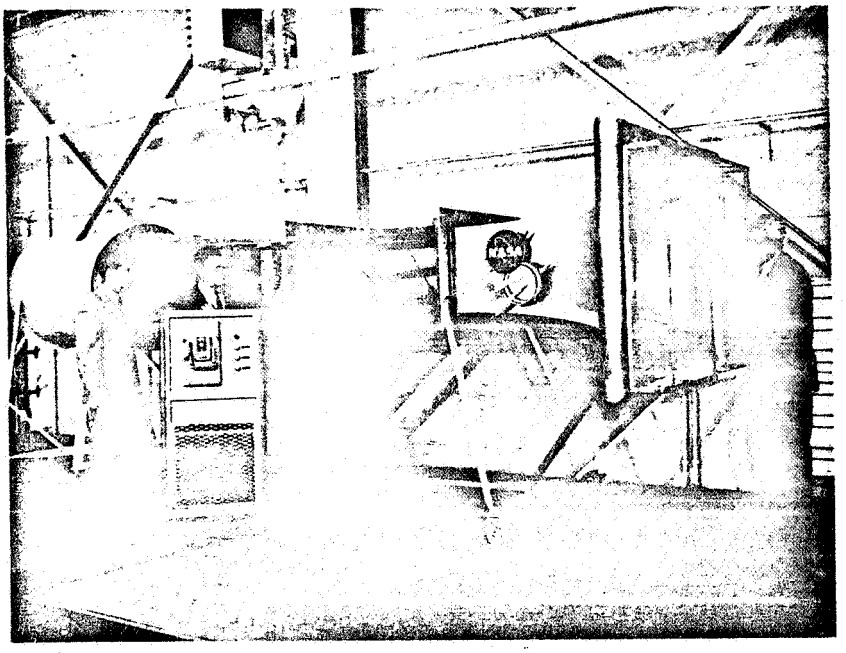

(a) Overall view of tunnel.

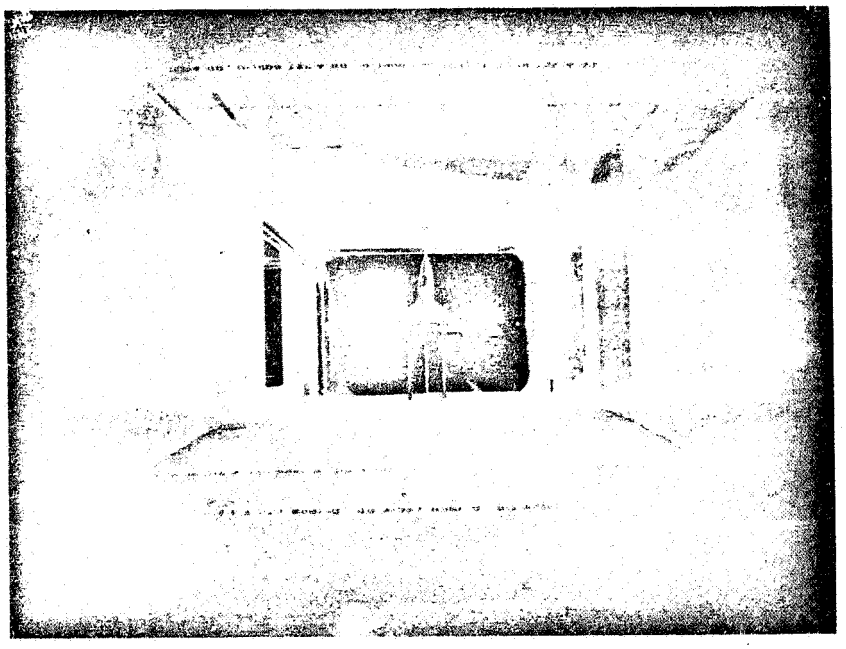

(b) View downstream through tunnel nozzle showing model installed in test section.

Figure 17-12. - Explorer wind tunnel.

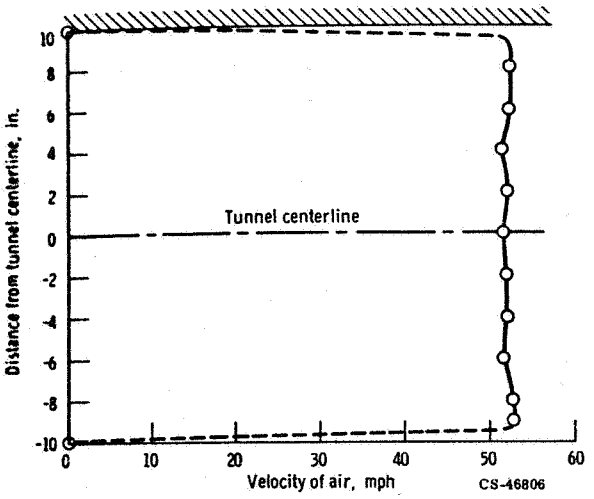

(a) Tunnel flow calibration at full power.

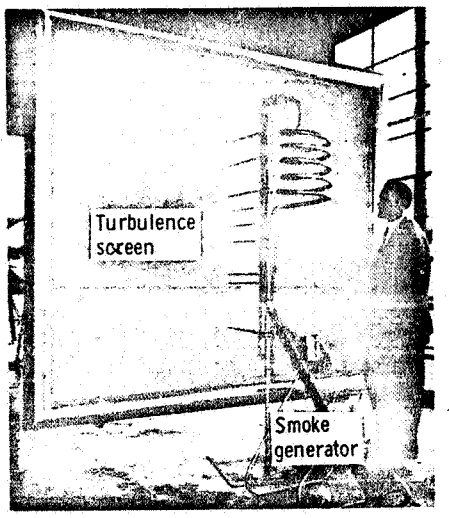

(b) Smoke generator and turbulence screen.

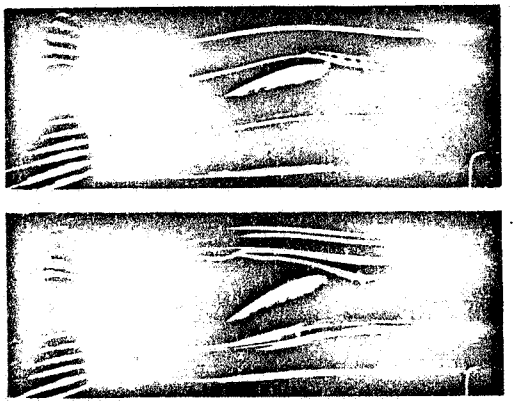

(c) Representative smoke pictures showing smooth and turbulent flow over airfoil.

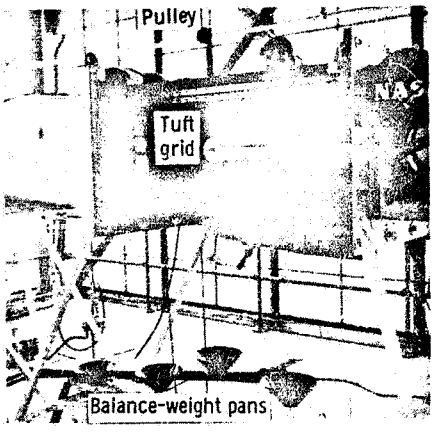

(d) Test section with balance-weight pans and tuft grid.

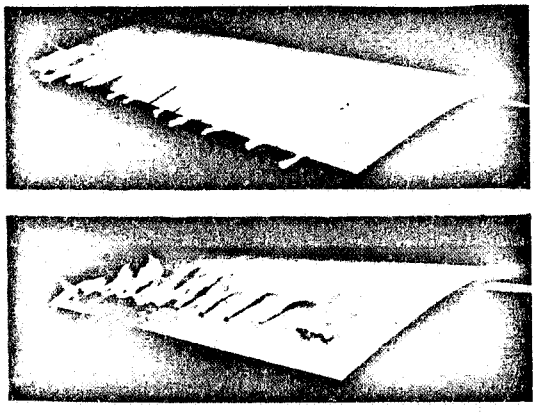

(e) Representative tuft pictures showing smooth and turbulent flow over airfoil.

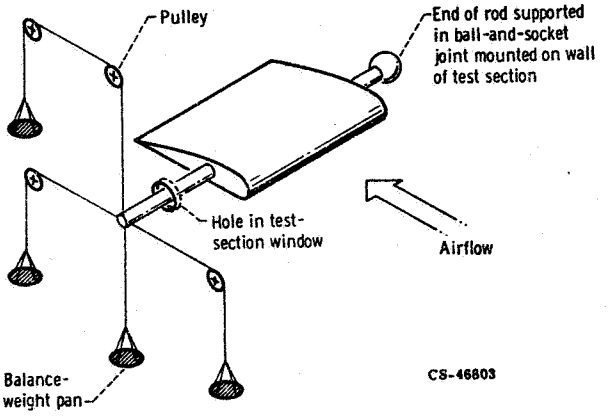

(f) Schematic of force-balance system for measuring lift and drag of airfoil.

Figure 17-13. - Explorer wind-tunnel details.

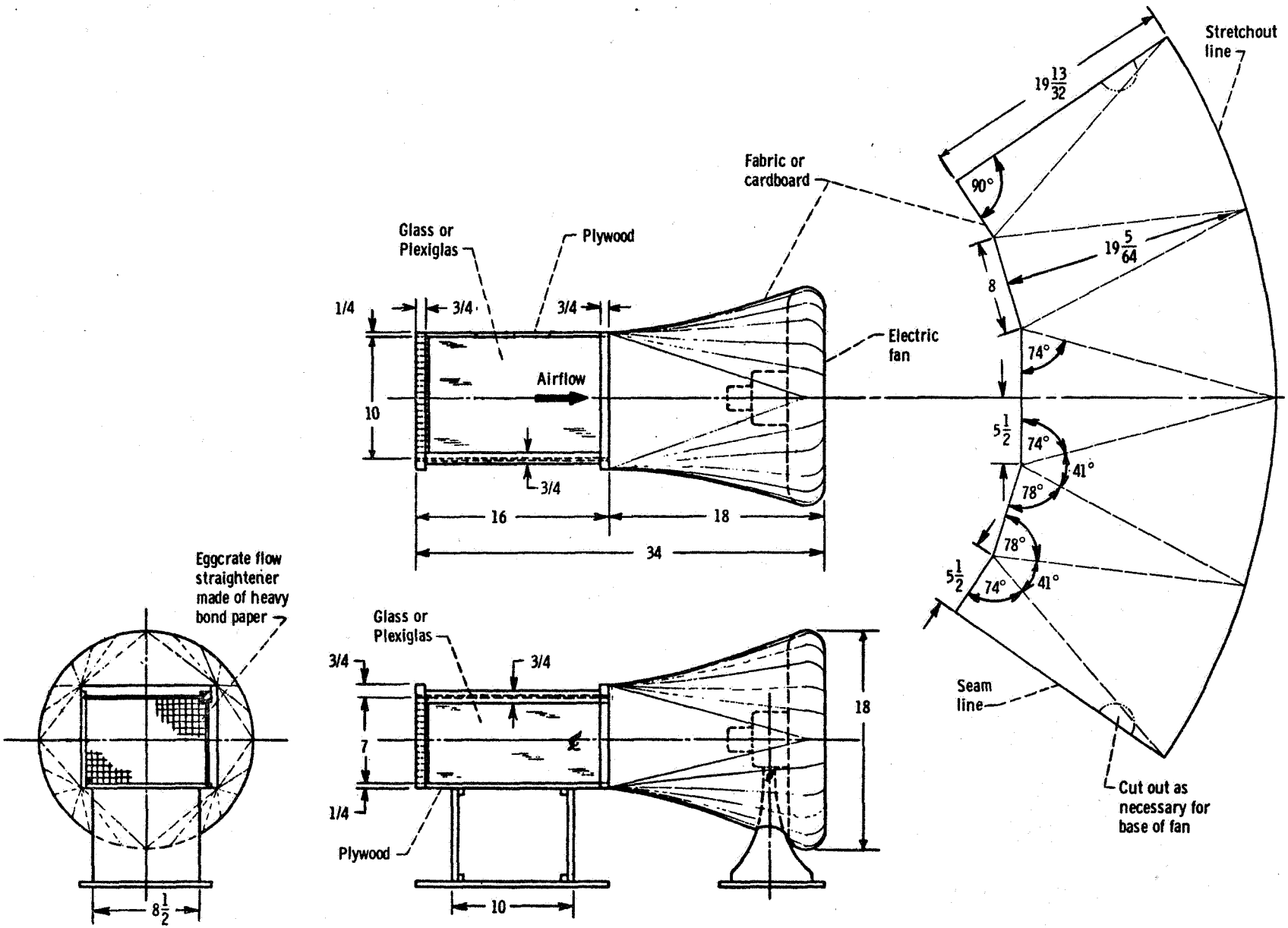

Figure 17-14. - Simple design for small, low-speed wind tunnel. (All linear dimensions in inches.)

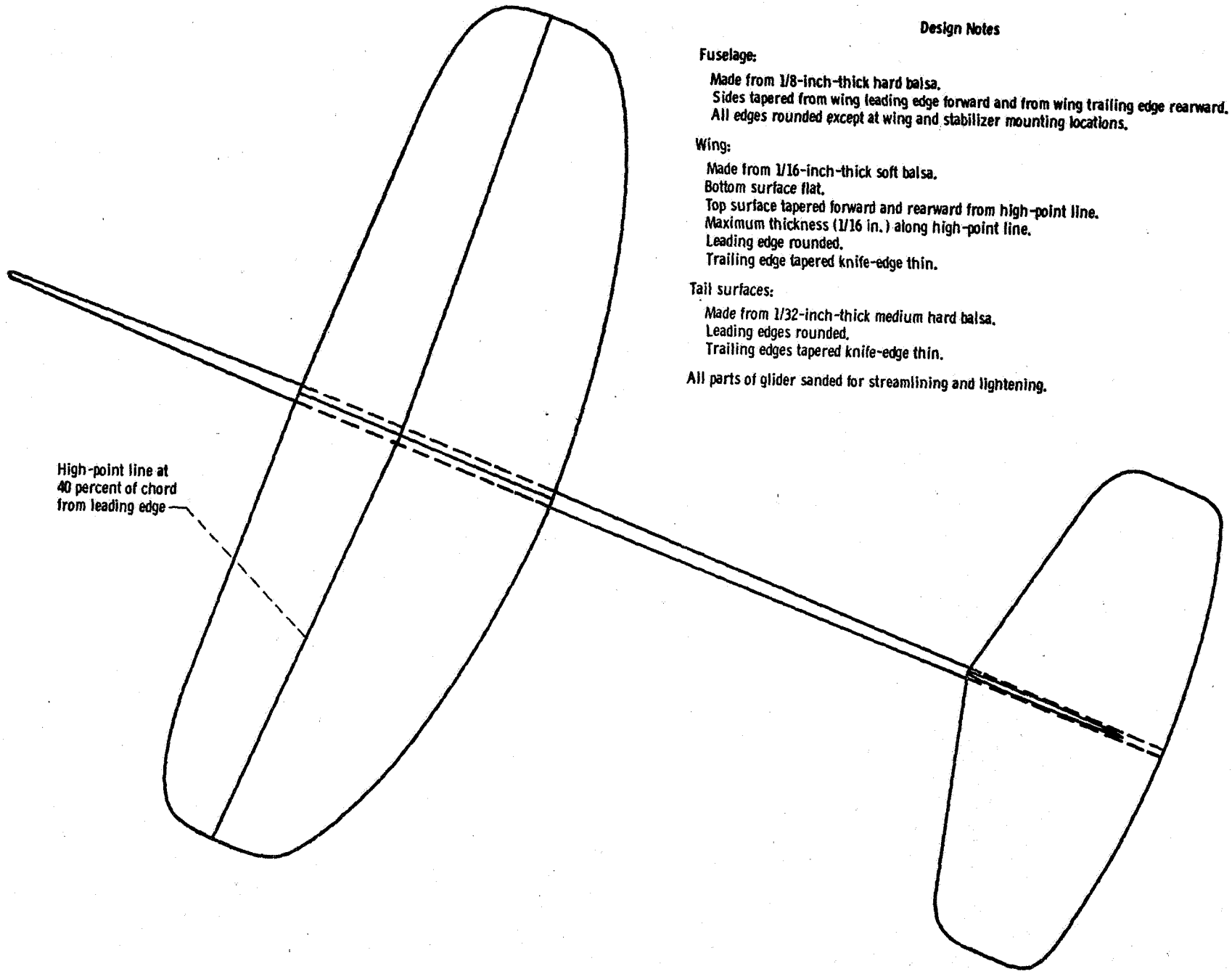

Design Notes

Fuselage:

Made from 1/8-inch-thick hard balsa.
Sides tapered from wing leading edge forward and from wing trailing edge rearward.
All edges rounded except at wing and stabilizer mounting locations.

Wing:

Made from 1/16-inch-thick soft balsa.
Bottom surface flat.
Top surface tapered forward and rearward from high-point line.
Maximum thickness (1/16 in.) along high-point line.
Leading edge rounded.
Trailing edge tapered knife-edge thin.

Tail surfaces:

Made from 1/32-inch-thick medium hard balsa.
Leading edges rounded.
Trailing edges tapered knife-edge thin.

All parts of glider sanded for streamlining and lightening.

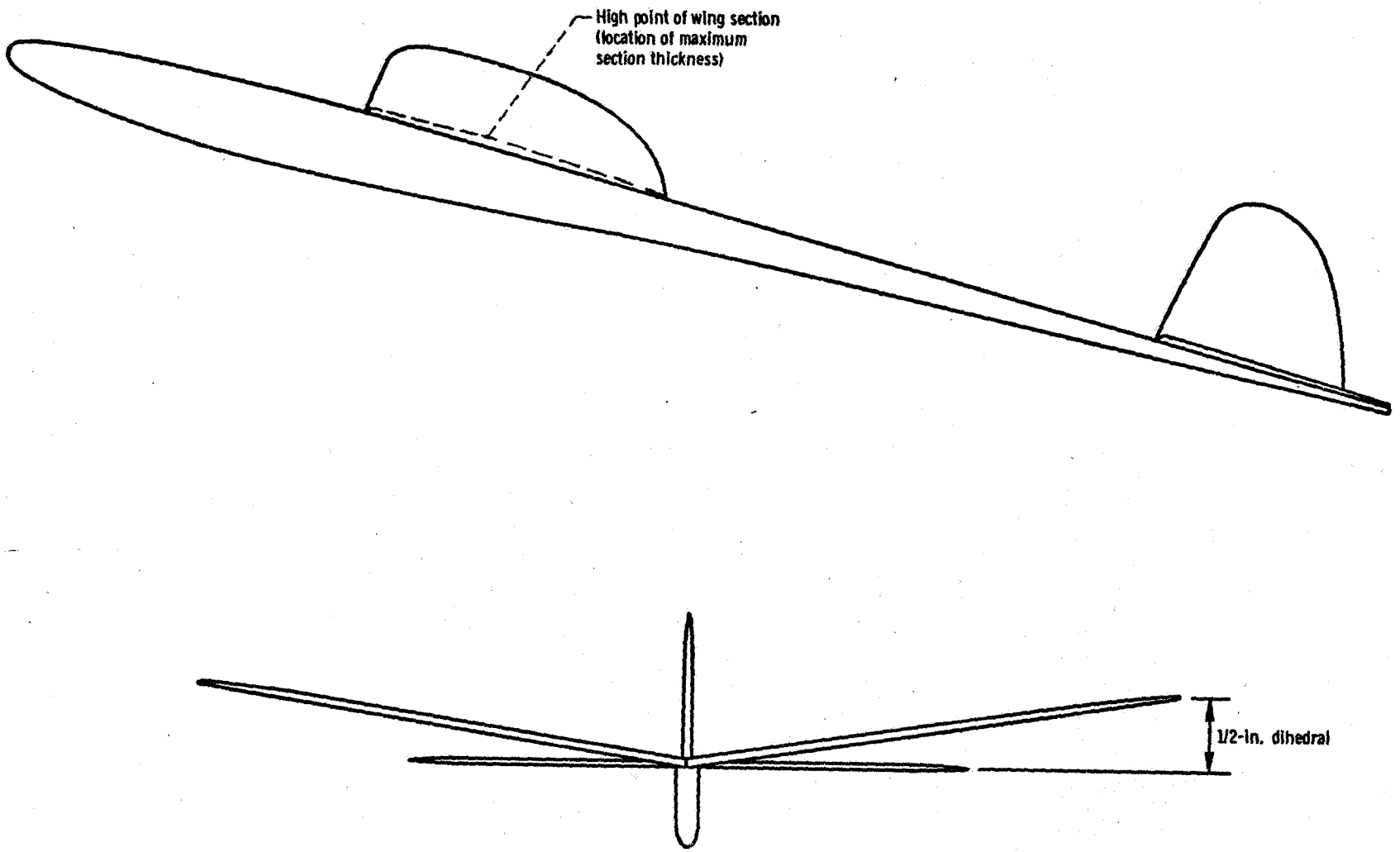

Figure 17-15. - Full-scale plans for small, hand-launched glider.

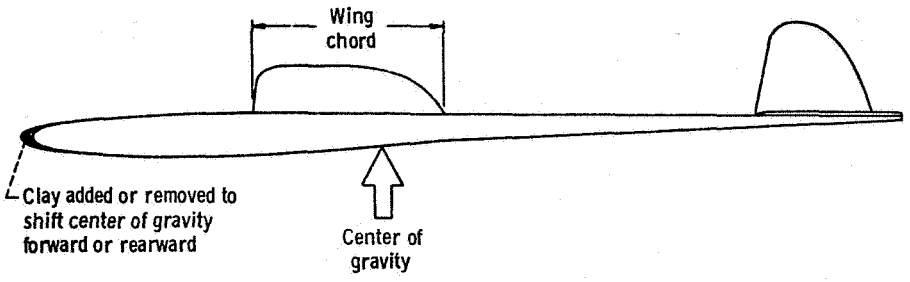

Figure 17-16. - Nose weight (clay) for adjustment of center of gravity.

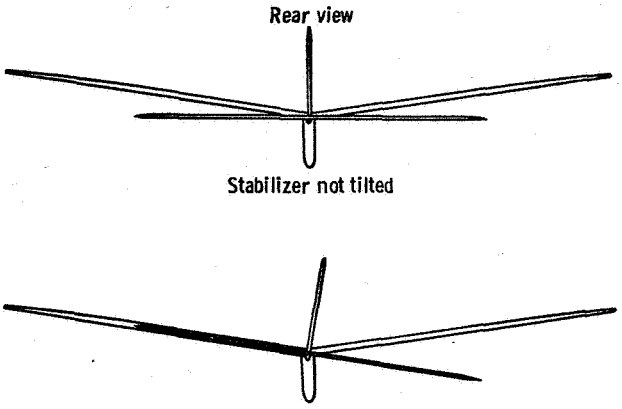

Figure 17-17. - Stabilizer tilt for adjustment of glide turning-circle diameter. (Direction of turn is opposite to direction of tilt.)

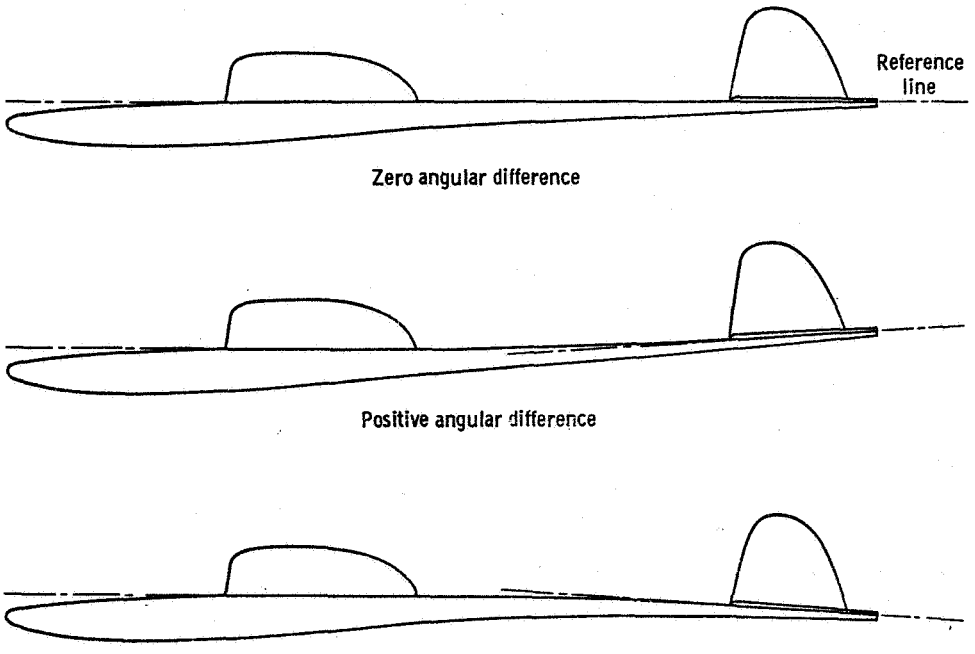

Figure 17-18. - Angular difference between wing and horizontal stabilizer.

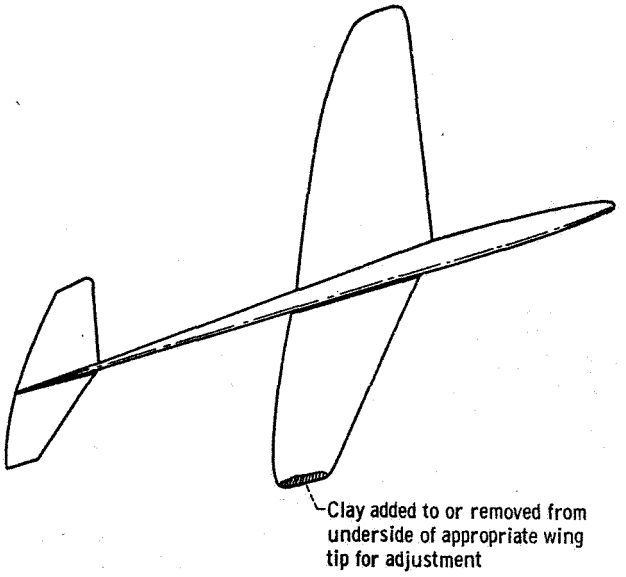

Figure 17-19. - Wing-tip weight (clay) for adjustment of glider roll characteristics.

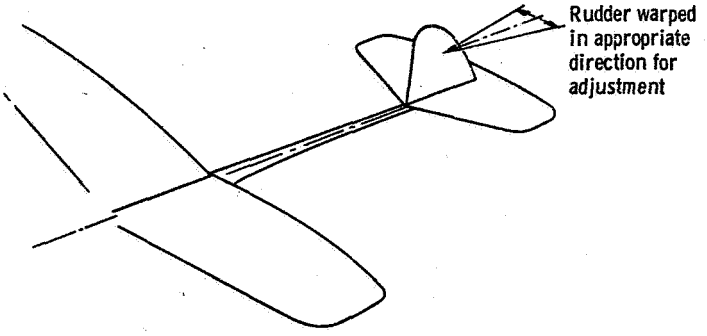

Figure 17-20. - Rudder offset for yaw adjustment to compensate for structural misalinement.

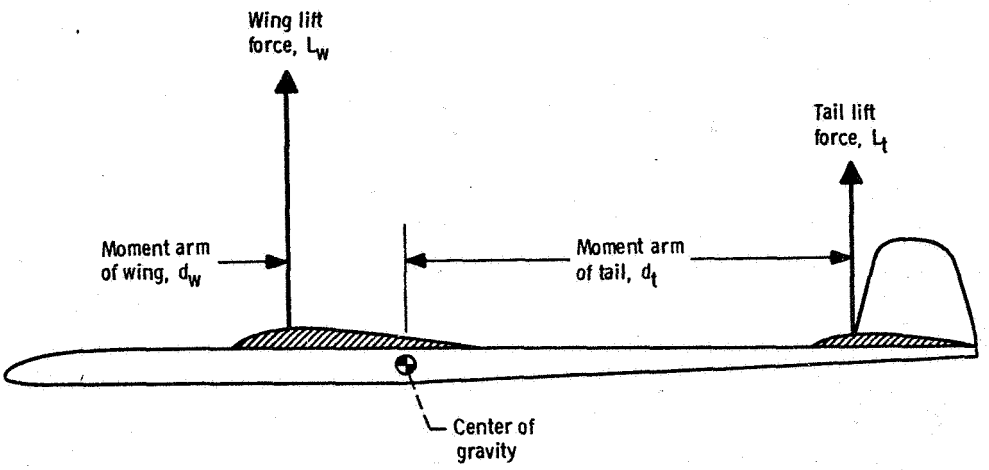

Figure 17-21. - Forces and moments acting in the pitch plane on a hand-launched glider.

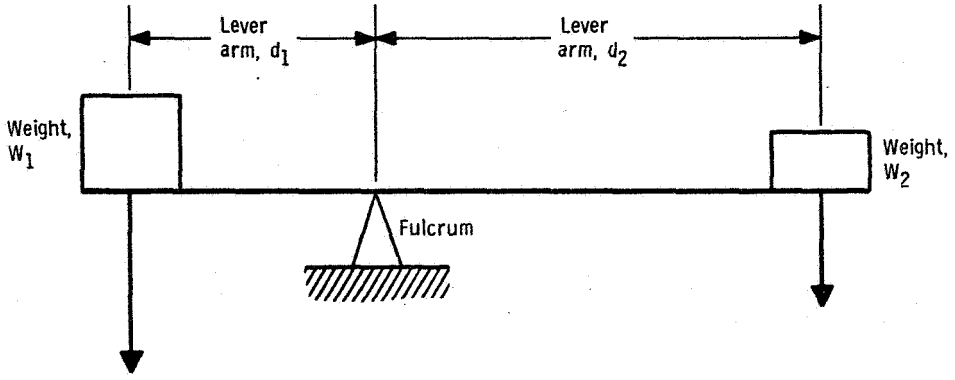

(a) Beam balanced ($W_1d_1 = W_2d_2$) but unstable - no restoring moments.

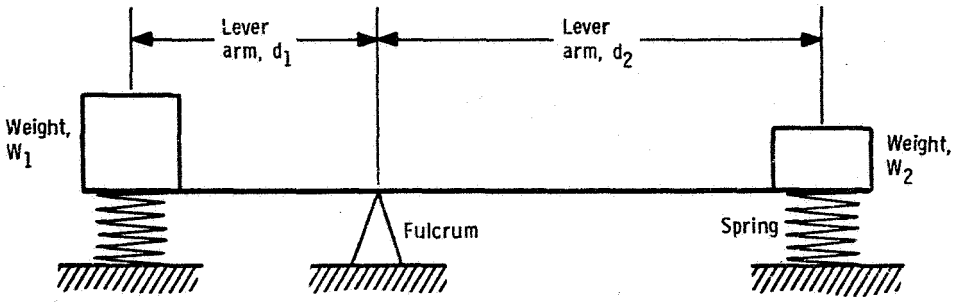

(b) Beam balanced ($W_1d_1 = W_2d_2$) and stable - restoring moments provided by springs.

Figure 17-22. - Unstable and stable balanced beams.

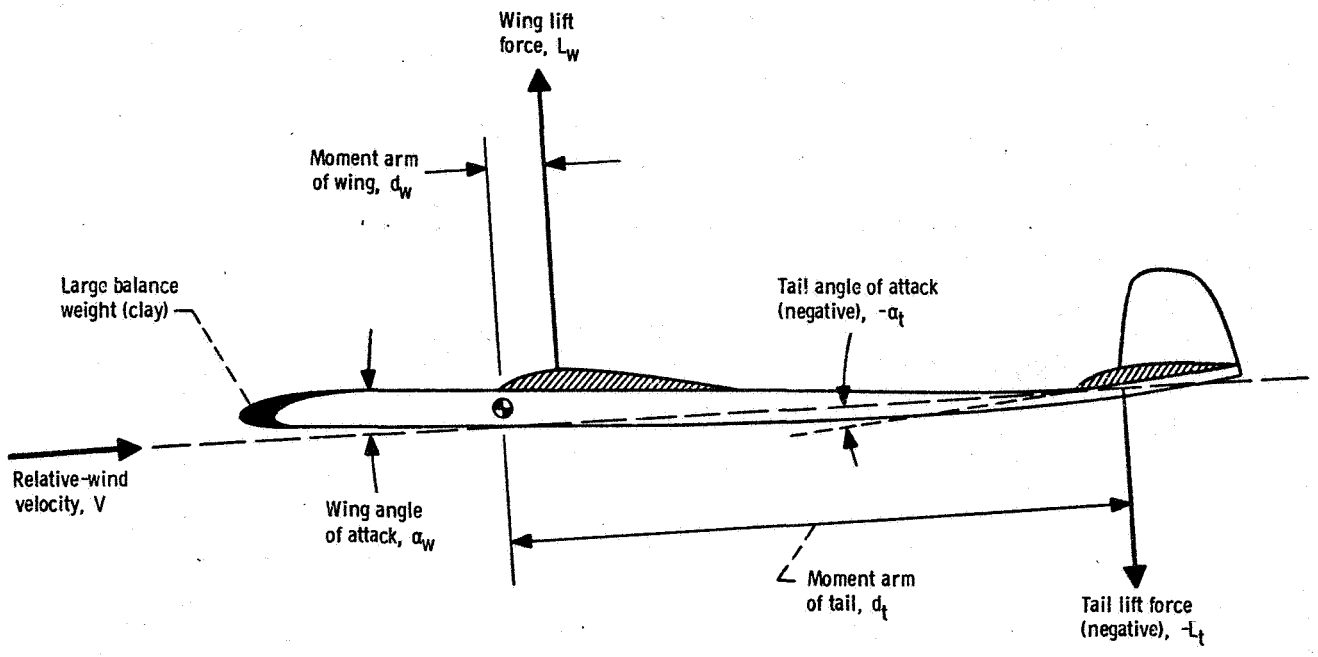

Figure 17-23. - Glider trimmed with the center of gravity ahead of the wing lift force.

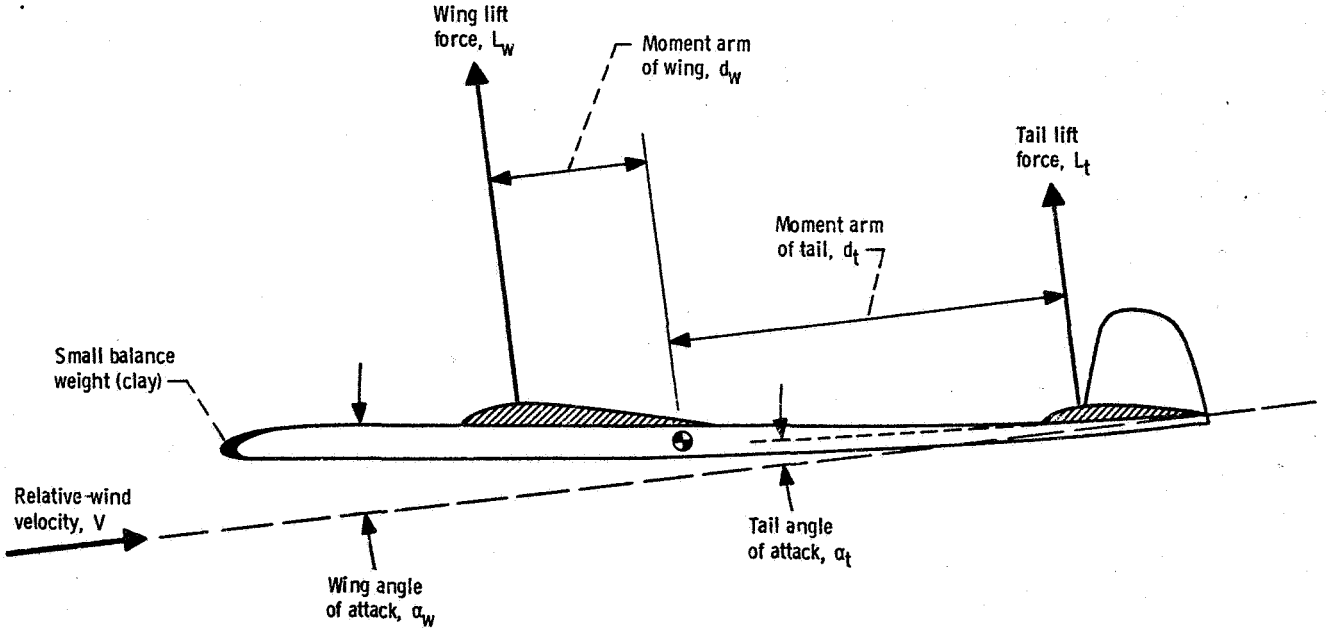

Figure 17-24. - Typical force and moment arrangement for an endurance glider.

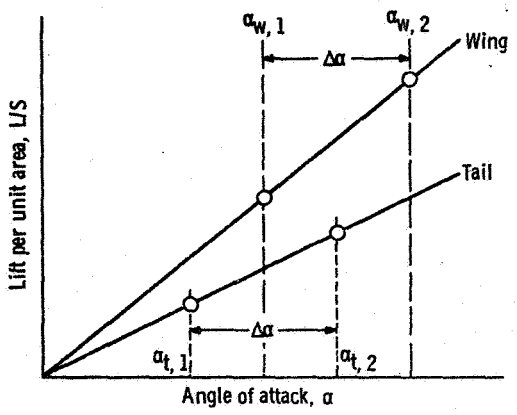

(a) Positive angular difference between wing and tail ($\alpha_w > \alpha_t$).

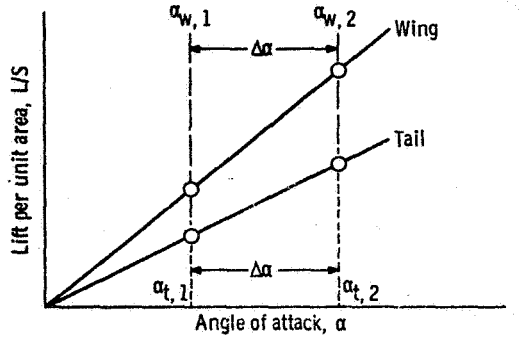

(b) Zero angular difference between wing and tail ($\alpha_w = \alpha_t$).

Figure 17-25. - Variation of lift force per unit area with angle of attack for wing and tail surfaces.

★ U. S. GOVERNMENT PRINTING OFFICE : 1971 O - 437-700